UNIVERSITY OF OKLAHOMA

GRADUATE COLLEGE

CASCADE REACTIONS TO ACCESS BIOACTIVE SCAFFOLDS

A DISSERTATION

SUBMITTED TO THE GRADUATE FACULTY

In partial fulfillment of the requirements for the

Degree of

DOCTOR OF PHILOSOPHY

by

STEVEN C. SCHLITZER

Norman, Oklahoma

2020

CASCADE REACTIONS TO ACCESS BIOACTIVE SCAFFOLDS

A DISSERTATION APPROVED FOR THE

DEPARTMENT OF CHEMISTRY AND BIOCHEMISTRY

BY THE COMMITTEE CONSISTING OF

Dr. Indrajeet Sharma, Chair

Dr. Eric R. I. Abraham

Dr. Daniel T. Glatzhofer

Dr. Adam S. Duerfeldt

Dr. George B. Richter-Addo

DEDICATION

I dedicate this dissertation to my wife Bre Schlitzer for her unending support and optimism throughout our journey in Oklahoma.

A man who fears will suffer twice.

ABSTRACT

In the recent decade there has been a shift in drug development to favor planar, aromatic small molecules with easy synthetic access, despite centuries of research in bioactive natural products, which are often highly rigid, three-dimensional structures like spirocycles. These scaffolds remain underexplored in drug development efforts, predominantly due to the challenges associated with their synthesis, and lack of a general, convergent methodology.

To address these challenges, we have designed an O–H Insertion/Conia-ene reaction cascade between homopropargylic alcohols and acceptor/acceptor diazo compounds, which uses dual Rh/Au^{+} catalytic system. This cascade occurs instantly at room temperature, and has been applied towards the synthesis of substituted tetrahydrofurans when linear diazo compounds are used. Thus far, the cascade accommodates a variety of substituted diazo compounds with carboxylic acids/alcohols to provide functionalized tetrahydrofurans, and γ-butyrolactones, with a high degree of regio- and stereo-selectivity.

Next, we were able to extend the utility of our O–H Insertion/Conia-ene reaction cascade towards the synthesis of spiroheterocycles by employing cyclic diazo substrates with propargylic alcohols. This convergent approach furnishes an array of spiroheterocycles by employing the same dual Rh/Au^{+} catalytic system in refluxing dichloromethane. This approach has proven general, and was used to synthesize a substrate scope of twenty-four substrates based on natural product scaffolds, including spirobarbituates, spiromeldrum's acids, spirooxindoles, and the spirocyclic core of the pseurotin natural products.

Lastly, we have extended our X–H Insertion/Conia-ene strategy towards uncommon nucleophiles, for the synthesis of sulfur- and all-carbon spirocycles. When propargylic thiols are employed as substrates with linear diazos, we have found that the S-H insertion reaction proceeds in high yield, and Conia-ene cyclization can be promoted when the reaction is conducted in a stepwise fashion. However, when the reaction is conducted in a single pot, we isolated a new, thiofuranofuran compound, which we expect forms via undesired 5-endo-dig cyclization of the propargylic thiol, followed by cyclopropanation and subsequent ring opening. Additionally, by changing our retrosynthetic approach to an intramolecular disconnection, we were able to synthesize an all-carbon spirocycle through a benzylic C-H Insertion/Conia-ene cascade, by using a catalytic mixture consisting of $Rh_2(HFB)_4$, $ClAuPPh_3$, and CuOTf in refluxing dichloromethane.

In an orthogonal research effort, we have also developed a metal-free cascade for the synthesis of aromatic heterocycles. This cascade uses precursors synthesized from readily accessible 2'-hydroxy/aminochalcones, and commences with a DBU-mediated intramolecular aldol condensation, which occurs within 90 minutes at room temperature, to generate a 1,3,5-triene. This triene is heated overnight (80 – 120 °C) to promote a 6π-electrocyclization, and oxidative aromatization to generate a new aromatic ring. This cascade has proven general, and has been applied towards the synthesis of benzo[c]coumarins, phenanthradinones, dibenzofurans, and carbazoles, up to a 1-gram scale.

The cascade reactions developed throughout the course of this dissertation research provide new retrosynthetic strategies for the formation of natural product cores, which could be used to expand the chemical space in drug discovery.

ACKNOWLEDGEMENTS

First, I would like to thank my loving wife Bre Schlitzer. I want to thank you for always believing in me, even in the times when I did not believe in myself. I could not have accomplished this feat without you; you are my drive to succeed and a constant source of inspiration, every day. I would like to thank my family, Carla Rauschenplat, Marlene 'Oma' Rauschenplat, and Manny Maldonado. Including but not limited to generous funding throughout my 'roaring twenties,' I am so thankful for the love and support that you have provided for the last ten years of my academic tenure. It is through you all that I have learned what family is, and guides what I am working towards with Bre.

Next, I would like to thank my undergraduate research adviser, Dr. Benjamin Gung, and the amazing young chemists that I had the pleasure of growing with at Miami University – Ethan Miller, John F. Manganaro, and Seth Filbrun. I would also like to thank my "batchmates," who started the Ph. D. program with me at OU – Eric Gardner, Jessi Gardner, and Quentin Avila. I could not have gotten to where I am today without your friendship and support. I cannot wait to see what our futures hold as STEM leaders, and I hope our paths converge once more.

Lastly, I would like to thank the University of Oklahoma and the Department of Chemistry and Biochemistry for providing a supportive venue to pursue my doctoral studies. I would like to thank my Ph. D. adviser and graduate committee chair, Dr. Indrajeet 'Inder' Sharma. Your unparalleled skills as a mentor and never-ending flow of ideas have given me a goalpost for what I would like to someday achieve not only as a scientist, but an educator. I would also like to thank my fellow Sharma lab teammates - senior students Dr. Arianne Hunter and Dr. Nick Massaro, and

junior students Joe Stevens, Anae Bain and Adam Alber. I would also like to thank undergraduate students Bilal Almutwalli and Katelyn Stevens for their contributions and providing opportunities to develop my skills as a mentor. I would also like to thank the post-docs who have helped guide my success along the way – Dr. Kiran Chinthpally, Dr. Dhanarajan 'Arun' Arunprasah and Dr. Santosh Rao. I would also like to thank the members of my graduate committee, Dr. Adam Duerfeldt, Dr. Daniel Glatzhofer, Dr. George Richter-Addo, and Dr. Eric Abraham; you have provided the fundamental education, support, and valuable feedback that helped guide me through my five years at OU. Finally, I would like to thank the amazing research support staff who have helped me on a near-daily basis – Dr. Susan Nimmo (NMR Spectroscopy), Dr. Steven Foster (HRMS), and Dr. Doug Powell (X-Ray Crystallography).

TABLE OF CONTENTES

LIST OF FIGURES

CHAPTER 1

CHAPTER 2

CHAPTER 4

LIST OF SCHEMES

CHAPTER 1

CHAPTER 2

CHAPTER 3

CHAPTER 4

LIST OF TABLES

CHAPTER 1

CHAPTER 2

CHAPTER 4

LIST OF ABBREVIATIONS

Å	Angstrom
A/A	Acceptor/Acceptor
$[\alpha]_D$	specific rotation at wavelength of sodium D line
Ac	acetyl
acac	acetylacetonate
Aq.	aqueous
Ar	aryl
atm	atmosphere
BF_4	tetrafluoroborate
Bn	benzyl
Boc	tert-butyloxycarbonyl
bp	boiling point
br	broad
brsm	based on recovered starting material
Bu	butyl
n-Bu	n-butyl
t-Bu	*tert*-butyl
bz	benzoyl
c	concentration for specific rotation measurements
^oC	degrees Celsius (centigrade)
calc'd	calculated
cat.	Catalytic
CCDC	Cambridge Crystallographic Data Centre
$CDCl_3$	deuterated chloroform
CI	chemical ionization
CM	complex mixture
CSA	camphorsulfonic acid
Cy	cyclohexyl
Δ	Reflux temperature
d	doublet
dba	dibenzylideneacetone
D/A	Donor/Acceptor
DBU	1,8-diazobicyclo[5.4.0]undec-7-ene
DCE	1,2-dichloroethane
DCM	dichloromethane
dec.	decomposition
DMAP	4-methylaminopyridine
DMB	2,4-dimethoxybenzyl
DMF	*N*,*N*-dimethylformamide

DMSO	dimethylsulfoxide
d.r.	diastereomeric ratio
E	entgegen (opposite)
E^+	electrophile
EDCI	1-ethyl-3-(3-dimethylaminopropyl)carbodiimide
EDG	electron donating group
ee	enantiomeric excess
E/H	ethyl acetate in hexanes
EI	electron impact
equiv.	equivalent
en	1,2-ethylenediamine
ESI	electrospray ionization
(esp)	$\alpha,\alpha,\alpha',\alpha'$-tetramethyl-1,3-benzenedipropionic acid
Et	ethyl
Et_3N	triethylamine
EtOH	ethanol
EWG	electron withdrawing group
FAB	fast atom bombardment
g	gram(s)
GC	gas chromatography
HFB	heptafluorobutyrate
HMDS	1,1,1,3,3,3-hexamethyldisilazane
HMPA	hexamethylphosphoramide
HPLC	high-performance liquid chromatography
hr	hour(s)
HRMS	high-resolution mass spectrometry
$h\nu$	light
Hz	Hertz
^iPr	isopropyl
IR	infrared (spectroscopy)
J	coupling constant
LG	leaving group
λ	wavelength
L	liter
L_n	ligand
m	multiplet or milli
m-	meta
m/z	mass-to-charge ratio
μ	micro
M	metal or molar
Me	methyl
MeCN	acetonitrile
MHz	megahertz
min	minute(s)

mol	mole(s)
mp	melting point
MS	molecular sieves
n	nano
N	normal (normality)
NMR	nuclear magnetic resonance
nOe	nuclear Overhauser effect
NR	no reaction
Nu	nucleophile
o-	ortho
p-	para
Ph	phenyl
pH	hydrogen ion concentration in aqueous solution
piv	pivaloyl
ppm	parts per million
i-Pr	isopropyl
p-ABSA	4-acetamidobenzenesulfonylazide
p-TSA	para-toluenesulfonic acid
Pyr	pyridine
q	quartet
ref	reference
R_f	retention factor
rt	room temperature
s	singlet
SAR	structure-activity relationship
sat.	saturated
t	triplet
TBAF	tetrabutylammonium fluoride
TBS	tert-butyldimethylsilyl
temp.	temperature
Tf	trifluoromethanesulfonyl (triflate)
TFA	trifluoroacetic acid
THF	tetrahydrofuran
TIPS	Triisopropylsilyl
TLC	thin layer chromatography
TMS	trimethylsilyl
Ts	p-toluenesulfonyl (tosyl)
X	anionic ligand or halide
Z	zusamman (together)

CHAPTER 1

Cascade Reactions: The Key to Molecular Complexity in Drug Development

1.1 Introduction

The rising cost of therapeutics has been a topic of great debate in the last decade, and this topic strikes at a core issue in America – public health. With the current outbreak of the novel COVID-19 virus, public health is at the forefront of public consideration, on a global scale. This attention has spurred an urgent need for the development of new bioactive entities for the treatment of diseases, novel or otherwise. The rising cost of therapeutics is caused by a number of factors, including but not limited to their development time, average success rate, and method

of their synthesis. Innovation in the field of synthetic methodologies can contribute to reducing these development costs.

A recent study published in the Journal of Health Economics has reported the cost of developing a new prescription medication is $2.6 billion, which has raised from $802 million in 2003.[1] These rising costs have several contributing factors, including the increased timeline of drug development and approval process in the 2010's, often lasting a decade or more. And it is best not forgotten that development costs are high for entities that do not receive FDA approval – placing a higher burden of cost on drugs that are approved. The majority of these compounds fail during phase II or III clinical trials, which are often 3.5-7 years into the development timeline, after submission of an Investigational New Drug Application (IND) with the FDA. To recoup development costs, many compounds that do not receive FDA approval for their initial treatment goals are screened for treating other diseases.

Even for drug compounds that are approved for production, one key factor contributing to the cost of their development is the number of steps associated with their synthesis. Currently the desire to minimize the number of synthetic steps in drug development, and the effort to prioritize combinatorial chemistry, the practice of high-throughput synthesis of compounds, has resulted in a number of blockbuster drugs however these compounds are primarily achiral, saturated, aromatic molecules.[2]

These features have severely limited the chemical space explored in current drug development efforts. Chemical space provides a representation of all possible carbon-based molecules than can be created.[3] Just like the number of planets, solar systems, and galaxies is

vast on a universal macroscale, the number of small molecules in chemical space is equally vast on the atomic microscale. By focusing modern drug development efforts on planar, aromatic molecules like those prepared in combinatorial chemistry, an entire realm of chemical space is being ignored, which could hold the key to highly potent, selective drug entities. Structurally complex, biologically relevant spirocycles, meanwhile, recently have been classified and their role in chemical space comprehensively mapped.[3b-e]

One area of chemical space that has been explored in drug development is the field of natural products. Natural products are generated as either primary or secondary metabolites of all living plants, animals, and marine organisms, and boast a high degree of structural complexity underexplored in chemical space. The enzymes responsible for the biosynthesis of these compounds are the ultimate chiral environment, often installing functional groups with a degree of stereocontrol that is unprecedented in synthetic chemistry. Natural products and their analogues had been a boon for pharmaceuticals throughout the 20th century, until the expansion of synthetic medicinal chemistry in the 1990's shifted attention away from structurally complex molecules towards smaller molecules with short, straightforward synthetic routes, which could be easily screened in a high-throughput fashion from a library of compounds.[4]

Indeed, a survey on four databases consisting of over 10,000 drugs and 3,000 natural products and has served to quantify the structural complexity lacking in modern pharmaceuticals. Namely, natural products typically contain more atoms (avg. M.W. 414 g/mol vs 340 g/mol), chiral centers (6.2 vs. 2.3), and H-Bond donors/acceptors. Likewise, successful drugs have more in common with compounds synthesized via combinatorial chemistry – these compounds have

an average molecular weight of 393 g/mol, 0.4 chiral centers per compound, and fewer H-Bond donors/acceptors.

The inherent disadvantage of pursuing natural products as drug candidates is that the methods to obtain large quantities needed for mass production rely on long total synthesis, often on the magnitude of 20 to 40 steps, or unsustainable depletion of their source material. Therefore, there is a great need to harness the structural complexity found in natural products, which breeds target binding specificity, while minimizing the number of steps required to install said complexity from readily available starting materials. To circumvent the lengthy synthesis required to prepare complex natural product structures, one can install a high degree of complexity using cascade reactions, in which two or more transformations occur in a single reaction vessel.

1.2 CASCADE REACTIONS IN TOTAL SYNTHESIS

In traditional organic synthesis, a multi-step reaction scheme is conducted by isolating the product of each individual reaction – this approach can be marred by time, characterization, and purification costs, especially when chromatographic purification is required. Ideally, one would perform multiple reactions without isolating intermediate products, in a process known as a reaction cascade. An ideal reaction cascade has to assure that the individual components are only involved in the reaction when they are required to do so, else byproducts arising from undesired reactivity pathways can result in a reduced yield. The literature contains many terms, used somewhat interchangeably, for the process of performing multiple reactions in a one-pot fashion, including cascade, domino, and tandem. For the purpose of this section, we will consider

cascade reactions only where all catalysts and reagents are present from the start of the reaction, and no additional additives are added throughout the course of the reaction.

The application of a reaction cascade lies at the pinnacle of synthetic design – generally producing complex, rigid scaffolds from simple starting materials. Because of their ability to install molecular complexity, cascade reactions have been a valuable tool in natural product total synthesis for decades, with R. Robinson's 1917 total synthesis of tropinone considered the seminal work in the field.[5-6]

Because the field of cascade reactions broadly encompasses all chemical transformations, classification of the cascades can be difficult; In a recent review of cascade reactions, K. C. Nicolaou and coworkers separated the field into five classes.[5c] Nicolaou et. al. classified a litany of cascade reactions used in total synthesis by their principal component reactivity – nucleophilic, electrophilic, radical-mediated, pericyclic, and transition-metal mediated processes. Notably, these classifications are restricted to the synthetic transformations of small molecules using organic reagents and transition-metal catalysts, and does not cover the wealth of advances made in enzymatic catalysis.

Nucleophilic cascade reactions generally employ the use of a base to generate the active nucleophile, or commence from pre-formed organometallic nucleophiles; this approach is exemplified in Sorenson's 2004 synthesis of (+)-harziphilone (**Scheme 1.1a**).[7a] Likewise, their electrophilic cascade counterparts use acid to increase the electrophilicity of pre-existing functional groups, or utilize traditional electrophilic reagents (e.g. $BF_3{\cdot}OEt_2$, organosilanes, organoselenates, etc.), as seen in Padwa et. al's 2002 synthesis of racemic jamine (**Scheme**

1.1b).[7b] In both cases, thermodynamic or photochemical conditions may need be employed to promote desired reactivity.

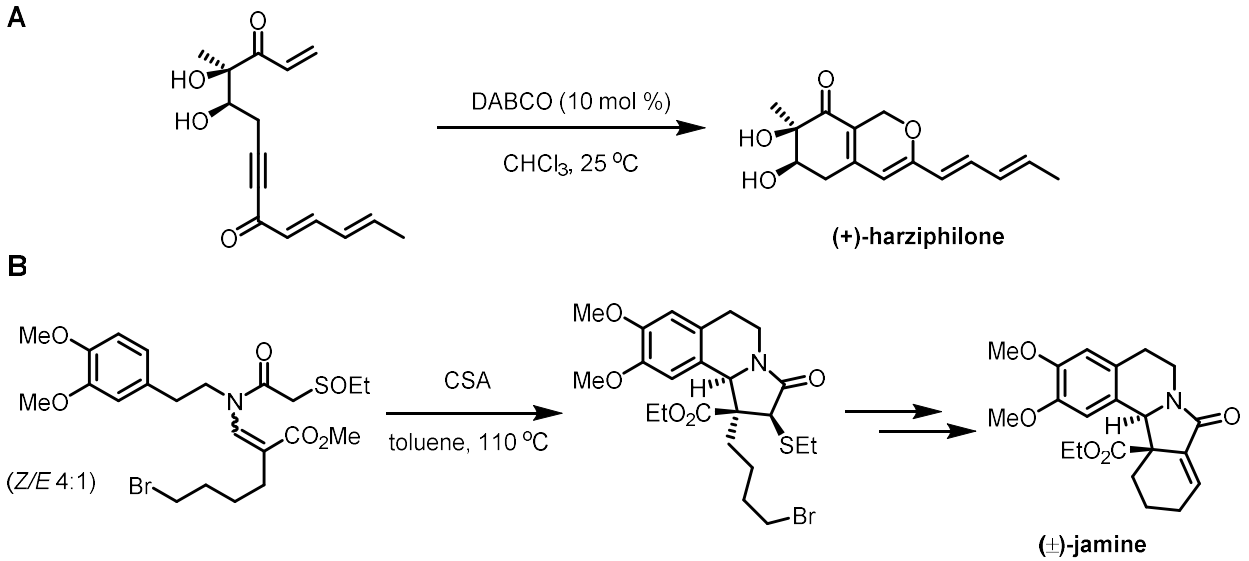

Scheme 1.1 a.) Representative example of nucleophilic cascade reactions b.) Representative example of electrophilic cascade reactions

Because organic radicals are, by definition, a highly reactive species, they represent the ideal candidate for cascade transformations. In many cases, an organic radical will break a pre-existing or create a new σ-bond, generating a new radical intermediate capable of continuing the cascade, until the radical is ultimately trapped or scavenged. Parker and Fokas' synthesis of morphine utilizes a radical cyclization cascade to form of the compound's core (**Scheme 1.2**).[7c]

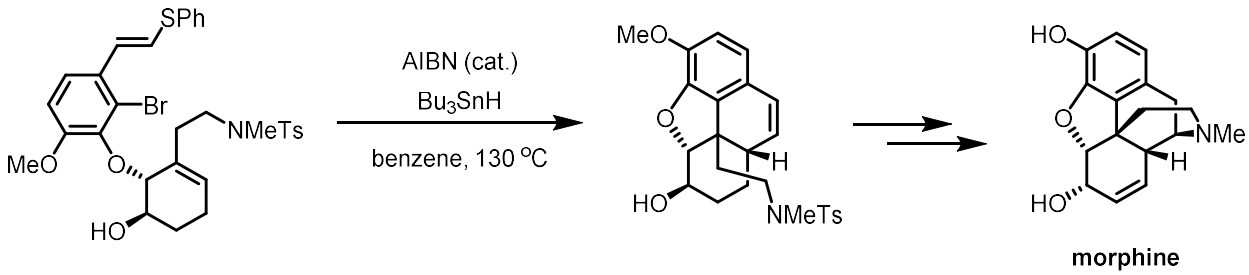

Scheme 1.2 Representative example of radical cascade reactions

Pericyclic reactions have also been used in cascades, and are perhaps the most common processes encountered in cascade reactions. Because pericyclic reactions typically only

require thermal or photochemical input to proceed, this reaction class boasts a high degree of functional group tolerance which is ideal in cascade methodology. This class broadly includes cycloadditions, sigmatropic rearrangements and electrocyclic reactions. Due to the concerted nature of their reaction mechanisms, pericyclic reactions often generate complex scaffolds with a high degree of stereocontrol. One key example of a pericyclic reaction cascade is Boger et. al's 2006 synthesis of vindorosine, in which a δ-lactone core is generated through a Diels-Alder reaction of an 1,3,4-oxadiazole, followed by intramolecular [3+2] cycloaddition (**Scheme 1.3**).[7d]

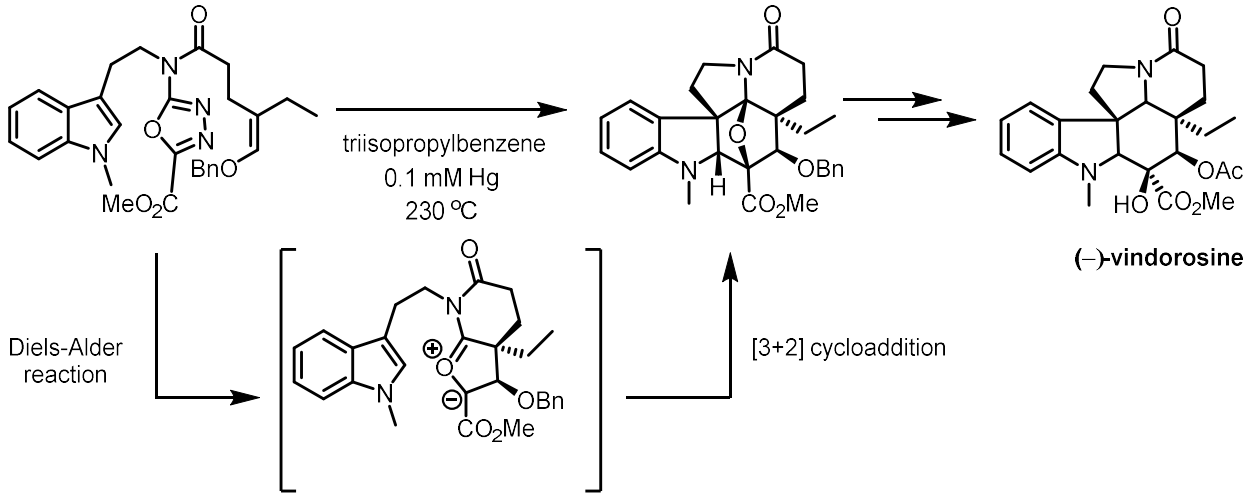

Scheme 1.3 Representative example of pericyclic cascade reactions

Lastly, the advances in transition metal catalysis has resulted in a wealth of examples in the development of multi-step cascade reactions; In recent years, development of chiral ligands for metal catalysts provides potential for cascades with a high degree of enantioselectivity. Palladium catalysis has provided a wealth of transformations for the synthetic chemist's toolbox in the past 50 years, and its catalytic cycle could be considered a reaction cascade in its own regard. Amongst the palladium-catalyzed C-C bond coupling reactions, the Heck reaction has found numerous applications in cascade development. This principle is

exemplified in Keay et. al's total synthesis of (+)-xestoquinone, in which a palladium (0) catalyst paired with a chiral BINAP ligand, promotes multiple 1,2-additions of palladium (II) intermediates to olefins, and terminates through β-hydride elimination (**Scheme 1.4**).[7e]

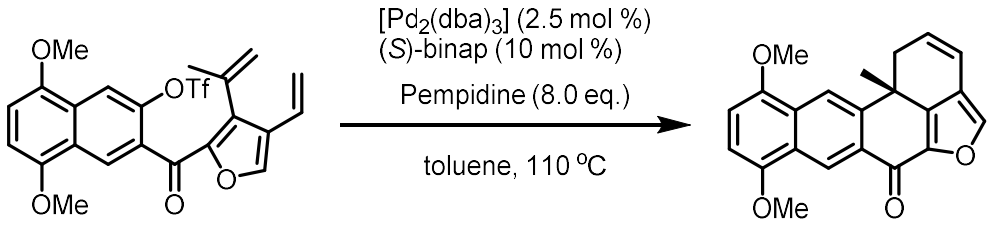

Scheme 1.4 Representative example of transition-metal mediated cascade reactions

Cascade reactions have been shown to generate complex scaffolds with a high degree of selectivity in a single step. This strategy has been applied to the total synthesis of several natural products, and can be an asset in drug discovery to reduce the cost of generating bioactive scaffolds in multi-step schemes. Despite significant advances in the field of cascade reactions, further development is needed to access underexplored scaffolds like spirocycles.

1.3 SPIROCYCLIC NATURAL PRODUCT SYNTHESIS

Spirocycles are valuable targets in drug discovery because their rigid scaffolds are capable of directing their substituents in a precise, 3D fashion. Although they are valuable targets, methodology remains limited for the convergent construction of spirocycles. This section will highlight some key spirocyclic natural products, and a recent example of their synthesis. Several of these syntheses utilize α-diazocarbonyls to generate carbenoids, but their ambiphilic reactivity is not exploited to generate the full spirocenter, with several additional steps needed to form the second ring. Examples such as these however have inspired our approach – designing a new reaction cascade, utilizing substrates containing a nucleophile and electrophile, in

combination with diazo compounds such as those explored in this section to generate spirocycles in a single step with a high degree of selectivity.

1.3.1 SYNTHESIS OF (±)-BERKELEYAMIDE D AND NATURAL (–)-BERKELEYAMIDE D

The spirocyclic γ-lactam natural product Berkeleyamide D was originally isolated by Stierle, et al. in 2008 from the acid lake fungus *Penicillium rubrum* from Berkeley Pit Lake in Butte, Montana. This potent natural product was found to inhibit MMP3 and caspase-1.[11] Berkeleyamide belongs to a family of related α-spiro-γ-lactam natural products including the Pseurotin family and Azaspirene (**Fig. 1.1**).

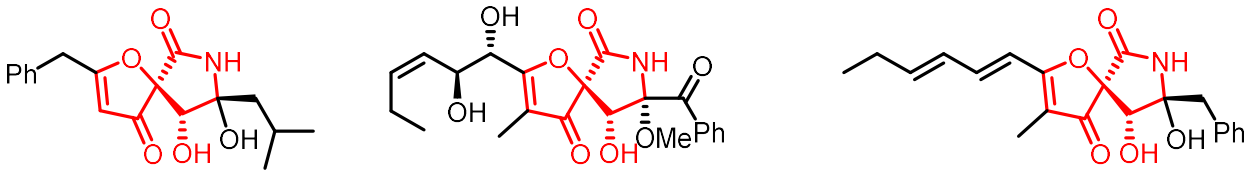

Figure 1.1. Spiro-γ-lactam natural products

While the absolute configuration of spiro-γ-lactams Pseurotin A and Azaspirene were able to be determined by extensive NMR characterization and X-Ray crystallography, the absolute configuration of Berkeleyamide D at C5 and relationship between substituents at C8 and C9 remained unknown until the first racemic synthesis was reported in 2014 by Tsubaki et al. The prepared racemate with separated by chiral HPLC gave both (+)- and (–)-enantiomers of Berkeleyamide D, with specific rotation values of $[\alpha]^{17}_{D}$ = +84.6 and -85.7, respectively.; the specific rotation of natural Berkeleyamide D was reported to be $[\alpha]^{25}_{D}$ = -55.9, which confirms the natural source as the (–)-enantiomer.[12]

The 2014 Tsubaki racemic synthesis of Berkeleyamide D was accomplished in four synthetic steps and relies on a Darzens reaction to form an α,β-epoxy-γ-lactam, a central structure of several natural products, followed by formation of the spirocenter through *C*-acylation. (**Scheme 1.5**).

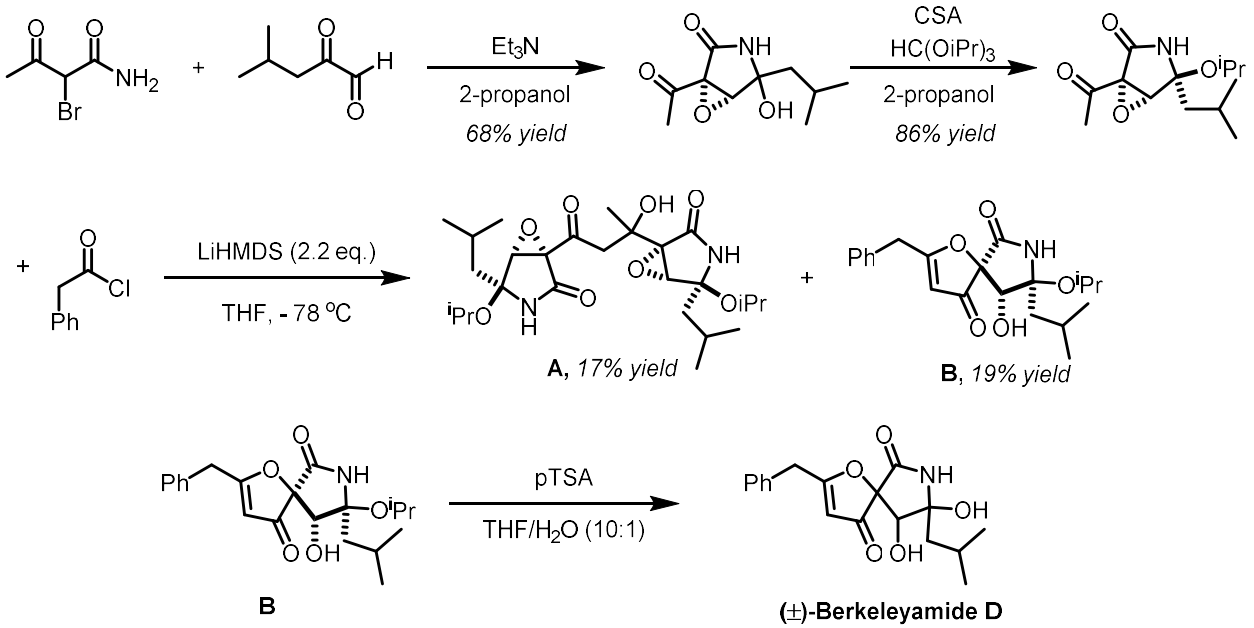

Scheme 1.5. Tsubaki et. al's first reported synthesis of (±)-Berkeleyamide D

Starting from an α-bromoketoamide, the authors developed a Darzens reaction using isobutyl glyoxyal to prepare an α,β-epoxy-γ-lactam in modest yield. This was treated with camphorsulfonic acid and exposed to triisopropyl orthoformate to generate the isopropyl ether as a single diastereomer; it is proposed that the nucleophile trajectory was dictated by the stearic bulk of the neighboring epoxide functionality. A lithium enolate of this ether was generated by exposure to LiHMDS which was quenched with phenylacetyl chloride to prepare the desired spirolactam **A**, along with the undesired homodimer **B**. Unfortunately, screening of alternative bases and additives were unable to improve the yield of **A**. Finally, hydrolysis of **A** using para-toluenesulfonic acid afforded racemic Berkeleyamide D.

The first asymmetric synthesis of Berkeleyamide D was recently completed in 2019, due to methodology developed by Shen, et al.[13] They describe a new asymmetric Darzens reaction to produce optically pure α,β-epoxy-γ-lactams (**Scheme 1.6**).

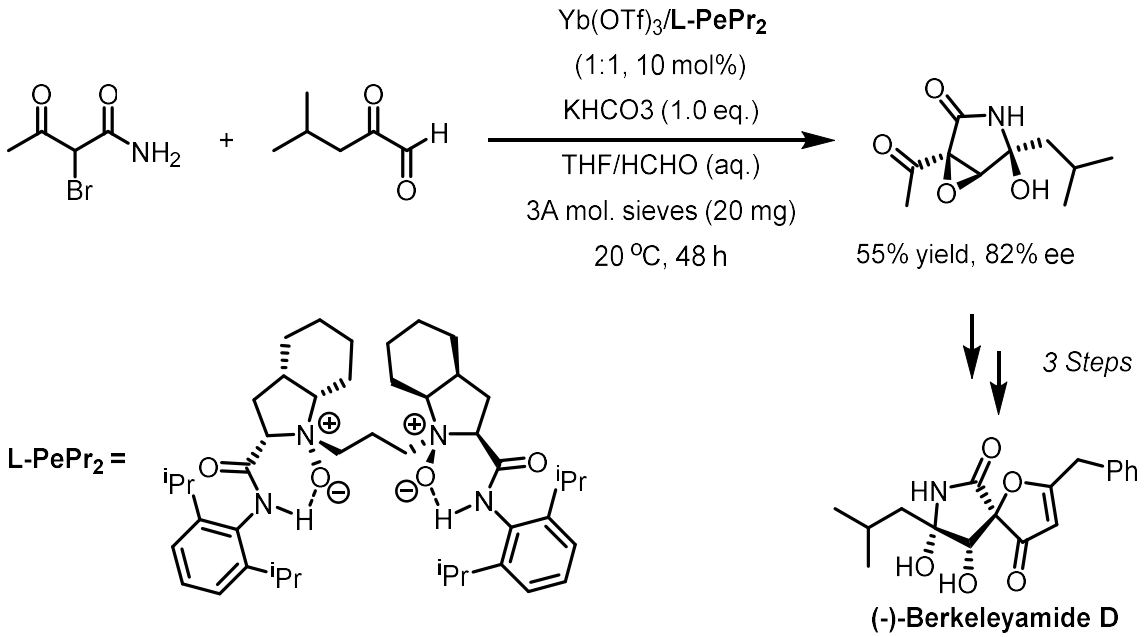

Scheme 1.6. Shen et. al's asymmetric Darzens reaction to access (–)-Berkeleyamide D

Shen's formal synthesis utilized a new method developed in their group for the asymmetric synthesis of α,β-epoxy-γ-lactams with a chiral Ytterbium (III) catalyst, generated *in situ* via the reaction between $Yb(OTf)_3$ and the chiral *N,N'*-dioxide ligand **L-PePr₂**. While both chiral organocatalysis and Lewis acid catalysis have been successfully employed for enantioselective Darzens reactions, the nucleophile had been limited to α-halo carbonyls, chloroacetonitrile, chloromethylsulfones, and 2-halo-1-indanones until this point. The authors describe challenges in the desired asymmetric Darzens cascade including the steric hindrance of the new α-bromo-β-ketoamide nucleophile hampering the S_N2 cyclization processes. Also, the diastereoselectivity of the aldol addition is directly related to the subsequent formation of the epoxide and lactam due to stereochemistry requirements, and the potential of a retro-aldol

process could reduce the enantioselectivity of the reaction. Nevertheless, using the new Yb-catalyzed conditions, the α,β-epoxy-γ-lactam was formed in good yields with excellent enantioselectivity, and the authors were then able to complete the synthesis of (–)-Berkleyamide D following the remaining steps as outlined by Tsubaki et al.

1.3.2 SYNTHESIS OF INDOLE ALKALOID (–)-SPIROTRYPROSTATIN B

(–)-Spirotryprostain B is a natural product classified as an indole alkaloid which was isolated in 1996 by Osada et al. from the fermentation broth of *Aspergillus fumigatus* BM939.[8] The compound, which can only be isolated in trace amounts (11 mg/400 mL fermentation broth), is known to inhibit the cell cycle in the G2/M phase and shows cytotoxic activity against the growth of human leukemia cell lines. While the first total synthesis of (–)-Spirotryprostatin B was reported in 2000,[8b] a total synthesis of the compound was reported by Meyers and Carreira in 2003 which utilizes cyclopropane formation from 3-diazooxindole (**Scheme 1.7**).[8] While this approach to (–)-Spirotryprostatin B is elegant in its own regard, it relies on multiple steps to generate the spirocenter, which could be reduced to a single step via novel cascade methodology.

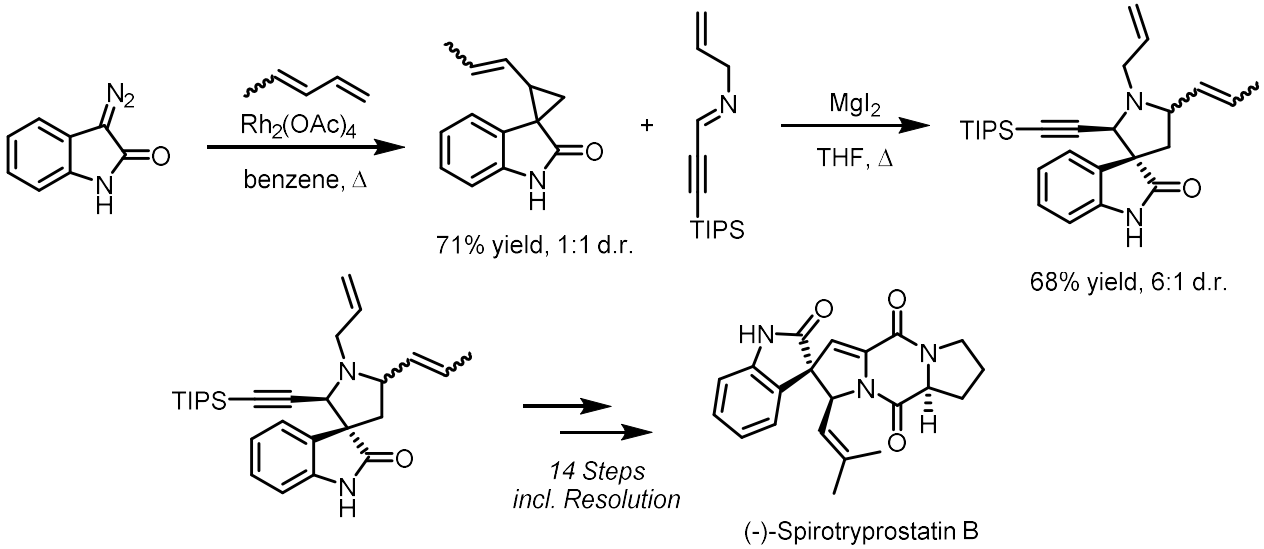

Scheme 1.7 Meyers and Carreira's Synthesis of (–)-Spirotryprostatin B

The first step in Carreira's synthesis involved a rhodium-catalyzed cyclopropanation between 3-diazooxindole and piperylene, which was achieved in good yields but no diastereoselectivity. The spirocyclic piperidine ring was then formed by MgI_2-mediated ring expansion of the resultant vinylcyclopropane in good yields, and with a 6:1 diastereomeric ratio favoring the desired stereoisomer. After cleavage of the *N*-allyic protecting group through palladium catalysis, the authors were then able to achieve asymmetry through coupling to the N-Boc-L-proline acid chloride, which generated a separable mixture of diastereomers and was incorporated in the final natural product structure.

1.3.3 SYNTHESIS OF CLINICALLY ADVANCED SPIROLACTONE (+)-GRISEOFULVIN

One of the most clinically relevant spirocyclic natural products is griseofulvin, who's development and chemistry dates back to the early 1940's which was recently reviewed.[9] The compound was first isolated from the mushroom *Penicillium griseofulvum* in 1939 by Oxford and coworkers. Efforts to elucidate the structure of griseofulvin were attempted by several groups over the next decade, until the absolute configuration was determined through single crystal X-

ray in 1977.[10] The compound has impressive biological activity – it was found in 2001 that it can potentiate the antitumorigenesis of nocodazole and induce apoptosis in cancer cell lines at concentrations as low as 1 μM.[10] Notably, the compound was launched in 1959 in the U.K. under the name "Grisovin" and in the U.S. as "Fulcin" for the treatment of ringworm in animals and humans. Several racemic total syntheses of griseofulvin have been reported as early as 1960, with only one asymmetric synthesis reported in 1991 by Pirrung et. al that utilizes a key intramolecular Rh-catalyzed O-R insertion/sigmatropic rearrangement sequence to form the vital spirocenter (**Scheme 1.8**).[10] This sequence is carried out in multiple steps however, and a reaction cascade could be considered to generate the full spirocycle in a single step.

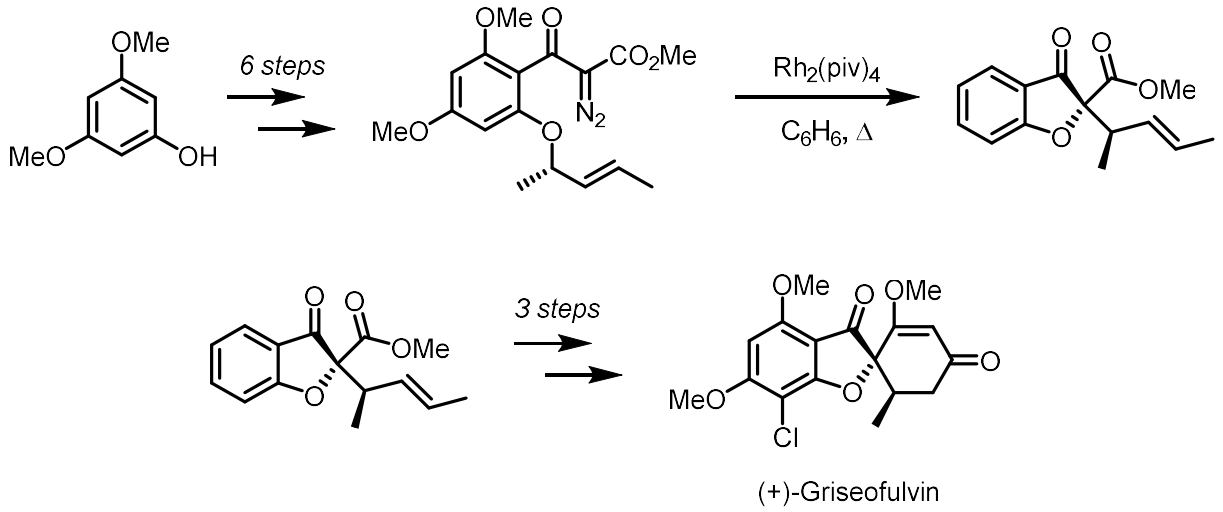

Scheme 1.8 Pirrung et al.'s asymmetric synthesis of (+)-Griseofulvin

Pirrung's synthesis began with a commercially available dimethoxyphenol, which was subjected to chlorination, acylation, and phenolic addition to (*R*)-pent-3-en-2-ol. This intermediate was condensed with Mander's reagent to provide a ketoester intermediate, which was then subjected to diazo transfer to give an Acceptor/Acceptor diazo. Carbenoid generation was conducted using $Rh_2(piv)_4$ to form the crucial spiro-junction in good yields, with complete diastereoselectivity. The synthesis was completed by conversion of the methyl ester to the

corresponding methyl ketone, followed by Diekmann cyclization and subsequent ether formation to furnish (+)-Griseofulvin in 5% yield over 10 steps.

1.4 ELECTROCYCLIC REACTIONS AND APPLICATIONS IN CASCADE REACTIONS

Electrocyclic reactions are a valuable tool in synthetic chemistry due to the convenient accessibility of their polyene precursors, high degree of selectivity, and atom economy, and have been utilized as key reactions in numerous natural product total synthesis in recent years.[14c] Not only this, but they are ideal candidates for cascade reactions, as they require only thermal input, with no additional reagents, to proceed – this overcomes functional group, reagent, and catalyst compatibility issues that are often encountered when designing new cascade reactions. The electrocyclic reaction is a subset of pericyclic reactions, in which electrons from multiple pi bonds interact in order to generate a new sigma bond, and a rearranged pi system (Scheme 1.9).

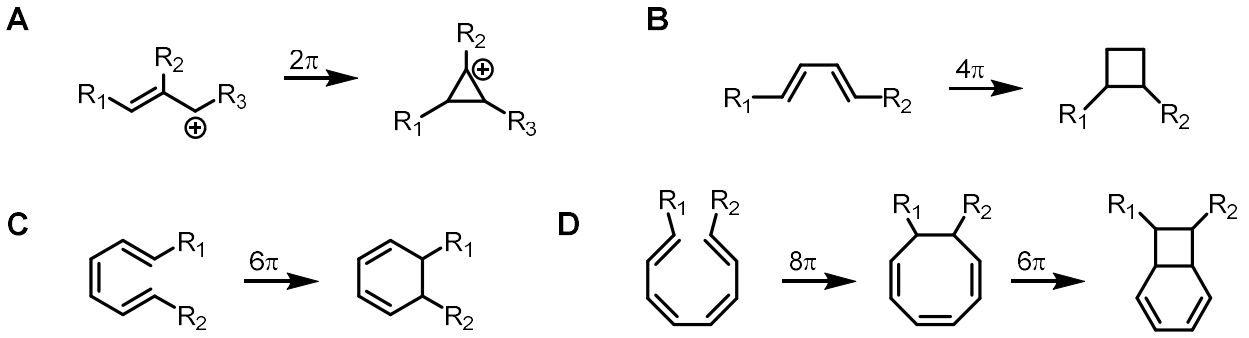

Scheme 1.9 Generalized electrocyclization reactions in a.) 2π systems b.) 4 π systems c.) 6 π systems d.) 8π systems

This process generally results in a high degree of stereocontrol, because of the principle of the conservation of orbital symmetry applies, as dictated by the Woodward-Hoffmann rules.[14a] These rules allow one to predict the stereochemical outcome of an electrocyclic reaction, by understanding whether the orbitals involved in bond formation are both rotating in the same direction (conrotatory), or opposite directions (disrotatory). Electrocyclization reactions are generally classified by the number of pi electrons interacting in a

given system – 2π, 4π, 6p, and 8π electrocyclizations have all been well documented. These reactions can be generated either under thermal or photochemical conditions, and the Woodward-Hoffman rules summarize the impact of number of participating pi bonds and reaction conditions on the resulting product stereochemistry (**Table 1**).

Electrocyclization Classification	Number of π -bonds	Thermal Outcome	Photochemical Outcome
2π	1	Conrotatory	Disrotatory
4π	2	Disrotatory	Conrotatory
6π	3	Conrotatory	Disrotatory
8π	4	Disrotatory	Conrotatory

Table 1.1 Summary of Woodward-Hoffman Rules for Electrocyclizations

It should be noted however that the 1,3,5,7-cyclooctatrienes, generated through 8π electrocyclization, are rarely isolated, and can undergo a subsequent 6π electrocyclization to yield bicyclo[4.2.0]octadienes (**Scheme 1.9d**).

In addition, oxo- and aza- variants of electrocyclization reactions are known and have been used to generate new heterocycles.[14b] This is most often exemplified in 6π electrocyclic substrates, whereby aldehydes and ketones are used to generate α-pyrans, and imines generate dihydropyridines, which are readily oxidized to their pyridine counterpart (**Scheme 1.10**).

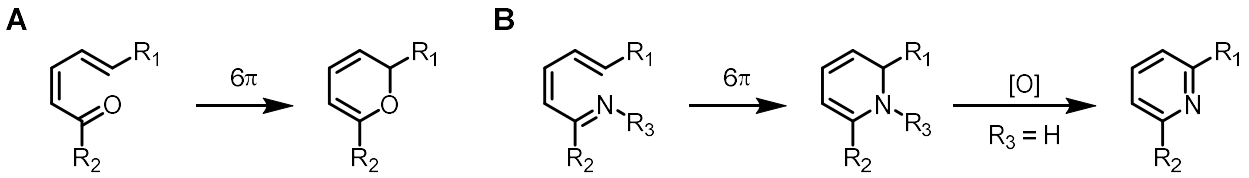

Scheme 1.10 Generalized reactivity of a.) oxo-electrocyclization b.) aza-electrocyclization

1.5 OBJECTIVE OF RESEARCH

The primary objective of this dissertation research is to develop new cascade reactions for the synthesis of bioactive scaffolds for drug discovery. Spirocyclic compounds, including those derived from natural products, represent a promising synthetic challenge because of their unique biological activities, arising from their 3-dimensional structure presenting functional groups in a well-defined manner to their protein targets. While many linear sequences have been successfully employed for the synthesis of spirocyclic compounds, our cascade approach provides a general, convergent method to generate these in a step-efficient fashion.

Cascade reactions have been utilized in numerous creative total synthesis in the last decade, exploiting cationic, anionic, electrocyclic, and radical reactivity. Because cascades employ multiple reactions in one pot without isolation of any intermediates, they have been valuable synthetic tools to address atom economy, reagent, and purification costs. In order to expand chemical space in the drug development process, we seek to develop a new retrosynthetic approach to spirocycles, bisecting the molecule at the quaternary spirocenter, which exploits the reactivity of diazo-derived metal carbenoids. In addition, we envision a new cascade approach to aromatic heterocycles, exploiting electrocyclic reactivity of triene intermediates to bisect the traditionally unreactive aromatic ring.

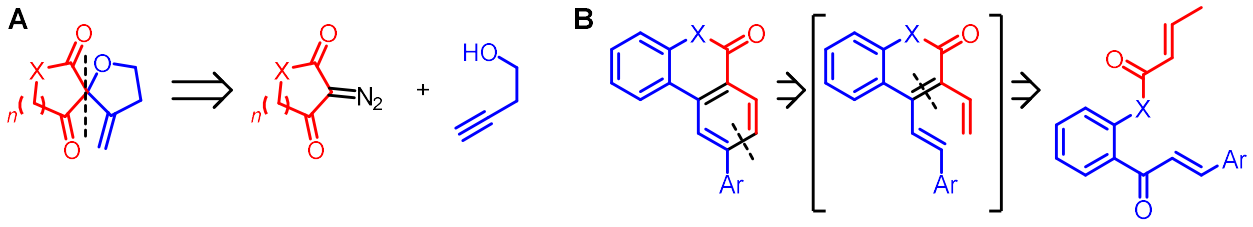

Scheme 1.11 a.) cascade approach towards spirocycles b.) cascade approach towards aromatic heterocycles

1.6 REFERENCES FOR CHAPTER 1

1. DiMasi, J. A., Grabowski, H. G., Hansen, R. W. "Innovation in the Pharmaceutical Industry: New Estimates of R&D Costs." *J. Health. Econ.* **2016**, *47,* 20–33.

2. a.) Lovering, F., Bikker, J., Humblet, C. "Escape from Flatland: Increasing Saturation as an Approach to Improving Clinical Success." *J. Med. Chem.* **2009**, *52*, 6752–6756. b.) Feher, M., Schmidt, J. M. "Property Distributions: Differences between Drugs, Natural Products, and Molecules from Combinatorial Chemistry." *J. Chem. Inf. Comput. Sci.* **2003**, *43,* 218–227. c.) Dobson, C. M. "Chemical Space and Biology." *Nature* **2004**, *432,* 824–829. d.) Lachance, H.; Wetzel, S.; Kumar, K.; Waldmann, H. "Charting, Navigating, and Populating Natural Product Chemical Space and Drug Discovery." *J. Med. Chem.* **2012**, *55*, 5989–6001.

3. a.) Brooks, W. H., Guida, W. C., Daniel, K. G. "The Significance of Chirality in Drug Design and Development." *Curr. Top. Med. Chem.* **2011**, *11,* 760–770. b.) Muller, G., Berkenbosch, T., Benningshof, J. C. J., Stumpfe, D., Bajorath, J. "Charting Biologically Relevant Spirocyclic Compound Space." *Chem. Eur. J.,* **2017**, *23,* 703–710. c.) Molvi, K. I., Haque, N., Awen, B. Z. S., Zameeruddin, M. "Synthesis of Spiro Compounds as Medicinal Agents; New Opportunities for Drug Design and Discovery. Part 1: A Review." *World. J. Pharmacy and Pharmaceutical Sci.,* **2014**, *3*, 536–563. d.) Zheng, Y., Tice, C. M., Singh, S. B. "The Use of Spirocyclic Scaffolds in Drug Discovery." *Bioorg. Med. Chem Lett.* **2014**, *24,* 3673–3682. e.) Zheng, Y- J., Tice, C. M. "The Utilization of Spirocyclic Scaffolds in Novel Drug Discovery." *Expert Opinion on Drug Discovery,* **2016**, 1–4.

4. Li, J. W. -H., Vederas, J. C. “Drug Discovery and Natural Products: End of an Era or an Endless Frontier?” *Science* **2009**, *325,* 161–167.

5. a.) Nicolaou, K. C.; Edmonds, D. J.; Bulger, P B. “Cascade Reactions in Total Synthesis.” *Angew. Chem. Int. Ed.* **2006**, *45*, 7134–7186. b.) Bur, S. K.; Padwa, A. “The Synthesis of Heterocycles using Cascade Chemistry.” *Adv. Het. Chem.* **2007**, *94*, 1–105. c.) Nicolaou, K. C.; Chen, J. S.; “The Art of Total Synthesis through Cascade Reactions.” *Chem. Soc. Rev.* **2009**, *38*, 2993–3009.

6. a.) Robinson, R.; “LXII – A Synthesis of Tropinone.” *J. Chem. Soc. Trans.* **1917**, 762–768. b.) Medley, J. W.; Movassaghi, M. “Robinson’s Landmark Synthesis of Tropinone.” *Chem. Comm.* **2013**, *9*, 10775–10777.

7. a.) Stark, L. M.; Pekari, K.; Sorensen, E. J. “A Nucleophile-Catalyzed Cycloisomerization Permits a Concise Synthesis of (+)-Harziphilone.” *Proc. Natal. Acad. Sci.* **2004**, *101*, 12064–12066. b.) Padwa, A.; Danca, M. D. “Total Synthesis of (±)-Jamtine using a Thonium/*N*-Acyliminium Ion Cascade.” *Org. Lett.* **2002**, *4*, 715–717. c.) Parker, K. A.; Fokas, D. “Enantioselective Synthesis of (–)-Dihydrocodeinone: A Short Formal Synthesis of (–)-Morphine.” *J. Org. Chem.* **2006**, *71*, 449–455. d.) Elliot, G. I.; Velcicky, J.; Ishikawa, H.; Li, Y.; Boger, D. L. “Total Synthesis of (–)- and *ent*-(+)-Vindorosine: Tandem Intramolecular Diels-Alder/1,3-Dipolar Cylcloaddition of 1,3,4-Oxadiazoles.” *Angew. Chem. Int. Ed.* **2006**, *45*, 620–622. e.) Maddaford, S. P.; Andersen, N. G.; Cristofoli, W. A.; Keay, B. A. “Total Synthesis of (+)-Xestoquinone using an Asymmetric Palladium-Catalyzed Polyene Cyclization.” *J. Am. Chem. Soc.* **1996**, *118*, 10766–10773.

8. a.) Cui, C.-B; Kakeya, H.; Osada, H. “Novel Mammalian Cell Cycle Inhibitors, Tryprostatins A, B and other Diketopiperazines Produced by *Aspergillus Fumigatus.” J. Antibiot*. **1996**, *49,* 832–835. b.) Sebahar, P. R.; Williams, R. M. “The Asymmetric Total Synthesis of (+)- and (–)-

Spirotryprostatin B." *J. Am. Chem. Soc.* **2000**, *122,* 5666–5667. c.) Meyers, C.; Carreira, E. "Total Synthesis of (–)-Spirotryprostatin B." M. *Angew. Chem. Int. Ed.* **2003**, *42*, 694–696.

9. Petersen, A. B.; Ronnest, M. H.; Larsen, T. O.; Clausen, M. H. "The Chemistry of Griseofulvin." *Chem Rev.* **2014***, 113,* 12088–12107.

10. a.) Oxford, A. E.; Raistrick, H.; Simonart, P. "XXIX. Studies in the Biochemistry of Micro-organisms. LX. Griseofulvin, $C_{17}H_{17}O_6Cl$, A Metabolic Product OF *Penicillium Griseo-fulvum Dierckx."* *Biochem. J.* **1939**, *33,* 240–248. b.) Malmros, G.; Wägner, A.; Maron, L. "7-Chloro-2',4,6,-trimethoxy-6'-methyl-spiro-(benzofuran-2(3h),2-(2')cyclohexene)-3-4'-dione $C_{17}H_{17}ClO_6$" *Cryst. Struct. Commun*. **1977***, 6,* 463. c.) Ho, Y.-S.; Duh, J.-S.; Jeng, J.-H.; Wang, Y.-J.; Liang, Y.-C.; Lin, C.-H.; Tseng, C.-J.; Yu, C.-F.; Chen, R.-J.; Lin, J.-K. "Griseofulvin Potentiates Antitumorigenesis Effects of Nocodazole through Induction of Apoptosis and G2/M Cell Cycle Arrest in Human Colorectal Cancer Cells." *Int. J. Cancer* **2001**, *91,* 393–401. d.) Pirrung, M. C.; Brown, W. L.; Rege, S.; Laughton, P. "Total Synthesis of (+)-Griseofulvin." *J. Am. Chem. Soc.* **1991***, 113,* 8561–8562.

11. Stierle, A. A.; Stierle D. B.; Patacini, B. "The Berkeleyamides, Amides from the Acid Lake Fungus *Penicillium rubrum." J. Nat. Prod.* **2008**, *71,* 856–860.

12. Komori, K.; Tnaiguchi, T.; Mizutani, S.; Monde, K.; Kuramochi, K.; and Tsubaki, K. "Short Synthesis of Berkeleyamide D and Determination of the Absolute Configuration by the Vibrational Circular Dichroism Exciton Chirality Method." *Org. Lett.* **2014***, 16,* 1386–1389.

13. Shen, B.; Liu, W.; Cao, W.; Liu, X.; Feng, X. "Asymmetric Synthesis of α,β-Epoxy-γ-lactams through Tandem Darzens/Hemiaminalization Reaction." *Org. Lett.* **2019**, *21,* 4713–4716.

14. a.) Meyers, E. L.; Trauner, D. “Selected Diastereoselective Reactions: Electrocyclizations.” *Comp. Chiral.* **2012**, *2*, 563–606. b.) Choshi, T.; Hibino, S. “Synthetic Studies on Nitrogen-Containing Fused-Heterocyclic Compounds Based on Thermal Electrocyclic Reactions of 6π-Electron and Aza-6π-Electron Systems.” *Heterocycles* **2011**, *83*, 1205–1239. c.) Bian, M.; Li, L.; Ding, H. “Recent Advances on the Application of Electrocyclic Reactions in Complex Natural Product Synthesis.” *Synthesis* **2017**, *49*, 4383–4413.

CHAPTER 2

Catalytic Cascade Approach to Tetrahydrofurans, γ-Butyrolactones, and Spiroethers

2.1 INTRODUCTION

The synthesis of small molecules containing a spirocenter continues to be a major challenge in organic synthesis, primarily because it involves the formation of a quaternary center. Quaternary centers, which are defined as one atom connected to four other atoms that are not hydrogen, are often chiral centers, which are difficult to form with a high degree of selectivity. This selectivity challenge stems from the geometry of the spirocyclic precursor – which is often a

functional group that sp^2 hybridized, or in a trigonal planar geometry. When an oncoming nucleophile reacts with a trigonal planar functional group to generate a chiral center, there is rarely any outside interference dictating its facial trajectory, resulting in the formation of a racemic stereocenter.

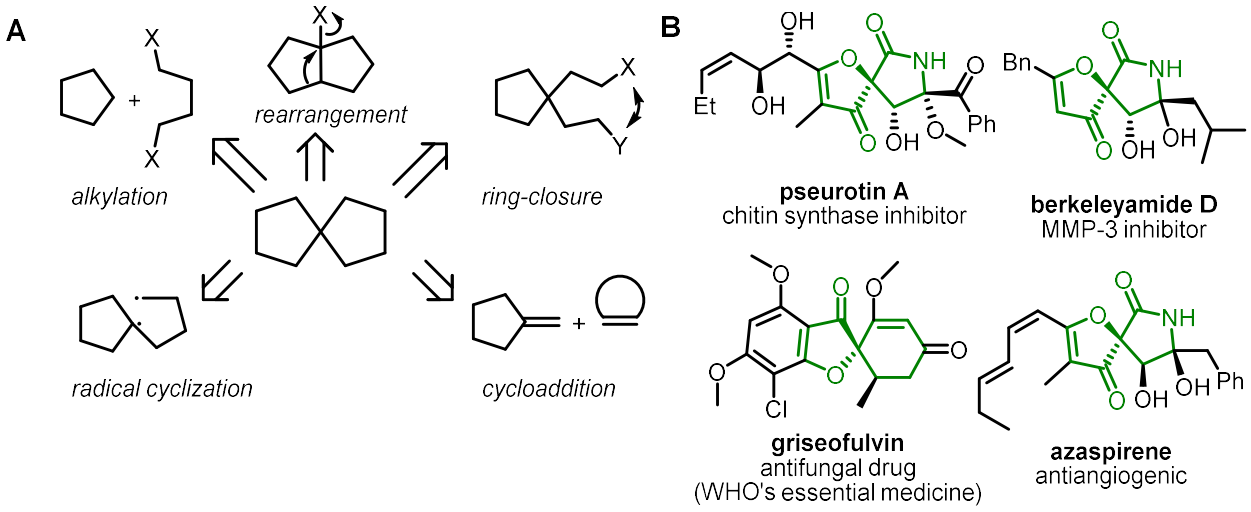

Figure 2.1. a.) Common Strategies Towards Spirocycles b.) Natural Products Bearing a Spiroether Core

Synthetic strategies have been developed to form spirocenters with a modest degree of stereocontrol, including alkylation, rearrangement, ring closure, cycloaddition, and radical cyclization, but these methods are all met with their own limitations (**Figure 2.1a**).[1a] Spirocyles comprise the core of numerous bioactive natural products, including the pseurotin family, Berkeleyamide D, azaspirene, and griseofulvin – which is on the World Health Organization's list of essential medicines (**Figure 2.2b**).[1b-1f]

With the abundance of bioactive natural products featuring a spirocyclic core, these scaffolds show promise as future drug leads. However, there does not appear to be a general route for spirocycle formation based on the intermolecular connection at the quaternary center

with high stereocontrol. Developing a general method would allow for the convenient construction of a diverse library of spirocycles. To this end, we have developed a convergent approach to spirocycle formation harnessing the ambiphilic reactivity of diazo-derived metal carbenoids in multi-step cascade reactions (**Figure 2.2a**).

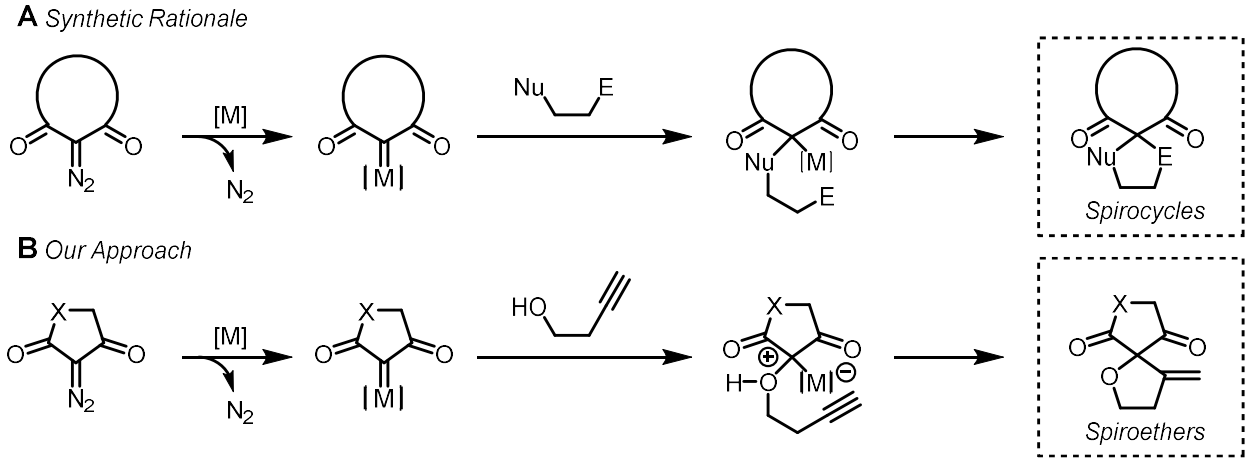

Figure 2.2. a.) General convergent approach to spirocycles b.) Carbene O–H Insertion/Conia-ene Approach to Spiroethers

We have developed an intermolecular reaction cascade which uses a two-component approach to spirocycles through cascade reactivity (**Figure 2.2b**). Our innovative approach first exploits the electrophilic reactivity of carbenoid intermediates in a carbene O–H insertion reaction. Then, 1,2-proton transfer of the zwitterionic intermediate is bypassed in favor of a Conia-ene cyclization, generating a new carbon-carbon bond. This convergent approach benefits from readily accessible diazo and alkynol precursors (generally one-step), and does not rely on forming highly functionalized linear precursors.

2.2 SYNTHESIS AND REACTIVITY OF THE DIAZO FUNCTIONAL GROUP

The diazo functional group is one that has been exploited for numerous creative transformations since their discovery in 1858.[2] Diazo compounds bear diatomic nitrogen gas

bonded to a single carbon atom, and have several resonance forms contributing to their reactivity (**Figure 2.3a**)[3a].

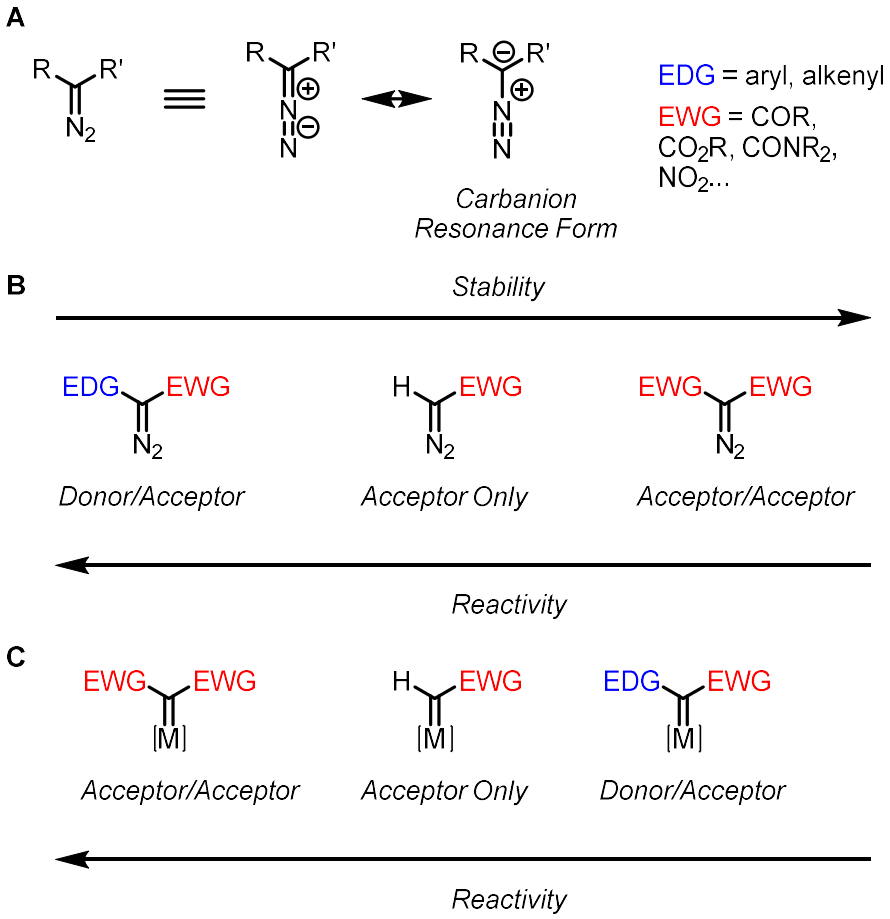

Figure 2.3. a.) Resonance forms of the diazo functional group b.) Classification of diazo compounds. c.) Inverse stability of diazo-derived carbenes

Diazo compounds can be sorted into three classifications, denoted by the presence of adjacent stabilizing or destabilizing functional groups (**Figure 2.3b**). The first and most stable diazo class is the Acceptor/Acceptor (A/A) diazo, which bears two electron withdrawing substituents stabilizing the carbanion resonance form. While azides and diazo compounds have a reputation for dangerous decomposition, many A/A diazos are benchtop stable, and can be stored in gram-quantities for months. A general guideline to assess azide and diazo reactivity has

been established, and is commonly known as the "rule of six." The rule of six states that six carbon (or other atoms of about the same size) per energetic functional group should provide enough dilution to render the compound safe to work with.[3b] Another method of generalizing diazo/azide reactivity is to assess their carbon-to-nitrogen ratio – if the sum of carbon and oxygen atoms in the molecule, divided by the number of nitrogen atoms exceeds 3, then the diazo is likely stable enough to isolate in large quantities.[3c]

The next diazo classification is the moderately stable acceptor-only diazo, which bears only one stabilizing electron-withdrawing substituent, with either a hydrogen or alkyl substituent. One of the most classical acceptor-only diazos, ethyl diazoacetate (EDA), is commercially available as a dilute solution in either toluene or dichloroethane. EDA has been widely studied in the field of diazo chemistry, in part due to its convenient availability, reactivity, and utility as a synthon in late-stage functionalization. The final diazo classification is the least stable Donor/Acceptor (D/A) diazo, which bears one stabilizing electron-withdrawing group and one destabilizing electron donating group; these electron-donating groups are most often alkynyl, alkenyl, or aryl substituents.

When a diazo compound is exposed to an appropriate metal catalyst, often using Rh, Cu, Ru, and recently Fe, N_2 gas is expelled to generate a metal-stabilized carbene. These reactive intermediates follow an inverse stability trend to their diazo precursors – the highly stable A/A diazo compounds generate the most reactive, highly electrophilic, carbenoids (**Figure 2.2c**).

Several methods are known for synthesizing stabilized diazo compounds – two of the most common utilize a methylene or ketone precursor (**Scheme 2.1**).

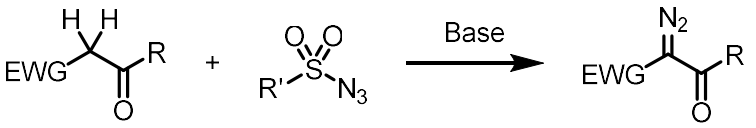

Scheme 2.1 Synthesis of diazo compounds by Regitz diazo transfer

By far, the most common method for synthesizing A/A diazo compounds is the diazo transfer reaction, also referred to as the Regitz diazo transfer. This named reaction, reported in 1964, employs the enolization of an active methylene compound, which then interacts with a sulfonyl azide reagent to transfer dinitrogen from the azide component.[4a] The method uses common sulfonyl azides like methanesulfonyl-, p-tolylsulfonyl-, and more recently the solid p-actamidobenzenesulfonyl azide (p-ABSA), which are generated via anion exchange between the corresponding sulfonyl chloride and sodium azide. Because the methylene precursors are typically quite acidic, mild organic bases like triethylamine and 1,8-diazabicyclo[5.4.0]undec-7-ene (DBU) are sufficient for the formation of most A/A diazo compounds. These diazos are conveniently isolated after chromatographic purification, simplified further by filtration of the sulfonamide byproduct.

A modification of the Regitz diazo transfer reaction was reported by Regitz and Menz in 1968 which extends its utility to a new classification of diazo compounds (**Scheme 2.2**).

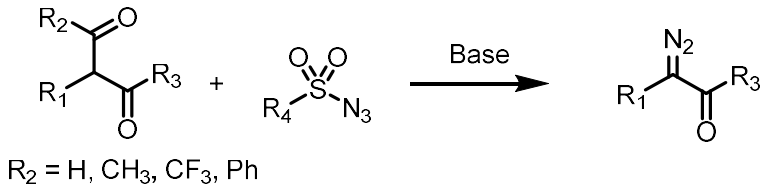

Scheme 2.2 Deformylative/Deacylative/Debenzoylative Diazo Transfer Reaction

Regitz originally reported α-formylketones can be exposed to diazo transfer conditions to generate acceptor–only diazo compounds, alongside the formation of an N-acylsulfonamide byproduct instead of the sulfonamide from standard diazo transfer conditions.[4b] In the same year, Hendrickson and Wolf independently reported the deacylative diazo transfer reaction, whereby diazo compounds were synthesized through diacylation, as opposed to deformylation[4c]. These discoveries were groundbreaking in the study of diazo compounds, as it allowed for the formation of stabilized diazos from scaffolds other than malonates and ketoesters. In the subsequent decades, Taber et. al reported an improved variation of Regitz' deformylative diazo transfer reaction utilizing a benzoyl leaving group.[4d]

Diazo transfer reactions can also be used to synthesize donor–acceptor diazo compounds, depending on the effect of surrounding substituents on the active methylene acidity; generally, a stronger organic base like DBU is required in these circumstances. In situations where diazo transfer is not suitable for diazo preparation, aryldiazos can also be generated in a two-step sequence from a ketones, α-ketoamides, and α-ketoesters, in a variation of the Bamford-Stevens reaction (**Scheme 2.3**)[5].

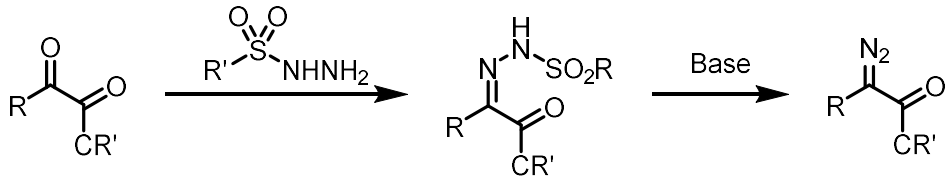

Scheme 2.3 Diazo formation through reduction of sulfonyl hydrazones.

2.3 TRAPPING OF ZWITTERIONIC INTERMEDIATE – THE CONIA–ENE REACTION

Broadly, an ene reaction can be classified as the concerted reaction between an alkene bearing an allylic hydrogen with a double- or triple-bond. These components are known as the "ene" and the "enophile," respectively. Such a rearrangement benefits from high atom economy – as all atoms present in the starting material are incorporated in the final product. Variants of the ene reaction are known; replacing the 'ene' portion of an ene reaction with an enol is known as a Conia-ene reaction. This reaction was first reported in 1966 by J. M. Conia, who performed numerous studies on the thermal cyclization of unsaturated ketones at temperatures often exceeding 300 °C (**Scheme 2.4a**).[6a] In the subsequent years since its report, numerous authors have reported the addition of particular Lewis acids can promote the reaction at milder reaction conditions, either by increasing the amount of the nucleophile in the enol form, or by polarizing the electrophilic pi-system.

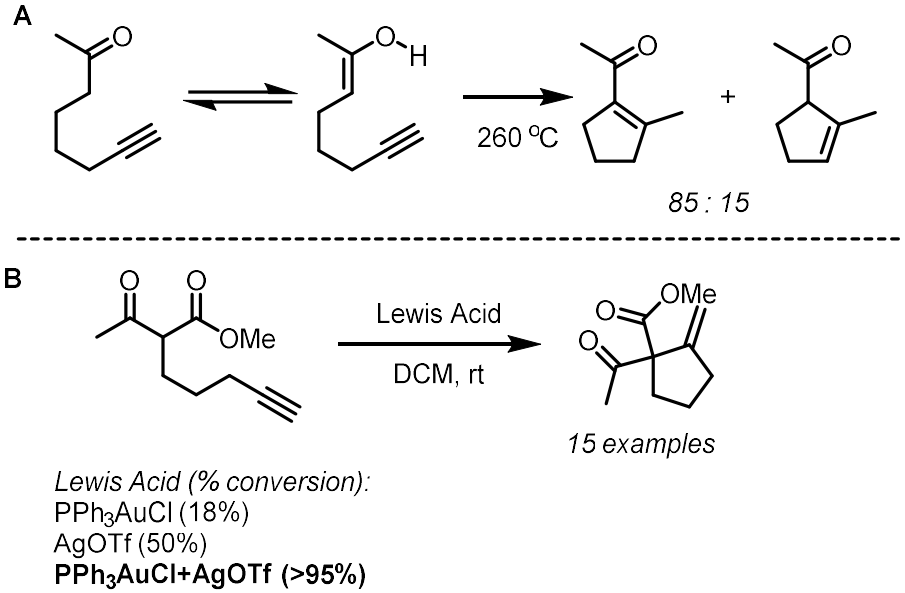

Scheme 2.4 a.) Conia's Thermal Ene Cyclization b.) Toste et. al.'s Au^+ Promoted Conia–Ene Cyclization

In 2004 Toste et. al. reported a method for inducing a Conia-ene cyclization under much more mild reaction conditions than previously reported (**Scheme 2.4b**).[7] After a screening of common Lewis acids and combinations thereof, Toste et. al. discovered that terminal alkynes could be polarized by cationic gold, generated via *in situ* reaction with various silver salts, and subsequently trapped intramolecularly with a large number of β-ketoesters. This report has guided our design for a new method of trapping zwitterionic intermediates, generated through carbene heteroatom–insertion chemistry.

2.4 CARBENOID CASCADE FOR THE FORMATION OF SUBSTITUTED TETRAHYDROFURANS AND γ-BUTYROLACTONES

In 2016 Hunter and Sharma reported a remarkable new method for the insertion of the carboxylic acid O–H bond into acceptor–acceptor diazo compounds, under mild conditions with an unprecedented reaction rate (**Scheme 2.5a**).[8a] This new method utilizes the catalyst Bis[rhodium)α,α,α',α'-tetramethyl-1,3-benzenedipropionic acid)] ($Rh_2(esp)_2$) to generate a reactive electrophilic carbenoid which reacts with carboxylic acids with reaction times of less than 10 minutes.

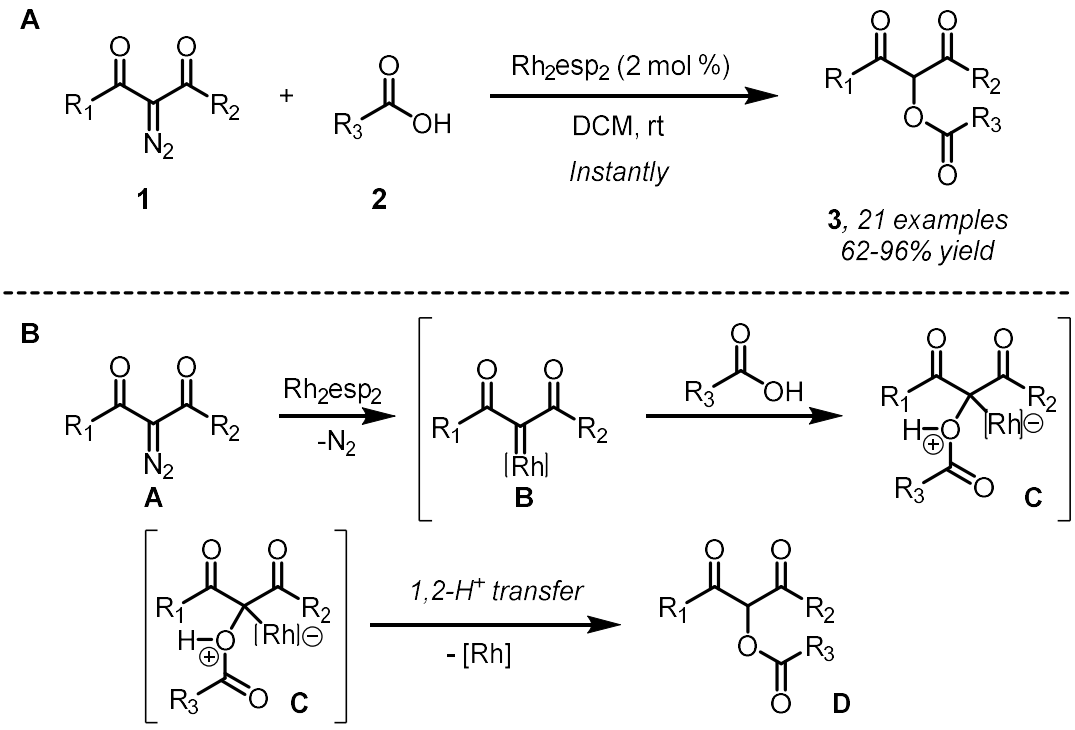

Scheme 2.5. a.) Sharma and Hunter's Carboxylic acid O–H Insertion to A/A Diazos b.) Mechanism of Carboxylic Acid O–H Insertion

The method reported by Sharma and Hunter displayed excellent chemoselectivity, favoring the acid O–H insertion over other known carbenoid–mediated processes such as olefin cyclopropanation, alkyne cyclopropenation, alcohol O–H insertion, and aryl sp^2 C–H activation. When exposed to the rhodium catalyst, diazo **A** extrudes nitrogen gas to generate the electrophilic carbenoid intermediate **B**. The carboxylic acid then attacks the carbenoid, generating zwitterionic intermediate **C**. Finally, a 1,2-proton transfer regenerates the rhodium catalyst, resulting in the formation of insertion product **D** (**Scheme 2.5b**). This method has proven to be general, with a substrate scope of over 20 insertion compounds having yields ranging from good to excellent.

2.4.1 SYNTHESIS OF γ-LACTONES THROUGH CARBENE O–H INSERTION/CONIA–ENE CASCADE

Expanding off of our earlier 2016 work, we hypothesized that the zwitterionic intermediate, generated in the process of acid O–H insertion, could be intercepted by a strong electrophile before 1,2-proton transfer occurs, to generate a new ring containing a quaternary center. Inspired by Toste's 2004 work in the cationic-gold catalyzed Conia-ene reaction, Hunter and Sharma envisioned that a properly activated alkynoic acid would be capable of undergoing an intermolecular carbene O–H insertion/Conia-ene cascade to furnish substituted lactones. By exposing insertion compound **3** to a variety of Lewis acid catalysts, they found that cationic gold, generated through *in situ* formation of AgCl using a silver salt bearing a weakly–coordinating anion, could indeed induce annulation to the corresponding γ-lactone **4** efficiently at room temperature, whereas heating and a longer reaction time was needed for the only other successful Lewis Acid, copper (I) triflate (**Scheme 2.6a**).

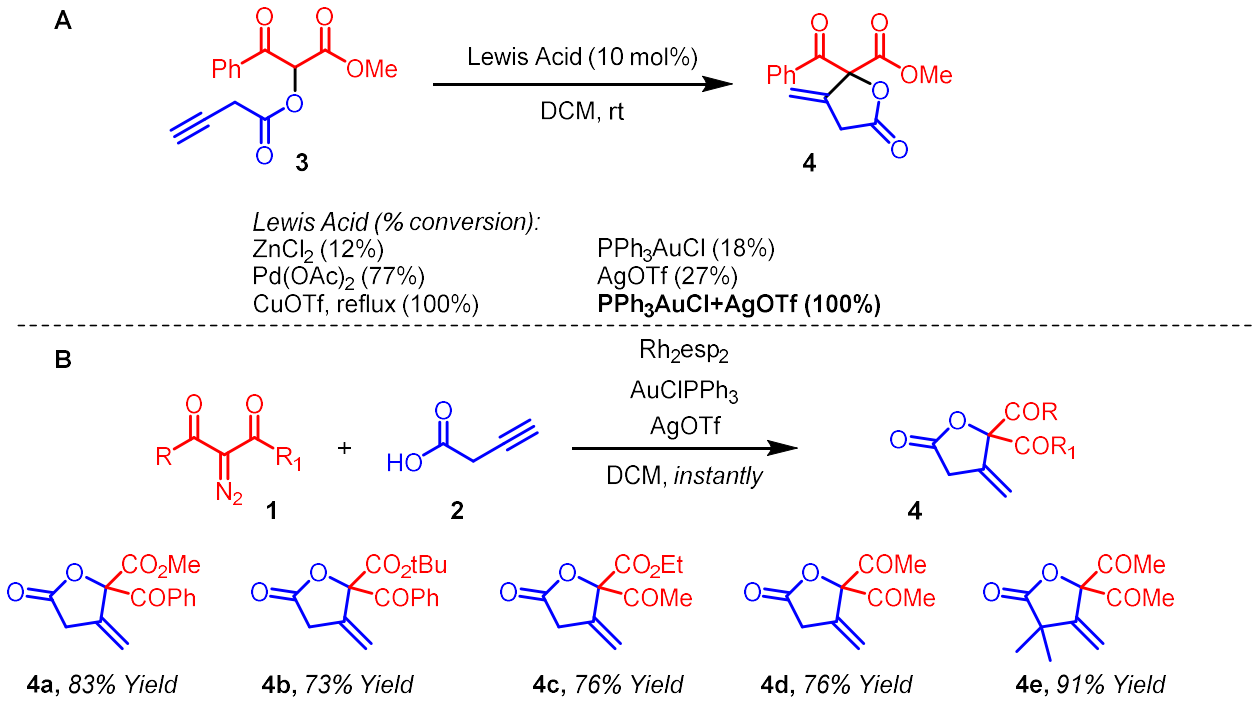

Scheme 2.6. a.) Lewis acid screening to promote intramolecular Conia-ene reaction b.) Carbene O–H Insertion/Conia-ene Cascade for γ–Lactones

Moreso, they found that butynoic acids are indeed capable of undergoing the desired reaction cascade in a one-pot fashion using a mixture of rhodium, gold, and silver catalysts with no trace of insertion products detected. This one-pot cascade approach was applied towards the synthesis of six different γ-lactones, with yields ranging from good to excellent (**Scheme 2.7b**).

2.4.2 SYNTHESIS OF TETRAHYDROFURANS VIA ALCOHOL O–H INSERTION/CONIA–ENE CASCADE

Inspired by the results of Hunter and Sharma, we turned our attention towards harnessing alternative nucleophiles for the O–H insertion portion of the reaction cascade. While there is literature precedent for the O–H insertion of alcohols to diazo–derived carbenoids,[9] an alcohol O–H insertion/Conia-Ene cascade would be a novel route to substituted

tetrahydrofurans. Indeed, when butynoic acid was replaced with commercially available 3-butyn-1-ol, the O–H insertion/Conia-ene reaction cascade was successful with a range of diazo compounds (**Scheme 2.7**).[8b]

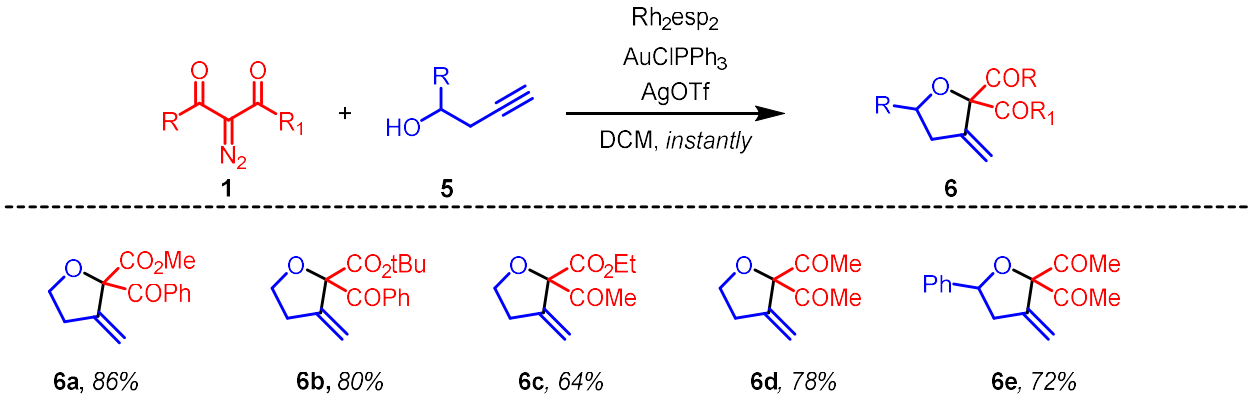

Scheme 2.7. O–H Insertion/Conia-ene Cascade Approach to Tetrahydrofurans

The reaction was successful with three different α-diazoketoesters, resulting in tetrahydrofurans **6a**-**6c**, bearing methyl, *tert*-butyl, and ethyl esters. The reaction cascade was also successful using diazo compounds derived from malonates; the methylmalonate diazo cleanly afforded diazo **6d** in good yields. Finally, we looked to the scope of the alcohol component – The cascade was successful with an unsubstituted primary alkynol but would the additional steric factors of a secondary dissuade O–H insertion? Fortunately, when racemic 1-phenyl-3-butyn-1-ol was exposed to the Rh/Au^{+} reaction conditions, tetrahydrofuran **6e** was formed and isolated in good yields. Since a new chiral center is formed throughout the course of this reaction cascade, we then prepared a number of chiral primary and secondary alkynols to probe the diastereoselectivity of the transformation (**Scheme 2.8**).

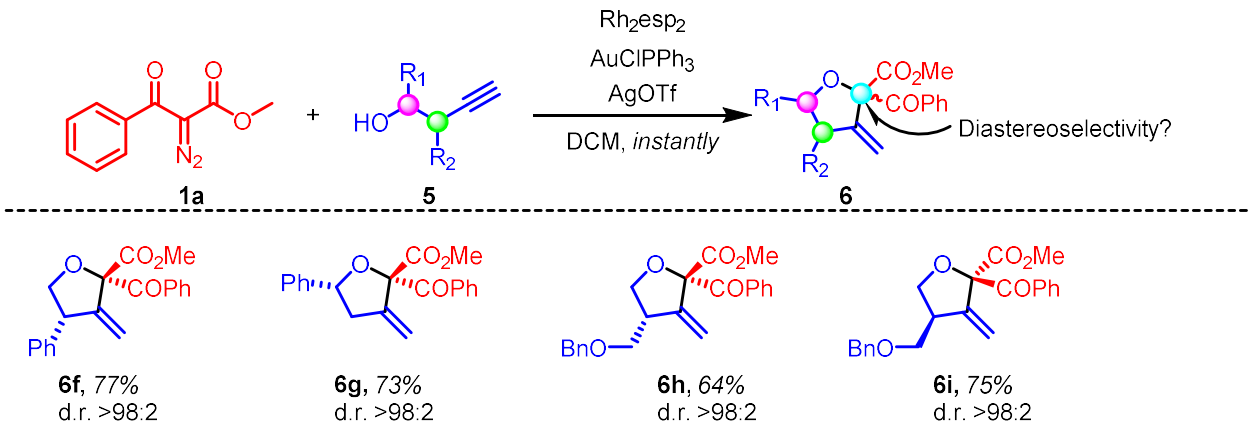

Scheme 2.8. Insertion of Chiral Primary and Secondary Alcohols to Probe Diastereoselectivity

To our delight, all prepared chiral primary and secondary alcohols withstood the reaction conditions well resulting in good yields of the corresponding furans. In the case of substituted primary alcohols, the reaction condition produced furan **6f** with excellent diastereoselectivity, as determined by ^{1}H NMR analysis. Next, a chiral secondary alcohol was employed to generate furan **6g**, also with excellent diastereoselectivity. Finally, an enantiomeric pair of substituted primary alcohols were exposed to the optimized reaction conditions in two parallel trials, and again we saw complete diastereoselectivity for compounds **6h** and **6i**. These products also had equal and opposite optical rotation values, as expected for a pair of enantiomers.

2.5 REACTION DESIGN – ACCESSING THE SPIRO-γ-LACTAM CORE OF BERKELEYAMIDE D

With the development of this successful reaction cascade we turned our attention toward our initial goal – The convergent formation of spirocycles. We targeted the core of Berkeleyamide D, as this would provide a similar route to the family of related α-spiro-γ-lactams.

We began our substrate design by analyzing a truncated form of Berkeleyamide D, and bisecting the molecule down the spiro junction (**Figure 2.4**).

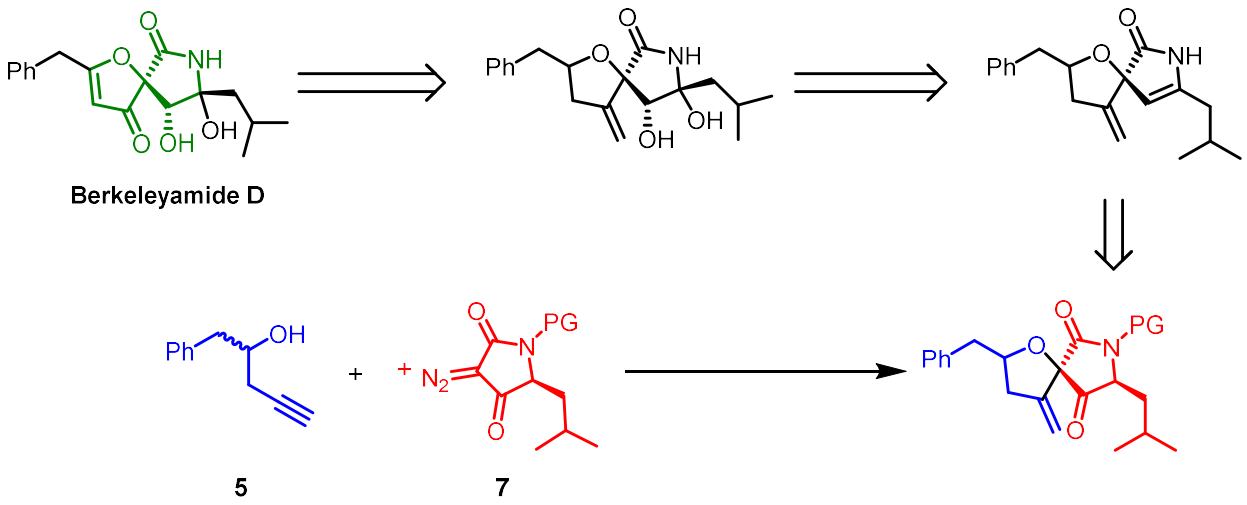

Figure 2.4. Retrosynthesis and Cascade Approach to the Berkeleyamide D Core

We envisioned that the truncated Berkeleyamide D core could be accessed via our O–H Insertion/Conia-ene cascade using secondary butynol **7** and γ-lactam diazo **8**. After forming the spirocore of Berkeleyamide D, we expect the remaining functionality could be installed through reduction and elimination of the ketone, dihydroxylation, oxidative cleavage of *exo*-olefin, and subsequent enolization/oxidation sequence to add unsaturation to the furan ring. With this strategy in hand, we pursued the synthesis of γ-lactam diazo **7**.

2.5.1 SYNTHESIS of γ–LACTAM DIAZOS

All γ-lactam diazos were synthesized using a modified procedure originally reported by Wood et. al (**Scheme 2.9**).[10]

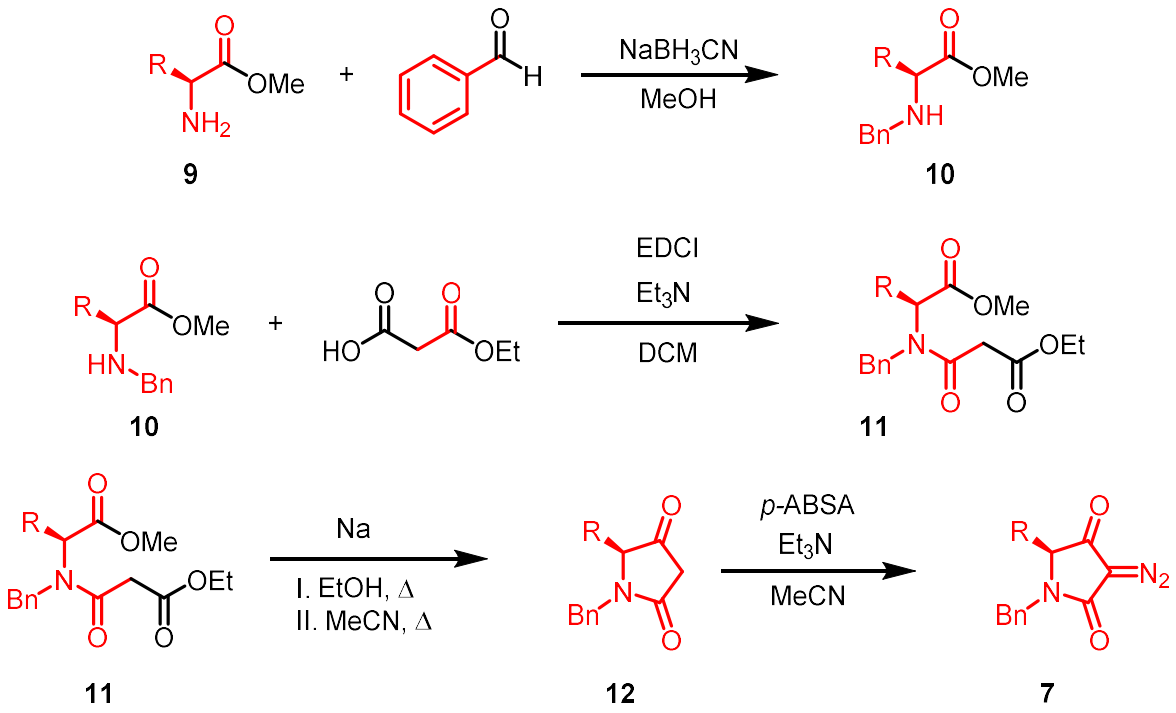

Scheme 2.9. Synthetic route to γ–Lactam diazo **7**

We began our synthesis using benzyl-protected γ-lactam diazo **7** as a model substrate. First, amino acid methyl ester hydrochlorides **9** were exposed to reductive amination conditions with benzaldehyde to furnish *N*-benzyl protected amines **10**. This secondary amine was coupled to ethyl hydrogen malonate using carbodiimide coupling conditions to furnish amides **11**. Next, the amides were exposed to Dieckmann cyclization conditions using *in situ* generated sodium ethoxide, followed by a hydrolysis/decarboxylation sequence to furnish γ-lactams **12**. Finally, lactams **12** were exposed to Regitz diazo transfer conditions to furnish desired diazos **7**. This

synthetic route provides a useful handle for substrate diversification – Altering amino acid **9** would affect the γ- alkyl substituent, and using leucine provides the exact alkyl chain present in natural Berkeleyamide D.

2.5.2 REACTION OPTIMIZATION

With a synthetic route to lactam diazos accomplished, we then turned our attention towards reaction condition optimization (**Table 2.1**).

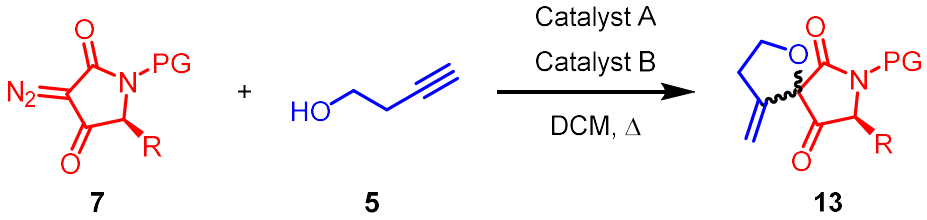

7 **5** **13**

Entry	R	P.G.	Catalyst A	Catalyst B	d.r.	Isolated Yield
1	Me	Bn	$Rh_2(esp)_2$ (2 mol %)	–	2.5:1.0	14%
2	Me	Bn	$Rh_2(esp)_2$ (2 mol %)	PPh_3AuCl (10 mol %) AgOTf (10 mol %)	2.5:1.0	53% yield
3	*i*Bu	Bn	$Rh_2(esp)_2$ (2 mol %)	PPh_3AuCl (10 mol %) AgOTf (10 mol %)	10:1.0	58% yield
4	*i*Bu	DMB	$Rh_2(esp)_2$ (2 mol %)	PPh_3AuCl (10 mol %) AgOTf (10 mol %)	>20:1.0	54% yield
5	***i*Bu**	**DMB**	**$Rh_2(esp)_2$ (2 mol %)**	**PPh_3AuCl (10 mol %) $AgSbF_6$ (10 mol %)**	**>20:1.0**	**68% yield**

Table 2.1 Reaction optimization for spiro–γ–lactam synthesis

Alanine–derived diazo **7a** was first exposed to $Rh_2(esp)_2$, which has proven successful for acid and alcohol O–H insertion to A/A carbenoids. We observed no reaction initially at room temperature, so the temperature was increased to DCM reflux. To our delight, rhodium alone produced desired spirocycle **13**, with no trace of insertion byproduct, albeit with a low yield and almost no

diastereoselectivity (**entry 1**). We hypothesized that the addition of cationic gold would increase the electrophilicity of the alkyne component, as was the case in our tetrahydrofuran synthesis. The addition of 10 mol % of PPh_3AuCl and AgOTf improved the yield of desired spirocycle **13a** to 53%, albeit with no major improvement in diastereoselectivity (**entry 2**). We then hypothesized that increasing the bulk on the alkyl component of diazo **7** would direct the trajectory of the incoming nucleophile better than a methyl substituent. In the case of leucine-derived diazo **7b** (R = *i*Bu), the reaction conditions cleanly afforded spirocycle **13b** in good yields, with a marked increase in diastereoselectivity (**entry 3**). We then turned our attention towards affecting the stearic bulk of the amide protecting group (PG). When the standard benzyl protecting group was changed to the bulkier 2,4-dimethoxybenzyl protecting group, the diastereoselectivity of the transformation improved to >20:1, the greatest that can be determined by NMR integration (**entry 4**). Finally, we turned our attention towards the role of the counter anion, paired with the gold catalyst. Since the active catalyst is cationic gold, effectively PPh_3Au^+, we hypothesized that a weakly coordinating anion would improve the yield of the overall Conia-ene reaction. We screened a variety of silver salts bearing weakly coordinating anions (OAc^-, OTf^-, BF_4^-, PF_6^-, SbF_6^-), and found a slight increase in yield using a silver salt bearing a hexafluoroantimonate (SbF_6^-) counter ion (**entry 5**). With optimized reaction conditions, we turned our attention toward determining the absolute configuration of the spirocenter formed during this reaction cascade.

2.5.3 DETERMINING THE ABSOLUTE CONFIGURATION OF SPIRO-γ-LACTAMS 13

We had hypothesized that the stearic bulk of the lactam γ-alkyl group would dictate the trajectory of the oncoming nucleophile to attack from the opposite face of the ring, after formation of the trigonal planar carbenoid intermediate. If this were indeed the case, the resulting product would have an *S*- configuration at the C5 spirocenter, while its diastereomer would have an *R*- configuration at the spirocenter (**Figure 2.5a**). We then performed Nuclear Overhauser effect (nOe) NMR experiments, which analyze through-space interactions of nearby protons, to glean insight into the configuration of this compound.

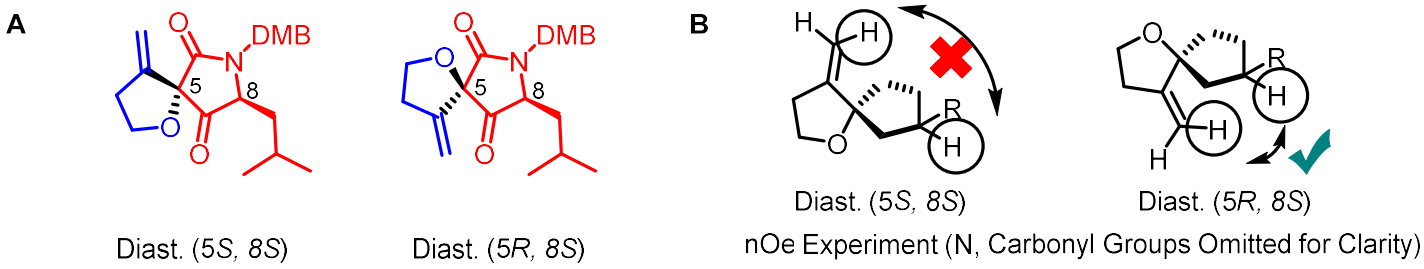

Figure 2.5. a.) Diastereomer options for spiro-γ-lactam 32b. b.) nOe experiment hypothesis

We envisioned that irradiating the chiral proton at C8 would provide valuable information into the orientation of the neighboring tetrahydrofuran ring. If the spirocenter was of the *R*- configuration, it may weakly couple to the olefin protons on the furan ring. Meanwhile, if the spirocenter was of the *S*- configuration, the olefin would lie on the same face of the C8 alkyl component, no such coupling would be present **(Figure 2.5b**). When these NMR experiments were performed however, we did indeed observe coupling between olefin protons and the chiral proton set at C8 (**Figure 2.6a**). These results serve to refute our initial hypothesis, and lead us to conclude that the configuration of the spirocenter at C5 is not dictated by the trajectory of the

incoming alcohol nucleophile, but rather the stearic bulk of the resulting olefin after Conia-ene cyclization.

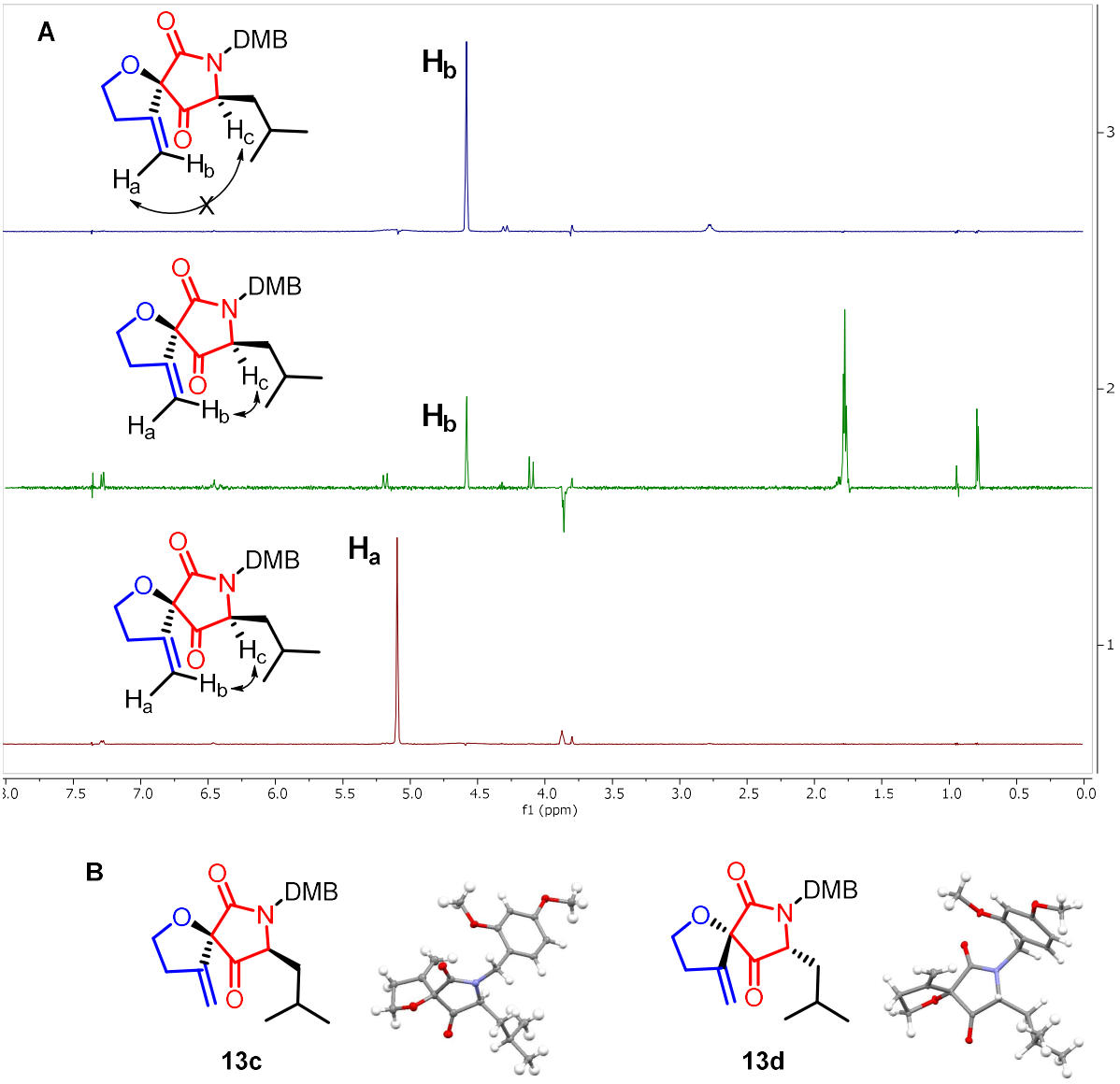

Figure 2.6. a.) nOe correlations between C8 H and olefin H. Signal suppression has been applied to irradiated protons for clarity. b.) Single crystal X-Ray results of 13c and its enantiomer

Finally, in order to support the new hypothesis, we pursued crystal growth for spirolactam **13c** and its enantiomer; fortunately, we were able to accomplish crystal growth by slow evaporation of the pure material in acetonitrile. The single crystal X-ray structure of **13c** and

its enantiomer supported our conclusion from the NMR experiments – when the diazo alkyl component is of the *S*- configuration, the resulting spirocenter will be the *R*- configuration. (**Figure 2.6b**). With this knowledge in hand, we explored the scope of diazos for this transformation.

2.5.4 SPIRO-γ-LACTAM SUBSTRATE SCOPE

The reaction conditions proved general with a range of *N*-Benzyl and *N*-dimethoxybenzyl protected diazo substrates (**Scheme 2.10**).

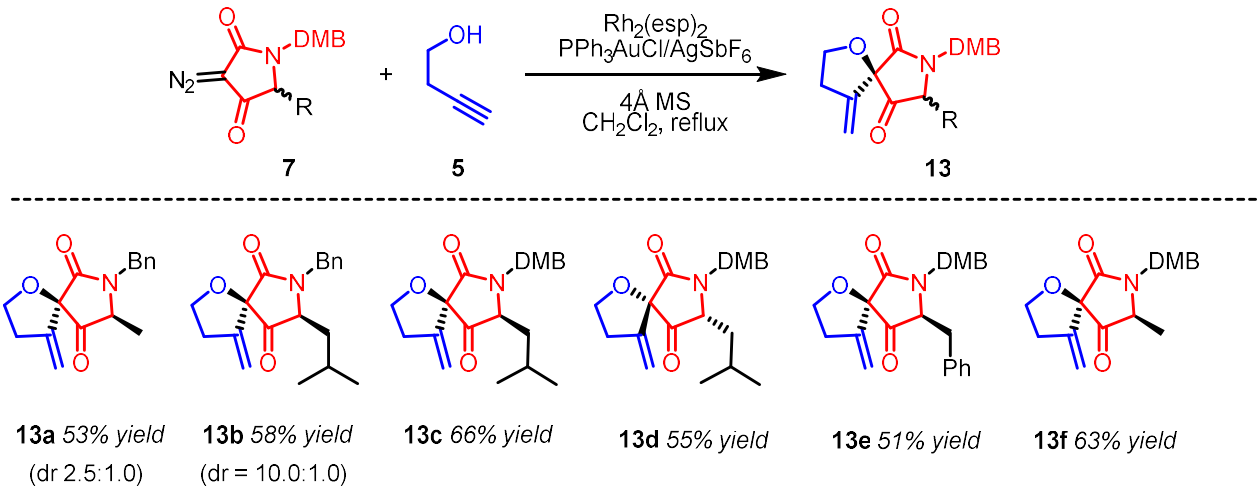

13a *53% yield* (dr 2.5:1.0) | **13b** *58% yield* (dr = 10.0:1.0) | **13c** *66% yield* | **13d** *55% yield* | **13e** *51% yield* | **13f** *63% yield*

Scheme 2.10 Scope of γ-lactam Diazos Employed

As discovered during optimization studies, N-benzyl protected substrates **13a** and **13b** could be prepared in modest yields, albeit with fair diastereoselectivity at best. Fortunately, when the protecting group was changed to N-dimethoxybenzyl, the analogous substrates could be prepared in similar yields with complete diastereosectivity (**13f** and **13c**). The reaction was also conducted with the enantiomer of leucine-derived diazo **7**, and we were able to isolate **13d** in good yields, which had an equal and opposite optical rotation to **13c**, which is expected for

enantiomers. Lastly, incorporation of a bulky benzyl alkyl group did not greatly impact overall yields or diasteroselecttivies (**13e**).

2.5.5 COMPUTATIONAL INSIGHTS ON SELECTIVITY OF SPIROCENTER FORMATION

Next, we turned to computational collaborators at the University of Pittsburgh (Prof. Peng Liu) for computational insights into the energetics of spirocycle formation for our reaction cascade (**Figure 2.7**).

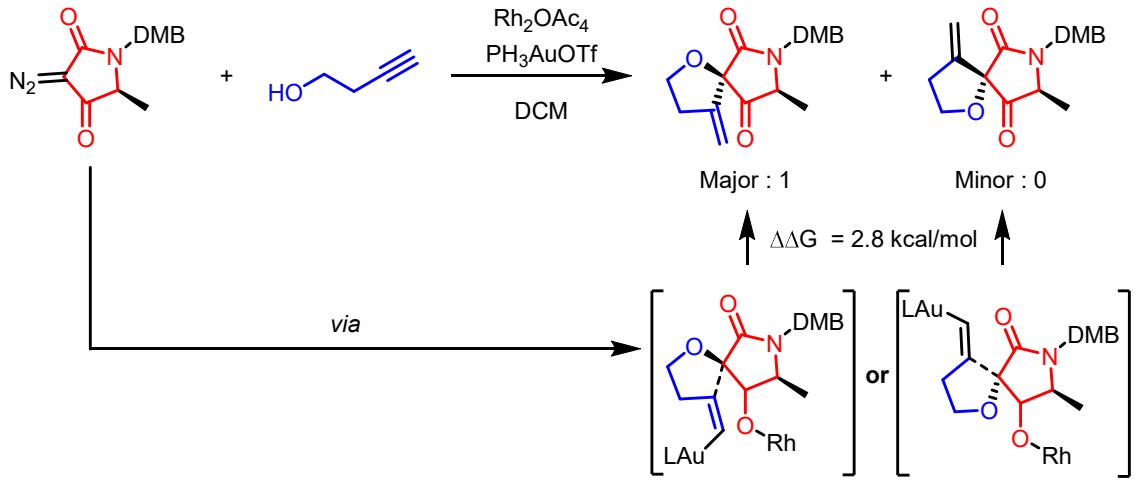

Figure 2.7. Transition State Calculation for Simplified Reaction Cascade Substrates

Ground state energy level calculations were performed using the B3LYP density functional and a mixed basis set of 6-31G(d) and SDD was used for Rh, Au, and non-metal atoms. To reduce computational resource strain, a simplified version of catalysts and substrates were used – $Rh_2(esp)_2$ ligands were simplified to acetate ligands, PPh_3AuCl truncated to PH_3AuOTf, and the alanine-derived diazo was used. Geometry optimizations were employed to determine the ground state energy level for starting materials and products, and transition state calculations were used to determine the energy of the transition states leading to the major and minor

diastereomers. Even in the case of this simplified model system, we observe a 2.8 kcal/mol difference in energy between the O–H nucleophile attacking from the same face as the diazo methyl groups versus the opposite face.

2.6 ROLE OF CHIRAL ALCOHOLS ON SPIROCENTER FORMATION

With the reaction cascade proving to be robust with respect to the γ-lactam diazo substrate, we then performed a series of experiments to probe the effect of pre-existing chirality of the O–H nucleophile on the resulting spirocenter formation (**Scheme 2.11**). Our previous success using chiral alcohols with linear diazos **1** led us to hypothesize that chiral alcohols would not have a major impact on the success of the reaction cascade. γ-lactam diazos **7** however, also contain a pre-existing chiral center, which was not a factor in linear diazos **1**.

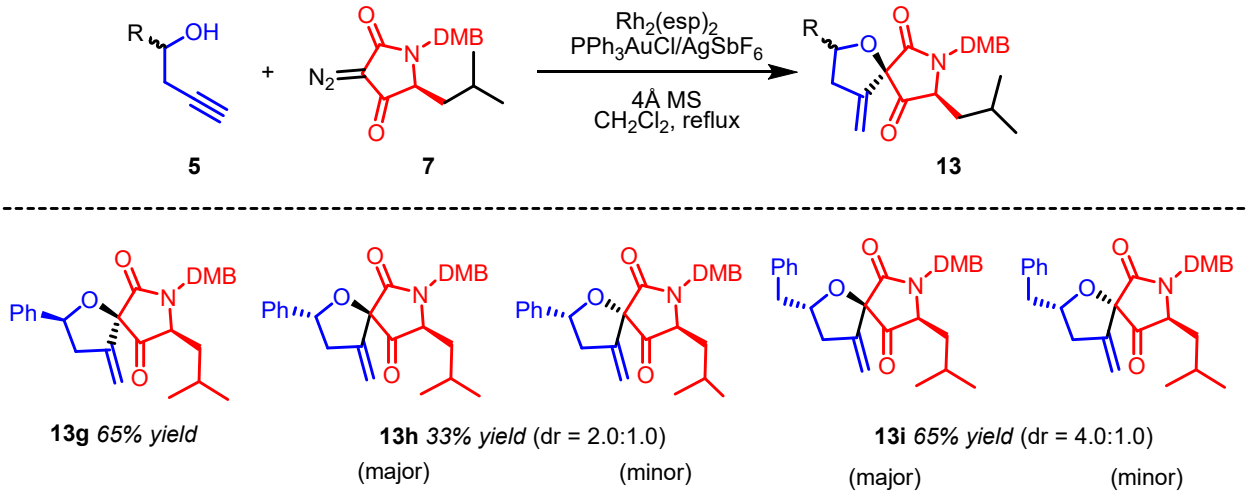

Scheme 2.11 Role of Alcohol Chirality on Reaction Cascade

In the case of secondary alkynol **5b** bearing the *S*-absolute configuration, which matched the *S*-configuration of diazo **7c**, the reaction proceeded cleanly and in good yields to provide a single diastereomer of spirocycle **13g**. When the absolute configuration of the secondary alcohol was changed

to *R*-, however, we observed a sluggish reaction overall and alcohol **5c** was not fully consumed. Indeed, in the mismatched case the reaction was sluggish and low yielding, resulting in poor diastereoselectivity for formation of spirocycle **13h**. Next, we hypothesized that adding a linker CH_2 to the mismatched secondary alcohol would result in a less-crowded transition state, leading to a higher diastereomeric ratio. In addition, Berkeleyamide D is substituted with a benzyl group at the C2 position. Indeed, when benzyl-substituted secondary alcohol **5d** was employed as a substrate, we observed an increase in yield and a modest increase in diastereoselectivity compared to its fellow mismatched substrate **13h**. Ultimately, if a full synthesis for Berkeleyamide D were to be pursued, the S- enantiomer of secondary alcohol 8d should be employed, which would result in good diastereoselectivity in the formation of the C5 spirocenter; since Berkeleyamide D features unsaturation between the C2 and C3 position, the preceding configuration at C2 would be inconsequential.

2.7 APPLICATION OF REACTION CASCADE TO *N*,*N*-DIMETHYLBARBITUATE AND MELDRUM'S ACID SYSTEMS

Lastly, we wanted to extend our application to other cyclic diazo substrates, to probe its utility in the synthesis of alternative spiroethers (**Scheme 2.12**).

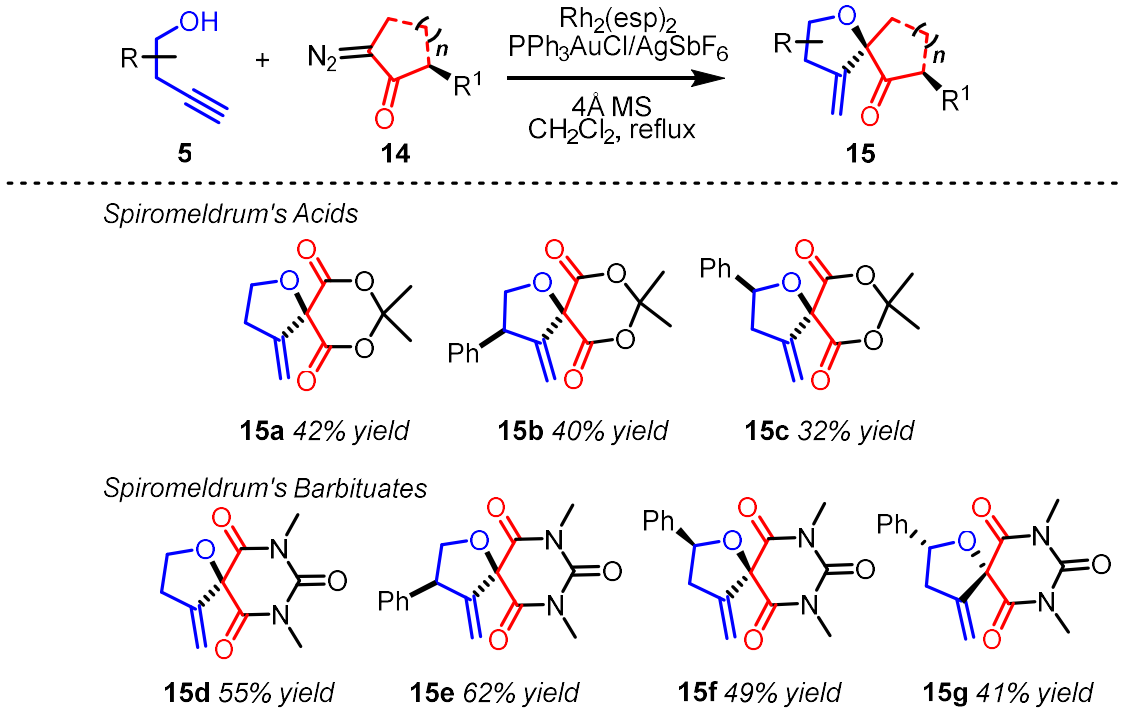

Scheme 2.12 Cascade Approach to Spirobarbituates and Spiromedrum's Acids

To our delight, known Meldrum's acid and *N*,*N*-dimethyl barbiturate diazos tolerated reaction conditions to afford the corresponding spiroethers in moderate to good yields. Lower yields were obtained broadly for spiromedrum's acids **15a**-**15c**, presumably due to their tendency to undergo fragmentation in the presence of Lewis Acids.[11]

2.8 SUMMARY & FUTURE DIRECTIONS

Completion of this research program has afforded a convergent cascade approach to substituted tetrahydrofuran, γ-butyrolactone, spiro-γ-lactam, and general spiroether scaffolds. This intermolecular reaction cascade employs the formation of an electrophilic carbenoid through the rhodium-catalyzed decomposition of stable A/A diazo compounds, followed by the O–H insertion reaction of alkynols and finally intramolecular trapping of the generated ylide with cationic gold-activated alkynes. The cascade has proven to be quite general in terms of reagent tolerance, with A/A diazos able to react with primary and secondary alkynols, resulting in a substrate scope of nine different tetrahydrofurans and over ten spirocycles prepared. Currently, the X-H Insertion/Conia-ene cascade has been successfully applied to O–H, N–H, and sp^2 C–H insertion substrates to produce a diverse set of spiroheterocycles; further developments to this cascade include harnessing S–H, sp^3 C–H, and Si–H reactivity to produce uncommon heterocyclic and spiroheterocyclic frameworks. While the reactivity of the X–H insertion reaction to carbenes is well developed, trapping their reactive intermediates with electrophiles in cascade reactions is still in its infancy – Our group has successfully utilized activated-alkynes and ketone electrophiles, however other electrophilic trapping agents can be explored, such as electron-deficient esters, cobalt acetylides, and silanes.

2.9 REFERENCES FOR CHAPTER 2

1. a.) Kotha, S.; Deb, A. C.; Lahiri, K.; Manivannan, E. "Selected Synthetic Strategies to Spirocyclics." *Synthesis* **2009**, *2,* 165–193. b.) Kuramochi, K.; Nagata, S.; Itaya, H.; Matsubara, Y.; Sunoki, T.; Uchiro, H.; Takao, K.; Kobayashi, S. "A Convergent Total Synthesis of Epolactaene: An Application of the Bridgehead Oxiranyl Anion Strategy." *Tetrahedron* **2003**, *59,* 9743–9758. c.) Nagumo, Y.; Kakeya, H.; Shoji, M.; Hayashi, Y.; Dohmae, N.; Oasda, H. "Epolactaene Binds Human Hsp60 Cys442 Resulting in the Inhibition of Chaperone Activity." *Biochem. J*. **2005**, *387,* 835–840. d.) Song, Z.; Cox, R. J.; Lazarus, C. M.; Simpson, T. J. "Fusarin C Biosynthesis in *Fusarium moniliforme* and *Fusarium venenatum*." *ChemBioChem* **2004**, *5,* 1196–1203. e.) Nicolaou, K. C.; Sun, Y.; Sarlah, D.; Zhan, W.; Wu, T. R. "Bioinspired Synthesis of Hirsutellones A, B, and C." *Org. Lett.* **2011***, 13,* 5708–5710. f.) Wang, L.; Su, H.; Yang, S.; Won, S.; Lin, C. "New Alkaloids and a Tetraflavonoid from *Cephalotaxus wilsoniana*." *J. Nat. Prod.* **2004***, 67,* 1182–1185.

2. Friess, P. "Preliminary Notice of the Reaction of Nitrous Acid with Picramic Acid and Aminonitrophenol." *Annalen der Chemie un Pharmacie* **1858**, *106*, 123–125.

3. a.) Carey, F. A., Sundberg, R. J. *Advanced Organic Chemistry,* 2nd ed; Springer US: 2007. b.) Kolb, H. C., Finn, M. G., Sharpless, K. B. "Click Chemistry: Diverse Chemical Function from a Few Good Reactions." *Angew. Chem. Int. Ed.* **2001**, *40*, 2004–2021. c.) Brase, S., Gil, C., Kepper, K., Zimmerman, V. "Organic Azides: An Exploding Diversity of a Unique Class of Compounds." *Angew. Chem. Int. Ed.* **2005**, *44*, 5188–5240.

4. a.) Regitz, M. "Reactions of Active Methylene Compounds with Azides. I. A New Synthesis for α-Diazo-β-dicarbonyl Compounds from Benzenesulfonylazides and β-Diketones." *Just. Lieb.*

Annal. Chem. **1964***,* 101–109. (Translated from German). b.) Regitz, M., Menz, F. "Deformylative Diazo Group Transfer – A New Route to α-Diazo-Ketones, Aldehydes, and Carboxylic Acid Esters." *Chem. Ber.* **1968**, 2622–2632. (Translated from German). c.) Hendrickson, J. B., Wolf, W. A. "The Direct Introduction of the Diazo Functional in Organic Synthesis." *J. Org. Chem.* **1986**, *33*, 3610–3618. d.) Taber, D. F., Gleave, D. M., Herr, R. J., Moody, K., Hennessy, M. J. "A New Method for the Construction of α-Diazoketones." *J. Org. Chem.* **1995**, *60,* 2283–2285.

5. a.) Bamford, W. R., Stevens, T. S. "The Decomposition of Toluene-p-sulphonylhydrazones by Alkalai." *J. Chem. Soc.* **1952**, 4635–4740. b.) Farnum, D. G. "Preparation of Aryldiazoalkanes by the Bamford-Stevens Reaction." *J. Org. Chem.* **1963**, *28,* 870–872.

9. a.) Conia, J. M.; Leperchec, P. "The Thermal Cyclisation of Unsaturated Carbonyl Compounds." *Synthesis* **1975***,* 1–19. b.) Clarke, M. L.; France, M. B. "The Carbonyl Ene Reaction." *Tetrahedron* **2008**, *64,* 9003–9031.

10. Kennedy-Smith, J. J.; Staben, S. T.; Toste, F. D. "Gold(I)-Catalyzed Conia-Ene Reaction of β-Ketoesters with Alkynes." *J. Am. Chem. Soc.* **2004**, *126,* 4526–4527.

11. a.) Hunter, A. C.; Chinthapally, K.; Sharma, I. "$Rh_2((esp))_2$: An Efficient Catalyst for O–H Insertion Reactions of Carboxylic Acids into Acceptor/Acceptor Diazo Compounds." *Eur. J. Org. Chem.* **2016**, 2260–2263. b.) Hunter, A. C.; Schlitzer, S. C.; Sharma, I. "Synergistic Diazo O–H Insertion/Conia–Ene Cascade Catalysis for the Stereoselective Synthesis of γ–Butyrolactones and Tetrahydrofurans." *Chem. Eur. J.* **2016**, *22,* 16062–16065.

12. a.) Miller, D. J.; Moody, C. J. "Synthetic Applications of the O−H Insertion Reactions of Carbenes and Carbenoids Derived from Diazocarbonyl and Related Diazo Compounds."

Tetrahedron **1995***, 51,* 10811–10843. b.) Peddibhotla, S.; Dang, Y.; Liu, J. O.; Romo, D. "Simultaneous Arming and Structure/Activity Studies of Natural Products Employing O−H Insertions: An Expedient and Versatile Strategy for Natural Products–Based Chemical Genetics." *J. Am. Chem. Soc.* **2007***, 129,* 12222–12231. c.) Maier, T. C.; Fu, G. C. "Catalytic Enantioselective O−H Insertion Reactions." *J. Am. Chem. Soc.* **2006***, 128,* 4594–4595. d.) Zhu, S.-F.; Cai, Y.; Mao, H.-X.; Xie, J.-H.; Zhou, Q.–L. "Enantioselective Iron-Catalyzed O−H Bond Insertions." *Nat. Chem.* **2010***, 2,* 546–551. e.) Zhu, S.–F.; Song, X.–G.; Li, Y.; Cai, Y.; Zhou, Q.–L. "Enantioselective Copper-Catalyzed Intramolecular O−H Insertion: An Efficient Approach to Chiral 2-Carboxy Cyclic Ethers." *J. Am. Chem. Soc.* **2010***, 132,* 16374–16376. f.) Paulissen, R.; Reimlinger, H.; Hayez, E.; Hubert, A.J.; Teyssie, P. "Transition Metal Catalyzed Reactions of Diazocompound – II Insertion in the Hydroxylic Bond." *Tetrahedron* **1973***, 14,* 2233–2236. g.) Noels, A. F.; Demonceau, A.; Petiniot, N; Hubert, A. J.; Teyssie, P. "Transition-Metal-Catalyzed Reaction of Diazocompounds, Efficient Synthesis of Functionalized Ethers by Carbene Insertion into the Hydroxylic Bond of Alcohols." *Tetrahedron* **1982**, *38,* 2733–2739.

13. Wood, J.; L., Petsch, D. T.; Stoltz, B. M.; Hawkins, E. M.; Elbaum, D.; Stover, D. R. "Total Synthesis and Protein Kinase Activity of C(7) Methyl Derivatives of K252a." *Synthesis* **1999***,* 1529–1533.

14. Armstrong, E. L., Grover, H. K., Kerr, M. A. "Scandium Triflate-Catalyzed Nucleophilic Additions to Indolylmethyl Meldrum's Acid Derivatives via a Gramine-Type Fragmentation: Synthesis of Substituted Indolemethanes." *J. Org. Chem.* **2013**, *78*, 10534–10540.

15. a.) V. Sandgren, T. Agback, P. Johansson, J. Lindberg, I. Kvarnström, B. Samuelsson, O. Belda, A. Dahlgren. "Design and Synthesis of Novel Arylketo-containing P1-P3 Linked Macro-cylic BACE-1 Inhibitors." *Bioinorg. & Med. Chem* **2012**, *20*, 4377–4389. b.) O. D. Montagnat, G. Lessene, A. B. Hughes. "Synthesis of Azide-Alkyne Fragments for "Click" Chemical Applications. Part 2. Formation of Oligomers from Orthogonally Protected Chiral Trialkylsilylhomopropargyl Azides and Homopropargyl Alcohols." *J. Org. Chem.* **2010**, *75*, 390–398.

2.10 EXPERIMENTAL SECTION

PUBLICATION AND CONTRIBUTION STATEMENT

The research presented in this chapter were published in the Chemistry – A European Journal (DOI: 10.1002/chem.201603934) and the Journal of Organic Chemistry (DOI: 10.1021/acs.joc.7b03196). Dr. Indrajeet Sharma and Arianne Hunter contributed with assistance in project design, manuscript writing, and editing. The examples presented in Schemes 2.7, 2.10, 2.11, and examples **15d** – **15g** were contributed by Steven Schlitzer, with starting material preparation assistance by co-author Bilal Almutwalli. Examples **15a** – **15b** were contributed by co-author Arianne Hunter. The examples presented in Scheme 2.8 were contributed equally by Steven Schlitzer and Arianne Hunter.

MATERIALS AND METHODS

Reagents

Reagents and solvents were obtained from Sigma-Aldrich (www.sigma-aldrich.com), ChemImpex (www.chemimpex.com) or Acros Organics (www.fishersci.com) and used without further purification unless otherwise indicated. Dry solvents (acetonitrile) were obtained from Acros Organics (www.fishersci.com), and dichloromethane was distilled over CaH_2 under N_2 unless otherwise indicated. THF purchased from Sigma-Aldrich was distilled over Na metal with benzophenone indicator. Diazo compounds were stored as a dilute solution frozen in benzene for periods longer than 24 hours.

Reactions

All reactions were performed in flame-dried glassware under positive N_2 pressure with magnetic stirring unless otherwise noted. Liquid reagents and solutions were transferred thru rubber septa via syringes flushed with N_2 prior to use. Cold baths were generated as follows: 0 °C with wet ice/water and −78 °C with dry ice/acetone. Syringe pump addition reactions were conducted using a CMA/100 microinjection pump.

Chromatography

TLC was performed on 0.25 mm E. Merck silica gel 60 F254 plates and visualized under UV light (254 nm) or by staining with potassium permanganate ($KMnO_4$), cerium ammonium molybdenate (CAM), phosphomolybdic acid (PMA), and ninhydrin. Silica flash chromatography was performed on Sorbtech 230–400 mesh silica gel 60.

Analytical Instrumentation

IR spectra were recorded on a Shimadzu IRAffinity-1 FTIR or a Nicolet 6700 FTIR spectrometer with peaks reported in cm^{-1}. NMR spectra were recorded on a Varian VNMRS 400, 500 and 600 MHz NMR spectrometer in $CDCl_3$ unless otherwise indicated. Chemical shifts are expressed in ppm relative to solvent signals: $CDCl_3$ ((^1H, 7.26 ppm, ^{13}C, 77.0 ppm); coupling constants are expressed in Hz. NMR spectra were processed using Mnova (www.mestrelab.com/software/mnova-nmr). Mass spectra were obtained at the OU Analytical Core Facility on an Agilent 6538 High-Mass-Resolution QTOF Mass Spectrometer and an Agilent 1290 UPLC. X-ray crystallography analysis was carried out at the University of Oklahoma using a Bruker APEX ccd area detector and graphite-monochromated Mo Kα radiation (λ = 0.71073 Å) source and a D8 Quest diffractometer with a Bruker Photon II cmos area detector and an Incoatec

Iμs microfocus Mo Kα source (λ = 0.71073 Å). Crystal structures were visualized using CCDC Mercury software (http://www.ccdc.cam.ac.uk/products/mercury/).

Nomenclature

N.B.: Atom numbers shown in chemical structures herein correspond to IUPAC nomenclature, which was used to name each compound.

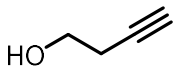

5a

3-butyn-1-ol is commercially available from Chem. Impex. and was used without further purification.

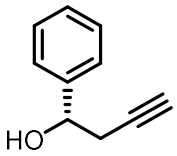

5b

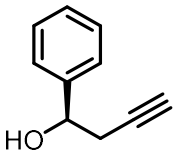

5c

(S)-1-phenylbut-3-yn-1-ol **5b** and (R)-1-phenylbut-3-yn-1-ol **5c** were synthesized in a four-step procedure as reported by Sandgren et. al[12a].

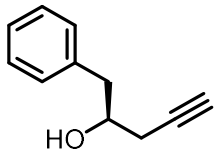

5d

(R)-1-phenylpent-4-yn-2-ol 5d was synthesized in a four-step procedure as reported by Montagnat et. al[12b].

2.10.1 GENERAL PROCEDURE FOR THE SYNTHESIS OF TETRAHYDROFURANS (GP1)

Alkynol (1 equiv.), $Rh_2((esp))^2$ (1 mol%), AgOTf (10 mol%), PPh_3AuCl (10 mol%), and activated 4Å molecular sieves (36 mg per mL of solvent) were added to a round bottom flask, dissolved in anhydrous dichloromethane (0.2 M), and allowed to pre–mix for 5 minutes. The diazo (1.2 equiv.) was dissolved in anhydrous dichloromethane (0.2 M making a total 0.1 M solution for the reaction) was then added dropwise via syringe over a span of 2 minutes. Once the release of N_2 gas ceased, reaction was observed to be complete by TLC. After completion, reaction mixture was filtered through a pad of celite and concentrated by rotary evaporation to provide the crude compound. Purification by flash chromatography (EtOAc/Hex) afforded pure tetrahydrofurans **29**.

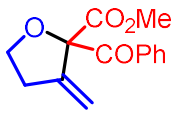

Methyl 2–benzoyl–3–methylenetetrahydrofuran–2–carboxylate (6a). Prepared from methyl 2–diazo–3–oxo–3–phenylpropanoate and 3–butyn–1–ol using general procedure **GP1**. Yellow liquid (52 mg, 86%). **^{1}H NMR** (400 MHz) δ 8.05–7.99 (m, 2H), 7.57–7.51 (m, 1H), 7.46–7.39 (m, 2H), 5.50 (t, J = 2.1 Hz, 1H), 5.41 (t, J = 2.3 Hz, 1H), 4.21 (q, J = 7.8 Hz, 1H), 4.08 (dt, J = 8.3, 6.4 Hz, 1H), 3.74 (s, 3H), 2.73 (ddt, J = 7.5, 4.4, 1.4 Hz, 2H). **^{13}C NMR** (101 MHz) δ 191.2, 170.0, 143.8, 134.3, 133.2, 129.7 (2C), 128.4 (2C), 112.6, 90.2, 68.9, 53.0, 32.9.

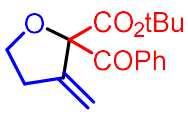

***tert*–Butyl 2–benzoyl–3–methylenetetrahydrofuran–2–carboxylate (6b).** Prepared from *tert*butyl 2–diazo–3–oxo–3–phenylpropanoate and 3–butyn–1–ol using general procedure **GP1**.

Yellow oil (47 mg, 80%). **TLC**: *Rf* 0.5 (4:1 hexanes/EtOAc). **IR** (NaCl) ν_{max}: 2958, 2924, 2854, 2127, 1722, 1598, 1583 cm^{-1}. **^{1}H NMR** (400 MHz) δ 8.07–8.03 (m, 2H), 7.57–7.50 (m, 1H), 7.47–7.39 (m, 2H), 5.50 (t, *J* = 2.1 Hz, 1H), 5.41 (t, *J* = 2.2 Hz, 1H), 4.23 (q, *J* = 7.8 Hz, 1H), 4.07 (dt, *J* = 8.2, 6.3 Hz, 1H), 2.73 (ddt, *J* = 8.3, 4.4, 1.7 Hz, 2H), 1.32 (s, 9H). **^{13}C NMR** (101 MHz) δ 191.3, 168.5, 144.3, 134.8, 132.9, 129.6 (2C), 128.3 (2C), 111.9, 90.1, 83.1, 68.8, 33.2, 29.7, 27.6. **ESI–MS** *m/z* calcd for $C_{17}H_{20}O_4$ ($[M+Na]^+$) 311.1; found 311.1.

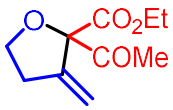

Ethyl 2–acetyl–3–methylenetetrahydrofuran–2–carboxylate (6c). Prepared from ethyl 2–diazo–3–oxobutanoate and 3–butyn–1–ol using general procedure **GP1**. Yellow oil (45 mg, 64%). **TLC**: *Rf* 0.60 (7:3 hexanes/EtOAc). **IR** (NaCl) ν_{max}: 2963, 2925, 1745, 1662 cm^{-1}. **^{1}H NMR** (400 MHz) δ 5.32 (t, *J* = 2.4 Hz, 1H), 5.30 (t, *J* = 2.2 Hz, 1H), 4.17 (qd, *J* = 7.1, 2.9 Hz, 2H), 4.09–3.97 (m, 2H), 2.70– 2.59 (m, 2H), 2.17 (s, 3H), 1.21 (t, *J* = 7.1 Hz, 3H). **^{13}C NMR** (101 MHz) δ 201.6, 168.1, 143.3, 112.0, 90.2, 68.4, 61.9, 32.7, 30.8, 25.4, 13.9. **HRMS** (ESI) *m/z* calcd for $C_{10}H_{14}O_4$ ($[M+Na]^+$) 221.0790; found 221.0784.

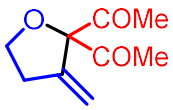

1,1'–(3–Methylenetetrahydrofuran–2,2–diyl)bis(ethan–1–one) (6d). Prepared from 3–diazopentane–2,4–dione and 3–butyn–1–ol using general procedure **GP1**. Orange oil (52 mg, 78%). **^{1}H NMR** (400 MHz) δ 5.34 (t, *J* = 2.2 Hz, 1H), 5.30 (t, *J* = 2.4 Hz, 1H), 4.08 (t, *J* = 7.1 Hz, 2H), 2.67 (ddd, *J* = 7.1, 4.9, 2.3 Hz, 2H), 2.23 (s, 6H). **^{13}C NMR** (101 MHz) δ 198.8, 178.9, 144.7, 112.9, 95.5, 42.3, 25.9.

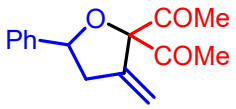

1,1'–(3–Methylene–5–phenyltetrahydrofuran–2,2–diyl)bis(ethan–1–one) (6e). Prepared from 3– diazopentane–2,4–dione and 1–phenylbut–3–yn–1–ol using general procedure **GP1**. Yellow oil (72mg, 72%). **TLC**: *Rf* 0.63 (7:3 hexanes/EtOAc). **^{1}H NMR** (400 MHz) δ 7.46–7.30 (m, 5H), 5.37 (dd, *J* = 2.8, 1.6 Hz, 1H), 5.34 (dd, *J* = 3.0, 1.6 Hz, 1H), 5.07 (dd, *J* = 10.3, 6.1 Hz, 1H), 3.03 (ddt, *J* = 15.7, 6.1, 1.6 Hz, 1H), 2.65 (ddt, *J* = 15.8, 10.3, 2.9 Hz, 1H), 2.31 (d, *J* = 5.4 Hz, 6H). **^{13}C NMR** (101 MHz) δ 203.3, 202.6, 142.6, 139.9, 128.7 (2C), 128.3 (2C), 126.1, 111.9, 81.4, 41.2, 26.3, 26.0. **HRMS** (ESI) *m/z* calcd for $C_{15}H_{16}O_3$ ([M+Na]$^+$) 267.0997; found 267.0993.

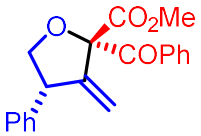

Methyl (*2S,4S*)–2–benzoyl–3–methylene–4–phenyltetrahydrofuran–2–carboxylate (6f). Prepared from methyl 2–diazo–3–oxo–3–phenylpropanoate and 2–phenylbut–3–yn–1–ol using general procedure **GP1**. Clear oil (47 mg, 77%). **TLC**: *Rf* 0.65 (4:1 hexanes/EtOAc). **^{1}H NMR** (400 MHz) δ 8.14–8.02 (m, 2H), 7.63–7.53 (m, 1H), 7.52–7.37 (m, 2H), 7.40–7.15 (m, 5H), 5.55 (d, *J* = 3.0 Hz, 1H), 5.13 (d, *J* = 2.7 Hz, 1H), 4.47 (t, *J* = 8.2 Hz, 1H), 4.27 (dd, *J* = 10.1, 8.3 Hz, 1H), 3.97 (ddt, *J* = 10.7, 8.1, 2.8 Hz, 1H), 3.80 (s, 3H). **^{13}C NMR** (101 MHz) δ 190.6, 170.2, 148.7, 138.5, 134.2, 133.4, 129.8 (2C), 128.9 (2C), 128.7 (2C), 128.5 (2C), 127.3, 114.4, 91.4, 76.1, 53.1, 50.6.

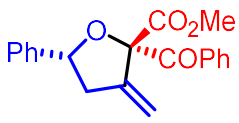

Methyl (2*S*,5*R*)–2–benzoyl–3–methylene–5–phenyltetrahydrofuran–2–carboxylate (6g). Prepared from methyl 2–diazo–3–oxo–3–phenylpropanoate and 1–phenylbut–3–yn–1–ol using

general procedure **GP1**. Clear oil (52 mg, 77%). **TLC**: *Rf* 0.64 (7:3 hexanes/EtOAc). **^{1}H NMR** (400 MHz) δ 8.16–8.03 (m, 4H), 7.60–7.50 (m, 1H), 7.48–7.39 (m, 1H), 7.37–7.19 (m, 4H), 5.53 (dd, *J* = 2.8, 1.3 Hz, 1H), 5.46 (dd, *J* = 3.1, 1.2 Hz, 1H), 5.42 (dd, *J* = 10.8, 5.6 Hz, 1H), 3.77 (s, 3H), 3.04 (ddt, *J* = 15.2, 5.7, 1.3 Hz, 1H), 2.67 (ddt, *J* = 15.1, 10.8, 2.9 Hz, 1H). **^{13}C NMR** (101 MHz) δ 190.8, 170.3, 144.2, 140.0, 134.4, 133.2, 129.9 (2C), 128.4 (2C), 128.4 (2C), 128.3 (2C), 127.9, 125.9, 112.6, 82.2, 52.9, 41.9. **HRMS** (ESI) *m/z* calcd for $C_{20}H_{18}O_4$ ([M+Na]$^+$) 345.1095; found 345.1102.

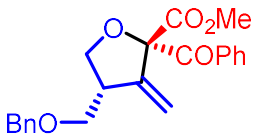

Methyl (2*R*,5*R*)–2–benzoyl–5–((benzyloxy)methyl)–3–methylenetetrahydrofuran–2–carboxylate (6h). Prepared from methyl 2–diazo–3–oxo–3–phenylpropanoate and (*R*)–1–(benzyloxy)pent–4–yn– 2–ol using general procedure **GP1**. Clear oil (62 mg, 64%): $[\alpha]^{21}_D$ +22.8 (c = 1, CHCl3). **TLC**: *Rf* 0.52 (7:3 hexanes/EtOAc). **^{1}H NMR** (400 MHz) δ 8.13–8.00 (m, 2H), 7.40 (t, *J* = 7.8 Hz, 3H), 7.23 (dd, *J* = 5.2, 1.7 Hz, 3H), 7.16 (dd, *J* = 6.9, 2.8 Hz, 2H), 5.48 (dd, *J* = 2.7, 1.6 Hz, 1H), 5.40 (dd, *J* = 2.9, 1.6 Hz, 1H), 4.43 (s, 2H), 3.75 (s, 3H), 3.66 (ddd, *J* = 14.6, 4.8, 2.4 Hz, 1H), 3.53 (t, *J* = 4.3 Hz, 2H), 2.84 – 2.72 (m, 1H), 2.68 (ddt, *J* = 8.9, 5.9, 2.7 Hz, 1H). **^{13}C NMR** (101 MHz) δ 191.3, 170.2, 143.8, 138.0, 134.4, 133.1, 129.9, 129.3, 128.6, 128.3, 128.3, 128.2, 127.5, 127.4, 112.8, 90.9, 79.9, 77.3, 73.2, 71.1, 53.0, 35.2. **HRMS** (ESI) *m/z* calcd for $C_{22}H_{22}O_5$ ([M+Na]$^+$) 389.1357; found 389.1365.

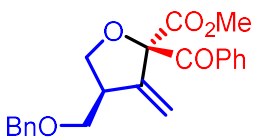

Methyl (2*R*,5*S*)–2–benzoyl–5–((benzyloxy)methyl)–3–methylenetetrahydrofuran–2–carboxylate (6i). Prepared from methyl 2–diazo–3–oxo–3–phenylpropanoate and (*S*)–1–

(benzyloxy)pent–4–yn–2–ol using general procedure **GP1**. Clear oil (47 mg, 75%): $[\alpha]^{21}_{D}$ –22.8 (c = 1, CHCl3). **TLC**: *Rf* 0.52 (7:3 hexanes/EtOAc). **^{1}H NMR** (400 MHz) δ 8.13–8.00 (m, 2H), 7.40 (t, *J* = 7.8 Hz, 3H), 7.23 (dd, *J* = 5.2, 1.7 Hz, 3H), 7.16 (dd, *J* = 6.9, 2.8 Hz, 2H), 5.48 (dd, *J* = 2.7, 1.6 Hz, 1H), 5.40 (dd, *J* = 2.9, 1.6 Hz, 1H), 4.43 (s, 2H), 3.75 (s, 3H), 3.66 (ddd, *J* = 14.6, 4.8, 2.4 Hz, 1H), 3.53 (t, *J* = 4.3 Hz, 2H), 2.84 – 2.72 (m, 1H), 2.68 (ddt, *J* = 8.9, 5.9, 2.7 Hz, 1H). **^{13}C NMR** (101 MHz) δ 191.3, 170.2, 143.8, 138.0, 134.4, 133.1, 129.9, 129.3, 128.6 (2C), 128.3, 128.2, 127.5, 127.4, 112.8, 90.9, 79.9, 77.3, 73.2, 71.1, 53.0, 35.2. **HRMS** (ESI) *m/z* calcd for $C_{22}H_{22}O_5$ ($[M+Na]^+$) 389.1357; found 389.1365.

2.10.3 GENERAL PROCEDURE FOR THE SYNTHESIS OF DIAZO COMPOUNDS (GP2)

To a flame dried round bottom flask equipped with a magnetic stir bar was added A prepared solution of lactam precursor in acetonitrile (0.2M, 1.0 equiv) and p–acetamidobenzenesulfonyl azide (1.2 equiv). The reaction mixture was cooled to 0 ºC and triethylamine (3.0 equiv) was added dropwise by hand. The reaction mixture was monitored via TLC until complete lactam consumption was observed. The reaction mixture was then diluted with ethyl acetate, and washed with a saturated solution of ammonium chloride. The aqueous layer was extracted with additional ethyl acetate, and combined organics were dried over sodium sulfate, filtered, and concentrated. The crude mixture was then purified via flash silica gel chromatography to furnish diazo compounds **31**.

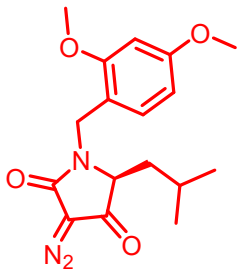

(S)–3–diazo–1–(2,4–dimethoxybenzyl)–5–isobutylpyrrolidine–2,4–dione (7c). Prepared using (S)–1–(2,4–dimethoxybenzyl)–5–isobutylpyrrolidine–2,4–dione and general procedure **E**. Bright yellow oil (600 mg, 77%). $[\alpha]^{21}_{D}$ –85.5 (c = 0.023, $CHCl_3$). **TLC**: R_f 0.51 (40% Ethyl acetate in hexanes). **IR** (NaCl) ν_{max}**:** 2999, 2957, 2872, 2839, 2360, 2335, 2123, 1762, 1689, 1612, 1508, 1402, 1363, 1209, 1157, 1122, 1037, 835 cm^{-1}. **^{1}H NMR** (500 MHz) δ 7.22 (d, *J* = 8.1 Hz, 1H), 6.48–6.42 (m, 2H), 4.99 (d, *J* = 14.8 Hz, 1H), 4.13 (d, *J* = 14.8 Hz, 1H), 3.80 (d, *J* = 1.0 Hz, 6H), 3.76 (dd, *J* = 7.5, 3.9 Hz, 1H), 1.89 (m, *J* = 13.4, 6.6, 5.4, 1.7 Hz, 1H), 1.78–1.65 (m, 2H), 0.92 (d, *J* = 6.7 Hz, 3H), 0.86 (d, *J* = 6.6 Hz, 3H). **^{13}C NMR** (126 MHz) δ 190.3, 161.6, 160.9, 158.4, 131.6, 128.3, 116.3, 104.4, 98.5, 62.7, 55.41, 55.4, 38.9, 38.1, 23.9, 23.6, 22.5. **LRMS** (ESI) m/z calcd for $C_{17}H_{24}N_3O_4Na$ ($[M+Na]^+$) 354.4; found 353.9.

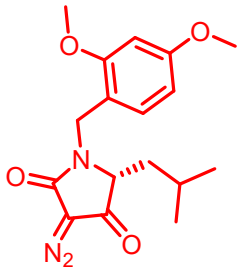

(R)–3–diazo–1–(2,4–dimethoxybenzyl)–5–isobutylpyrrolidine–2,4–dione (7d). Prepared using (R)–1–(2,4–dimethoxybenzyl)–5–isobutylpyrrolidine–2,4–dione and general procedure **E**. Bright yellow oil (255mg, 71%). $[\alpha]^{21}_{D}$ +85.3 (c = 0.017, $CHCl_3$). **TLC** : R_f 0.51 (40% Ethyl acetate in hexanes). **IR** (NaCl) ν_{max}**:** 2957, 2870, 2396, 2388, 2123, 1683, 1614, 1589, 1506, 1404, 1361, 1209, 1157, 1122, 1035, 858 cm^{-1}. **^{1}H NMR** (500 MHz) δ 7.23 (d, *J* = 8.1 Hz, 1H), 6.52–6.41 (m, 2H), 5.00 (d, *J* = 14.8 Hz, 1H), 4.14 (d, *J* = 14.8 Hz,

1H), 3.81 (s, 6H), 3.77 (dd, *J* = 7.6, 3.9 Hz, 1H), 1.96 – 1.84 (m, 1H), 1.73 (m, 2H), 0.93 (d, *J* = 6.7 Hz, 3H), 0.87 (d, *J* = 6.5 Hz, 3H). **^{13}C NMR** (101 MHz) δ 190.2, 161.6, 160. 8, 158.3, 131.5, 128.3, 116.1, 104.3, 98.3, 62.6, 55.3, 55.3, 38.8, 38.0, 23.8, 23.6, 22.4. **LRMS** (ESI) m/z calcd for $C_{17}H_{24}N_3O_4Na$ ([M+Na]$^+$) 354.4; found 353.9.

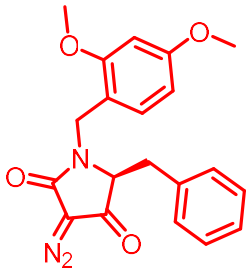

(S)–5–benzyl–3–diazo–1–(2,4–dimethoxybenzyl)pyrrolidine–2,4–dione (7e). Prepared using (S)–5–benzyl–1–(2,4–dimethoxybenzyl)pyrrolidine–2,4–dione and general procedure **E**. Bright yellow oil (126 mg, 47%). $[\alpha]^{21}_D$ –40.2 (c = 0.024, $CHCl_3$). **TLC** : R_f 0.62 (50% Ethyl acetate in hexanes). **IR** (NaCl) ν_{max}**:** 3028, 3001, 2935, 2937, 2360, 2335, 1768, 1695, 1612, 1506, 1456, 1415, 1259, 1207, 1157, 1122, 1035, 925, 833 cm^{-1}. **^{1}H NMR** (400 MHz) δ 7.36 (s, 2H), 7.31–7.22 (m, 3H), 7.17 (d, *J* = 9.0 Hz, 1H), 7.12 (m, 2H), 6.49 – 6.42 (m, 2H), 5.03 (d, *J* = 14.6 Hz, 1H), 4.24 (d, *J* = 14.6 Hz, 1H), 4.02 (t, *J* = 4.4 Hz, 1H), 3.81 (d, *J* = 5.7 Hz, 6H), 3.19 (t, *J* = 4.8 Hz, 2H). **^{13}C NMR** (126 MHz) δ 189.3, 161.8, 161.0, 158.5, 134.5, 131.8, 129.7 (2C), 128.5(2C), 128.3 (2C), 127.2, 116.1, 104.5, 98.5, 64.6, 55.4, 39.4, 34.8. **LRMS** (ESI) m/z calcd for $C_{20}H_{19}N_3O_4Na$ ([M+Na]$^+$) 388.4; found 387.9.

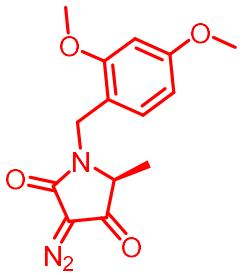

(S)–3–diazo–1–(2,4–dimethoxybenzyl)–5–methylpyrrolidine–2,4–dione (7f). Prepared using (S)–1–(2,4–dimethoxybenzyl)–5–methylpyrrolidine–2,4–dione and general procedure **E**. Faint yellow oil (499 mg, 93%). $[\alpha]^{21}_{D}$ –162.2 (c = 0.024, $CHCl_3$). **TLC :** R_f 0.63 (50% Ethyl acetate in hexanes). **IR** (NaCl) ν_{max}**:** 2939, 2837, 2360, 2335, 2214, 1664, 1612, 1508, 1462, 1265, 1213, 1157, 1122, 1037, 974, 935, 835 cm^{-1}. **^{1}H NMR** (400 MHz) δ 7.22–7.15 (m, 1H), 6.42 (d, *J* = 6.8 Hz, 2H), 4.92 (d, *J*=14.8 Hz, 1H), 4.15 (d, *J* = 14.8 Hz, 1H), 3.77 (d, *J* = 7.4 Hz, 6H), 3.73 (q, 1H), 1.36 (d, *J* = 6.9 Hz, 3H). **^{13}C NMR** (101 MHz) δ 190.2, 161.0, 160.9, 158.4, 131.4, 116.3, 104.5, 98.4, 60.1, 55.4, 55.4, 43.5, 38.6, 15.3. **LRMS** (ESI) m/z calcd for $C_{14}H_{15}N_3O_4Na$ ($[M+Na]^+$) 312.3; found 311.9.

2.10.3 GENERAL PROCEDURE FOR THE SYNTHESIS OF SPIRO–γ–LACTAMS (GP3)

To a 4.0 mL vial equipped with a magnetic stir bar was added powdered 4Å molecular sieves (70 mg/ mL solvent). The molecular sieves were activated via heat and allowed to cool to room temperature under vacuum. $Rh_2((esp))_2$ (1 mol %), $AuClPPh_3$ (10 mol %), and $AgSbF_6$ (10 mol %) were then measured directly into the reaction vessel. A solution of alkynol (1.2 equiv.) and diazo (1.0 equiv.) in dichloromethane (0.3M) was added, and the mixture was sonicated for 30 seconds. The reaction vessel was sealed, and heated to reflux. The reaction was monitored by TLC until complete consumption of diazo was observed (between 30 minutes – 5 h). The crude reaction mixture was then cooled to room temperature, filtered through a pad of celite, concentrated, and analyzed via ^{1}H NMR. The crude mixture was then purified via flash chromatography to furnish spirocyclic compounds.

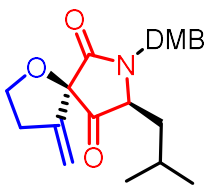

(5R,8S)–7–(2,4–dimethoxybenzyl)–8–isobutyl–4–methylene–1–oxa–7–azaspiro[4.4]nonane–6,9–dione (13c). Prepared from (S)–3–diazo–1–(2,4–dimethoxybenzyl)–5–isobutylpyrrolidine–2,4–dione and but–3–yn–1–ol using general procedure **GP3** (Conversion of Diazo observed in 1 hour). Yellow–orange crystalline solid (38 mg, 68%). m.p. 128–136 °C. $[\alpha]^{21}_{D}$ –22.5 (c = 0.006, $CHCl_3$). **TLC :** R_f 0.30 (40% Ethyl acetate in hexanes). **IR** (NaCl) ν_{max}**:** 2956, 2929, 2973, 2360, 2335, 1772, 1702, 1612, 1589, 1508, 1463, 1438, 1413, 1365, 1294, 1267, 1209, 1159, 1126, 1035, 914, 833, 786 cm^{-1}. **^{1}H NMR** (500 MHz) δ 7.29 (m, 1H), 6.47 (m, 2H), 5.19 (d, *J* = 14.3 Hz, 1H), 5.10 (s, 1H), 4.59 (s, 1H), 4.33 (t, J = 7.1 Hz, 2H), 4.11 (d, *J* = 14.4 Hz, 1H), 3.88 (t, *J* = 5.3 Hz, 1H), 3.81 (d, *J* = 3.3 Hz, 6H), 2.78 (m, 2H), 1.90 – 1.72 (m, 3H), 0.95 (d, *J* = 6.3 Hz, 3H), 0.80 (d, *J* = 6.2 Hz, 3H). **^{13}C NMR** (126 MHz) δ 208.0, 170.1, 161.0, 158.5, 148.0, 132.2, 116.0, 107.9, 104.4, 98.5, 83.2, 70.1, 61.1, 55.4, 55.3, 38.7, 37.1, 33.2, 24.3, 23.6, 22.5. **HRMS** (ESI) m/z calcd for $C_{21}H_{27}NO_5Na$ ($[M+Na]^+$) 396.1787; found 396.1783.

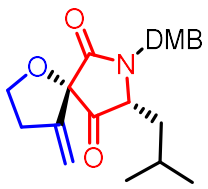

(5S,8R)–7–(2,4–dimethoxybenzyl)–8–isobutyl–4–methylene–1–oxa–7–azaspiro[4.4]nonane–6,9–dione (13d). Prepared from (R)–3–diazo–1–(2,4–dimethoxybenzyl)–5–isobutylpyrrolidine–2,4–dione and but–3–yn–1–ol using general procedure **GP3** (Conversion of Diazo observed in 1 hour). Yellow crystalline solid (37 mg, 66%). m.p. 127–139 °C. $[\alpha]^{21}_{D}$ +22.9 (c = 0.011, $CHCl_3$). **TLC** : R_f 0.30 (40% Ethyl acetate in hexanes). **IR** (NaCl) ν_{max}**:** 2956, 2875, 2841, 2360, 2335, 1772, 1703, 1612, 1587, 1508, 1462, 1413, 1294, 1267, 1209, 1159, 1128, 1089, 1033, 910, 833 cm^{-1}. **^{1}H NMR**

(500 MHz) δ 7.29 (m, 1H), 6.49 – 6.45 (m, 2H), 5.19 (d, *J* = 14.4 Hz, 1H), 5.10 (s, 1H), 4.58 (s, 1H), 4.33 (t, *J* = 7.8, 2H), 4.11 (d, *J* = 14.4 Hz, 1H), 3.88 (t, *J* = 5.3 Hz, 1H), 3.81 (d, *J* = 3.2 Hz, 6H), 2.86 – 2.73 (m, 2H), 1.89 – 1.72 (m, 3H), 0.95 (d, *J* = 6.3 Hz, 3H), 0.79 (d, *J* = 6.2 Hz, 3H). **^{13}C NMR** (126 MHz) δ 208.0, 170.1, 161.0, 158.5, 148.0, 132.2, 116.0, 107.9, 104.4, 98.4, 83.2, 70.1, 61.3, 55.4, 55.3, 38.7, 37.1, 33.2, 24.3, 23.6, 22.5. **HRMS** (ESI) m/z calcd for $C_{21}H_{27}NO_5Na$ ($[M+Na]^+$) 396.1787; found 396.1787.

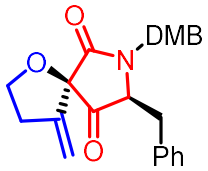

(5R,8S)–8–benzyl–7–(2,4–dimethoxybenzyl)–4–methylene–1–oxa–7–azaspiro[4.4]nonane–6,9–dione (13e). Prepared from (S)–5–benzyl–3–diazo–1–(2,4–dimethoxybenzyl)pyrrolidine–2,4–dione and but–3–yn–1–ol using general procedure **GP3** (Conversion of Diazo observed in 30 minutes). Vibrant yellow oil (23 mg, 64%). $[\alpha]^{21}_D$ –37.8 (c = 0.017, $CHCl_3$). **TLC :** R_f 0.33 (50% Ethyl acetate in hexanes). **IR** (NaCl) ν_{max}**:** 3294, 3076, 2958, 2872, 2841, 2360, 2335, 1772, 1703, 1612, 1589, 1508, 1462, 1413, 1294, 1267, 1209, 1126, 1035, 916, 833, 732 cm^{-1}. **^{1}H NMR** (400 MHz) δ 7.32 – 7.18 (m, 4H), 7.13 – 7.09 (m, 2H), 6.51 – 6.43 (m, 2H), 5.14 (d, *J* = 14.4 Hz, 1H), 5.06 (s, 1H), 4.54 (s, 1H), 4.28 – 4.23 (m, 2H), 4.21 – 4.15 (m, 2H), 3.81 (d, *J* = 2.1 Hz, 6H), 3.30 (dd, *J* = 14.7, 3.4 Hz, 1H), 3.17 (dd, *J* = 14.7, 6.4 Hz, 1H), 2.72 (m, 2H). **^{13}C NMR** (101 MHz) δ 207.2, 170.0, 161.0, 158.5, 147.9, 135.1, 132.3, 129.57 (2C), 128.6 (2C), 127.1, 115.9, 108.0, 104.5, 98.5, 83.2, 70.0, 63.2, 55.4, 55.4, 39.1, 34.5, 33.1. **HRMS** (ESI) m/z calcd for $C_{24}H_{25}NO_5Na$ ($[M+Na]^+$) 430.1630; found 430.1635.

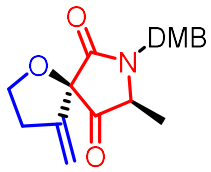

(5R,8S)–7–(2,4–dimethoxybenzyl)–8–methyl–4–methylene–1–oxa–7–azaspiro[4.4]nonane–6,9–dione (13f). Prepared from (S)–3–diazo–1–(2,4–dimethoxybenzyl)–5–methylpyrrolidine–2,4–dione and but–3–yn–1–ol using general procedure **GP3** (Conversion of Diazo observed in 1 hour). Faint yellow oil (32 mg, 63%). $[\alpha]^{21}_{D}$ –68.0 (c = 0.011, $CHCl_3$). **TLC :** R_f 0.28 (50% Ethyl acetate in hexanes). **IR** (NaCl) ν_{max}**:** 2956, 2873, 2841, 2360, 2335, 2125, 2096, 1772, 1701, 1612, 1508, 1462, 1413, 1367, 1294, 1207, 1161, 1126, 1089, 1035, 833 cm^{-1}. **^{1}H NMR** (500 MHz) δ 7.33 – 7.25 (m, 1H), 6.47 (m, 2H), 5.20 (d, *J* = 14.5 Hz, 1H), 5.12 (s, 1H), 4.63 (s, 1H), 4.34 (t, *J* = 7.0 Hz, 2H), 4.11 (d, *J* = 14.5 Hz, 1H), 3.90 (q, *J* = 6.8 Hz, 1H), 3.82 (s, 6H), 2.84 – 2.73 (m, 2H), 1.41 (d, *J* = 6.7 Hz, 3H). **^{13}C NMR** (126 MHz) δ 207.2, 169.4, 161.0, 158.5, 147.5, 132.1, 116.0, 108.0, 104.5, 98.5, 83.6, 70.0, 58.1, 55.4, 55.4, 38.3, 33.0, 14.3. **HRMS** (ESI) m/z calcd for $C_{18}H_{21}NO_5Na$ ($[M+Na]^+$) 354.1317; found 354.1299.

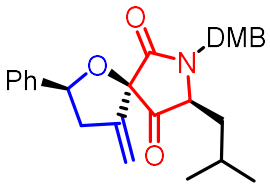

(2S,5R,8S)–7–(2,4–dimethoxybenzyl)–8–isobutyl–4–methylene–2–phenyl–1–oxa–7–azaspiro[4.4]nonane–6,9–dione (13g). Prepared from (S)–3–diazo–1–(2,4–dimethoxybenzyl)–

5–isobutylpyrrolidine–2,4–dione and (S)–1–phenylbut–3–yn–1–ol using general procedure **GP3** (Conversion of Diazo observed in 45 minutes). Vibrant yellow oil (16 mg, 65%). $[\alpha]^{21}_{D}$ –72.4 (c = 0.006, $CHCl_3$). **TLC :** R_f 0.61 (40% Ethyl acetate in hexanes). **IR** (NaCl) ν_{max}**:** 3001, 2958, 2933, 2870, 2358, 2341, 2123, 1770, 1699, 1614, 1587, 1506, 1456, 1409, 1294, 1265, 1209, 1157, 1128, 1089, 1033, 918, 835, 754, 736, 700 cm^{-1}. **^{1}H NMR** (500 MHz) δ 7.54 – 7.51 (m, 2H), 7.39 – 7.28 (m, 4H), 6.50 – 6.45 (m, 2H), 5.45 (dd, *J* = 10.6, 5.6 Hz, 1H), 5.19 (d, *J* = 14.4 Hz, 1H), 5.09 (s, 1H), 4.62 (s, 1H), 4.14 (d, *J* = 14.4 Hz, 1H), 3.96 (t, *J* = 7.2 Hz, 1H), 3.82 (d, *J* = 3.1 Hz, 6H), 3.01 (m, 1H), 2.75 (m, 1H), 1.94 – 1.83 (m, 1H), 1.82 – 1.77 (m, 2H), 0.95 (d, *J* = 6.6 Hz, 3H), 0.81 (d, *J* = 6.5 Hz, 3H). **^{13}C NMR** (126 MHz) δ 206.9, 170.5, 161.0, 158.4, 147.7, 140.5, 132.4, 128.4 (2C), 128.1, 126.6, 116.1, 108.1, 104.5, 98.5, 84.0, 82.9, 61.0, 55.4, 55.3, 42.1, 38.7, 37.3, 24.3, 23.7, 22.4, 20.8. **HRMS** (ESI) m/z calcd for $C_{27}H_{31}NO_5Na$ ($[M+Na]^+$) 472.2100; found 472.2099.

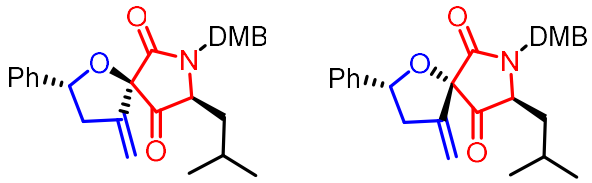

Major **Minor**

In this mismatch diazo/alcohol case, the reaction became sluggish after 5 hours and full consumption of alcohol compound was not observed. The overall yields based on recovered alcohol starting material 28c was 68%.

(2R,5R,8S)–7–(2,4–dimethoxybenzyl)–8–isobutyl–4–methylene–2–phenyl–1–oxa–7–azaspiro[4.4]nonane–6,9–dione (13h major). Prepared from (S)–3–diazo–1–(2,4–dimethoxybenzyl)–5–isobutylpyrrolidine–2,4–dione and (R)–1–phenylbut–3–yn–1–ol using general procedure **GP3** (Partial conversion of diazo observed in 5 hours). Vibrant yellow oil (14

mg, 23%) $[\alpha]^{21}_D$ –38.1 (c = 0.008, $CHCl_3$). **TLC :** R_f 0.61 (40% Ethyl acetate in hexanes). **IR** (NaCl) ν_{max}**:** 3001, 2956, 2931, 2872, 2841, 2123, 1772, 1703, 1612, 1587, 1506, 1460, 1411, 1294, 1265, 1209, 1159, 1128, 1087, 1033, 1004, 918, 833, 754, 700 cm^{-1}. **^{1}H NMR** (500 MHz) δ 7.60 – 7.56 (m, 2H), 7.40 – 7.33 (m, 2H), 7.32 – 7.28 (m, 2H), 6.48 (m, 2H), 5.47 (dd, *J* = 9.1, 6.6 Hz, 1H), 5.23 (d, *J* = 14.3 Hz, 1H), 5.11 (s, 1H), 4.62 (sm, 1H), 4.14 (d, *J* = 14.4 Hz, 1H), 3.90 – 3.86 (m, 1H), 3.82 (d, *J* = 2.8 Hz, 6H), 3.11 (m, 1H), 2.86 (m, 1H), 1.92 – 1.80 (m, 1H), 1.81 – 1.73 (m, 2H), 0.94 (d, *J* = 6.6 Hz, 3H), 0.81 (d, *J* = 6.4 Hz, 3H). **^{13}C NMR** (101 MHz) δ 209.2, 169.4, 160.95, 158.5, 148.0, 140.8, 132.1, 128.4 (2C), 128.1 (2C), 126.5, 115.8, 108.0, 104.4, 98.4, 82.7, 61.3, 55.4, 55.3, 42.1, 38.8, 37.4, 29.7, 24.3, 23.7, 22.4. **HRMS** (ESI) m/z calcd for $C_{27}H_{31}NO_5Na$ ($[M+Na]^+$) 472.2100; found 472.2107.

(2R,5S,8S)–7–(3,4–dimethylbenzyl)–8–isobutyl–4–methylene–2–phenyl–1–oxa–7–azaspiro[4.4]nonane–6,9–dione (13h minor). Prepared from (S)–3–diazo–1–(2,4–dimethoxybenzyl)–5–isobutylpyrrolidine–2,4–dione and (R)–1–phenylbut–3–yn–1–ol using general procedure **GP3** (Partial conversion of diazo observed in 5 hours). Yellow oil (7 mg, 11%) **^{1}H NMR** (400 MHz, Chloroform–*d*) δ 7.54 – 7.48 (m, 2H), 7.40 – 7.28 (m, 5H), 6.47 (d, *J* = 2.2 Hz, 1H), 5.45 (dd, *J* = 10.6, 5.6 Hz, 1H), 5.19 (d, *J* = 14.4 Hz, 1H), 5.09 (d, *J* = 2.6 Hz, 1H), 4.61 (d, *J* = 2.9 Hz, 1H), 4.13 (d, *J* = 14.4 Hz, 1H), 3.96 (t, *J* = 5.5 Hz, 1H), 3.82 (d, *J* = 2.5 Hz, 6H), 3.01 (dd, *J* = 15.1, 5.4 Hz, 1H), 2.82 – 2.67 (m, 1H), 1.92 – 1.74 (m, 3H), 0.94 (d, *J* = 6.5 Hz, 2H), 0.81 (d, *J* = 6.4 Hz, 2H). **^{13}C NMR** (101 MHz, $cdcl_3$) δ 206.9, 170.5, 161.0, 158.4, 147.7, 140.5, 132.3, 128.4 (2C), 128.1, 126.6, 125.6, 116.1, 108.0, 104.4, 98.5, 84.0, 82. 9, 61.0, 55.3, 42.1, 38.7, 37.3, 29.7, 24.3, 23.6, 22.4. **HRMS** (ESI) m/z calcd for $C_{27}H_{32}NO_5N$ ($[M+H]^+$) ; 450.2280; found 450.2281.

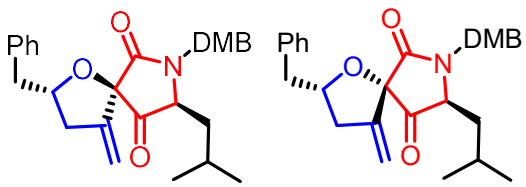

Major **Minor**

(2S,5R,8S)–2–benzyl–7–(2,4–dimethoxybenzyl)–8–isobutyl–4–methylene–1–oxa–7–azaspiro[4.4]nonane–6,9–dione (13i major). Prepared from (S)–3–diazo–1–(2,4–dimethoxybenzyl)–5–isobutylpyrrolidine–2,4–dione and using general procedure **GP3** (Conversion of Diazo observed in 4 hours). Vibrant yellow oil (41 mg, 49%). $[\alpha]^{21}_{D}$ –63.5 (c = 0.012, $CHCl_3$). **TLC :** R_f 0.69 (50% Ethyl acetate in hexanes). **IR** (NaCl) ν_{max}**:** 3032, 3001, 2956, 2926, 2870, 2362, 2335, 2121, 1772, 1699, 1612, 1587, 1506, 1462, 1411, 1363, 1294, 1265, 1207, 1159, 1126, 1089, 1037, 918, 833, 756, 700 cm^{-1}. **^{1}H NMR** (500 MHz) δ 7.28 m, 2H), 7.26 – 7.18 (m, 4H), 6.45 (m, 2H), 5.16 (d, *J* = 14.4 Hz, 1H), 5.01 (s, 1H), 4.78 – 4.68 (m, 1H), 4.53 (s, 1H), 4.10 (d, *J* = 14.4 Hz, 1H), 3.89 – 3.86 (m, 1H), 3.80 (d, *J* = 3.2 Hz, 6H), 3.23 (dd, *J* = 13.6, 6.0 Hz, 1H), 2.84 (dd, *J* = 13.6, 7.7 Hz, 1H), 2.69 (m, 1H), 2.52 – 2.44 (m, 1H), 1.84 (m, 1H), 1.77 (m, 2H), 0.95 (d, *J* = 6.5 Hz, 3H), 0.80 (d, *J* = 6.4 Hz, 3H). **^{13}C NMR** (101 MHz) δ 207.2, 170.4, 160.9, 158.4, 147. 9, 137.7, 132.2, 129.3, 128.4 (2C), 126.4, 116.0, 108.1, 104.4, 98.4, 84.1, 82.2, 61.0, 55.4, 55.3, 41.8, 38.6, 37.2, 29.7, 24.3, 23.7, 22.4, 14.1. **HRMS** (ESI) m/z calcd for $C_{28}H_{33}NO_5Na$ ($[M+Na]^+$) 486.2256; found 486.2264.

(2S,5S,8S)–2–benzyl–7–(3,4–dimethylbenzyl)–8–isobutyl–4–methylene–1–oxa–7–azaspiro[4.4]nonane–6,9–dione (13i minor). Prepared from (S)–3–diazo–1–(2,4–dimethoxybenzyl)–5–isobutylpyrrolidine–2,4–dione and using general procedure **GP3** (Conversion of Diazo observed in 4 hours). Yellow oil (11 mg, 12%). **^{1}H NMR** (500 MHz,

Chloroform–*d*) δ 7.36 – 7.28 (m, 4H), 7.25 – 7.14 (m, 3H), 6.48 (d, *J* = 7.9 Hz, 2H), 5.21 (d, *J* = 14.4 Hz, 1H), 5.05 (d, *J* = 2.2 Hz, 1H), 4.72 (p, *J* = 6.8 Hz, 1H), 4.58 (d, *J* = 2.5 Hz, 1H), 4.14 (d, *J* = 14.4 Hz, 1H), 3.87 (t, *J* = 5.5 Hz, 1H), 3.82 (d, *J* = 4.1 Hz, 6H), 3.26 (dd, *J* = 13.6, 6.4 Hz, 1H), 2.86 (dd, *J* = 13.6, 7.7 Hz, 1H), 2.78 – 2.70 (m, 1H), 2.61 – 2.54 (m, 1H), 1.89 – 1.81 (m, 1H), 1.77 (dd, *J* = 7.5, 5.3 Hz, 2H), 0.95 (d, *J* = 6.6 Hz, 3H), 0.80 (d, *J* = 6.4 Hz, 3H). **^{13}C NMR** (126 MHz, $cdcl_3$) δ 206.9, 171.1, 158.5, 147.7, 132.3, 129.4 (2C), 128.4 (2C), 126.3, 116.0, 108.22, 104.4, 98.4, 82.1, 60.9, 55.4, 41.9, 38.8, 38.2, 37.3, 30.9, 29.7, 24.3, 23.7, 22.4. **HRMS** (ESI) m/z calcd for $C_{28}H_{33}NO_5$ ($[M+H]^+$]) 464.2437 ; found 464.2427.

Appendix I

Spectra Relevant to Chapter 2

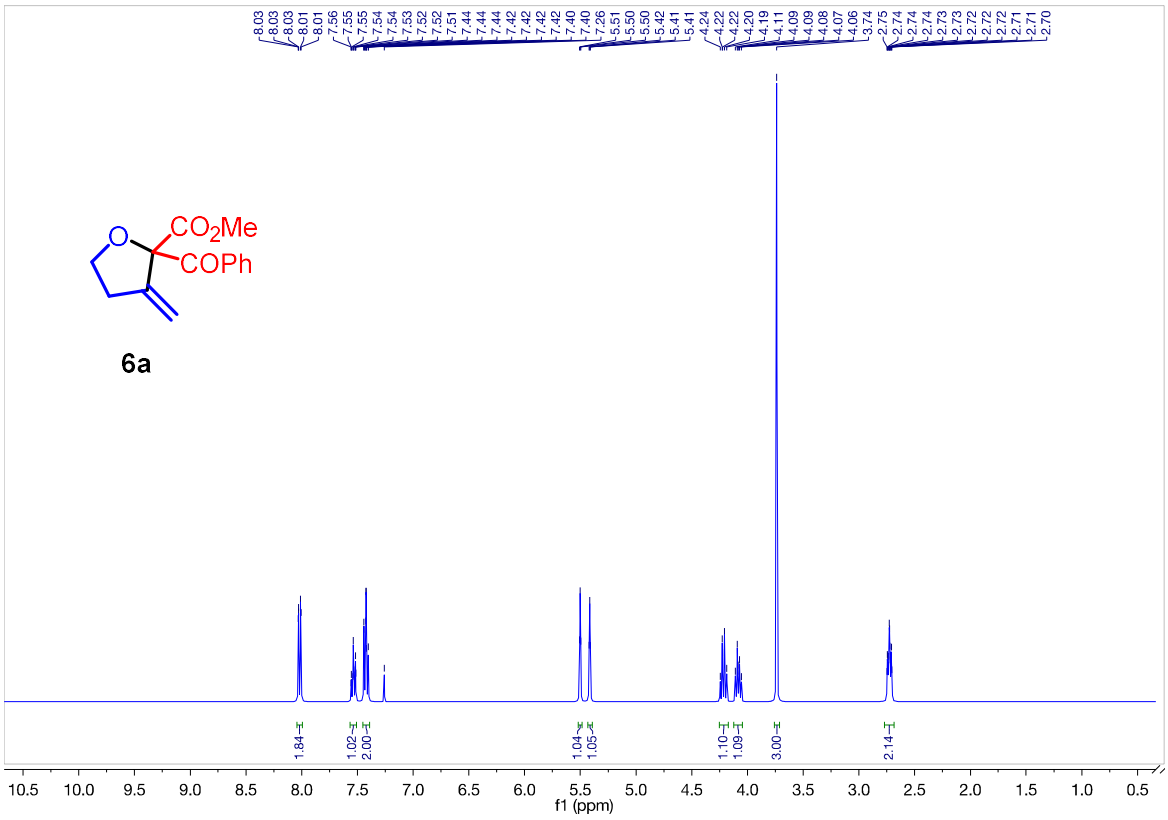
CO2Me
COPh
6a
f1 (ppm)

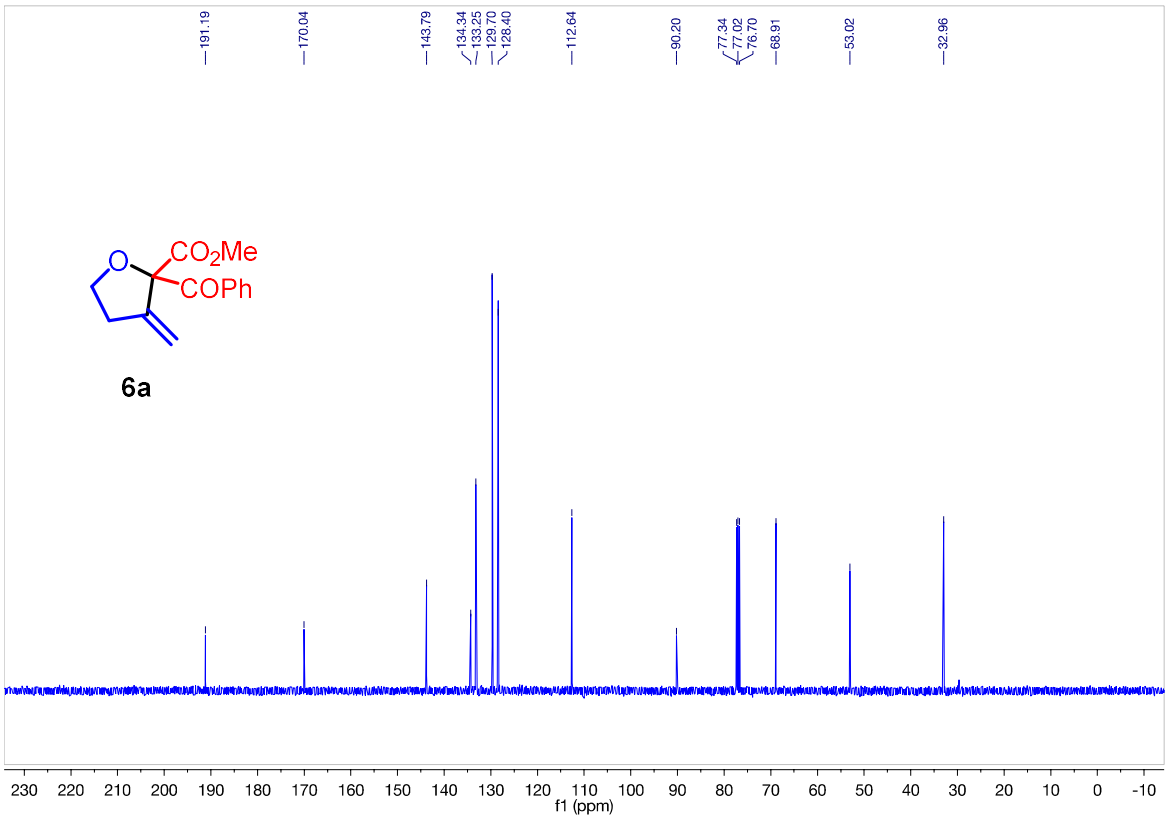
CO2Me
COPh
6a
f1 (ppm)

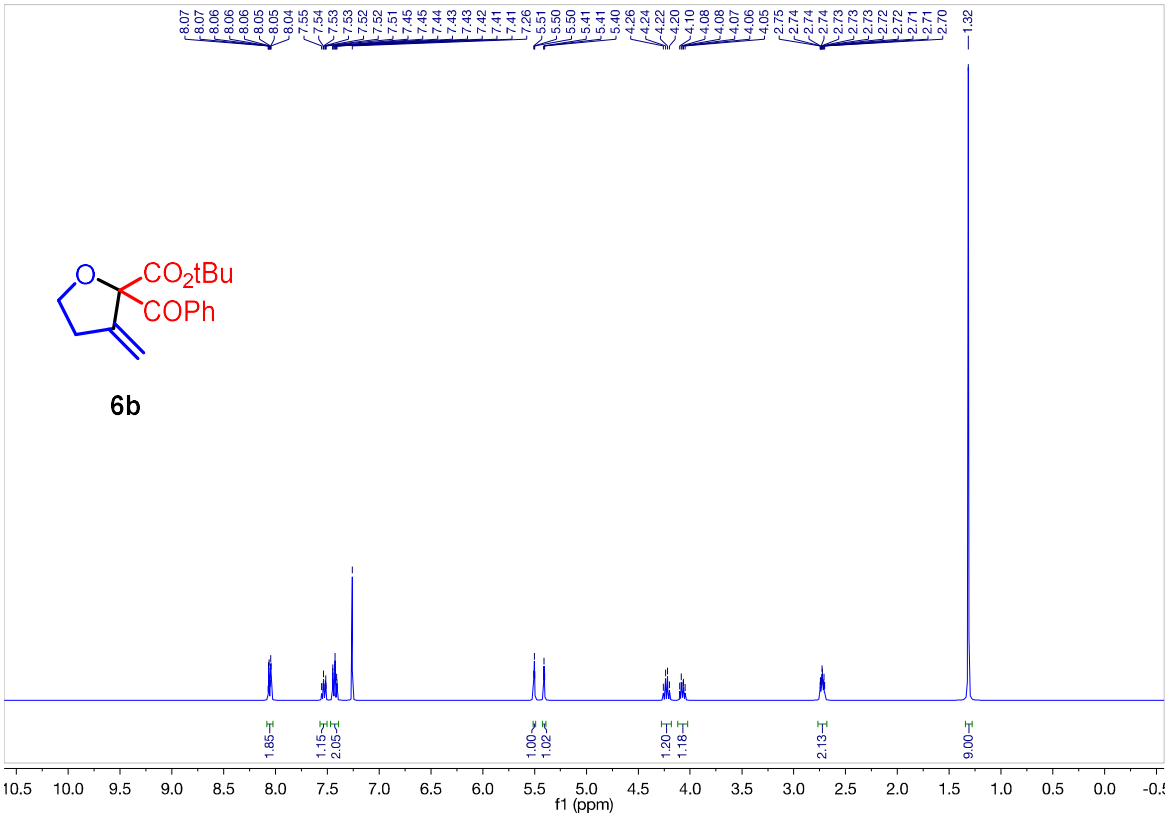
CO2tBu
COPh
6b
f1 (ppm)

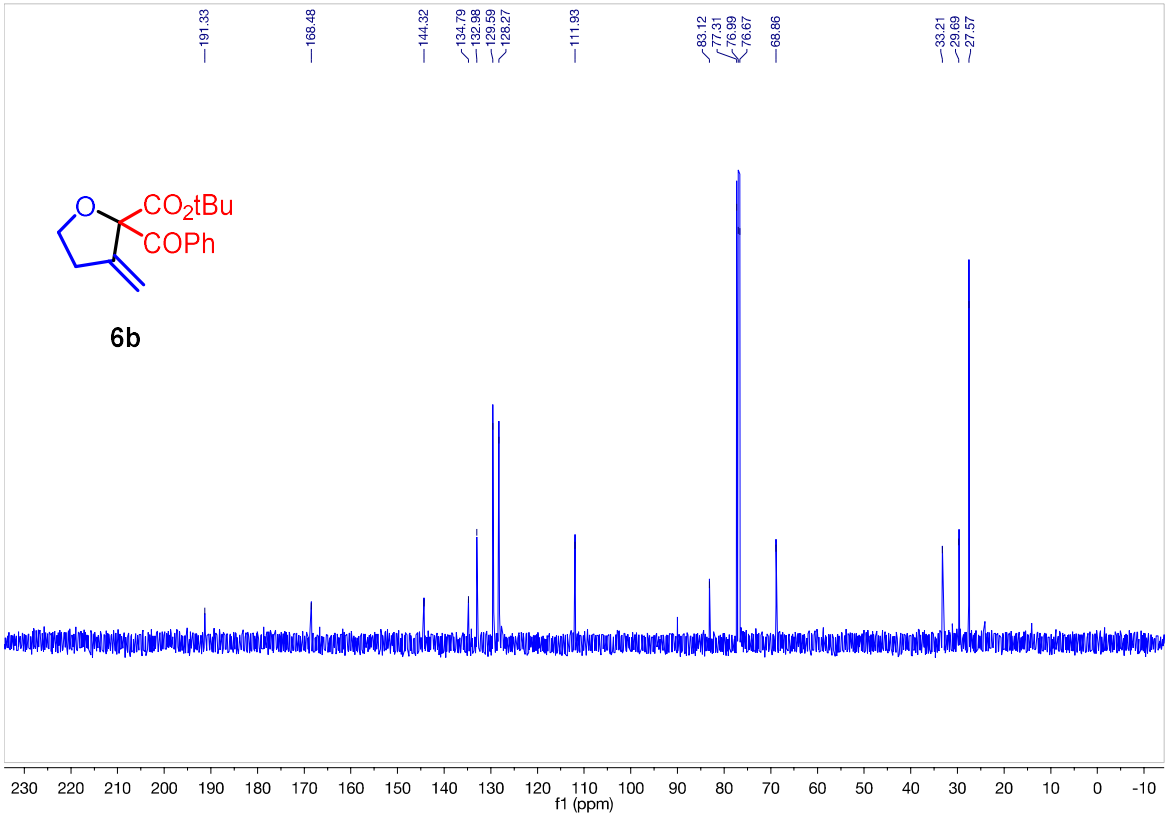
CO2tBu
COPh
6b
f1 (ppm)

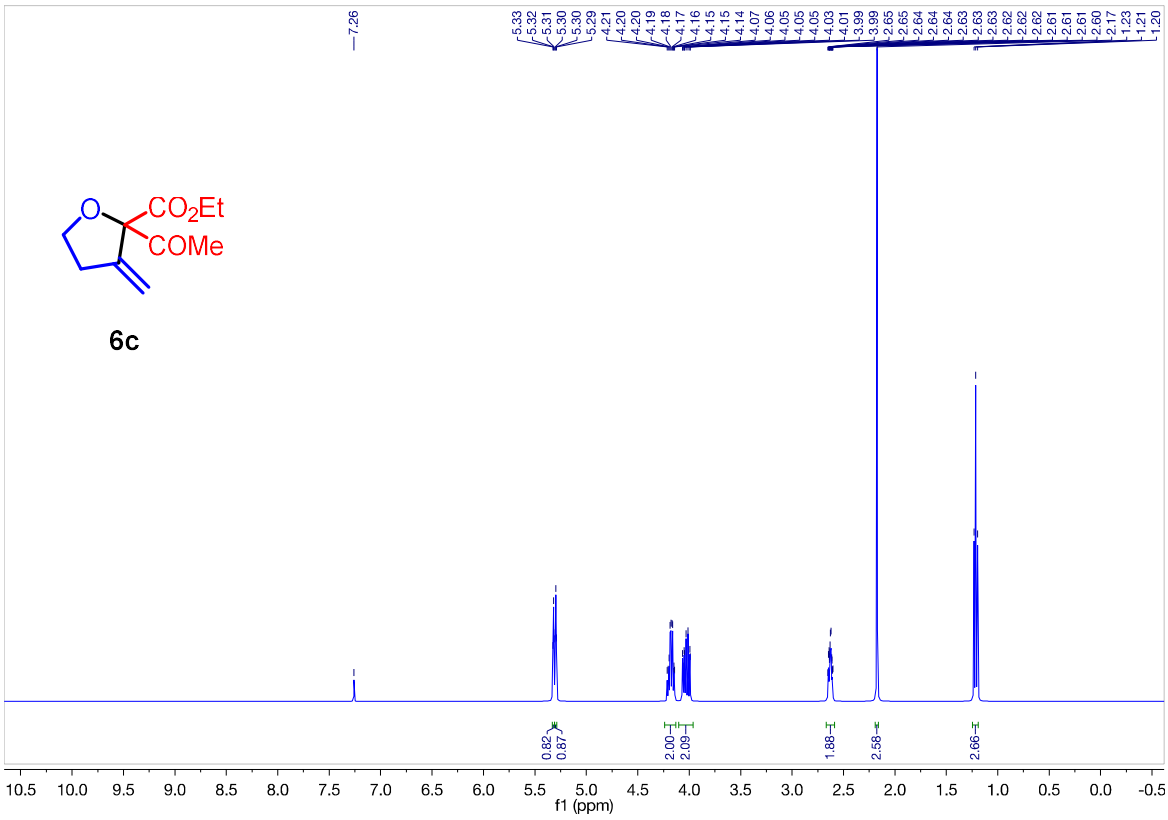
7.26
5.33
5.32
5.31
5.30
5.30
5.29
4.21
4.20
4.20
4.19
4.18
4.17
4.16
4.15
4.15
4.14
4.07
4.06
4.05
4.05
4.05
4.03
4.01
3.99
3.99
2.65
2.65
2.64
2.64
2.64
2.63
2.63
2.63
2.62
2.62
2.62
2.61
2.61
2.61
2.60
2.17
1.23
1.21
1.20
O
CO2Et
COMe
6c
0.82
0.87
2.00
2.09
1.88
2.58
2.66
10.5 10.0 9.5 9.0 8.5 8.0 7.5 7.0 6.5 6.0 5.5 5.0 4.5 4.0 3.5 3.0 2.5 2.0 1.5 1.0 0.5 0.0 -0.5
f1 (ppm)

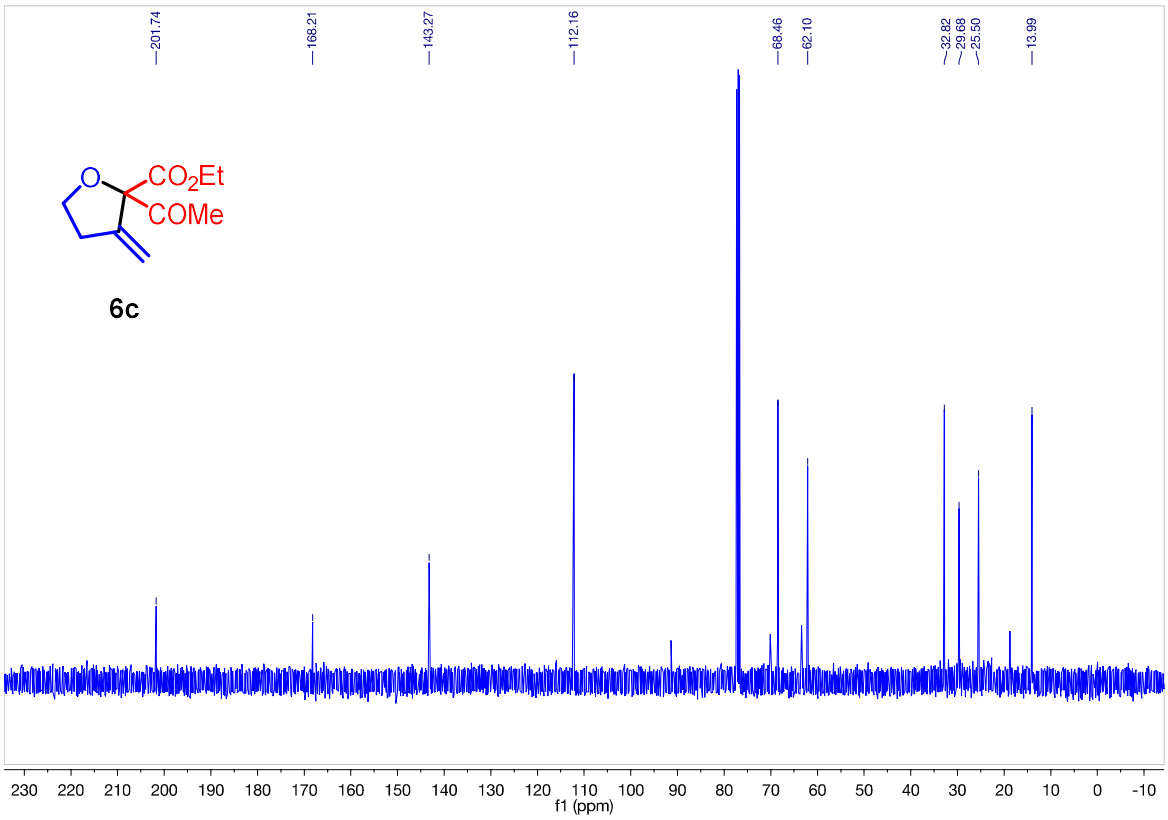
201.74
168.21
143.27
112.16
68.46
62.10
32.82
29.68
25.50
13.99
O
CO2Et
COMe
6c
230 220 210 200 190 180 170 160 150 140 130 120 110 100 90 80 70 60 50 40 30 20 10 0 -10
f1 (ppm)

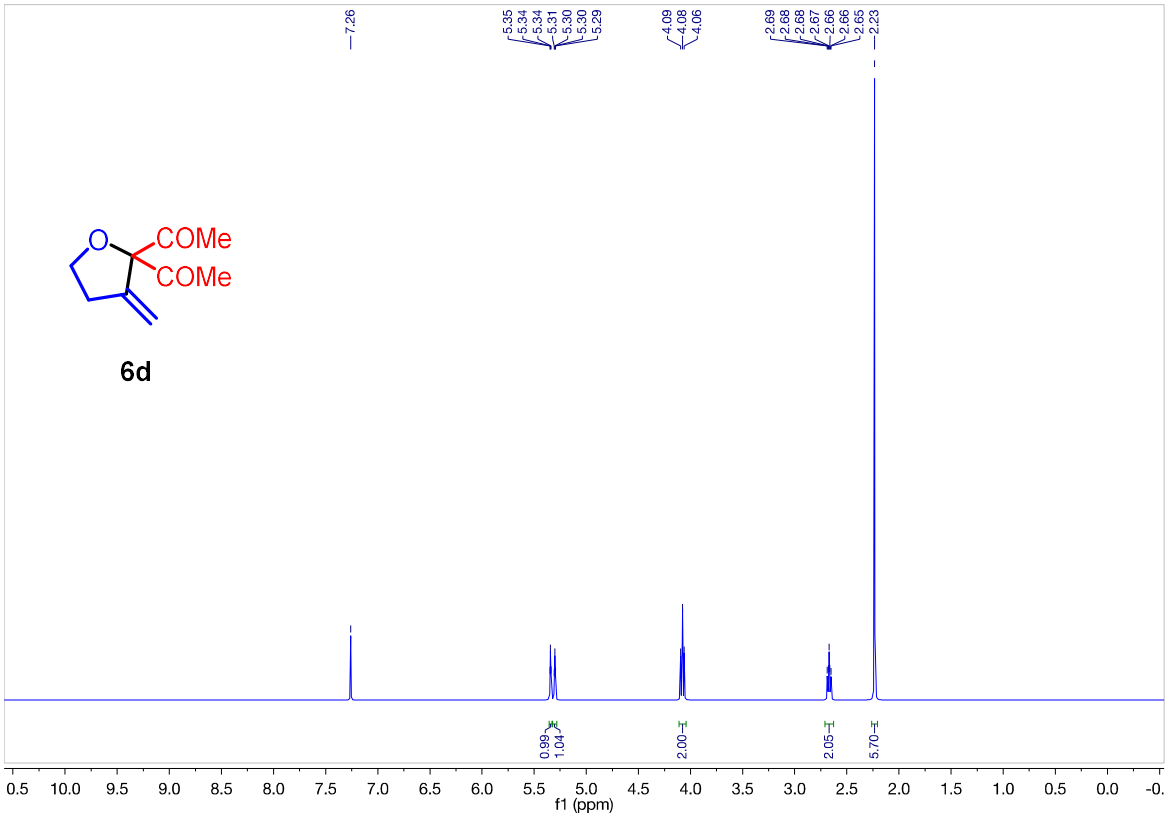
7.26
5.35
5.34
5.34
5.31
5.30
5.30
5.29
4.09
4.08
4.06
2.69
2.68
2.68
2.67
2.66
2.66
2.65
2.23
COMe
COMe
6d
0.99
1.04
2.00
2.05
5.70
f1 (ppm)

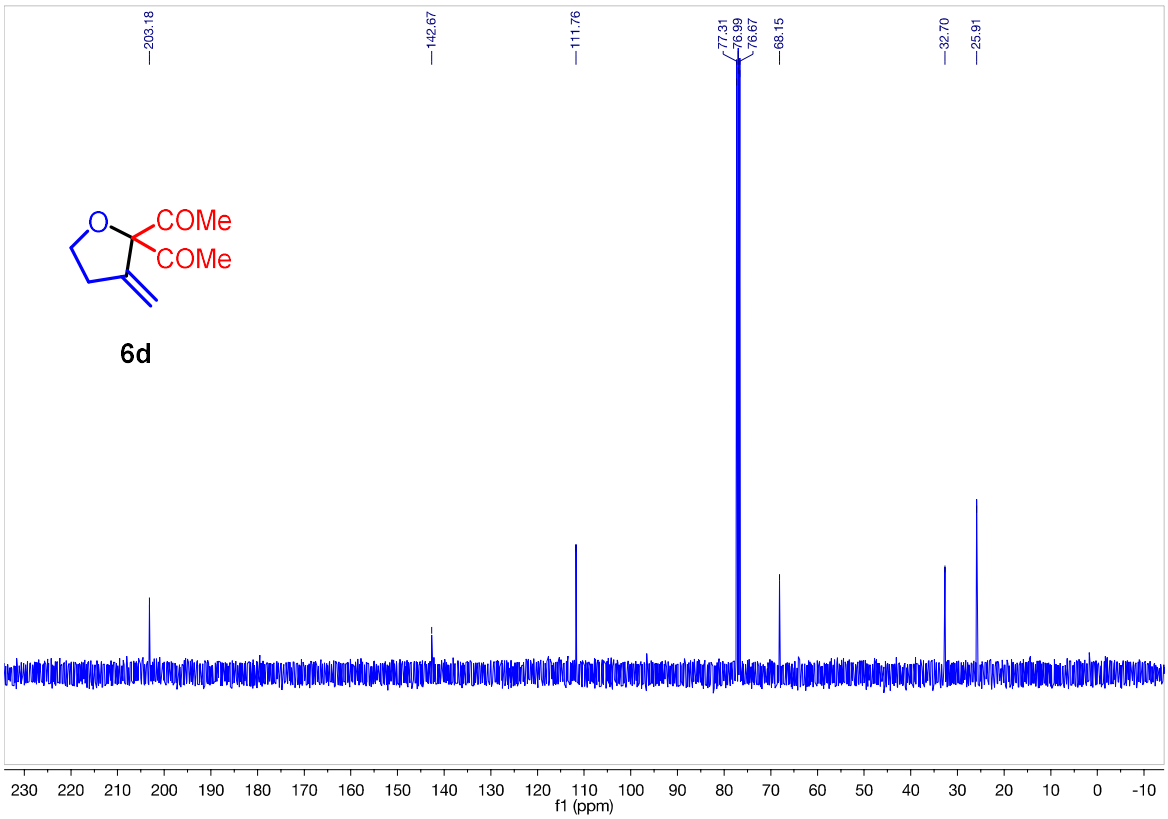
203.18
142.67
111.76
77.31
76.99
76.67
68.15
32.70
25.91
COMe
COMe
6d
f1 (ppm)

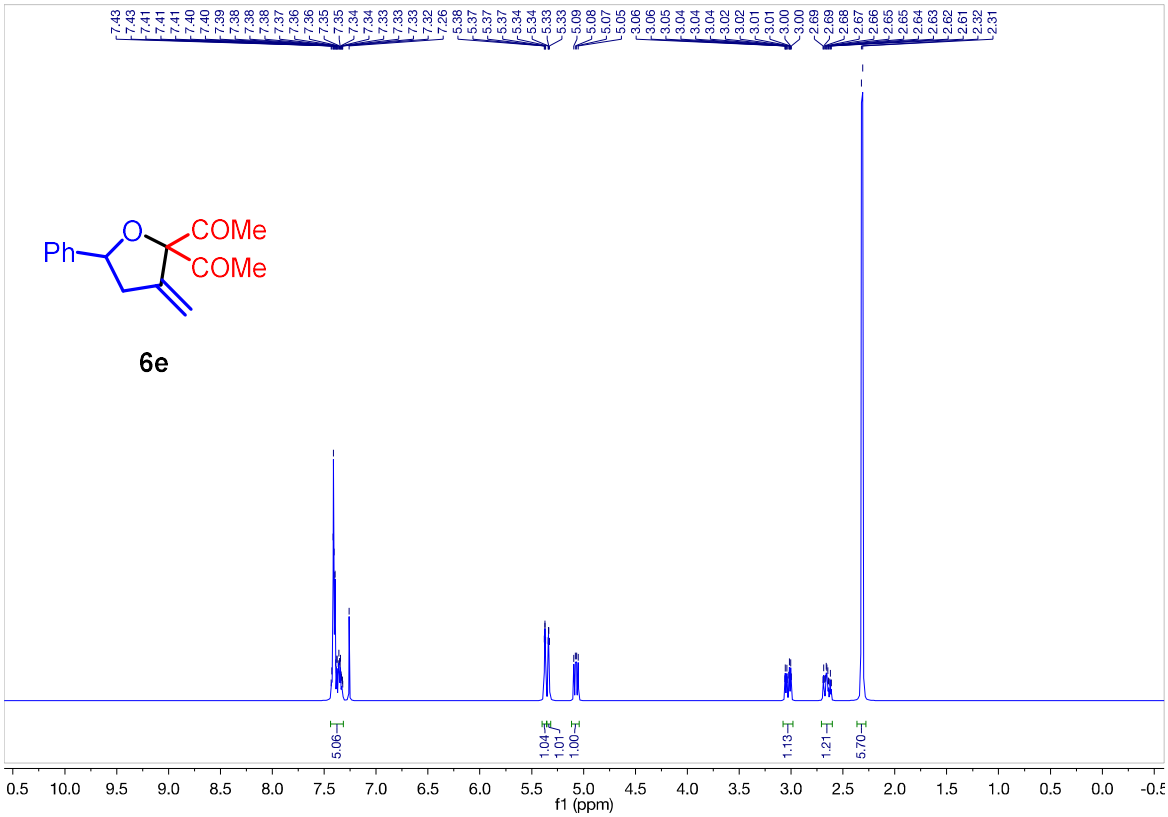
Ph
O
COMe
COMe
6e
f1 (ppm)

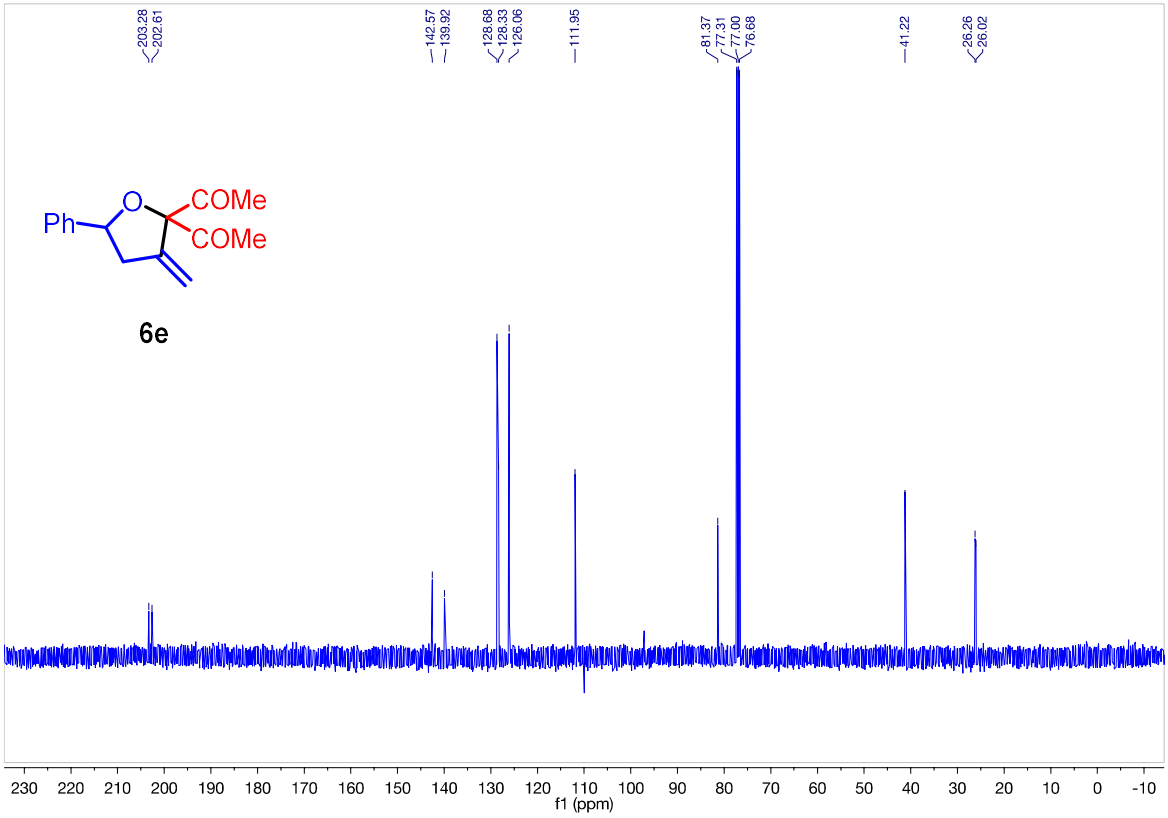
Ph
O
COMe
COMe
6e
f1 (ppm)

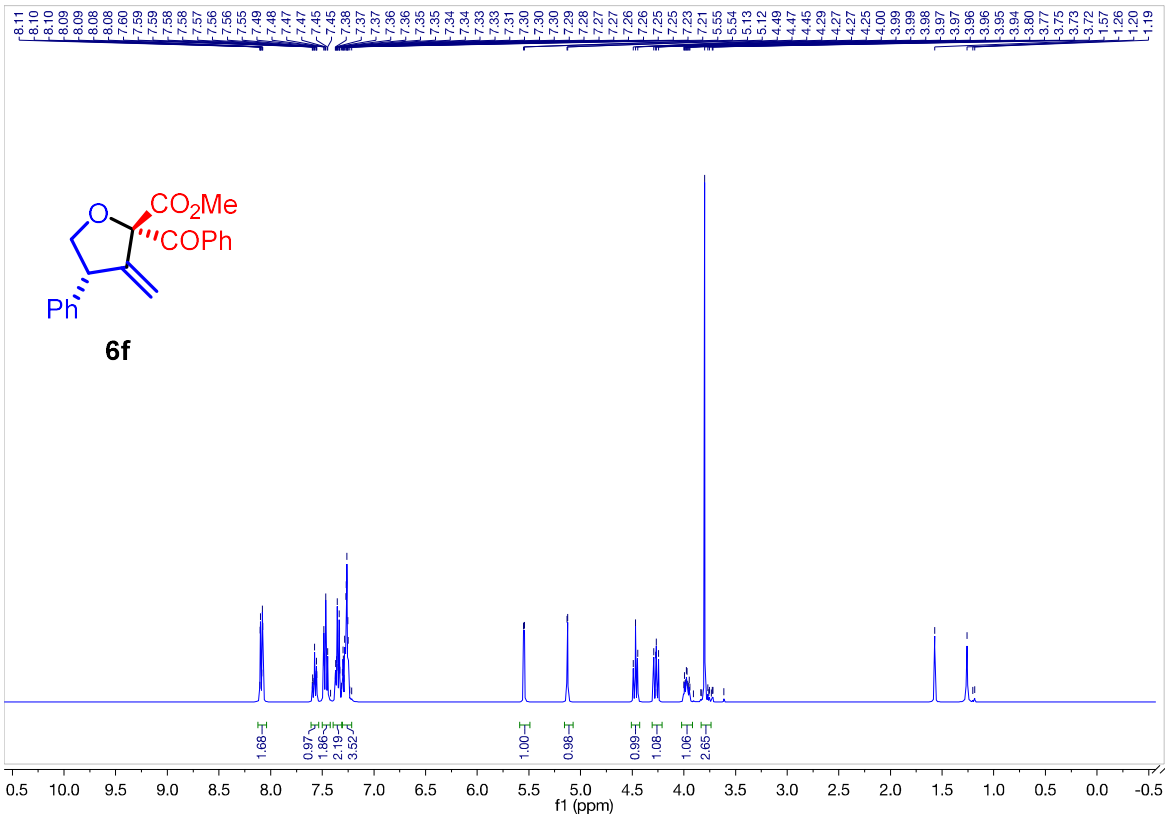
CO2Me
COPh
Ph
6f
f1 (ppm)

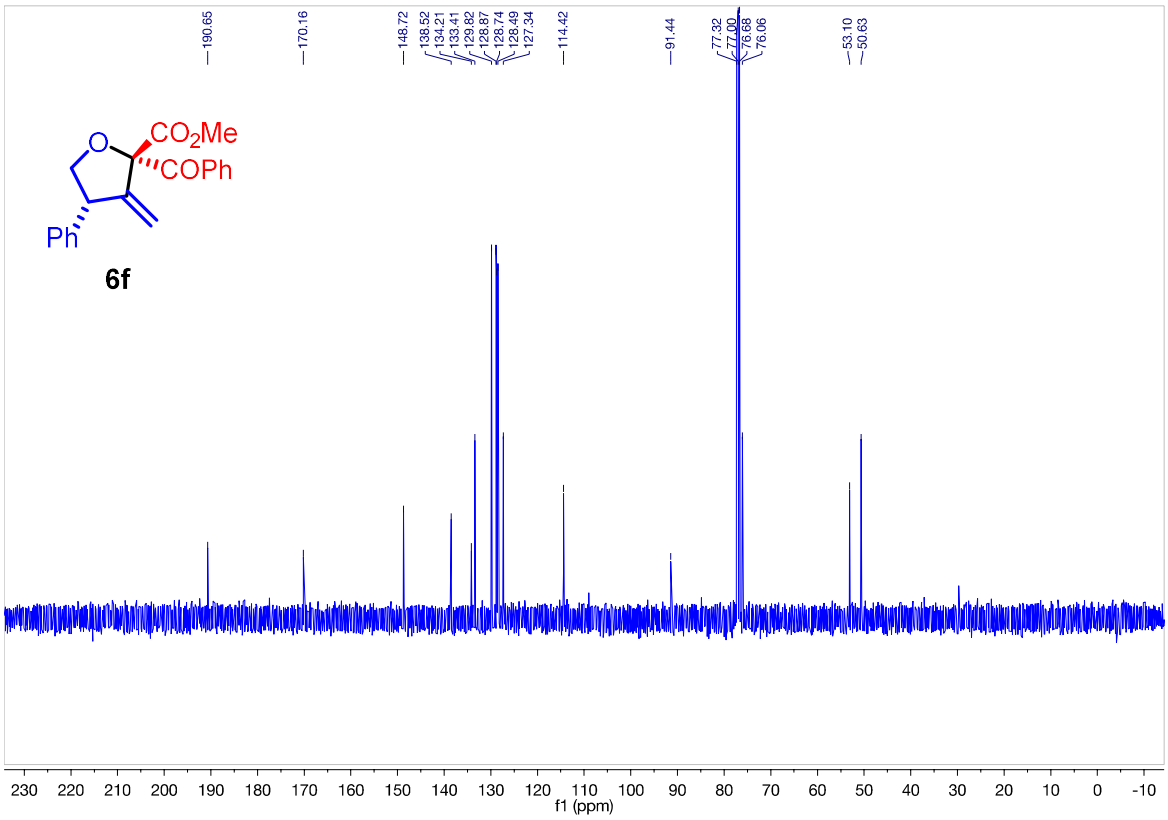
CO2Me
COPh
Ph
6f
f1 (ppm)

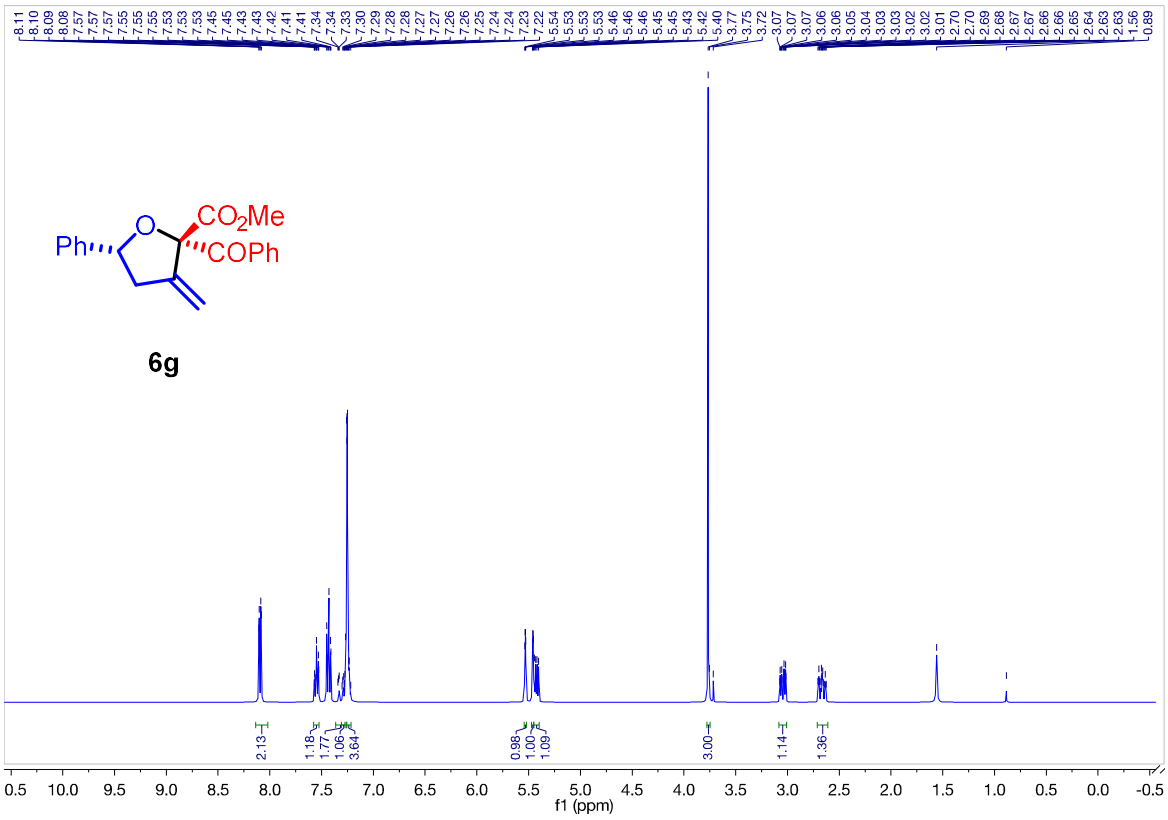
Ph
O
CO2Me
COPh
6g
f1 (ppm)

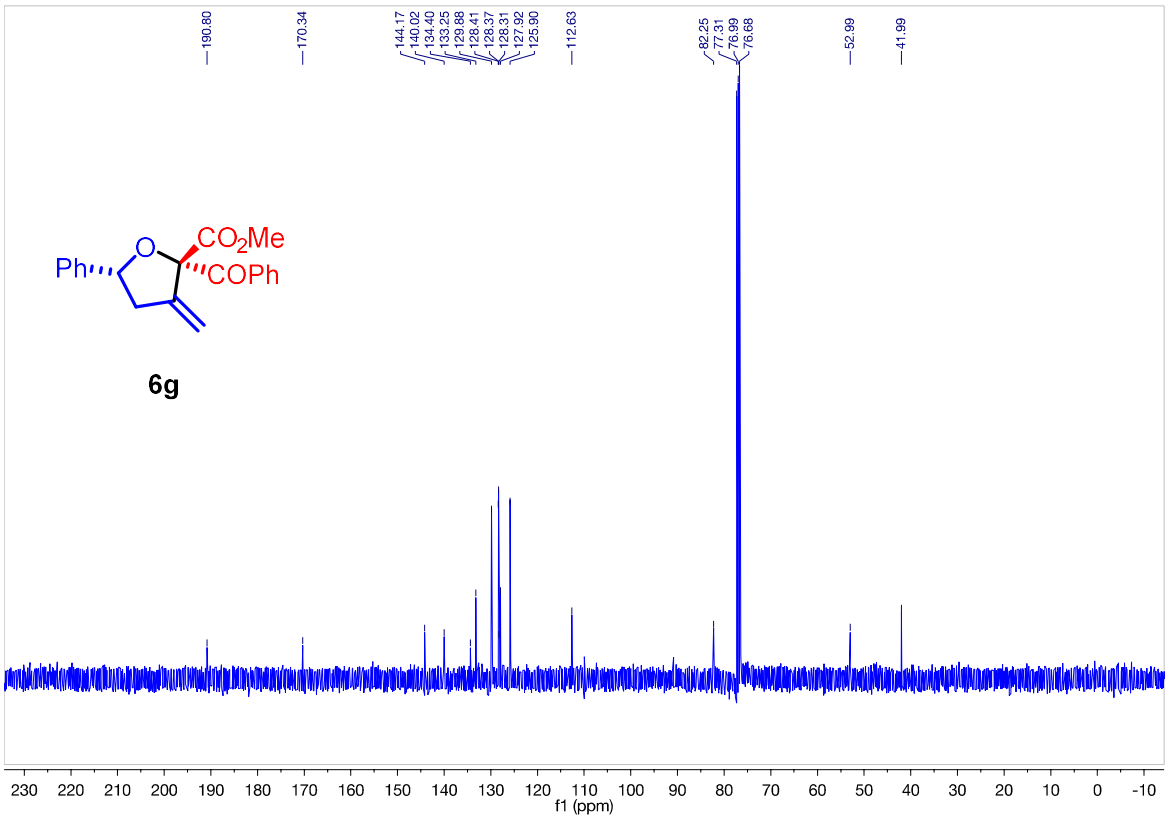
Ph
O
CO2Me
COPh
6g
f1 (ppm)

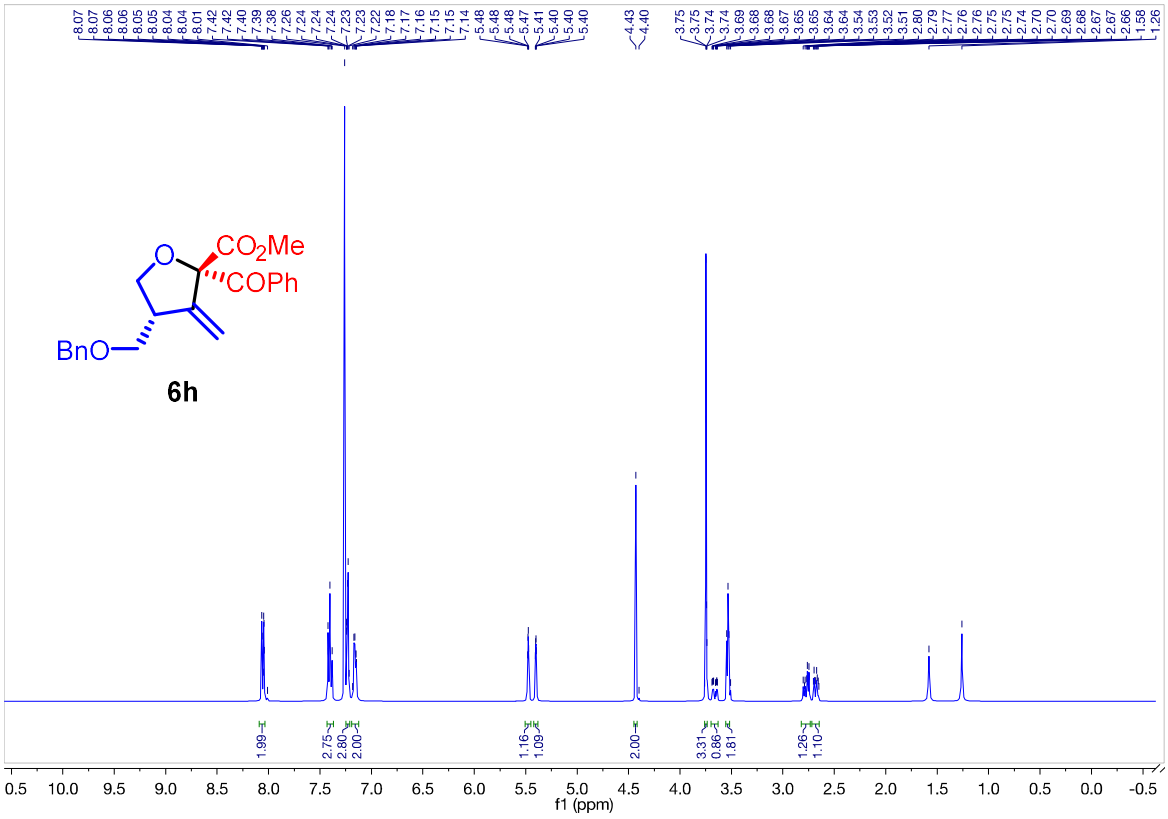
CO2Me
COPh
BnO
6h
f1 (ppm)

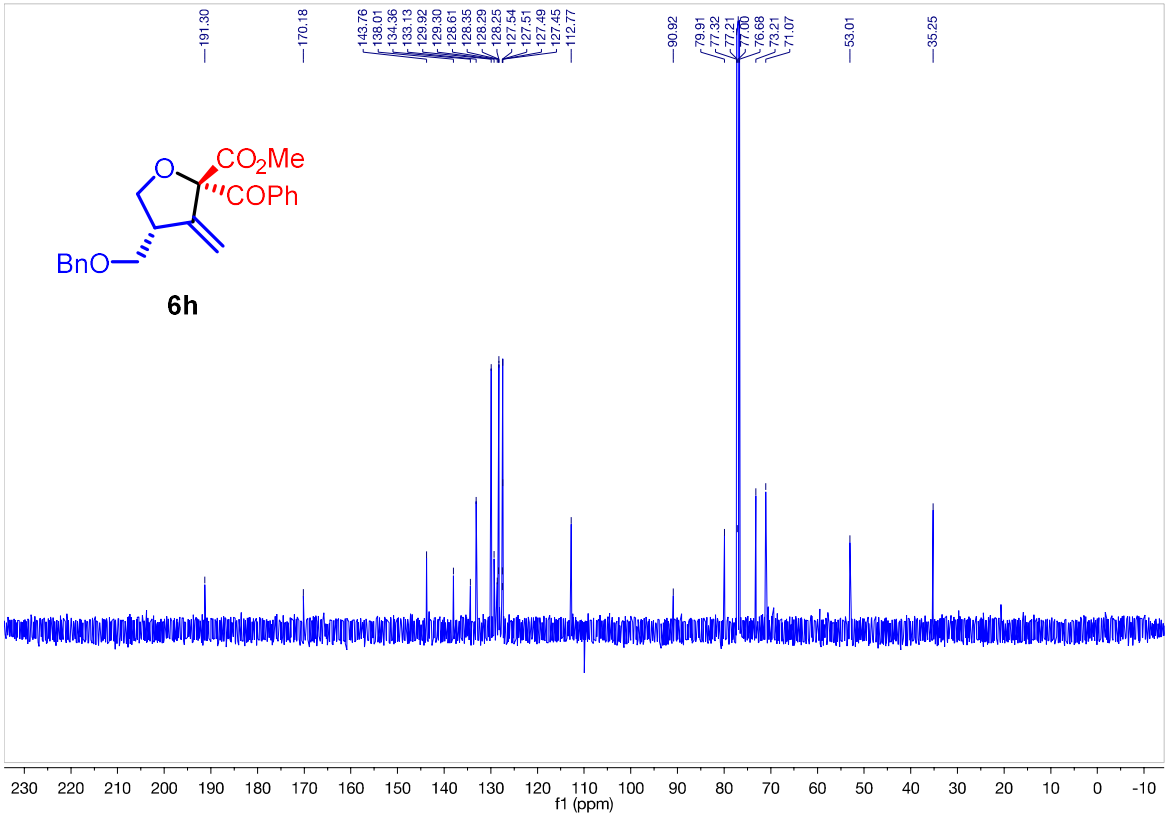
CO2Me
COPh
BnO
6h
f1 (ppm)

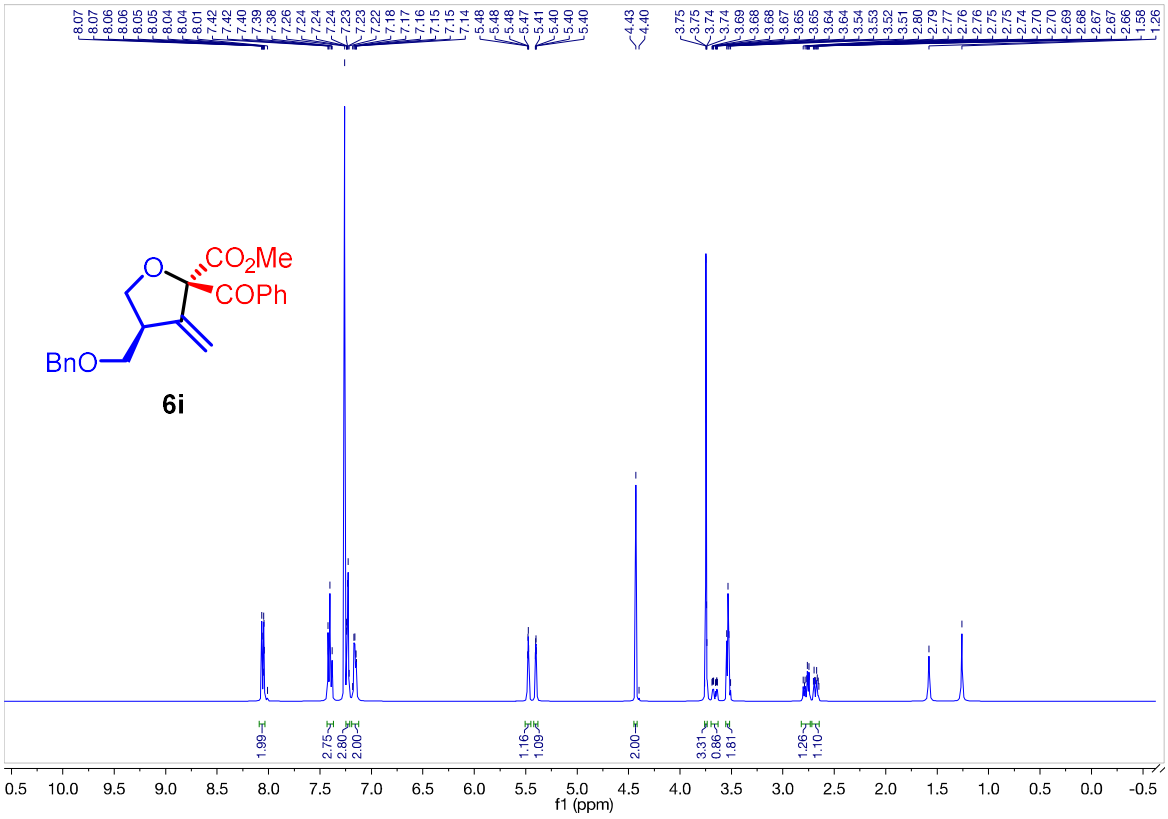
CO2Me
COPh
BnO
6i
f1 (ppm)

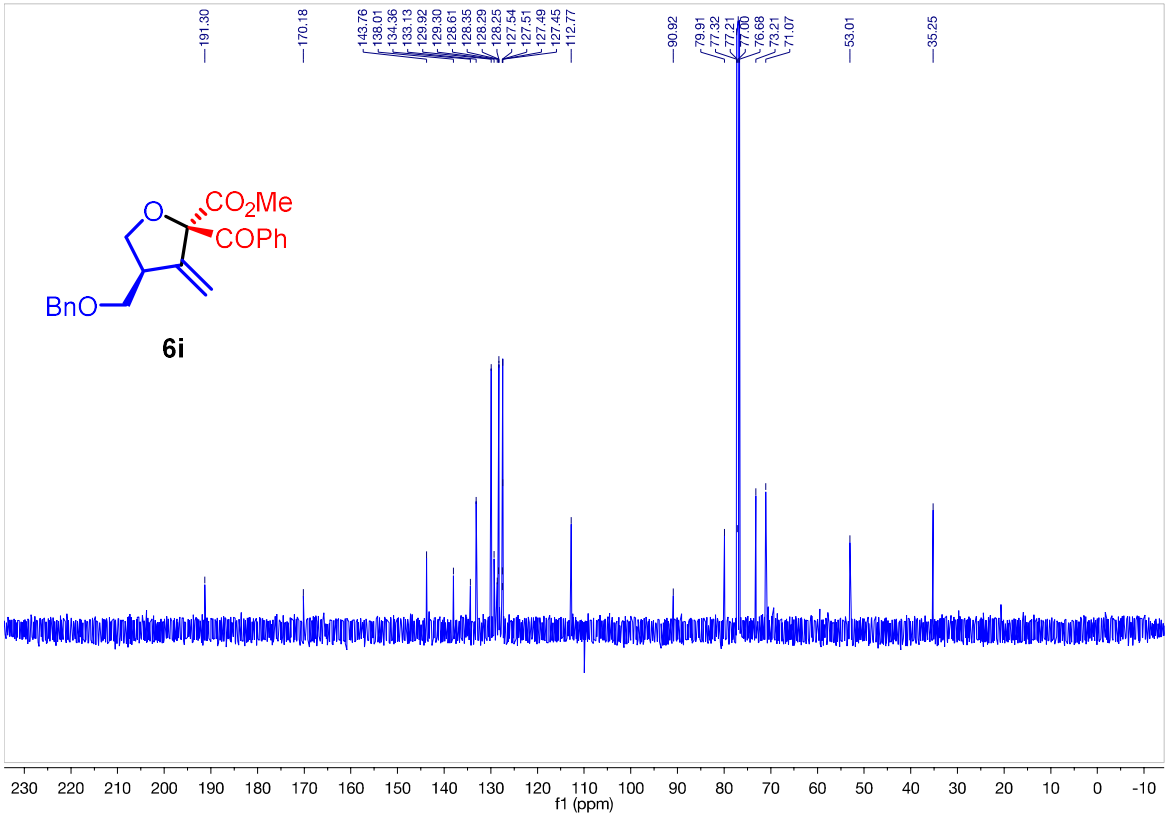
CO2Me
COPh
BnO
6i
f1 (ppm)

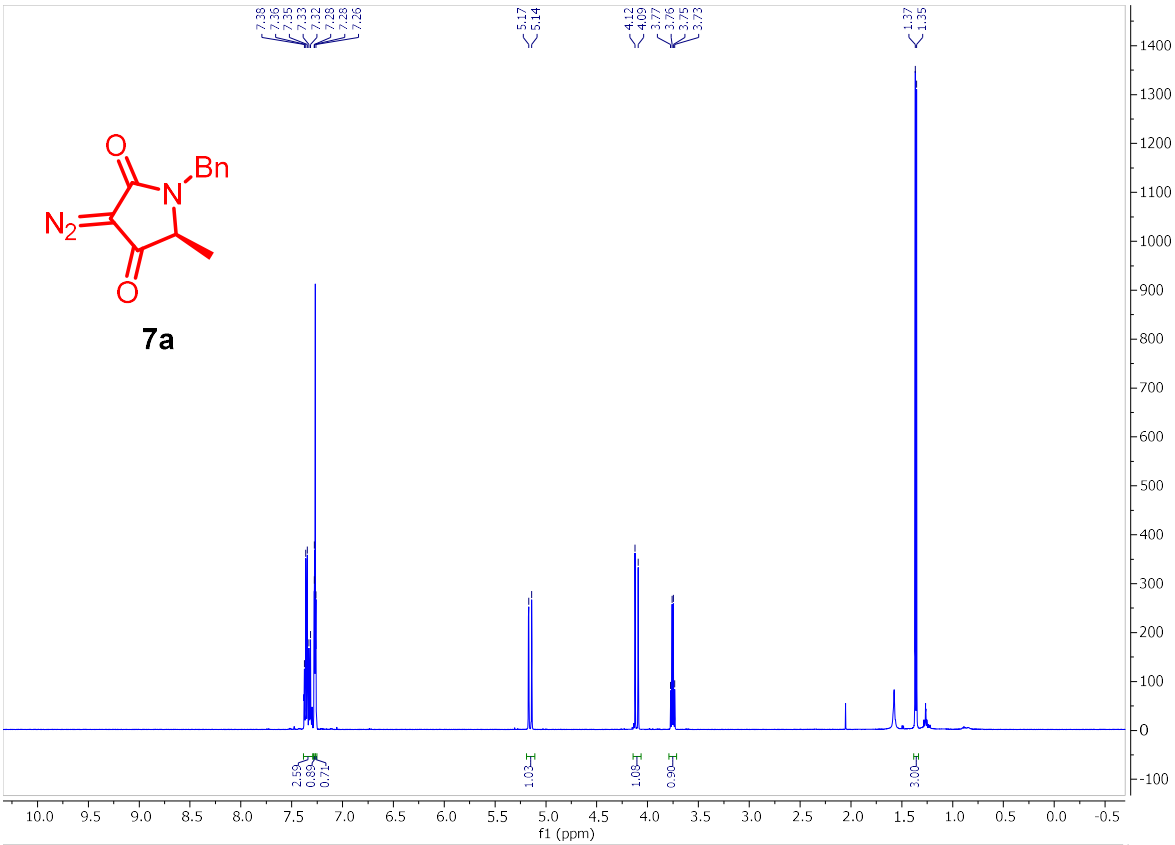
7a
f1 (ppm)

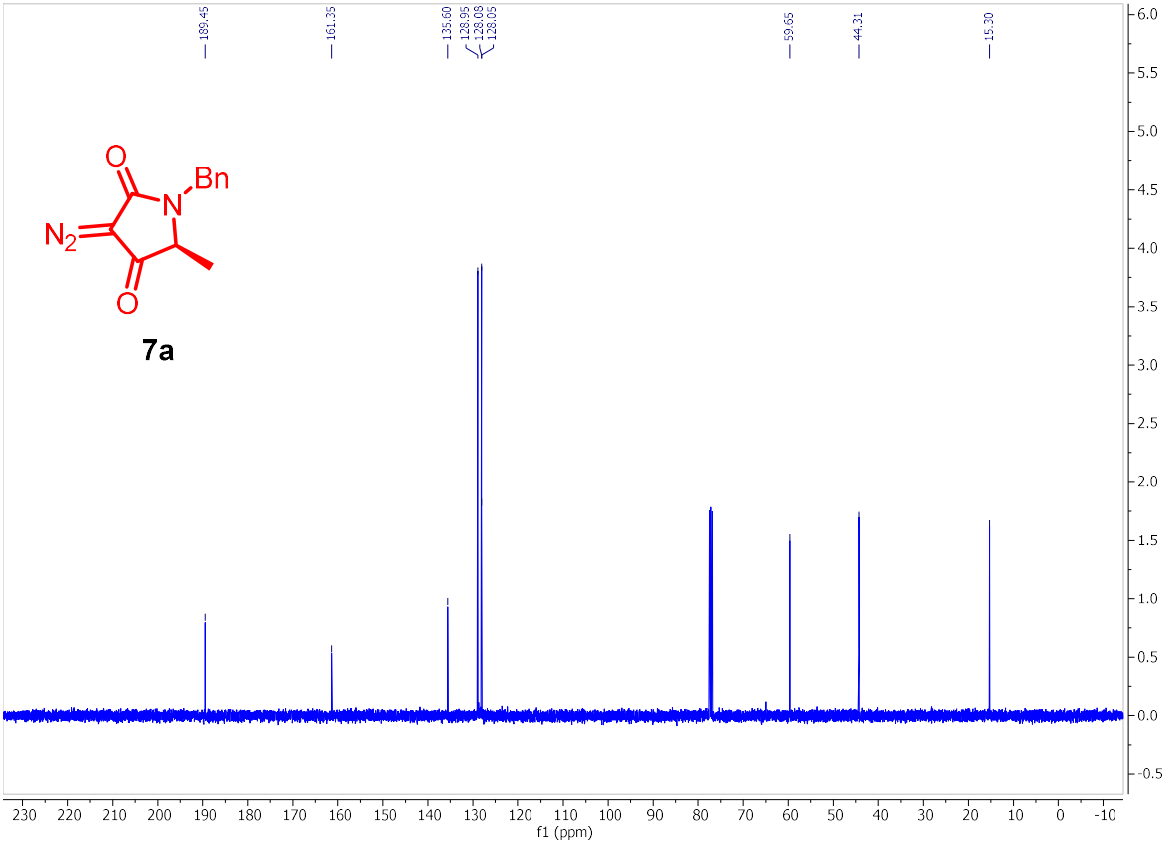
7a
f1 (ppm)

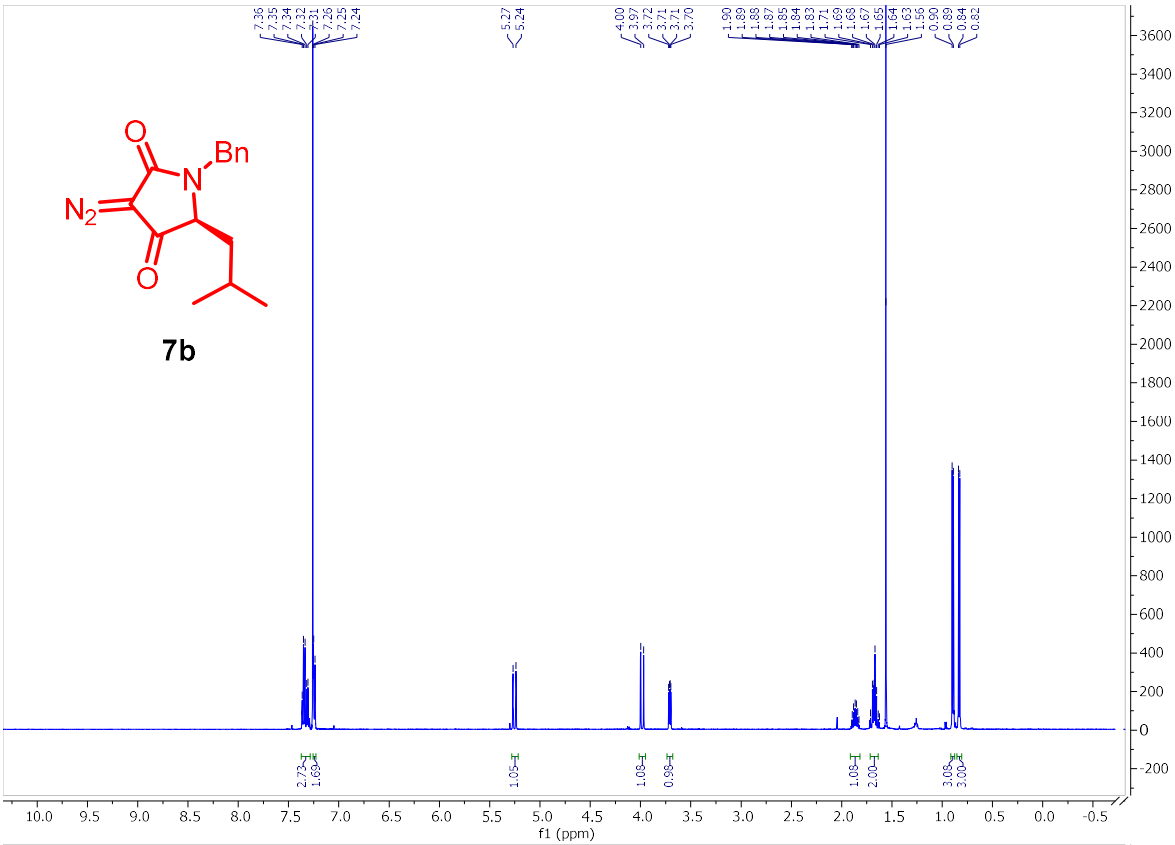
7.36
7.35
7.34
7.32
7.31
7.26
7.25
7.24
5.27
5.24
4.00
3.97
3.72
3.71
3.71
3.70
1.90
1.89
1.88
1.87
1.85
1.84
1.83
1.71
1.69
1.68
1.67
1.65
1.64
1.63
1.56
0.90
0.89
0.84
0.82
2.73
1.69
1.05
1.05
0.98
1.05
2.00
3.05
3.00
f1 (ppm)
Bn
N
O
O
N2
7b

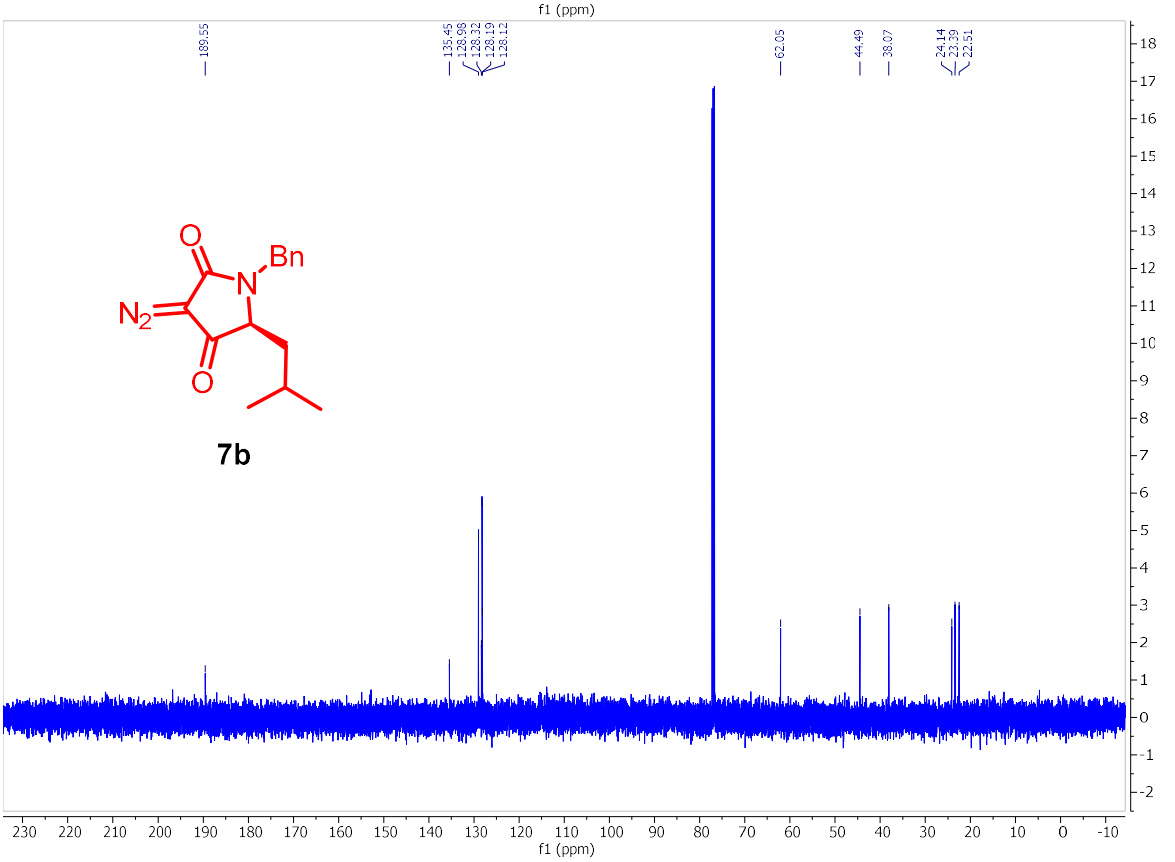
189.55
135.45
128.98
128.32
128.19
128.12
62.05
44.49
38.07
24.14
23.39
22.51
f1 (ppm)
Bn
N
O
O
N2
7b

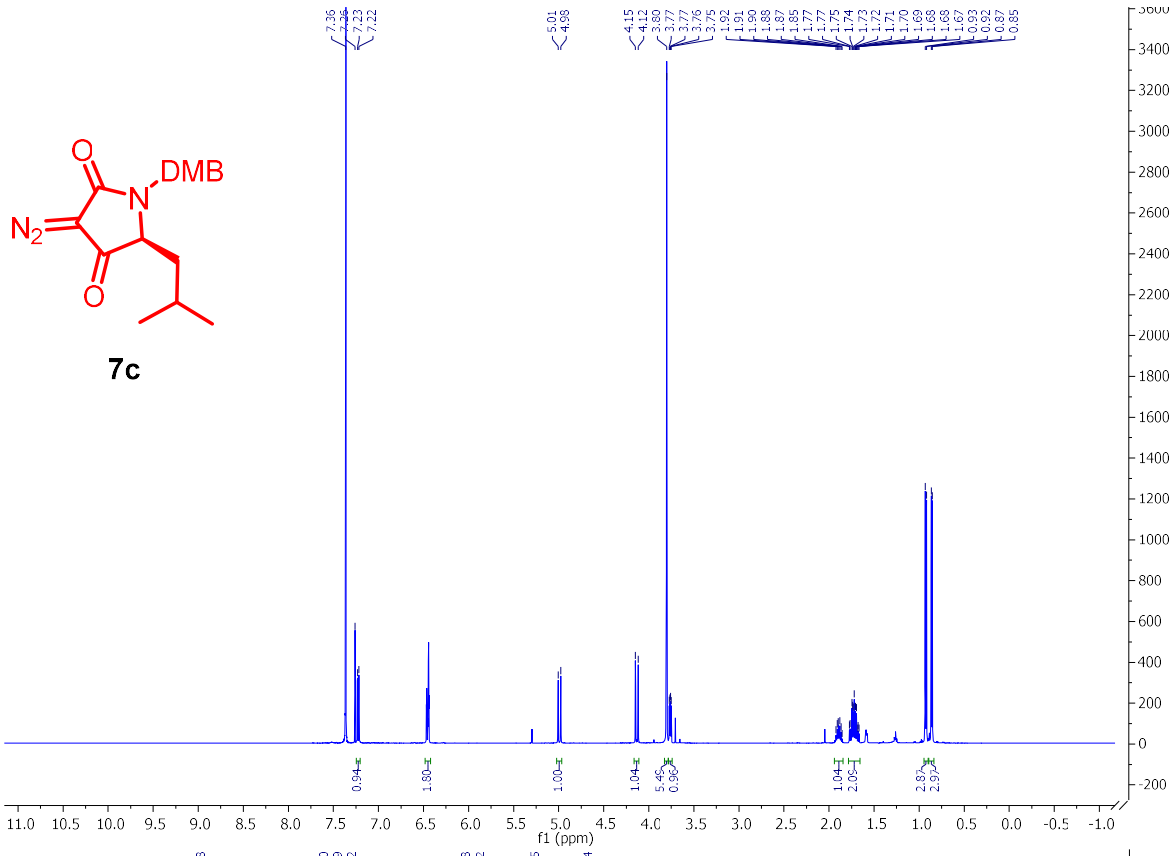
DMB
N2
O
O
N
7c
f1 (ppm)

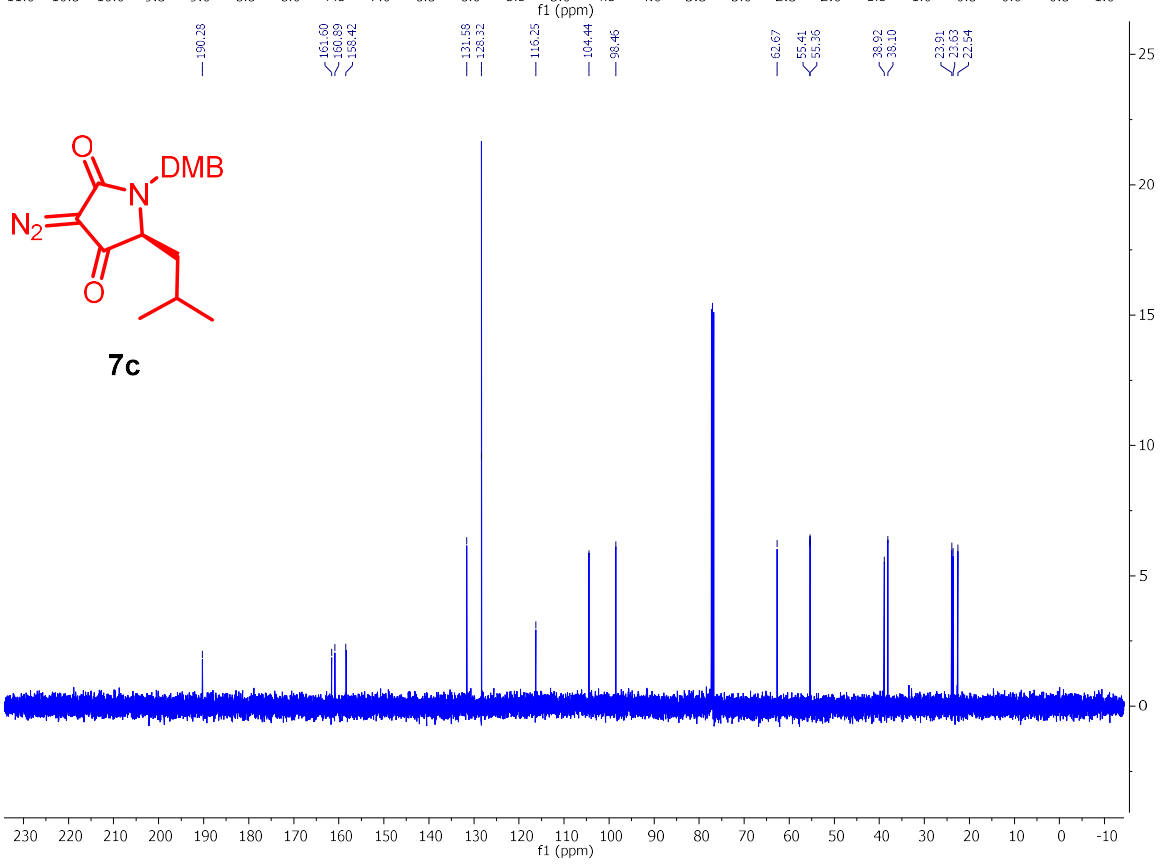
DMB
N2
O
O
N
7c
f1 (ppm)

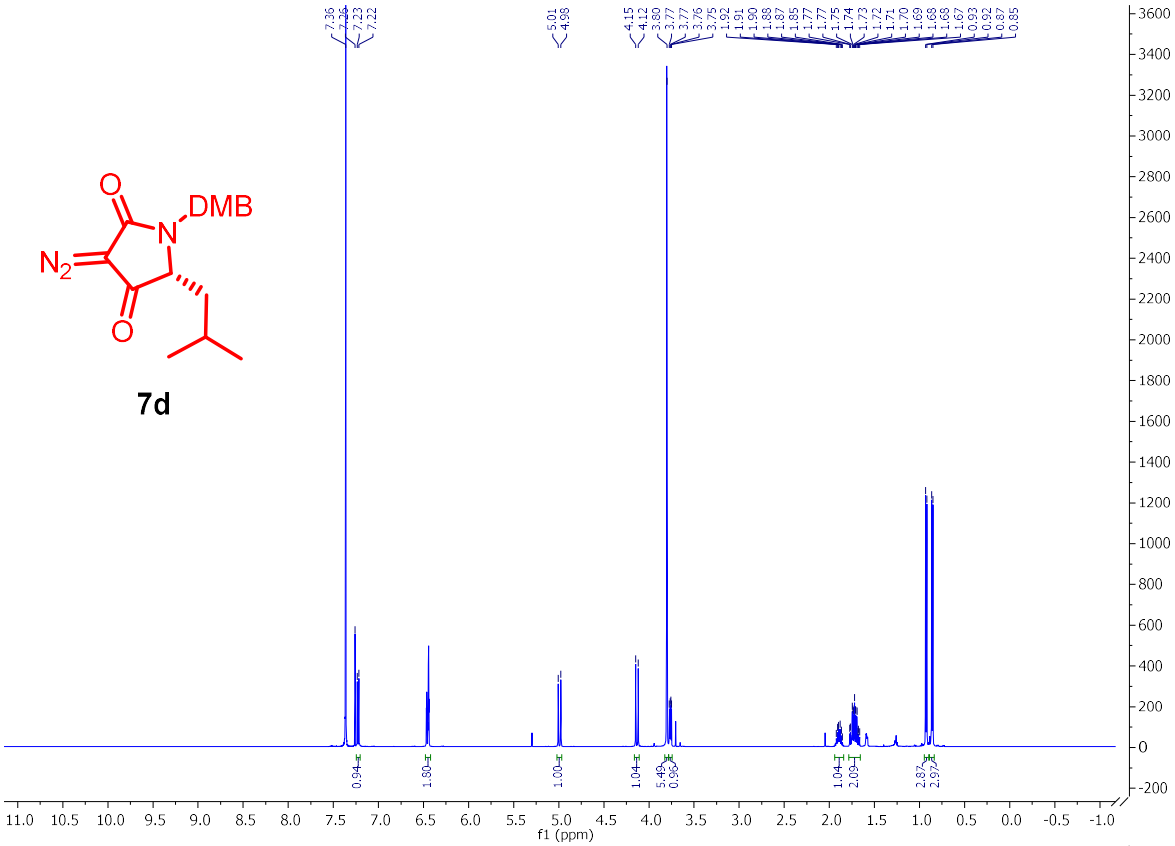
DMB
N2
O
N
O
7d
f1 (ppm)

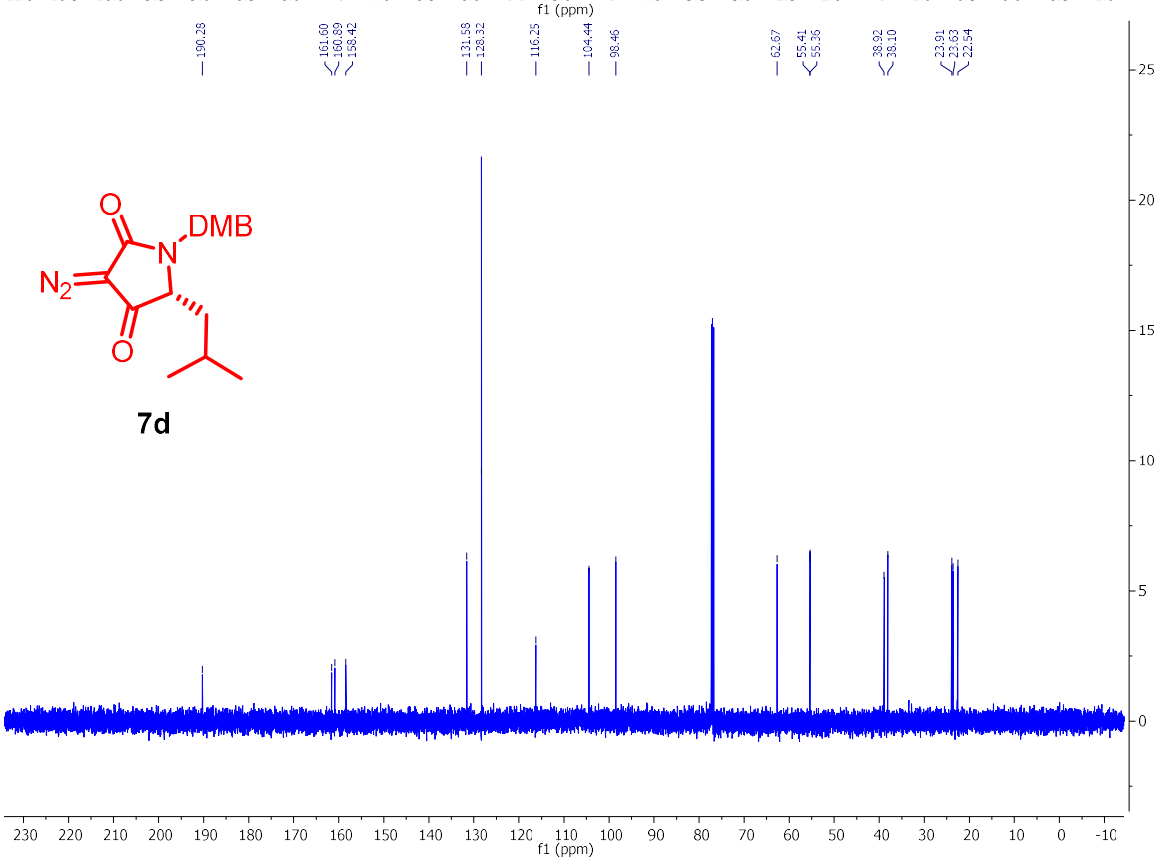
DMB
N2
O
N
O
7d
f1 (ppm)

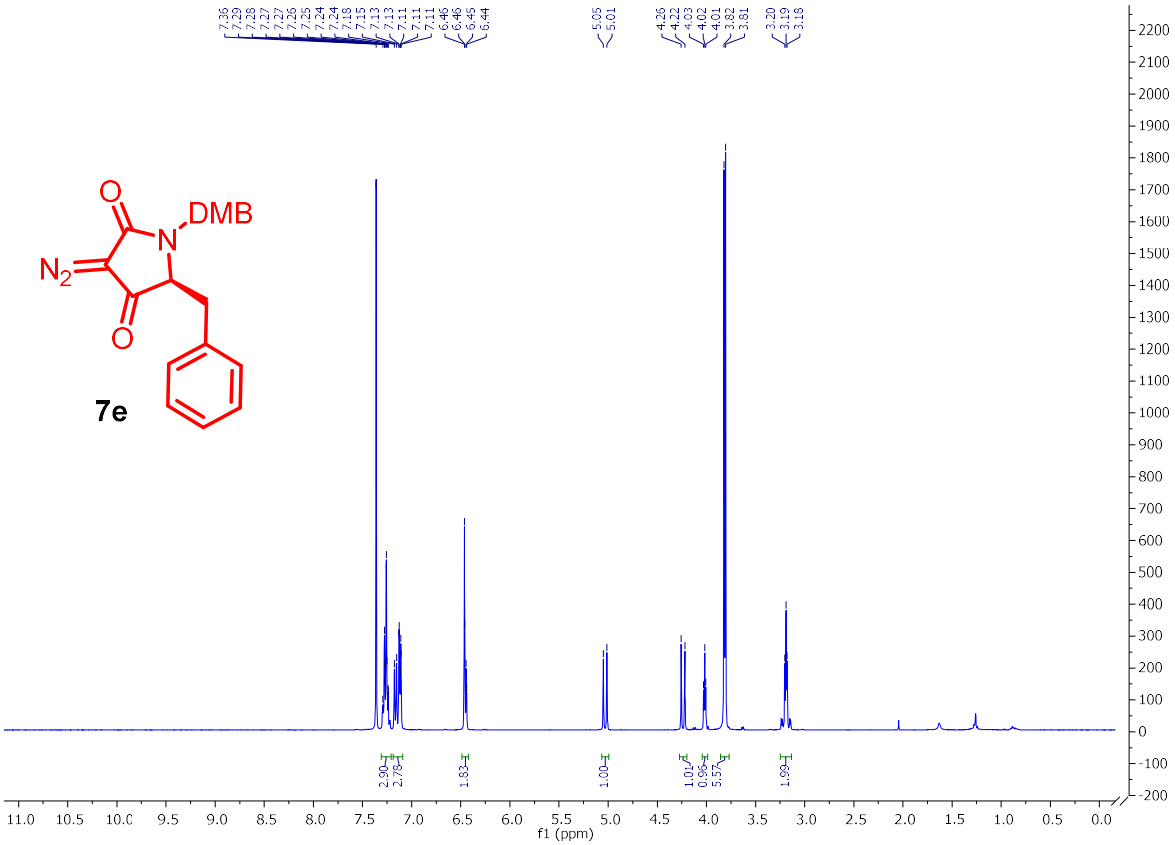
7.36
7.29
7.28
7.27
7.27
7.25
7.25
7.24
7.24
7.15
7.15
7.13
7.13
7.11
7.11
7.11
6.46
6.46
6.45
6.44
5.05
5.01
4.26
4.22
4.03
4.02
4.01
3.82
3.81
3.20
3.19
3.18
DMB
N2
O
N
O
7e
2.90
2.78
1.83
1.00
1.01
0.96
5.57
1.99
f1 (ppm)

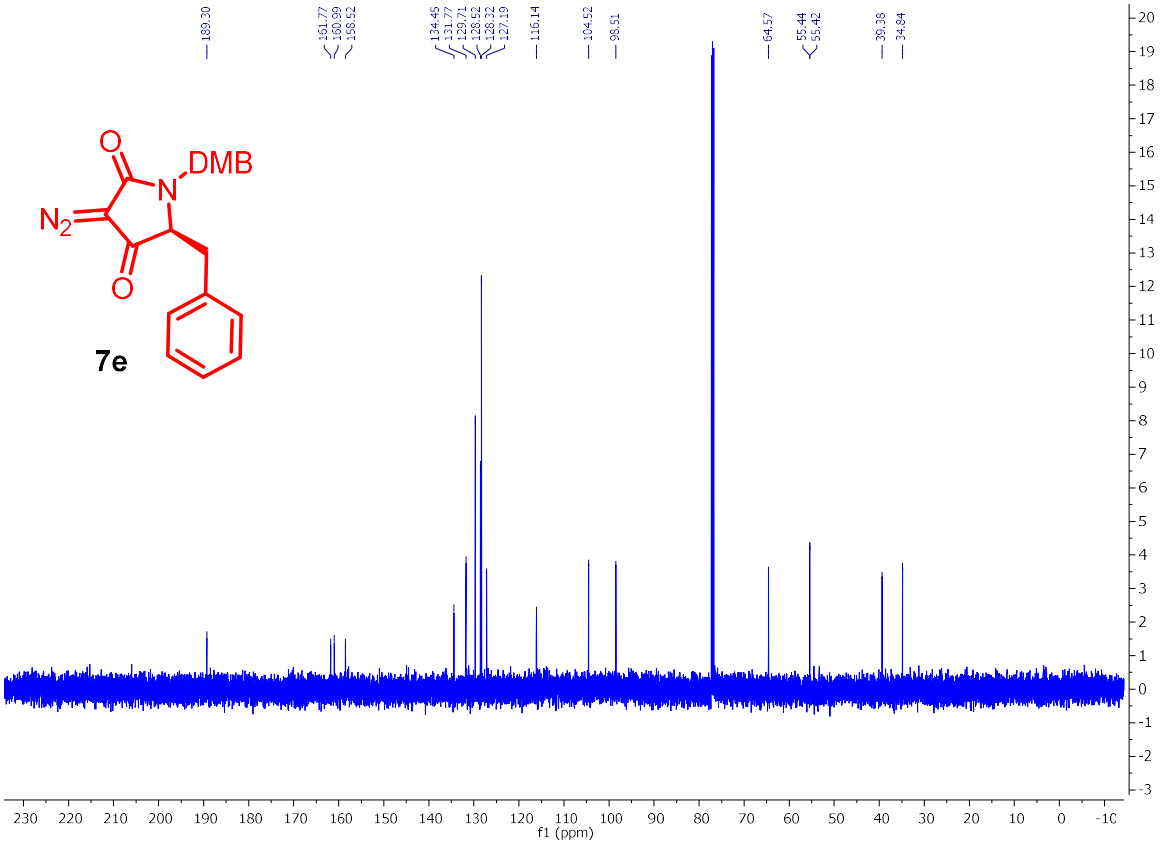
189.30
161.77
160.99
158.52
134.45
131.77
129.71
128.52
128.32
127.19
116.14
104.52
98.51
64.57
55.44
55.42
39.38
34.84
DMB
N2
O
N
O
7e
f1 (ppm)

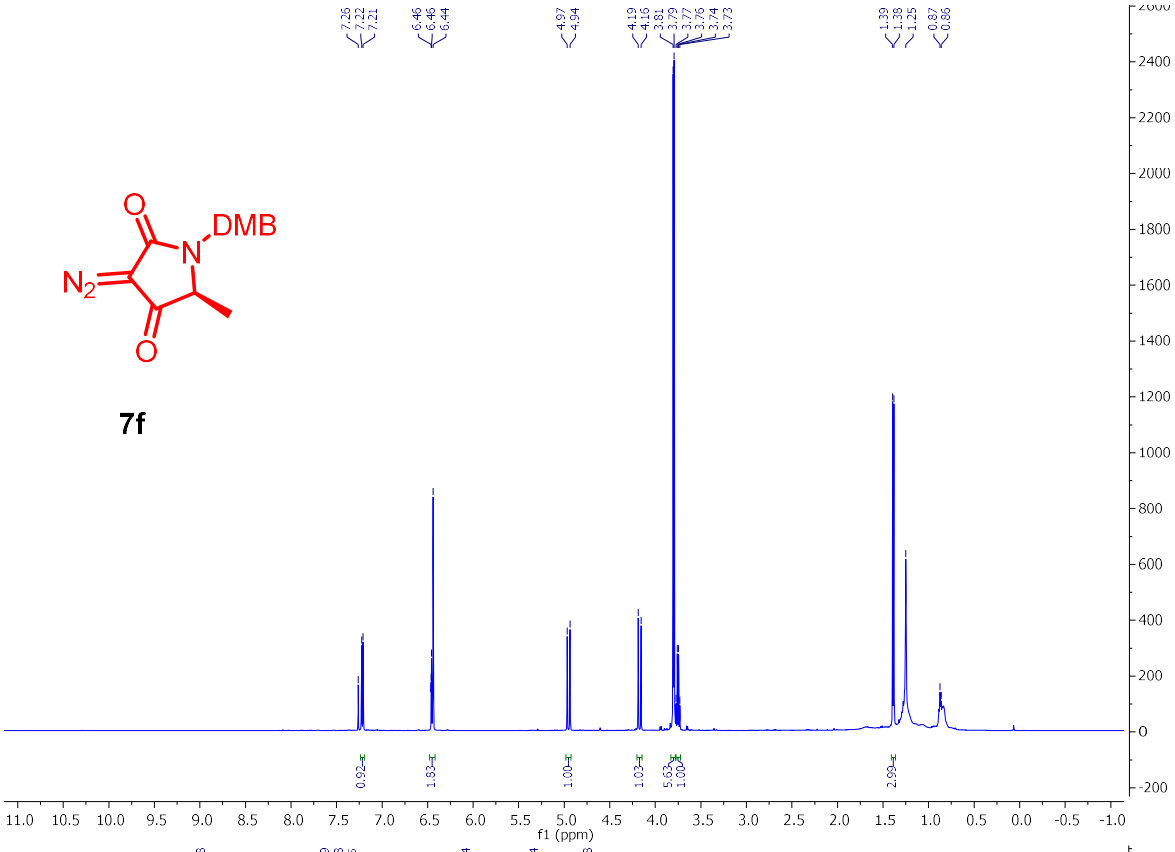
7.26
7.22
7.21
6.46
6.45
6.44
4.97
4.94
4.19
4.16
3.81
3.79
3.77
3.76
3.74
3.73
1.39
1.38
1.25
0.87
0.86
0.92
1.83
1.00
1.03
5.63
1.00
2.99
f1 (ppm)

O
DMB
N
N2
O

7f

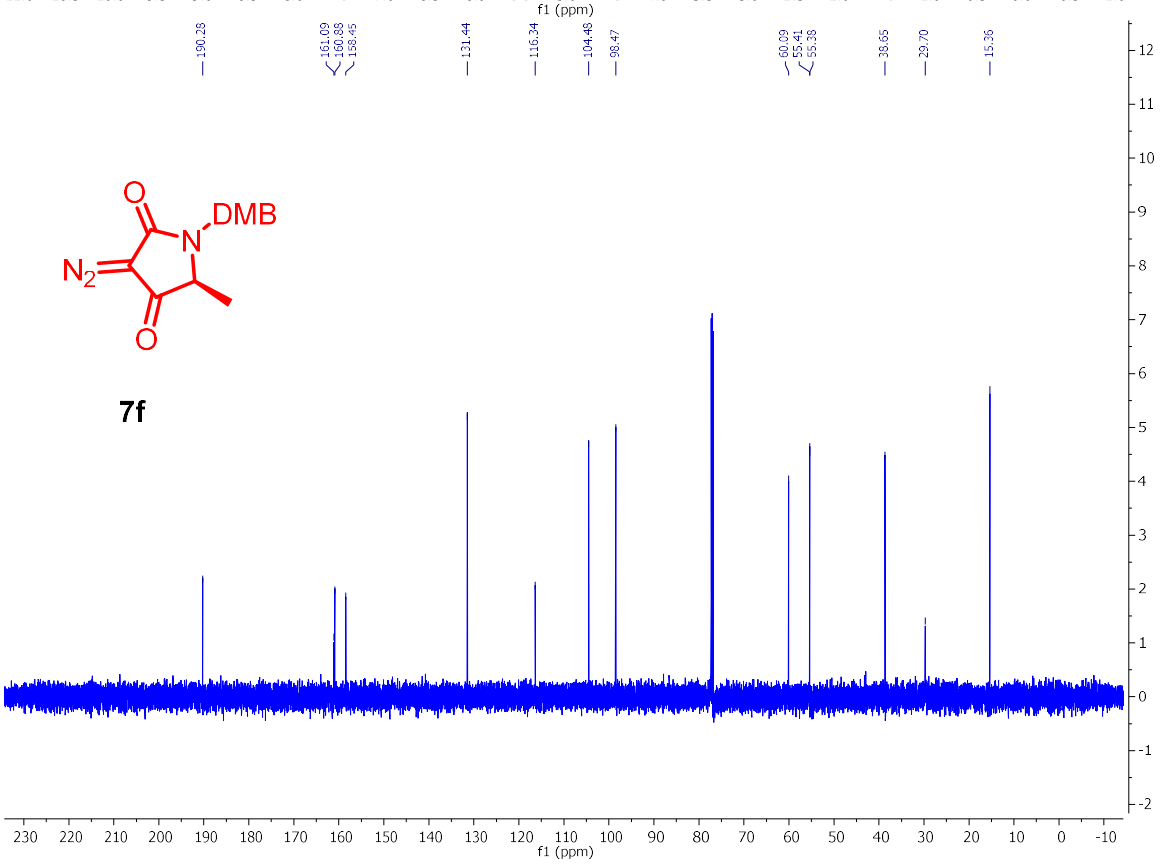
190.28
161.09
160.88
158.45
131.44
116.34
104.48
98.47
60.09
55.41
55.38
38.65
29.70
15.36
f1 (ppm)

O
DMB
N
N2
O

7f

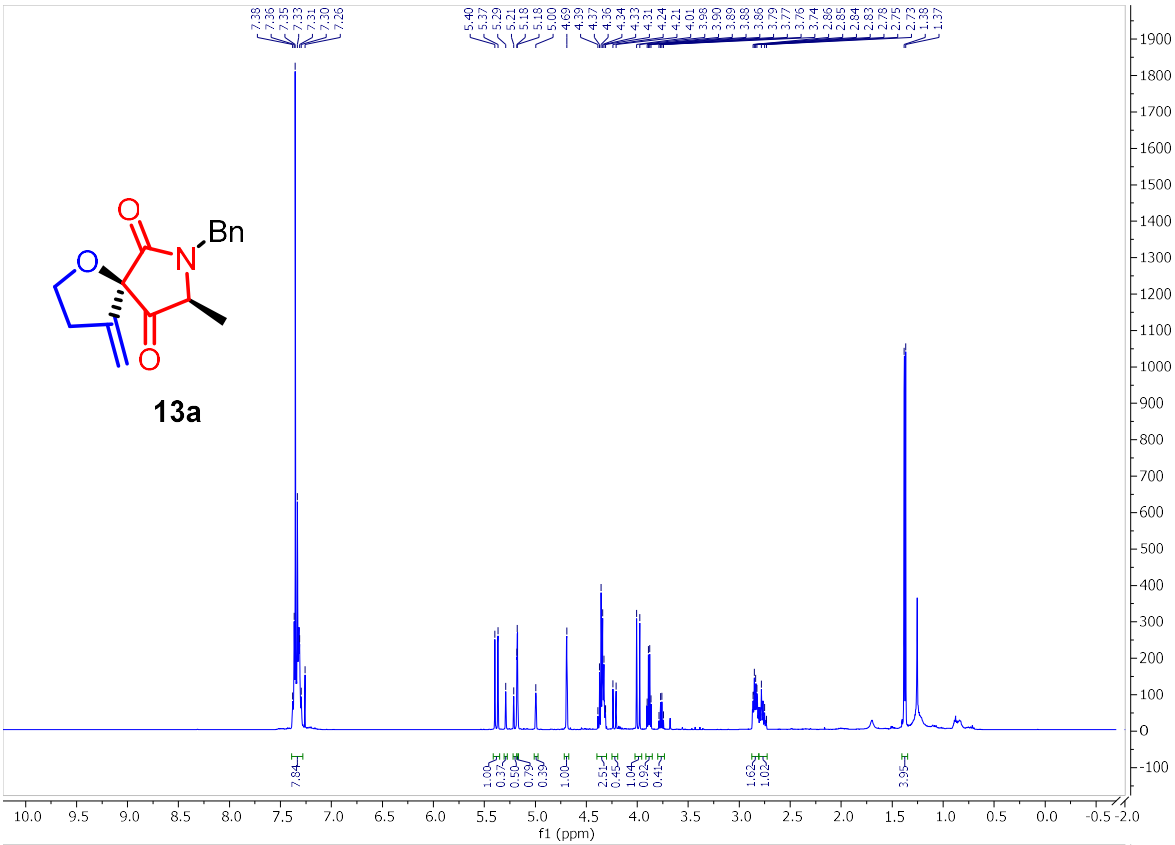
Bn
13a
f1 (ppm)

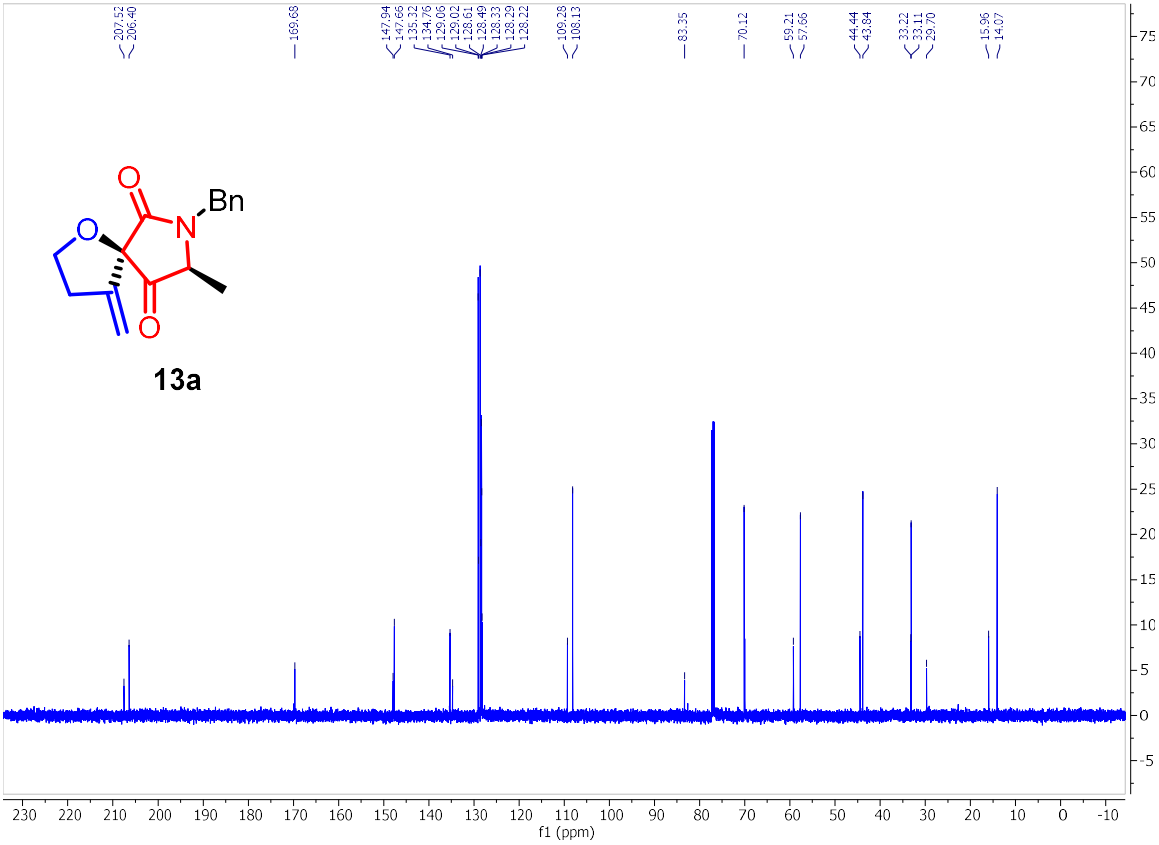
Bn
13a
f1 (ppm)

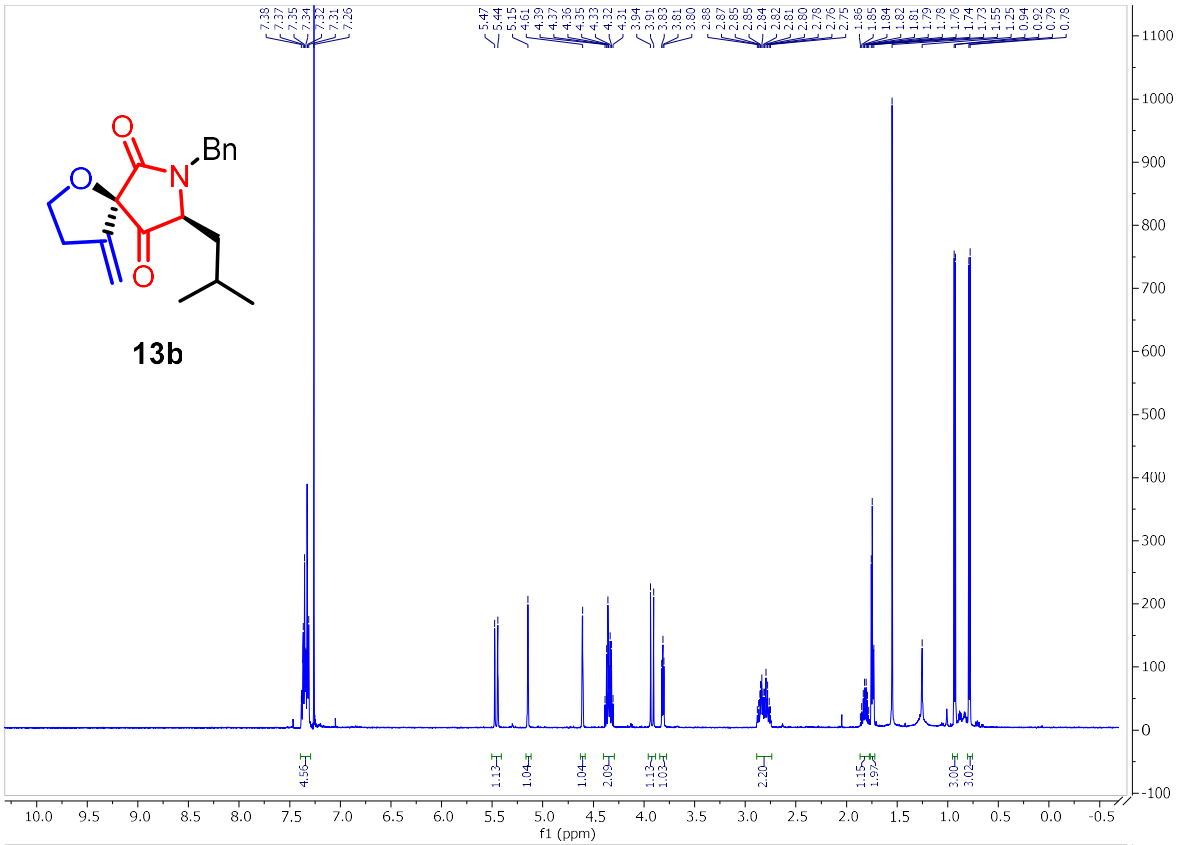
Bn
13b
f1 (ppm)

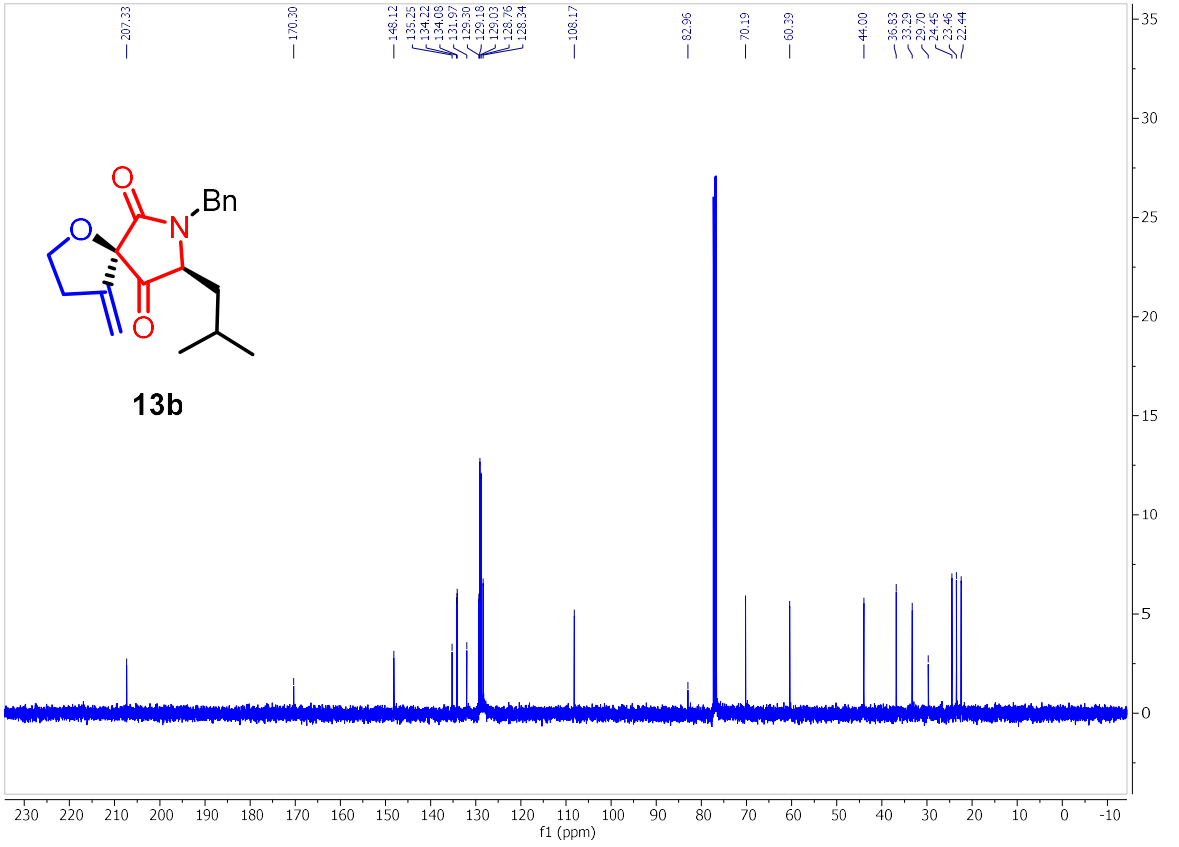
Bn
13b
f1 (ppm)

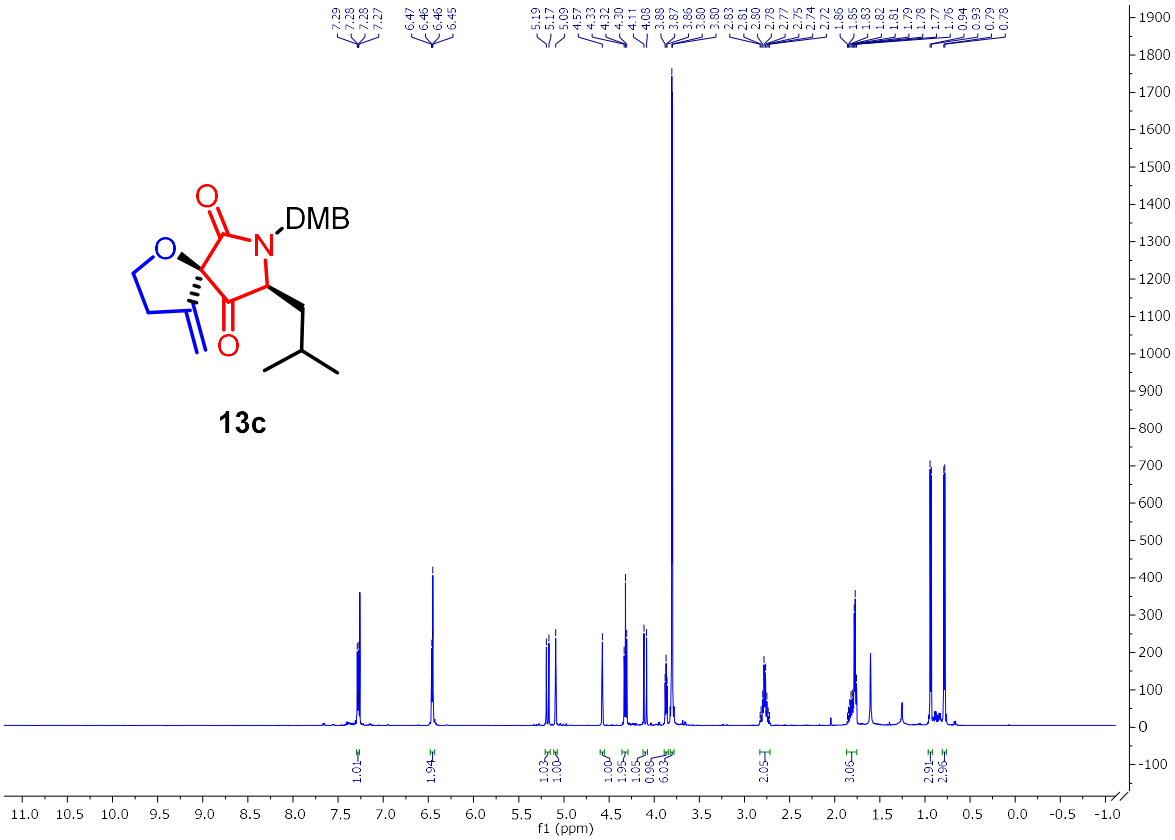
DMB
13c
f1 (ppm)

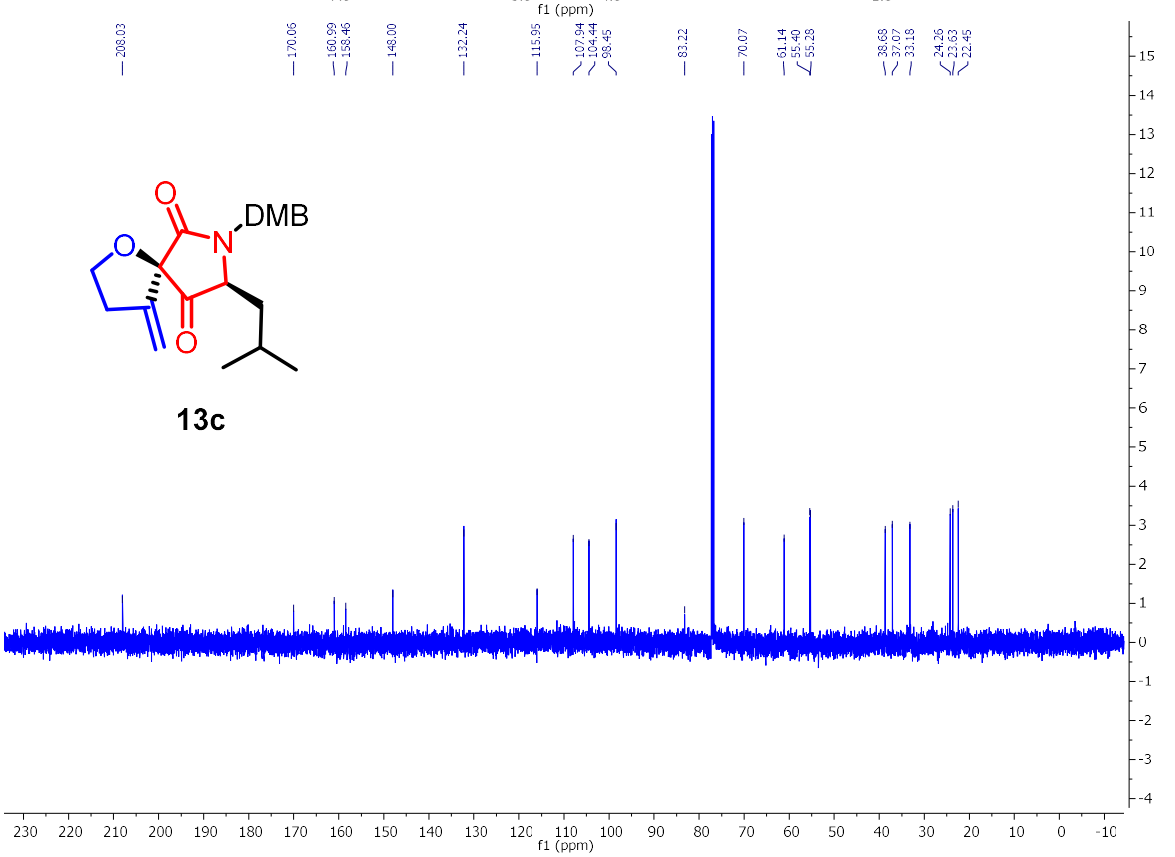
DMB
13c
f1 (ppm)

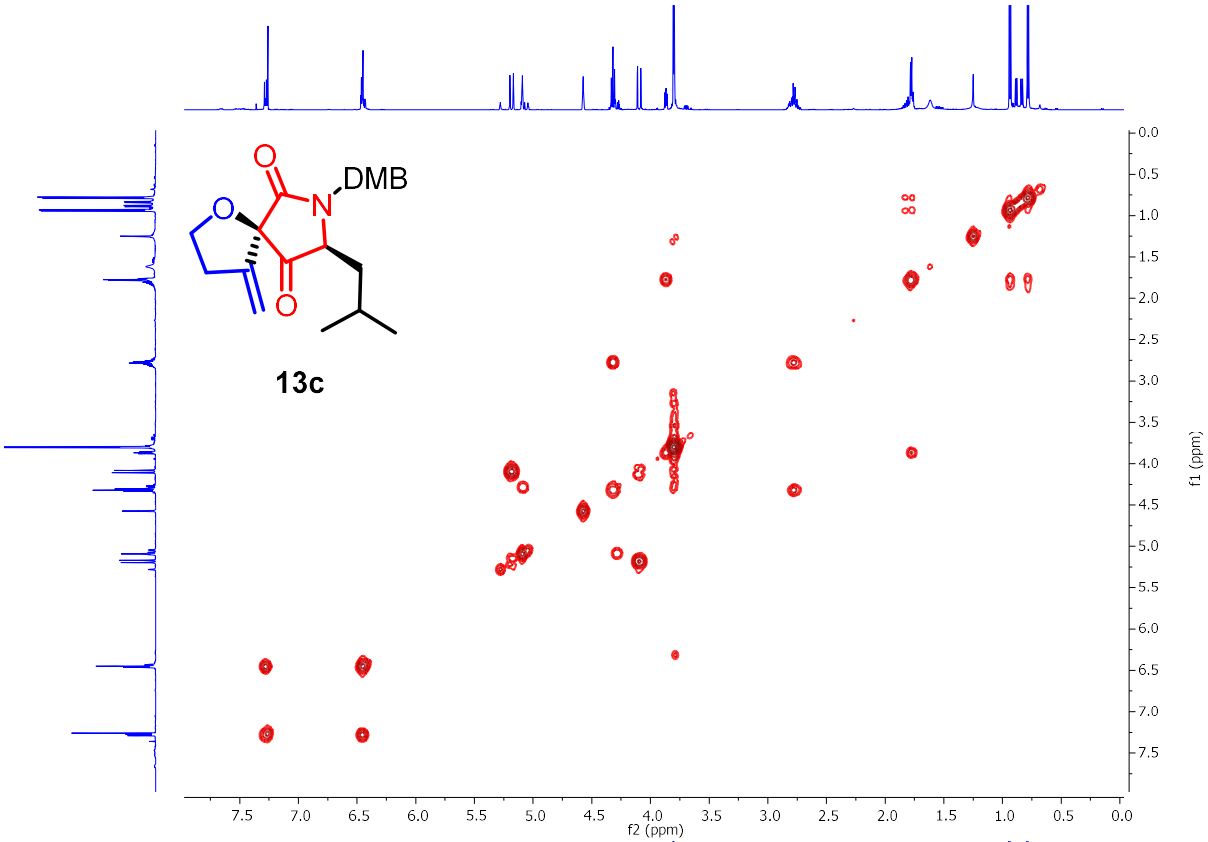
DMB
13c
f2 (ppm)
f1 (ppm)

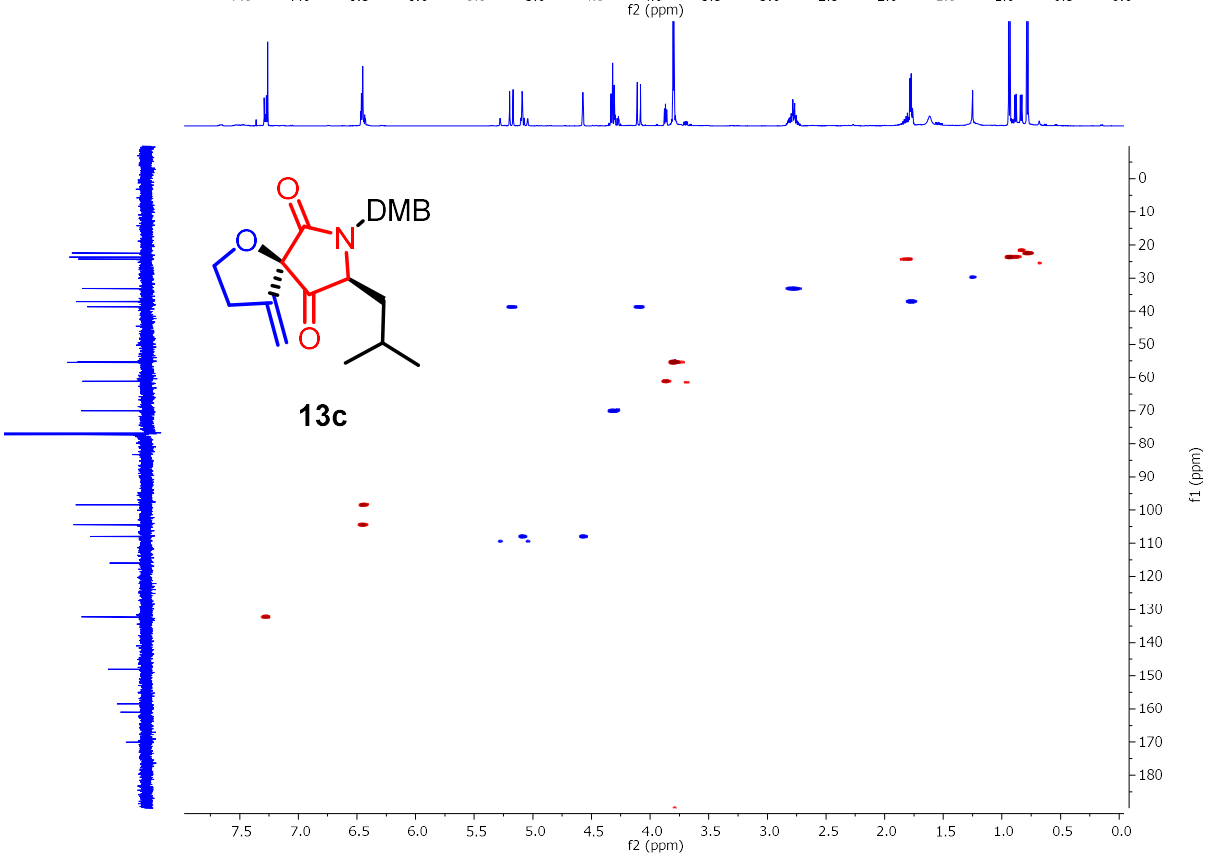
DMB
13c
f2 (ppm)
f1 (ppm)

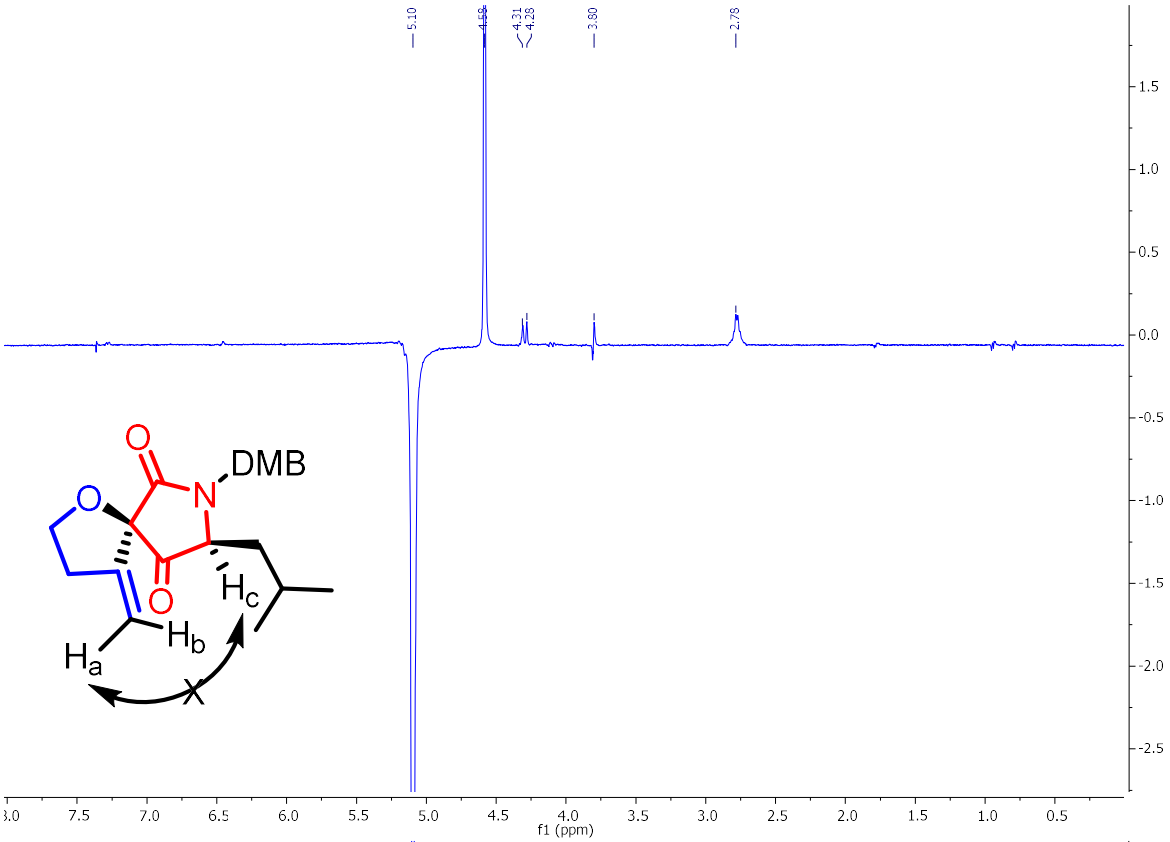
5.10
4.58
4.31
4.28
3.80
2.78
DMB
O
N
O
O
Hc
Hb
Ha
f1 (ppm)

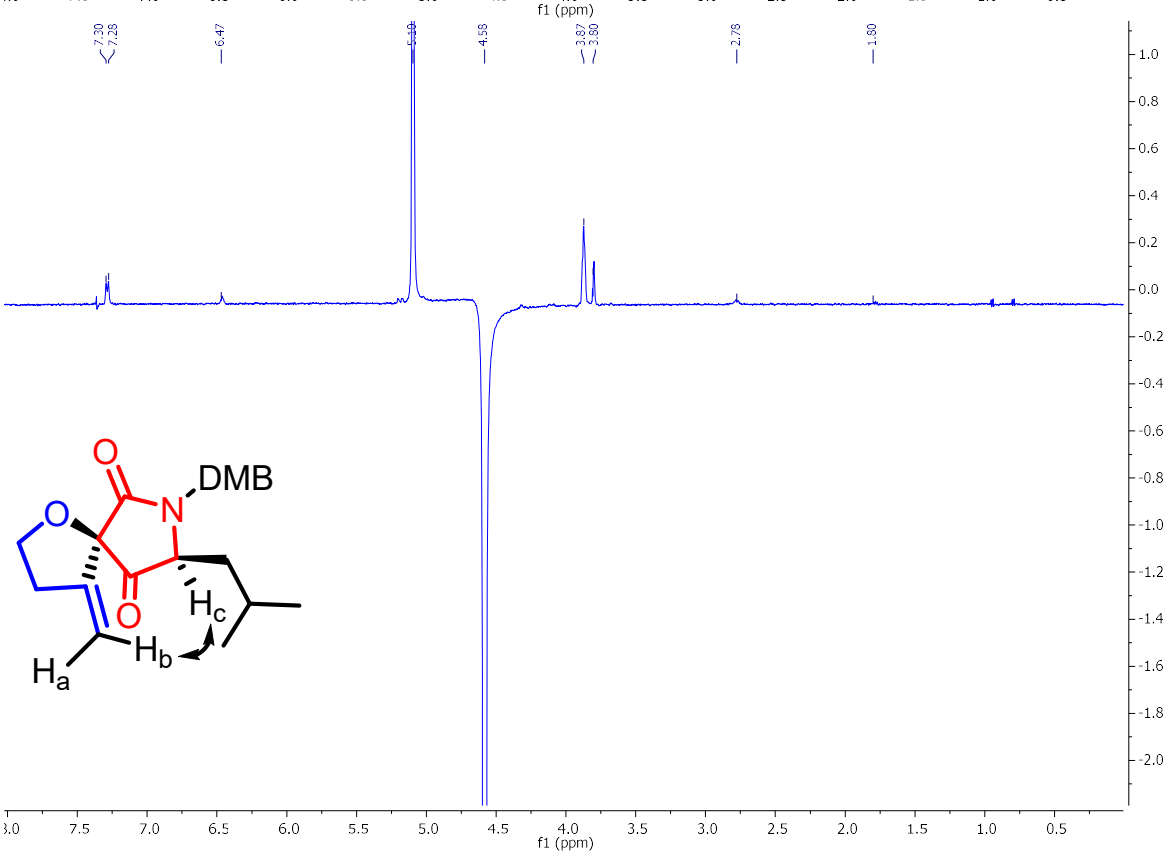
7.30
7.28
6.47
5.49
4.58
3.87
3.80
2.78
1.80
DMB
O
N
O
O
Hc
Hb
Ha
f1 (ppm)

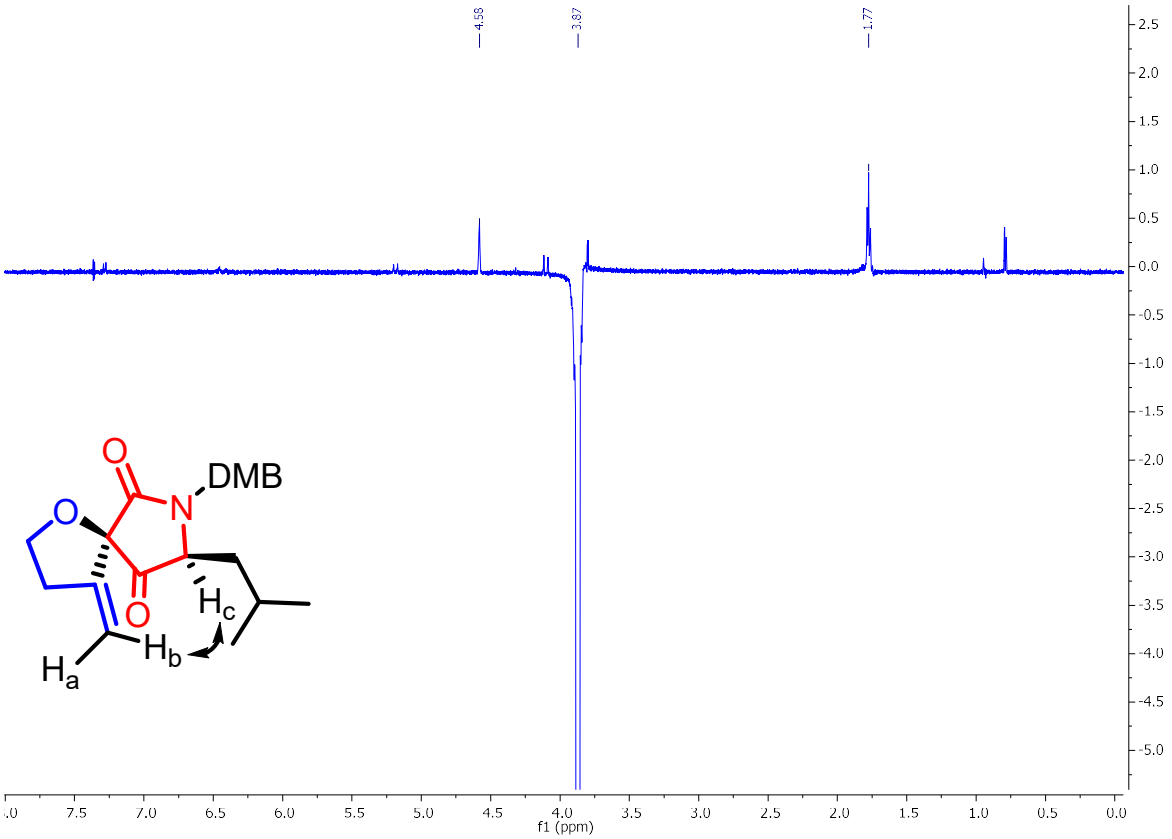
4.58
3.87
1.77
2.5
2.0
1.5
1.0
0.5
0.0
-0.5
-1.0
-1.5
-2.0
-2.5
-3.0
-3.5
-4.0
-4.5
-5.0
7.5
7.0
6.5
6.0
5.5
5.0
4.5
4.0
3.5
3.0
2.5
2.0
1.5
1.0
0.5
0.0
f1 (ppm)
O
N
DMB
O
O
Hc
Hb
Ha

Compound : 1**3c** (A colourless, block-shaped crystal of dimensions 0.20 x 0.28 x 0.32 mm)

Sample : SCS-2017-429

User : Steven Schlitzer

Formula : $C_{21}H_{27}NO_5$

CCDC 1572604

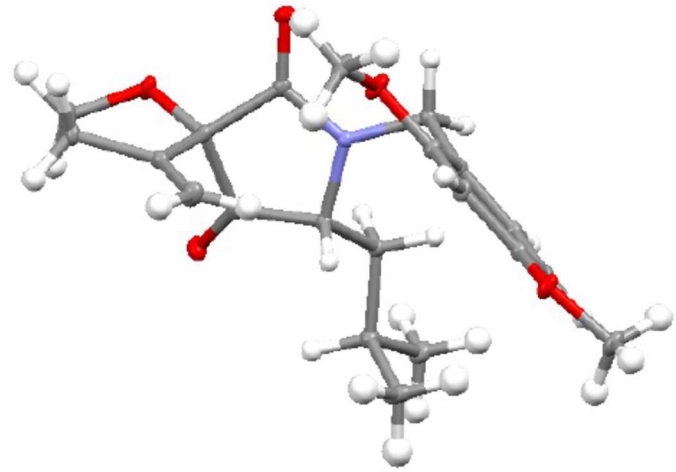

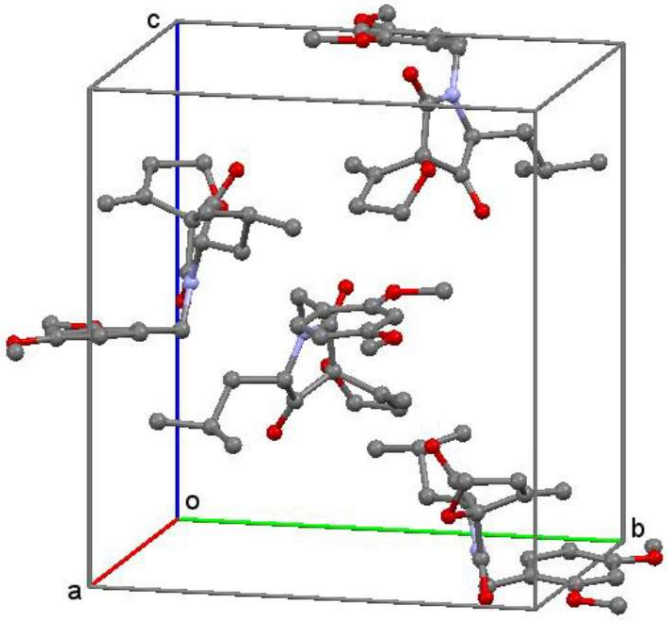

Comment

The displacement ellipsoids were drawn at the 50% probability level.

Table S1. Crystal data and structure refinement for SCS-2017-429.

Empirical formula	$C_{21}H_{27}NO_5$	
Formula weight	373.43	
Crystal system	orthorhombic	
Space group	$P2_12_12_1$	
Unit cell dimensions	*a*=10.098(4) Å	α= 90°
	b=13.103(5) Å	β= 90°
	c=14.443(5) Å	γ= 90°
Volume	1911.0(12) Å^3	
Z, Z'	4, 1	
Density (calculated)	1.298 Mg/m^3	
Wavelength	0.71073 Å	
Temperature	100(2) K	
F(000)	800	
Absorption coefficient	0.092 mm-1	
Absorption correction	semi-empirical from equivalents	
Theta range for data collection	2.099 to 25.993°	
Reflections collected	29580	
Independent reflections	3739 [R(int)=0.1052]	
Data / restraints / parameters	3739 / 0 / 244	
wR(F^2 all data)	*wR*2=0.1478	
R(*F* obsd data)	*R*1=0.0514	
Goodness-of-fit on F^2	1.027	
Observed data [I > 2σ(I)]	2537	
Absolute structure parameter	-0.6(10)	
Largest and mean shift / s.u.	0.000 and 0.000	
Largest diff. peak and hole	0.223 and -0.214 e/Å^3	

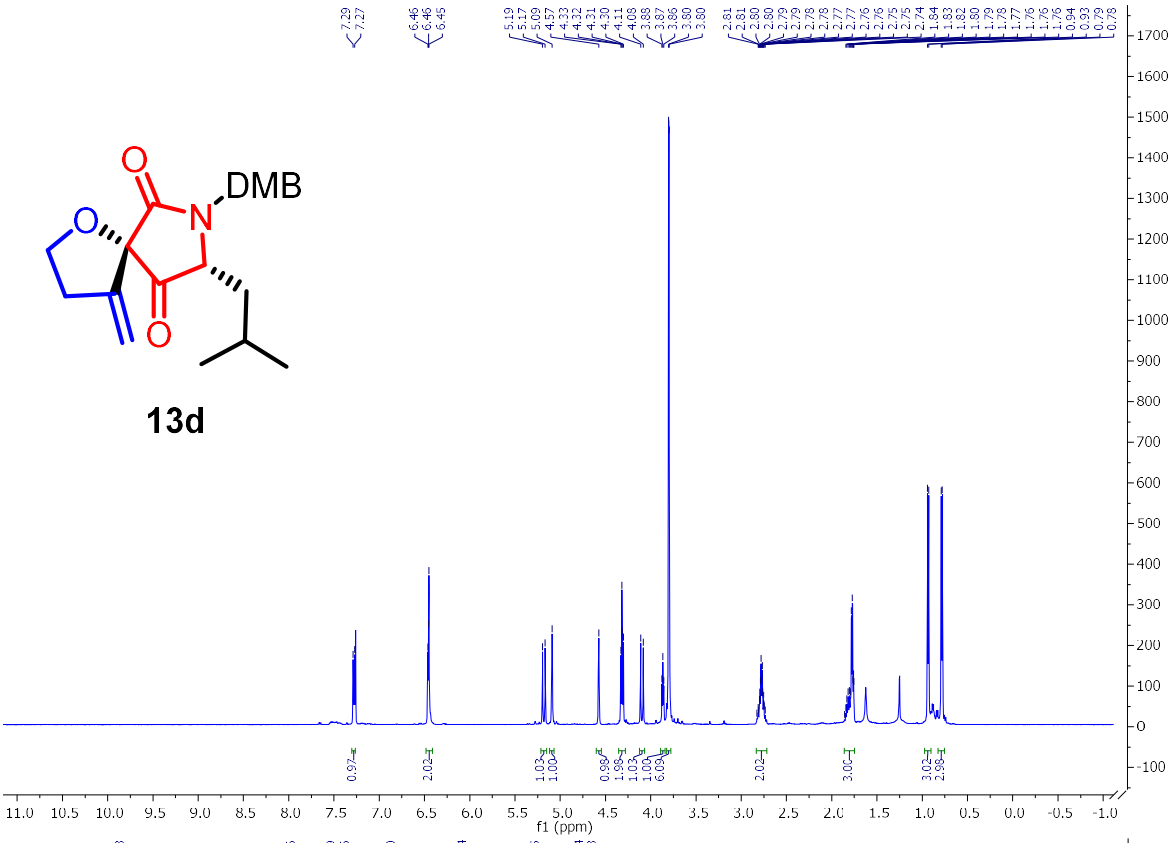
DMB
13d
f1 (ppm)

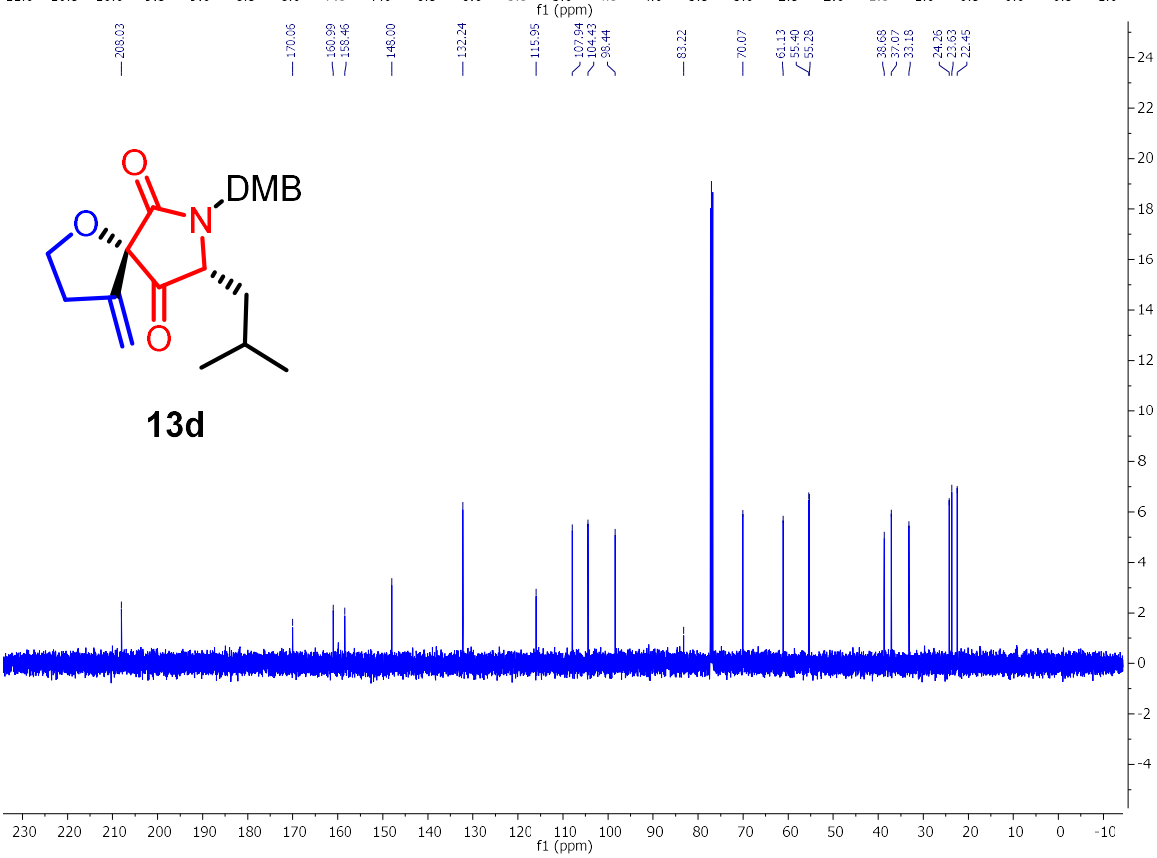
DMB
13d
f1 (ppm)

Compound : 1**3d (**A colourless, rod-shaped crystal of dimensions 0.05 x 0.15 x 0.41 mm)

Sample : SCS-2017-439

User : Steven Schlitzer

Formula : $C_{21}H_{27}NO_5$

CCDC 1572603

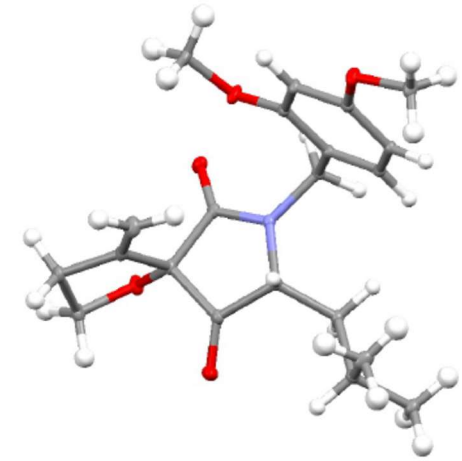

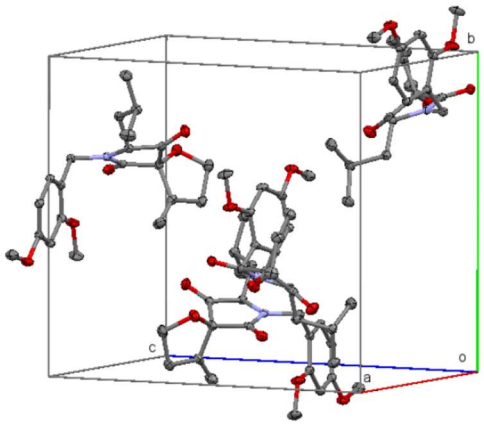

Comment
The displacement ellipsoids were drawn at the 50% probability level.

Table S2. Crystal data and structure refinement for SCS-2016-439.

Empirical formula	$C_{21}H_{27}NO_5$	
Formula weight	373.43	
Crystal system	orthorhombic	
Space group	$P2_12_12_1$	
Unit cell dimensions	*a*=10.1147(7) Å	α= 90°
	b=13.1272(9) Å	β= 90°
	c=14.4524(10) Å	γ= 90°
Volume	1919.0(2) Å^3	
Z, Z'	4, 1	
Density (calculated)	1.293 Mg/m^3	
Wavelength	0.71073 Å	
Temperature	100(2) K	
F(000)	800	
Absorption coefficient	0.092 mm^{-1}	
Absorption correction	semi-empirical from equivalents	
Max. and min. transmission	0.995 and 0.963	
Theta range for data collection	2.096 to 27.498°	
Reflections collected	37767	
Independent reflections	4407 [R(int)=0.0354]	
Data / restraints / parameters	4407 / 0 / 244	
wR(F^2 all data)	*wR*2=0.0794	
R(*F* obsd data)	*R*1=0.0302	
Goodness-of-fit on F^2	0.990	
Observed data [I > 2σ(I)]	4105	
Absolute structure parameter	0.1(3)	
Largest and mean shift / s.u.	0.000 and 0.000	
Largest diff. peak and hole	0.229 and -0.179 e/Å^3	

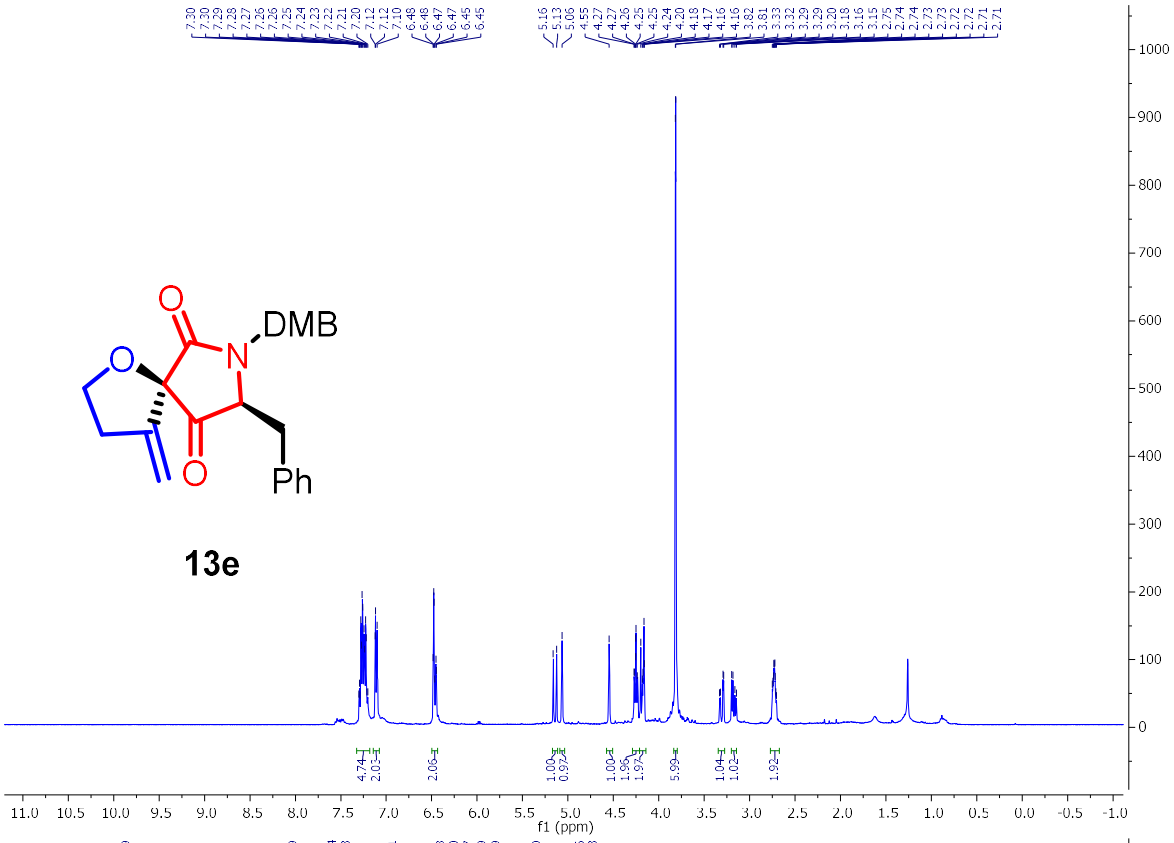
DMB
Ph
13e
f1 (ppm)

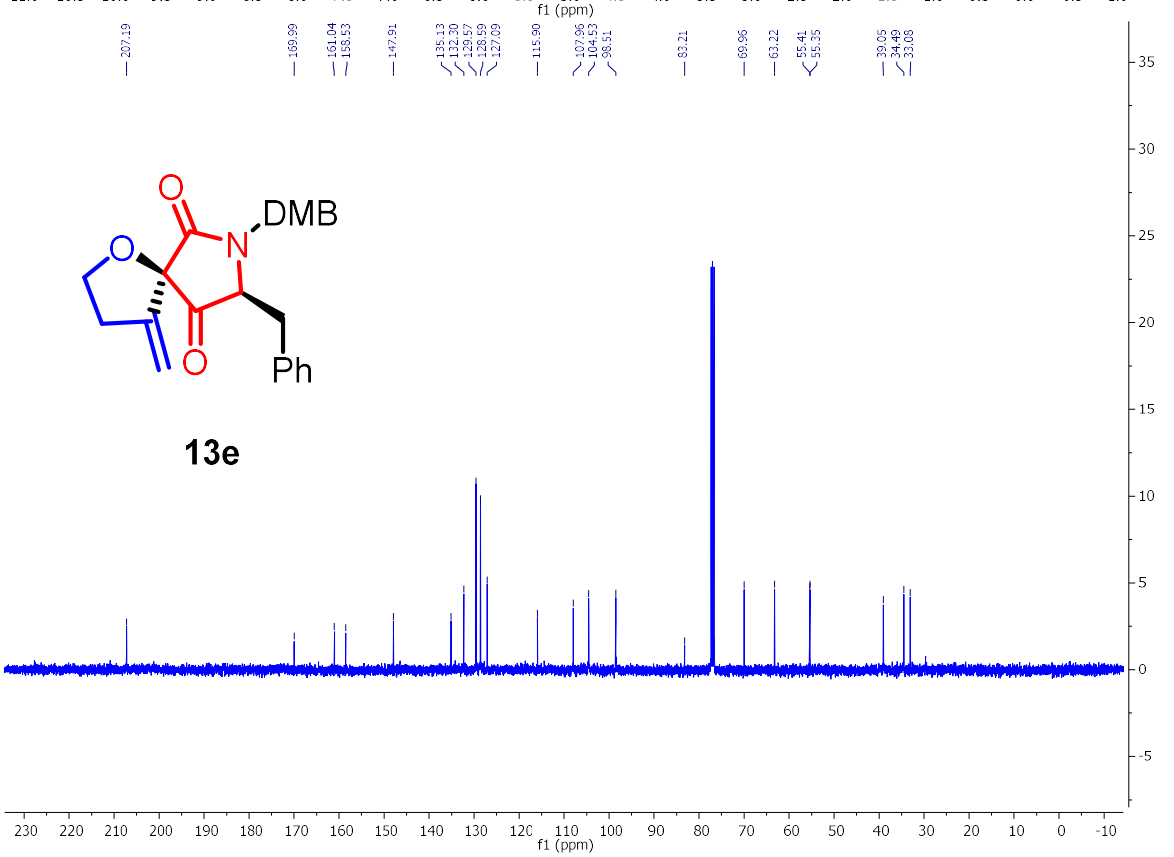
DMB
Ph
13e
f1 (ppm)

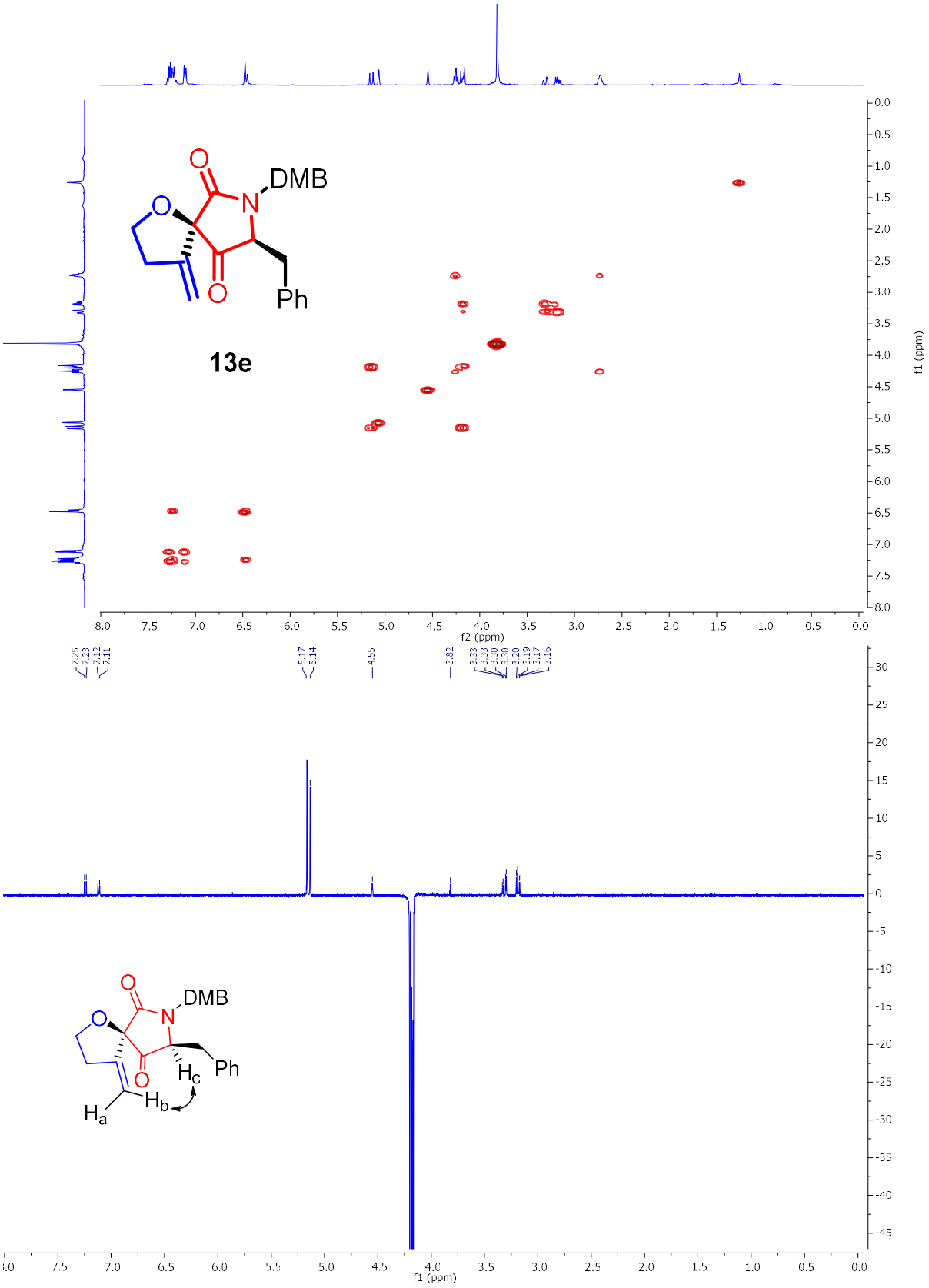
DMB
Ph
13e
f2 (ppm)
f1 (ppm)
7.25
7.23
7.12
7.11
5.17
5.14
4.55
3.82
3.33
3.33
3.30
3.30
3.20
3.19
3.17
3.16
DMB
Ph
Hc
Hb
Ha
f1 (ppm)

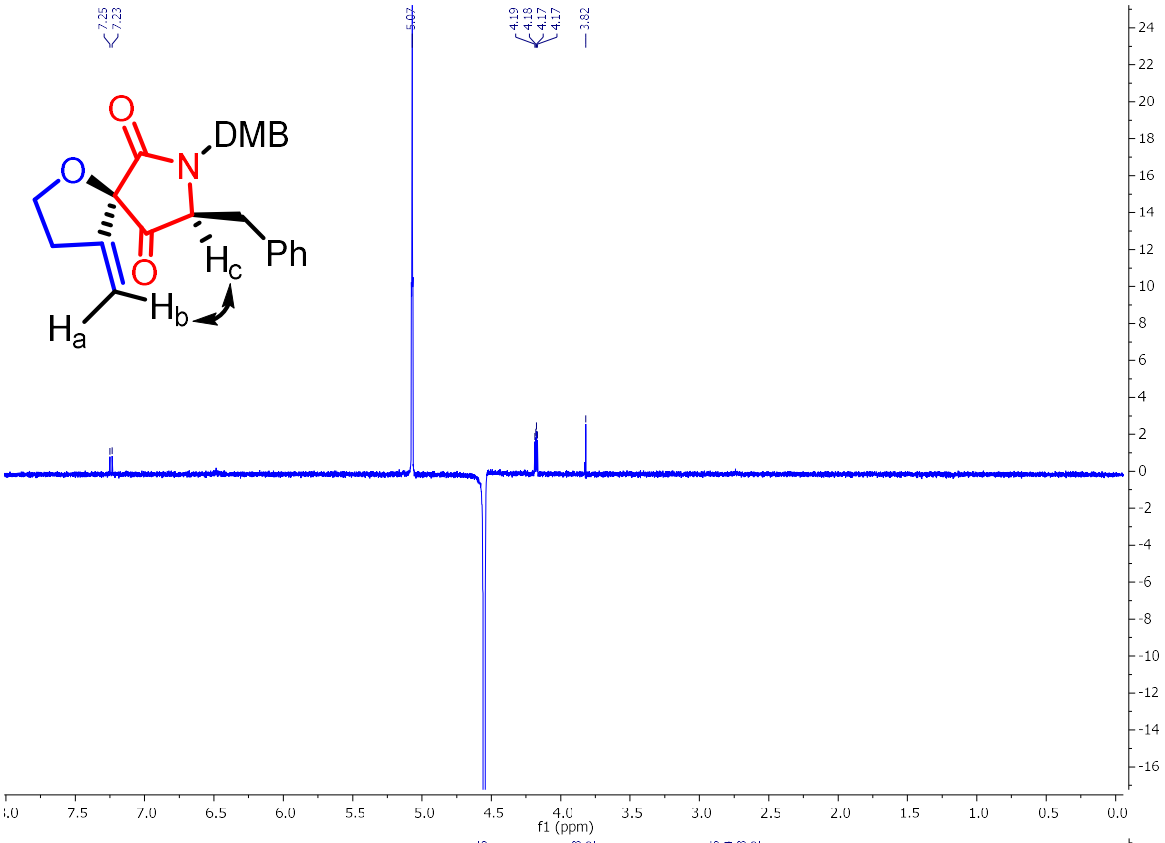
DMB
Ph
Hc
Hb
Ha
f1 (ppm)

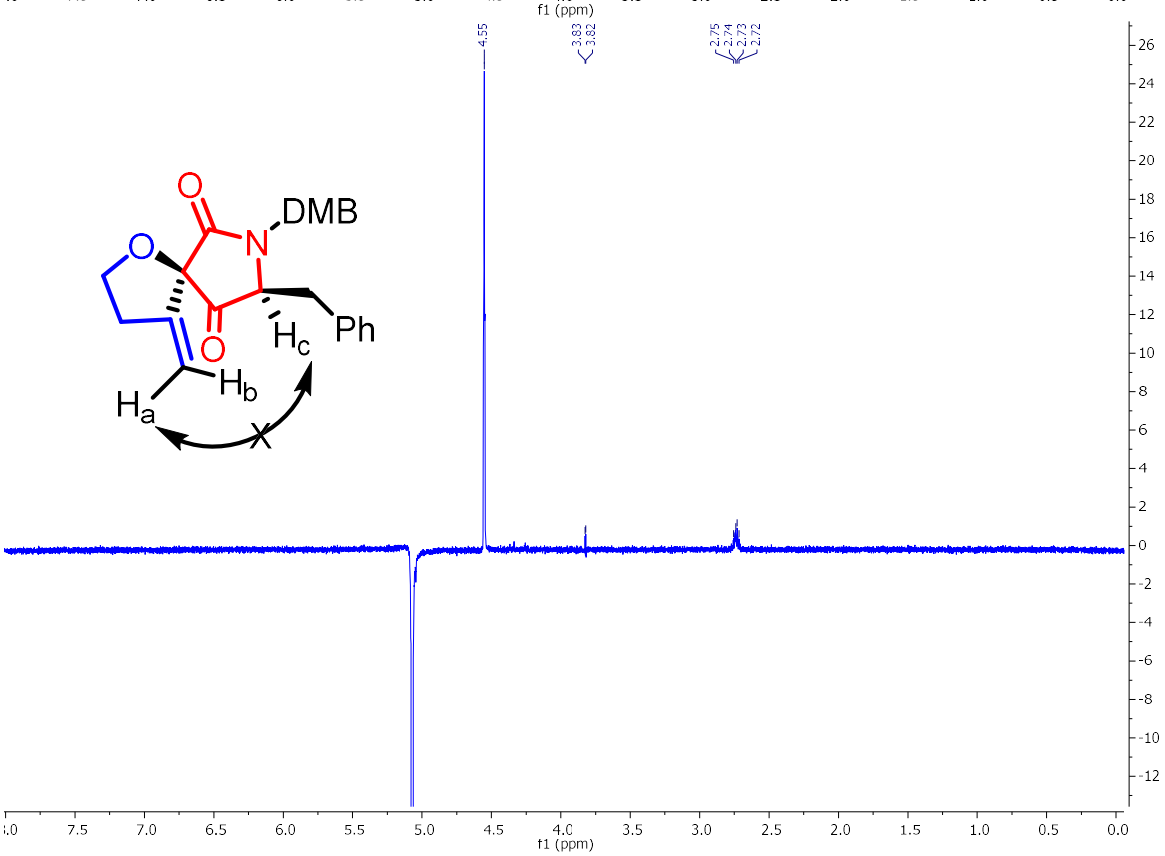
DMB
Ph
Hc
Hb
Ha
X
f1 (ppm)

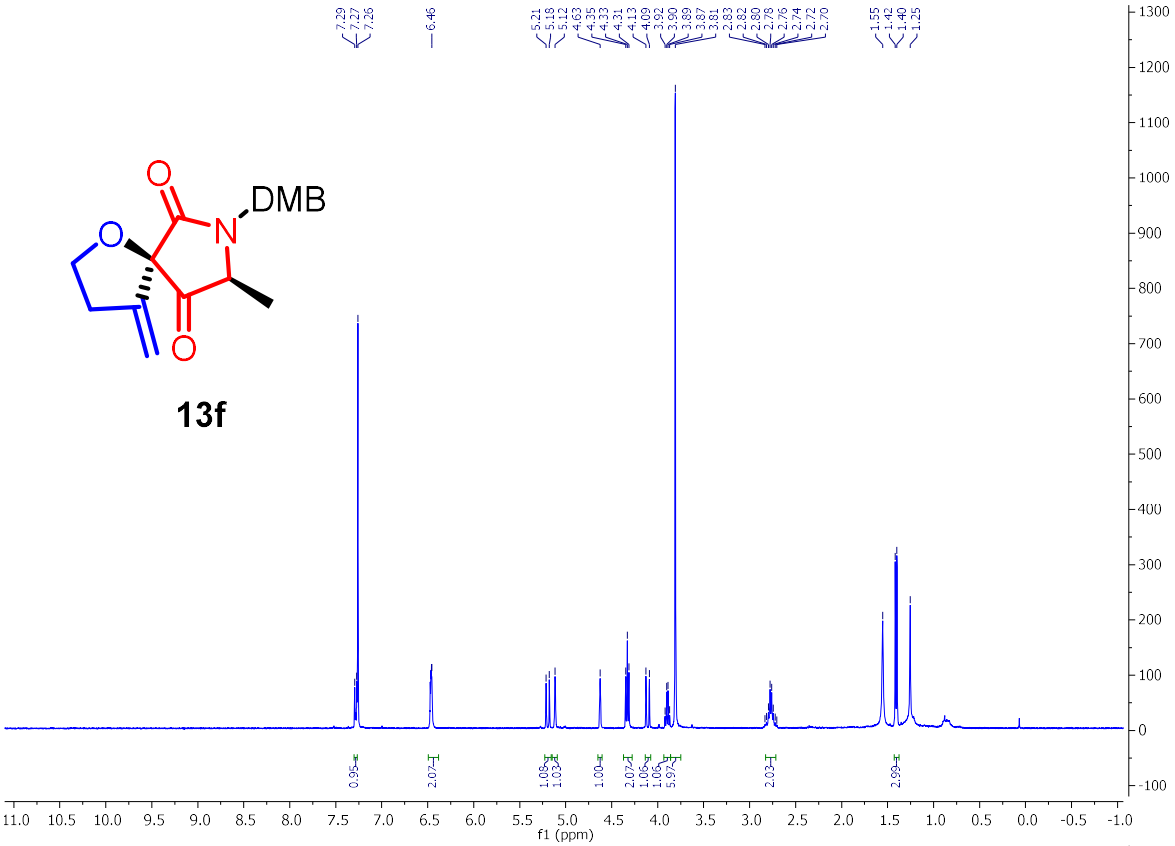
DMB
13f
f1 (ppm)

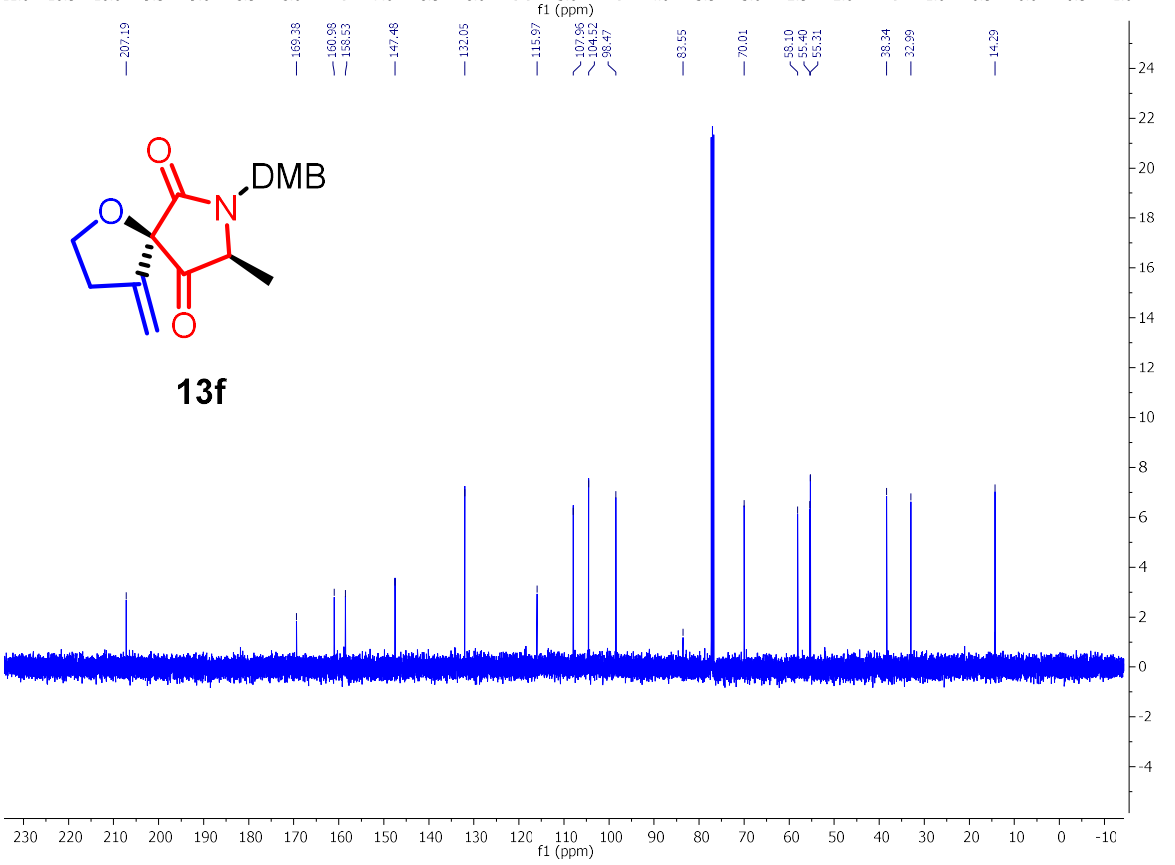
DMB
13f
f1 (ppm)

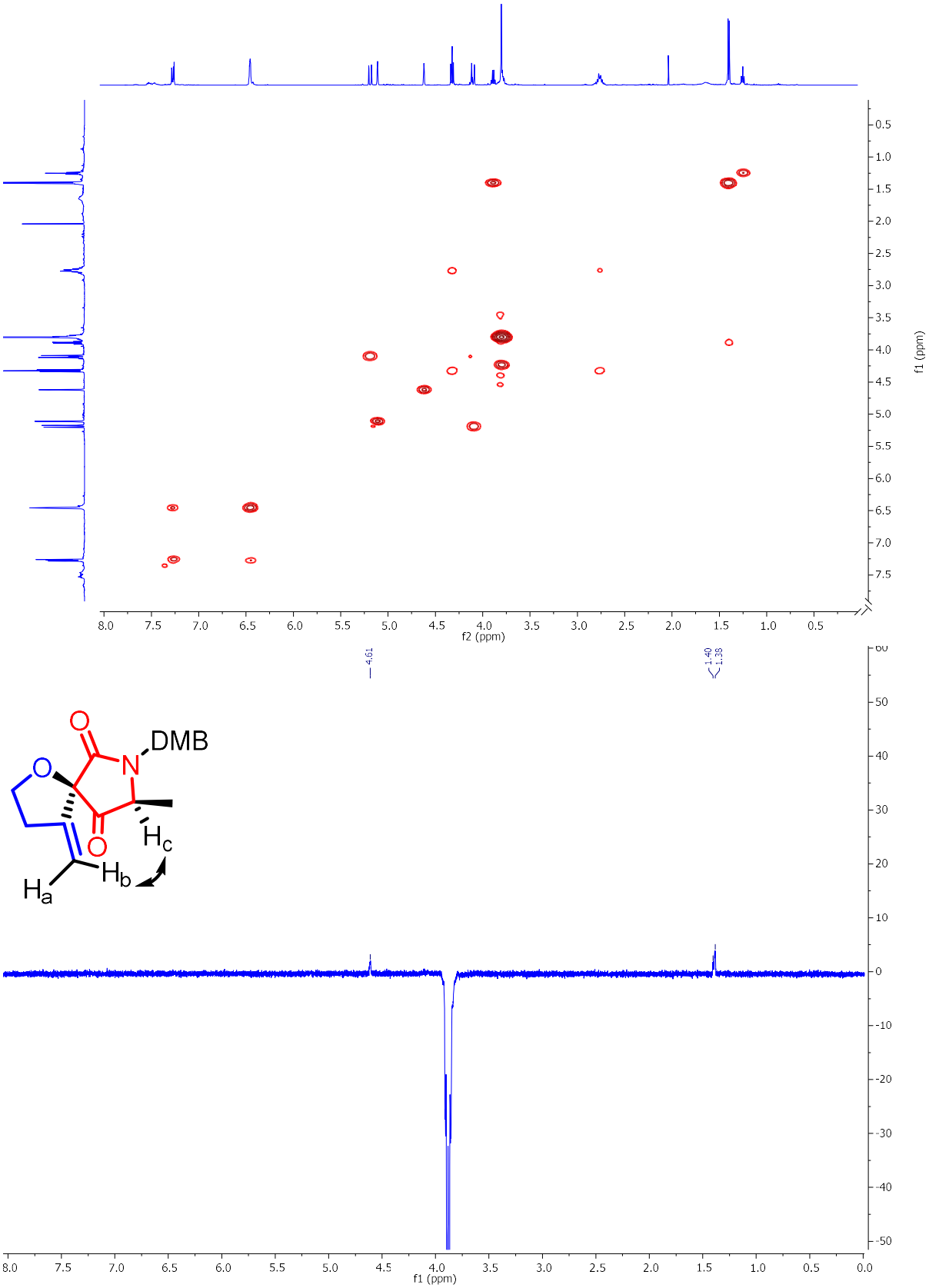
f2 (ppm)
f1 (ppm)
4.61
1.40
1.38
DMB
Ha
Hb
Hc
f1 (ppm)

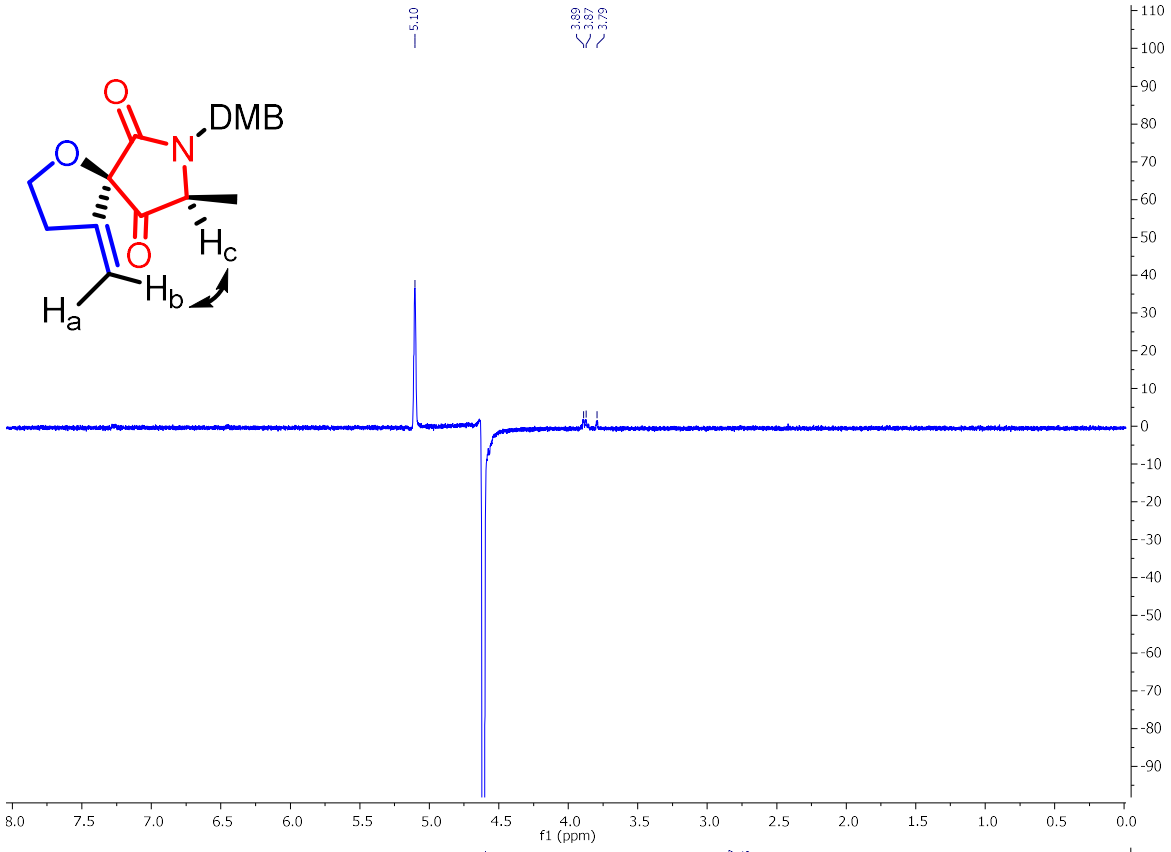
5.10
3.89
3.87
3.79
DMB
O
N
O
O
Hc
Hb
Ha
f1 (ppm)

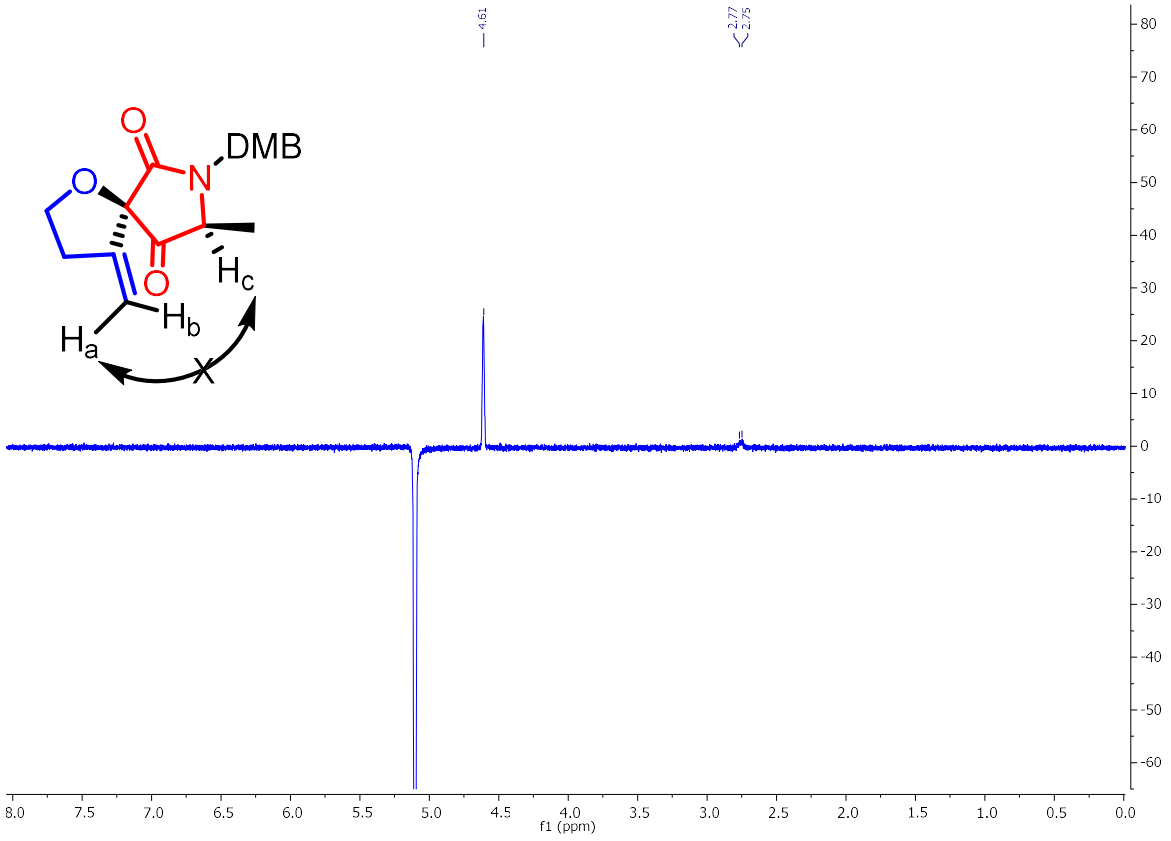
4.61
2.77
2.75
DMB
O
N
O
O
Hc
Hb
Ha
X
f1 (ppm)

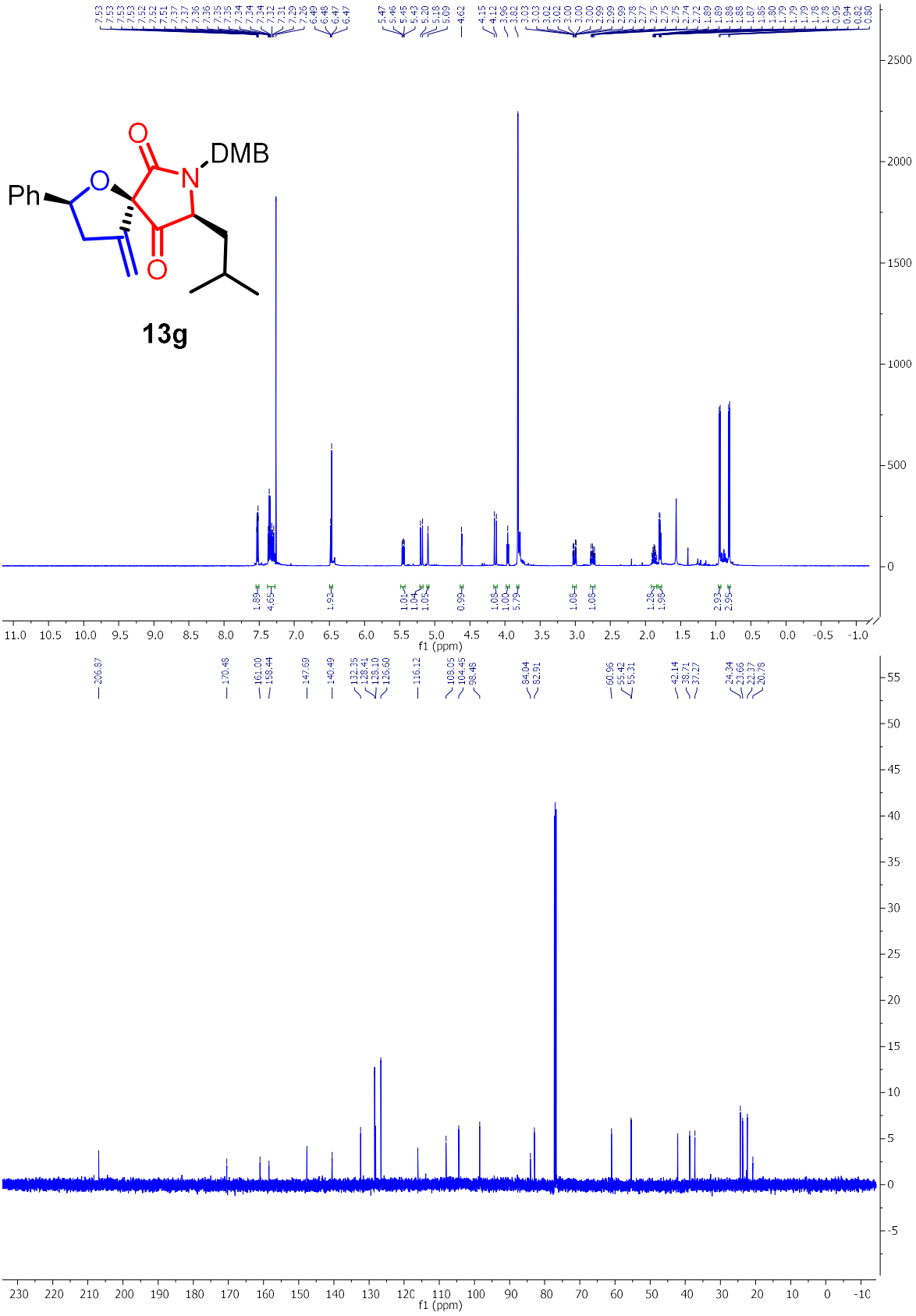
DMB
Ph
O
N
O
O
13g
f1 (ppm)
f1 (ppm)

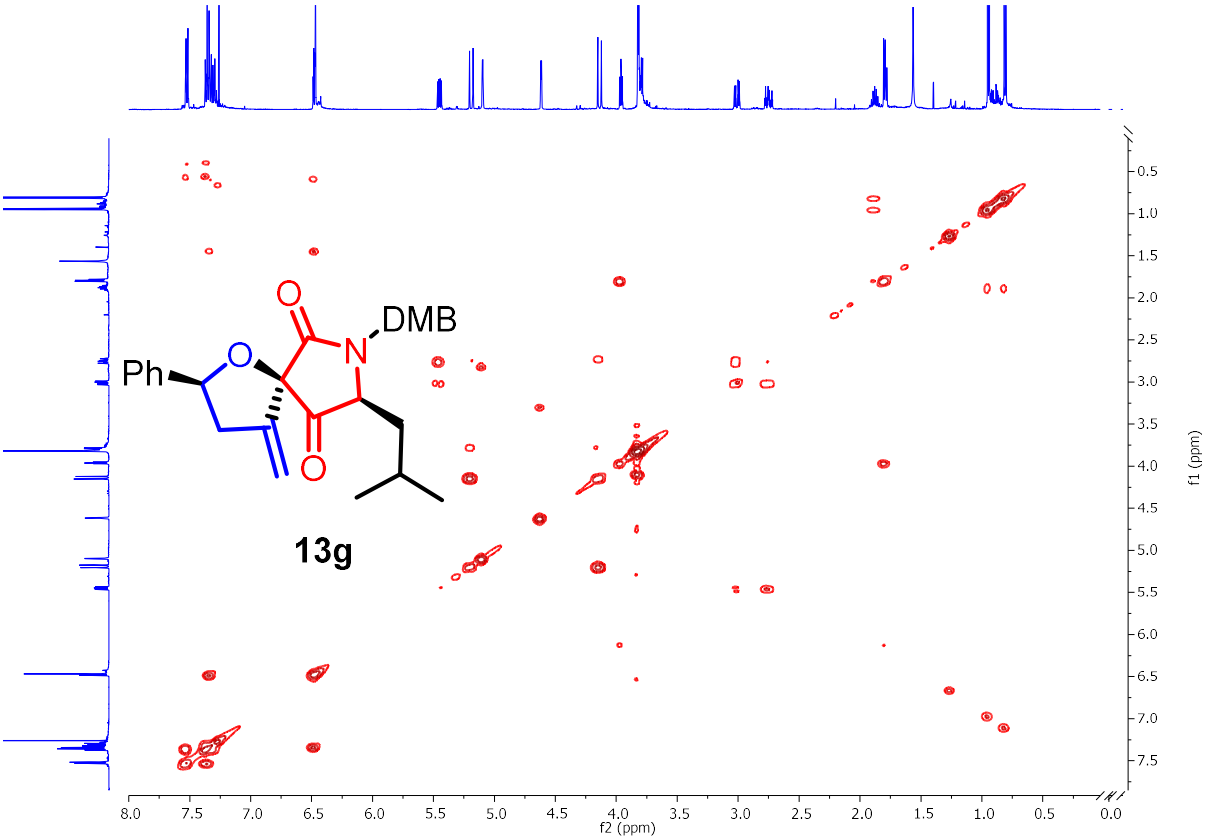
DMB
Ph
O
N
O
O
13g
f2 (ppm)
f1 (ppm)

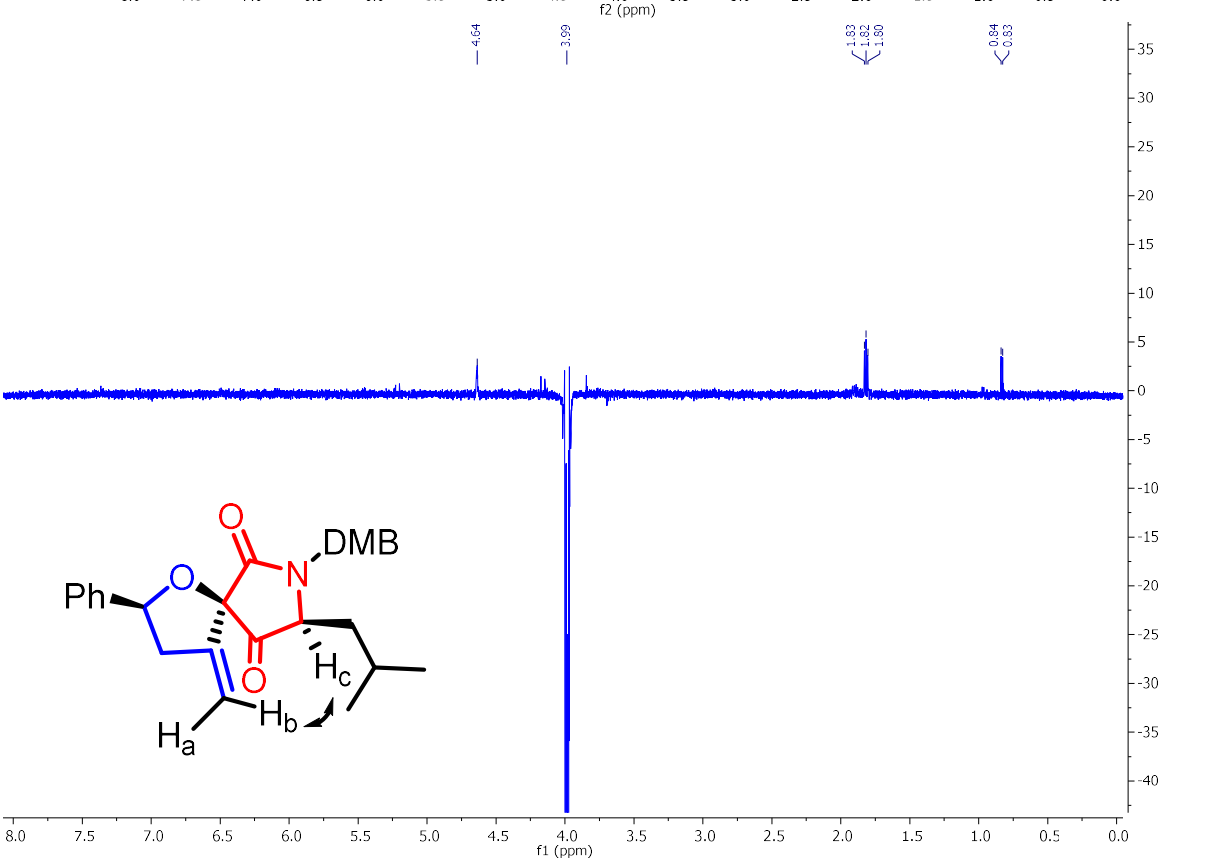
4.64
3.99
1.83
1.82
1.80
0.84
0.83
DMB
Ph
O
N
O
O
Hc
Hb
Ha
f1 (ppm)

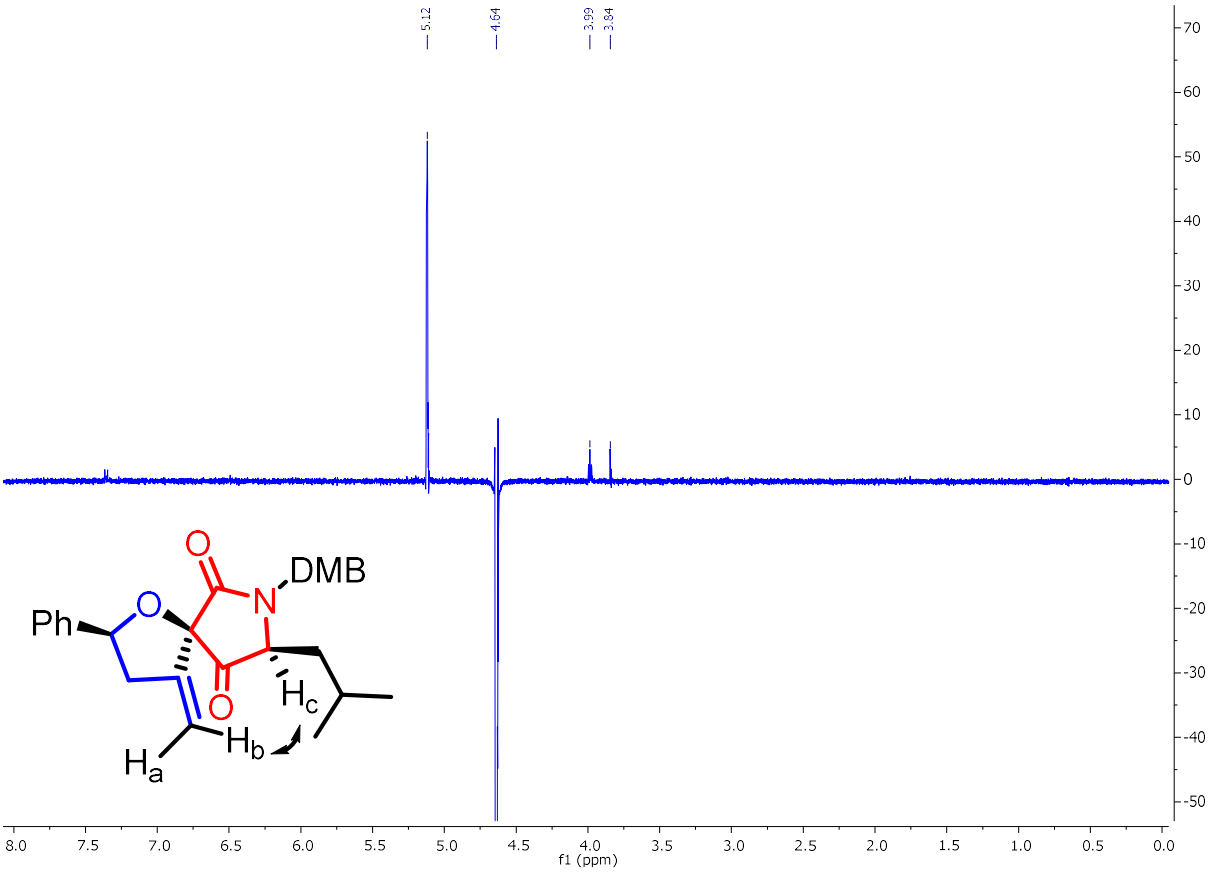
5.12
4.64
3.99
3.84
70
60
50
40
30
20
10
0
-10
-20
-30
-40
-50
8.0
7.5
7.0
6.5
6.0
5.5
5.0
4.5
4.0
3.5
3.0
2.5
2.0
1.5
1.0
0.5
0.0
f1 (ppm)
O
DMB
N
Ph
O
O
Hc
Hb
Ha

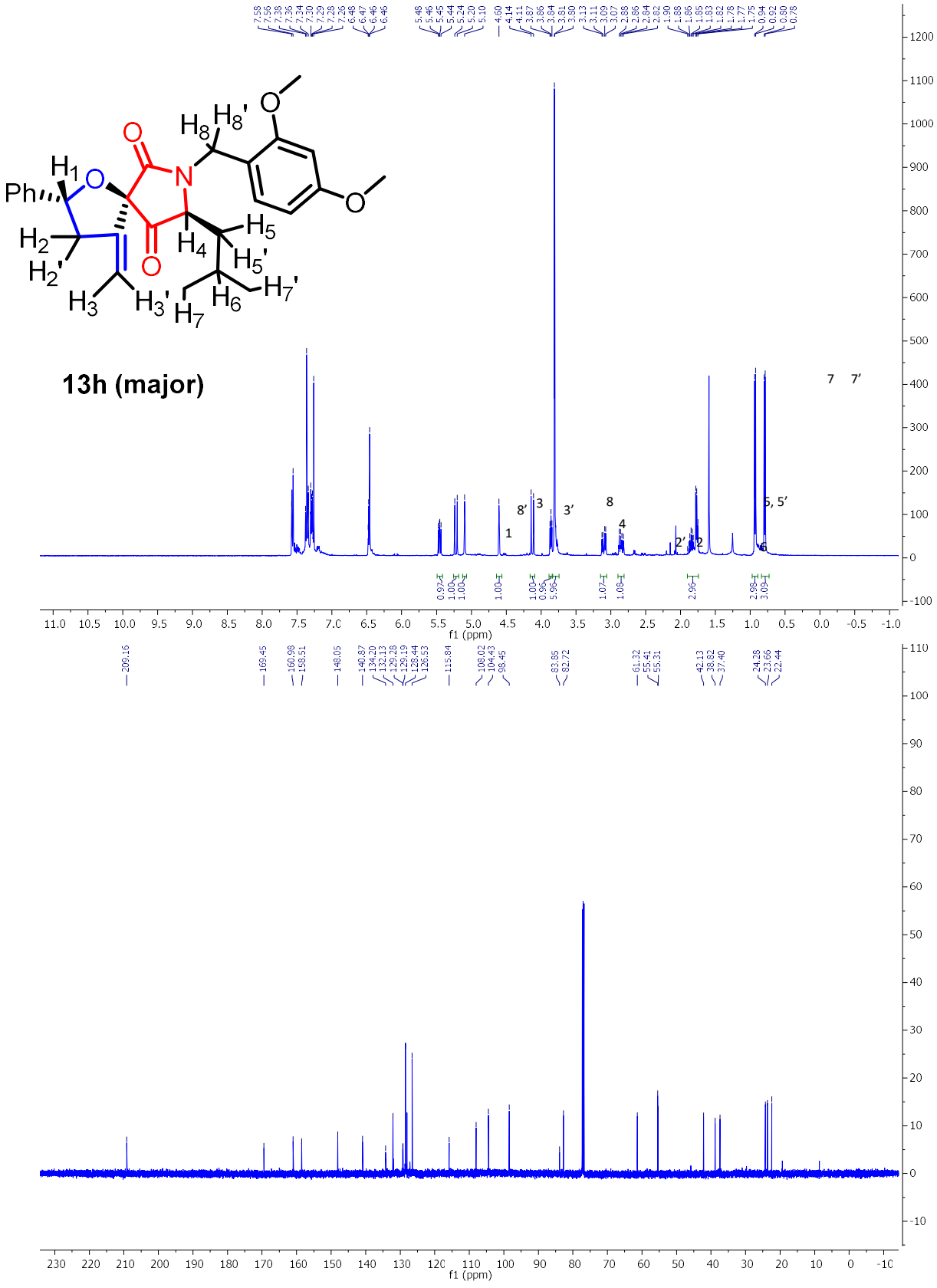
13h (major)
Ph
H1
H2
H2'
H3
H3'
H4
H5
H5'
H6
H7
H7'
H8
H8'
O
N
7.58 7.56 7.38 7.36 7.34 7.30 7.29 7.28 7.26 6.48 6.47 6.46 6.46
5.48 5.46 5.45 5.44 5.24 5.20 5.10
4.60 4.14 4.11 3.87 3.86 3.84 3.81 3.80 3.13 3.11 3.09 3.07 2.88 2.86 2.84 2.82 1.90 1.88 1.86 1.85 1.83 1.82 1.78 1.77 1.75 0.94 0.92 0.80 0.78
1 8' 3 3' 8 4 2' 2 6 5, 5' 7 7'
0.97 1.00 1.00 1.00 1.00 0.96 5.96 1.07 1.08 2.96 2.98 3.09
f1 (ppm)
209.16 169.45 160.98 158.51 148.05 140.87 134.20 132.13 129.28 129.19 128.44 126.53 115.84 108.02 104.43 98.45 83.85 82.72 61.32 55.41 55.31 42.13 38.82 37.40 24.28 23.66 22.44
f1 (ppm)

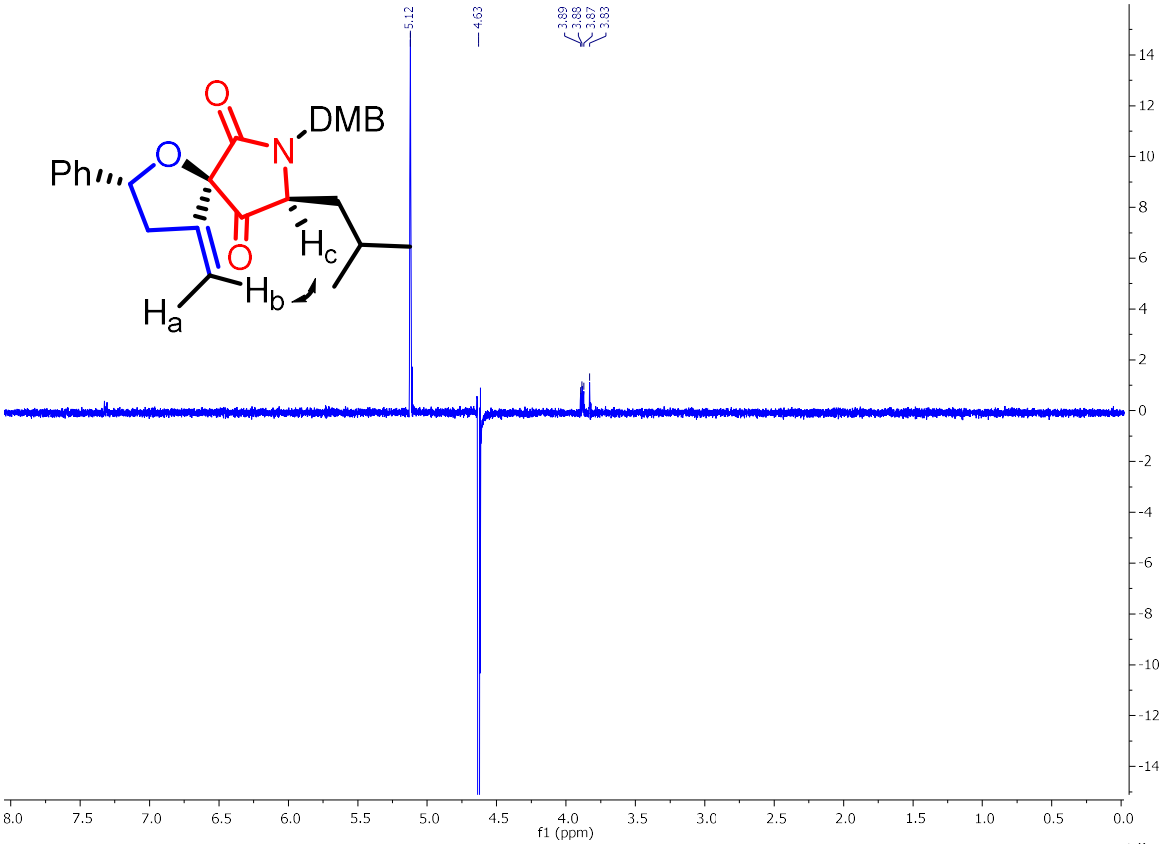
5.12
4.63
3.89
3.88
3.87
3.83
DMB
Ph
O
N
O
O
Hc
Hb
Ha
f1 (ppm)

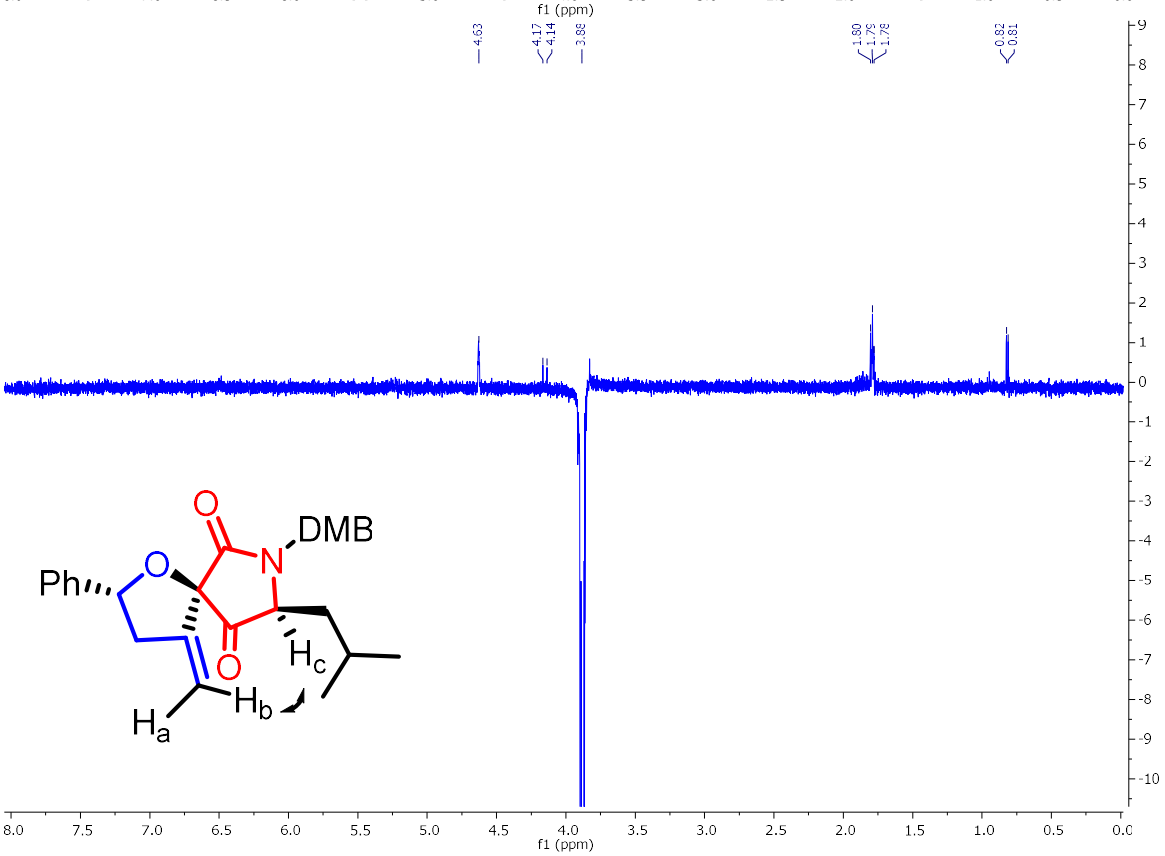
4.63
4.17
4.14
3.88
1.80
1.79
1.78
0.82
0.81
DMB
Ph
O
N
O
O
Hc
Hb
Ha
f1 (ppm)

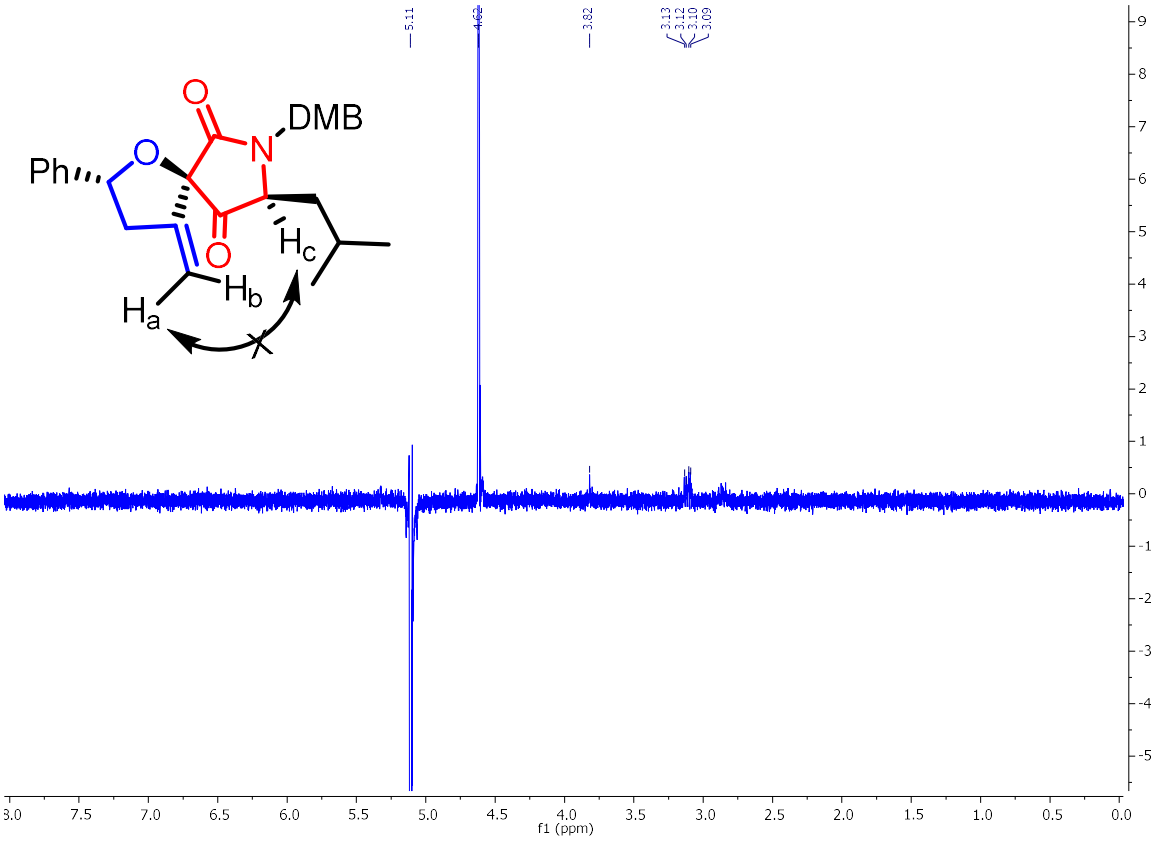
5.11
4.66
3.82
3.13
3.12
3.10
3.09
DMB
Ph
O
N
O
O
Hc
Hb
Ha
f1 (ppm)

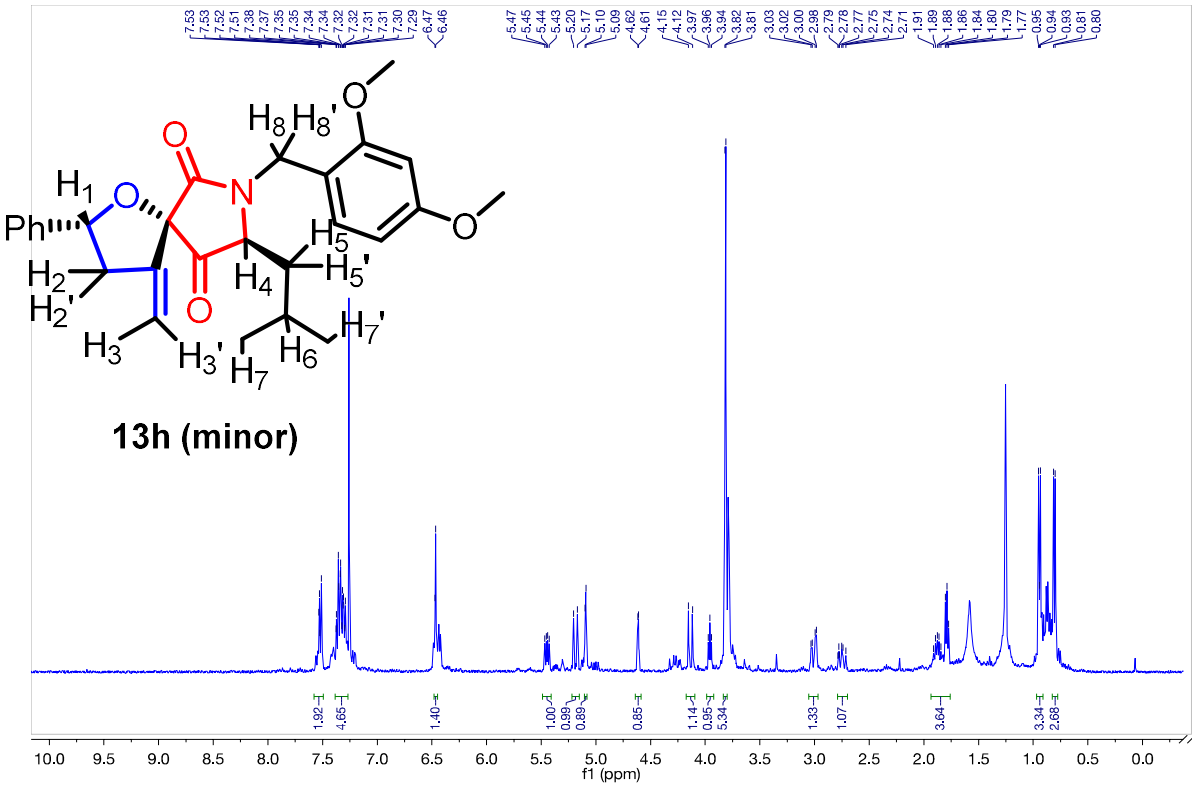
13h (minor)
f1 (ppm)

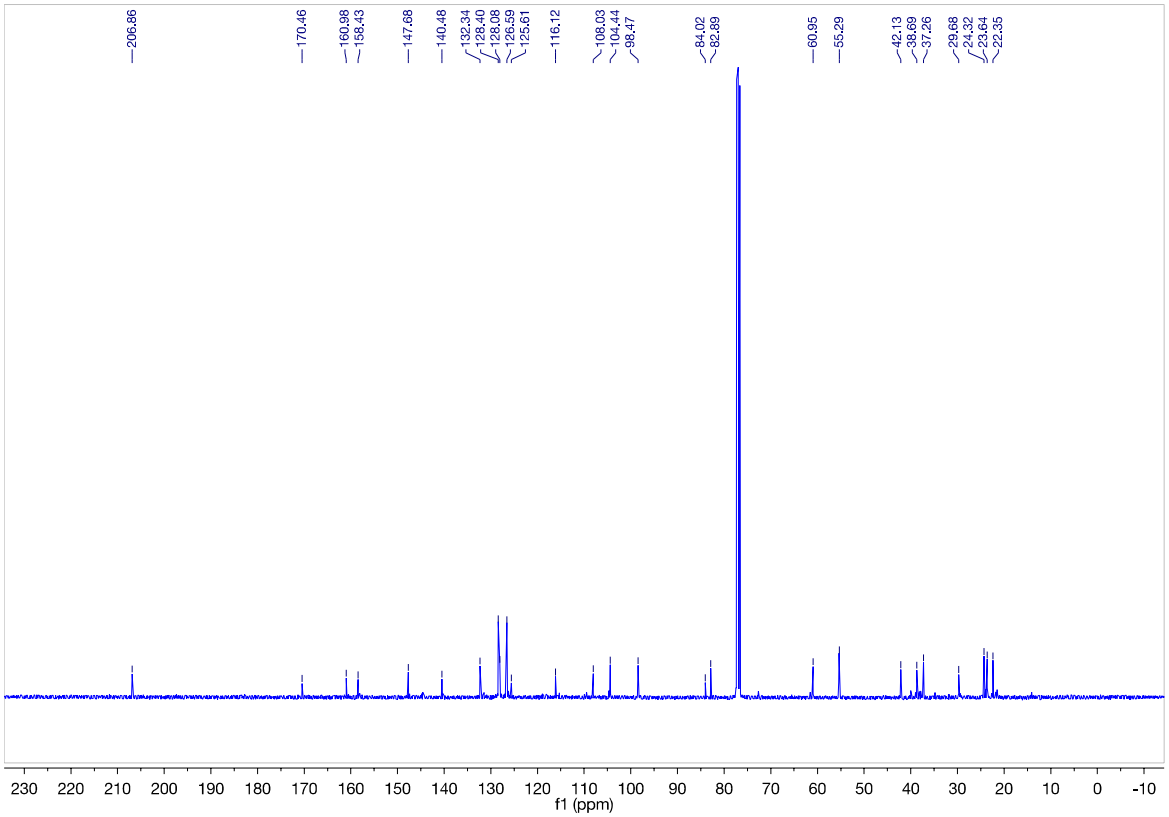
f1 (ppm)

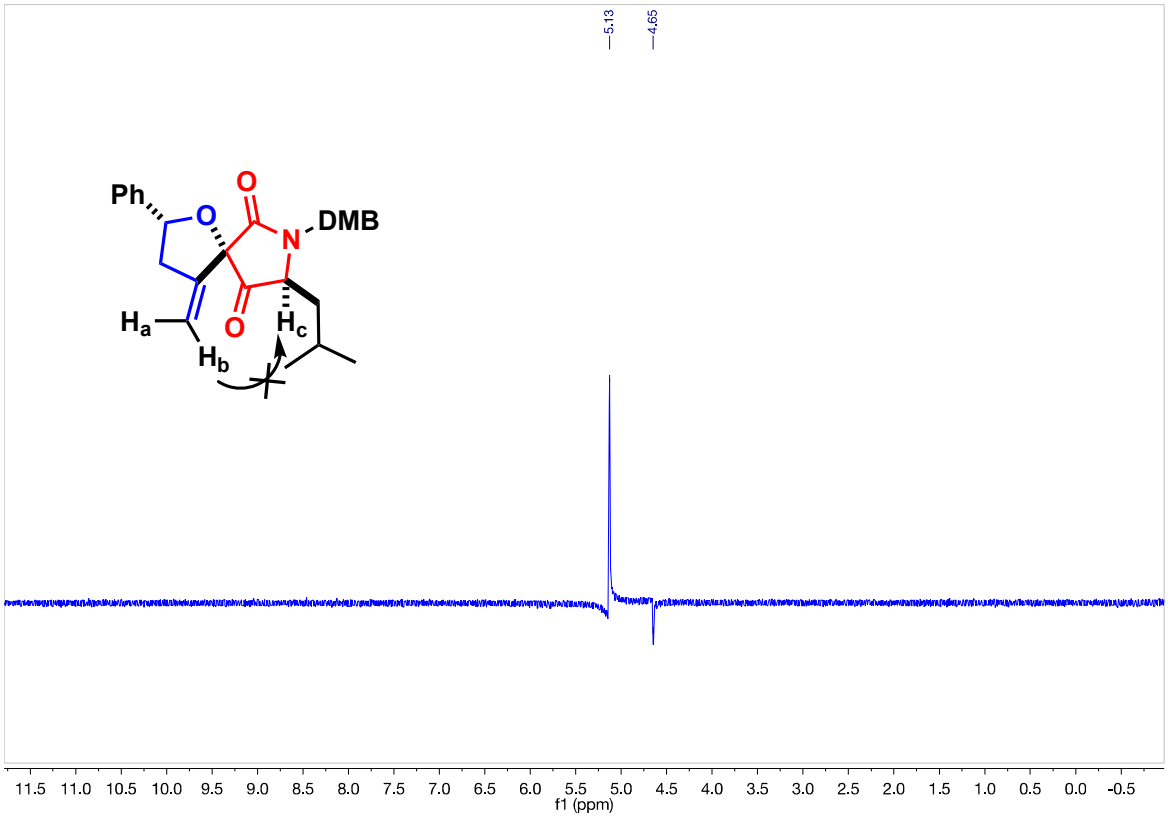
5.13
4.65
Ph
O
DMB
N
O
O
Ha
Hb
Hc
11.5 11.0 10.5 10.0 9.5 9.0 8.5 8.0 7.5 7.0 6.5 6.0 5.5 5.0 4.5 4.0 3.5 3.0 2.5 2.0 1.5 1.0 0.5 0.0 -0.5
f1 (ppm)

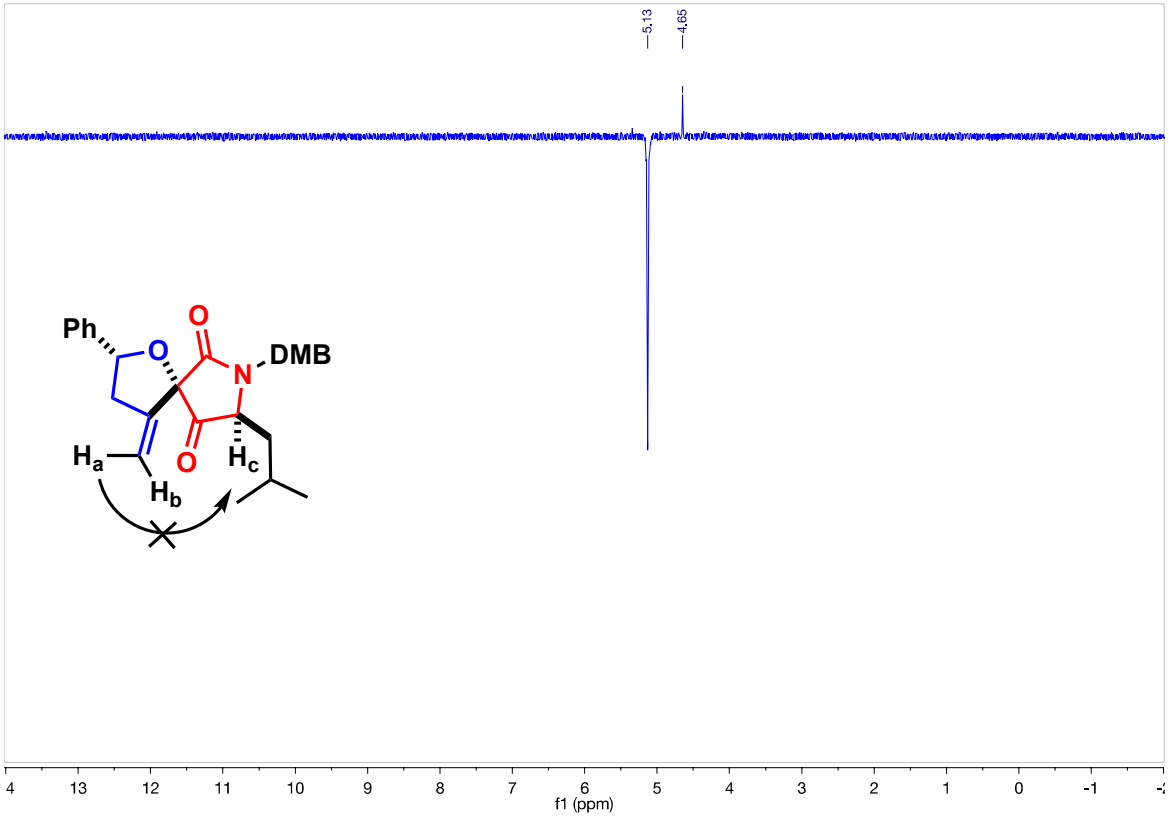
5.13
4.65
Ph
O
DMB
N
O
O
Ha
Hb
Hc
4 13 12 11 10 9 8 7 6 5 4 3 2 1 0 -1
f1 (ppm)

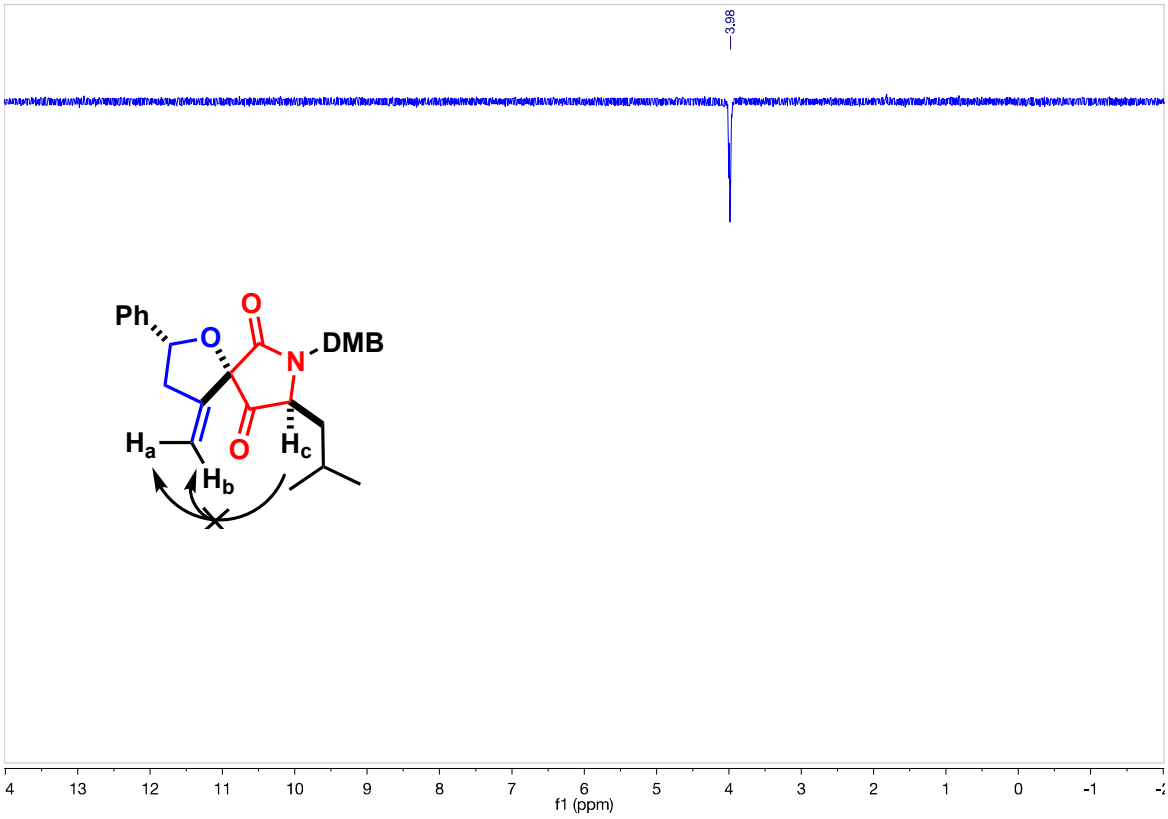
3.98
Ph
O
O
N
DMB
O
Ha
Hb
Hc
4
13
12
11
10
9
8
7
6
5
4
3
2
1
0
-1
f1 (ppm)

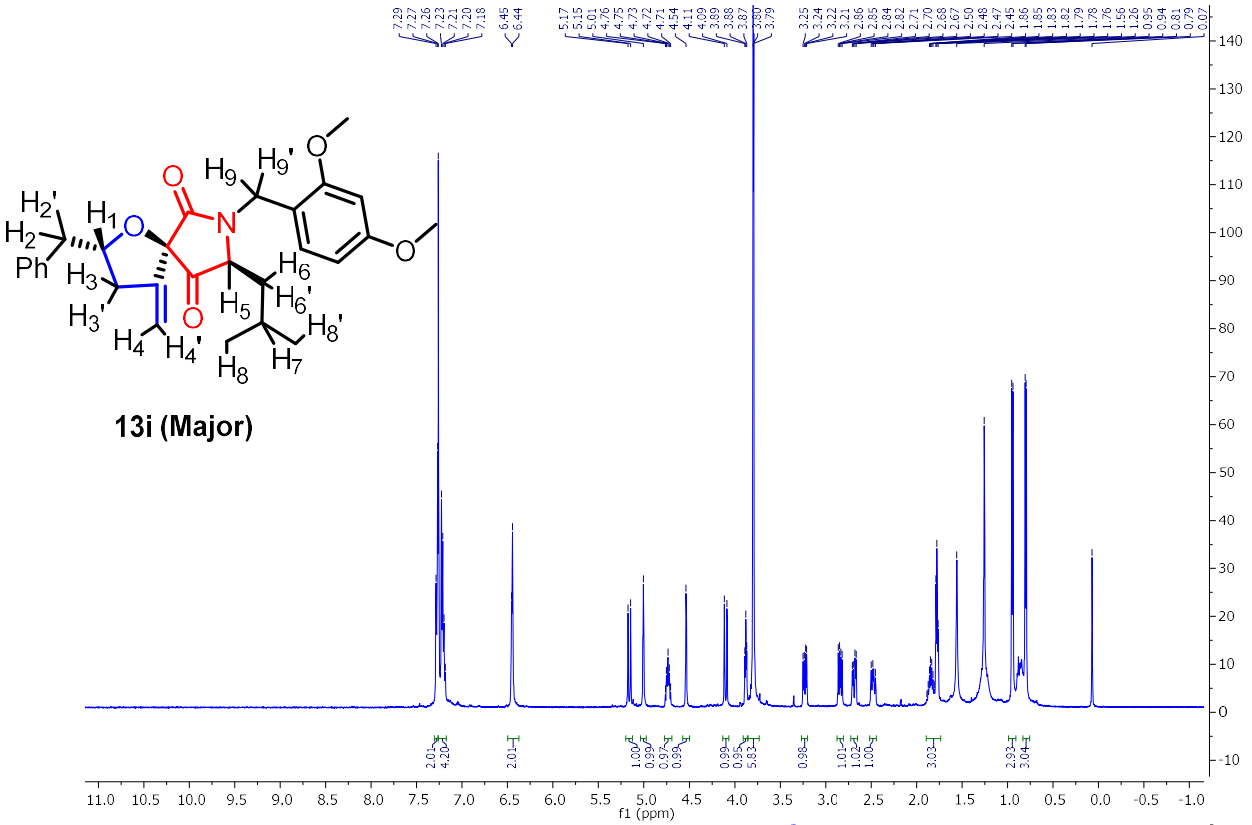
13i (Major)
f1 (ppm)

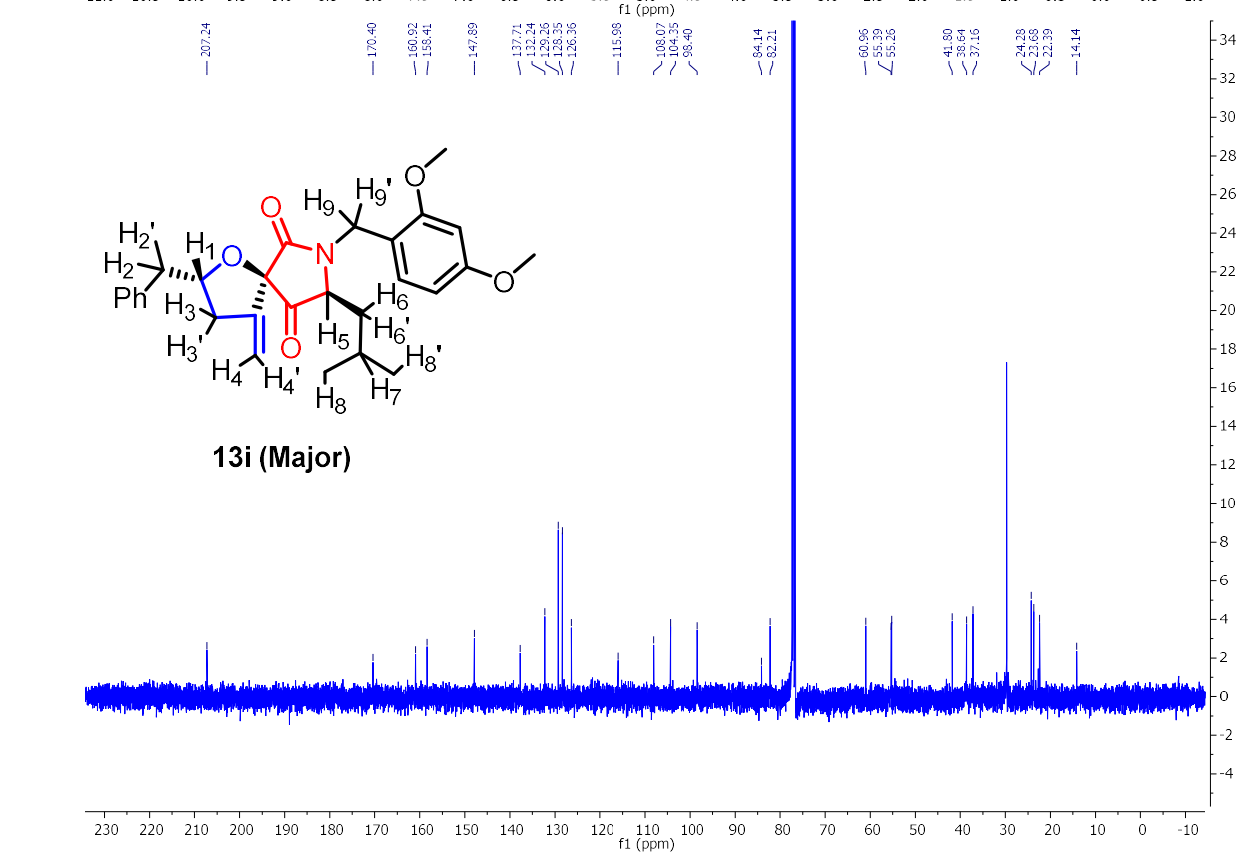
13i (Major)
f1 (ppm)

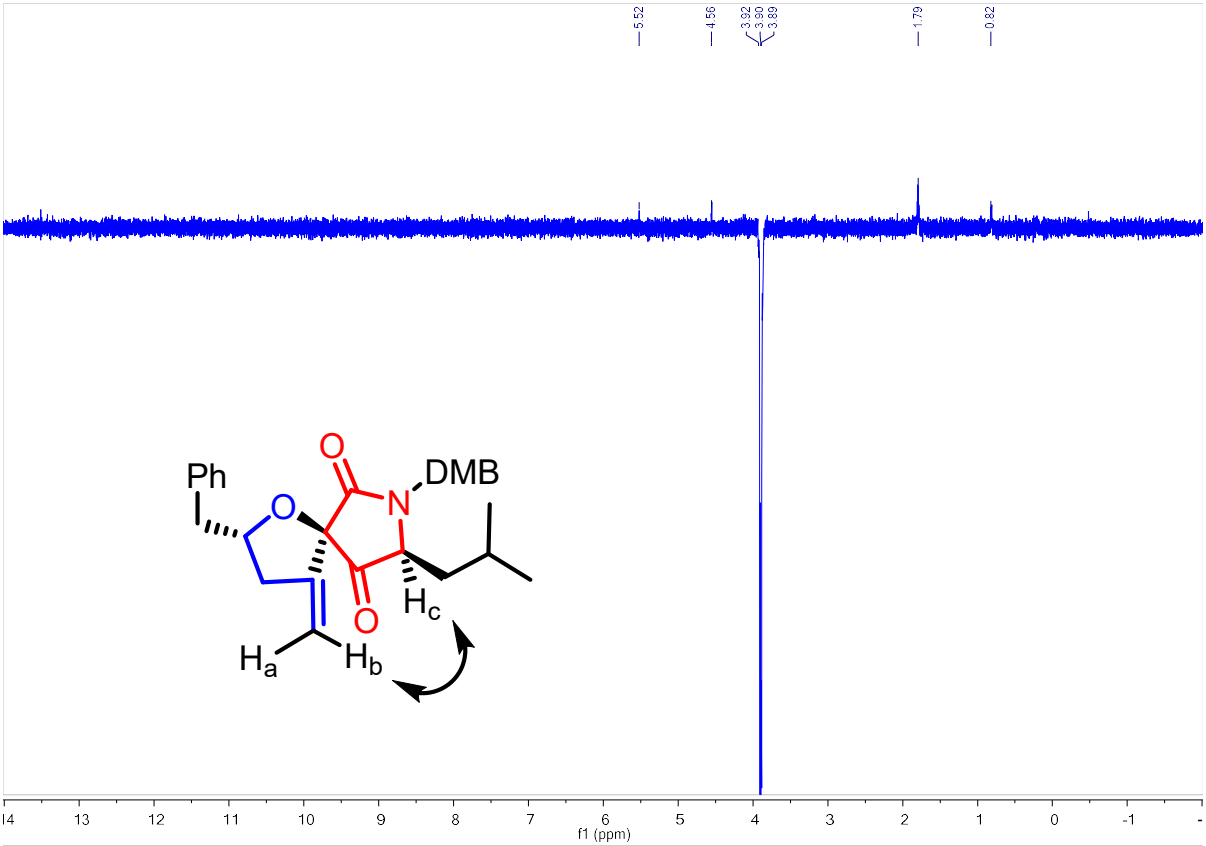
5.52
4.56
3.92
3.90
3.89
1.79
0.82
Ph
O
N
DMB
O
O
H_c
H_a
H_b
14 13 12 11 10 9 8 7 6 5 4 3 2 1 0 -1
f1 (ppm)

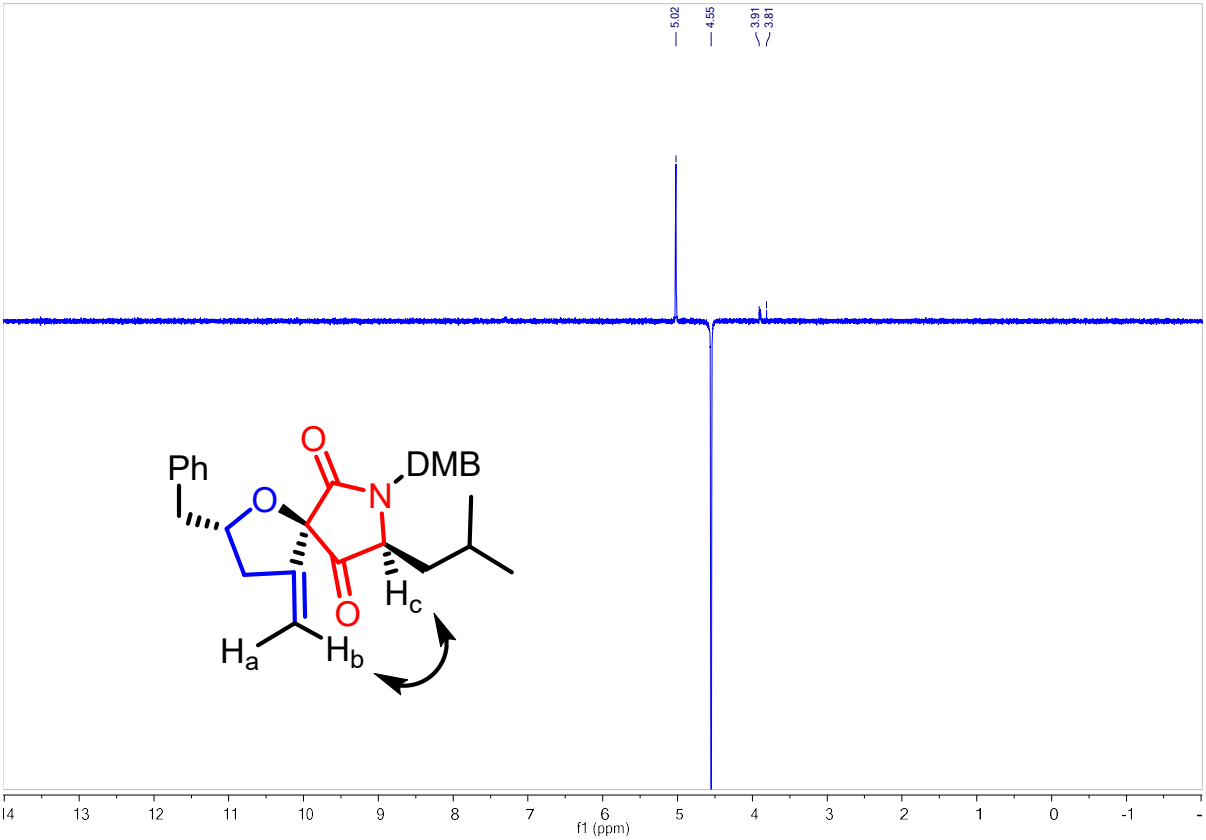
5.02
4.55
3.91
3.81
Ph
O
N
DMB
O
O
H_c
H_a
H_b
14 13 12 11 10 9 8 7 6 5 4 3 2 1 0 -1
f1 (ppm)

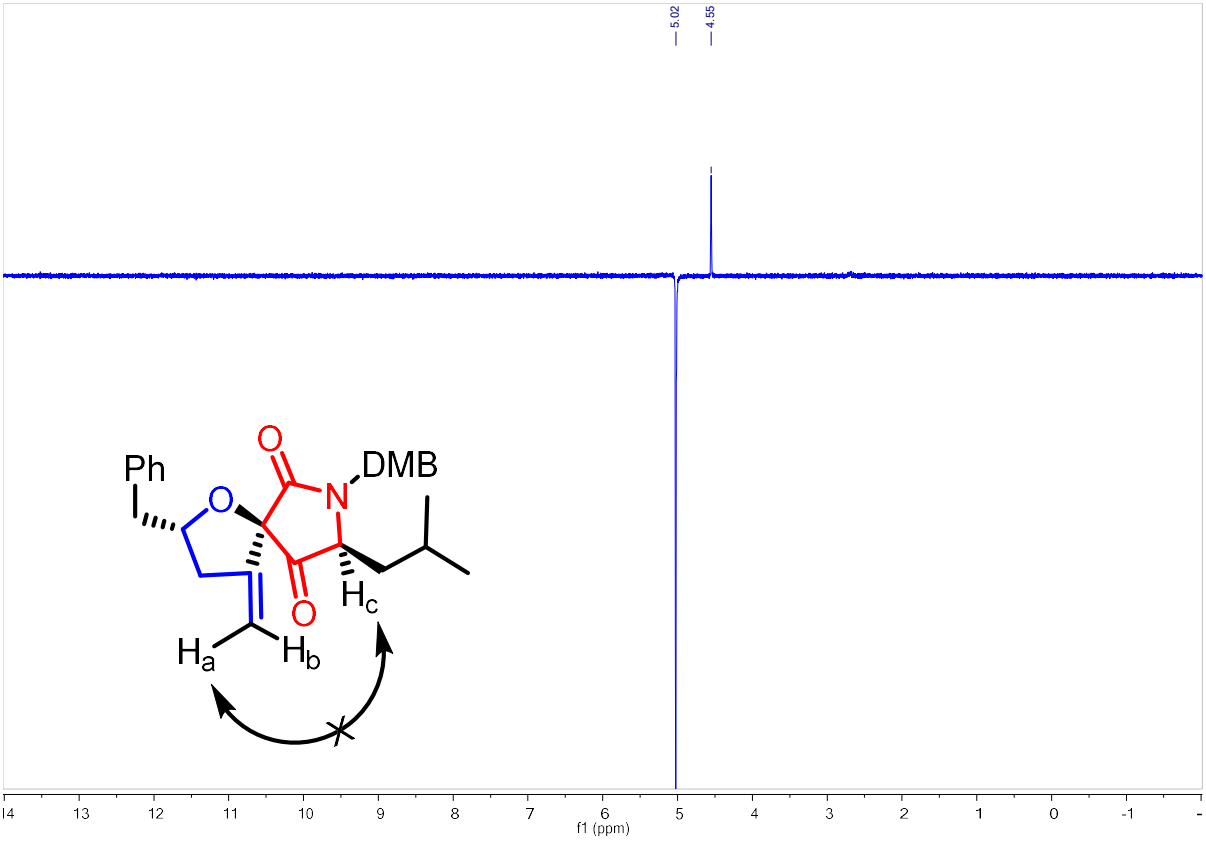
5.02
4.55
Ph
O
O
N
DMB
O
Hc
Ha
Hb
14
13
12
11
10
9
8
7
6
5
4
3
2
1
0
-1
f1 (ppm)

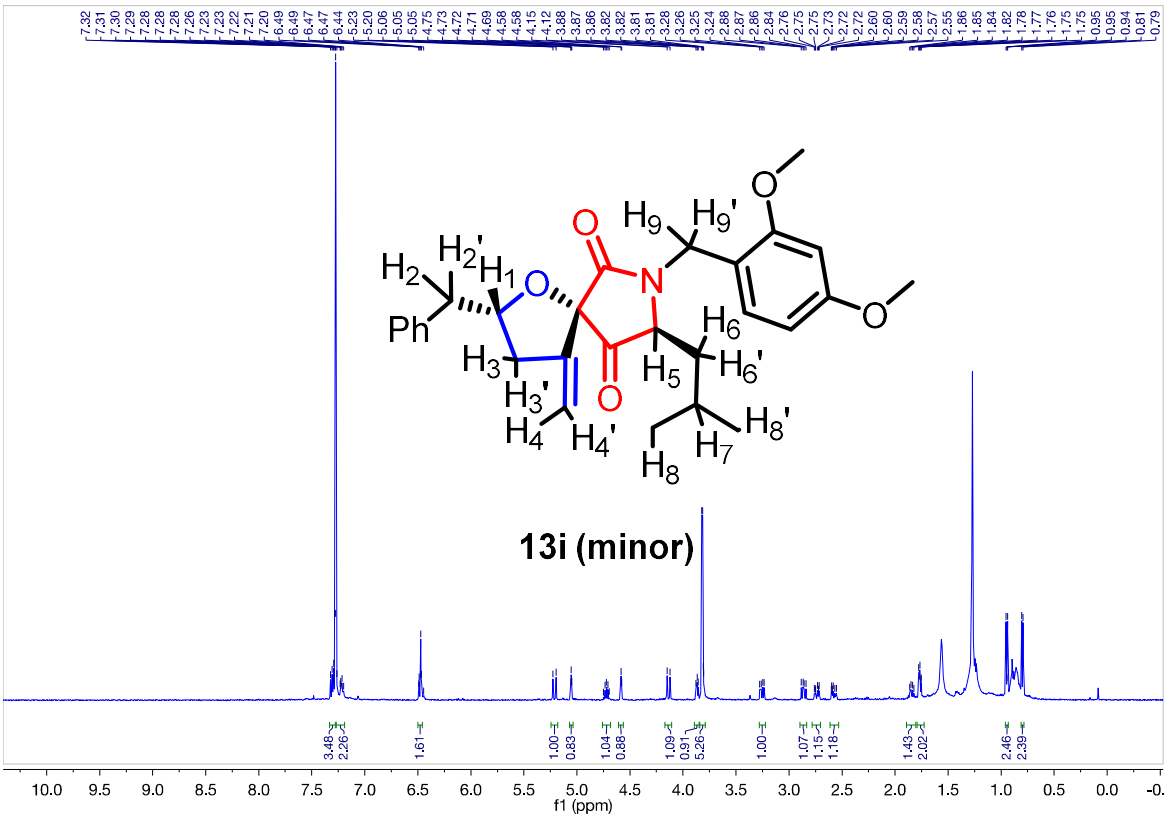
13i (minor)
f1 (ppm)

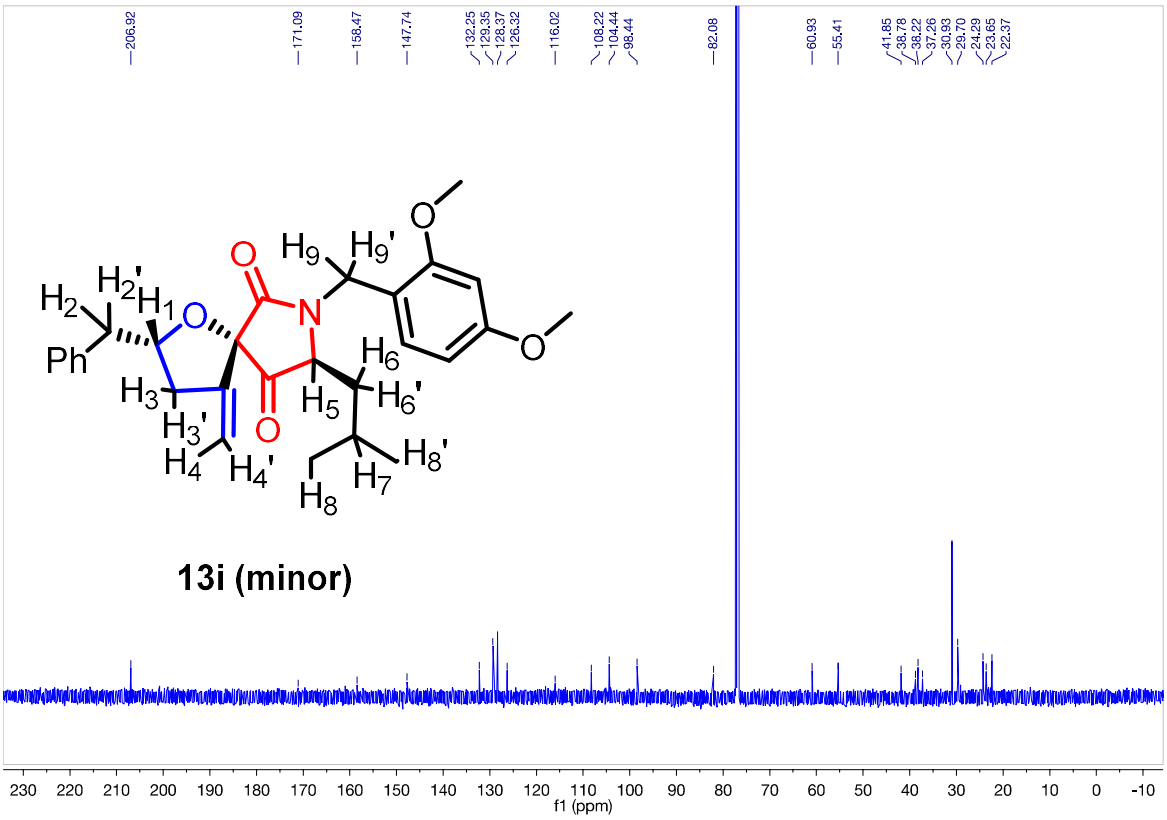
13i (minor)
f1 (ppm)

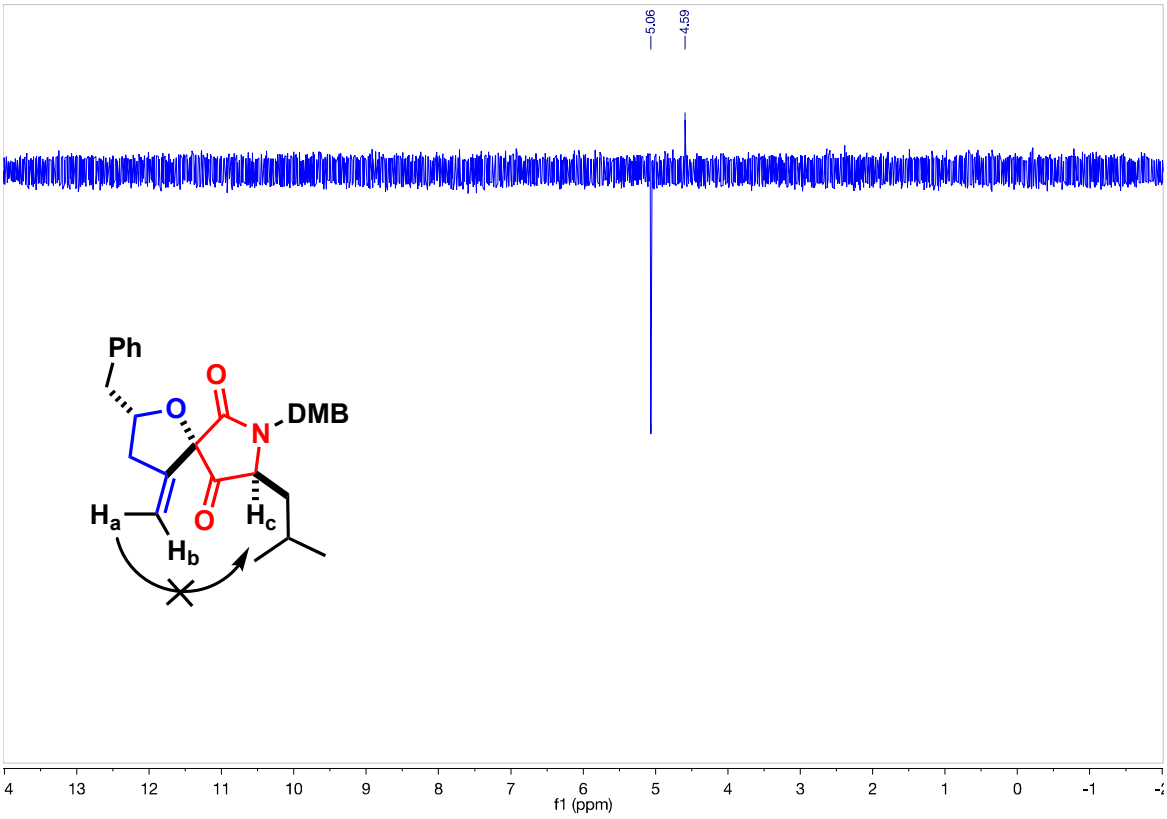
5.06
4.59
Ph
O
O
N
DMB
O
H_a
H_c
H_b
4
13
12
11
10
9
8
7
6
5
4
3
2
1
0
-1
f1 (ppm)

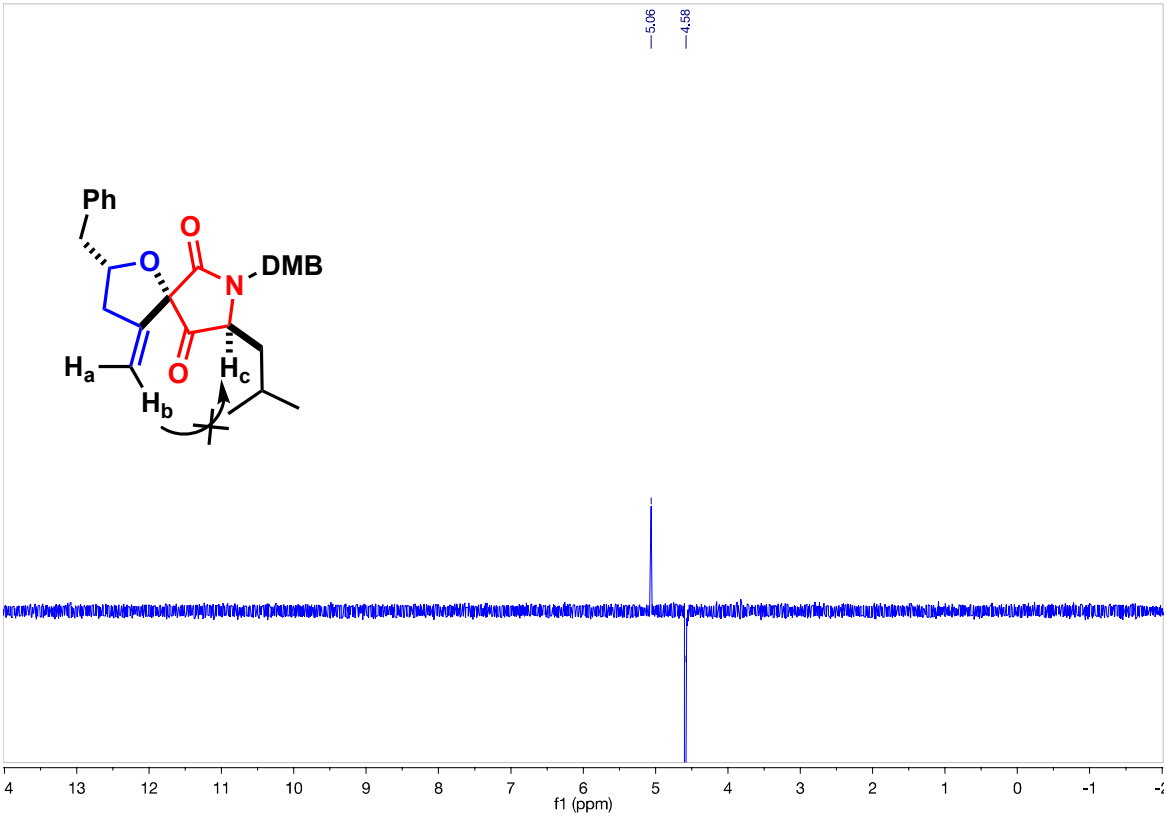
5.06
4.58
Ph
O
O
N
DMB
O
H_a
H_c
H_b
4
13
12
11
10
9
8
7
6
5
4
3
2
1
0
-1
f1 (ppm)

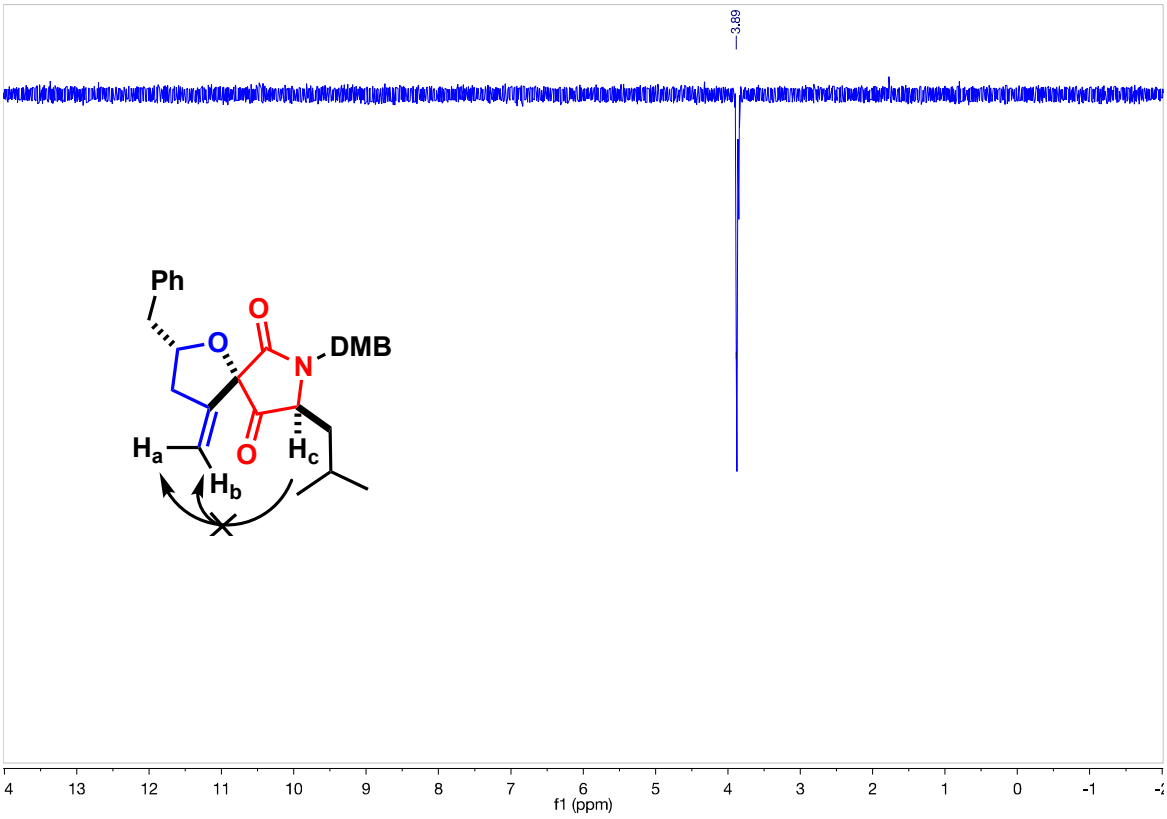
3.89
Ph
O
O
N
DMB
O
H_a
H_b
H_c
4
13
12
11
10
9
8
7
6
5
4
3
2
1
0
-1
f1 (ppm)

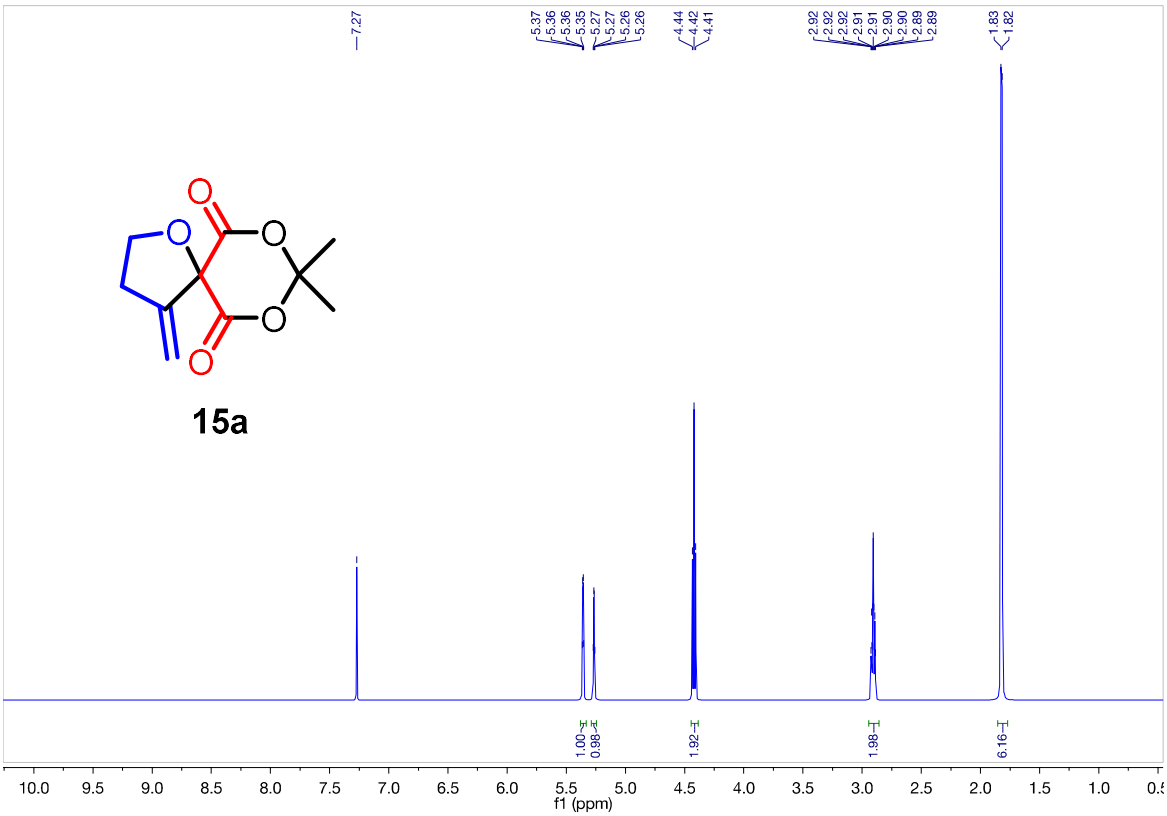
7.27
5.37
5.36
5.36
5.35
5.27
5.27
5.26
5.26
4.44
4.42
4.41
2.92
2.92
2.92
2.91
2.91
2.90
2.90
2.89
2.89
1.83
1.82
1.00
0.98
1.92
1.98
6.16
f1 (ppm)

15a

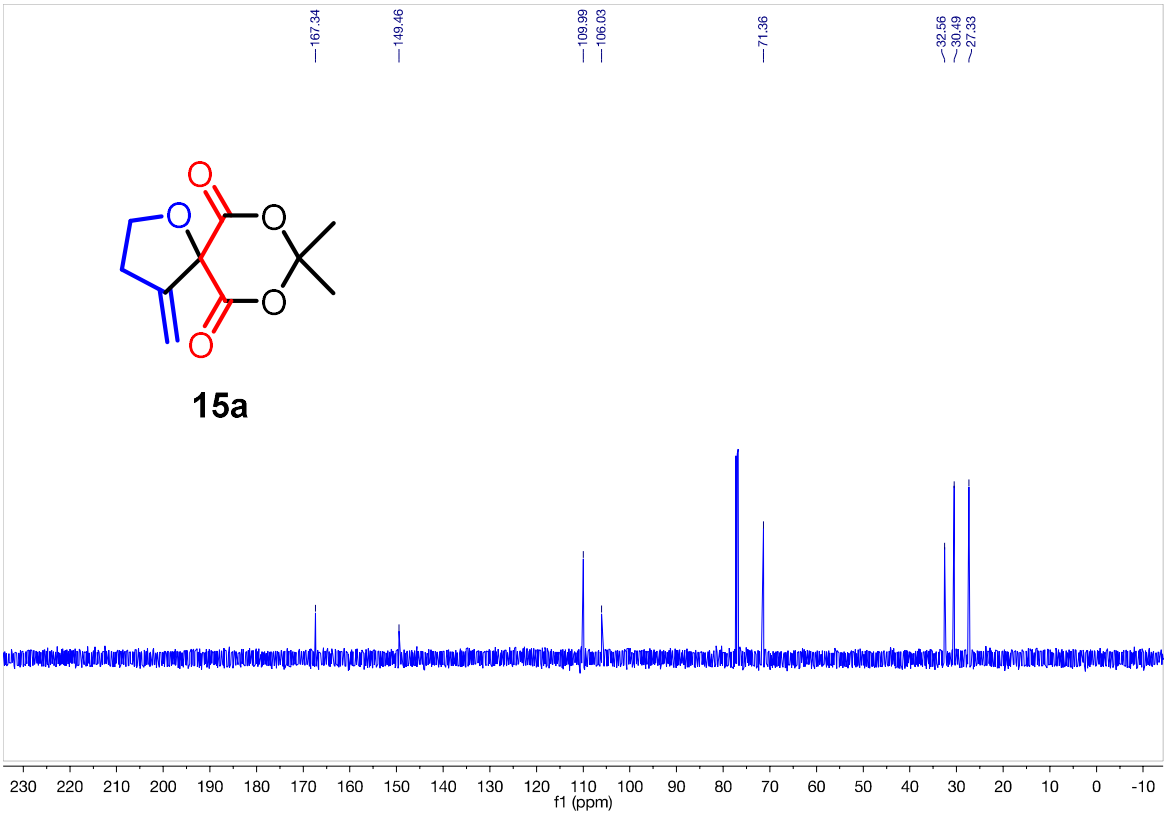
167.34
149.46
109.99
106.03
71.36
32.56
30.49
27.33
f1 (ppm)

15a

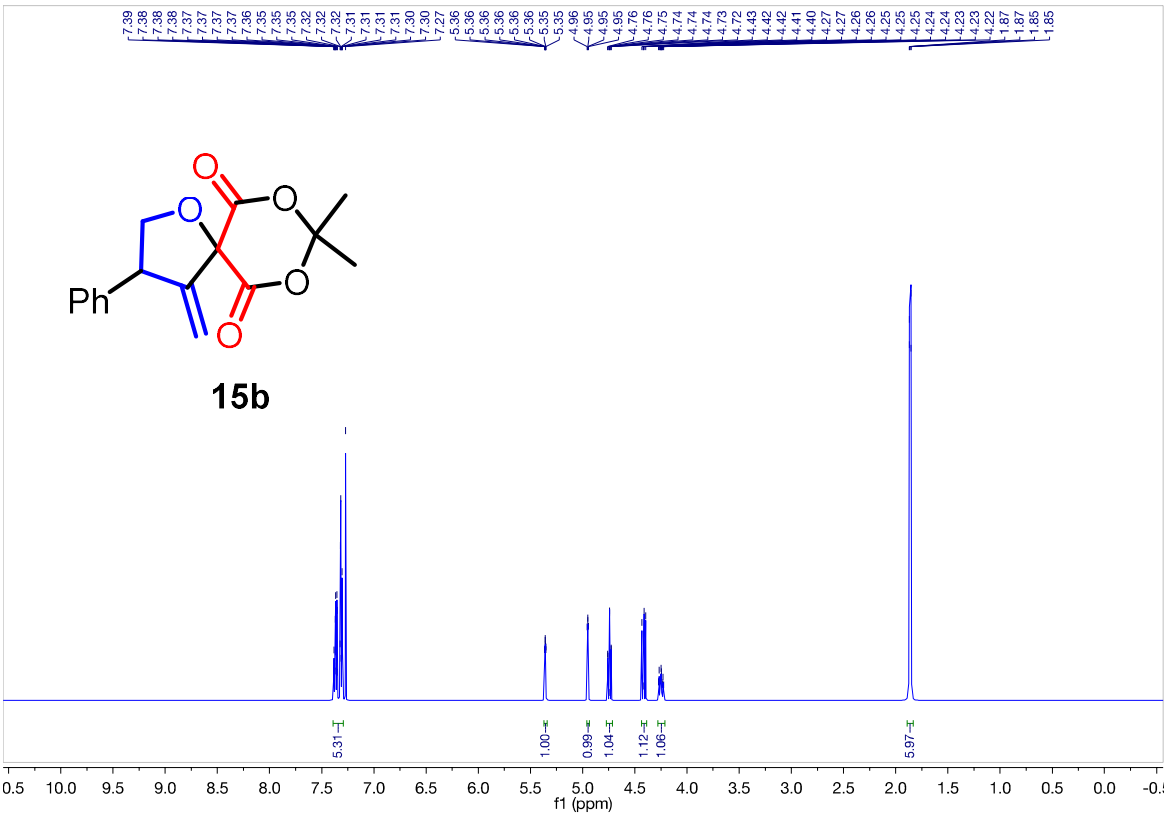
Ph
15b
f1 (ppm)

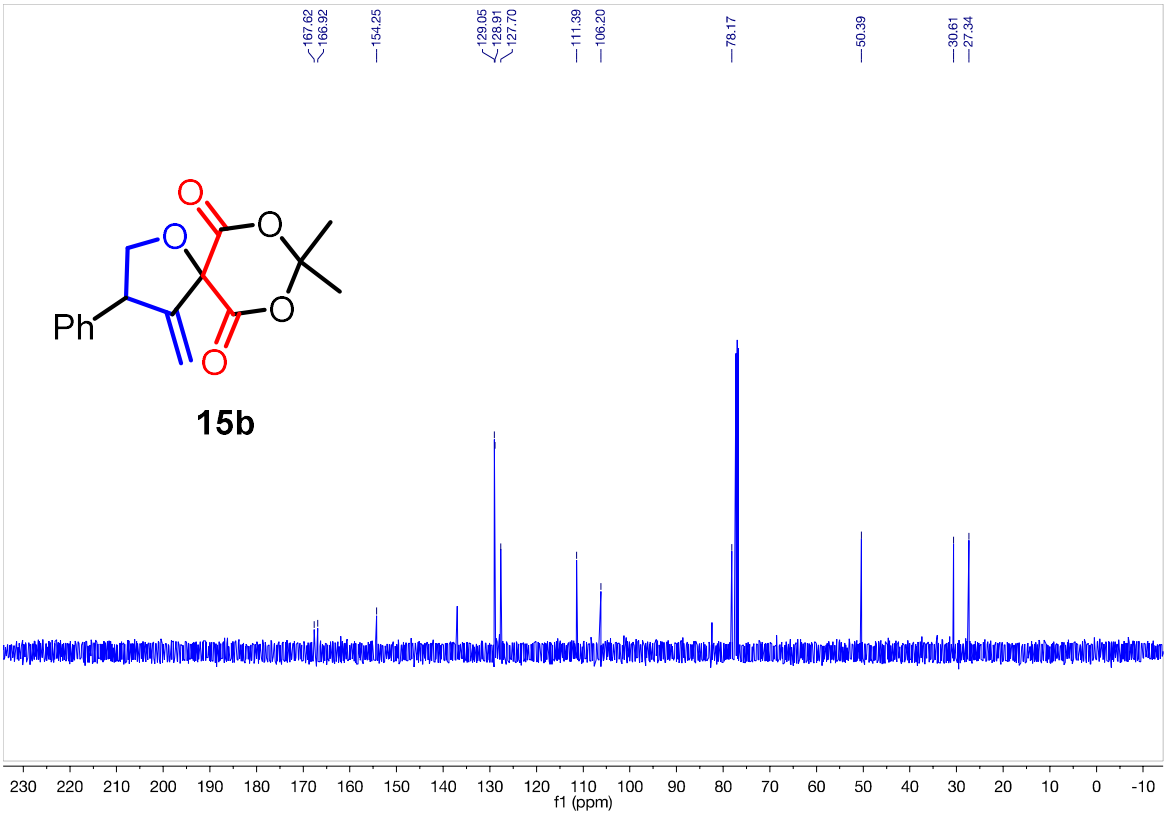
Ph
15b
f1 (ppm)

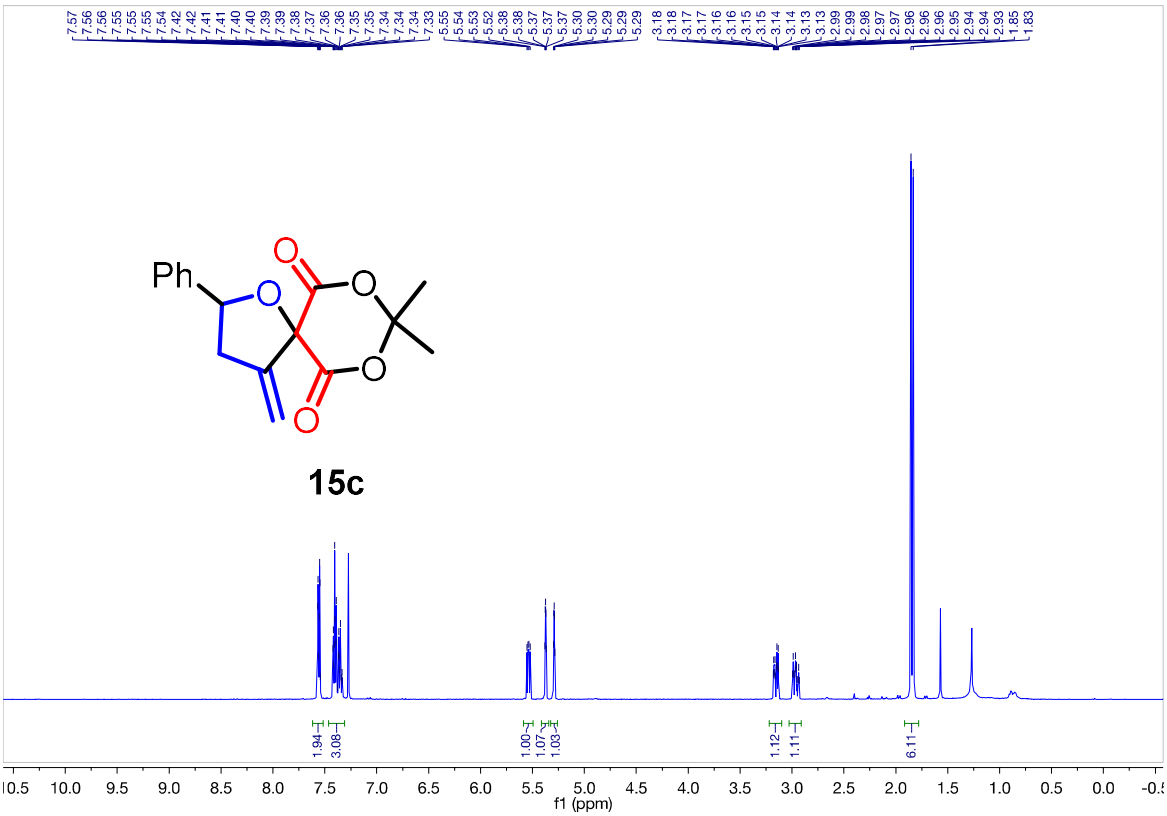
Ph
O
O
O
O
O
15c
1.94
3.08
1.00
1.07
1.03
1.12
1.11
6.11
f1 (ppm)

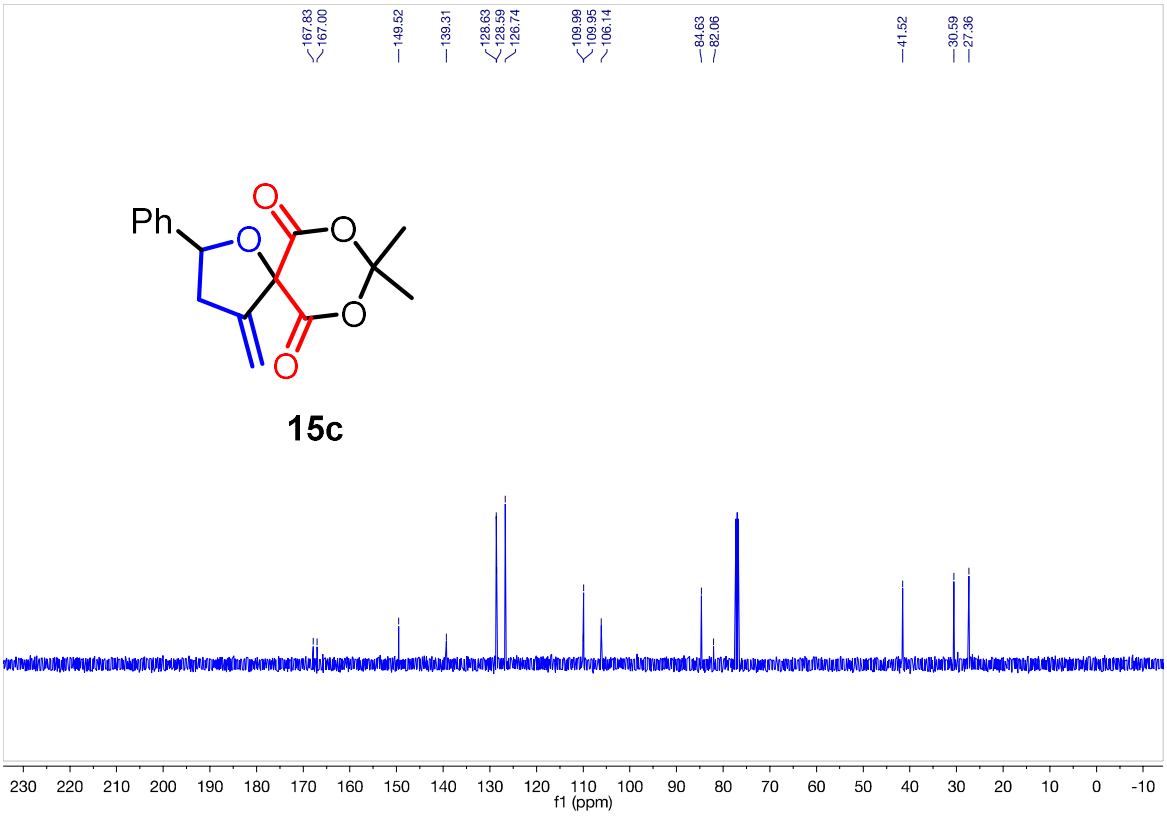
167.83
167.00
149.52
139.31
128.63
128.59
126.74
109.99
109.95
106.14
84.63
82.06
41.52
30.59
27.36
Ph
O
O
O
O
O
15c
f1 (ppm)

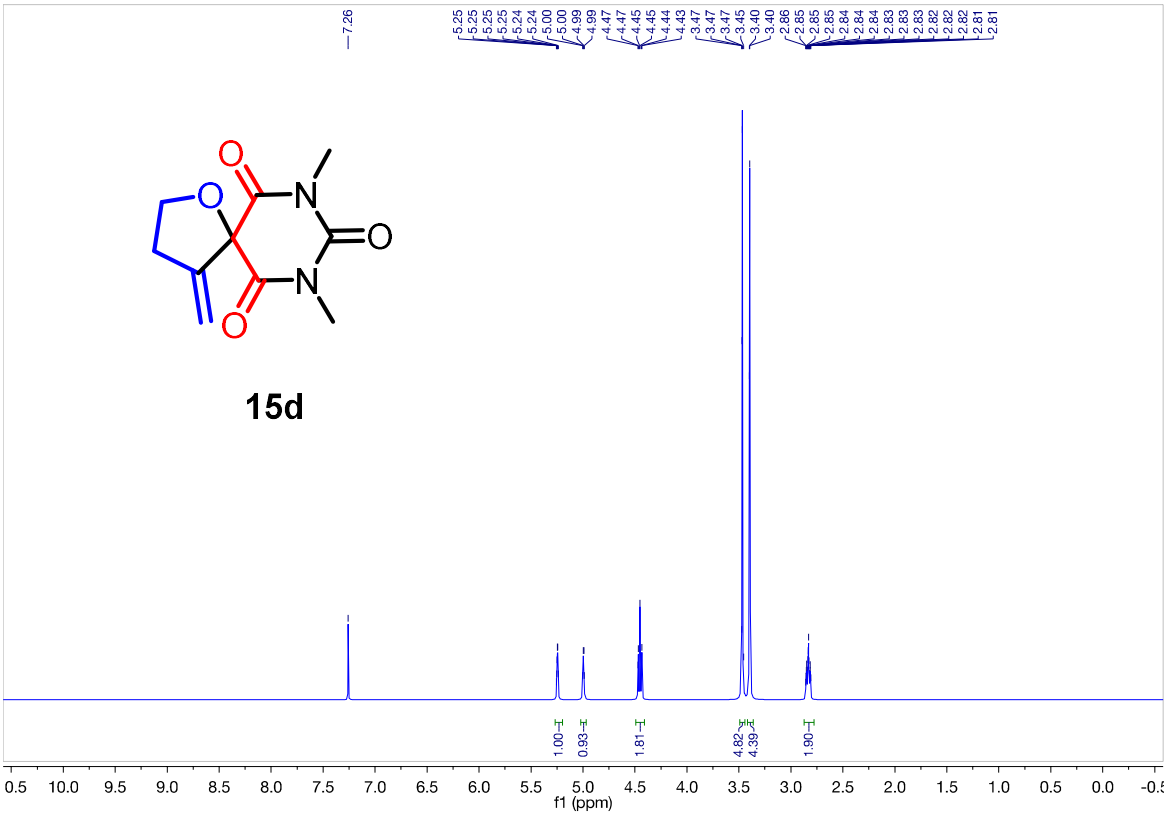
15d
f1 (ppm)

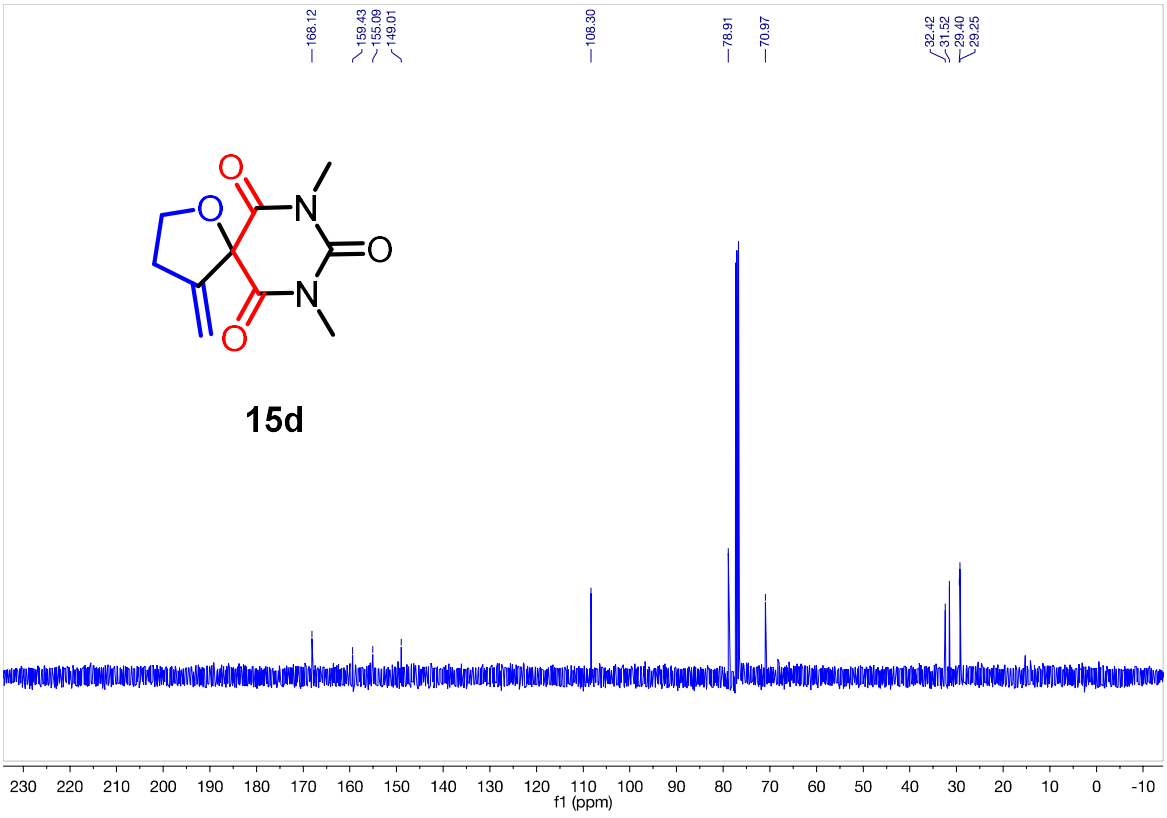
15d
f1 (ppm)

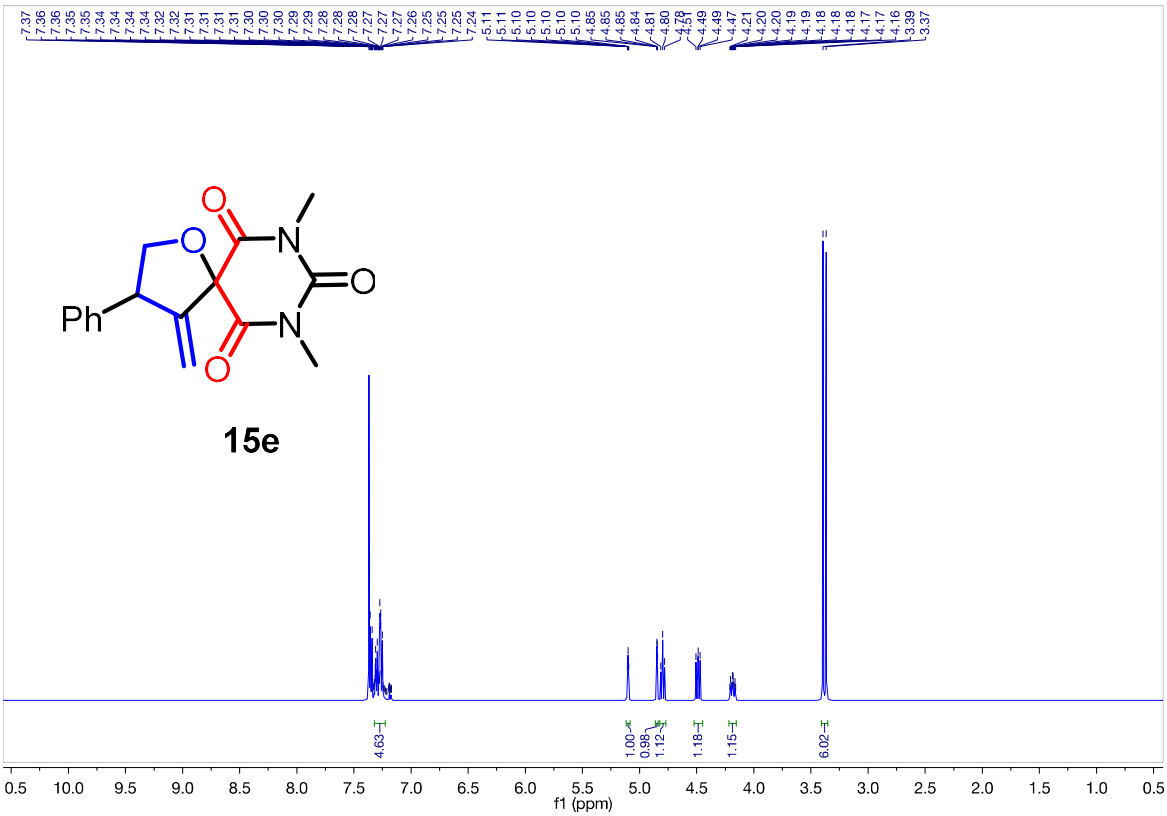
Ph
O
N
O
N
O
O
15e
4.63
1.00
0.98
1.12
1.18
1.15
6.02
f1 (ppm)

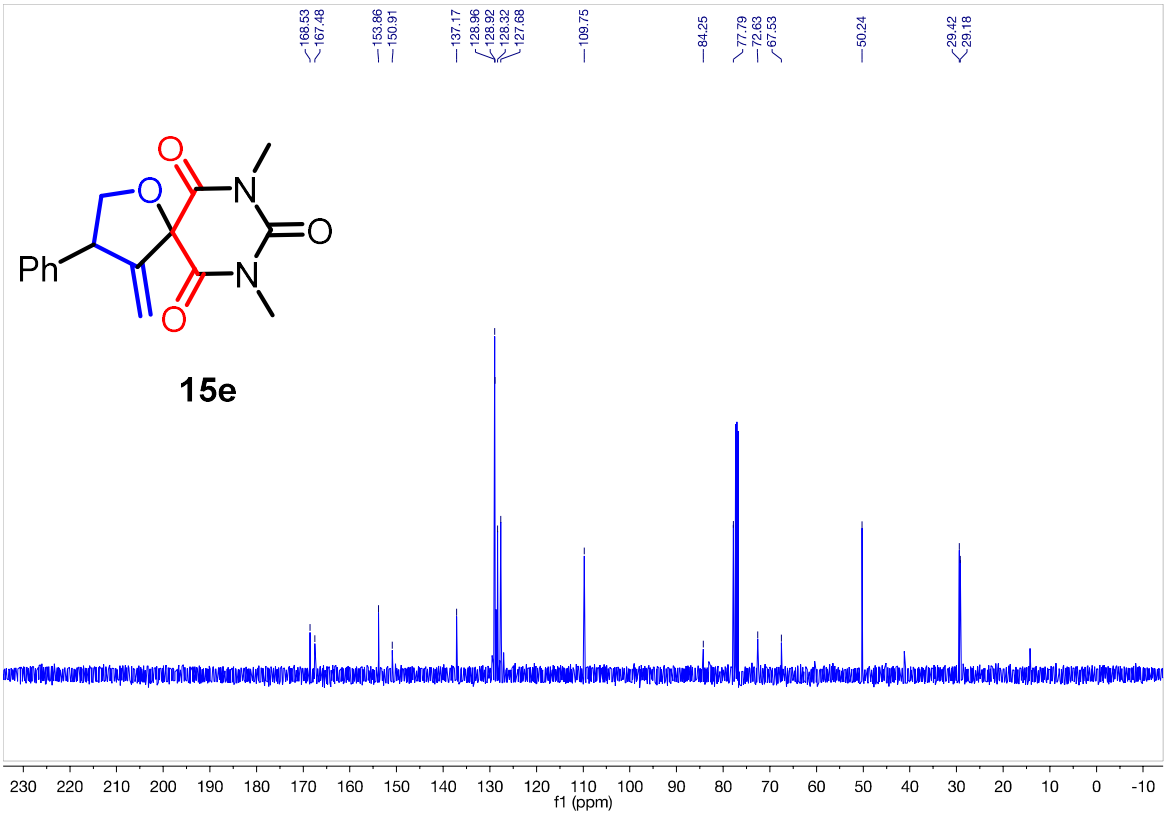
168.53
167.48
153.86
150.91
137.17
128.96
128.92
128.32
127.68
109.75
84.25
77.79
72.63
67.53
50.24
29.42
29.18
Ph
O
N
O
N
O
O
15e
f1 (ppm)

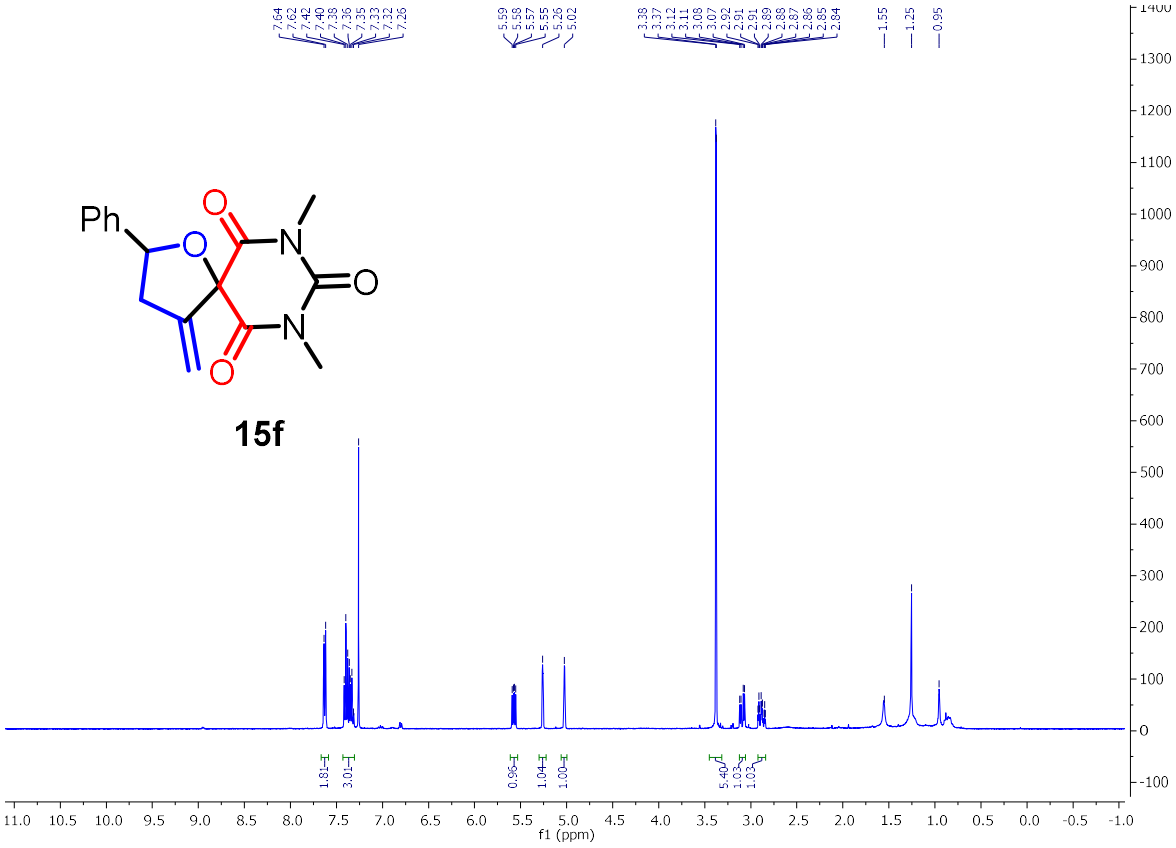
Ph
O
N
O
N
O
O
15f
f1 (ppm)

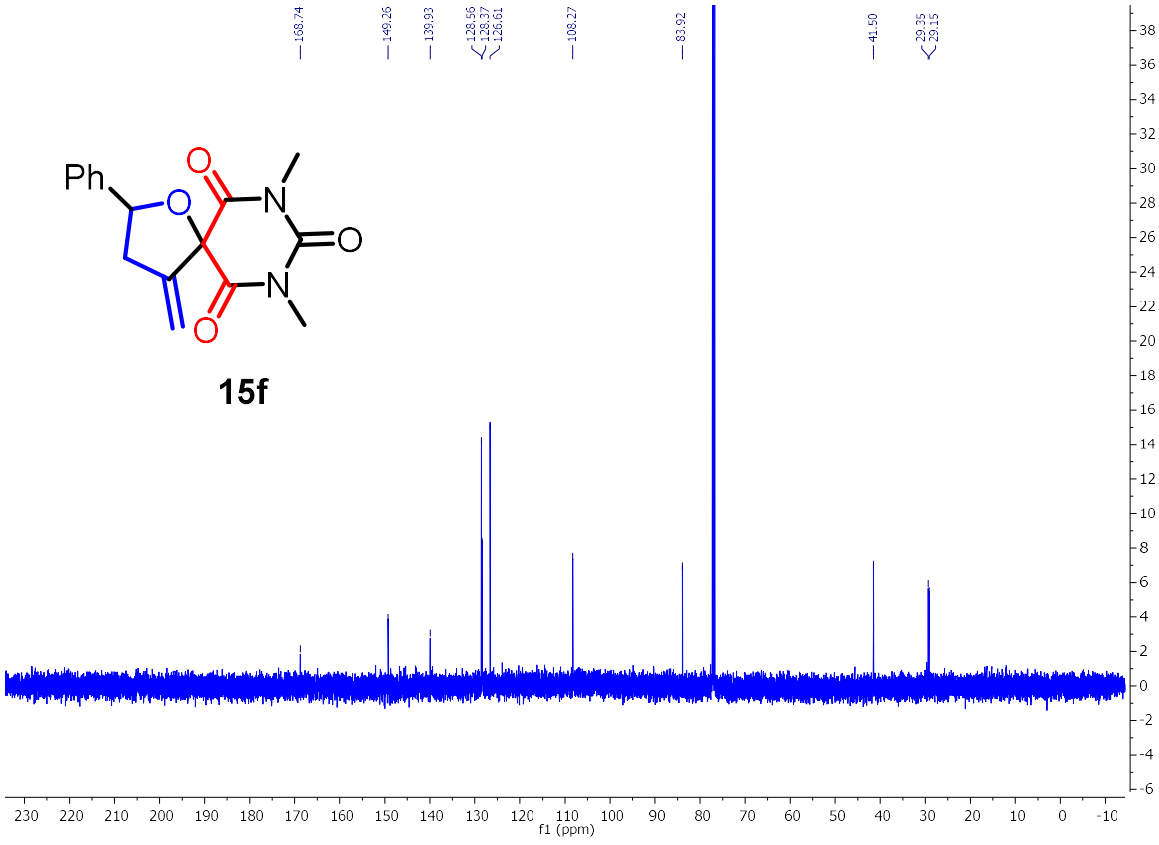
Ph
O
N
O
N
O
O
15f
f1 (ppm)

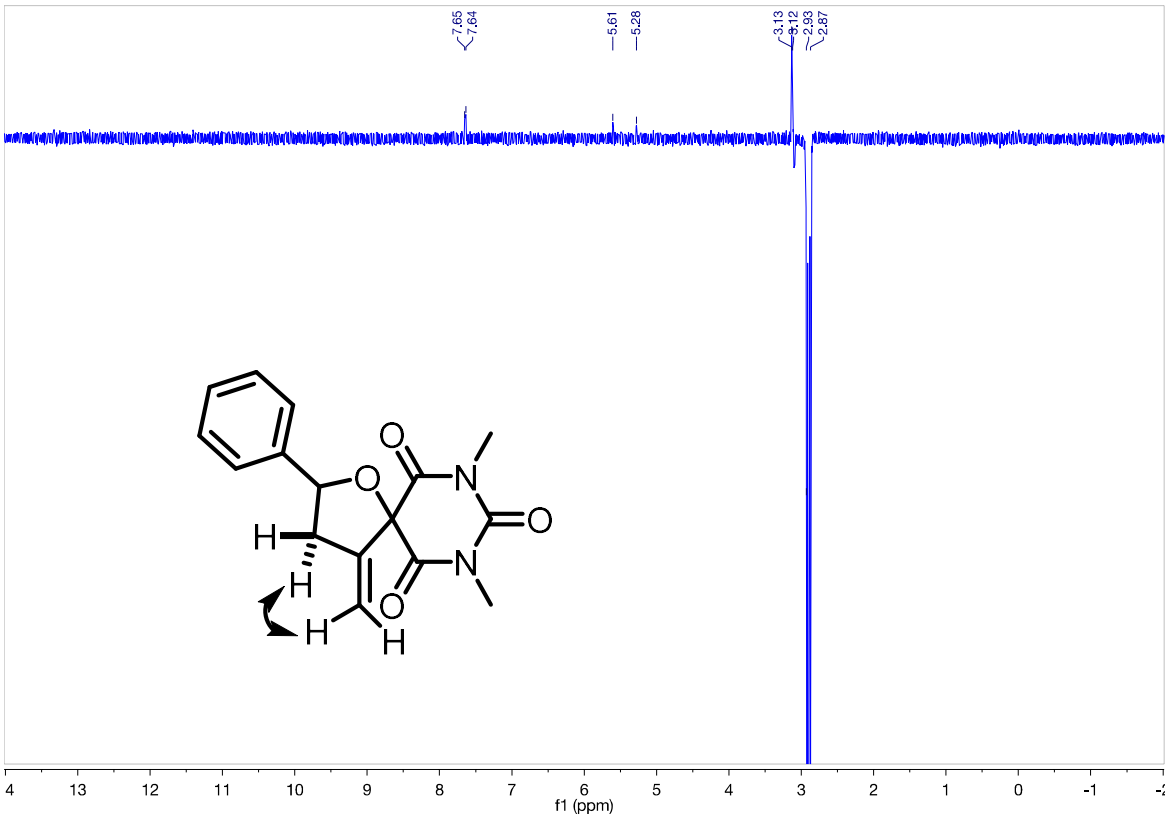
7.65
7.64
5.61
5.28
3.13
3.12
2.93
2.87
O
O
N
O
N
O
H
H
H
H
O
H
4
13
12
11
10
9
8
7
6
5
4
3
2
1
0
-1
f1 (ppm)

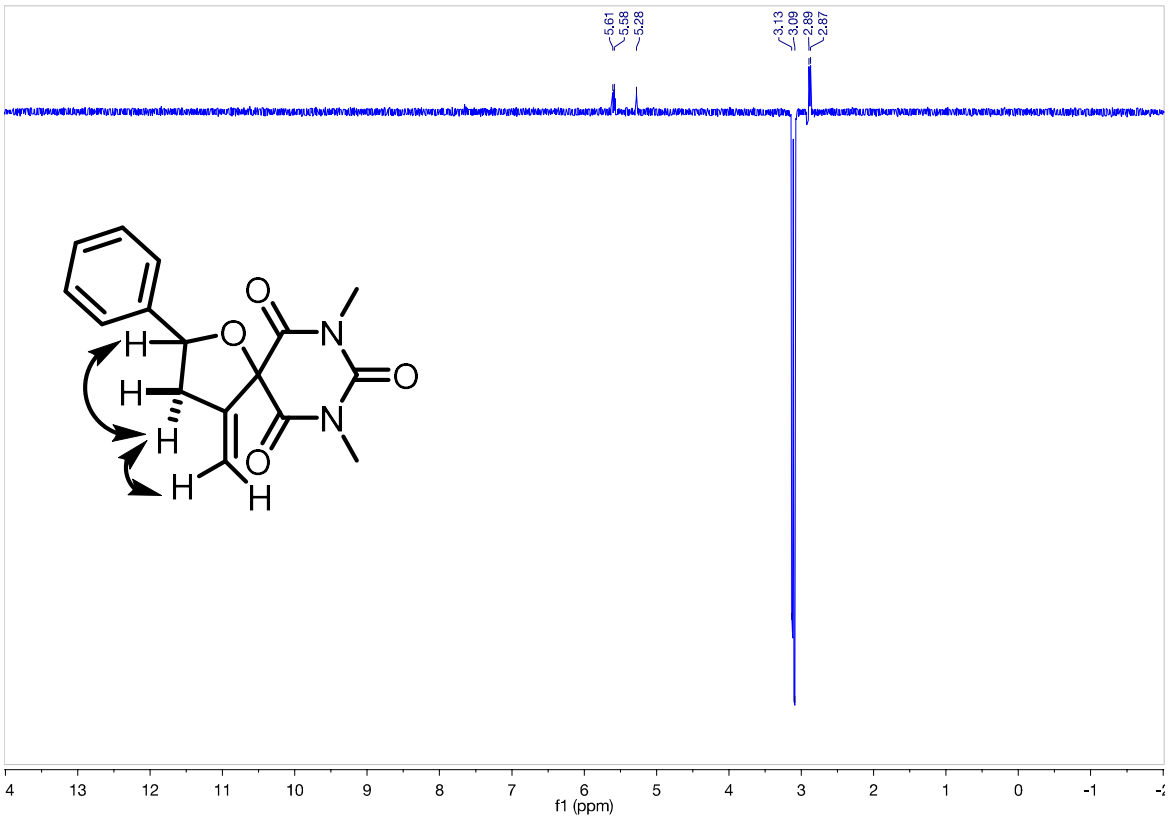
5.61
5.58
5.28
3.13
3.09
2.89
2.87
O
O
N
O
N
O
H
H
H
H
O
H
4
13
12
11
10
9
8
7
6
5
4
3
2
1
0
-1
f1 (ppm)

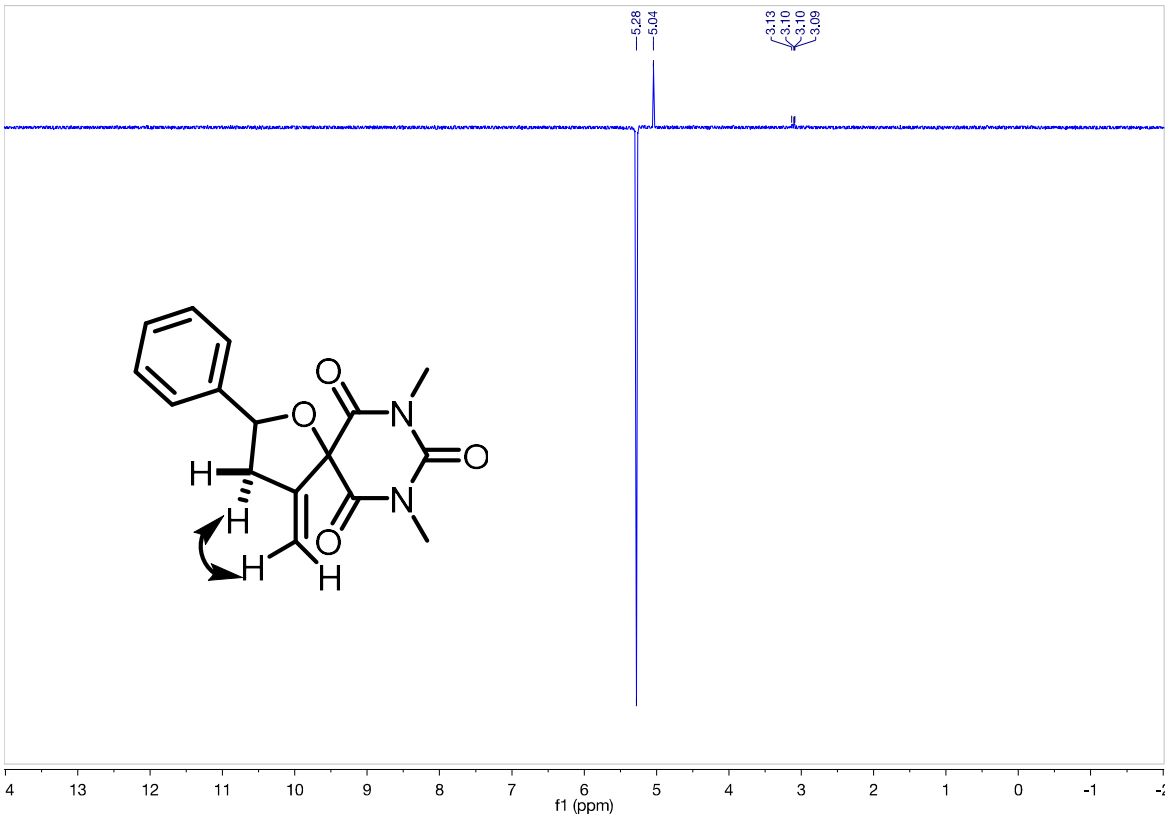
5.28
5.04
3.13
3.10
3.10
3.09
O
O
N
O
N
O
H
H
H
H
4
13
12
11
10
9
8
7
6
5
4
3
2
1
0
-1
f1 (ppm)

CHAPTER 3

Method Development for the Synthesis of Spirothiophenes and All-Carbon Spirocycles

3.1 INTRODUCTION

Our research team has had considerable success with combining carbene-insertion chemistry with Conia-ene electrophilic trapping chemistry to prepare a diverse library of heterocyclic scaffolds; so far, our methodology has successfully utilized carboxylic acid O–H, alcohol O–H, amine N–H, and sp^2 C–H insertion approaches to the corresponding heterocycle, and in all cases the cascade could be used to access spirocyclic scaffolds. We continue to explore

carbene-insertion chemistry of lesser-studied nucleophiles, namely the S-H insertion of thiols, and sp^3 C-H insertion of alkanes **(Scheme 3.1**).

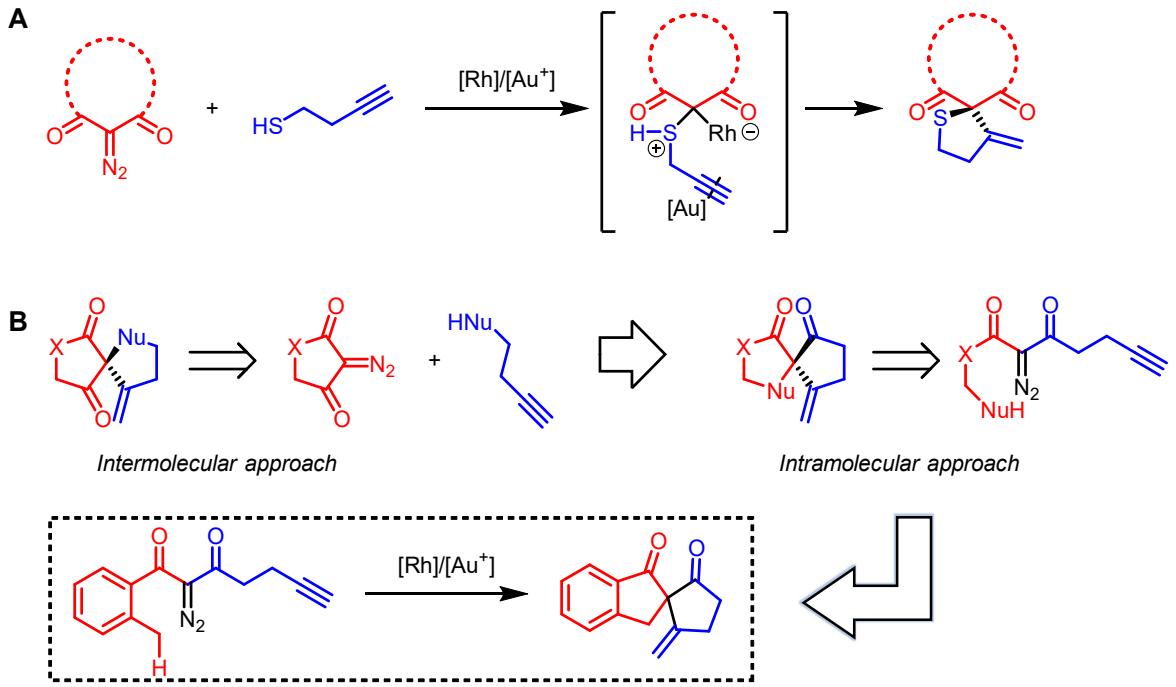

Scheme 3.1 a.) Rationale for carbene S–H insertion/Conia-ene cascade b.) Modified retrosynthetic disconnection for sp^3 C–H insertion/Conia-ene cascade

In order to address the challenge of forming all-carbon spirocycles, we needed to adjust our strategic rationale from an intermolecular approach, to an intramolecular one (**Scheme 3.1b**). Site-selective reactivity remains a major challenge in the field of C-H insertion, and intramolecular variants have been the most successful substrates due to the reduced entropic factor, arising from the close proximity between nucleophile and carbenoid. Additionally, we expect that constraining our desired site of C-H insertion through ring constraint would improve the entropic driving force for the reaction.

Sulfur heterocycles have received attention in the field of medicinal chemistry, and are often used in bioiosteric replacement of the corresponding nitrogen- and oxygen-

heterocycles. While the field also includes scaffolds bearing nitrogen in addition to sulfur, like thiazoles, isothiazoles, and thiazolidines – 5-membered thiophenes and 6-membered thiopyrans all well represented in biologically active scaffolds.[1a] Additionally, all-carbon spirocycles are found in a number of synthetic and naturally-occurring compounds with unique biological activity.[1b-1d] Our innovative carbene cascade methodology seeks to provide new step- and atom-economic methods to provide such heterocycles.

3.1.1 S–H INSERTION TO DIAZO-DERIVED CARBENES

While the carbene O–H insertion reaction has been well studied for nearly a half-century, the reactivity of the isoelectronic sulfur S–H insertion reaction has only received moderate attention. These studies employed the use of reactive Donor/Acceptor diazo compounds, and predominantly benzylic/aromatic thiol substrates.[2] Only a handful of somewhat dated reports exist, however, into the S-H insertion of Acceptor/Acceptor carbenoids.[3]

There are many similarities between the reactivity of O–H and S–H nucleophiles with carbenes, but one key difference leads to an entirely different reactive pathway for thiols (**Scheme 3.2**).

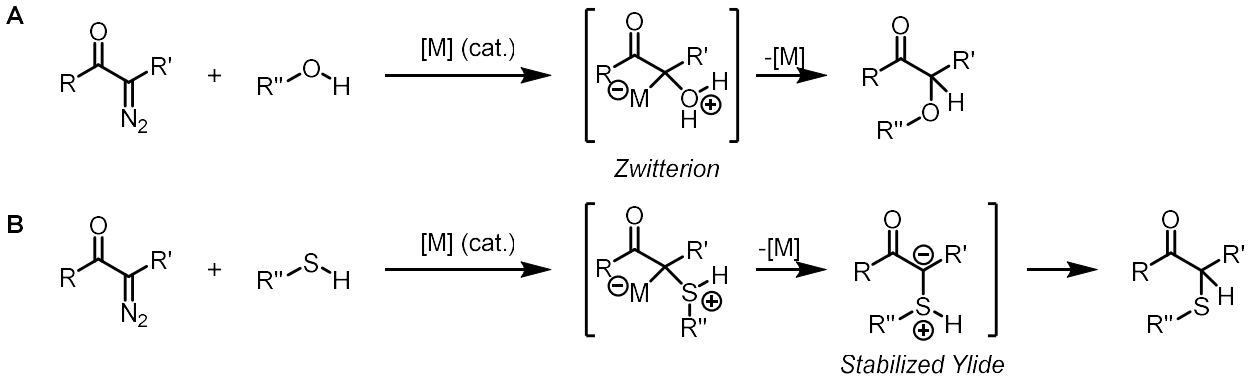

Scheme 3.2. a.) General mechanism for carbene O–H insertion b.) Analogous reaction mechanism for S–H insertion

In both cases, a suitable metal catalyst decomposes the diazo compound to generate the reactive carbenoid, which bonds to either the oxygen- or sulfur-lone pair electrons. In the case of O–H insertion, the zwitterionic intermediate then undergoes 1,2-proton transfer to give the corresponding insertion compound, but in the case of S–H insertion the metal is capable of dissociation to generate a stabilized ylide. 1,2-proton transfer of this intermediate then provides the S–H insertion product. In addition, this ylide intermediate is capable of undergoing a number of sigmatropic rearrangements if thioethers are employed as substrates in place of thiols.

3.1.2 S–R INSERTION TO CARBENES & REARRANGEMENT REACTIONS

Because they proceed through a somewhat stable ylide intermediate, thioethers are able to undergo a number of rearrangements, dependent on the identity of their substituent (**Scheme 3.3**).[4]

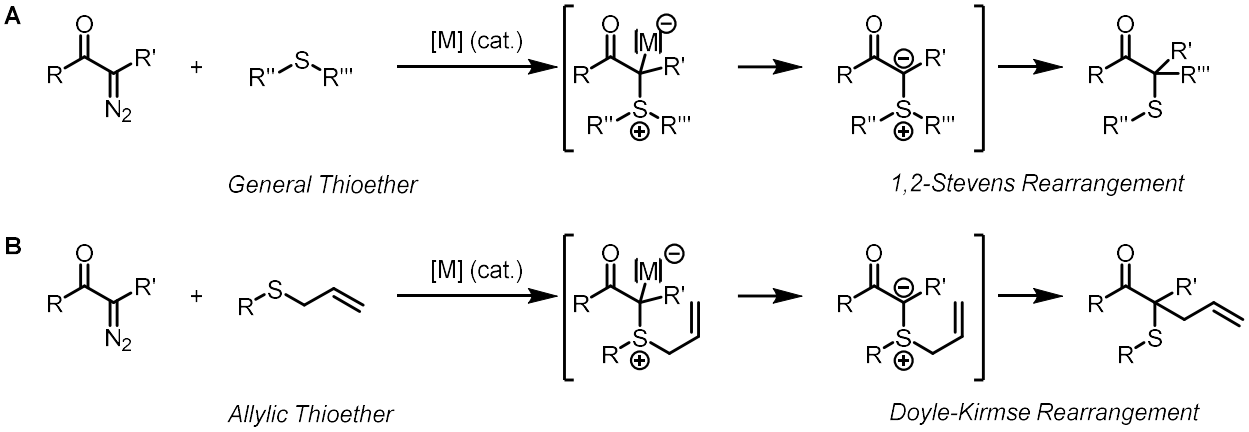

Scheme 3.3. a.) 1,2-Stevens rearrangement of sulfur ylide intermediates b.) Doyle-Kirmse rearrangement of sulfur ylide intermediates

Generally, sulfur-ylide intermediates are capable of undergoing a 1,2-Stevens rearrangement, in which an alkyl migration occurs to provide a thioether product (**Scheme 3.2a**). These ylide intermediates have shown to be suitably stable for isolation, then photochemically

converted to the rearranged product.[4d] In the case of strongly electron deficient benzylic migrating groups, the related Sommelet-Hauser rearrangement is possible, in which the bond migration occurs to the *ortho*- ring position.

A similar rearrangement reaction, the Doyle-Kirmse rearrangement, occurs in the case of allylic thioethers under carbene-insertion conditions. (**Scheme 3.3b**). This concerted [2,3]-sigmatropic rearrangement is known to occur under thermodynamic or photochemical conditions, and in the case of propargylic thioethers, has produced isolable allene products. Notably, there have been developments in both earth abundant catalysis and asymmetric induction for the Doyle-Kirmse reaction.[4g,4h] Unlike the related S–H insertion reaction, S–R insertion has been well studied for Acceptor/Acceptor diazo substrates, and has even been used as a key step in several total synthesis.[4a,4d]

3.1.3 C–H INSERTION TO DIAZO-DERIVED CARBENES: REACTIVITY & MECHANISM

The C–H bond is ubiquitous in organic compounds, and selective utilization of this fundamentally inert functionality, remains a major challenge in organic synthesis. The field of C–H functionalization, which has received considerable attention in the last decade, has established several unique strategies to promote C–H reactivity. Such strategies have been comprehensively collected in a number of reviews.[5]

The process of C-H functionalization, broadly describing the cleavage of a C–H bond which then binds to a new functionality, includes two distinct strategies – C–H activation, and C–H insertion. C-H activation is classified by stepwise cleavage of a C–H bond by oxidative addition of an appropriate metal catalyst, followed by further functionalization using an organic substrate.

A representative example of this includes the common catalytic cycle of Rhodium(III) cylopentadenyl dimers (**Scheme 3.4a**).[5a]

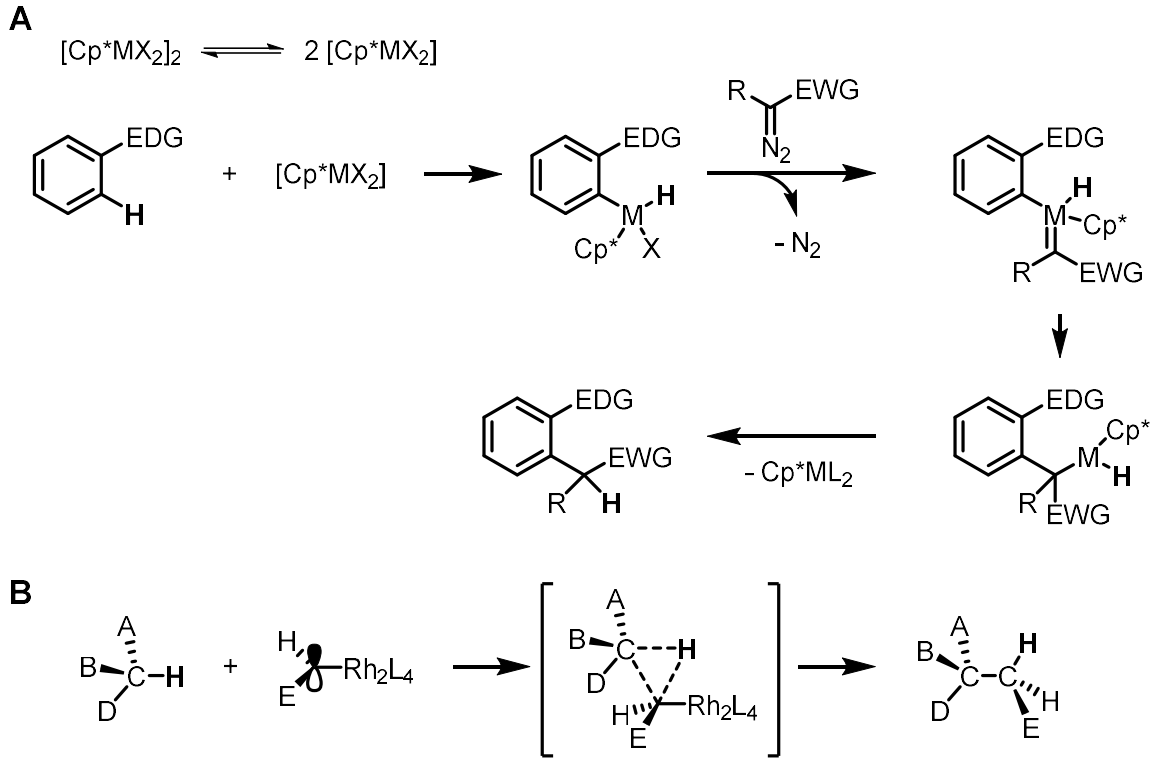

Scheme 3.4. a.) Doyle's proposed mechanism for C–H insertion to rhodium carbenoids. b.) general mechanism for sp^2 C–H activation by metal(III) catalysts.

In this C–H activation approach, the rhodium (III) catalyst undergoes oxidative addition to the sp^2 C–H bond of electron-rich arenes to generate a rhodium (II) intermediate, capable of decomposing diazo substrates. Migratory insertion of the carbenoid ultimately generates the C–H functionalized product.

C–H Insertion, meanwhile, can occur using carbenes generated with dirhodium(II) carboxylate dimers. C-H Insertion occurs through concerted homolysis the C-H bond, with simultaneous bond formation to the carbenoid (**Scheme 3.4b**).[5f,5h]

A major challenge in C–H functionalization is site-selectivity. Because the C–H bond is so prevalent, trying to promote reactivity commonly results in a complex mixture of products, especially in the case of intermolecular reactions. In fact, an early quote by diazo pioneer Mike Doyle states that "Intermolecular C–H insertion reactions… are not synthetically useful." This challenge has been addressed, and predominantly overcome, in the subsequent decades through efforts by research teams of Davies, Teyssie, and Moody, among others. Early reports by the Teyssie group showcase the intramolecular C–H insertion reactivity of ethyl diazoacetate to unactivated alkanes, which was moderately tunable by altering the electronics of the accompanying dirhodium(II) carboxylate dimer (**Scheme 3.5**).[5i,j]

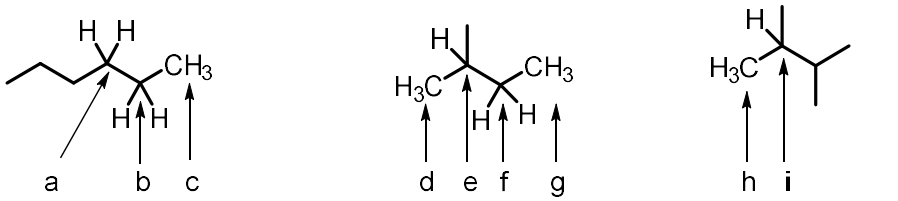

n-Hexane *2-methylbutane* *2,3-dimethylbutane*

Catalyst	a	b	c	d	e	f	g	h	i	Comments
$Rh_2(OAc)_4$	33	63	4	5	8	90	1	5	95	*Low yielding*
$Rh_2(TFA)_4$	31	64	5	5	25	66	4	12	88	*Higher Yields*
$Rh_2(9\text{-trp})_4$	9	61	30	18	18	27	37	33	67	*Highest Yields*

Scheme 3.5. Teyssie's survey on selectivity in intermolecular C–H insertion to ethyl diazoacetate.

As preliminarily shown by Teyssie's bulky $Rh_2(9\text{-trp})_4$ catalyst results, further developments of dirhodium(II) carboxylate catalysts can help overcome the selectivity issues rampant in the field of C-H insertion. The group of Huw Davies disclosed a new bulky, chiral

dirhodium(II) catalyst in 1996 – tetrakis[(S)-(-)-N-(p-dodecylphenylsulfonyl)prolinato]dirhodium(II) (Rh_2(*S*-DOSP)$_4$). In the years to follow, Davies and coworkers would go on to showcase Rh_2(*S*-DOSP)$_4$'s excellent reactivity in the intermolecular C-H Insertion of donor-acceptor diazos into an array of C-H substrates (**Scheme 3.6**).[5f]

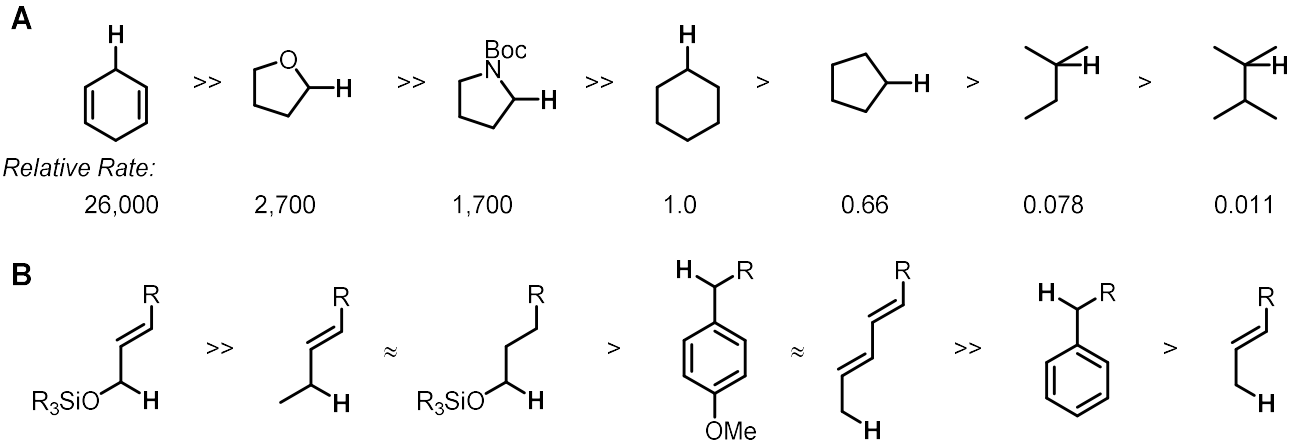

Scheme 3.6. a.) Davies' study towards the reaction rates of C-H substrates towards insertion. b.) Survey of reactivity for allylic and benzylic substrates towards with aryldiazo acetates.

In a series of competition studies, Davies' was able to observe a high reaction rate for substrates capable of stabilizing a positive charge (**Scheme 3.6a**). Namely, the allylic system and adjacent to a heteroatom. Interestingly, in the case of 1,3-cyclohexadiene, the rate of C–H insertion overcame the rate of cyclopropanation of styrene. Later, the group would determine a relative reactivity spectrum of allylic and benzylic systems (**Scheme 3.6b**). It was shown that allylic systems bearing conjugation to silyl ethers displayed remarkable reactivity. Electron-neutral and electron-rich benzylic substrates meanwhile produced moderate reaction rates, while not overcoming the rate of secondary allylic substrates. With insight towards harnessing C–H insertion reactivity, we designed a substrate which would employ benzylic C–H insertion in a cascade manner.

3.2 DIVERGENT S-H INSERTION/CONIA-ENE CASCADE APPROACH TO SPIROTHIOPHENES

In order to access a new realm of heterocycles and spiroheterocycles based on sulfur, we pursued the synthesis of mercaptyne substrates, capable of undergoing a S–H insertion/Conia-ene cascade.

3.2.1 SYNTHESIS OF SECONDARY MERCAPTYNE PRECURSORS

Thiols were prepared in a four-step sequence from commercially available styrene oxide (**Scheme 3.7**).

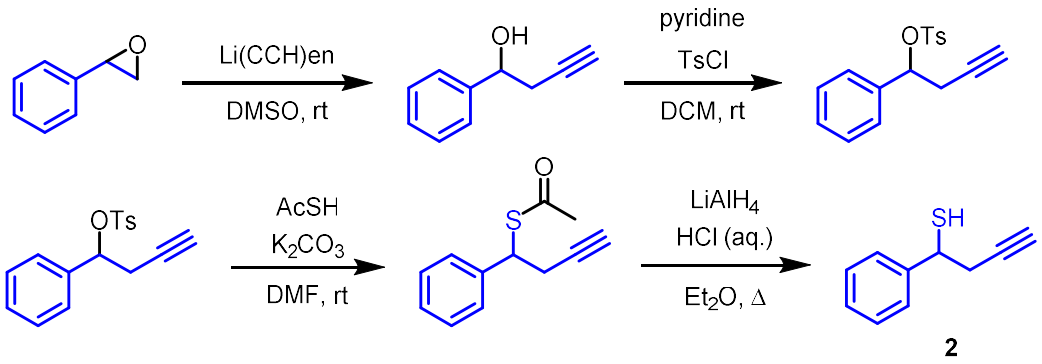

Scheme 3.7. Synthesis of secondary mercaptyne **2**

First, styrene oxide was exposed to ring-opening conditions with lithium actylide to produce racemic 2-phenylbutyn-1-ol. The alcohol was then converted to the corresponding tosylate, which was exposed to substitution conditions with *in situ* generated potassium thioacetate. The material could be stored as the thioacetate for long periods of time, and is converted to corresponding thiol **2** through hydride reduction conditions. While the route could be used to synthesize primary 3-butyn-1-thiol, we had difficulties during thiol isolation,

predominantly due to the volatility of the compound under vacuum. For this reason, we proceeded using secondary thiol **2**.

3.2.2 STEPWISE APPROACH TO SPIROTHIOPHENES

With a route established to the desired mercaptyne substrates, we turned our attention towards reaction optimization (**Scheme 3.8**). We began our optimization studied by using $Rh_2(esp)_2$, our previously established catalyst for O–H insertion. We had previously observed success in the stepwise Conia-ene cyclization of Acceptor/Acceptor O–H insertion products, so we envisioned being able to optimize the insertion and Conia-Ene steps individually, then proceed to a one-pot trial.

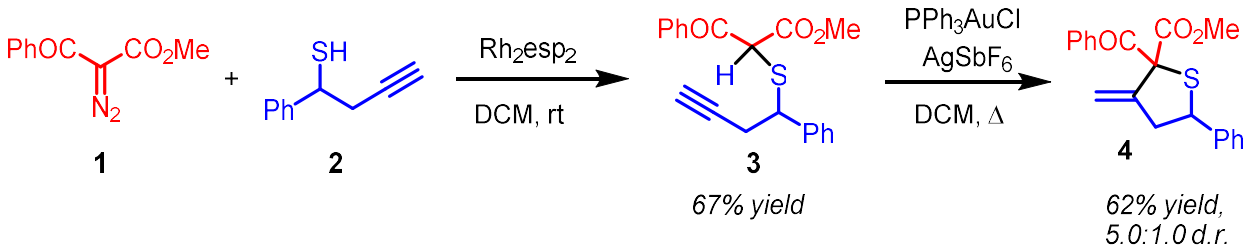

Scheme 3.8 Stepwise S-H insertion/Conia-ene sequence to hydrothioufuran **4**

First, ketoester diazo **1** and secondary mercaptyne **2** were exposed to $Rh_2(esp)_2$, and we were able to isolate insertion compound **3** with a moderate yield in dichloromethane at room temperature. Characterization of **3** by ^1H NMR was complication by the compound's tendency to undergo keto-enol tautomerization, and the diastereotopic peaks arising from a racemic nucleophile. We next exposed insertion product **3** to cationic gold catalytic conditions. We did not observe any conversion at room temperature, but quickly achieved conversion of **3** after

elevating temperatures to reflux. To our delight, we were able to isolate desired hydrothiofuran **4**, characterized by its diagnostic *exo*-olefin protons in ^{1}H NMR.

3.2.3 ONE-POT APPROACH TO THIOFURANOFURANS

Encouraged by this stepwise trial, we next turned our attention to one-pot conditions (**Scheme 3.9**).

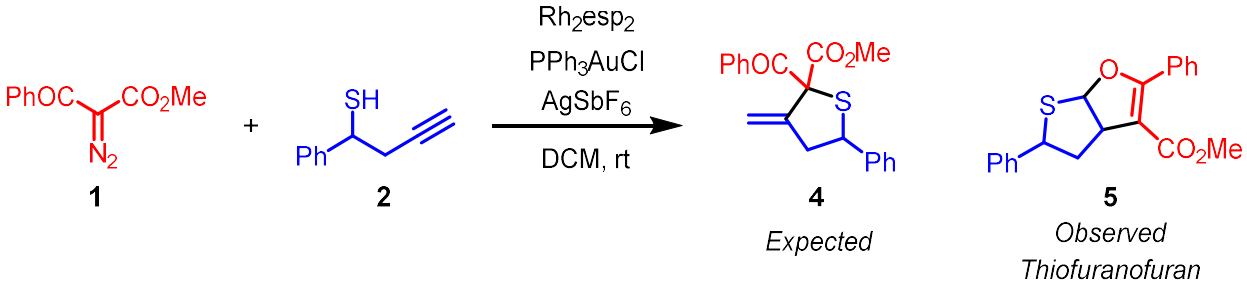

Scheme 3.9 One-pot S-H insertion/Conia-Ene trial

When diazo **1** and mercaptyne **2** were exposed to one-pot catalytic conditions, however, we did not observe any evidence of hydrothiophenes **4**. Instead, we characterized a product distinctly lacking a ketone peak, and with 2 new olefin peaks observable on ^{13}C NMR. We rationalize the formation of thiofuranofuran **5** due to interaction between mercaptyne **2** and the cationic gold catalytic conditions (**Scheme 3.10**).

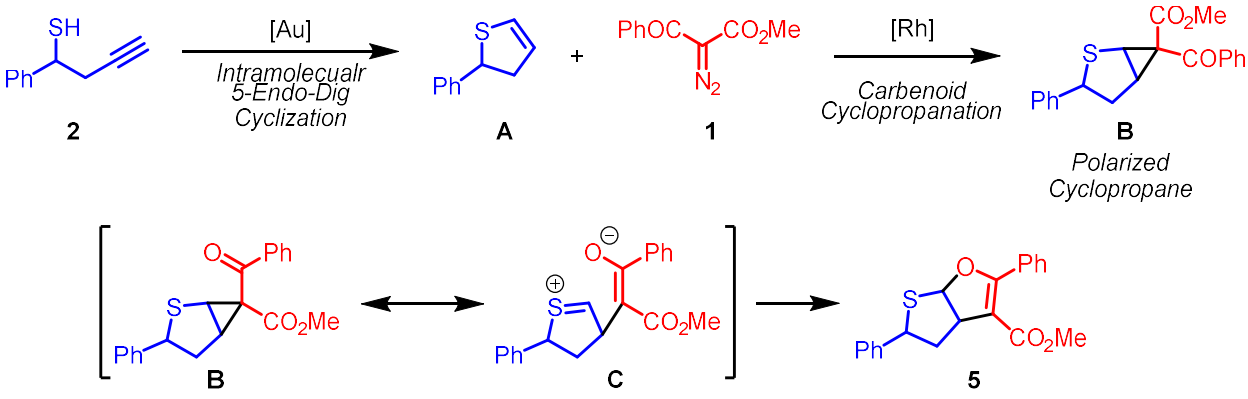

Scheme 3.10 Proposed mechanism for thiofuranofuran formation

We propose that, in the presence of cationic gold, mercaptyne **2** underwent a 5-*endo*-dig cyclization to produce thiophene **A** before diazo 1 was able to undergo S–H insertion. Instead, with the formation of a new olein, thiophene 1 underwent carbenoid cyclopropanation to produce polarized cyclopropane **B**. **C**, a resonance form of **B** showcases the electrophilicity of the thiophene C2 once a polarized cyclopropane is generated. Lastly, the enolate resulting from ring opening underwent O-alkylation to quench the sulfonium ion, resulting in formation of thiofuranofuran **5**.

While these preliminary results are not entirely encouraging, we have determined a novel new reactive pathway for secondary mercaptynes to generate a fused, heterocyclic scaffold. While these results may not bode well for a one-pot S–H insertion/Conia-ene approach to hydrothiophenes, reaction condition optimization may be able to circumvent the undesired 5-*endo*-dig cyclization of mercaptyne **2**.

For example, we could utilize slow addition of the diazo and gold mixture to a mixture of mercaptyne **2** and rhodium, which may circumvent the undesired 5-*endo*-dig cyclization; generation of carbenoids from diazos through gold catalysis is a known process however and should be anticipated from this approach. In addition, screening other additives besides silver salt for the generation of cationic gold could mitigate the undesired annulation reactivity. Copper and zinc salts are also well-known to generate cationic gold from AuRCl pre-catalysts. Lastly, the coordination ability of the paired silver counterion could be tuned; typically, weakly coordinating anions like $AgSbF_6^-$ and OTf^- produce highly cationic gold species, which were successful in cases where there were no chemoselectivity issues. It is possible that stronger anion coordination could affect the catalytic activity of the gold cation.

3.3 sp^3 C-H INSERTION APPROACH TO ALL-CARBON SPIROCYCLES

Without being able to take advantage of the fundamental reactivity of functional groups, C–H insertion cascades represent a challenge in organic synthesis. The analogous all-carbon spirocenters required a new retrosynthetic disconnection from our previous X–H insertion/Conia-ene strategies, now reliant on intramolecular C–H insertion to minimize entropic driving force for the process.

3.3.1 HUNTER AND SHARMA'S sp^2 C-H INSERTION/CONIA–ENE CASCADE FOR THE SYNTHESIS OF CARBOCYCLIC OXINDOLES

In 2018, Hunter et. al. disclosed a new reaction cascade using an interrupted C–H insertion strategy for the synthesis of carbocyclic oxindoles (**Scheme 3.11**).[6]

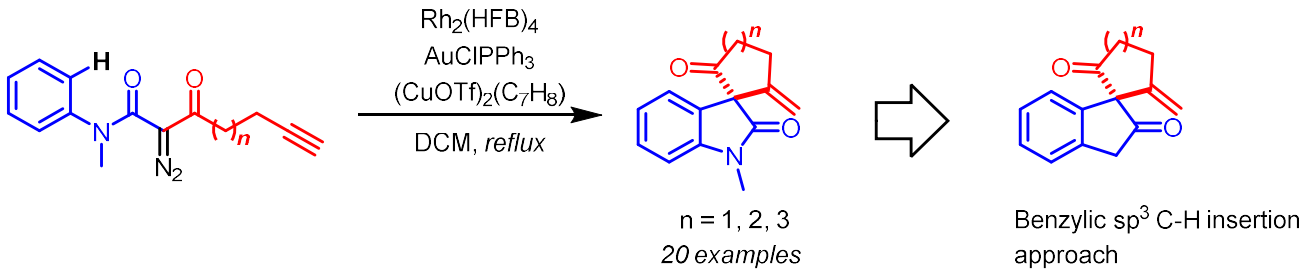

Scheme 3.11. Hunter et. al's sp^2 C–H Insertion/Conia-ene cascade to synthesize spirocarbocycles

In their report, the group discloses a successful intramolecular C–H insertion/Conia-ene reaction cascade using rhodium(II) carboxylate dimers, and gold-activated alkynes. The reaction conditions proved general for the formation of 5-, 6-, and 7- membered carbocycles, and was even suitable for the decomposition of acceptor-only diazos, with minor modifications of the optimized reaction conditions. This development led our hypothesis for the formation of a new

spirocyclic scaffolds – If a substrate could undergo *ortho*- sp^2 C–H insertion and subsequent Cona-ene cyclization, could a substrate be designed to harness the analogous sp^3 C–H insertion strategy? Guided by Davies' survey of intermolecular sp^3 C–H insertion, we suspected that a benzylic C–H bond would be the ideal site for our approach.

3.3.2 SYNTHESIS OF C-H INSERTION LINEAR PRECURSOR

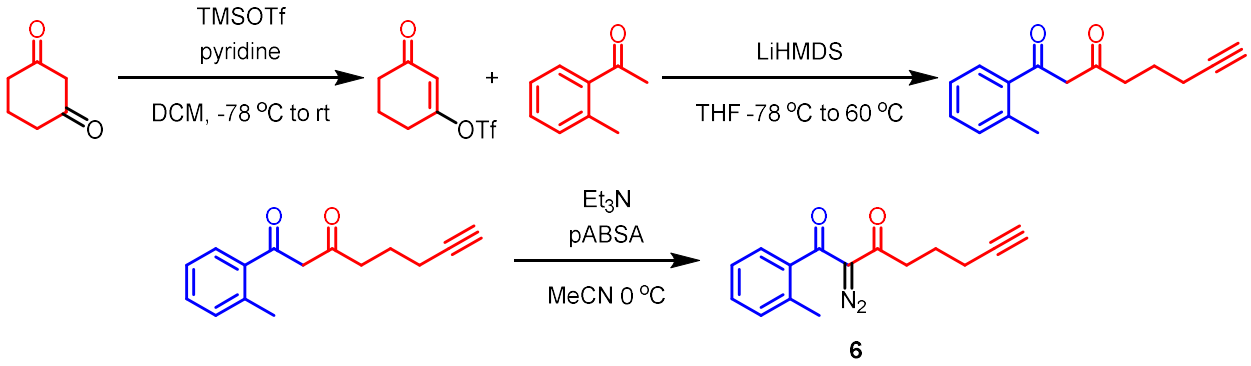

Scheme 3.12. Synthetic approach to C–H insertion precursor **6**

To access diazo **6**, first 1,3-cyclohexandione was exposed to soft enolization conditions, and trapped with TMSOTf to generate the corresponding vinyl triflate. Next, the enolate of 2'-methylacetophenone was generated using LiHMDS, and quenched with the vinyl triflate, which undergoes ring opening to produce the desired methylene precursor.[7a] Lastly, diazo transfer conditions to the active methylene using *p*-ABSA cleanly afforded parent diazo **6**.

To access 5-membered and 7-membered precursors, an alternative synthesis was sought due to 1,3-cylopenanedione's incompatibility in vinylogous triflate ring opening, and the high cost of 1,3-cycloheptanedione (**Scheme 3.13**).

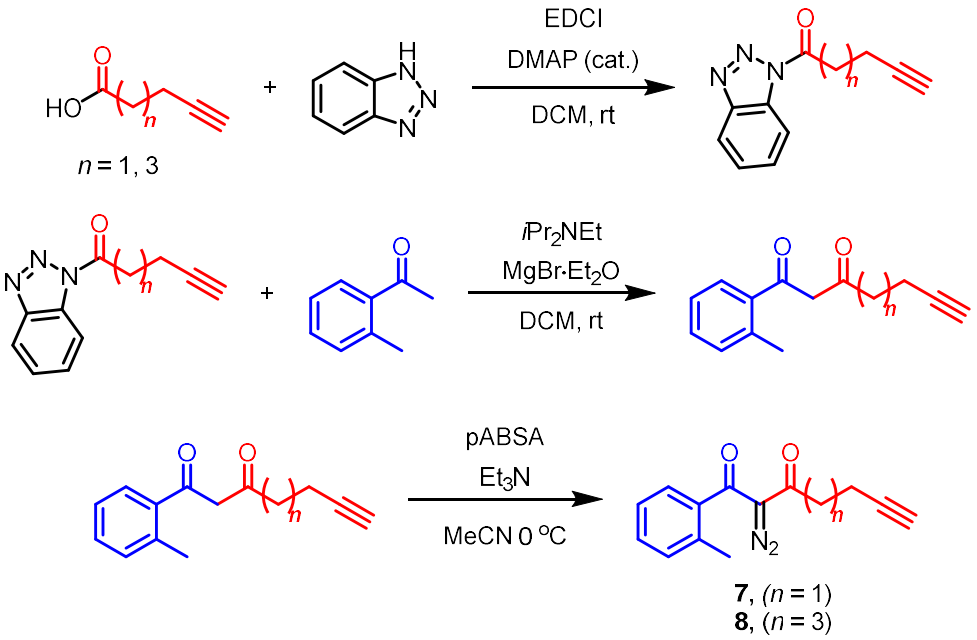

Scheme 3.13. Synthesis of diazos **7** and **8** through acyl substitution of benzotriazoleamides

In both cases the correspond alkynoic acid, readily accessible via Jones oxidation of the commercially available alkynol, was converted to the triazole amide via carbodiimide coupling conditions. Next, inspired by a recent report,[7b] 2'-methylacetophenone was exposed to soft enolization conditions in the presence of a Lewis acid to afford the resulting methylene precursors. Lastly, diazo transfer conditions using *p*-ABSA afforded desired diazos **7** and **8**.

3.3.3 OPTIMIZATION STUDIES – BENZYLIC C–H INSERTION/CONIA-ENE CASCADE

Having established a convenient route to diazos **6**-**8**, we turned our attention towards promoting the desired benzylic C–H reactivity. As was the case will acceptor/acceptor diazo substrates, we envisioned that we could optimize the insertion and Conia-ene processes sequentially, then combine these insights for a one pot approach (**Scheme 3.14**).

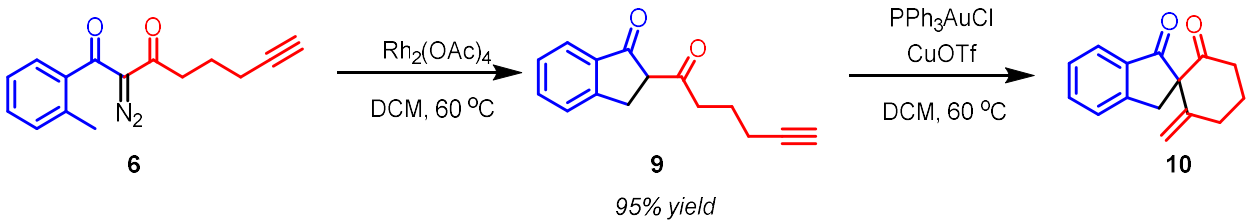

Scheme 3.14 Proof-of-concept study: stepwise Benzylic sp^3 C-H Insertion/Conia-ene of **6**

Using basic carboxylate dimer Rh_2OAc_4, diazo **6** cleanly underwent the desired sp^3 C–H insertion to provide enol **9**. The insertion compound then successfully underwent Conia-ene cyclization to produce carbocycle **10**. The previously established Ag salt, used for in situ generation of Au^+, needed to be switched to a Cu salt as was in the case in Hunter's study, due to the propensity for these terminal alkynes to undergo hydrolysis to the resulting ketone. Inspired by these stepwise results, we next attempted the cascade reactions in a one-pot fashion (**Scheme 3.15**).

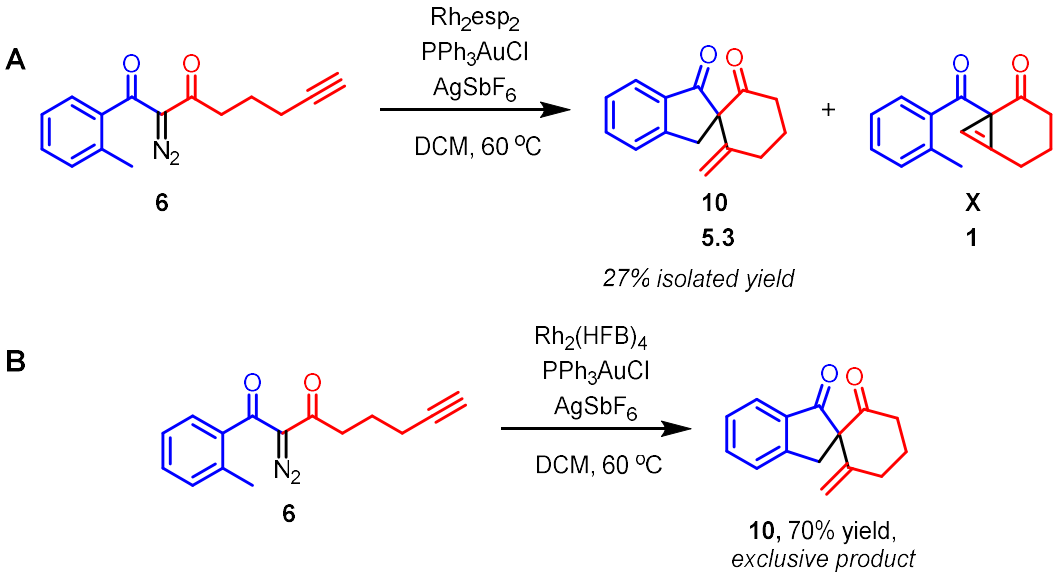

Scheme 3.15 a.) One-pot cascade trial using $Rh_2(esp)_4$ b.) One-pot cascade trial using $Rh_2(HFB)_4$

When **6** was exposed to Rh/Au/Ag in a one pot fashion however, we observed only a small amount of **10**, and the presence of byproduct **X,** we expect formed due to a competing cyclopropanation pathway due to activation of the alkyne. We hypothesized that altering the electrophilicity of the rhodium catalyst could affect the nucleophilicity of the generated Rhoda-enolate, favoring the desired insertion/Conia-ene pathway over the undesired cyclopropanation. Indeed, when $Rh_2(esp)_2$ was replaced with the highly electron deficient dirhodium(II) heptafluorobutyrate ($Rh_2(HFB)_4$), we observed no trace of diagnostic cyclopropane peaks on the crude 1H NMR, and instead clean formation of **10**, which was isolated in 70% yield.

Inspired by Hunter and Sharma's success generating 5- and 7- membered rings through their sp^2 C–H Insertion/Conia-ene cascades, we next evaluated diazos **7** and **8** towards stepwise C–H insertion and resulting Conia-ene (**Scheme 3.16**).

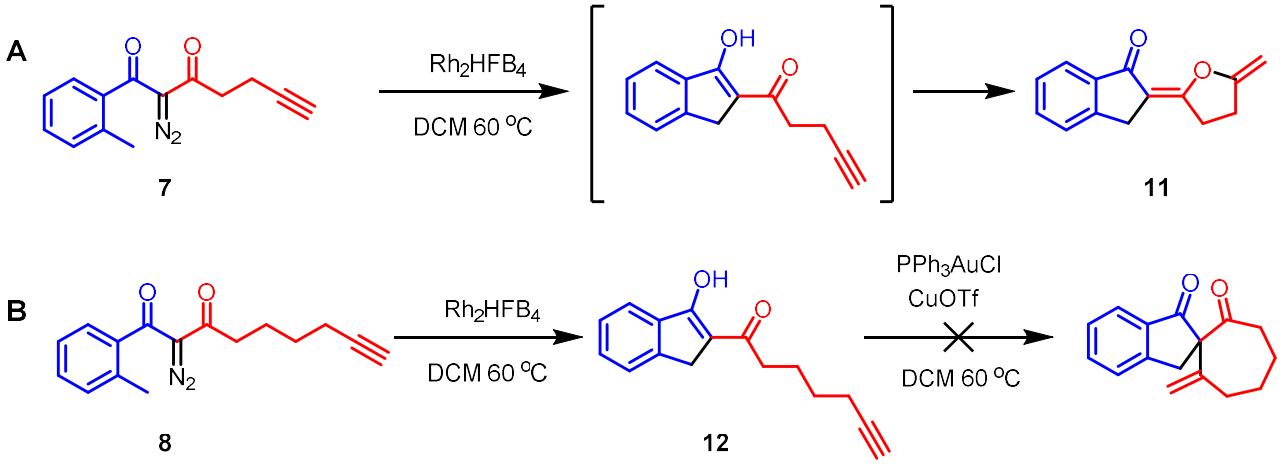

Scheme 3.16 a.) Stepwise-approach to five-membered carbocycles b.) Stepwise-approach to seven-membered carbocycles

When diazo **7** was exposed to Rh_2HFB_4, we observed evidence of C–H insertion, but appears the substrate underwent further o-alkylation to produce *exo*-glycal **11**. Hunter and Sharma also encountered this form of reactivity in their sp^2 C–H Insertion/Conia-ene approach,

and cited the disfavored 5-*enolendo*-*exo*-dig cyclization encouraging undesired ketone alkylation. The authors were able to address this limitation by utilizing a donor/acceptor diazo without the reactive ketone, to circumvent its reactivity. When diazo 8 was exposed to Rh_2HFB_4 the reaction resulted in complete conversion to the C-H insertion compound **11.** Then, when insertion product **12** was exposed to the Au^+ conditions, we did not observe any diagnostic *exo*-olefin protons indicative of successful Conia-ene cyclization, and recovered a complex mixture of products.

3.4 SUMMARY & FUTURE DIRECTIONS

In this chapter, we have described an extension of our insertion/Conia-ene cascade methodology to underutilized S–H and benzylic C–H bonds. Success in these cascade reactions generate hydrothiophenes and all-carbon spirocycles, which are valuable bioisosteres and are found in bioactive natural products. By applying secondary mercaptynes to Rh/Au^+ catalytic conditions, we were able to accomplish stepwise S–H insertion and Conia-ene cyclization to produce the desired hydrothiophenes. In a one-pot approach using the secondary mercaptyne and diazo substrates however, we obtained a thiofuranofuran product, which we expect formed by way of intramolecular 5-*endo*-dig cyclization of the mercaptyne in the presence of Au^+, before diazo addition. Employing our knowledge of sp^3 C–H insertion reactivity, we also applied our Rh/Au^+ methodology for an intramolecular approach to 3-spiroindenones. While this approach has not proven as general as Hunter and Sharma's previously disclosed method for generating 3-spriooxindoles, we were able to apply our method to form 6-membered spiroindenes through a Conia-ene reaction. Efforts in these pursuits are ongoing and warrant future study.

3.5 REFERENCES FOR CHAPTER 3

1.) a.) Pathania, S.; Narang, R. K.; Rawal, R. K. "Role of Sulphur-heterocycles in Medicinal Chemistry: An Update." *E. J. Med. Chem.* **2019**, *180*, 486–508. B.) D'yakonov, V. A.; Trapeznikova, O. A.; de Meijere, A. D.; Dzhemilev, U. M. "Metal Complex Catalysis in the Synthesis of Spirocarbocycles." *Chem. Rev.* **2014**, *114*, 5775–5814. c.) Sudhapria, N.; Perumal, P. T.; Balachandra, C.; Ignacimuthu, I.; Sangeetha, M.; Doble, M. "Synthesis of New Class of Spirocarbocycle Derivatives by Multicomponent Domino Reaction and their Evaluation for Antimicrobial, Anticancer Activity and Molecular Docking Studies." *E. J. Med. Chem.* **2014**, *83*, 190–207. d.) Lokesh, K.; Kesavan, V. "Efficient Synthesis of Highly Functionalized Spirocarbocyclic Oxindoles through Hauser Annulation." *Eur. J. Org. Chem.* **2017**, 5689–5695.

2.) a.) Zhang, X., Ma, M., Wang, J. "Catalytic Asymmetric S–H Insertion Reaction of Carbenoids." *ARKIVOC* **2003**, 84–91. b.) Xu, B., Zhu, S- F., Zhang, Z- C., Uy, Z- X., Ma, Y., Zhou, Q- L. "Highly Enantioselective S–H Bond Insertion Cooperatively Catalyzed by Dirhodium Complexes and Chiral Spiro Phosphoric Acids." *Chem. Sci*. **2014**, *5*, 1442–1449. c.) Bernardim, B., Couch, E. D., Hardman-Baldwin, A. M., Burtoloso, A. C. B., Mattson, A. E. "Divergent Roles of Urea and Phosphoric Acid Derived Catalysts in Reactions of Diazo Compounds." *Synthesis* **2016**, *48*, 677–686. d.) Keipour, H., Jalba, A., Delange-Laurin, L., Ollevier, T. "Copper-Catalyzed Carbenoid Insertion Reactions of α-Diazoesters and α-Diazoketones into Si–H and S–H Bonds." *J. Org. Chem.* **2017**, *82*, 3000–3010. e.) Xiao, G., Chen, T., Ma, C., Xing, D., Hu, W. "Rh(II)/Chiral Phosphoric Acid-Cocatalyzed Enantioselective Synthesis of Spirooxindole-Fused Thiaindanes." *Org. Lett.* **2018**, *20*, 4531–4535. f.) Keipour, H., Jalba, A., Tanbouza, N., Carreras, V., Ollevier, T. "α-Thiocarbonyl Synthesis via the

Fe(II)-Catalyzed Insertion Reaction of α-Diazocarbonyls into S–H Bonds." *Org. Biomol. Chem.* **2019**, *17*, 3098–3103. g.) Barkhatova, D., Zhukovsky, D., Dar'in, D., Krasavin, M. "Employing α-Diazocarbonyl Compound Chemistry in the Assembly of Medicinally Important Aryl(alkyl)thiolactam Scaffold." *Eur. J. Org. Chem.* **2019**, 5798–5800.

3.) a.) Moyer, M. P., Feldman, P. L., Rapoport, H. "Intramolecular N–H, O–H, and S–H Insertion Reactions. Synthesis of Heterocycles from α-Diazo-β-Keto Esters." *J. Org. Chem.* **1985**, *50*, 5223–5230. b.) Moody, C. J., Taylor, R. J. "Rhodium Carbenoid Mediated Cyclisations. Use of Ethyl Lithiodiazoacetate in the Preparation of ω-Hydroxy-, -Mercapto-, and -Boc-Amino-α-Diazo-β-Keto Esters." *Tet. Lett.* **1987**, *28*, 5351–5352 c.) Moody, C. J., Taylor, R. D. "Rhodium Carbenoid Mediated Cyclisations. Synthesis and Rearrangement of Cyclic Sulphonium Ylides." *Tet. Lett.* **1988**, *29*, 6005–6008. d.) Moody, C. J., Taylor, R. J. "Rhodium Carbenoid Mediated Cyclizations. Part 5. Synthesis and Rearrangement of Cyclic Sulphonium Ylides; Preparation of 6- and 7-Membered Sulphur Heterocycles." *Tetrahedron* **1990**, *46*, 6501–6524.

4.) a.) Lin, R.; Cao, Y.; West, F. G. "Medium-Sized Cyclic Ethers via Stevens [1,2]-Shift of Mixed Monotihoacetal-Derived Sulfonium Ylides: Application to Formal Synthesis of (+)-Laurencin." *Org. Lett.* **2017,** *19*, 552–555. b.) Xu, X.; Li, C.; Tao, Z.; Pan, Y. "Hemin-Catalyzed Sulfonium Ylide Formation and Subsequently Reactant-Controlled Chemoselective Rearrangements." *Chem. Comm.* **2017,** *53*, 6219–6222. c.) Qu, J- P.; Hu, Z- H.; Zhou, J.; Cao, C- L., Sun, X- L.; Dai, L- X.; Tang, Y. "Ligand-Accelerated Asymmetric [1,2]-Stevens Rearrangement of Sulfur Ylides via Decomposition of Diazomalonates Catalyzed by Chiral Bisoxazoline/Copper Complex." *Adv. Synth. Catal.* **2009**, *351*, 308–312. d.) Mortimer, A. J. P.; Aliev, A. E.; Tocher, D. A.; Porter, M. J.

"Synthesis of the Tagetitoxin Core via Photo-Stevens Rearrangement." *Org. Lett.* **2008**, *10*, 5477–5480. e.) Thomson, T.; Stevens, T. S. "Degradation of Quaternary Ammonium Salts. Part V. Molecular Rearrangement in Related Sulphur Compounds." *J. Chem. Soc.* **1932***,* 69–73. f.) Orlowska, K.; Rybica-Jasninska, K.; Krajewski, P.; Gryko, D. "Photochemical Doyle-Kirmse Reaction: A Route to Allenes." *Org. Lett.* **2020**, *22*, 1019–2021. g.) Lin, X.; Tang, Y.; Yang, W.; Tan, F.; Lin, L.; Liu, X.; Fend, X. "Chiral Nickel(II) Complex Catalyzed Enantioselective Doyle-Kirmse Reaction of α-Diazo pyrazoleamides." *J. Am. Chem. Soc.* **2018**, *140*, 3299–3305. h.) Holzwarth, M. S.; Alt, I.; Plietker, B. "Catalytic Activation of Diazo Compounds Using Electron-Rich, Defined Iron Complexes for Carbene-Transfer Reactions." *Angew. Chem. Int. Ed.* **2012,** *51*, 5341–5354. i.) Davies, P. W.; Albrecht, S. G.-C.; Assanelli, G. "Silver-catalyzed Doyle-Kirmse Reaction of Allyl and Propargyl Sulfides." *Org. Biomol. Chem.* **2009**, *7*, 1276–1279. j.) Doyle, M. P.; Tamblyn, W. H.; Bagheri, V. "Highly Effective Catalytic Methods for Ylide Generation from Diazo Compounds. Mechanism of the Rhodium- and Copper-Catalyzed Reactions with Allylic Compounds." *J. Org. Chem.* **1921**, *46*, 5094–5102.

5.) a.) Xiang, Y.; Wang, C.; Ding, Q.; Peng, Y. "Diazo Compounds: Versatile Synthons for the Synthesis of Nitrogen Heterocycles via Transition Metal-Catalyzed Cascade C–H Activation/Carbene Insertion/Annulation Reactions." *Adv. Synth. Catal.* **2019**, *361*, 919–944. b.) Zhu, C.; Wang, C- Q.; Feng, C. "Recent Advance in Transition-Metal-Catalyzed Oxidant Free [4+1] Annulation through C-H Bond Activation." *Tet. Lett.* **2018**, *59*, 430–437. c.) Gurmessa, G. T.; Singh, G. S. "Recent Progress in Insertion and Cyclopropanation Reactions of Metal Carbenoids from α-Diazocarbonyl Compounds." *Res. Chem. Intermed.* **2017**, *43*, 6447–6504. d.) Sultanova, R. M.; Khanova, M. D.; Zlotskii, S. S. "The Insertion Reaction of Diazocarbonyl Compounds at C–H Bonds

in the Synthesis of Biologically Active Nitrogen- and Oxygen-Containing Heterocycles." *Chem. Het. Comp.* **2015**, *51*, 775–784. e.) Hu, F.; Xia, Y.; Ma, C.; Zhang, Y.; Wang, J. "C–H Bond Functionalization Based on Metal Carbene Migratory Insertion." *Chem. Comm.* **2015**, *51*, 7986–7995. f.) Davies, H. M. L.; Morton, D. "Guiding Principles for Site Selective and Stereoselective C–H Functionalization by Donor/Acceptor Rhodium Carbenes." *Chem. Soc. Rev.* **2011**, *40*, 1857–1869. g.) Slattery, C. N.; Ford, A.; Maguira, A. R. "Catalytic Asymmetric C–H Insertion Reactions of α-Diazocarbonyl Compounds." *Tetrahedron* **2010**, *66*, 6681–6705. h.) Doyle, M. P.; Duffy, R.; Ratnikov, M.; Zhou, L. "Catalytic Carbene Insertion into C–H Bonds." *Chem. Rev.* **2010**, *110*, 704–724. i.) Demonceau, A.; Noels, A. F.; Hubert, A. J.; Teyssie, P. "Transition-Metal-Catalyzed Reactions of Diazoesters. Insertion into C-H Bonds of Paraffins by Carbenoids." *J. Chem. Soc. Chem. Comm.* **1981**, 688-689. j.) Demonceau, A.; Noels, A. F.; Hubert, A. J.; Teyssie, P. "Transition-Metal-Catalyzed Reactions of Diazoesters. Insertion into C-H Bonds of Paraffins Catalyzed by Bulky Rhodium(II) Carboxylates: Enhanced Attack on Primary C-H Bonds." *Bull. Soc. Chim. Belg.* **1984**, *93*, 945-948.

6.) Hunter, A. C.; Chinthapally, K.; Bain, A. I.; Stevens, J. C.; Sharma, I. "Rhodium/Gold Dual Catalysis in Carbene sp^2 C–H Functionalization/Conia-ene Cascade for the Stereoselective Synthesis of Diverse Carbocycles." *Adv. Synth. Catal.* **2019**, *361*, 2951-2958.

7.) a.) Kamijo, S.; Dudley, G. B. "Tandem Nucleophilic Addition/Fragmentation Reactions and Synthetic Versatility of Vinylogous Acyl Triflates." *J. Am. Chem. Soc.* **2006**, *128*, 6499-6507. b.) Lim, D.; Zhou, G.; Livanos, A. E.; Fang, F.; Coltart, D. M. "$MgBr_2 \cdot OEt_2$-Promoted Coupling of Ketones and Activated Acyl Donor via Soft Enolization: A Practical Synthesis of 1,3-Diketones." *Synthesis* **2008**, *13*, 2148-2152.

3.6 EXPERIMENTAL SECTION

PUBLICATION AND CONTRIBUTION STATEMENT

The material presented in this chapter is unpublished and the sole contributor is Steven Schlitzer. Dr. Indrajeet Sharma contributed with assistance in project design and NMR analysis.

MATERIALS AND METHODS

Reagents

Reagents and solvents were obtained from Sigma-Aldrich (www.sigma-aldrich.com), ChemImpex (www.chemimpex.com) or Acros Organics (www.fishersci.com) and used without further purification unless otherwise indicated. Dry solvents (acetonitrile) were obtained from Acros Organics (www.fishersci.com), and dichloromethane was distilled over CaH_2 under N_2 unless otherwise indicated. THF purchased from Sigma-Aldrich was distilled over Na metal with benzophenone indicator. Diazo compounds were stored as a dilute solution frozen in benzene for periods longer than 24 hours.

Reactions

All reactions were performed in flame-dried glassware under positive N_2 pressure with magnetic stirring unless otherwise noted. Liquid reagents and solutions were transferred thru rubber septa via syringes flushed with N_2 prior to use. Cold baths were generated as follows: 0 °C with wet ice/water and −78 °C with dry ice/acetone. Syringe pump addition reactions were conducted using a CMA/100 microinjection pump.

Chromatography

TLC was performed on 0.25 mm E. Merck silica gel 60 F254 plates and visualized under UV light (254 nm) or by staining with potassium permanganate ($KMnO_4$), cerium ammonium molybdenate (CAM), phosphomolybdic acid (PMA), and ninhydrin. Silica flash chromatography was performed on Sorbtech 230–400 mesh silica gel 60.

Analytical Instrumentation

IR spectra were recorded on a Shimadzu IRAffinity-1 FTIR or a Nicolet 6700 FTIR spectrometer with peaks reported in cm^{-1}. NMR spectra were recorded on a Varian VNMRS 400, 500 and 600 MHz NMR spectrometer in $CDCl_3$ unless otherwise indicated. Chemical shifts are expressed in ppm relative to solvent signals: $CDCl_3$ ((^1H, 7.26 ppm, ^{13}C, 77.0 ppm); coupling constants are expressed in Hz. NMR spectra were processed using Mnova (www.mestrelab.com/software/mnova-nmr). Mass spectra were obtained at the OU Analytical Core Facility on an Agilent 6538 High-Mass-Resolution QTOF Mass Spectrometer and an Agilent 1290 UPLC. X-ray crystallography analysis was carried out at the University of Oklahoma using a Bruker APEX ccd area detector and graphite-monochromated Mo Kα radiation (λ = 0.71073 Å) source and a D8 Quest diffractometer with a Bruker Photon II cmos area detector and an Incoatec Iμs microfocus Mo Kα source (λ = 0.71073 Å). Crystal structures were visualized using CCDC Mercury software (http://www.ccdc.cam.ac.uk/products/mercury/).

Nomenclature

N.B.: Atom numbers shown in chemical structures herein correspond to IUPAC nomenclature, which was used to name each compound.

3.6.1 SYNTHESIS OF SECONDARY MERCAPTYNE 2

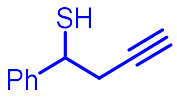

1-Phenylbut-3-yne-1-thiol (2). To a suspension of $LiAlH_4$ (1.25 eq.) in anhydrous diethyl ether (0.4 M) was added a solution of 1-phenylbut-3-yn-1-yl ethanethioate in minimal diethyl ether under N_2. The mixture was heated to reflux with stirring for 3 hours, then cooled to 0 °C, whereby residual $LiAlH_4$ was destroyed by careful addition of acetone. The precipitate was dissolved by adding 1N HCl. The organic layer was separated, and aqueous layer extracted into Et_2O (3x). Combined organics were washed with 1N HCl (2x), water (2x), and brine, then concentrated by rotatory evaporating, using a water bath set no higher than 35 °C. The resulting thiol was used without further purification. Foul-smelling yellow liquid (368 mg, 99%). ^{1}H NMR (600 MHz, Chloroform-*d*) δ 7.39 – 7.24 (m, 5H), 4.23 (dt, *J* = 7.6, 5.5 Hz, 1H), 2.84 (m, *J* = 60 Hz, 2H), 2.40 (d, *J* = 5.2 Hz, 1H), 2.09 (s, 1H). ^{13}C NMR (151 MHz, Chloroform-*d*) δ 142.2, 128.7 (2C), 127.8, 126.9 (2C), 81.4, 71.0, 42.8, 30.2.

3.6.2 REACTIVITY OF MERCAPTYNE 2 TOWARDS INSERTION AND CONIA-ENE CHEMISTRY

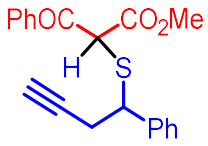

Methyl 3-oxo-3-phenyl-2-((1-phenylbut-3-yn-1-yl)thio)propanoate (3). To a solution of 1-phenylbut-3-yne-1-thiol (1.0 eq) in dichloromethane (0.2 M) was added Rh2(esp)2 (2 mol %). The system was degassed with N_2, followed by slow dropwise addition of a solution of 2-diazo-3-oxo-3-phenylpropanoate (1.2 eq.) in dichloromethane (0.2 M). The reaction mixture was stirred at

room temperature while monitoring by TLC. After complete conversion of thiol was observed, the reaction was passed through a short celite pad, eluting with excess dichloromethane. The organics were concentrated and purified by column chromatography to provide insertion product **3** as a diastereomeric mixture of keto and enol tautomers. ^{1}H NMR (600 MHz, Chloroform-*d*) δ 13.8z1 (s, 1H), 7.84 – 7.79 (m, 2H), 7.70 – 7.65 (m, 2H), 7.58 – 7.52 (m, 2H), 7.48 – 7.45 (m, 2H), 7.44 – 7.27 (m, 24H), 7.22 – 7.17 (m, 4H), 6.97 (dd, *J* = 6.7, 3.0 Hz, 3H), 4.91 (s, 1H), 4.73 (s, 1H), 4.29 (s, 1H), 4.20 (s, 1H), 3.90 (s, 1H), 3.82 (s, 5H), 3.72 (s, 4H), 3.63 (s, 3H), 2.87 – 2.78 (m, 4H), 2.67 – 2.54 (m, 3H), 1.98 (dt, *J* = 3.7, 2.6 Hz, 2H), 1.88 (t, *J* = 2.6 Hz, 1H). ^{13}C NMR (151 MHz, Chloroform-*d*) δ 190.5, 180.6, 174.2, 168.2, 168.0, 139.7, 133.8, 133.7, 130.1, 129.4, 128.9, 128.7, 128. 7, 128.6, 128.6, 128.2, 128.2, 128.1, 128.1, 128.0, 127.7, 127.4, 127.4, 81.3, 80.5, 80.3, 71.1, 70.1, 54.3, 53.4, 53.2, 52.8, 51.9, 48. 6, 48.4, 26.6, 26.1, 24.8.

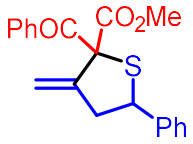

Methyl 2-benzoyl-3-methylene-5-phenyltetrahydrothiophene-2-carboxylate (4). To a stirred solution of $AuClPPh_3$ (10 mol%) and $AgSbF_6$ (10 mol %) in minimal dichloromethane was added a solution of insertion product **3** in dichloromethane (0.2 M) dropwise by syringe. The reaction was stirred at room temperature while monitoring by TLC, and after full conversion of **3** was observed, the reaction was diluted with excess dichloromethane. Organics were washed with sat. $NaHCO_3$ (2x), water (2x), and brine (1x), then dried over Na_2SO_4. Removal of solvent followed by purification by column chromatography furnished the title compound as a 5.2:1.0 mixture of diastereomers. Yellow oil (20 mg, 40%).

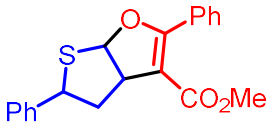

Methyl 2,5-diphenyl-3a,4,5,6a-tetrahydrothieno[2,3-b]furan-3-carboxylate (5). A solution of 1-phenylbut-3-yne-1-thiol (1.0 eq.), $Rh_2(esp)_2$, $AuClPPh_3$, and $AgSbF_6$ in dichloromethane (0.2 M) was prepared and degassed with N_2. The mixture was stirred at room temperature, while a solution of methyl 2-diazo-3-oxo-3-phenylpropanoate (1.2 eq.) was added dropwise by syringe. The reaction was stirred at room temperature while monitoring by TLC, and after full conversion of thiol was observed, the reaction was diluted with excess dichloromethane. Organics were washed with sat. $NaHCO_3$ (2x), water (2x), and brine (1x), then dried over Na_2SO_4. Removal of solvent followed by purification by column chromatography furnished the title compound. ^{1}H NMR (600 MHz, Chloroform-*d*) δ 7.38 – 7.26 (m, 26H), 4.34 (s, 1H), 4.29 (s, 1H), 4.12 (dd, *J* = 8.1, 6.3 Hz, 1H), 3.78 – 3.72 (m, 2H), 3.71 (s, 3H), 3.58 (s, 4H), 2.79 – 2.68 (m, 6H), 1.99 (t, *J* = 2.6 Hz, 1H), 1.96 (t, *J* = 2.7 Hz, 1H). ^{13}C NMR (151 MHz, Chloroform-*d*) δ 171.1, 170.6, 140.0, 136.0, 128. 7, 128.6, 128.6, 128. 6, 128.5, 128.4, 128.3, 128.2, 128.0, 127.9, 80.6, 70.8, 52.7, 52.4, 51.6, 48.8, 48.1, 26.5, 26.3. Yellow oil (23 mg, 68%).

3.6.3 SYNTHESIS OF C-H ACTIVATION DIAZO SUBSTRATES 6-8

General Procedure A for Diazo Transfer : Diketone (1.0 eq.) and *p*-ABSA (1.2 eq.) were dissolved in anhydrous MeCN (0.2 M) and cooled to 0 °C. Et3N (1.5 eq.) was added dropwise by syringe, and after 15 minutes the reaction was allowed to warm to room temperature. The reaction was stirred at this temperature while monitoring by TLC. After full conversion of diketone was observed (Typically within 2 hours), the reaction mixture was diluted with excess diethyl ether.

The organic layer was washed with sat. NH_4Cl (2x), water (2x), and brine (1x), then dried over Na_2SO_4. Concentration of the organic layer followed by purification of the residue by column chromatography (EtOAc/Hex) furnished diazos **6**-**8**.

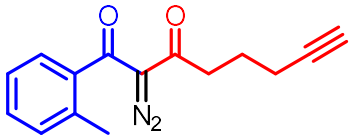

2-Diazo-1-(o-tolyl)oct-7-yne-1,3-dione (6). Prepared from (Z)-1-hydroxy-1-(o-tolyl)oct-1-en-7-yn-3-one using General Procedure **A**. Yellow oil (476 mg, 50%). ^{1}H NMR (300 MHz, Chloroform-*d*) δ 7.43 – 7.27 (m, 4H), 3.05 (s, 2H), 2.40 (s, 3H), 2.31 (s, 2H), 1.98 (t, *J* = 2.6 Hz, 1H), 1.92 (t, *J* = 7.1 Hz, 2H). ^{13}C NMR (126 MHz, Chloroform-*d*) δ 192.2, 186.7, 137. 6, 135.4, 131.4, 131.0, 126.1, 126.0, 86.12, 83.5, 69.2, 40.0, 22.9, 19.03, 17.8.

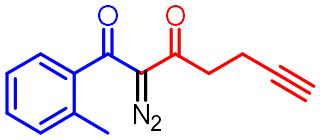

2-Diazo-1-(o-tolyl)hept-6-yne-1,3-dione (7). Prepared from (Z)-1-hydroxy-1-(o-tolyl)hept-1-en-6-yn-3-one using general procedure **A**. Yellow oil (322 mg, 59%). ^{1}H NMR (300 MHz, Chloroform-*d*) δ 7.43 – 7.27 (m, 4H), 3.20 (t, *J* = 7.1 Hz, 2H), 2.59 (td, *J* = 7.1, 2.7 Hz, 2H), 2.40 (d, *J* = 0.6 Hz, 3H), 1.99 (t, *J* = 2.7 Hz, 1H). ^{13}C NMR (101 MHz, Chloroform-*d*) δ 190.6, 186.4, 137.2, 135.4, 131.4, 131.0, 125.9, 125.9, 85.9, 82.7, 68.8, 40.0, 18.9, 13.1.

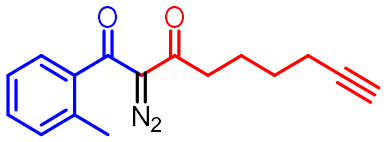

2-Diazo-1-(o-tolyl)non-8-yne-1,3-dione (8). Prepared from (Z)-1-hydroxy-1-(o-tolyl)non-1-en-8-yn-3-one using general procedure **A**. Yellow oil (138 mg, 62%). ^{1}H NMR (300 MHz, Chloroform-*d*) δ 7.41 – 7.27 (m, 3H), 7.25 (m, 1H), 2.93 (dd, *J* = 7.8, 6.9 Hz, 2H), 2.38 (s, 3H), 2.22 (td, *J* = 7.0, 2.7 Hz, 2H), 1.94 (t, *J* = 2.6 Hz, 1H), 1.85 – 1.71 (m, 2H), 1.65 – 1.51 (m, 2H). ^{13}C NMR (75 MHz, Chloroform-*d*) δ 192.6, 186.7, 137.6, 135.4, 131.4, 131.0, 126.0 (2C), 86.1, 84.0, 68.6, 40.7, 27.9, 23.3, 19.0, 18.3.

3.6.4 REACTIVITY OF DIAZOS 6-8 TOWARDS INSERTION AND CONIA-ENE CHEMISTRY

General Procedure B for C-H insertion: A solution of Rh_2HFB_4 (2 mol%) in minimal dichloromethane was prepared and degassed using N_2. The system was heated to reflux, and a solution of diazo **6**-**8** (1.0 eq.) in dichloromethane (0.2 M) was added dropwise by syringe. The reaction progress was monitored by TLC, and after full conversion of starting material was observed, the reaction was filtered through a celite plug, eluting with excess dichloromethane. Concentration of the organic layer followed by purification of the residue by column chromatography furnished insertion compounds **9**, **11** and **12**.

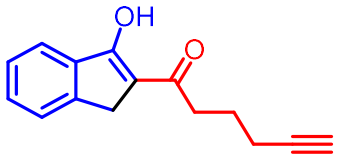

1-(3-Hydroxy-1H-inden-2-yl)hex-5-yn-1-one (9). Prepared from 2-Diazo-1-(o-tolyl)oct-7-yne-1,3-dione **6** using General Procedure **B**. Yellow oil (32 mg, 95%). ^{1}H NMR (500 MHz, Chloroform-*d*) δ

7.83 (d, *J* = 7.7 Hz, 1H), 7.56 (td, *J* = 7.4, 1.2 Hz, 1H), 7.51 (d, *J* = 7.5 Hz, 1H), 7.42 (t, *J* = 7.4 Hz, 1H), 3.65 (s, 3H), 2.61 (t, *J* = 7.3 Hz, 2H), 2.32 (td, *J* = 6.8, 2.6 Hz, 2H), 2.03 (t, *J* = 2.6 Hz, 1H), 2.00 – 1.93 (m, 2H). ^{13}C NMR (126 MHz, Chloroform-*d*) δ 179.9, 147.5, 138.2, 135.4, 132. 8, 127.7, 127.3, 125.7, 123.2, 83.5, 69.3, 33.2, 30.1, 24.3, 17.9.

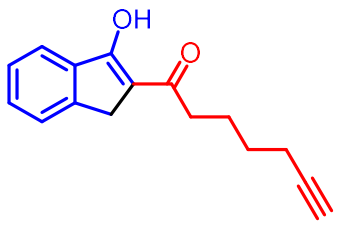

1-(3-Hydroxy-1H-inden-2-yl)hept-6-yn-1-one (12). Prepared from 2-Diazo-1-(o-tolyl)non-8-yne-1,3-dione **7** using General Procedure **B**. Yellow oil (10 mg, 35%). ^{1}H NMR (300 MHz, Chloroform-*d*) δ 7.83 (dt, *J* = 7.7, 1.0 Hz, 1H), 7.57 – 7.47 (m, 2H), 7.46 – 7.38 (m, 1H), 3.61 (s, 3H), 2.47 (t, *J* = 7.5 Hz, 2H), 2.31 – 2.21 (m, 2H), 2.02 (t, *J* = 2.6 Hz, 1H), 1.92 – 1.80 (m, 2H), 1.72 – 1.55 (m, 2H). ^{13}C NMR (75 MHz, Chloroform-*d*) δ 191.5, 147. 5, 138.2, 132. 8, 127.4, 125.7, 123.2, 110.2, 68.7, 61.2, 34.2, 30.2, 29.7, 28.0, 24.8, 18.2.

General Procedure C for Conia-ene Cyclization: A solution of $AuClPPh_3$ (10 mol%) and $(Cu(OTf))_2(C_6H_6)$ (10 mol %) in minimal dichloromethane was prepared and degassed using N_2. The system was heated to reflux, and a solution of insertion product **9** (1.0 eq.) in dichloromethane (0.2 M) was added dropwise by syringe. The reaction progress was monitored by TLC, and after full conversion of starting material was observed, the reaction was filtered through a celite plug, eluting with excess dichloromethane. The organic solution was washed with sat. $NaHCO_3$ (2x), water (2x), and brine, then dried over Na_2SO_4. Concentration of the organic

layer followed by purification of the residue by column chromatography furnished insertion compounds **9**, **11** and **12**.

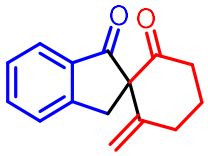

2-Methylenespiro[cyclohexane-1,2'-indene]-1',6(3'H)-dione (10). Prepared from 1-(3-Hydroxy-1H-inden-2-yl)hex-5-yn-1-one **9** using General Procedure **C**. Yellow oil (22 mg, 75%). ^{1}H NMR (600 MHz, Chloroform-*d*) δ 7.66 (d, *J* = 7.7 Hz, 1H), 7.60 (t, *J* = 7.4 Hz, 1H), 7.50 (d, *J* = 7.7 Hz, 1H), 7.35 (t, *J* = 7.4 Hz, 1H), 4.90 (s, 1H), 4.77 (s, 1H), 4.17 (d, *J* = 17.5 Hz, 1H), 3.26 (d, *J* = 17.5 Hz, 1H), 3.14 – 3.06 (m, 2H), 2.65 (d, 1H, *J* = 14.4 Hz, 1H), 2.50 (d, *J* = 14.4 Hz, 1H), 2.14 (m, 1H), 1.76 (m, *J* = 13.1 Hz, 1H). ^{13}C NMR (151 MHz, Chloroform-*d*) δ 204.9, 199.1, 153.3, 145. 8, 135.3, 132.2, 127.7, 126.0, 125.3, 109.7, 73.8, 39.8, 32.9, 31.8, 23.9, 14.1.

Appendix II

Spectra Relevant to Chapter 3

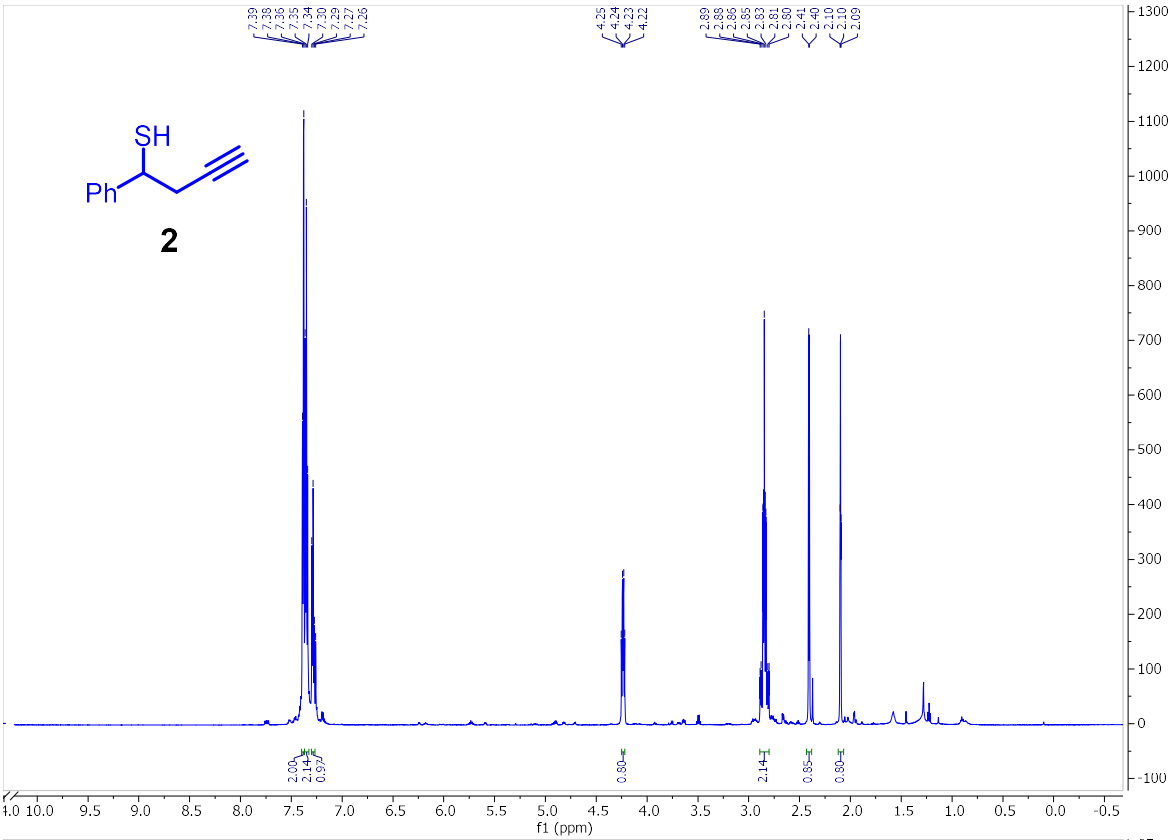
SH
Ph
2
f1 (ppm)

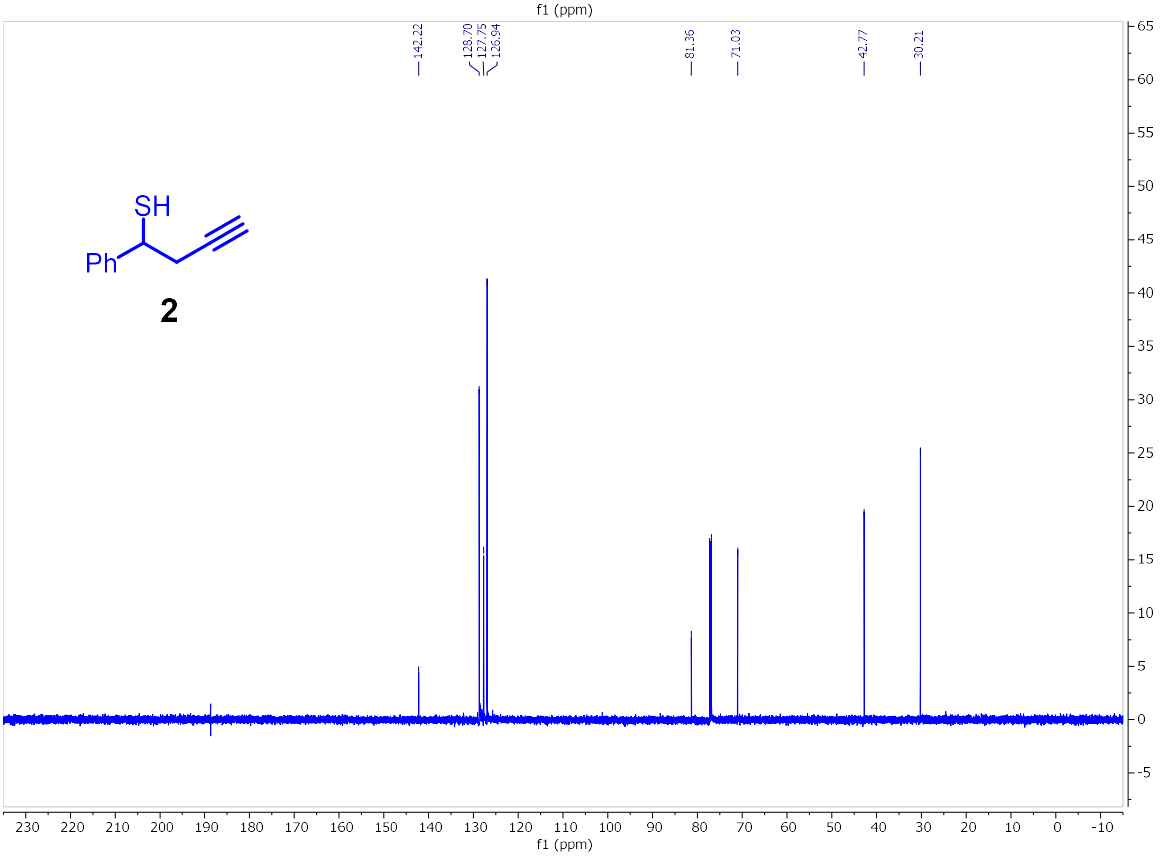
SH
Ph
2
f1 (ppm)

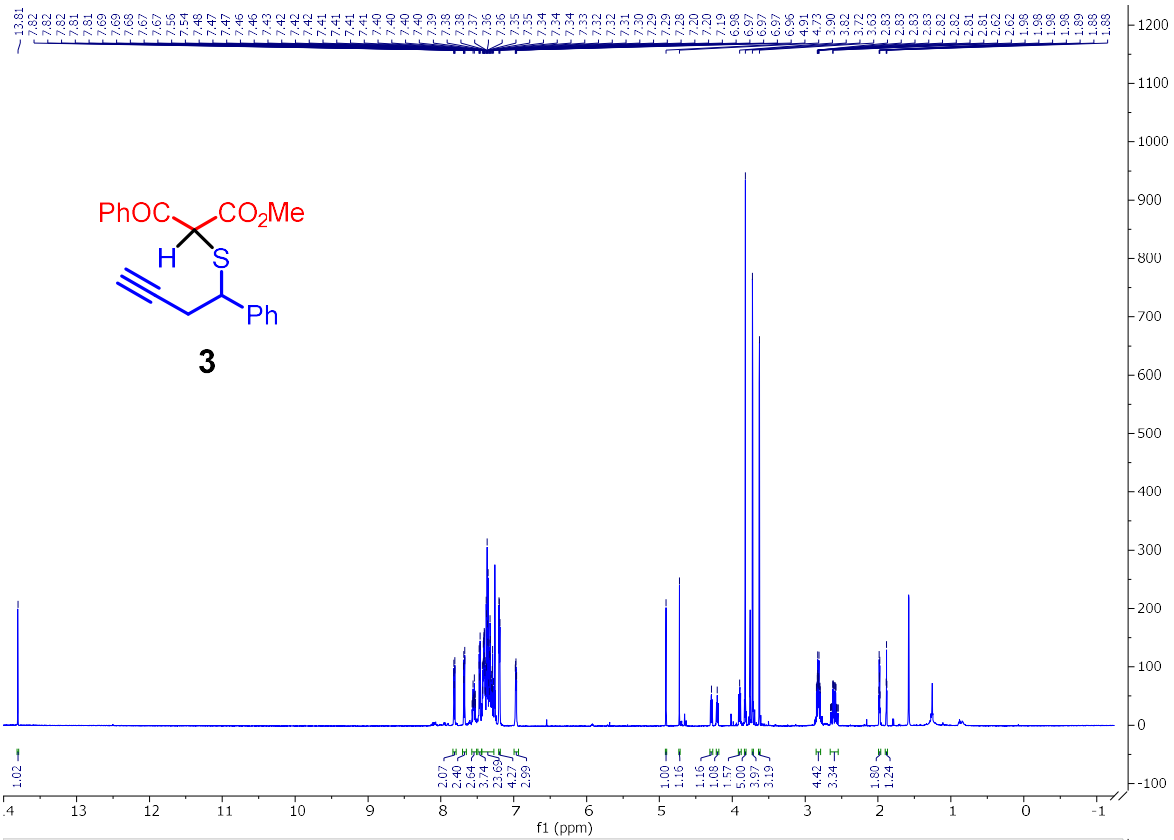
PhOC
CO2Me
H
S
Ph
3
f1 (ppm)

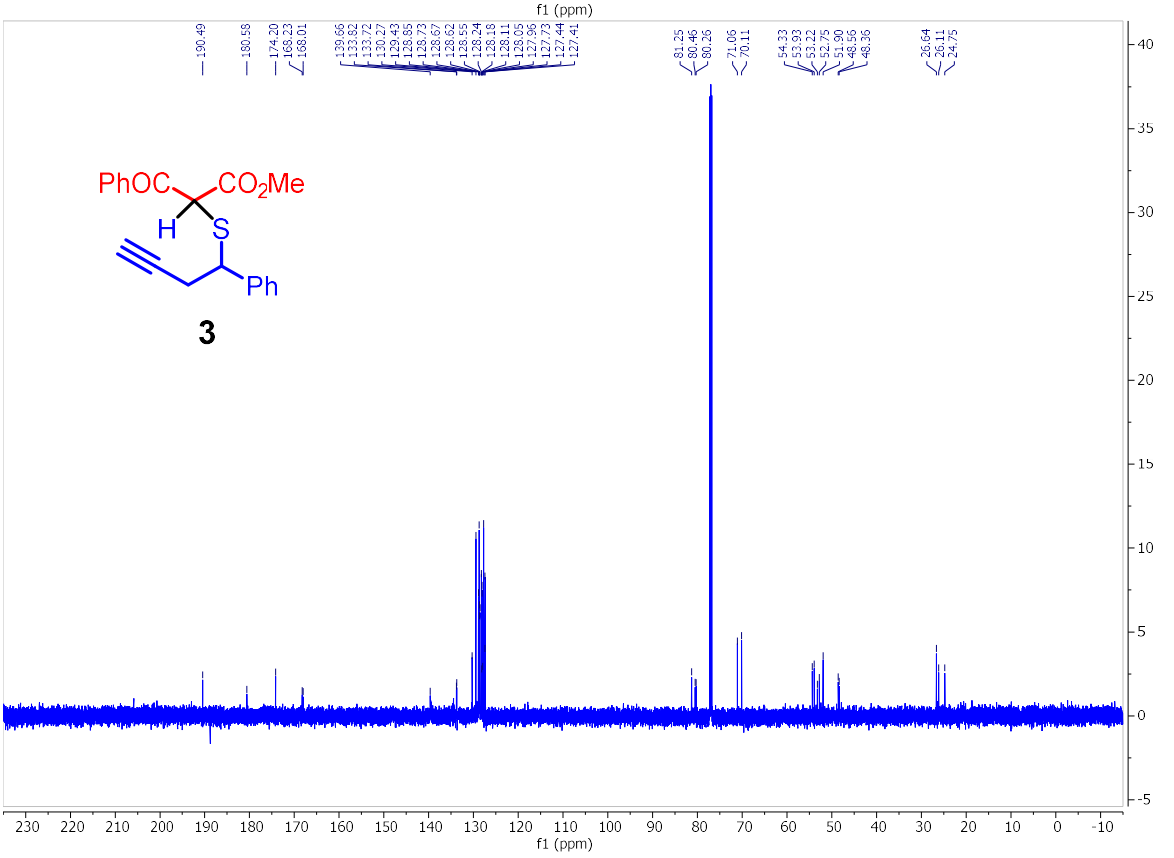
PhOC
CO2Me
H
S
Ph
3
f1 (ppm)

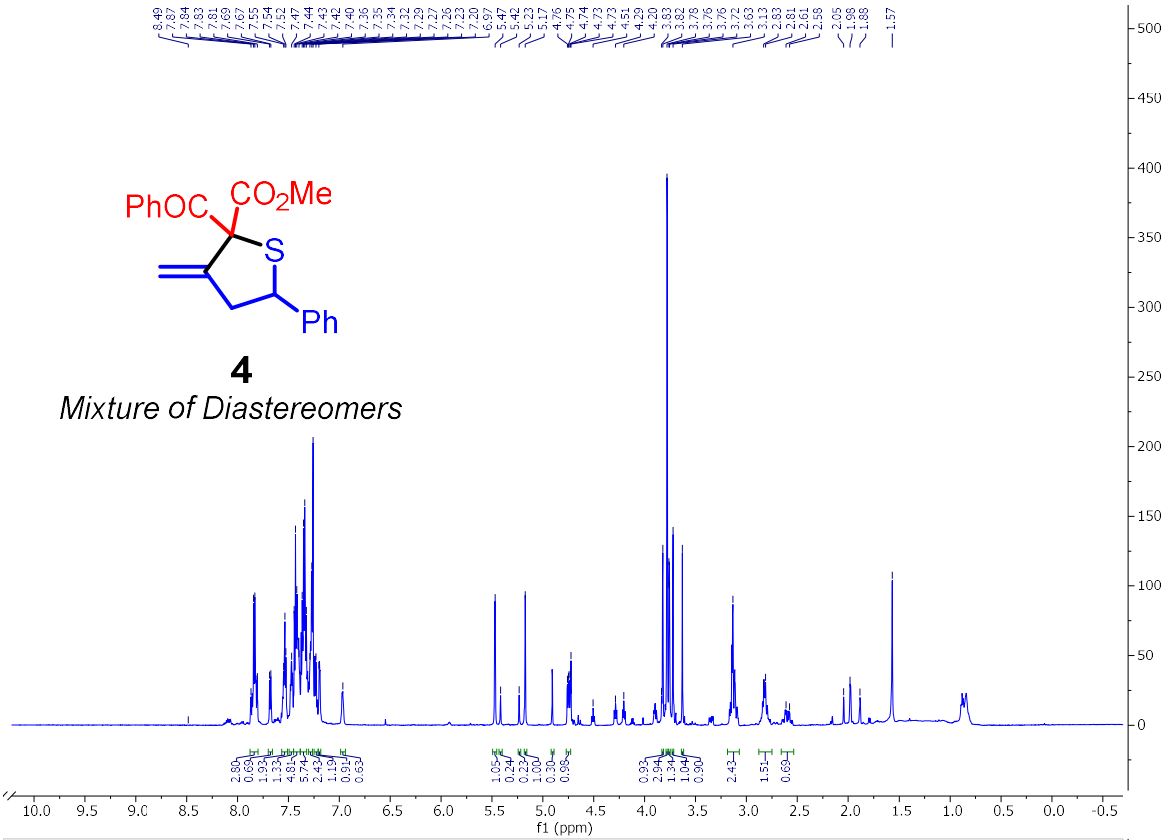

4

Mixture of Diastereomers

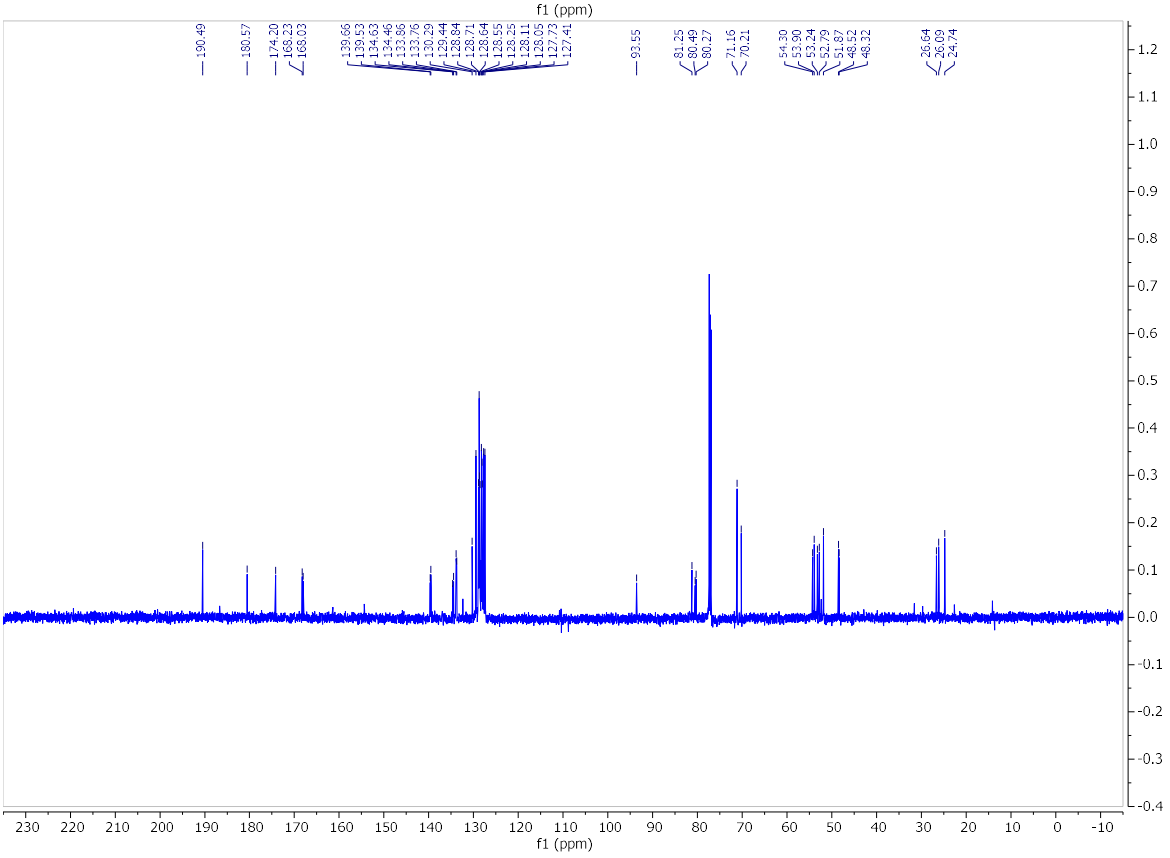

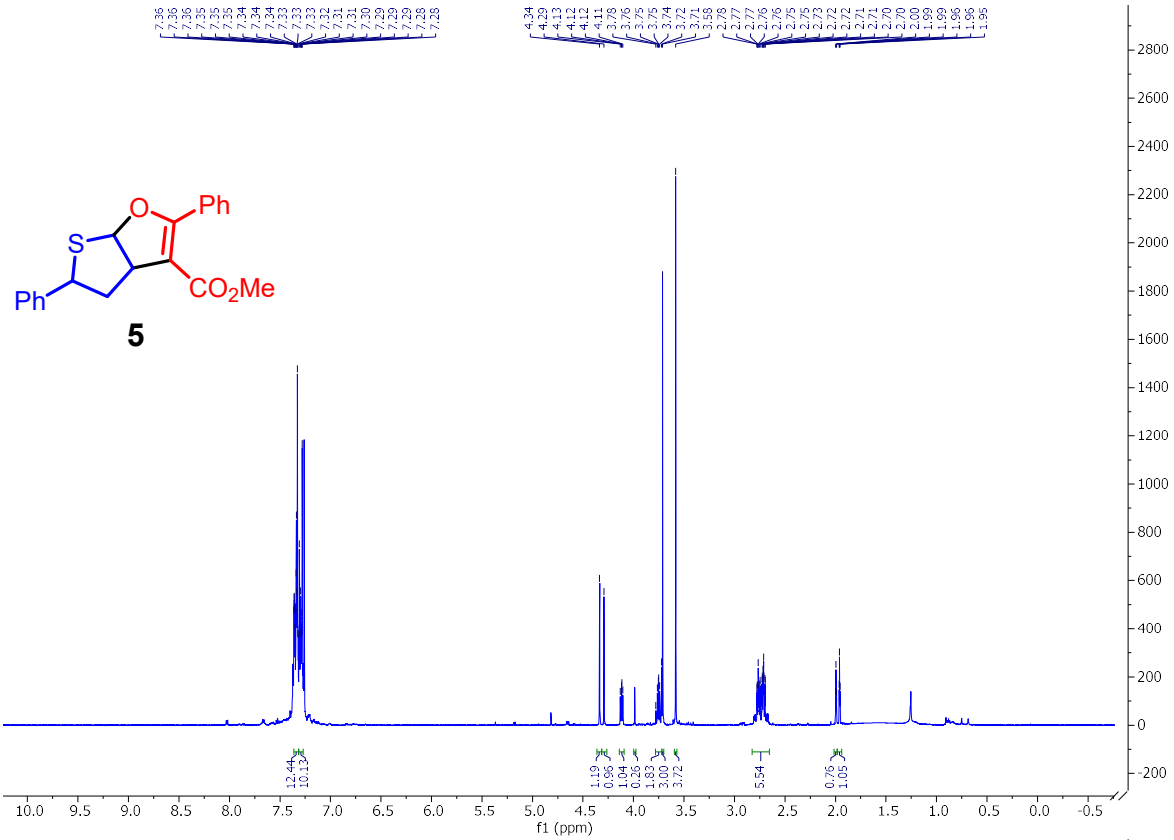
Ph
O
S
Ph
CO2Me
5
f1 (ppm)

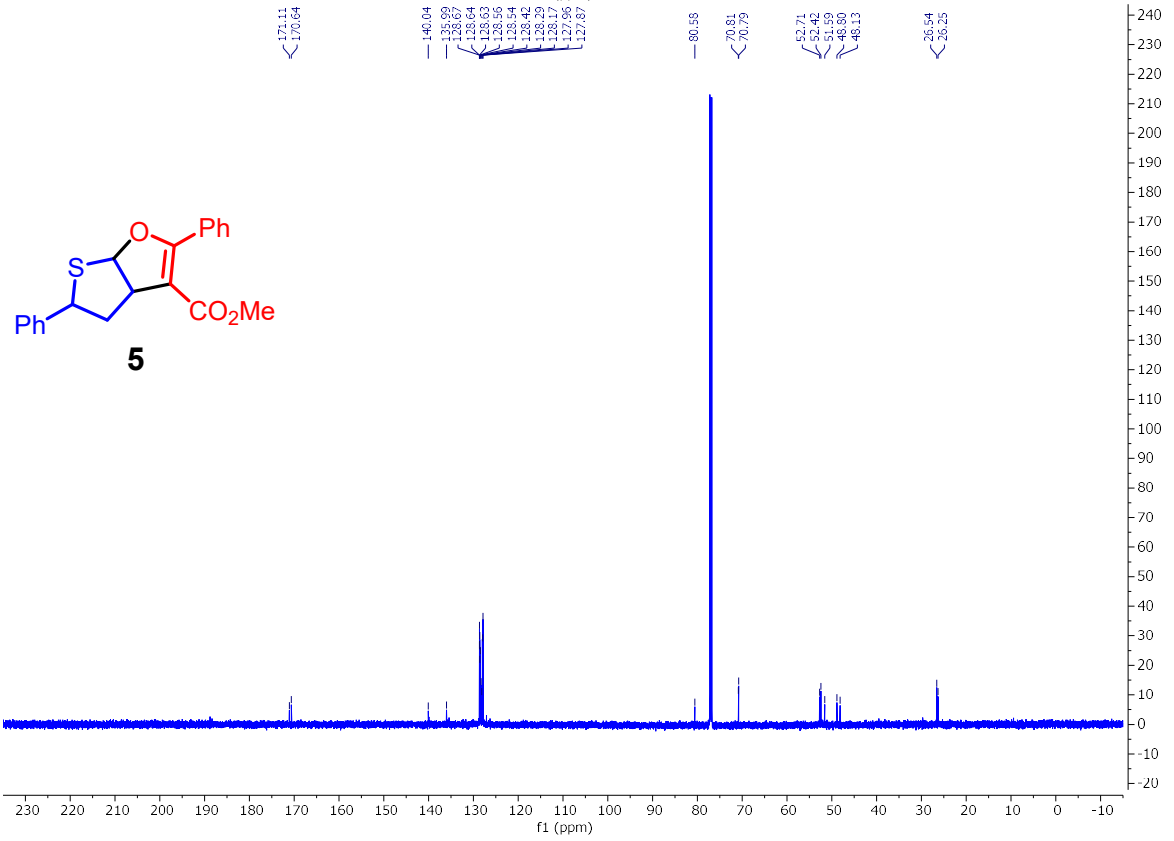
Ph
O
S
Ph
CO2Me
5
f1 (ppm)

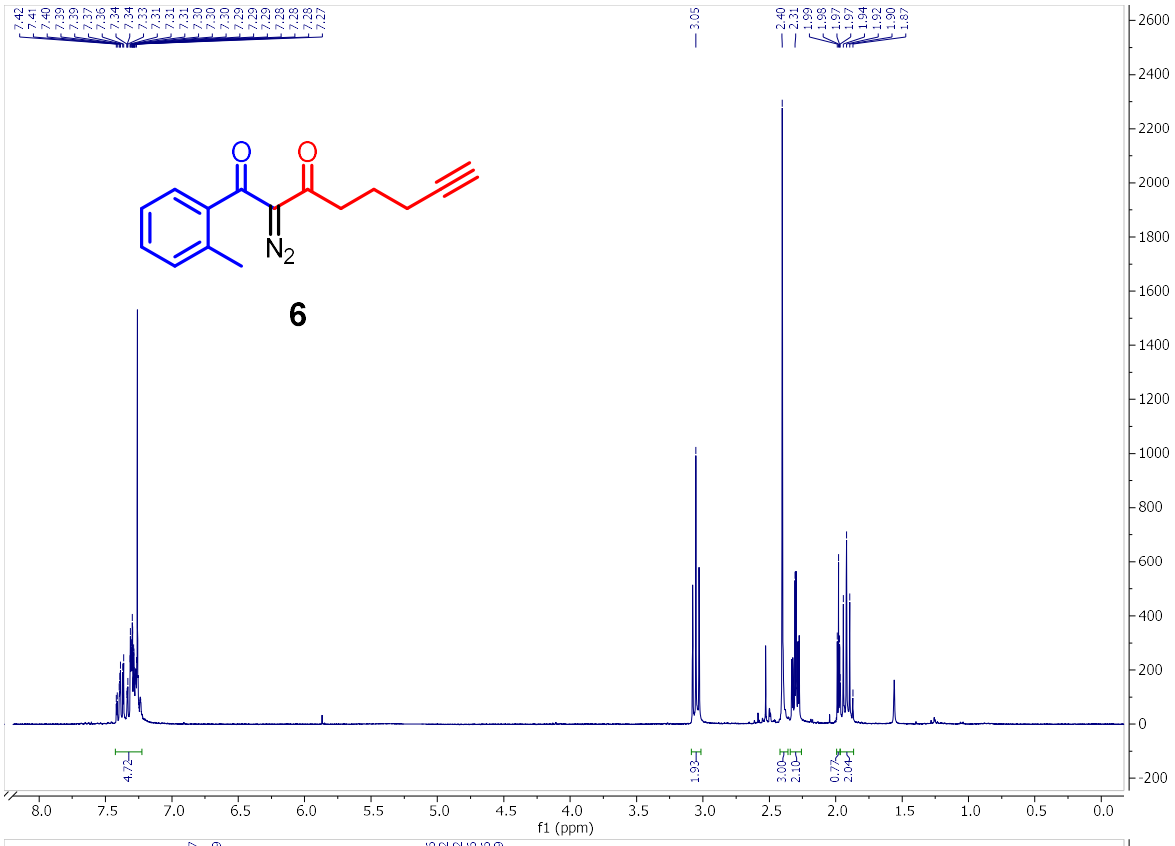
7.42
7.41
7.40
7.39
7.39
7.37
7.36
7.34
7.34
7.33
7.31
7.31
7.31
7.30
7.30
7.30
7.29
7.29
7.28
7.28
7.28
7.27
3.05
2.40
2.31
1.99
1.98
1.97
1.97
1.94
1.92
1.90
1.87
N2
6
4.72
1.93
3.09
2.10
0.77
2.04
f1 (ppm)

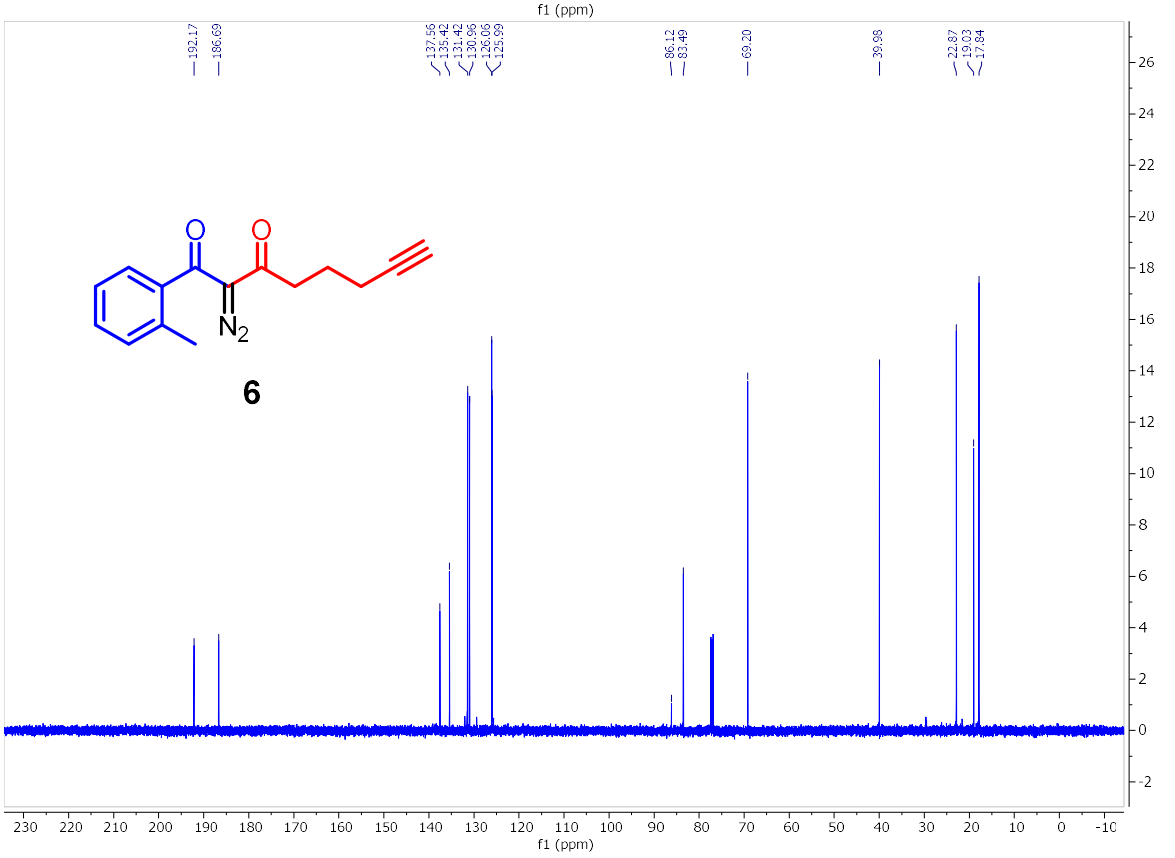
192.17
186.69
137.56
135.42
131.42
130.96
126.06
125.99
86.12
83.49
69.20
39.98
22.87
19.03
17.84
N2
6
f1 (ppm)

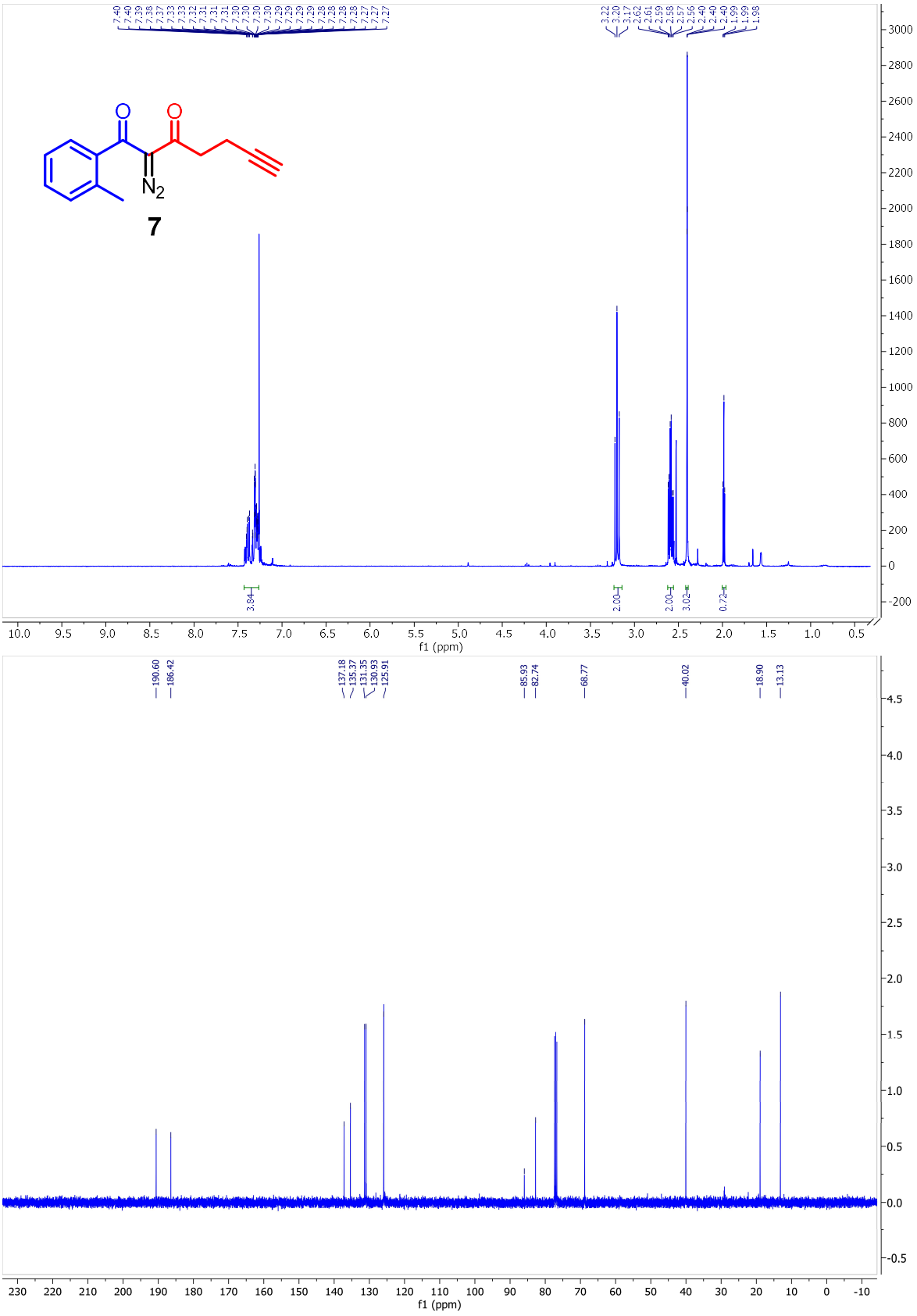
7.40
7.40
7.39
7.38
7.37
7.33
7.32
7.31
7.31
7.30
7.30
7.30
7.29
7.29
7.29
7.28
7.28
7.28
7.27
7.27
7.27
3.22
3.20
3.17
2.62
2.61
2.59
2.58
2.57
2.56
2.40
2.40
1.99
1.99
1.98
O
O
N2
7
3.84
2.00
2.00
3.02
0.72
f1 (ppm)
190.60
186.42
137.18
135.37
131.35
130.93
125.91
85.93
82.74
68.77
40.02
18.90
13.13
f1 (ppm)

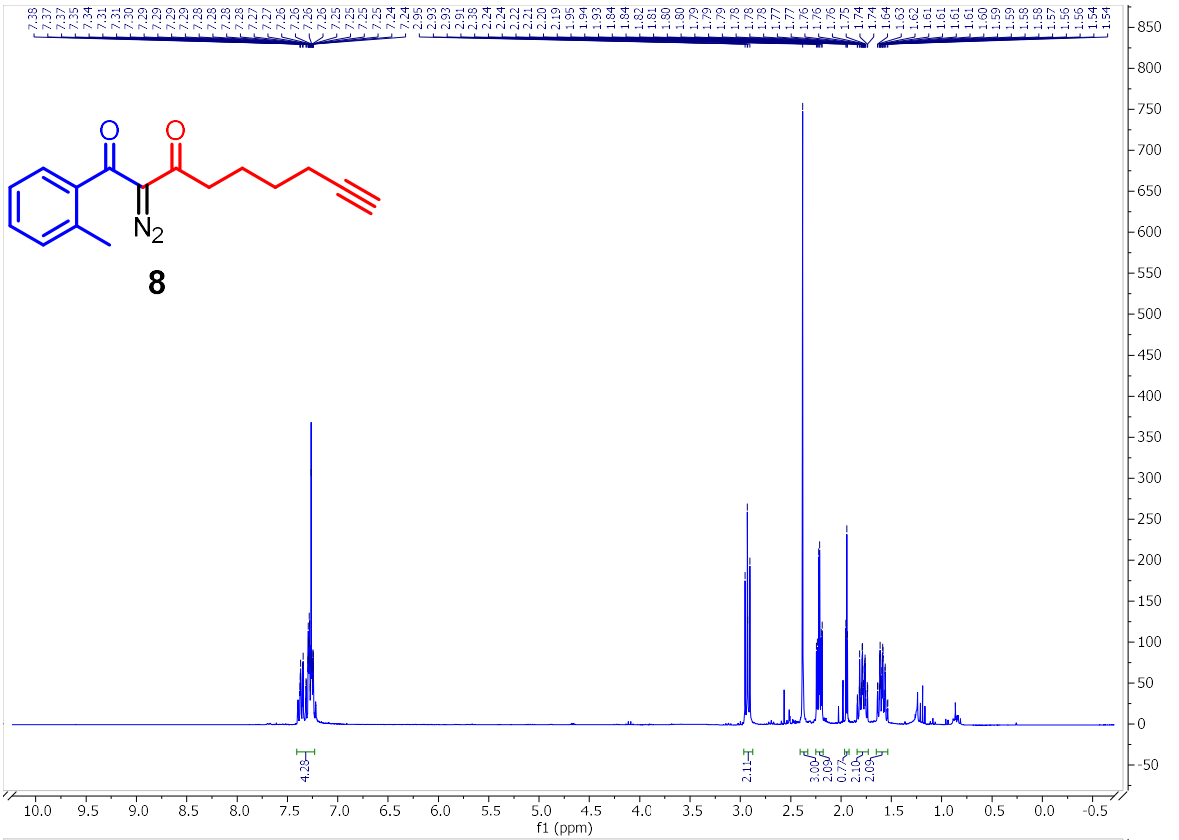
8
f1 (ppm)

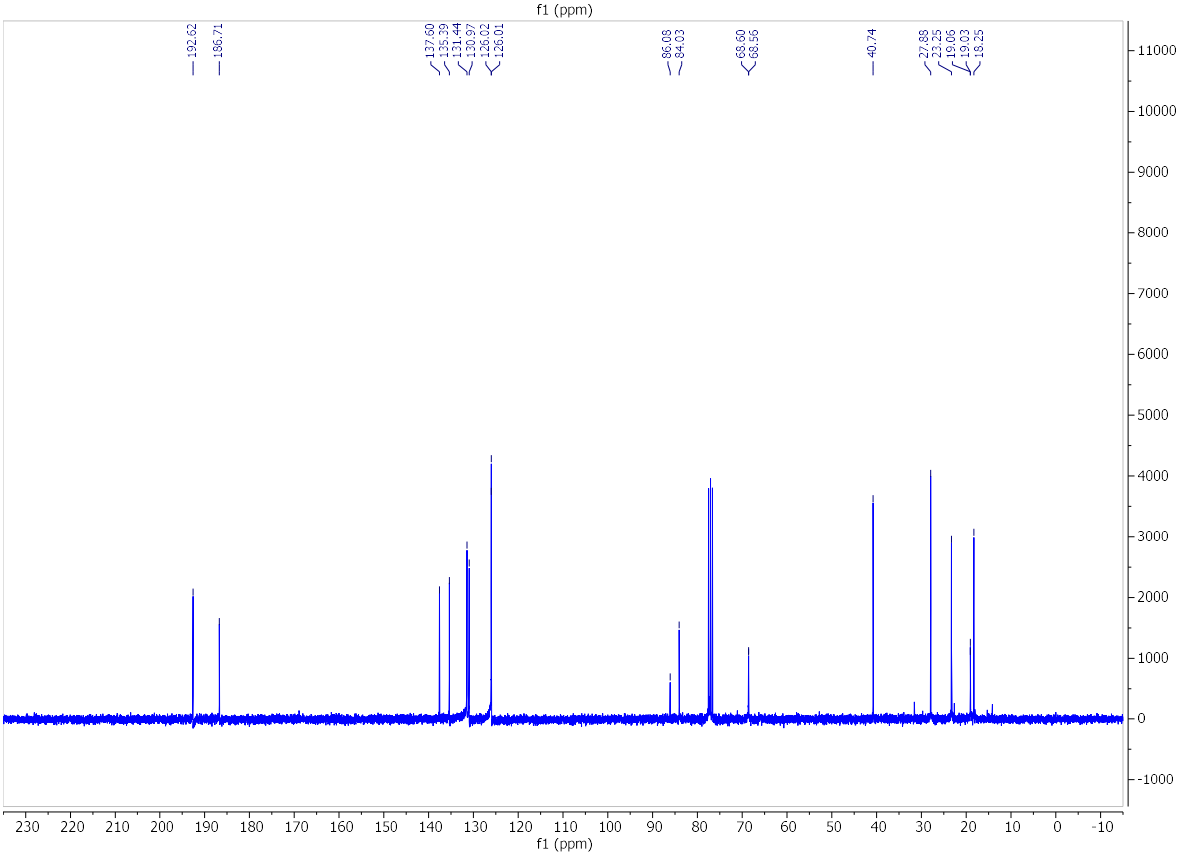
f1 (ppm)

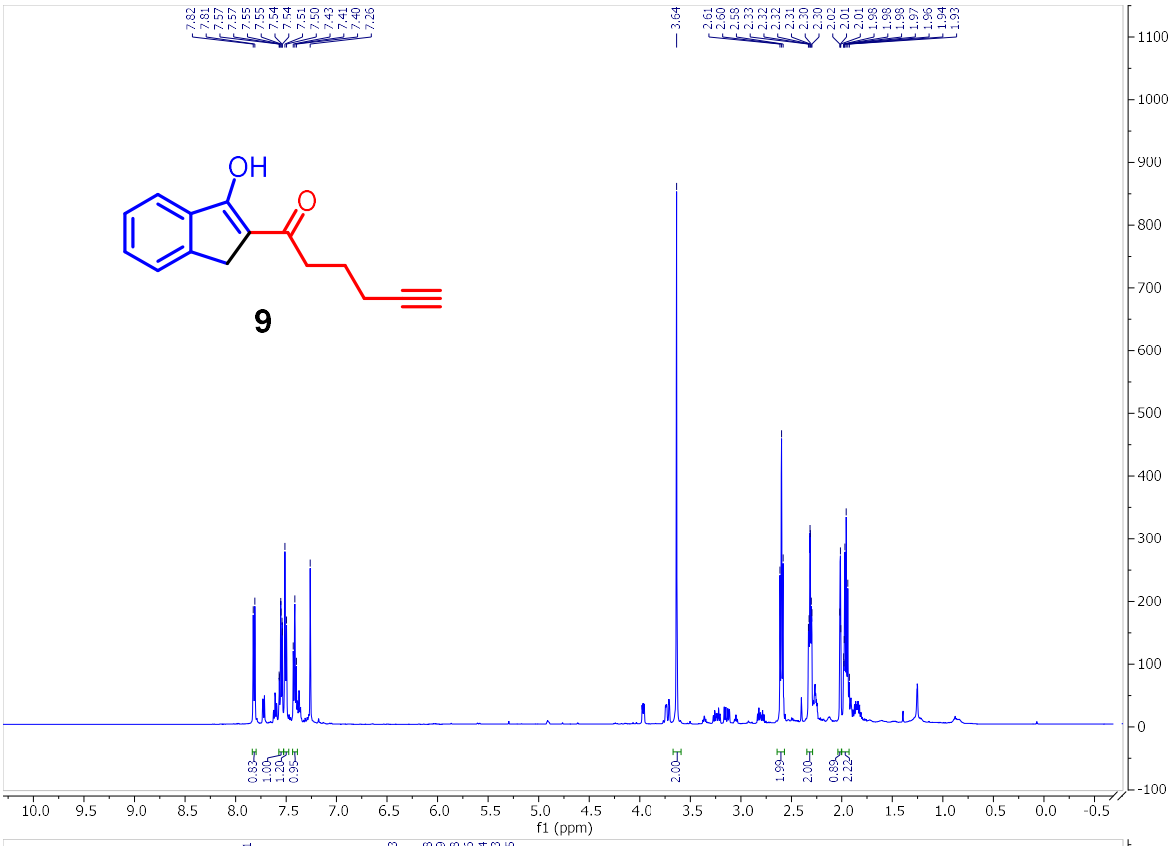
OH
O
9
f1 (ppm)

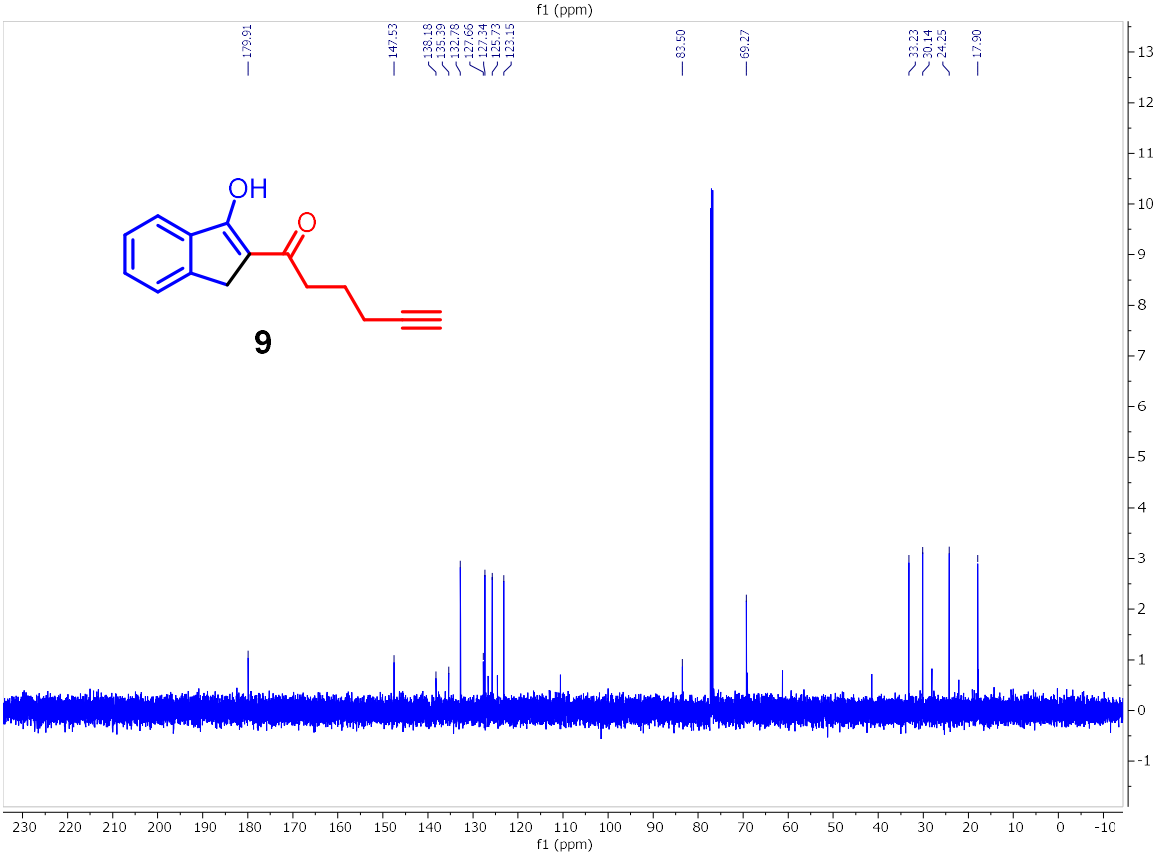
OH
O
9
f1 (ppm)

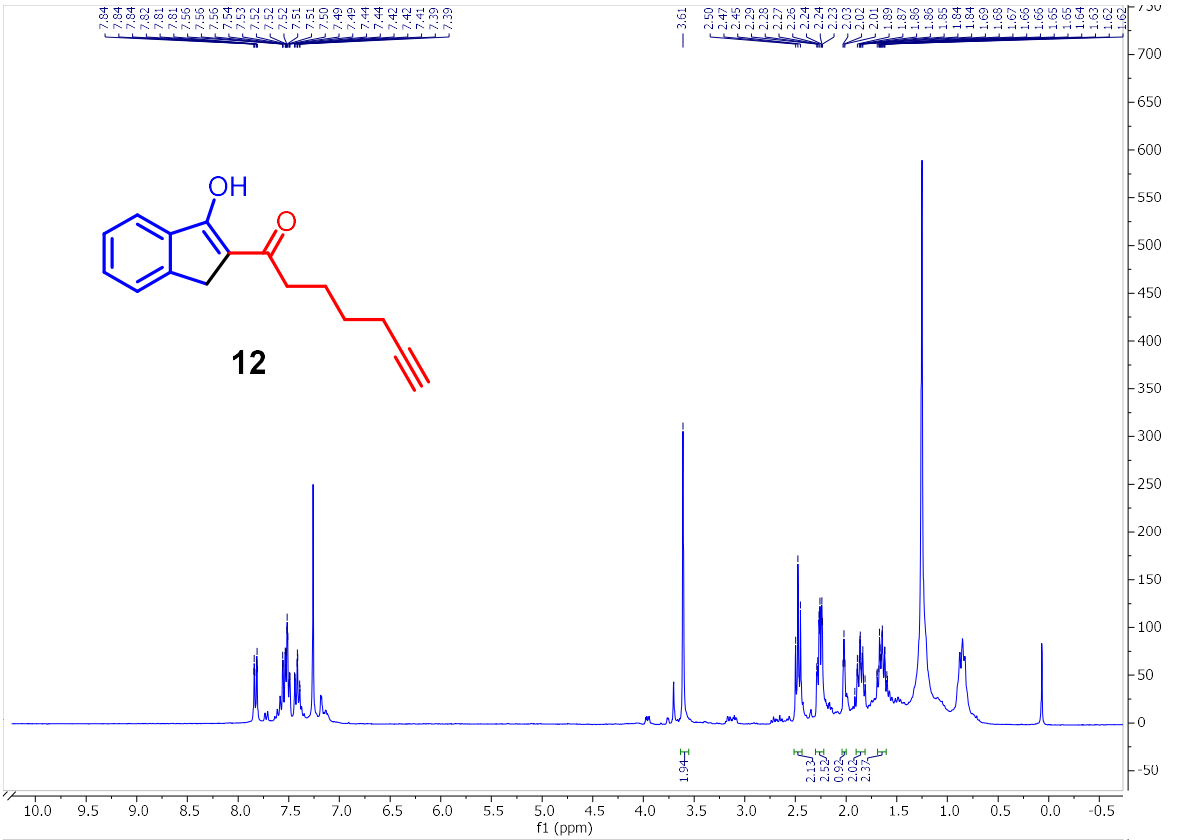
OH
O
12
f1 (ppm)

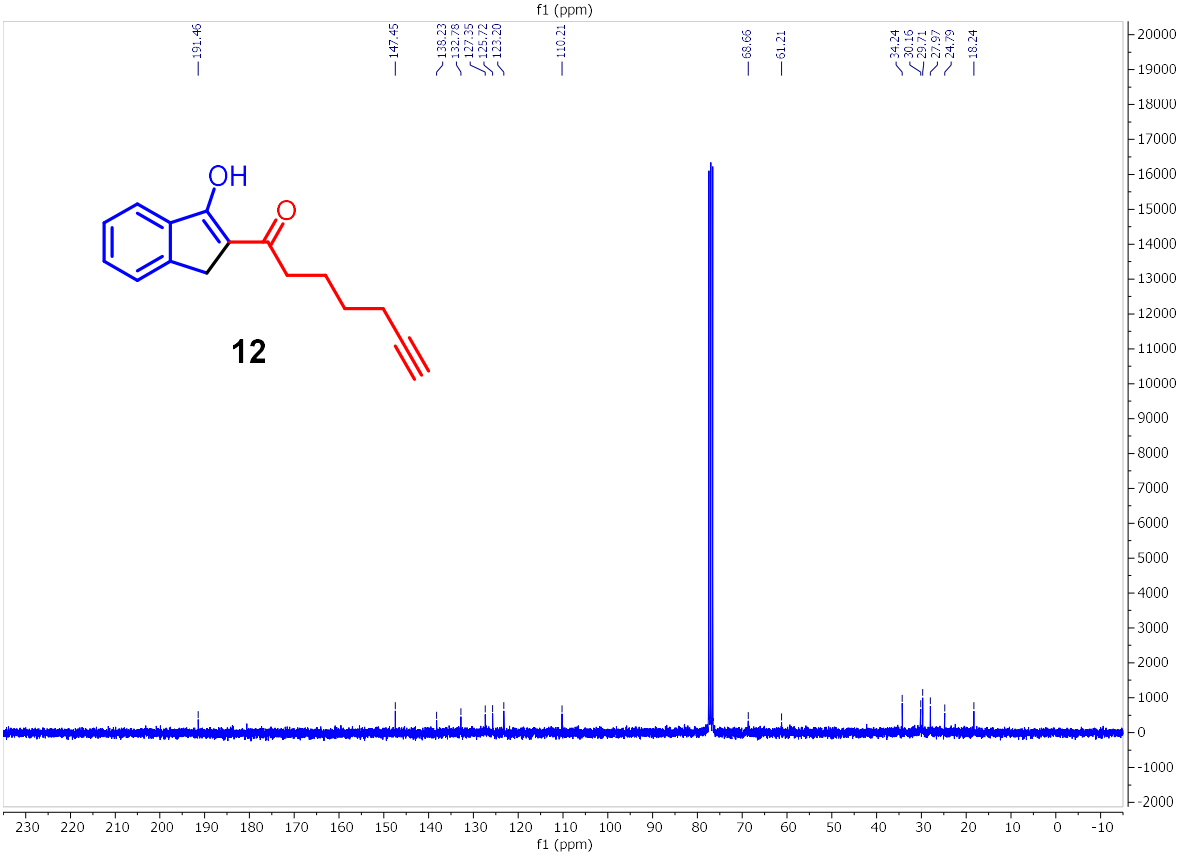
OH
O
12
f1 (ppm)

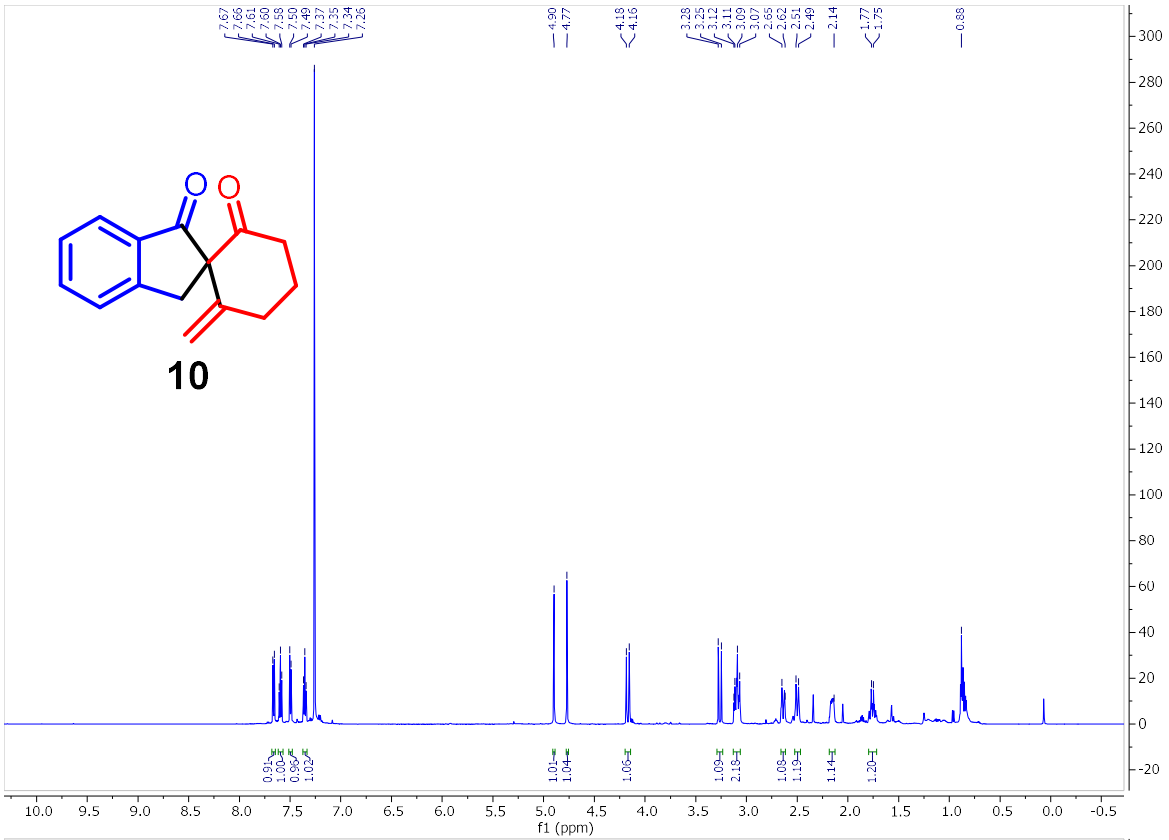
10
f1 (ppm)

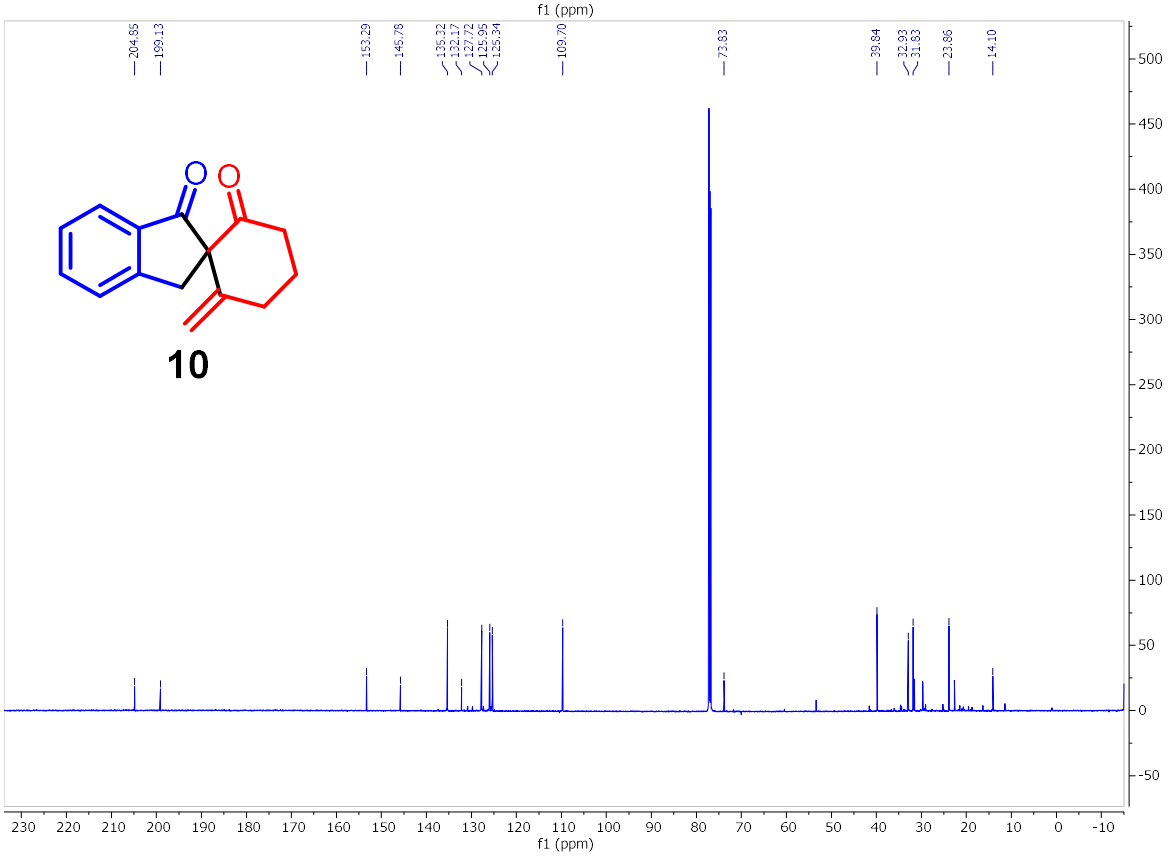
10
f1 (ppm)

CHAPTER 4

Development of a Metal-Free Cascade Approach to Aromatic Heterocycles

4.1 INTRODUCTION

The efficient formation of medium-sized rings, broadly classified as rings containing between 8-12 atoms, remains a challenge in organic synthesis. Medium-sized rings are represented in numerous bioactive scaffolds, and challenges in their formation result from high angular and torsional strain, associated with the preferred bond angle of sp^3 hybridized carbons. A study towards the rate of intramolecular lactonization (k(intra)) showcases this unique trend (**Figure 1**);[1] This report shows the relative stability of small rings, between 5-7 atoms, met with a marked decrease in reaction rate to generate medium sized rings. As the ring size extends past

12 atoms, the increased size allows for conformational flexibility of the atoms, and resulting stabilization.

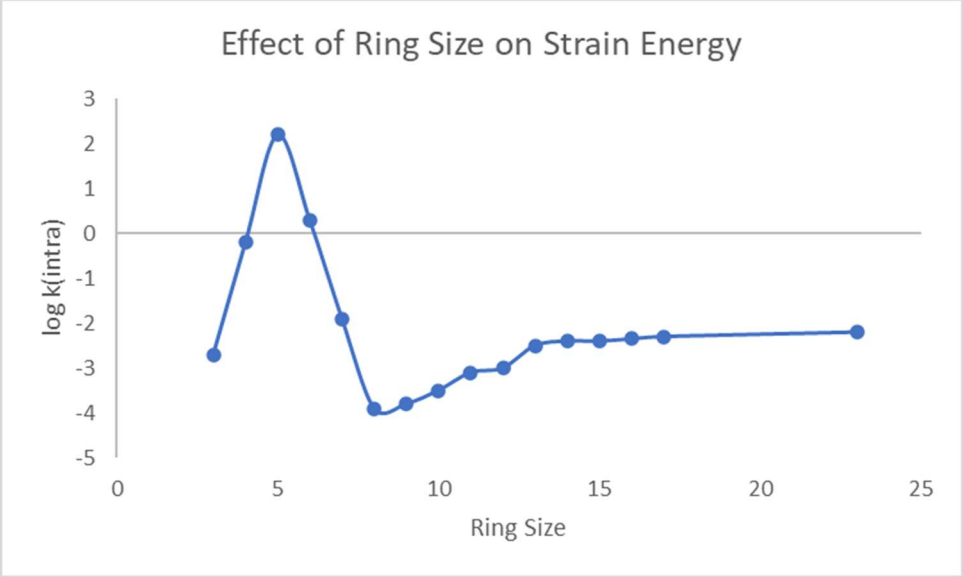

Figure 4.1 Impact of ring size on rate of intramolecular lactonization

Recently, our group has developed a new method to access medium-sized rings, which utilizes carbene an X—H insertion/aldol/oxy-cope cascade.[2] In continuing our interest in the formation of complex macrocyclic scaffolds, we initially designed a substrate that would lead to a metal-free approach to benzannulated oxacycles. We hypothesized that coupling readily accessible 2'-hydroxychalcones with crotonic acid would provide a substrate capable of enolization, intramolecular aldol addition, followed by an anionic oxy-cope rearrangement to access 10-membered Oxacycles (**Figure 4.1a**).

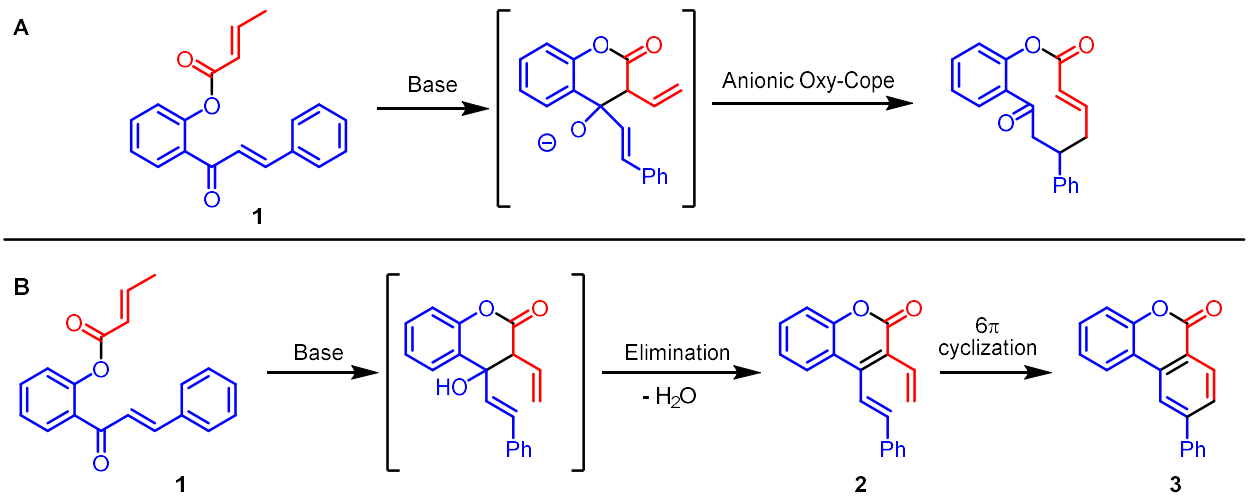

Scheme 4.1 a.) Cascade approach to 10-membered oxacycles b.) Observed formation of Benzo[c]coumarins

When crotonate **1** was exposed to base however, we observed the clean formation of a product that, after NMR analysis, completely lacked any aliphatic protons, as would be expected in the desired macrolactone product. Upon full characterization, we discovered that the product was instead aromatic benzo[c]coumarin **3**, which had formed through a base-mediated aldol-elimination to generate 1,3,5-triene **2**. This triene intermediate presumably underwent a thermal 6π-electrocyclization[3] and subsequent aerial oxidation to form a new aromatic ring (**Scheme 4.1b**). After surveying the literature, this tricyclic aromatic scaffold and related scaffolds are the core structures of several notable natural products (**Figure 4.1**).

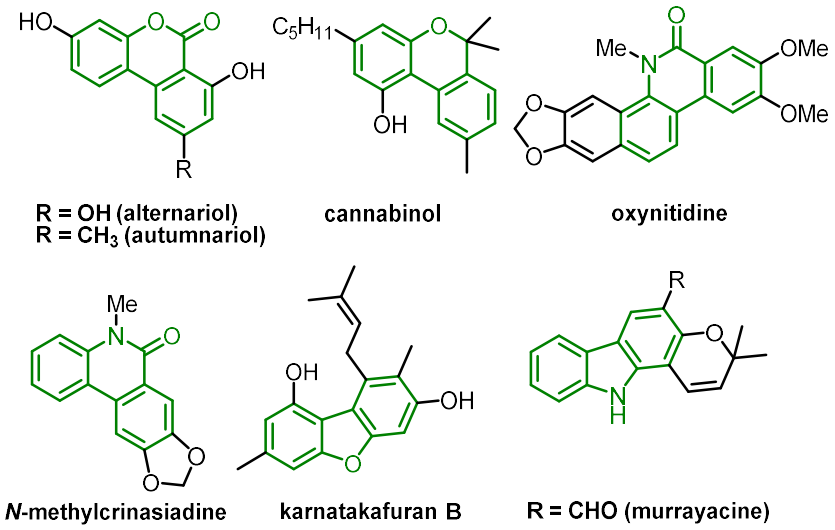

Figure 4.2 Fused Aromatic Heterocycles in Natural Products

Alternariol and autumnariol both feature a benzo[c]coumarin core directly, and the natural product cannabinol was recently synthesized from a benzo[c]coumarin intermediate in three steps.[4a-e] Likewise, the lactam counterparts, Phenanthradin-6(5*H*)-ones, comprise the core scaffold of oxynitidine and N-methylcrinasiadine.[4g-h] Lastly, similar *bis*-benzannulated scaffolds, dibenzofurans and carbazoles, are well represented in natural product cores, including karnatakafuran B and murrayacine.[4i-j] Although there are examples in literature of 6π-electrocyclization employed in the synthesis of biologically relevant natural products,[5] this serendipitous cascade represents a unique retrosynthetic disconnection for the construction of benzannulated heterocycles that does not rely on modification of a pre-formed heterocyclic scaffold.[6]

4.2 CASCADE APPROACH TO BENZO[C]COUMARINS

4.2.1 SUBSTRATE SYNTHESIS

The desired crotonate ester starting materials can be accessed via a high-yielding two-step route from commercially available acetophenones and aryl aldehydes (**Scheme 4.2**). All reactions could be conveniently performed on a multi-gram scale.

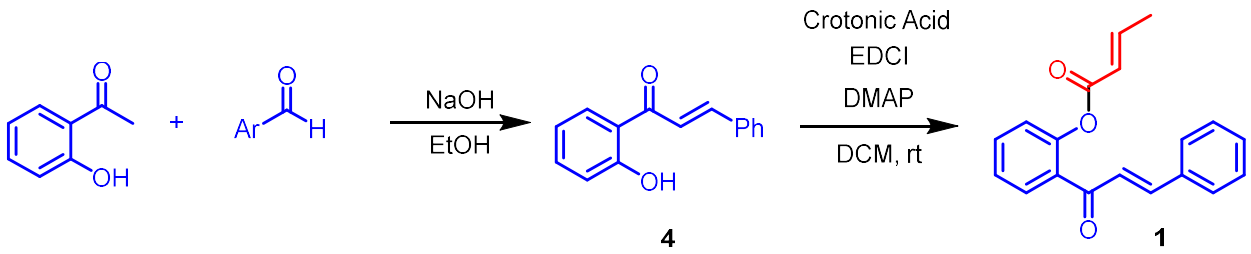

Scheme 4.2 Synthesis of Croconate esters **1**

Condensation between 2'-hydroxycetophenone and benzaldehydes under Claisen-Schmidt conditions afford 2'-hydroxychalcones **4** in excellent yields; These products are easily purified by crystallization in ethanol. Next, carbodiimide coupling of **4** to crotonic acid produces desired ester **1** after acid/base purification. With desired crotonate ester in hand, we began searching for conditions that could encourage the desired intramolecular aldol addition/oxy-cope cascade.

4.2.2 REACTION OPTIMIZATION

With our preliminary observation, we then directed our attention towards optimizing reaction conditions for the formation of benzo[c]coumarin **3** (**Table 4.1**).

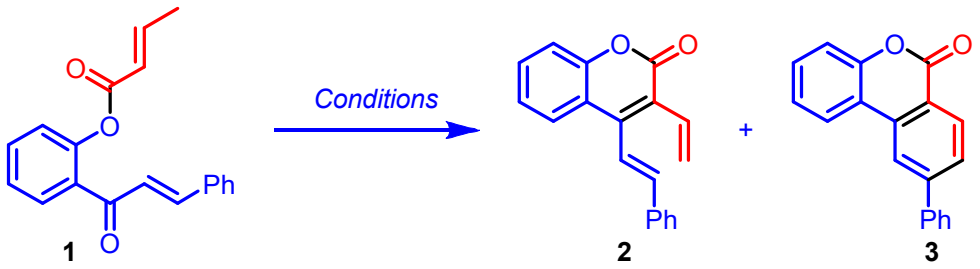

Entry	**Base (eq.)**	**Solvent**	**Temperature**	**2:3**
1	K_2CO_3 (3.0)	Acetone	Reflux	1:2 (23)[c]
2	Et_3N (3.0)	DCM	Reflux	N.R.
3	DBU (3.0)	DCM	rt	95:5
4	DBU (3.0)	DMSO	rt	90:10
5	**DBU (3.0)**	**DMSO**	**rt → 80 °C**	**0:100 (82)[c]**
6	DBU (2.0)	DMSO	rt → 80 °C	0:100 (64)[c]
7	DBU (1.0)	DMSO	rt → 80 °C	0:100 (45)[c]
8	DBU (0.1)	DMSO	rt → 80 °C	trace

Table 4.1 Reaction optimization for aldol elimination/electrocyclization sequence. All optimization reactions were performed by adding base at room temperature to a solution of **1** in DMSO (0.15 M). The reaction vessel was sealed and heated at the indicated temperature for 16 hours. [b]The percent ratio of **2** and **3** was determined by crude ^{1}H NMR integration. [c]Isolated yield of **3** obtained after column chromatography.

When we exposed crotonate 1 to potassium carbonate in refluxing acetone, we observed full conversion to triene **2,** with a 66% conversion to **3**; these reaction conditions however were low yielding, so we explored using common organic bases. We observed no reaction between crotonate **1** in dichloromethane, even when the reaction temperature was elevated to reflux over 24 hours. When DBU was used as the base, we observed full conversion of **1** to triene **2**, with partial conversion to **3**; this suggested that the desired thermal

electrocyclization could proceed at room temperature, however elevated temperatures may be needed to encourage this reactivity. Inspired by recent reports into the 6π-electrocyclization of 1,3,5-triene systems,[6] DMSO was then used as the reaction solvent and we observed a slight increase in the formation of **3** at room temperature. Finally, we elevated reaction temperatures to 80 °C, and full conversion of **2** to **3** was observed after heating for 16 hours, with an excellent isolated yield.

Lastly, we performed experiments to observe the effect on reducing base equivalency. Although reducing the amount of DBU still resulted in complete conversion of **1** to triene **2**, and **2** to **3**, we observed a marked decrease in isolated yield when compared to using 3.0 equivalents. When a catalytic amount of DBU was employed, we observed only trace conversion of **1** to **2**.

4.2.3 BENZO[C]COUMARIN SUBSTRATE SCOPE

With optimized reaction conditions established, we then explored the effects of substituents on crotonate ester **1** (**Scheme 4.3**).

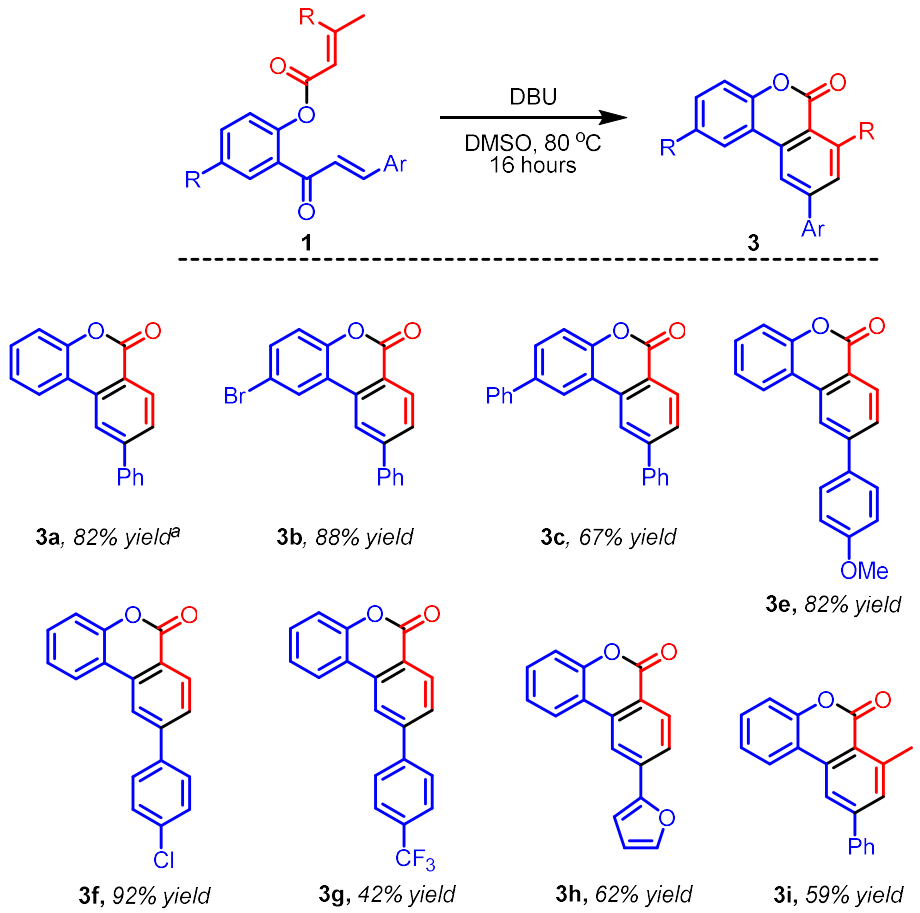

3a, *82% yield*[a] **3b**, *88% yield* **3c**, *67% yield* **3e**, *82% yield*

3f, *92% yield* **3g**, *42% yield* **3h**, *62% yield* **3i**, *59% yield*

Scheme 4.3 Cascade approach to benzo[c]coumarins – Substrate scope

Parent crotonate ester 1 cleanly underwent optimized reaction conditions to give **3a** in good yields. This reaction was also scaled-up to the 1-gram scale, with only a slight decrease in yield (76%). Aromatic bromination of acetophenone and subsequent coupling furnished ester **1b**, which underwent cascade conditions cleanly, producing 2-bromobenzocoumarin **3b** in excellent yield. **1b** bears an aryl bromide functionality, which was converted to an additional phenyl substituent

through palladium catalyzed coupling conditions. This substrate produced the corresponding benzocoumarin **3c** in a good yield. Next, we examined the effects of altering the electronics of the chalcone functionality, conveniently accessed by using 4-substituted benzaldehyde starting materials. Overall, the reaction proceeded smoothly with electron-neutral and electron-donating substituents (**3d** – **3f**), however strongly electron-withdrawing substituents resulted in diminished yield (**3g**). We also probed the effect of alternative heterocyclic scaffolds on the reactivity of crotonate **1**; by condensing 2'-hydroxyacetophenone with 2-furaldehyde, **1g** was cleanly prepared and withstood reaction conditions to furnish furan-substituted benzylcoumarin **3g** in good yield. Lastly, we observed the effects on alkylation of the crotonate ester in the β-position. Compound **1i** was prepared by coupling 2'-hydroxychalcone with 3-methyl-2-butenoic acid, and did successfully undergo the desired aldol/electrocyclication cascade, however we noticed the reaction became sluggish, and evidence of incomplete electrocyclization was observed.

4.3 SYNTHESIS OF PHENANTHRADIN-6(5H)-ONES

With a substrate scope of 9 substituted benzo[c]coumarins prepared, we then explored the possibility of utilizing the amide analogue of 1 in the reaction cascade, for the synthesis of phenanthradin-6(5*H*)-ones.

4.3.1 SUBSTRATE SYNTHESIS

Amide substrate 6 could be prepared in a three-step sequence beginning with 2'-aminoacetophenone (**Scheme 4.4**).

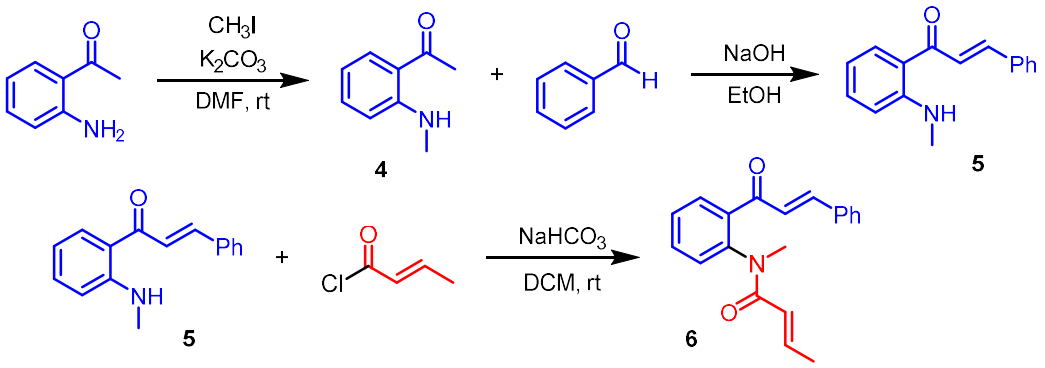

Scheme 4.4 Synthesis of *N*-methylcrotonamides **6**

First, 2'-aminoacetophenone was mono-methylated using iodomethane in the presence of potassium carbonate in DMF. Mono-alkylation proved to be a challenge for this substrate, as the electron-deficient nature of the amine made reductive amination conditions unsuitable. Fortunately, the mono-methyl amine **4** could be separated from its bis-methyl counterpart and unreacted starting material by crystallization. Then, condensation with various aryl aldehydes provided 2'-methylaminochalcones **5** in good, reliable yields. Lastly, acyl substitution with crotonyl chloride produced desired N-methylcrotonylamide **6**. Notably, **5** was unresponsive towards carbodiimide coupling conditions with crotonic acid, so the acyl chloride counterpart was used in its stead. With amide **5** in hand, we determined its efficacy in the reaction cascade.

4.3.2 PHENANTHRADIN-6(5H)-ONE SUBSTRATE SCOPE

To our delight, N-methyl-N-crotonylamide **6** withstood optimized conditions smoothly to cleanly afford the desired phenanthradin-6(5H)-one product. We then explored the substrate scope of this transformation with respect to crotonylamides **6** (**Scheme 4.5**).

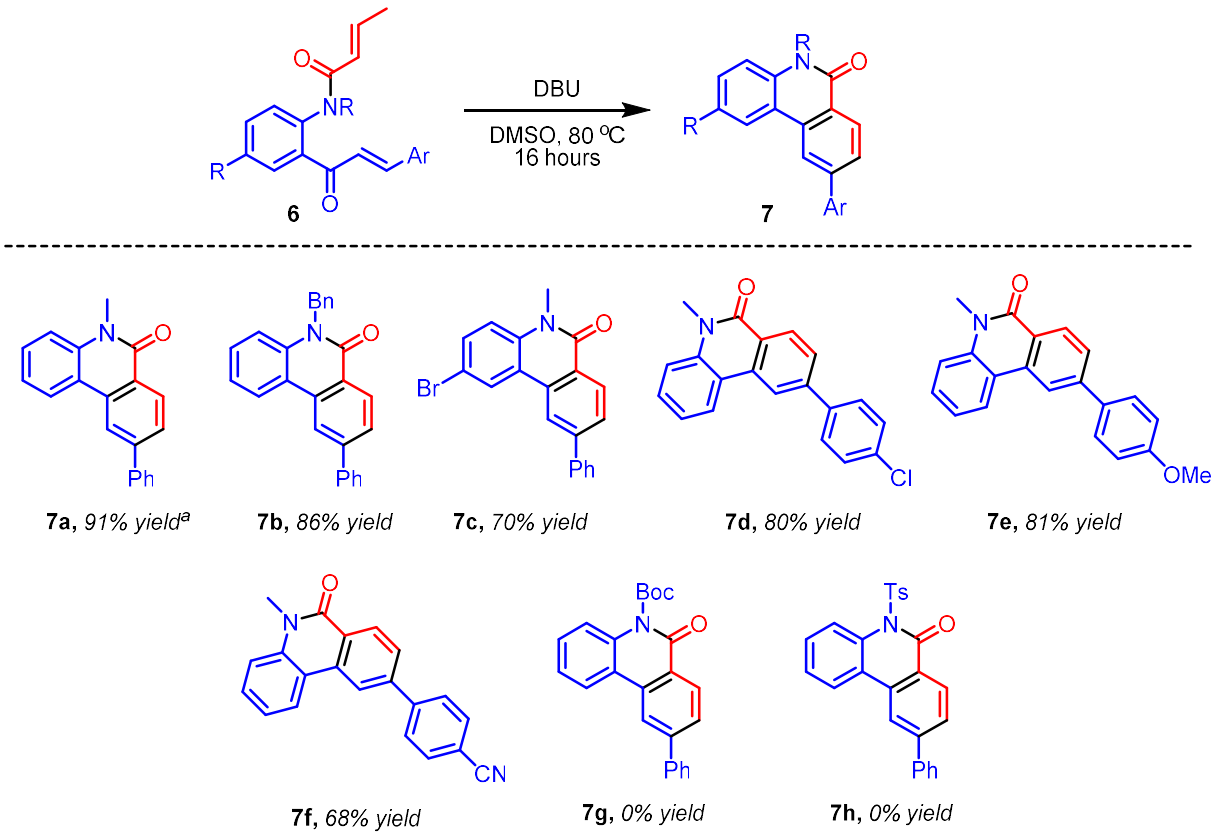

Scheme 4.5 Scope of Phenanthradin-6(5*H*)-one substrates prepared

Parent N-Methyl-N-crotonylamide **6a** cleanly underwent the desired aldol/electrocyclization cascade to give **7a** in excellent yields. This reaction was amenable to a scale up to 1-gram, with negligible loss in yield (89%). The reaction conditions also withstood the N-Benzyl protecting group to give **7b** in good yields. As in the case of benzo[c]coumarins, bromo-functionalized precursor also underwent the desired cascade to give **7c** in good yields. We then

observed the effect of altering the electronics of the 1,3,5-triene intermediate, and isolated electron-neutral and electron-rich products **7d** and **7e** in good yields, with a slight decrease in yield for electron-poor **7f**. Lastly, we explored linear substrates **6** bearing labile amide protecting groups. Unfortunately, the reaction conditions did not withstand the common electron-withdrawing protecting groups tert-butyl carbamate (boc) and 4-toluenesulfonate (Ts). In the case of *boc*-protected **6g**, the reaction produced a complex mixture of products, resulting from cleavage of the *boc*- protecting group. There are several examples of boc- protected amines undergoing deprotection in the presence of DBU.[7] In the case of tosyl-protected **6h**, exposure to DBU resulted in cleavage of the crotonylamide resulting in clean recovery of *N*-Tosyl-2'-aminochalcone.

4.4 ARYL-ELECTROCYCLIZATION

We next explored the possibility of exchanging one olefin component of 1,3,5-trine intermediate **2** to an aromatic ring. 6p electrocyclizations including an aromatic ring have been documented.[8] Generation of the requisite aryl-diene intermediate would rely on direct α-enolization and attack of an active methylene precursor, as opposed to our established indirect γ-enolization and α-enolate attack. If this approach proves successful, it will provide an expedient route to several new tetracyclic frameworks.

4.4.1 SUBSTRATE SYNTHESIS

We envisioned a route to linear precursors **8** involving coupling of prepared 2'-heterochalcones to commercially available arylacetic acids (**Scheme 4.6**). Fortunately, the pre-established coupling conditions between chalcones and crotonic acid, used to prepare precursors **1** and **6**, were well suited to coupling with the arylacetic acids, resulting in precursors **8** being formed in excellent yields in most cases.

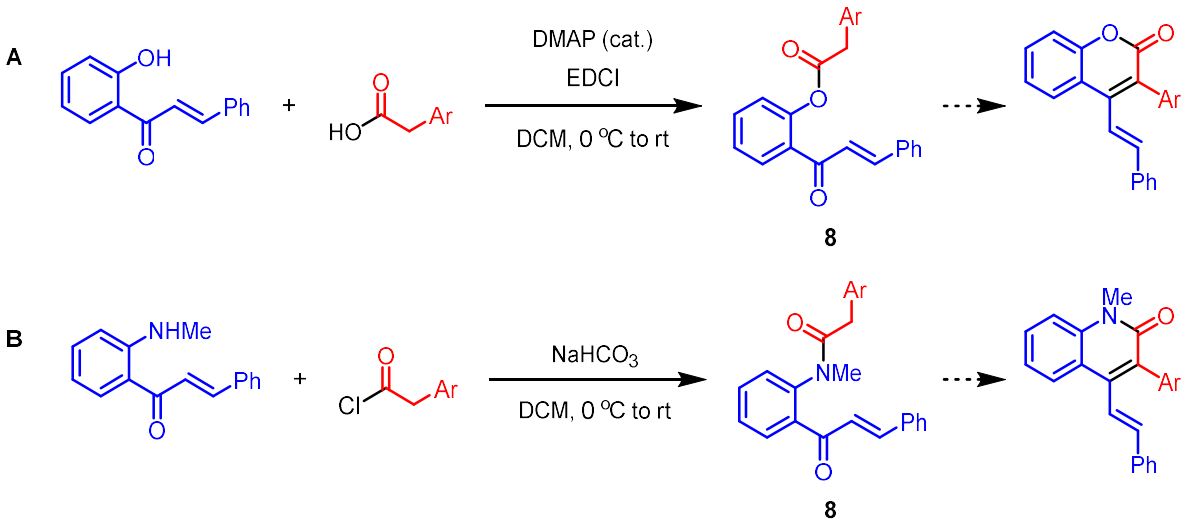

Scheme 4.6 a.) Synthesis of Hetroarylbenzo[c]coumarin Precursors b.) Synthesis of Hetroarylphenanthradin-6(5H)-one Precursors

Some of the linear substrates **8** however were prone to enolization and intramolecular aldol condensation during coupling conditions, likely due to the reduced pK_a of the α-methylene relative to the γ-crotonyl protons – In these cases the resulting aryl-diene was exposed to the reaction cascade conditions directly.

4.4.2 SUBSTRATE SCOPE AND LIMITATIONS

Phenyl-substituted precursor **8a** was prepared and we proceeded to test our aryl-electrocyclization hypothesis. The precursor underwent the desired aldol condensation in good yields at room temperature, but this intermediate did not undergo 6π-electrocyclization at 80 °C, even after 24 hours. Unfortunately, this substrate did not undergo electrocyclization, even after 48 hours at 180 °C. We hypothesized that exchanging the phenyl ring with electron-rich heterocycles would provide a driving force for the desired electrocyclization to occur. After exchanging the phenyl ring for an electron-rich furan ring, we were delighted to observe the formation of **9b**, although a slight increase in temperature (120 °C) was required to induce electrocyclization. We next pursued the scope of aryl-donors that could undergo electrocyclization (**Scheme 4.7**).

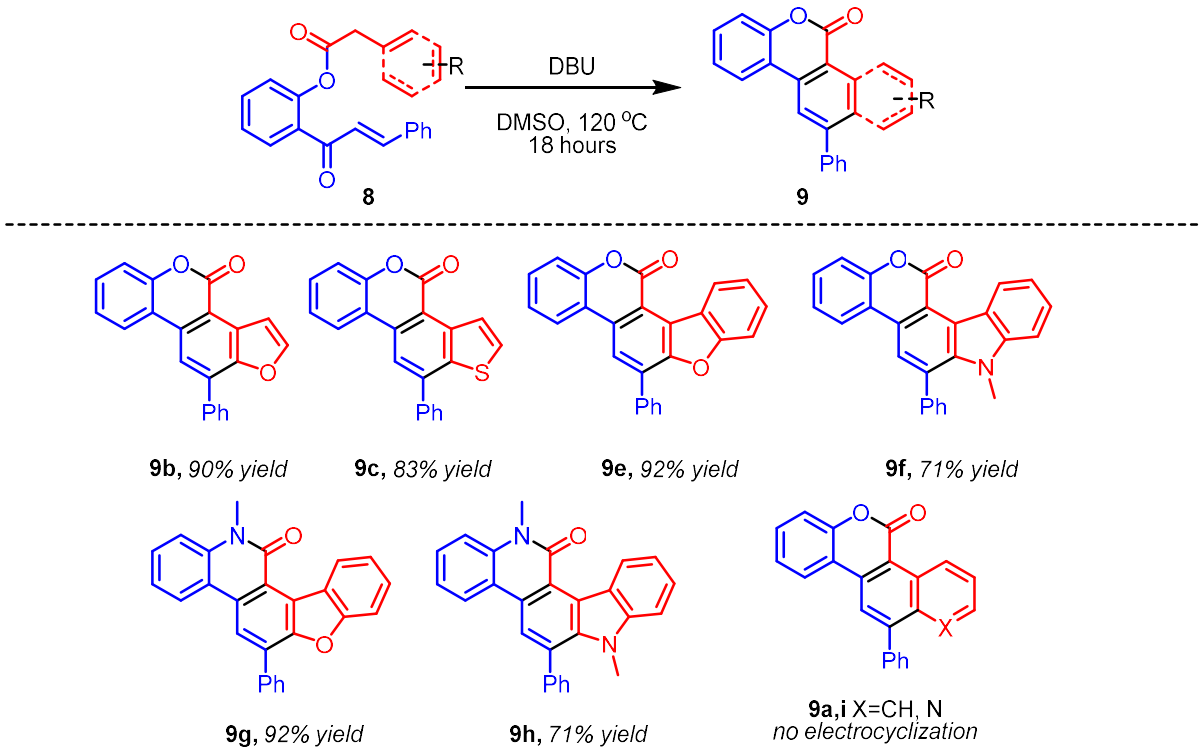

Scheme 4.7 Substrate Scope for Aryl-Electrocyclization Cascade

Furan-substituted **9b** was prepared in an excellent 90% yield, and the reaction was also well-suited to a thiofuran donor, resulting in an 83% yield of **9c**. Notably, this thiofuran precursor was prone to intramolecular aldol condensation during coupling conditions, so the reaction was performed using the resulting aryl-diene. Next, we explored the possibility of using bicyclic aromatic heterocycle donors – To our delight, the reaction conditions also tolerated dibenzofuran and N-methylindole donors **8e** and **8f** well, resulting in good yields of **9e** and **9f**. The lactam analogs were also successful candidates, and phenanthradin-6(5H)-ones **9g** and **9h** were prepared in comparable yields to their lactone counterparts. Lastly, we attempted the reaction conditions with pyridine-donor **8i**, however this compound did not undergo aryl-electrocyclization even after 24 hours at 180 °C.

4.5 SYNTHESIS OF DIBENZOFURANS AND CARBAZOLES

We next explored the possibility of synthesizing other heterocyclic scaffolds using our Aldol condensation/electrocyclization cascade. We were happy to find that this cascade could be applied to the synthesis of dibenzofurans and carbazoles (**Scheme 4.8**).

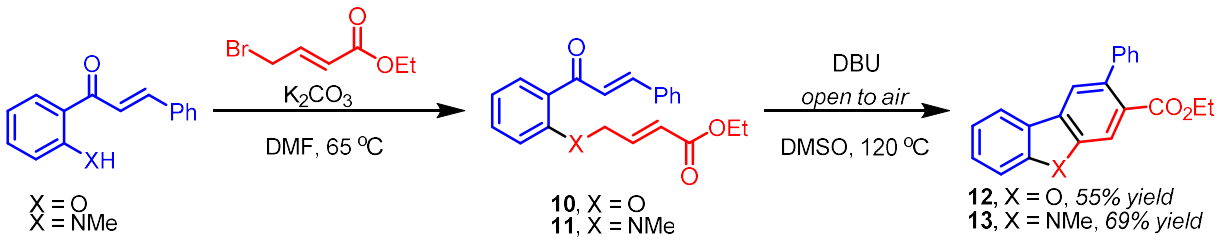

Scheme 4.8 Cascade approach to dibenzofurans and carbazoles

2'-functionalized chalcones underwent substitution with ethyl 4-bromocrotonate in the presence of base to cleanly give electrocyclization precursors **8** and **9**. These compounds

underwent the desired γ-deprotonation and α-enolate attack to give the desired triene intermediate at room temperature. When the reaction was heated to 80 °C, no desired electrocyclization occurred, but when heated to 120 °C 8 and 9 were converted to dibenzofuran **10** and carbazole **11** were isolated in good yields.

4.6 ATTEMPTED FORMAL SYNTHESIS OF CANNABINOL

The natural product cannabinol (CBN), an agonist of the CB_1 and CB_2 receptors, was synthesized recently from a benzo[c]coumarin precursor.[4d] In their report, Wang et al. reported the synthesis of Benzo[c]coumarin **B** through intramolecular palladium-catalyzed lactonization of a biphenyl *ortho*-benzoic acid. Then a functionalization route employed by Teske et. al. was employed, involving addition of methyllithium followed by acid-catalyzed ring closure of the resulting diol, and subsequent ester cleavage.[4e] We envisioned that we could accomplish a formal synthesis of cannabinol by synthesizing **B** through an aldol/electrocyclization cascade of precursor **A** (**Scheme 4.9**).

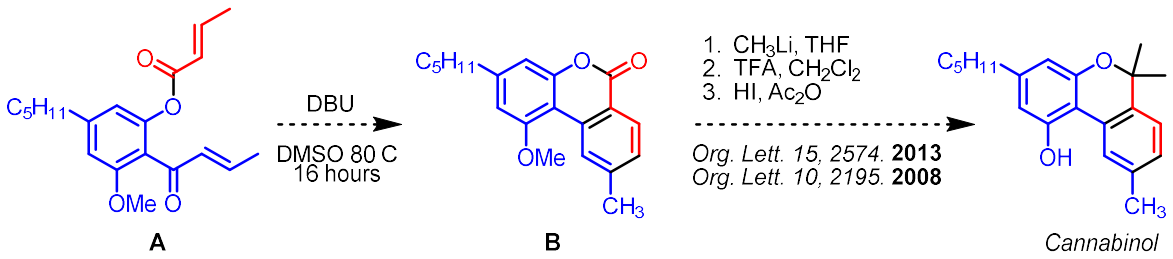

Scheme 4.9 Planned formal synthesis of Cannabinol, using methods from Teske et. al.

We proceeded forward towards the synthesis of **A**. We designed a three-step route that would afford desired electrocyclization precursor **B** (**Scheme 4.10**).

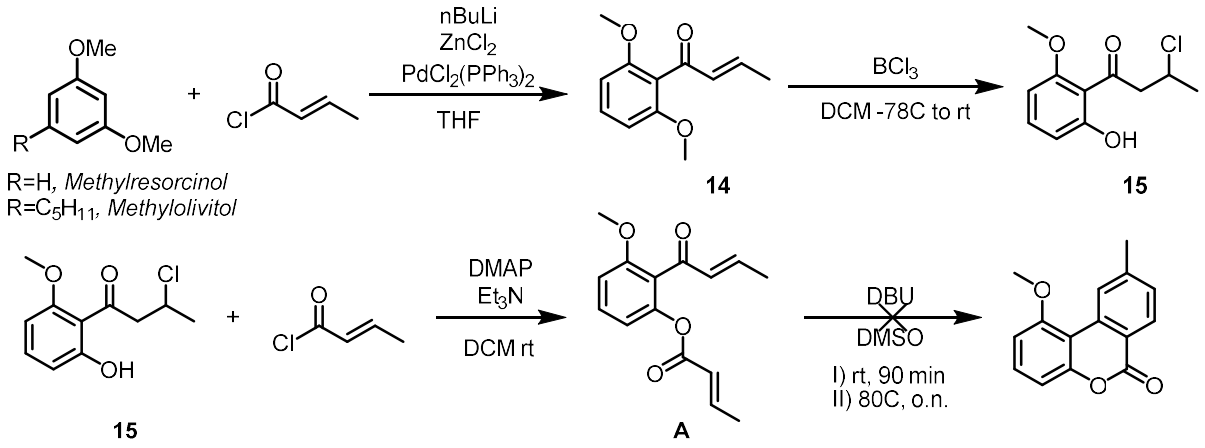

Scheme 4.10 Synthesis of precursor **A** and exposure to cascade conditions

Methylresorcinol, which differs from methylolivitol, the actual precursor to CBN, was used as a model substrate to test our electrocyclization hypothesis. First, methylresorcinol underwent palladium-catalyzed arylation to give crotonophenone **14**, which was exposed to a stoichiometric amount of boron trichloride. We envisioned that these conditions would result in mono-deprotection of a methyl ether, which occurred, but also resulted in Michael addition of chloride to the α,β-unsaturated ketone. We expected this alkyl chloride to undergo elimination in the presence of a base to restore the α,β-unsaturation, so we proceeded forward. Acyl substitution of crotonyl chloride then cleanly afforded desired precursor **A**.

Unfortunately, when **A** was exposed to the optimized reaction conditions, we were unable to isolate any quantity of desired CBN precursor, but rather observed a complex mixture of products. We then exposed **A** to DBU at room temperature, and quenched the reaction after 90 minutes, to determine whether there was an issue with the aldol condensation step, or the subsequent electrocyclization. In this case, we obtained a mixture of products featuring distinct ^{1}H NMR peaks around 12.0 ppm – characteristic of 2'-hydroxychalcones. This leads us to suspect

that this compound, now bearing acidic protons at the ketone γ-position, underwent undesired enolization and subsequent attack on the ester component. Collapse of the resulting tetrahedral intermediate would lead to ester cleavage and fragmentation of the resulting phenol. These findings lead us to infer that a major limitation in substrate scope includes compounds that lack conjugation of the α,β-unsaturated ketone to another functional group.

4.7 SUMMARY & FUTURE DIRECTIONS

In summary, while pursuing a new pathway to generate 10-membered oxacycles, we have discovered a reaction cascade whereby benzo[c]coumarins are formed through an aldol condensation/6π-electrocyclization cascade; The cascade conditions proved general and resulted in a substrate scope of nine benzo[c]coumarins. Conditions were also well-suited to synthesize the lactam analogs, and eight N-alkylphenanthridin-6(5H)-ones were prepared. The parent benzo[c]coumarin and phenanthridine-6(5H)-one compounds were amenable to scale-up, and could be prepared at gram-scale. The 6π-electrocyclization could also include an aromatic heterocycle, and by heating at 120 ^{o}C six different tetracycles were prepared. By changing the cascade precursor slightly, we were also able to extend this approach to dibenzofuran and carbazole scaffolds. Lastly, insights gained during an attempted formal synthesis of the natural product cannabinol revealed that the reaction cascade undergoes an undesired decomposition pathway in the case of substrates containing enolizable protons on the ketone component, by way of ester cleavage and resulting phenolic fragmentation. The developed cascade methodology has shown an impressive substrate scope, but a limitation requires the α,β-unsaturated ketone be in conjugation with an aromatic ring or ester. Identification of a labile conjugating group, which could be cleaved after electrocyclization, would greatly improve the merit of this methodology. In addition, electrocyclization methodology could be employed in diazo-derived carbene chemistry – carbene-carbene coupling is a well-known process to generate alkenes. Utilizing vinyl, styryl, or aryl diazo compounds could provide a triene intermediate suitable for electrocyclization, as a new approach to substituted heterocycles.

4.8 REFERENCES FOR CHAPTER 4

1. Illuminati, G.; Mandolini, L. “Ring Closure Reactions of Bifunctional Chain Molecules.” *Acc. Chem. Res.,* **1981**, *14*, 95-102.

2. a.) Chinthapally, K., Massaro, N. P., Sharma, I. “Rhodium Carbenoid Initiated O-H Insertion/Aldol/Oxy-Cope Cascade for the Stereoselective Synthesis of Functionalized Oxacycles.” *Org. Lett*., **2016**, *18*, 6340−6343; b.) Chinthapally, K., Massaro, N. P., Padgett, H. L., Sharma, I. “A Serendipitous Cascade of Rhodium Vinylcarbenoids with Aminochalcones for the Synthesis of Functionalized Quinolines.” *Chem. Comm.* **2017**, *53*, 12205−12208; c.) Massaro, N. P., Stevens, J. C., Chatterji, A., Sharma, I. “Stereoselective Synthesis of Diverse Lactones through a Cascade Reaction of Rhodium Carbenoids with Ketoacids.” *Org. Lett*. **2018**, *20*, 7585−7589.

3. a.) Okamura, W. H., De Lera, A. R. *In Comprehensive Organic Synthesis*; Trost, B. M., Fleming, I. Paquette, L. A. Eds.; Pergamon Press: New York, **1991**; Vol. 5, p 699; b.) Von Essen, R., Frank, D., Sunnemann, H. W., Vidovic, D., Magull, J., de Meijere, A. “Domino 6π-Electrocyclization/Diels-Alder Reactions on 1,6-Disubstituted (*E,Z,E*)-1,3,5-Hexatrienes: Versatile Access to Highly Substituted Tri- and Tetracyclic Systems.” *Chem. Eur. J.* **2005**, *11*, 6583−6592; c.) Voigt, K., von Zezschwitz, P., Rosauer, K., Lanksy, A., Adams, A., Reiser, O., de Meijere, A. “The Twofold Heck Reaction on 1,2-Dihalocycloakenes and Subsequent 6π-Electrocyclization of the Resulting (*E,Z,E*)-1,3,5-Hexatrienes: A New Formal {2+2+2}-Assembly of Six-Membered Rings.” *Eur. J. Org. Chem.* **1998**, 1521−1534; d.) von Zezschwitz, P., Petry, F., de Meijere, A. “A One-Pot Sequence of Stille and Heck Couplings: Synthesis of Various 1,3,5-Hexatrienes and Their Subsequent 6π-Electrocyclizations.” *Chem. Eur. J.* **2001**, *7*, 4035−4046; e.) Sunnemann, H. W., de Meijere, A. “Steroids and Steroid Analogues from

Stille-Heck Coupling Sequences." *Angew. Chem. Int. Ed*. **2004**, *43*, 895−897; f.) von Essen, R., von Zezschwitz, P., Vidovic, D., de Meijere, A. "A New Phototransformation of Methoxycarbonyl-Substituted (*E,Z,E*)-1,3,5-Hexatrienes: Easy Access to Ring-Annelated 8-Oxabicyclo[3.2.1]octa-2,6-diene Derivatives." *Chem. Eur. J.* **2004**, *10*, 4341−4352.

4. a.) Turner, C. E., Elsohla. M. A., Boeren, E. G. J. "Constituents of Cannabis Sativa L. XVII. A Review of the Natural Constituents." *Nat. Prod*. **1980**, *43*, 169−234; .b.) ElSohly, M. A., and Slade, D. "Chemical Constituents of Marijuana: The Complex Mixture of Natural Cannabinoids." *Life Sci.* **2005**, *79*, 539−548; c.) Raistrick, H., Stickings C. E., Thomas, R. "Studies in the Biochemistry of Micro-organisms. 90. Alternariol and Alternariol Monomethyl Ether, Metabolic Products of *Alternaria Tenuis*." *Biochemical Journal*, **1953**, *55*, 421−433; d.) Li, Y., Ding, Y., Wang, J., Su, Y., Wang, X. "Pd-Catalyzed C-H Lactonization for Expedient Synthesis of Biaryl Lactones and Total Synthesis of Cannabinol." *Org. Lett.* **2013**, *15*, 2574-2577; e.) Teske, J. A., Deiters, A. "A Cyclotrimerization Route to Cannabinoids." *Org. Lett.,* **2008**, *10*, 2195-2198. f.) Sidwell, W. R. L., Fritz, H., Tamm, C. "Autumnariol und Autumnariniol, zwei neue Dibenzo-α-pyone aus *Eucomis Autumnalis Graeb.* Nachweis einer Fernkopplung uber Sechs Bindungen in den Magnetischen Protonenresonanz-Spektren." *Helv. Chim. Act.* **1971**, *54*, 207−215. (Translated from German); g.) Nakamura, M., Aoyama, A., Salim, M. T. A., Okamoto, M., Baba, M., Miyachi, H., Hashimoto, Y., Aoyama, H. "Structural Development Studies of Anti-Hepititis C Virus Agents with a Phenanthridinone Skeleton." *Bioorg. & Med. Chem*. **2010**, *18*, 2402−2411; h.) Patil, S., Kamath, S., Sanchez, T., Neamati, N., Schinazi, R. F., Buolamwini, J. K. "Synthesis and Biological Evaluation of Novel 5(*H*)-Phenanthradin-6-ones, 5(*H*)-Phanthradin-6-one Diketo Acid, and Polyclic Aromatic Diketo Acid Analogs as New HIV-1 Integrase Inhibitors." *Bioorg. & Med. Chem*. **2007**, *15*,

1212−1228; i.) Manniche, S., Sprogoe, K., Dalsgaard, P. W., Christophersen, C., Larsen, T. O. "Karntakafurans A and B: Two Dibenzofurans Isolated from the Fungus *Aspergillus Karnatakaensis*." *J. Nat. Prod.* **2004**, *67*, 2111−2112; j.) Schmidt, A. W., Reddy, K. R., Knoller, H. "Occurrence, Biogenesis, and Synthesis of Biologically Active Carbazole Alkaloids." *Chem. Rev*. **2012**, *112*, 3193−3328.

5. a.) Myers, E. L., Trauner, D. (2012). 2.19 *Selected Diastereoselective Reactions: Electrocyclizations. Comprehensive Chirality.* b.) Carreira, E. M., and Yamamoto, H. Amsterdam, Elsevier: 563–606; c.) Bian, M., Li, L., and Ding, H., "Recent Advances on the Application of Electrocyclic Reactions in Complex Natural Product Synthesis." *Synthesis*, **2017**, *49*, 4383–4413; c.) Choshi, T., and Hibino, S., "Synthetic Studies on Nitrogen-Containing Fused-Heterocyclic Compounds Based on Thermal Elecrocyclic Reactions of 6π-Electron and Aza 6π-Electron Systems." *Heterocycles*, **2011**, *6*, 1205−1240; d.) Sunnemann, H. W., Banwell, M. G., de Meijere, A. "Synthesis and Use of New Substituted 1,3,5-Hexatrienes in Studying Thermally Induced 6π-Electrocyclizations." *Eur. J. Org. Chem*. **2007**, 3879−3893; e.) Itoh, T., Abe, T., Choshi, T., Nishiyama, T., Yanada, R., Ishikura, M. "Concise Total Synthesis of Pyrido[4,3-b]carbazole Alkaloids using Copper-Mediated 6π-Electrocyclization." *Eur. J. Org. Chem*. **2016**, 2290−2299.

6. a.) Mou, C., Zhu, T., Zheng, P., Yang, S., Song, B. A., Chi, Y. R. "Green and Rapid Access to Benzocoumarins *via* Direct Benzene Construction through Base-Mediated Formal [4+2] Reaction and Air Oxidation." *Adv. Synth. Catal*. **2016**, *358*, 707−712; b.) Poudel, T. N., Lee, Y. R. "An Advanced and Novel One-Pot Synthetic Method for Diverse Benzo[c]chromen-6-ones by Transition-Metal Free Mild Base-Promoted Domino Reactions of Substituted 2-

Hydroxychalcones with β-Ketoesters and its Application to Polysubstituted Terhenyls." *Org. Biomol. Chem*. **2014**, *12*, 919−930.

7. a.) Yang, M.C., Peng, C., Huang, H., Yang, L., He, X. H., Huang, W., Cui, H. L., He, G., Han, B. "Organocatalytic Asymmetric Synthesis of Spiro-oxindole Piperidine Derivatives that Reduce Cancer Cell Proliferation by Inhibiting MDM2-p53 Interaction." *Org. Lett*. **2017**, *19*, 6752−6755. b.) Millington, E. L., Dondas, H. A., Fishwick, C. W. G., Kilner, C., Grigg, R. "Catalytic Bimetalic [Pd(0)/Ag(I) Heck-1,3-dipolar Cycloaddition Cascade Reactions Accessing Spiro-oxindoles. Concominant *in situ* Generation of Azomethine Ylides and Dipolarophile." *Tetrahedron,* **2018**, *74*, 3564−3577; c.) Trost, B. M., Bringley, D. A., Zhang, T., Cramer, N. "Rapid Access to Spirocyclic Oxindole Alkaloids: Application of the Asymmetric Palladium-Catalyzed [3+2] Trimethylenemethane Cycloaddition." *J. Am. Chem. Soc*., **2013**, *135*, 16720−16735; d.) Trost, B. M., Cramer, N., Bernsmann, H. "Concise Total Synthesis of (±)-Marcfortine B." *J. Am. Chem. Soc*., **2007**, *129*, 3086−3087.

8. a.) Li, A., DeSchepper, D. J., Klumpp, D. A. "Triflic Acid Promoted Synthesis of Polycyclic Aromatic Compounds." *Tet. Lett.,* **2009**, *50*, 1924-1927. B.) Kim, K. H., Lim, C. H., Lim, J. W., Kim, J. N. "2,3-Dichloro-5,6-dicyaco-para-benzoquinone (DDQ)/Methanesulfonic Acid (MsOH)-Mediated Intramolecular Arene-Alkene Oxidative Coupling." *Adv. Synth. Catal.,* **2014**, *356*, 697-704. c.) Nogi, K., Yorimitsu, H. "Aromatic Metamorphosis: Conversion of an Aromatic Skeleton into a Different Ring System." *Chem. Comm.,* **2017**, *53*, 4055-4065. d.) Zhu, C., Zhao, Y., Wang, D., Sun, W-Y., Shi, Z. "Palladium-Catalyzed Direct Arylation and Cyclization of o-Iodobiaryls to a Library of Tetraphenylenes." *Sci. Report.,* **2016**, *6*, 33131, 1-9. e.) Nagode, S. B., Kant, R., Rastogi, N. "Synthesis of Phenanthrenes through Visible-Light Photoredox Catalyzed Intramolecular

Cyclization of α-Bromochalcones."*E. J. Org. Chem.,* **2018**, *13*, 1533-1537. f.) Zhao, Z., Britt, L. H., Murphy, G. K. "Oxidative, Iodoarene-Catalyzed Intramolecular Alkene Arylation for the Synthesis of Polycyclic Aromatic Hydrocarbons." *Chem. Eur. J.,* **2018**, *24*, 17002-17005. g.) Akbar, S., Tamilarasan, V. J., Srinivasan, K. "Iodine-Mediated Synthesis of Benzo[*a*]fluorenones from Yne-enones." *RSC Adv.,* **2019**, *9*, 23652-23657.

9. Xiao, J.; Chen, Y.; Zhu, S.; Wang, L.; Xu, L.; Wei, H. "Diversified Construction of Chromeno[3,4-*c*]pyridine-5-one and Benzo[c]chromen-6-one Derivatives by Domino Reaction of 4-Alkynyl-2-oxo-2*H*-chromene-3-carbaldehydes." *Adv. Synth. Catal.* **2014**, *356*, 1835-1845.

10. Castaing, M.; Wason, S. L.; Estepa, B.; Hooper, J. F.; Willis, M. C. "2-Aminobenzaldehydes as Versatile Substrates for Rhodium-Catalyzed Alkyne Hydroacylation: Application to Dihydroquinolone Synthesis." *Angew. Chem. Int. Ed.* **2013**, *52*, 13280-13283.

11. Litkei, G.; Totildekes, A. L. "Oxidation of the 2'NHR Analogs of 2'-OR Chalcones; Conversion of 2'-NHR Chalcone Epoxides." *Synth. Comm.* **2006**, *21*, 1597-1609.

12. Li, L.; Chen, J.; Kan, X.; Zhang, L.; Zhao, Y. "One-Pot Synthesis of Phenanthridinones Using a Base-Catalyzed/Promoted Bicyclization of α,β-Unsaturated Carbonyl Compounds with Dimethyl Glutaconate." *Eur. J. Org. Chem.* **2015**, *22*, 4892-4899.

13. Tang, E.; Chen, B.; Zhang, L.; Li, W.; Lin, J. "$ZnCl_2$-Catalyzed Intramolecular Cyclization Reaction of 2-Aminochalcones Using Polymer-Supported Selenium Reagent: Synthesis of 2-Phenyl-4-Quinolones and 2-Phenyl-2,3-Dihydroquinolin-4(1*H*)-one." *Synlett* **2011**, *5*, 707-711.

14. Bernini, R.; Cacchi, S.; Fabrizi, G.; Sferrazza, A. “A Simple General Approach to Phenanthridinones via Palladium-Catalyzed Intramolecular Direct Arene Arylation.” *Synthesis* **2008,** *5*, 729-738.

4.9 EXPERIMENTAL SECTION

PUBLICATION AND CONTRIBUTION STATEMENT

The material in this chapter was published as a cover article in Organic Chemistry Frontiers (DOI: 10.1039/c9qo01336a). Dr. Indrajeet Sharma contributed with assistance in project design, manuscript writing, and editing. The compound examples produced in this chapter are contributed by Steven Schlitzer, with starting material preparation assistance contributed by co-author Katelyn Stevens and purification assistance by co-author Dr. Dhanarajan 'Arun' Arunprasath.

MATERIALS AND METHODS

Reagents

Reagents and solvents were obtained from Sigma-Aldrich (www.sigma-aldrich.com), ChemImpex (www.chemimpex.com) or Acros Organics (www.fishersci.com) and used without further purification unless otherwise indicated. Dry solvents (acetonitrile) were obtained from Acros Organics (www.fishersci.com), and dichloromethane was distilled over CaH_2 under N_2 unless otherwise indicated. THF purchased from Sigma-Aldrich was distilled over Na metal with benzophenone indicator.

Reactions

All reactions were performed in flame-dried glassware under positive N_2 pressure with magnetic stirring unless otherwise noted. Liquid reagents and solutions were transferred thru rubber septa via syringes flushed with N_2 prior to use. Cold baths were generated as follows: 0 °C with wet

ice/water and −78 °C with dry ice/acetone. Syringe pump addition reactions were conducted using a CMA/100 microinjection pump.

Chromatography

TLC was performed on 0.25 mm E. Merck silica gel 60 F254 plates and visualized under UV light (254 nm) or by staining with potassium permanganate ($KMnO_4$), cerium ammonium molybdenate (CAM), phosphomolybdic acid (PMA), and ninhydrin. Silica flash chromatography was performed on Sorbtech 230–400 mesh silica gel 60.

Analytical Instrumentation

IR spectra were recorded on a Shimadzu IRAffinity-1 FTIR or a Nicolet 6700 FTIR spectrometer with peaks reported in cm^{-1}. NMR spectra were recorded on a Varian VNMRS 400, 500 and 600 MHz NMR spectrometer in $CDCl_3$ unless otherwise indicated. Chemical shifts are expressed in ppm relative to solvent signals: $CDCl_3$ ((^1H, 7.26 ppm, ^{13}C, 77.0 ppm); coupling constants are expressed in Hz. NMR spectra were processed using Mnova (www.mestrelab.com/software/mnova-nmr). Mass spectra were obtained at the OU Analytical Core Facility on an Agilent 6538 High-Mass-Resolution QTOF Mass Spectrometer and an Agilent 1290 UPLC. X-ray crystallography analysis was carried out at the University of Oklahoma using a Bruker APEX ccd area detector and graphite-monochromated Mo Kα radiation (λ = 0.71073 Å) source and a D8 Quest diffractometer with a Bruker Photon II cmos area detector and an Incoatec Iμs microfocus Mo Kα source (λ = 0.71073 Å). Crystal structures were visualized using CCDC Mercury software (http://www.ccdc.cam.ac.uk/products/mercury/).

Nomenclature

N.B.: Atom numbers shown in chemical structures herein correspond to IUPAC nomenclature, which was used to name each compound.

4.9.1 GENERAL PROCEDURE 1 FOR THE SYNTHESIS OF CROTONYLHYDROXYCHALCONES (1)

To a round bottom flask was measured 2'-hydroxyacetophenones (**1**) (1.0 equiv.), which was then dissolved in dichloromethane (0.2 M). This solution was cooled in an ice/water bath then crotonic acid (1.2 equiv.) and DMAP (0.1 equiv.) were added, followed by the addition of 1-Ethyl-3-(3-dimethylaminopropyl)carbodiimide hydrochloride (EDCI, 1.5 equiv.). The reaction vessel was allowed to warm naturally to room temperature with stirring over 16 hours. The reaction mixture was then diluted with excess dichloromethane and washed sequentially with 1N HCl (2x) and sat. $NaHCO_3$ (2x). Organics were dried over anhydrous Na_2SO_4, concentrated in vacuo, then purified by flash chromatography eluting with 1:20 ethyl acetate:hexanes gradient to 2:5 ethyl acetate:hexanes to furnish crotonylhydroxychalcones **1a**-**1h**.

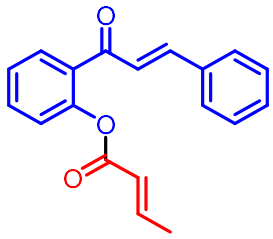

2-cinnamoylphenyl (*E*)-but-2-enoate (1a). Synthesized using general procedure 1. Yellow oil (272 mg, 79% yield). **TLC**: R_f 0.23 (ethyl acetate/hexanes = 1: 4). **IR** (neat) ν_{max}: 3032, 1733, 1604, 1448, 1331, 1194, 1146, 1098, 964, 748 cm^{-1}. **^{1}H NMR** (600 MHz) δ 7.70 (dd, *J* = 7.6, 1.7 Hz, 1H), 7.60–7.51 (m, 4H), 7.41–7.31 (m, 4H), 7.20 (dd, *J* = 8.2, 1.1 Hz, 1H), 7.17–7.08 (m, 2H), 5.97 (dd, *J* = 15.5, 1.8 Hz, 1H), 1.82 (dd, *J* = 6.9, 1.7 Hz, 3H). **^{13}C NMR** (151 MHz) δ 191.6, 164.4, 148.7, 147.7,

145.1, 134.6, 132.6, 132.3, 130.5, 129.8, 128.9 (2C), 128.4 (2C), 125.9, 125.7, 123.4, 121.6, 18.1. **HRMS** (ESI) *m/z* calcd for $C_{19}H_{16}O_3Na$ ([M + Na]$^+$) 315.0997; found 315.0995.

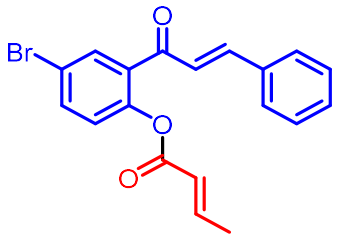

4-bromo-2-cinnamoylphenyl (*E*)-but-2-enoate (1b). Synthesized using general procedure 1. Yellow oil (103 mg, 74% yield). **TLC**: R_f 0.29 (ethyl acetate/hexanes = 3: 7). **IR** (neat) ν_{max}: 3060, 3026, 2973, 1736, 1651, 1598, 1448, 1189, 1144, 966, 863, 741, 691 cm^{-1}. **^{1}H NMR** (600 MHz) δ 7.79 (d, *J* = 2.4 Hz, 1H), 7.63 (dd, *J* = 8.6, 2.4 Hz, 1H), 7.59–7.50 (m, 3H), 7.39 (m, 3H), 7.16–7.06 (m, 4H), 5.94 (dd, *J* = 15.6, 1.7 Hz, 1H), 1.82 (dd, *J* = 7.0, 1.7 Hz, 3H). **^{13}C NMR** (151 MHz) δ 190.1, 164.1, 148.4, 147.6, 145.9, 135.07, 134.3, 134.2, 132.4, 130.8, 128.9 (2C), 128.5 (2C), 125.2, 125.0, 121.2, 119.1, 18.2. **HRMS** (ESI) *m/z* calcd for $C_{19}H_{15}BrO_3Na$ ([M + Na]$^+$) 393.0102; found 393.0102.

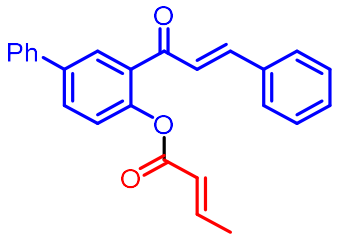

3-cinnamoyl-[1,1'-biphenyl]-4-yl (*E*)-but-2-enoate (1c). Synthesized using general procedure 1. Yellow oil (154 mg, 35% yield). **TLC**: R_f 0.27 (ethyl acetate/hexanes = 3: 7). **IR** (neat) ν_{max}: 3029, 1734, 1652, 1596, 1477, 1330, 1189, 1097, 964, 789 cm^{-1}. **^{1}H NMR** (600 MHz) δ 7.89 (d, *J* = 2.3 Hz, 1H), 7.75 (dd, *J* = 8.4, 2.3 Hz, 1H), 7.65–7.59 (m, 3H), 7.59–7.53 (m, 2H), 7.46 (t, *J* = 7.7 Hz,

2H), 7.42–7.35 (m, 4H), 7.28 (d, *J* = 8.4 Hz, 1H), 7.18 (m, 2H), 5.99 (dd, *J* = 15.5, 1.8 Hz, 1H), 1.84 (dd, *J* = 6.9, 1.7 Hz, 3H). **^{13}C NMR** (75 MHz) δ 191.7, 164.6, 148.0, 145.4, 139.5, 139.2, 134.6, 132.8, 130.9, 130.7, 129.0, 128.9 (2C), 128.5 (2C), 128.4 (2C), 127.8, 127.2, 125.6, 123.8, 121.5, 18.3. **HRMS** (ESI) *m/z* calcd for $C_{25}H_{20}O_3Na$ ($[M + Na]^+$) 391.1310; found 391.1316.

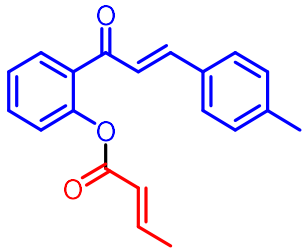

2-((*E*)-3-(p-tolyl)acryloyl)phenyl (*E*)-but-2-enoate (1d). Synthesized using general procedure 1. Yellow oil (328 mg, 12% yield). **TLC**: R_f 0.39 (ethyl acetate/hexanes = 1: 4). **IR** (neat) ν_{max}: 2916, 1713, 1605, 1443, 1395, 1271, 1076, 887, 811, 781 cm^{-1}. **^{1}H NMR** (600 MHz) δ 7.68 (dd, *J* = 7.7, 1.7 Hz, 1H), 7.55 (d, *J* = 16.0 Hz, 1H), 7.51 (ddd, *J* = 8.2, 7.4, 1.7 Hz, 1H), 7.43 (d, *J* = 7.9 Hz, 2H), 7.32 (td, *J* = 7.5, 1.2 Hz, 1H), 7.19 (dd, *J* = 8.2, 1.1 Hz, 1H), 7.17 (d, *J* = 7.8 Hz, 2H), 7.15–7.07 (m, 2H), 5.96 (dd, *J* = 15.5, 1.7 Hz, 1H), 2.35 (s, 3H), 1.82 (dd, *J* = 6.9, 1.7 Hz, 3H). **^{13}C NMR** (151 MHz) δ 191.7, 164.4, 148.7, 147.7, 145.4, 141.1, 132.7, 132.3, 131.8, 129.8, 129.7 (2C), 128.5 (2C), 125.9, 124.6, 123.5, 121.6, 21.5, 18.2. **HRMS** (ESI) *m/z* calcd for $C_{20}H_{19}O_3$ ($[M + H]^+$) 307.1334; found 307.1325.

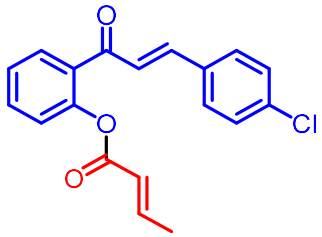

2-((*E*)-3-(4-chlorophenyl)acryloyl)phenyl (*E*)-but-2-enoate (1e). Synthesized using general procedure 1. Yellow oil (525 mg, 52% yield). **TLC**: R_f 0.25 (ethyl acetate/hexanes = 3: 7). **IR** (neat) ν_{max}: 2915, 1732, 1603, 1489, 1293, 1192, 1092, 964, 820, 730 cm^{-1}. **^{1}H NMR** (600 MHz) δ 7.68 (dd, *J* = 7.6, 1.9 Hz, 1H), 7.53 (m, 1H), 7.52–7.47 (d, *J* = 18 Hz, 1H), 7.45 (m, 2H), 7.33 (m, 3H), 7.19 (dd, *J* = 8.3, 1.9 Hz, 1H), 7.15–7.07 (m, 2H), 5.96 (d, *J* = 15.6 Hz, 1H), 1.85–1.81 (d, *J* = 6 Hz, 3H). **^{13}C NMR** (151 MHz) δ 191.4, 164.4, 148.7, 147.9, 143.6, 136.4, 133.1 (2C), 132.5 (2C), 129.8 (2C), 129.5 (2C), 129.2, 126.0, 123.5, 121.5, 18.2. **HRMS** (ESI) *m/z* calcd for $C_{19}H_{15}ClO_3Na$ ($[M + Na]^+$) 349.0607; found 349.0612.

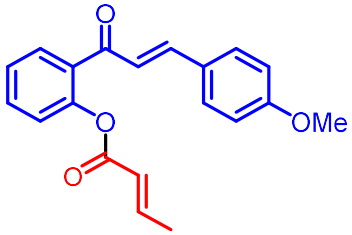

2-((*E*)-3-(4-methoxyphenyl)acryloyl)phenyl (*E*)-but-2-enoate (1f). Synthesized using general procedure 1. Yellow oil (146 mg, 45% yield). **TLC**: R_f 0.13 (ethyl acetate/hexanes = 3: 7). **IR** (neat) ν_{max}: 2936, 1733, 1589, 1509, 1194, 1171, 1098, 1021, 966, 826, 730 cm^{-1}. **^{1}H NMR** (600 MHz) δ 7.67 (dd, *J* = 7.6, 1.7 Hz, 1H), 7.55–7.47 (m, 4H), 7.33 (td, *J* = 7.6, 1.1 Hz, 1H), 7.19 (dd, *J* = 8.1, 1.1 Hz, 1H), 7.11 (dq, *J* = 15.5, 6.9 Hz, 1H), 7.01 (d, *J* = 15.8 Hz, 1H), 6.89 (d, *J* = 8.8 Hz, 2H), 5.97 (dd, *J* = 15.5, 1.8 Hz, 1H), 3.83 (s, 3H), 1.84 (dd, *J* = 7.0, 1.7 Hz, 3H). **^{13}C NMR** (151 MHz) δ 191.8, 164.5,

161.7, 148.6, 147.7, 145.2, 132.8, 132.1, 130.2, 129.7 (2C), 127.3 (2C), 125.8, 123.4, 121.6, 114.4, 113.5, 55.4, 18.2. **HRMS** (ESI) *m/z* calcd for $C_{20}H_{18}O_4Na$ ([M + Na]$^+$) 345.1103; found 345.1109.

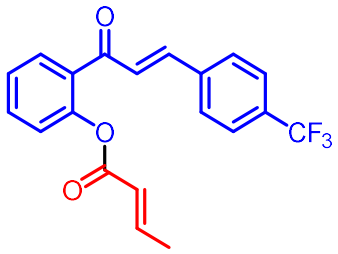

2-((*E*)-3-(4-(trifluoromethyl)phenyl)acryloyl)phenyl (*E*)-but-2-enoate (1g). Synthesized using general procedure 1. Yellow solid (565 mg, 68% yield, m.p. 55–56 ºC). **TLC**: R_f 0.47 (ethyl acetate/hexanes = 1:4). **IR** (neat) ν_{max}: 3014, 1734, 1655, 1597, 1442, 1321, 1289, 1211, 1145, 1066, 963, 836, 771 cm^{-1}. **^{1}H NMR** (400 MHz) δ 7.70 (dd, *J* = 7.7, 1.7 Hz, 1H), 7.58 (d, *J* = 14.9 Hz, 4H), 7.54–7.43 (m, 2H), 7.31 (td, *J* = 7.6, 1.2 Hz, 1H), 7.24–7.17 (m, 2H), 7.09 (m, *J* = 15.6, 1H), 5.95 (dd, *J* = 15.5, 1.7 Hz, 1H), 1.79 (dd, *J* = 7.0, 1.8 Hz, 3H). **^{13}C NMR** (151 MHz) δ 191.0, 164.4, 148.8, 148.0, 142.7, 138.0, 132.8, 131.7, 132.1, 129.9, 128.5, 127.6, 126.0, 125.7 (q, $J_{C\text{-}F}$ = 3.4 Hz), 123.5, 121.44, 18.1 [Note : While peaks corresponding to the CF_3 were observed, some portion of the peaks were lost in signal noise]. **HRMS** (ESI) *m/z* calcd for $C_{20}H_{15}F_3O_3Na$ ([M + Na]$^+$) 383.0871; found 383.0869.

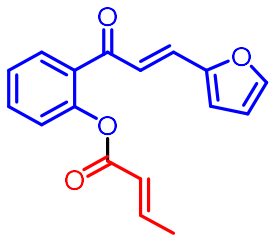

2-((*E*)-3-(furan-2-yl)acryloyl)phenyl (*E*)-but-2-enoate (1h). Synthesized using general procedure 1. Yellow oil (190 mg, 42% yield). **TLC**: R_f 0.30 (ethyl acetate/hexanes = 3: 7). **IR** (neat) ν_{max}: 3057,

1732, 1655, 1598, 1550, 1477, 1037, 1217, 1194, 1098, 1012, 934, 750 cm^{-1}. **^{1}H NMR** (300 MHz) δ 7.71–7.65 (m, 1H), 7.53–7.48 (m, 1H), 7.47 (td, *J* = 1.4, 0.8 Hz, 1H), 7.37–7.25 (m, 2H), 7.20–7.01 (m, 3H), 6.63 (dd, *J* = 3.4, 0.6 Hz, 1H), 6.45 (dd, *J* = 3.4, 1.8 Hz, 1H), 5.98 (dd, *J* = 15.5, 1.8 Hz, 1H), 1.85 (dd, *J* = 6.9, 1.7 Hz, 3H). **^{13}C NMR** (75 MHz) δ 190.8, 164.4, 151.3, 148.8, 147.6, 145.1, 132.4, 131.0, 129.8, 125.9, 123.5, 122.9 (2C), 121.6, 116.4, 112.7, 18.2. **HRMS** (ESI) *m/z* calcd for $C_{17}H_{14}O_4Na$ ($[M + Na]^+$) 305.0790; found 305.0790.

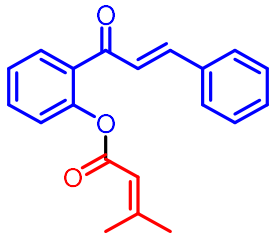

2-cinnamoylphenyl 3-methylbut-2-enoate (1i). Synthesized using general procedure 1. Yellow oil (350 mg, 88% yield). **TLC**: R_f 0.48 (ethyl acetate/hexanes = 1: 4). **IR** (neat) ν_{max}: 3061, 2917, 2359, 1738, 1605, 1448, 1332, 1200, 1119, 1063, 749 cm^{-1}. **^{1}H NMR** (600 MHz) δ 7.70 (dd, *J* = 7.6, 1.7 Hz, 1H), 7.59–7.51 (m, 4H), 7.37 (m, 3H), 7.35–7.31 (t, 2H), 7.19–7.13 (m, 2H), 5.85 (d, *J* = 1.4 Hz, 1H), 2.11 (s, 3H), 1.83 (s, 3H). **^{13}C NMR** (151 MHz) δ 191.8, 164.5, 161.0, 148.8, 144.9, 134.7, 132.6, 132.4, 130.5, 129.8, 128.8 (2C), 128.4 (2C), 125.8, 125.7, 123.6, 114.7, 27.6, 20.5. **HRMS** (ESI) *m/z* calcd for $C_{20}H_{18}O_3Na$ ($[M + Na]^+$) 329.1154; found 329.1153.

4.9.2 SYNTHESIS OF (*E*)-4-STYRYL-3-VNIYL-2*H*-CHROMEN-2-ONE (2)

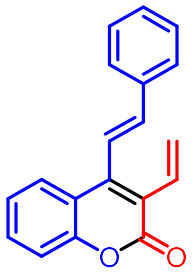

(*E*)-4-styryl-3-vinyl-2*H*-chromen-2-one (2). To a 4.0 mL vial was measured crotonylhydroxychalcone (**1**) (1.0 equiv.). DMSO (0.15M) was then added, followed by the addition of DBU (3.0 equiv.). The reaction vessel was equipped with a magnetic stir bar, sealed, and stirred at room temperature for 90 minutes. The reaction mixture was then diluted into ethyl acetate. Organics were washed sequentially with sat. NH_4Cl (2x) and water (2x) then dried over anhydrous Na_2SO_4. Organics were concentrated in vacuo and purified by flash chromatography to furnish (E)-4-styryl-3-vinyl-2H-chromen-2-one (2). Yellow oil (375 mg, 60% yield). **TLC**: R_f 0.53 (ethyl acetate/hexanes = 1:1). **IR** (neat): 3025, 1709, 1603, 1449, 1320, 1100, 984, 712. **^{1}H NMR** (400 MHz) δ 7.72 (d, *J* = 8.0 Hz, 1H), 7.57 (d, *J* = 7.5 Hz, 2H), 7.42 (tq, *J* = 14.3, 7.5 Hz, 4H), 7.30–7.20 (m, 2H), 7.15–7.06 (m, 1H), 6.91–6.76 (m, 2H), 6.41 (dd, *J* = 17.6, 1.9 Hz, 1H), 5.60 (dd, *J* = 11.9, 1.9 Hz, 1H). **^{13}C NMR** (101 MHz) δ 159.8, 152.4, 146.5, 139.6, 135.6, 131.3, 129.6, 129.3, 129.0 (2C), 128.6 (2C), 127.0, 126.3, 124.1, 122.9, 120.8, 119.4, 116.7. **HRMS** (ESI) *m/z* calcd for $C_{19}H_{15}O_2$ ($[M + H]^+$) 275.1072; found 275.1081.

4.9.3 GENERAL PROCEDURE 2 FOR THE SYNTHESIS OF BENZO[*C*]COUMARINS (3)

To a 15 mL round bottom flask was measured crotonylhydroxychalcone (**1**) (1.0 equiv.). DMSO (0.15M) was then added, followed by the addition of DBU (3.0 equiv.). The reaction vessel was

equipped with a magnetic stir bar and stirred open to air at room temperature for 90 minutes. The reaction mixture was then heated to 80 °C and stirred at this temperature for 16 hours. The reaction mixture was then cooled to room temperature and diluted into ethyl acetate. Organics were washed sequentially with sat. NH_4Cl (2x) and water (2x) then dried over anhydrous Na_2SO_4. Organics were concentrated in vacuo and purified by flash chromatography 1:20 ethyl acetate:hexanes gradient to 2:5 ethyl acetate:hexanes to furnish benzo[c]coumarins **3a**-**3h**.

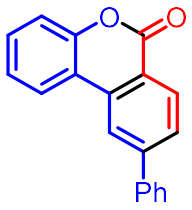

9-phenyl-6*H*-benzo[*c*]chromen-6-one (3a). Synthesized using general procedure 2. (223 mg, 82% yield). Characterization data was in accordance with previous reports.[9]

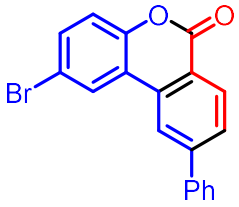

2-bromo-9-phenyl-6*H*-benzo[*c*]chromen-6-one (3b). Synthesized using general procedure 2. (46 mg, 88% yield). Characterization data was in accordance with previous reports. [6a]

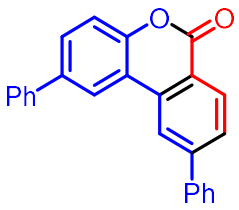

2,9-diphenyl-6*H*-benzo[*c*]chromen-6-one (3c). Synthesized using general procedure 2. Gray solid (35 mg, 67% yield, m.p. 184–185 ºC). **TLC**: R_f 0.54 (ethyl acetate/hexanes = 1:4). **IR** (neat) ν_{max}: 3057, 2925, 1723, 1611, 1484, 1270, 1076, 883, 761 cm^{-1}. **^{1}H NMR** (600 MHz) δ 8.44 (dd, *J* = 8.1, 1.5 Hz, 1H), 8.31 (s, 1H), 8.26 (s, 1H), 7.78 (s, 1H), 7.71 (d, *J* = 7.3 Hz, 2H), 7.68 (d, *J* = 8.6, 1H), 7.64 (d, *J* = 7.4 Hz, 2H), 7.53 (t, *J* = 7.4 Hz, 2H), 7.51–7.45 (m, 3H), 7.44–7.37 (m, 2H). **^{13}C NMR** (151 MHz) δ 161.0, 150.9, 147.8, 140.1, 139.6, 137.9, 135.0, 131.2, 129.5, 129.1, 129.0 (2C), 128.8 (2C), 128.0 (2C), 127.7 (2C), 127.5 (2C), 127.2, 121.2, 120.1, 120.0, 118.2. **HRMS** (ESI) *m/z* calcd for $C_{25}H_{16}O_2Na$ ($[M + Na]^+$) 371.1048; found 371.1047.

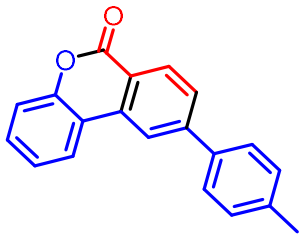

9-(p-tolyl)-6*H*-benzo[*c*]chromen-6-one (3d). Synthesized using general procedure 2. (33 mg, 77% yield). Characterization data was in accordance with previous reports. [6a]

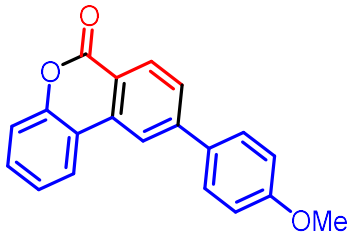

9-(4-methoxyphenyl)-6*H*-benzo[*c*]chromen-6-one (3e). Synthesized using general procedure 2. (37 mg, 82% yield). Characterization data was in accordance with previous reports. [9]

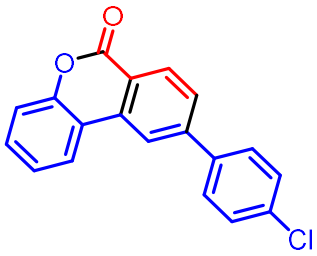

9-(4-chlorophenyl)-6*H*-benzo[*c*]chromen-6-one (3f). Synthesized using general procedure 2. (42 mg, 92% yield). Characterization data was in accordance with previous reports. [9]

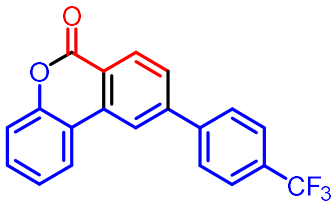

9-(4-(trifluoromethyl)phenyl)-6*H*-benzo[*c*]chromen-6-one (3g). Synthesized using general procedure 2. Beige solid (24 mg, 46% yield, m.p. 172–174 ºC). **TLC**: R_f 0.27 (ethyl acetate/hexanes = 1:5). **IR** (neat) ν_{max}: 3021, 2160, 1977, 1712, 1611, 1449, 1322, 1165, 1107, 1087, 826, 871 cm^{-1}. **^{1}H NMR** (400 MHz) δ 8.51 (d, *J* = 8.2 Hz, 1H), 8.30 (d, *J* = 1.8 Hz, 1H), 8.16 (dd, *J* = 7.9, 1.6 Hz, 1H), 7.85–7.76 (m, 5H), 7.53 (m, *J* = 8.5 Hz, 1H), 7.44–7.35 (m, 2H). **^{13}C NMR** (101 MHz) δ 160.9, 151.5, 146.2, 143.2, 135.3, 131.4, 130.8, 127.9, 126.1 (d, *J* = 3.8 Hz), 124.7, 122.7, 120.7, 120.4, 119.1 (q, $J_{C\text{-}F}$ = 272.1 Hz, 1C), 117.8 [Note : While peaks corresponding to the CF_3 were observed, some portion of the peaks were lost in signal noise]. **HRMS** (ESI) *m/z* calcd for $C_{20}H_{12}F_3O_2$ ($[M + H]^+$) 341.0789; found 341.0794.

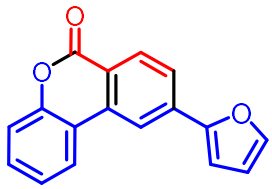

9-(furan-2-yl)-6*H*-benzo[*c*]chromen-6-one (3h). Synthesized using general procedure 2. Yellow oil (24 mg, 62% yield). **TLC**: R_f 0.40 (ethyl acetate/hexanes = 1:4). **IR** (neat) ν_{max}: 2922, 2852, 1716, 1612, 1476, 1275, 1208, 1105, 916, 898, 734 cm^{-1}. **^{1}H NMR** (400 MHz) δ 8.39 (dd, *J* = 5.0, 3.3 Hz, 2H), 8.19–8.11 (m, 1H), 7.83 (dd, *J* = 8.4, 1.6 Hz, 1H), 7.60 (d, *J* = 1.8 Hz, 1H), 7.50 (ddd, *J* = 8.4, 7.0, 1.6 Hz, 1H), 7.37 (t, *J* = 7.6 Hz, 2H), 6.95 (d, *J* = 3.4 Hz, 1H), 6.58 (dd, *J* = 3.5, 1.8 Hz, 1H). **^{13}C NMR** (101 MHz) δ 161.0, 152.3, 151.5, 143.9, 136.4, 135.4, 131.1, 130.6, 124.5, 124.1, 122.9, 119.5, 118.0, 117.8, 116.0, 112.4, 108.7. **HRMS** (ESI) *m/z* calcd for $C_{17}H_{11}O_3$ ($[M + H]^+$) 263.0708; found 263.0710.

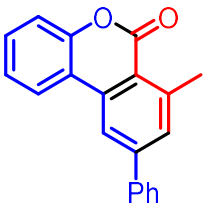

7-methyl-9-phenyl-6*H*-benzo[*c*]chromen-6-one (3i). Synthesized using general procedure 2. (25 mg, 59% yield). Characterization data was in accordance with previous reports. [6a]

4.9.4 GENERAL PROCEDURE 3 FOR THE SYNTHESIS OF *N*-ALKYLAMINOCHALCONES

To a solution of *N*-methylacetophenones (1.0 equiv.) in ethanol (2.5 M) was added solid NaOH (3.0 equiv.). After the solid was fully dissolved, the appropriate benzaldehyde (1.2 equiv.) was added, and the mixture was stirred at room temperature overnight. The reaction mixture was then cooled to 0 ºC in an ice/water bath and the mixture was carefully neutralized using 1N HCl. The crude mixture was extracted with dichloromethane (3x) then washed with water (2x) and brine (2x). Organics were dried over Na_2SO_4 and concentrated to furnish chalcones which were purified by flash chromatography 1:20 ethyl acetate:hexanes gradient to 2:5 ethyl acetate:hexanes to furnish *N*-alkylaminochalcones.

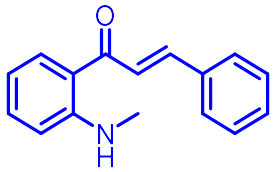

(*E*)-1-(2-(methylamino)phenyl)-3-phenylprop-2-en-1-one. Synthesized using general procedure 3. (1.17 g, 66% yield). Characterization data was in accordance with previous reports.[10]

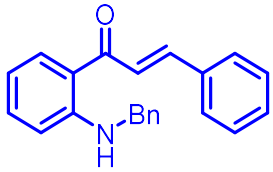

(*E*)-1-(2-(benzylamino)phenyl)-3-phenylprop-2-en-1-one. Synthesized using general procedure 3. (55 mg, 35% yield). Characterization data was in accordance with previous reports. [11]

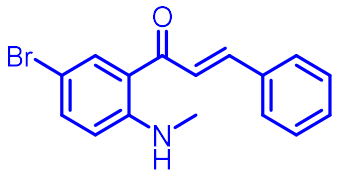

(*E*)-1-(5-bromo-2-(methylamino)phenyl)-3-phenylprop-2-en-1-one. Synthesized using general procedure 3. Orange solid (270 mg, 28% yield, mp 73 – 75 ºC). **TLC**: R_f 0.70 (ethyl acetate/hexanes = 1:4). **IR** (neat) ν_{max}: 3309, 3924, 2907, 1642, 1585, 1447, 1187, 1165, 984, 813 cm^{-1}. **^{1}H NMR** (400 MHz) 8.98 (bs, 1H), 7.96 (s, 1H), 7.72 (d, J = 15.5 Hz, 1H), 7.64 (m, J = 9.1 Hz, 2H), 7.55 (d, J = 15.5 Hz, 1H), 7.41 (s, 4H), 6.62 (d, J = 9.1 Hz, 1H), 2.92 (s, 3H). **^{13}C NMR** (101 MHz) δ 190.5, 151.5, 143.4, 137.5, 135.0, 133.5, 130.3, 128.9 (2C), 128.4 (2C), 122.4, 119.5, 113.3, 105.2, 29.5. **HRMS** (ESI) *m/z* calcd for $C_{16}H_{15}BrNO$ ($[M+H]^+$) 316.0337; found 316.0338.

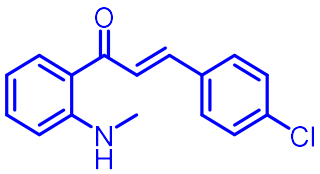

(*E*)-3-(4-chlorophenyl)-1-(2-(methylamino)phenyl)prop-2-en-1-one. Synthesized using general procedure 3. (273 mg, 88% yield). Characterization data was in accordance with previous reports.[12]

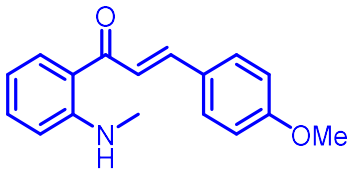

(*E*)-3-(4-methoxyphenyl)-1-(2-(methylamino)phenyl)prop-2-en-1-one. Synthesized using general procedure 3. (315 mg, quant. yield). Characterization data was in accordance with previous reports. [13]

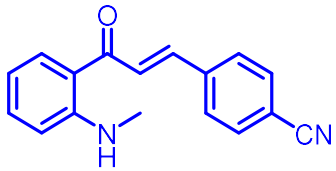

(*E*)-4-(3-(2-(methylamino)phenyl)-3-oxoprop-1-en-1-yl)benzonitrile. Synthesized using general procedure 3. (251 mg, 83% yield). Characterization data was in accordance with previous reports.[14]

4.9.5 GENERAL PROCEDURE 4 FOR THE SYNTHESIS OF *N*-ALKYL-*N*-CROTONYLAMINOCHALCONES (6)

To a solution of *N*-alkylaminochalcone (1.0 equiv.) in dichloromethane (0.2M) at 0 °C was added solid $NaHCO_3$ (1.5 equiv.). The mixture was stirred at this temperature for 10 minutes before crotonyl chloride (1.2 equiv.) was added slowly by syringe. The reaction mixture was allowed to warm naturally to room temperature and stirred at this temperature overnight. The reaction mixture was diluted with dichloromethane, then washed with water (2x). The organic layer was then dried over Na_2SO_4 and concentrated to give crude *N*-alkyl-*N*-crotonylaminochalcones (**5**) as a separable mixture of E/Z isomers, which were then purified via column chromatography 1:10 ethyl acetate:hexanes gradient to 1:1 ethyl acetate:hexanes to furnish pure *N*-alkyl-*N*-crotonylaminochalcones **6a**-**6i**.

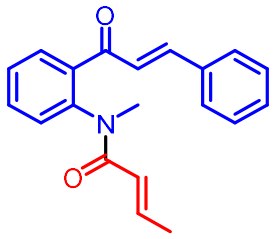

(*E*)-*N*-(2-cinnamoylphenyl)-*N*-methylbut-2-enamide (6a). Synthesized using general procedure 4. Orange oil (970 mg, 81% yield). **TLC**: R_f 0.23 (ethyl acetate/hexanes = 2:5). **IR** (neat) ν_{max}: 3033, 1664, 1631, 1595, 1478, 1367, 1288, 1206, 1095, 963, 771 cm^{-1}. **^{1}H NMR** (500 MHz) δ 7.68 (dd, *J* = 7.6, 1.6 Hz, 1H), 7.59 (td, *J* = 7.7, 1.7 Hz, 1H), 7.56–7.47 (m, 6H), 7.40 (m, 4H), 7.28 (d, *J* = 6.1 Hz, 1H), 7.01 (d, *J* = 16.0 Hz, 1H), 6.90 (dq, *J* = 15.0, 6.9 Hz, 1H), 5.74 (dd, *J* = 15.0, 1.7 Hz, 1H), 3.28 (s, 3H). **^{13}C NMR** (75 MHz) δ 192.9, 165.8, 145.8, 141.8, 138.1, 134.2, 132.1, 130.8, 129.9, 129.6,

129.3, 128.9, 128.4 (2C), 128.1 (2C), 125.1, 122.5, 37.7, 18.0. HRMS (ESI) *m/z* calcd for $C_{20}H_{10}NO_2$ ($[M + H]^+$) 306.1494; found 306.1486.

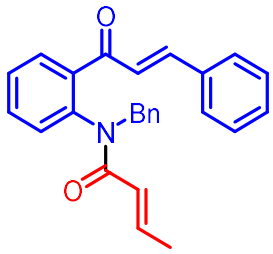

(*E*)-*N*-benzyl-*N*-(2-cinnamoylphenyl)but-2-enamide (6b). Synthesized using general procedure 4. Yellow oil (44 mg, 47% yield). **TLC**: R_f 0.43 (ethyl acetate/hexanes = 3:7). **IR** (neat) ν_{max}: 3028, 2245, 1662, 1595, 1446, 1386, 1354, 1288, 1203, 907, 725 cm^{-1}. **^{1}H NMR** (300 MHz) δ 7.66–7.61 (m, 1H), 7.52–7.45 (m, 2H), 7.40 (m, *J* = 8.5 Hz, 5H), 7.21–7.14 (m, 4H), 7.03–6.92 (m, 2H), 6.90–6.85 (m, 1H), 5.74 (dq, *J* = 15.0, 1.6 Hz, 1H), 5.48 (d, *J* = 14.3 Hz, 1H), 4.24 (d, *J* = 14.4 Hz, 1H), 1.70 (dd, *J* = 6.9, 1.7 Hz, 3H). **^{13}C NMR** (75 MHz) δ 192.9, 165.9, 145.9, 142.4, 139.8, 138.4, 137.1, 134.3, 131.6, 131.0, 130.9, 129.5, 129.3, 129.0 (2C), 128.5 (2C), 128.3 (2C), 128.1 (2C), 127.4, 125.1, 122.9, 53.3, 18.1. **HRMS** (ESI) *m/z* calcd for $C_{26}H_{24}NO_2$ ($[M+H]^+$ 382.1807; found 382.1806.

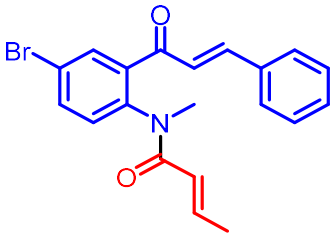

(*E*)-*N*-(4-bromo-2-cinnamoylphenyl)-*N*-methylbut-2-enamide (6d). Synthesized using general procedure 4. Yellow oil (347 mg, 90% yield). **TLC**: R_f 0.26 (ethyl acetate/hexanes = 3:7). **IR** (neat) ν_{max}: 3055, 2631, 1597, 1447, 1393, 1293, 1198, 1102, 962, 823, 774 cm^{-1}. **^{1}H NMR** (400 MHz) 7.77 (d, J = 2.4 Hz, 1H), 7.68 (dd, J = 8.3, 2.5 Hz, 1H), 7.56–7.48 (m, 3H), 7.39 (d, J = 6.7 Hz, 3H),

7.14 (d, J = 8.4 Hz, 1H), 6.99–6.83 (m, 2H), 5.75–5.66 (m, 1H), 3.23 (s, 3H), 1.71 (dd, J = 7.0, 1.7 Hz, 3H). **^{13}C NMR** (101 MHz) δ 191.3, 165.7, 146.6, 142.8, 140.7, 139.8, 135.1, 134.0, 132.5, 131.2, 131.0, 129.1 (2C), 128.6 (2C), 124.4, 122.1, 121.8, 37.7, 18.1. **HRMS** (ESI) *m/z* calcd for $C_{20}H_{19}BrNO_2$ ($[M + H]^+$) 384.0599; found 384.0601.

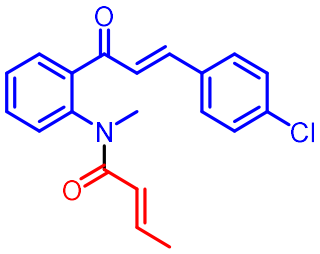

(*E*)-*N*-(2-((*E*)-3-(4-chlorophenyl)acryloyl)phenyl)-*N*-methylbut-2-enamide (6f). Synthesized using general procedure 4. Yellow oil (337 mg, 99% yield). **IR** (neat) ν_{max}: 2911, 1663, 1590, 1488, 1367, 1290, 1204, 1089, 962, 768 cm^{-1}. **TLC**: R_f 0.30 (ethyl acetate/hexanes = 2:5). **^{1}H NMR** (300 MHz) δ 7.65 (dd, *J* = 7.5, 1.7 Hz, 1H), 7.57 (td, *J* = 7.6, 1.7 Hz, 1H), 7.45 (m, *J* = 16.3, 4H), 7.33 (d, *J* = 8.5 Hz, 2H), 7.25 (dd, *J* = 7.9, 1.2 Hz, 1H), 6.94 (d, *J* = 15.9 Hz, 1H), 6.89–6.79 (m, 1H), 5.75–5.64 (m, 1H), 3.24 (s, 3H), 1.67 (dd, *J* = 7.0, 1.7 Hz, 3H). **^{13}C NMR** (75 MHz) δ 192.5, 165.8, 144.1, 142.2, 141.7, 138.0, 136.7, 132.8, 132.3, 129.7, 129.6, 129.3, 129.3 (2C), 128.1 (2C), 125.4, 122.4, 37.8, 18.1. **HRMS** (ESI) *m/z* calcd for $C_{20}H_{18}ClNO_2Na$ ($[M + Na]^+$) 362.0924 ; found 362.0920.

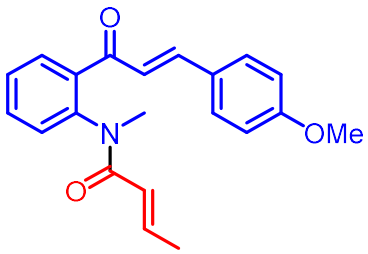

(*E*)-*N*-(2-((*E*)-3-(4-methoxyphenyl)acryloyl)phenyl)-*N*-methylbut-2-enamide (6g). Synthesized using general procedure 4. Yellow oil (295 mg, 75% yield). **IR** (neat) ν_{max}: 2933, 1663, 1592, 1444,

1329, 1303, 1171, 1020, 962, 826, 730 cm^{-1}. **TLC**: R_f 0.18 (ethyl acetate/hexanes = 2:5). **^{1}H NMR** (300 MHz) δ 7.61 (dd, *J* = 7.5, 1.8 Hz, 1H), 7.52 (td, *J* = 7.6, 1.8 Hz, 1H), 7.48–7.39 (m, 4H), 7.21 (dd, *J* = 7.8, 1.3 Hz, 1H), 6.92–6.78 (m, 4H), 5.70 (dd, *J* = 15.0, 1.7 Hz, 1H), 3.79 (s, 3H), 3.22 (s, 3H), 1.65 (dd, *J* = 6.9, 1.7 Hz, 3H). **^{13}C NMR** (75 MHz) δ 193.1, 165.9, 161.9, 145.9, 141.8, 141.5, 138.5, 131.9, 130.3, 129.5, 129.3 (2C), 128.4 (2C), 126.9, 122.9, 122.5, 114.5, 55.4, 37.7, 18.0. **HRMS** (ESI) *m/z* calcd for $C_{21}H_{21}NO_3Na$ ($[M + Na]^+$) 358.1419 ; found 358.1418.

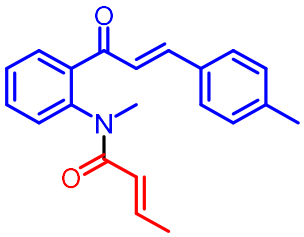

(E)-N-methyl-N-(2-((E)-3-(p-tolyl)acryloyl)phenyl)but-2-enamide (6h). Synthesized using general procedure 4. Yellow oil (495 mg, 77% yield). **IR** (neat) ν_{max}: 3050, 2915, 1664, 1628, 1596, 1445, 1370, 1297, 1205, 1040, 963, 813, 731 cm^{-1}. **TLC**: R_f 0.48 (ethyl acetate/hexanes = 1:1). **^{1}H NMR** (300 MHz) δ 7.61 (d, *J* = 9.1 Hz, 1H), 7.53 (t, *J* = 7.6 Hz, 1H), 7.48 – 7.40 (m, 2H), 7.36 (d, *J* = 8.1 Hz, 2H), 7.22 (d, *J* = 8.8 Hz, 1H), 7.14 (d, *J* = 7.9 Hz, 2H), 6.92 (d, *J* = 15.9 Hz, 1H), 6.88 – 6.77 (m, 1H), 5.70 (d, *J* = 16.7 Hz, 1H), 3.23 (s, 3H), 2.32 (s, 3H), 1.67 – 1.59 (m, 3H). **HRMS** (ESI) *m/z* calcd for $C_{21}H_{22}NO_2$ ($[M + H]^+$) 320.1651; found 320.1649.

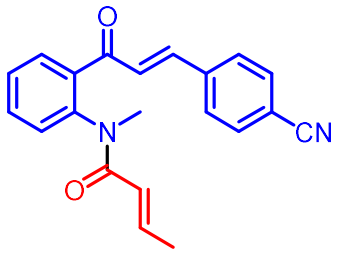

(*E*)-*N*-(2-((*E*)-3-(4-cyanophenyl)acryloyl)phenyl)-*N*-methylbut-2-enamide (6i). Synthesized using general procedure 4. Yellow oil (102 mg, 32% yield). **IR** (neat) ν_{max}: 3462, 3054, 2226, 1661, 1445, 1295, 1096, 963, 827, 770 cm^{-1}. **TLC**: R_f 0.18 (ethyl acetate/hexanes = 2:5). **^{1}H NMR** (300 MHz) δ 7.72–7.52 (m, 9H), 7.50–7.43 (m, 2H), 7.29–7.21 (m, 1H), 7.03 (d, *J* = 15.9 Hz, 1H), 6.95–6.79 (m, 1H), 5.68 (dd, *J* = 15.0, 1.7 Hz, 1H), 3.24 (s, 3H), 1.67 (dd, *J* = 7.0, 1.6 Hz, 3H). **^{13}C NMR** (75 MHz) δ 191.8, 165.8, 142.5, 142.4, 141.9, 138.7, 137.5, 132.9, 132.7, 129.9, 129.3, 128.7, 128.2, 127.8, 122.2, 118.3, 113.6, 37.8, 18.1. **HRMS** (ESI) *m/z* calcd for $C_{21}H_{18}N_2O_2Na$ ($[M + Na]^+$) 352.1266; found 352.1266.

4.9.6 GENERAL PROCEDURE 5 FOR THE SYNTHESIS OF PHENANTHRADIN-6(5*H*)-ONES (7) :

To a 15 mL round bottom flask was measured *N*-aklyl-*N*-crotonylaminochalcone (**6**) (1.0 equiv.). DMSO (0.15M) was then added, followed by the addition of DBU (3.0 equiv.). The reaction vessel was equipped with a magnetic stir bar and stirred open to air at room temperature for 90 minutes. The reaction mixture was then heated to 80 °C and stirred at this temperature for 16 hours. The reaction mixture was then cooled to room temperature and diluted with ethyl acetate. Organics were washed sequentially with sat. NH_4Cl (2x) and water (2x) then dried over anhydrous

Na_2SO_4. Organics were concentrated in vacuo and purified by flash chromatography using a 1:10 ethyl acetate:hexanes gradient to 1:1 ethyl acetate:hexanes to furnish phenanthradinones **7a-7i**.

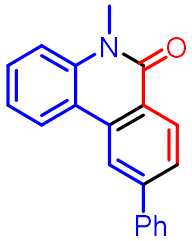

5-methyl-9-phenylphenanthridin-6(5*H*)-one (7a). Synthesized using general procedure 5. Yellow oil (259 mg, 91% yield). **TLC**: R_f 0.43 (ethyl acetate/hexanes = 3:10). **IR** (neat) ν_{max}: 3029, 2252, 1625, 1584, 1466, 1417, 1277, 1158, 1075, 866, 744 cm^{-1}. **^{1}H NMR** (500 MHz) δ 8.63 (d, *J* = 8.2 Hz, 1H), 8.47 (d, *J* = 1.7 Hz, 1H), 7.82 (dd, *J* = 8.3, 1.6 Hz, 1H), 7.75 (dd, *J* = 8.2, 1.3 Hz, 2H), 7.59 (ddd, *J* = 8.6, 7.1, 1.5 Hz, 1H), 7.54 (t, *J* = 7.6 Hz, 2H), 7.48–7.44 (m, 2H), 7.36 (ddd, *J* = 8.1, 7.2, 1.1 Hz, 1H), 3.85 (s, 3H). **^{13}C NMR** (75 MHz) δ 161.5, 145.1, 140.4, 138.2, 133.8, 129.7, 129.5, 129.0 (2C), 128.3 (2C), 127.5, 127.1, 124.4, 123.2, 122.5, 120.1, 119.3, 115.1, 30.0. **HRMS** (ESI) *m/z* calcd for $C_{20}H_{16}NO$ ($[M + H]^+$) 286.1232; found 286.1237.

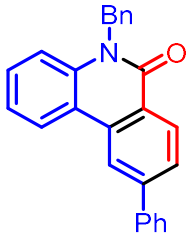

5-benzyl-9-phenylphenanthridin-6(5*H*)-one (7b). Synthesized using general procedure 5. (36 mg, 86% yield). Characterization data was in accordance with previous reports.[15]

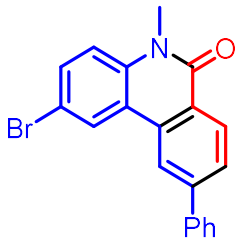

2-bromo-5-methyl-9-phenylphenanthridin-6(5*H*)-one (7e). Synthesized using general procedure 5. Yellow oil (29 mg, 70% yield). **TLC**: R_f 0.45 (ethyl acetate/hexanes = 3:10). **IR** (neat) ν_{max}: 3085, 2920, 2120, 1639, 1582, 1361, 1187, 1033, 853, 625 cm^{-1}. **^{1}H NMR** (600 MHz) □ 8.59 (d, J = 8.3 Hz, 1H), 8.44 (s, 1H), 8.35 (d, J = 1.7 Hz, 1H), 7.84 (dd, J = 8.3, 1.7 Hz, 1H), 7.76–7.70 (m, 2H), 7.65 (dd, J = 8.8, 2.2 Hz, 1H), 7.54 (t, J = 7.5 Hz, 2H), 7.46 (t, J = 7.5 Hz, 1H), 7.31 (d, J = 8.9 Hz, 1H), 3.81 (s, 3H). **^{13}C NMR** (151 MHz) δ 161.2, 145.6, 140.1, 137.3, 132.6, 132.3, 129.6, 129.0 (2C), 128.4 (2C), 127.8, 127.5, 126.0, 124.6, 121.1, 120.2, 116.8, 115.7, 30.1. **HRMS** (ESI) *m/z* calcd for $C_{20}H_{15}BrNO$ ($[M + H]^+$) 364.0337; found 364.0342.

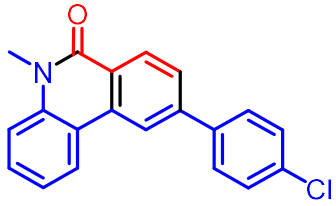

9-(4-chlorophenyl)-5-methylphenanthridin-6(5*H*)-one (7f). Synthesized using general procedure 5. Yellow Oil (38 mg, 80% yield). **TLC**: R_f 0.28 (ethyl acetate/hexanes = 1:4). **IR** (neat) ν_{max}: 2923, 1644, 1585, 1444, 1389, 1343, 1092, 1005, 814, 689 cm^{-1}. **^{1}H NMR** (300 MHz) δ 8.61 (dd, *J* = 8.3, 0.5 Hz, 1H), 8.42–8.39 (m, 1H), 8.36 (dd, *J* = 8.1, 1.5 Hz, 1H), 7.78–7.73 (m, 1H), 7.70–7.63 (m, 2H), 7.58 (ddd, *J* = 8.5, 7.1, 1.5 Hz, 1H), 7.52–7.47 (m, 2H), 7.47–7.42 (m, 1H), 7.35 (ddd, *J* = 8.3, 7.3, 1.2 Hz, 1H), 3.84 (s, 3H). **^{13}C NMR** (75 MHz) δ 161.4, 143.9, 138.8, 138.3, 134.5, 133.9, 129.8,

129.7, 129.2 (2C), 128.8 (2C), 126.9, 124.7, 123.2, 122.5, 120.0, 119.1, 115.2, 30.0. **HRMS** (ESI) *m/z* calcd for $C_{20}H_{15}ClNO$ ([M + H]$^+$) 320.0842; found 320.0851.

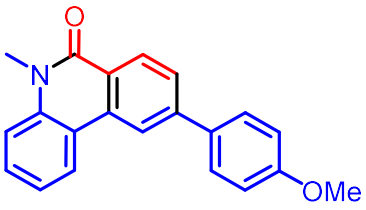

9-(4-methoxyphenyl)-5-methylphenanthridin-6(5*H*)-one (7g). Synthesized using general procedure 5. Yellow oil (45 mg, 81% yield). **TLC**: R_f 0.21 (ethyl acetate/hexanes = 1:4). **IR** (neat) ν_{max}: 2927, 1643, 1585, 1520, 1444, 1298, 1246, 1178, 1032, 826, 750 cm^{-1}. **^{1}H NMR** (300 MHz) δ 8.58 (d, *J* = 8.3 Hz, 1H), 8.41 (d, *J* = 1.7 Hz, 1H), 8.38 (dd, *J* = 8.2, 1.5 Hz, 1H), 7.78 (dd, *J* = 8.3, 1.7 Hz, 1H), 7.72–7.65 (m, 2H), 7.57 (ddd, *J* = 8.5, 7.1, 1.5 Hz, 1H), 7.44 (dd, *J* = 8.5, 1.2 Hz, 1H), 7.35 (ddd, *J* = 8.2, 7.1, 1.2 Hz, 1H), 7.05 (d, *J* = 8.7 Hz, 2H), 3.89 (s, 3H), 3.84 (s, 3H). **^{13}C NMR** (75 MHz) δ 159.9, 144.8, 138.3, 133.9, 129.6 (2C), 129.5, 128.6, 126.8, 124.0, 123.2 (2C), 122.4 (2C), 121.8, 119.4 (2C), 115.1, 114.4, 55.4, 30.0. **HRMS** (ESI) *m/z* calcd for $C_{21}H_{18}NO_2$ ([M + H]$^+$) 316.1338; found 316.1345.

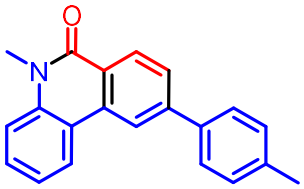

5-methyl-9-(p-tolyl)phenanthridin-6(5H)-one (7h). Synthesized using general procedure 5. Yellow solid (269 mg, 89% yield, m.p. 136–138 ºC). **TLC**: R_f 0.33 (ethyl acetate/hexanes = 1:3). **IR** (neat) ν_{max}: 2914, 1920, 1642, 1614, 1584, 1445, 1338, 1306, 1101, 1044, 814, 781, 684 cm^{-1}. **^{1}H NMR** (300 MHz) δ 8.51 (d, *J* = 8.3 Hz, 1H), 8.30 (s, 1H), 8.23 (d, *J* = 7.8 Hz, 2H), 7.70 (d, *J* = 8.1 Hz,

1H), 7.58 (d, *J* = 7.8 Hz, 2H), 7.48 (t, *J* = 7.4 Hz, 1H), 7.29 (q, *J* = 7.2 Hz, 4H), 3.73 (s, 3H), 2.42 (s, 3H). **^{13}C NMR** (75 MHz). δ 161.4, 144.9, 138.2, 137.3, 133.7, 129.7, 129.5, 129.4 (2C), 127.3, 126.8, 124.1 (2C), 123.1, 122.3 (2C), 119.6, 119.2, 115.0, 29.9, 21.2. **HRMS** (ESI) *m/z* calcd for $C_{21}H_{18}NO$ ($[M + H]^+$) 300.1388; found 300.1389.

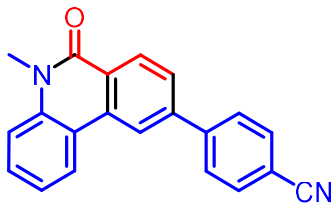

4-(5-methyl-6-oxo-5,6-dihydrophenanthridin-9-yl)benzonitrile (7i). Synthesized using general procedure 5. Yellow oil (31 mg, 68% yield,). **TLC**: R_f 0.14 (ethyl acetate/hexanes = 1:4). **IR** (neat) ν_{max}: 3090, 3035, 2219, 1645, 1604, 1478, 1347, 1035, 824 cm^{-1}. **^{1}H NMR** (300 MHz) δ 8.64 (dd, *J* = 8.3, 0.5 Hz, 1H), 8.43 (d, *J* = 1.8 Hz, 1H), 8.35 (dd, *J* = 8.1, 1.5 Hz, 1H), 7.82 (d, *J* = 1.5 Hz, 4H), 7.77 (dd, *J* = 8.3, 1.7 Hz, 1H), 7.60 (ddd, *J* = 8.5, 7.1, 1.5 Hz, 1H), 7.45 (dd, *J* = 8.5, 1.1 Hz, 1H), 7.36 (ddd, *J* = 8.2, 7.1, 1.2 Hz, 1H), 3.83 (s, 3H). **^{13}C NMR** (75 MHz) δ 161.2, 144.8, 143.0, 138.3, 134.1, 132.8, 130.1, 129.9, 128.2 (2C), 126.8, 125.4, 123.2 (2C), 122.6, 120.5, 118.9, 118.7, 115.3, 111.9, 30.1. **HRMS** (ESI) *m/z* calcd for $C_{21}H_{15}N_2O$ ($[M + H]^+$) 311.1184; found 311.1191.

4.9.7 GENERAL PROCEDURE 6 FOR THE SYNTHESIS OF ARYLACETYLCHALCONES (8)

a.) To a round bottom flask was measured 2'-hydroxyacetophenones (**1**) (1.0 equiv.), which was then dissolved in dichloromethane (0.2 M). This solution was cooled in an ice/water bath then arylacetic acid (1.2 equiv.) and DMAP (0.1 equiv.) were added, followed by the addition of 1-Ethyl-3-(3-dimethylaminopropyl)carbodiimide hydrochloride (EDCI, 1.5 equiv.). The reaction

vessel was allowed to warm naturally to room temperature and stirred for 4 hours. The reaction mixture was then diluted with excess dichloromethane and washed sequentially with 1N HCl (2x) and sat. $NaHCO_3$ (2x). Organics were dried over anhydrous Na_2SO_4, concentrated in vacuo, then purified by flash chromatography eluting with 1:20 ethyl acetate:hexanes gradient to 2:5 ethyl acetate:hexanes to furnish arylacetichydroxychalcones **8a**-**8d**.

b.) To a stirred solution of corresponding arylacetic acid (1.2 equiv.) was added one drop of DMF. The reaction vessel was equipped with a reflux condenser and a 2M solution of $(COCl)_2$ (1.5 equiv.) was slowly added by syringe. The mixture was heated to reflux with stirring for 90 minutes, then cooled to room temperature. Solvent was removed by rotary evaporation and the crude acyl chloride was carried forward without further purification. To a solution of *N*-methylaminochalcone (1.0 equiv.) in dichloromethane (0.2M) at 0 ^oC was added solid $NaHCO_3$ (1.5 equiv.). The mixture was stirred at this temperature for 10 minutes before crude acyl chloride (1.2 equiv.) was added slowly by syringe. The reaction mixture was allowed to warm naturally to room temperature and stirred at this temperature overnight. The reaction mixture was diluted with dichloromethane, then washed with water (2x). The organic layer was then dried over Na_2SO_4 and concentrated to give crude *N*-alkyl-*N*-arylaceticaminochalcones (**8**), which were then purified via column chromatography 3:10 ethyl acetate:hexanes gradient to 1:1 ethyl acetate:hexanes to furnish pure *N*-alkyl-*N*-arylaminochalcones **8f**-**8h**.

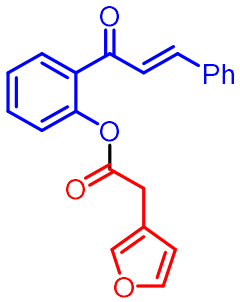

2-cinnamoylphenyl 2-(furan-3-yl)acetate (8a). Synthesized using general procedure 6a. Yellow oil (467 mg, 80% yield). **TLC**: R_f 0.33 (ethyl acetate/hexanes = 1:4). **IR** (neat) ν_{max}: 3058, 2915, 1761, 1666, 1604, 1448, 1303, 1194, 1112, 1020, 998, 872, 731 cm^{-1}. **^{1}H NMR** (300 MHz, Chloroform-*d*) δ 7.70 (dd, *J* = 7.7, 1.7 Hz, 1H), 7.60 – 7.50 (m, 4H), 7.44 – 7.31 (m, 6H), 7.21 – 7.10 (m, 2H), 6.38 (s, 1H), 3.68 (s, 3H). **^{13}C NMR** (75 MHz, Chloroform-*d*) δ 191.7, 169.6, 148.6, 145.7, 143.0, 140.7, 134.4, 132.5, 132.2, 130.9, 129.9, 129.0, 128.5 (2C), 126.2, 125.3, 123.4, 116.4, 111.4, 30.7. **HRMS** (ESI) *m/z* calcd for $C_{21}H_{16}O_4Na$ ($[M + Na]^+$) 355.0946; found 355.0948.

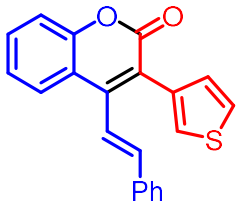

(*Z*)-4-(2-phenyl-2-(thiophen-2-yl)vinyl)-2*H*-chromen-2-one (8b). Synthesized using general procedure 6a. Yellow oil (690 mg, 77% yield). **TLC**: R_f 0.32 (ethyl acetate/hexanes = 1:4). **IR** (neat) ν_{max}: 3028, 2923, 2854, 1703, 1603, 1450, 1282, 1110, 1051, 970 cm^{-1}. **^{1}H NMR** (400 MHz, Chloroform-*d*) δ 7.95 (d, *J* = 8.1 Hz, 1H), 7.55 (d, *J* = 7.0 Hz, 1H), 7.54 – 7.47 (m, 3H), 7.43 (t, *J* = 7.0 Hz, 4H), 7.38 (d, *J* = 7.0 Hz, 1H), 7.32 (d, *J* = 9.2 Hz, 1H), 7.12 – 7.09 (m, 1H), 7.04 (d, *J* = 4.7 Hz, 2H). **^{13}C NMR** (101 MHz, Chloroform-*d*) δ 160.3, 153.0, 146.5, 138.6, 135.8, 134.7, 131.5, 131.26,

129.2 (2C), 129.0 (2C), 128.2 (2C), 127.1, 126.6, 124.3, 122.5, 119.0, 118.7, 117.2. **HRMS** (ESI) *m/z* calcd for $C_{21}H_{15}O_2S$ ($[M + H]^+$) 331.0793; found 331.0788.

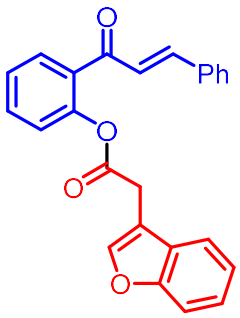

2-cinnamoylphenyl 2-(benzofuran-3-yl)acetate (8c). Synthesized using general procedure 6a. Yellow oil (260 mg, 76% yield). **TLC**: R_f 0.25 (ethyl acetate/hexanes = 1:4). **IR** (neat) ν_{max}: 3060, 2954, 1760, 1604, 1449, 1331, 1303, 1196, 1097, 731 cm^{-1}. **^{1}H NMR** (300 MHz, Chloroform-*d*) δ 7.69 (dd, *J* = 7.7, 1.7 Hz, 1H), 7.59 – 7.49 (m, 6H), 7.45 (d, *J* = 8.1 Hz, 1H), 7.43 – 7.33 (m, 4H), 7.32 – 7.25 (m, 1H), 7.21 (d, *J* = 7.5 Hz, 1H), 7.16 (d, *J* = 8.0 Hz, 1H), 7.09 (d, *J* = 16.1 Hz, 1H), 3.92 (s, 2H). **^{13}C NMR** (101 MHz, Chloroform-*d*) δ 191.7, 169.2, 155.1, 148.6, 145.8, 143.2, 134.3, 132.5, 132.2, 130.9, 129.8, 129.0 (2C), 128.5 (2C), 127.5, 126.3, 125.2, 124.5, 123.5, 122.7, 119.8, 112.3, 111.5, 29.6. **HRMS** (ESI) *m/z* calcd for $C_{25}H_{19}O_4$ ($[M + H]^+$) 383.1283; found 383.1289.

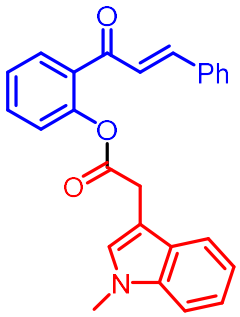

2-cinnamoylphenyl 2-(1-methyl-1*H*-indol-3-yl)acetate (8d). Synthesized using general procedure 6b. Yellow oil (140 mg, 19% yield). **TLC**: R_f 0.22 (ethyl acetate/hexanes = 1:4). **IR** (neat) ν_{max}: 3057, 2929, 1756, 1603, 1474, 1447, 1330, 1193, 1104, 1013, 916, 775 cm^{-1}. **^{1}H NMR** (300 MHz, Chloroform-*d*) δ 7.66 (d, *J* = 7.6 Hz, 1H), 7.58 (d, *J* = 7.9 Hz, 1H), 7.54 – 7.45 (m, 4H), 7.41 – 7.29 (m, 4H), 7.24 (t, *J* = 6.7 Hz, 2H), 7.20 – 7.10 (m, 2H), 7.07 (m, 1H), 6.99 (d, *J* = 19.7 Hz, 1H), 3.96 (s, 2H), 3.66 (s, 3H). **^{13}C NMR** (151 MHz, Chloroform-*d*) δ 192.1, 170.3, 148.7, 145.5, 136.8, 134.5, 132.5, 132.2, 130.6, 129.7 (2C), 128.9 (2C), 128.5, 128.0, 127.7, 126.0, 125.6, 123.4, 121.8, 119.3, 118.9, 109.3, 105.6, 32.6, 31.2. **HRMS** (ESI) *m/z* calcd for $C_{26}H_{21}NO_3Na$ ($[M + Na]^+$) 418.1419; found 418.1411.

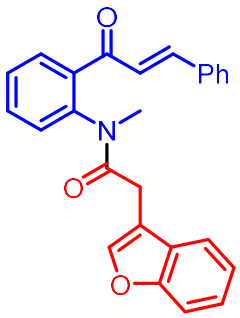

2-(benzofuran-3-yl)-N-(2-cinnamoylphenyl)-N-methylacetamide (8e). Synthesized using general procedure 6b. Yellow oil (184 mg, 93% yield). **TLC**: R_f 0.53 (ethyl acetate/hexanes = 1:1). **IR** (neat) ν_{max}: 3060, 2924, 2247, 1731, 1644, 1596, 1449, 1330, 1207, 1095, 906, 856, 725 cm^{-1}.

^{1}H NMR (300 MHz, Chloroform-*d*) δ 7.73 – 7.68 (m, 1H), 7.57 – 7.53 (m, 2H), 7.52 – 7.48 (m, 2H), 7.47 – 7.43 (m, 2H), 7.42 – 7.32 (m, 5H), 7.28 – 7.22 (m, 1H), 7.22 – 7.19 (m, 1H), 7.19 – 7.12 (m, 1H), 7.00 (d, *J* = 16.0 Hz, 1H), 3.25 (s, 3H). **^{13}C NMR** (75 MHz, Chloroform-*d*) δ 192.5, 170.2, 155.0, 146.5, 142.9, 141.8, 137.6, 134.1, 132.4, 131.1, 129.7, 129.6, 129.0 (2C), 128.6 (2C), 128.6 (2C), 127.9, 124.8, 124.2, 122.5, 119.9, 114.08, 111.3, 29.9. **HRMS** (ESI) *m/z* calcd for $C_{26}H_{21}NO_2$ ([M + H]$^+$) 396.1600; found 396.1604.

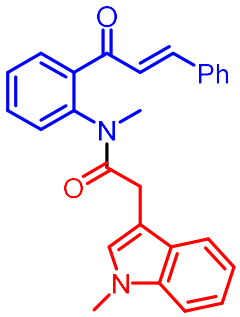

N-(2-cinnamoylphenyl)-N-methyl-2-(1-methyl-1H-indol-3-yl)acetamide (8f). Synthesized using general procedure 6b. Yellow oil (117 mg, 65% yield). **TLC**: R_f 0.40 (ethyl acetate/hexanes = 1:1). **IR** (neat) ν_{max}: 3055, 2928, 2240, 1644, 1596, 1484, 1447, 1371, 1329, 1206, 1109, 1012, 908, 728 cm^{-1}. **^{1}H NMR** (300 MHz, Chloroform-*d*) δ 7.65 (d, *J* = 8.9 Hz, 1H), 7.50 (dd, *J* = 15.8, 9.0 Hz, 3H), 7.36 (s, 5H), 7.23 (d, *J* = 7.6 Hz, 2H), 7.12 (s, 2H), 7.01 (s, 1H), 6.84 (s, 1H), 6.72 (d, *J* = 15.9 Hz, 1H), 3.61 (d, *J* = 5.2 Hz, 2H), 3.55 (s, 3H), 3.29 (s, 3H). **^{13}C NMR** (75 MHz, Chloroform-*d*) δ 192.3, 171.5, 145.6, 142.3, 137.8, 136.6, 134.1, 132.4, 130.9, 129.7, 128.9 (2C), 128.6 (2C), 128.3 (2C), 127.9, 127.7, 124.5, 121.4, 118.9, 118.7, 109.2, 107.3, 38.1, 32.6, 31.1. **HRMS** (ESI) *m/z* calcd for $C_{27}H_{25}N_2O_2$ ([M + H]$^+$) 409.1916; found 409.1922.

4.9.8 GENERAL PROCEDURE 7 FOR THE SYNTHESIS OF HETEROBENZO[*C*]COUMARINS AND HETEROARYLPHENANTHRADIN-6(5*H*)-ONES (9)

To a 15 mL round bottom flask was measured arylaceticchalcone (**9**) (1.0 equiv.). DMSO (0.15M) was then added, followed by the addition of DBU (3.0 equiv.). The reaction vessel was equipped with a magnetic stir bar, and stirred open to air at room temperature for 90 minutes. The reaction mixture was then heated to 120 °C and stirred at this temperature for 16 hours. The reaction mixture was then cooled to room temperature and diluted into ethyl acetate. Organics were washed sequentially with sat. NH_4Cl (2x) and water (2x) then dried over anhydrous Na_2SO_4. Organics were concentrated in vacuo and purified by flash chromatography 1:20 ethyl acetate:hexanes gradient to 2:5 ethyl acetate:hexanes to furnish heteroarylbenzo[c]coumarins **9a**-**9d**.

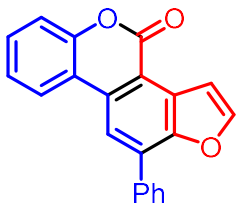

11-phenyl-4*H*-benzofuro[4,5-c]chromen-4-one (9a). Synthesized using general procedure 7. Beige solid (61 mg, 90% yield, m.p. 204–206 ºC). **TLC**: R_f 0.50 (ethyl acetate/hexanes = 1:4). **IR** (neat) ν_{max}: 3027, 2921, 1726, 1607, 1482, 1350, 1251, 1200, 1109, 1025, 873, 684 cm^{-1}. **^{1}H NMR** (300 MHz, Chloroform-*d*) δ 8.15 (d, *J* = 9.1 Hz, 2H), 7.94 (dd, *J* = 8.2, 1.4 Hz, 2H), 7.86 (dd, *J* = 24.4, 2.1 Hz, 2H), 7.63 – 7.50 (m, 3H), 7.50 – 7.38 (m, 2H), 7.36 (d, *J* = 7.8 Hz, 1H). **^{13}C NMR** (75 MHz, Chloroform-*d*) δ 160.3, 152.2, 151.3, 148.0, 135.0, 132.6, 132.1, 129.9, 129.2, 129.2, 129.1 (2C),

128.9 (2C), 124.5, 122.9, 118.4, 117.8, 117.1, 112.7, 108.8. **HRMS** (ESI) *m/z* calcd for $C_{21}H_{13}O_3$ ([M + H]$^+$) 313.0865; found 313.0867.

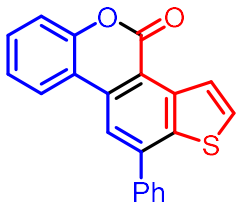

11-phenyl-4*H*-thieno[2',3':5,6]benzo[1,2-c]chromen-4-one (9b). Synthesized using general procedure 7. Beige solid (19 mg, 83% yield, m.p. 206–208 ºC). **TLC**: R_f 0.50 (ethyl acetate/hexanes = 1:4). **IR** (neat) ν_{max}: 2923, 2359, 1702, 1583, 1498, 1332, 1280, 1199, 967, 746 cm^{-1}. **^{1}H NMR** (400 MHz, Chloroform-*d*) δ 8.22 (d, *J* = 8.0 Hz, 1H), 8.12 (s, 1H), 7.74 (d, *J* = 5.6 Hz, 1H), 7.68 (d, *J* = 6.8 Hz, 2H), 7.62 – 7.47 (m, 6H), 7.40 (t, *J* = 7.4 Hz, 1H). **^{13}C NMR** (126 MHz, Chloroform-*d*) δ 160.6, 151.2, 144.4, 139.8, 139.1, 132.8, 131.0, 130.4, 129.2 (2C), 128.9 (2C), 128.7 (2C), 124.7, 123.3, 123.0, 118.3 (2C), 117.9 (2C). **HRMS** (ESI) *m/z* calcd for $C_{21}H_{14}O_2S$ ([M + H]$^+$) 329.0636; found 329.0643.

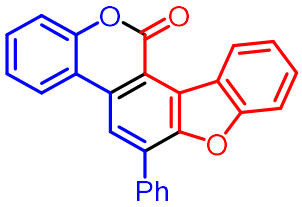

6-phenyl-12*H*-benzo[2,3]benzofuro[4,5-c]chromen-12-one (9c). Synthesized using general procedure 7. Beige solid (12 mg, 89% yield, m.p. 247–249 ºC). **TLC**: R_f 0.42 (ethyl acetate/hexanes = 1:4). **IR** (neat) ν_{max}: 2919, 2849, 1723, 1599, 1451, 1364, 1252, 1195, 1142, 966, 874, 767 cm^{-1}. **^{1}H NMR** (300 MHz, Chloroform-*d*) δ 9.41 (d, *J* = 9.3 Hz, 1H), 8.30 (s, 1H), 8.15 (d, *J* = 8.0 Hz, 1H), 7.97 (d, *J* = 6.8 Hz, 2H), 7.67 – 7.51 (m, 5H), 7.51 – 7.45 (m, 2H), 7.45 – 7.38 (m, 1H), 7.37 – 7.29

(m, 1H). **^{13}C NMR** (126 MHz, Chloroform-*d*) δ 160.2, 157.5, 153.6, 151.1, 135.2, 132.8, 132.1, 130.0, 129.4, 129.2, 129.0 (2C), 128.3 (2C), 125.7, 124.5, 123.4, 123.1, 123.0 (2C), 120.4, 118.3, 117.6, 115.2, 111.4. **HRMS** (ESI) *m/z* calcd for $C_{25}H_{15}O_3$ ([M + H]$^+$) 363.1021; found 363.1029.

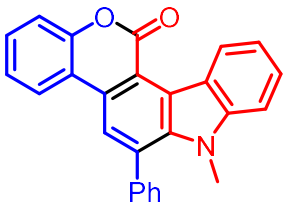

7-methyl-6-phenylchromeno[4,3-c]carbazol-12(7*H*)-one (9d). Synthesized using general procedure 7. Yellow solid (19 mg, 71% yield, m.p. 251–253 ºC). **TLC**: R_f 0.40 (ethyl acetate/hexanes = 1:4). **IR** (neat) ν_{max}: 2919, 2850, 1712, 1594, 1400, 1321, 1143, 1005, 873, 738 cm^{-1}. **^{1}H NMR** (400 MHz, Chloroform-*d*) δ 9.66 (d, *J* = 8.7 Hz, 1H), 8.09 – 8.01 (m, 2H), 7.56 (s, 6H), 7.41 – 7.32 (m, 4H), 7.27 (d, *J* = 4.6 Hz, 1H), 3.40 (s, 3H). **^{13}C NMR** (101 MHz, Chloroform-*d*) δ 160.8, 150.8, 143.4, 139.5 (2C), 139.1, 133.2, 129.5, 129.0, 128.4 (2C), 128.4 (2C), 128.2 (2C), 127.4, 124.1, 123.4, 122.7, 121.9, 120.1, 118.9, 117.2, 115.1, 108.7, 33.4. **HRMS** (ESI) *m/z* calcd for $C_{26}H_{18}NO_2$ ([M + H]$^+$) 376.1338; found 376.1340.

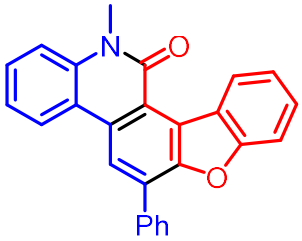

13-methyl-6-phenylbenzofuro[3,2-i]phenanthridin-12(13H)-one (9e). Synthesized using general procedure 7. Beige solid (58 mg, 86% yield, m.p. 234–236 ºC). **TLC**: R_f 0.38 (ethyl acetate/hexanes = 1:1). **IR** (neat) ν_{max}: 3032, 2921, 1915, 1642, 1604, 1486, 1328, 1219, 1047, 866, 743 cm^{-1}. **^{1}H**

NMR (300 MHz, Chloroform-*d*) δ 9.60 (d, *J* = 8.1 Hz, 1H), 8.38 (s, 1H), 8.27 (d, *J* = 9.4 Hz, 1H), 7.94 (d, *J* = 6.9 Hz, 2H), 7.60 (t, *J* = 7.2 Hz, 3H), 7.54 (d, *J* = 7.0 Hz, 1H), 7.46 (q, *J* = 8.3 Hz, 3H), 7.36 (d, *J* = 9.3 Hz, 1H), 7.26 (t, 1H), 3.85 (s, 3H). **^{13}C NMR** (75 MHz, Chloroform-*d*) δ 161.3, 157.2, 153.4, 137.6, 135.8, 130.7, 130.5, 129.3, 129.2, 129.0, 128.8 (2C), 128.7, 128.0, 124.3, 124.1, 123.4, 123.0, 122.3, 120.86, 120.7, 119.5, 114.8, 111.1, 30.0. **HRMS** (ESI) *m/z* calcd for $C_{25}H_{18}NO_2$ ([M + H]$^+$) 376.1338; found 376.1338.

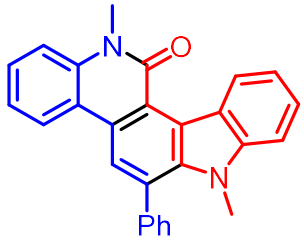

7,13-dimethyl-6-phenyl-7,13-dihydro-12H-indolo[3,2-i]phenanthridin-12-one (9f). Synthesized using general procedure 7. Yellow oil (48 mg, 63% yield). **TLC**: R_f 0.46 (ethyl acetate/hexanes = 1:1). **IR** (neat) ν_{max}: 3050, 2925, 2241, 1629, 1598, 1448, 1307, 1246, 1078, 907, 729 cm^{-1}. **^{1}H NMR** (300 MHz, Chloroform-*d*) δ 8.13 (dd, *J* = 8.2, 1.5 Hz, 1H), 7.59 (ddd, *J* = 8.5, 7.1, 1.5 Hz, 1H), 7.45 (dd, *J* = 8.1, 1.1 Hz, 2H), 7.37 – 7.30 (m, 1H), 7.30 – 7.25 (m, 4H), 7.24 (d, *J* = 8.7 Hz, 1H), 7.22 – 7.17 (m, 1H), 7.10 – 7.03 (m, 2H), 6.86 (d, *J* = 16.8 Hz, 1H), 3.84 (s, 3H), 3.79 (s, 3H). **^{13}C NMR** (126 MHz, Chloroform-*d*) δ 161.7, 142.7, 139.6, 136.9, 136.7, 136.2, 131.3, 129.7, 128.7 (2C), 128.1 (2C), 127.6, 127.4, 126.6, 125.0, 124.6, 121.8, 121.5, 121.3, 120.4, 119.6, 114.4, 109.5, 109.3, 33.0, 30.3. **HRMS** (ESI) *m/z* calcd for $C_{27}H_{21}N_2O$ ([M + H]$^+$) 389.1654; found 389.1654.

4.9.9 SYNTHESIS OF ETHYL 2-PHENYLDIBENZO[B,D]FURAN-3-CARBOXYLATE (11)

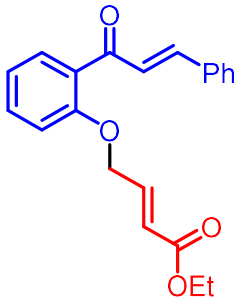

ethyl (*E*)-4-(2-cinnamoylphenoxy)but-2-enoate (10). To a suspension of anhydrous potassium carbonate (6.0 mmol, 829 mg, 3.0 equiv.) in DMSO (2 mL) was added hydroxychalcone (448 mg, 2.0 mmol, 1.0 equiv.). Ethyl 4-bromocrotonate (0.736 mL, 4.0 mmol, 2.0 equiv.) was then added dropwise via syringe. The mixture was then stirred at room temperature for 6 hours. The inorganic solids were removed via filtration and organics were quenched via addition of cold water. The aqueous solution was extracted with dichloromethane (3x 20 mL) and the organics were washed with water (3x 15 mL). Organics were dried over dried over anhydrous Na_2SO_4, concentrated, and purified by flash chromatography to furnish Ethyl (E)-4-(2-cinnamoylphenoxy)but-2-enoate **10**. Yellow oil (362 mg, 54% yield). **TLC**: R_f = 0.21 (ethyl acetate/hexanes = 1:4). **IR** (neat) ν_{max}: 2980, 1715, 1660, 1599, 1448, 1303, 1271, 1177, 1021, 970, 753 cm^{-1}. **^{1}H NMR** (300 MHz) δ 7.67–7.59 (m, 2H), 7.58–7.51 (m, 2H), 7.47–7.38 (m, 2H), 7.38–7.30 (m, 3H), 7.09–6.97 (m, 2H), 6.92 (dd, *J* = 8.4, 0.9 Hz, 1H), 6.15 (dt, *J* = 15.8, 2.1 Hz, 1H), 4.75 (dd, *J* = 3.9, 2.1 Hz, 2H), 4.05 (q, *J* = 7.1 Hz, 2H), 1.13 (t, *J* = 7.1 Hz, 3H). **^{13}C NMR** (75 MHz) δ 192.6, 165.9, 156.4, 143.4, 141.4, 134.8, 132.9, 130.6, 130.3, 129.7, 128.8 (2C), 128.5 (2C), 126.9, 122.2, 121.5, 112.7, 67.1, 60.4, 14.1. **HRMS** (ESI) *m/z* calcd for $C_{21}H_{21}O_4$ ($[M + H]^+$) 337.1440; found 337.1431.

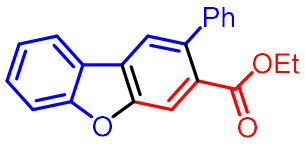

ethyl 2-phenyldibenzo[b,d]furan-3-carboxylate (12). To a 15 mL round bottom flask was measured ethyl (*E*)-4-(2-cinnamoylphenoxy)but-2-enoate (**10**) (1.0 equiv.). DMSO (0.15M) was then added, followed by the addition of DBU (3.0 equiv.). The reaction vessel was equipped with a magnetic stir bar, and stirred open to air at room temperature for 90 minutes. The reaction mixture was then heated to 120 °C and stirred at this temperature for 16 hours. The reaction mixture was then cooled to room temperature and diluted into ethyl acetate. Organics were washed sequentially with sat. NH_4Cl (2x) and water (2x) then dried over anhydrous Na_2SO_4. Organics were concentrated in vacuo and purified by flash chromatography to furnish dibenzofuran **11**. Yellow oil (26 mg, 55% yield). **TLC**: R_f 0.57 (ethyl acetate/hexanes = 1:4). **IR** (neat) ν_{max}: 3057, 2979, 2358, 1707, 1458, 1217, 1106, 1017,786 cm^{-1}. **^{1}H NMR** (600 MHz) δ 8.07 (d, *J* = 2.2 Hz, 1H), 7.96 (d, *J* = 7.8 Hz, 1H), 7.92 (d, *J* = 2.2 Hz, 1H), 7.62 (d, *J* = 8.3 Hz, 1H), 7.53 (t, *J* = 7.9 Hz, 1H), 7.45–7.33 (m, 6H), 4.13 (q, *J* = 7.0 Hz, 2H), 1.02 (t, *J* = 7.1 Hz, 3H). **^{13}C NMR** (151 MHz) δ 168.4, 157.5, 154.7, 141.9, 137.8, 130.0, 128.7 (2C), 128.4 (2C), 128.0, 127.0, 126.8, 123.4, 123.1, 122.6, 121.2, 113.2, 112.0, 61.12 13.6. **HRMS** (ESI) *m/z* calcd for $C_{21}H_{16}O_3Na$ ($[M + Na]^+$) 339.0997; found 339.0986.

4.9.10. SYNTHESIS OF ETHYL- 9-METHYL-3-PHENYL-9H-CARBAZOLE-2-CARBOXYLATE (13)

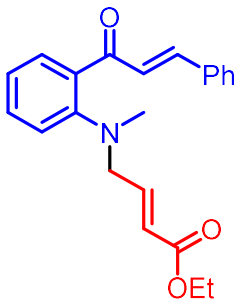

ethyl (*E*)-4-((2-cinnamoylphenyl)(methyl)amino)but-2-enoate (11). To a solution of N-methylaminochalcone (356 mg, 1.50 mmol, 1.0 equiv.) and ethyl 4-bromocrotonate (0.310 mL, 1.80 mmol, 1.2 equiv.) in MeCN (3 mL) was added anhydrous potassium carbonate (207 mg, 1.50 mmol, 1.0 equiv.). The reaction vessel was sealed and heated to reflux with stirring for 16 hours. The reaction mixture was cooled to room temperature and inorganic salts were removed via filtration. Organics were then concentrated and purified by flash chromatography to furnish Ethyl (E)-4-((2-cinnamoylphenyl)(methyl)amino)but-2-enoate **9**. Yellow oil (468 mg, 89% yield). **TLC**: R_f 0.32 (ethyl acetate/hexanes = 1:4). **IR** (neat) ν_{max}: 2980, 1715, 1658, 1597, 1485, 1448, 1367, 1265, 1173, 1030, 974, 704 cm^{-1}. **^{1}H NMR** (400 MHz) δ 7.65 (d, *J* = 16.0 Hz, 1H), 7.59–7.54 (m, 2H), 7.50 (dd, *J* = 7.6, 1.7 Hz, 1H), 7.44–7.34 (m, 3H), 7.30 (d, *J* = 16.0 Hz, 1H), 7.03 (qd, *J* = 7.8, 7.4, 1.0 Hz, 2H), 6.87 (dt, *J* = 15.7, 5.7 Hz, 1H), 5.93 (dt, *J* = 15.7, 1.7 Hz, 1H), 4.09 (q, *J* = 7.1 Hz, 2H), 3.80 (dd, *J* = 5.7, 1.6 Hz, 2H), 2.79 (s, 3H), 1.18 (t, *J* = 7.1 Hz, 3H). **^{13}C NMR** (101 MHz) δ 195.2, 165.9, 150.8, 143.8, 143.2, 134.9, 132.8, 131.8, 130.3 (2C), 128.9 (2C), 128.4 (2C), 126.3, 123.5, 121.4, 118.5, 60.4, 57.9, 41.3, 14.1. **HRMS** (ESI) *m/z* calcd for $C_{22}H_{24}NO_3$ ($[M + H]^+$) 350.1756; found 350.1758.

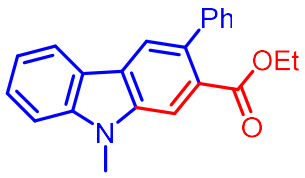

ethyl 9-methyl-3-phenyl-9H-carbazole-2-carboxylate (13). To a 15 mL round bottom flask was measured ethyl (*E*)-4-((2-cinnamoylphenyl)(methyl)amino)but-2-enoate (**12**) (1.0 equiv.). DMSO (0.15M) was then added, followed by the addition of DBU (3.0 equiv.). The reaction vessel was equipped with a magnetic stir bar, and stirred open to air at room temperature for 90 minutes. The reaction mixture was then heated to 120 ^{o}C and stirred at this temperature for 16 hours. The reaction mixture was then cooled to room temperature and diluted into ethyl acetate. Organics were washed sequentially with sat. NH_4Cl (2x) and water (2x) then dried over anhydrous Na_2SO_4. Organics were concentrated in vacuo and purified by flash chromatography to furnish carbazole **9**. Orange oil (64 mg, 69% yield). **TLC**: R_f 0.36 (ethyl acetate/hexanes = 1:4). **IR** (neat) ν_{max}: 2978, 1701, 1493, 1460, 1368, 1234, 1095, 1018, 908, 785, 699 cm^{-1}. **^{1}H NMR** (500 MHz) δ 8.11 (d, *J* = 7.8 Hz, 1H), 8.07 (d, *J* = 1.5 Hz, 1H), 7.95 (d, *J* = 1.5 Hz, 1H), 7.56 (t, *J* = 7.9 Hz, 1H), 7.46 (d, *J* = 8.3 Hz, 1H), 7.45–7.34 (m, 4H), 7.30–7.26 (m, 2H), 4.14 (qd, *J* = 7.1, 1.4 Hz, 2H), 3.94 (d, *J* = 1.6 Hz, 3H), 1.01 (t, *J* = 7.1 Hz, 3H). **^{13}C NMR** (101 MHz) δ 169.6, 142.8, 142.4, 139.5, 133.6, 128.9 (2C), 128.5 (2C), 127.9, 126.9, 126.5, 125.0, 122.2 (2C), 121.0, 119.4, 110.4, 108.8, 61.0, 29.3, 13.6. **LRMS*** (ESI) *m/z* calcd for $C_{22}H_{22}NO_3$ ($[M + H + H_2O]^+$) 348.2; found 348.5.

*We were unable to obtain an accurate HRMS in ESI for this compound.

Appendix III

Spectra Relevant to Chapter 4

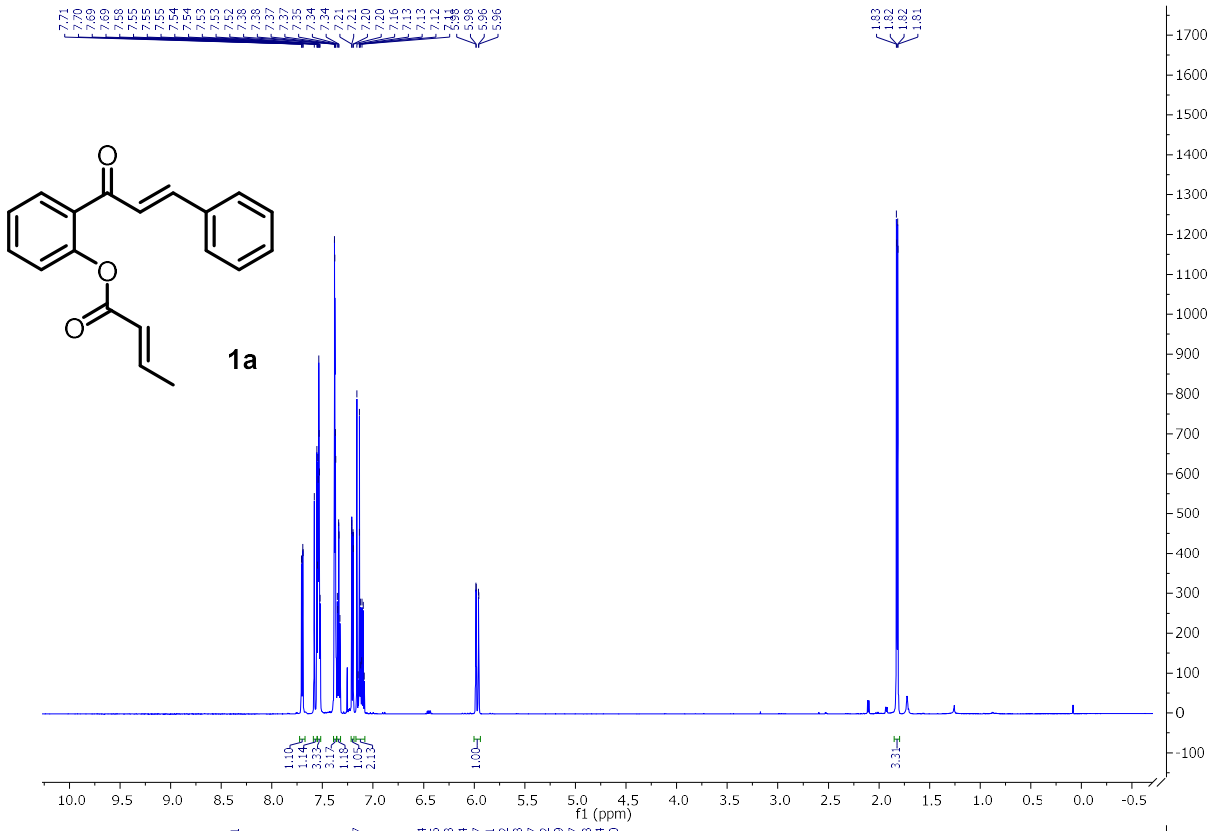
1a
f1 (ppm)

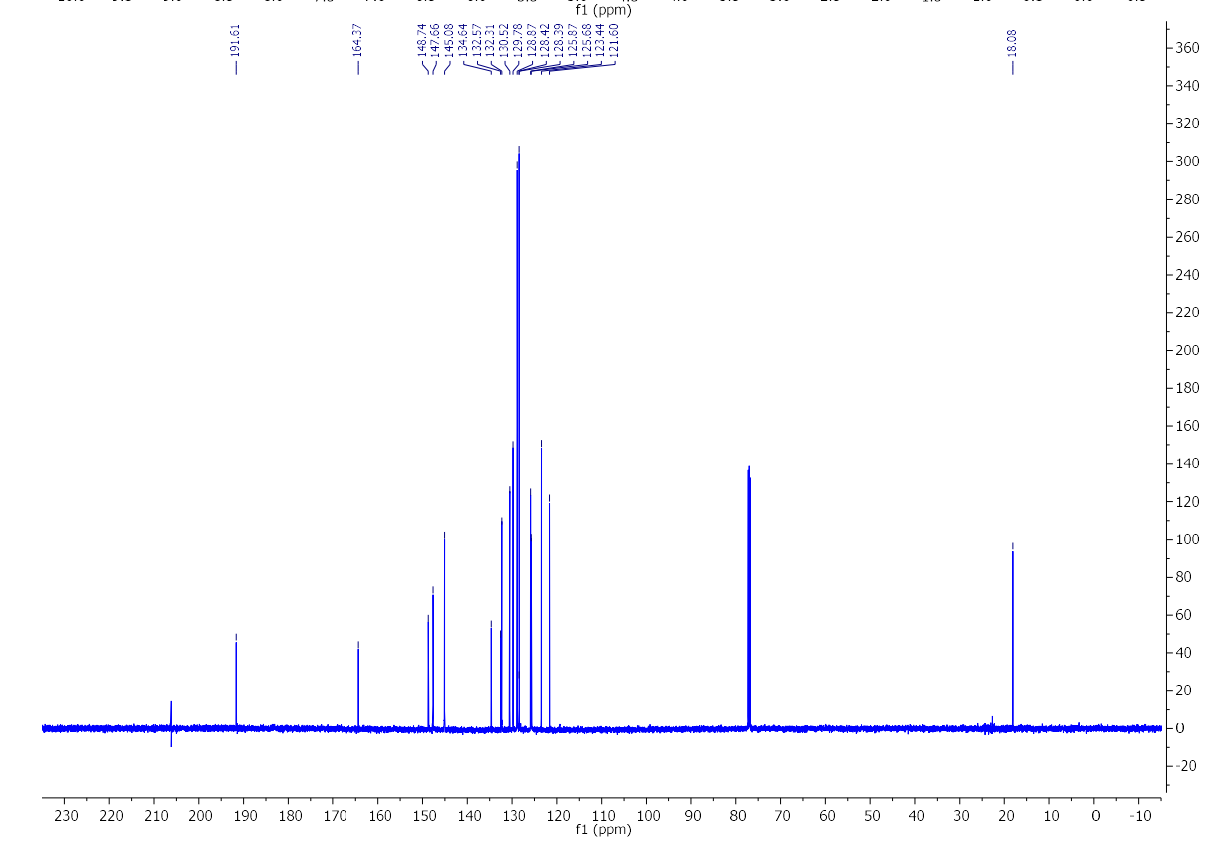
f1 (ppm)

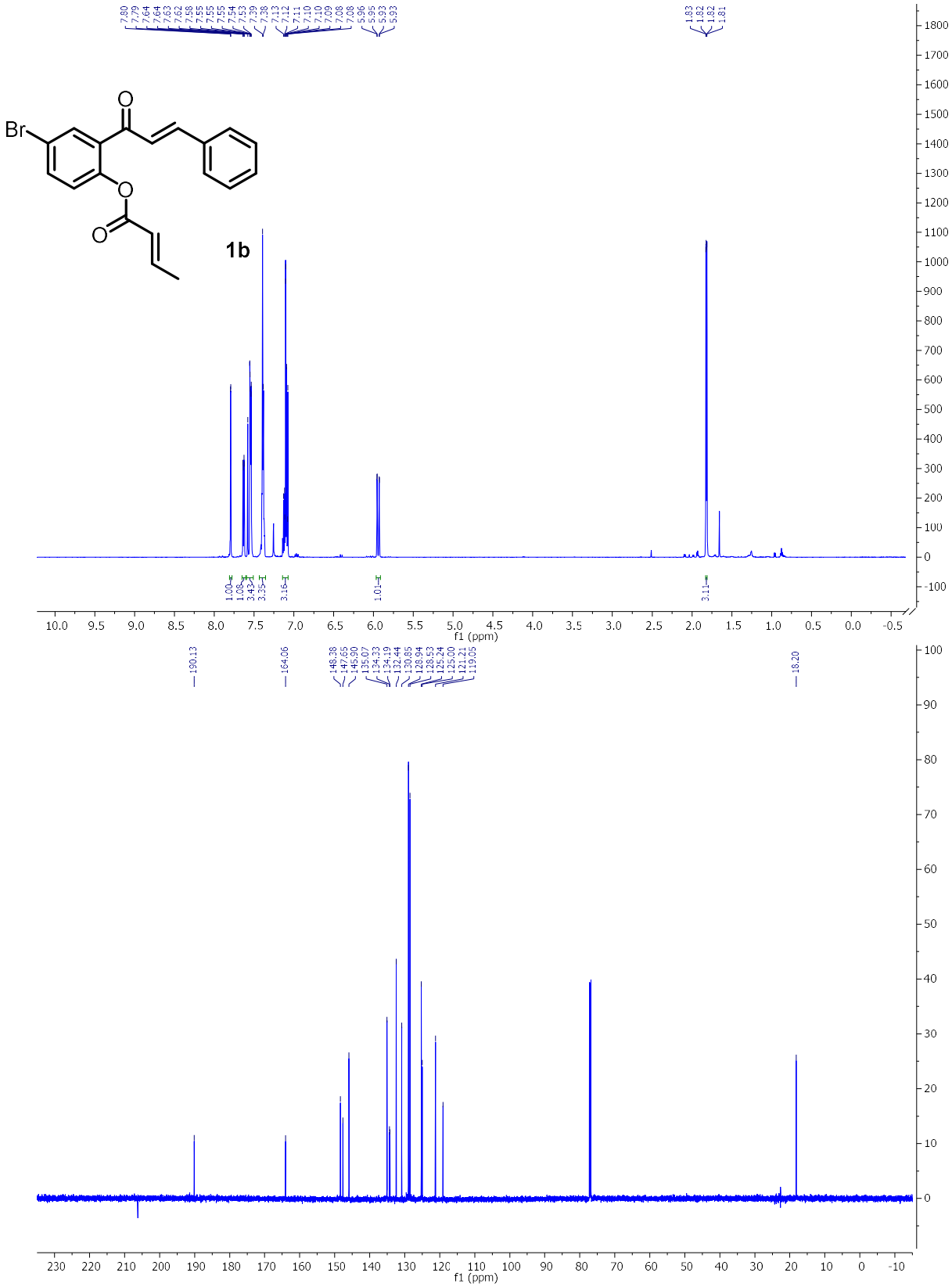
Br
O
O
O
1b
f1 (ppm)
f1 (ppm)

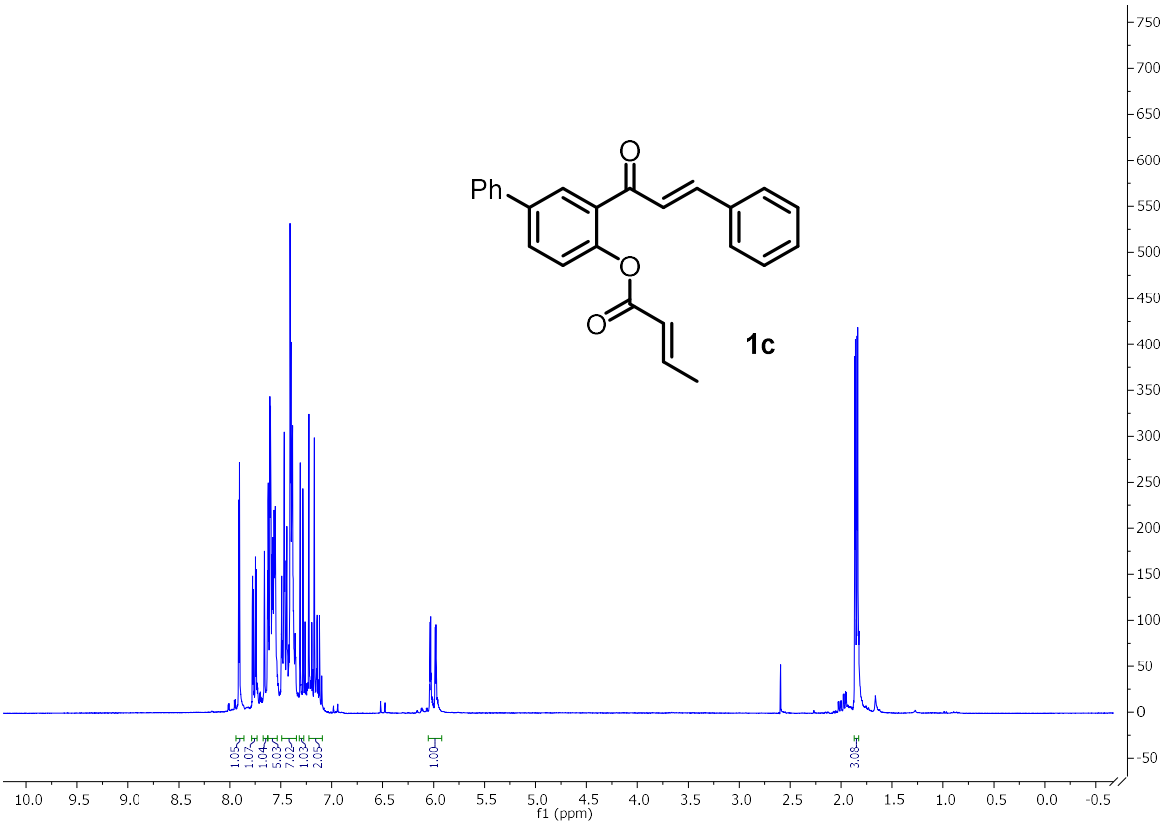
Ph
O
O
O
1c
f1 (ppm)

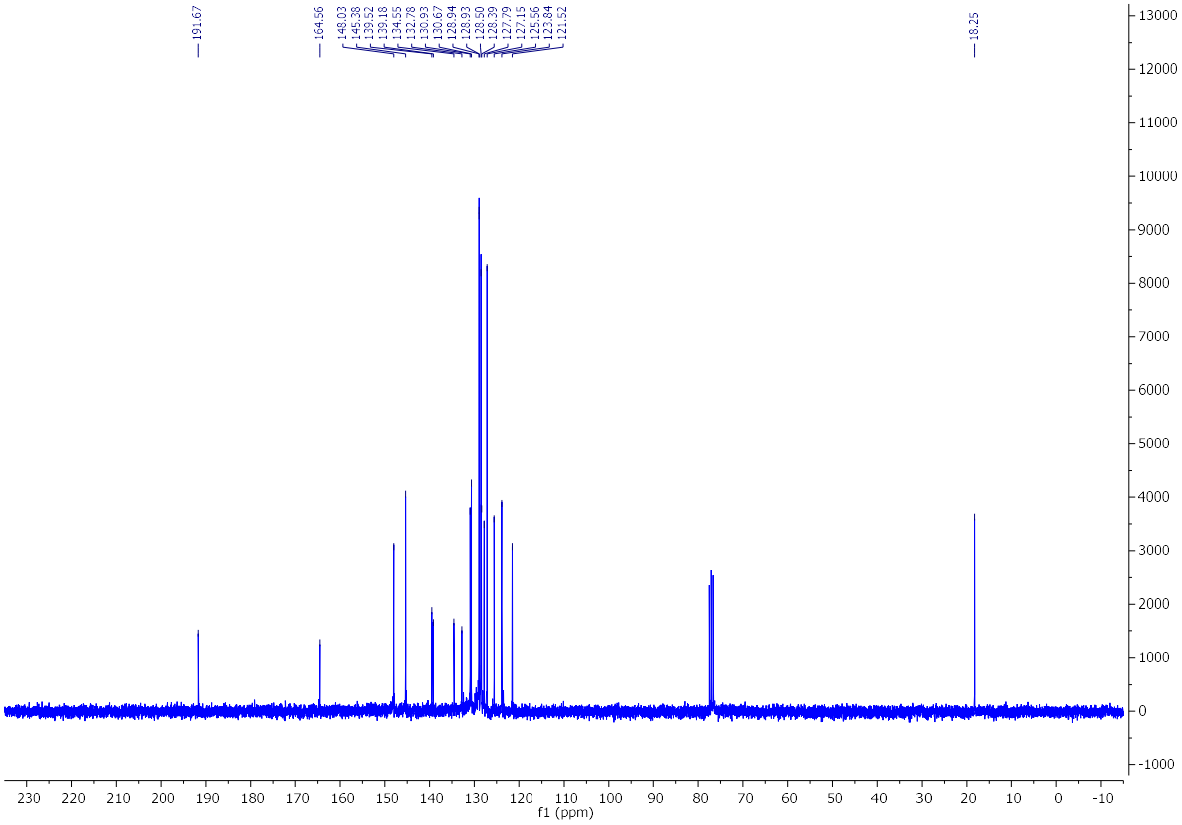
191.67
164.56
148.03
145.38
139.52
139.18
134.55
132.78
130.93
130.67
128.94
128.93
128.50
128.39
127.79
127.15
125.56
123.84
121.62
18.25
f1 (ppm)

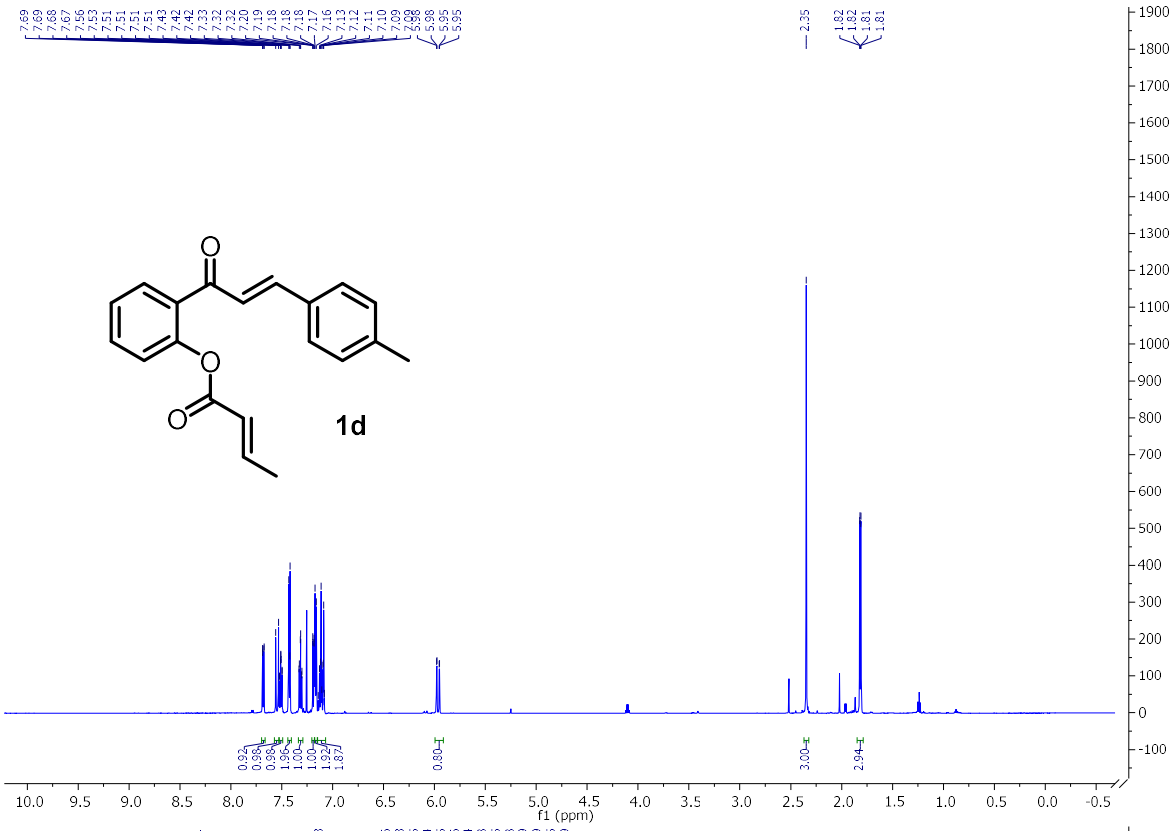
1d
f1 (ppm)

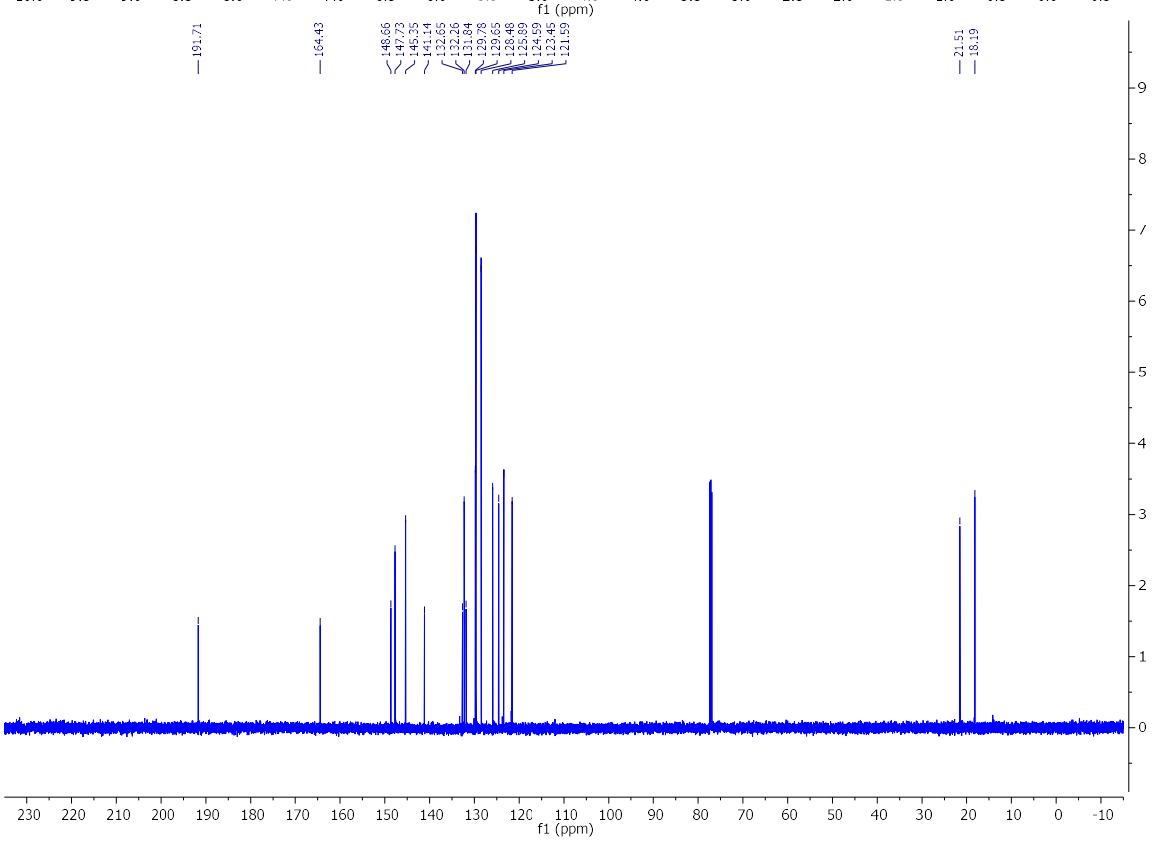
f1 (ppm)

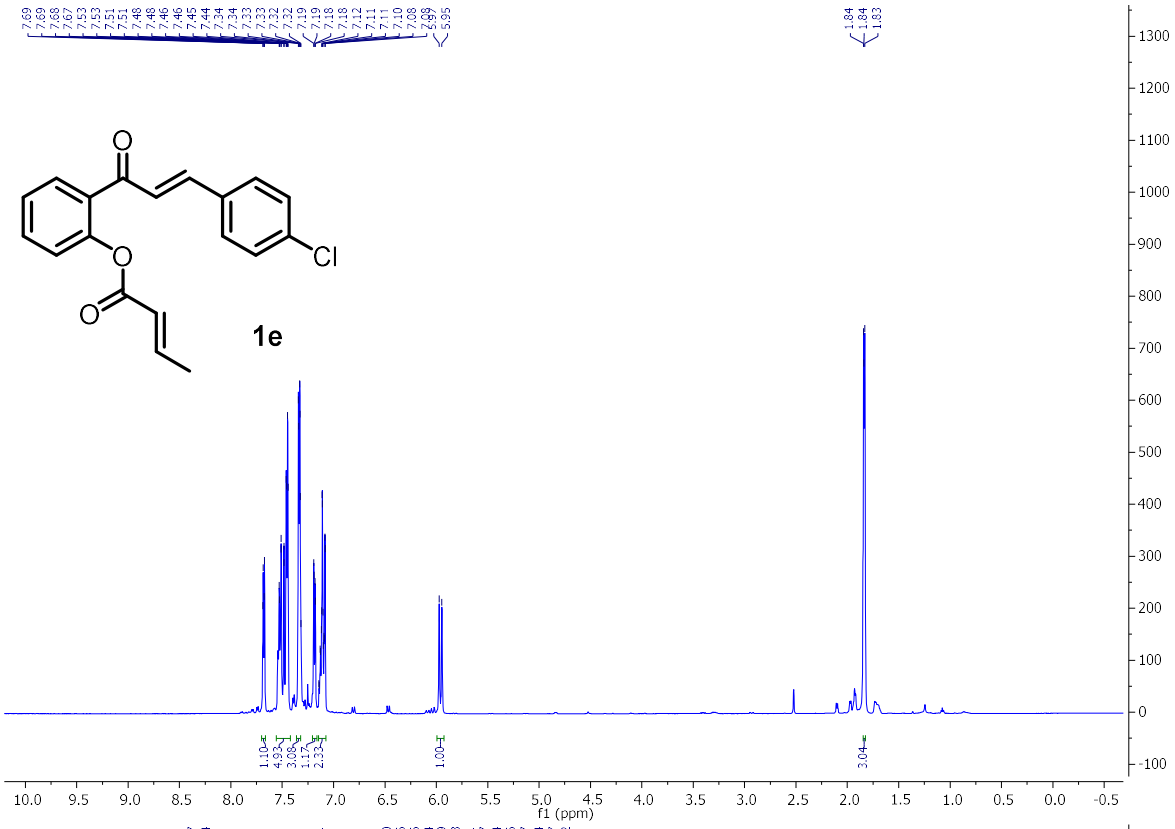
1e
Cl
O
O
O
f1 (ppm)

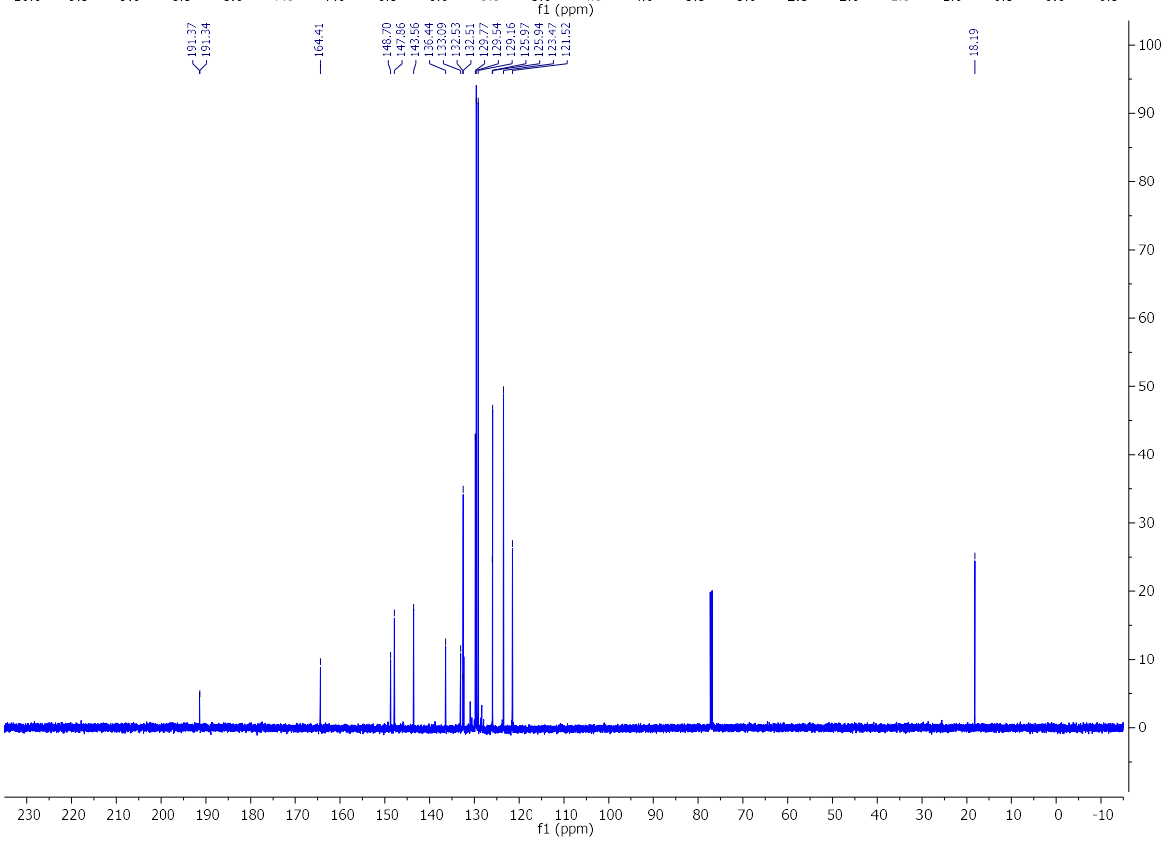
191.37
191.34
164.41
148.70
147.86
143.56
136.44
133.09
132.53
132.51
129.77
129.54
129.16
125.97
125.94
123.47
121.52
18.19
f1 (ppm)

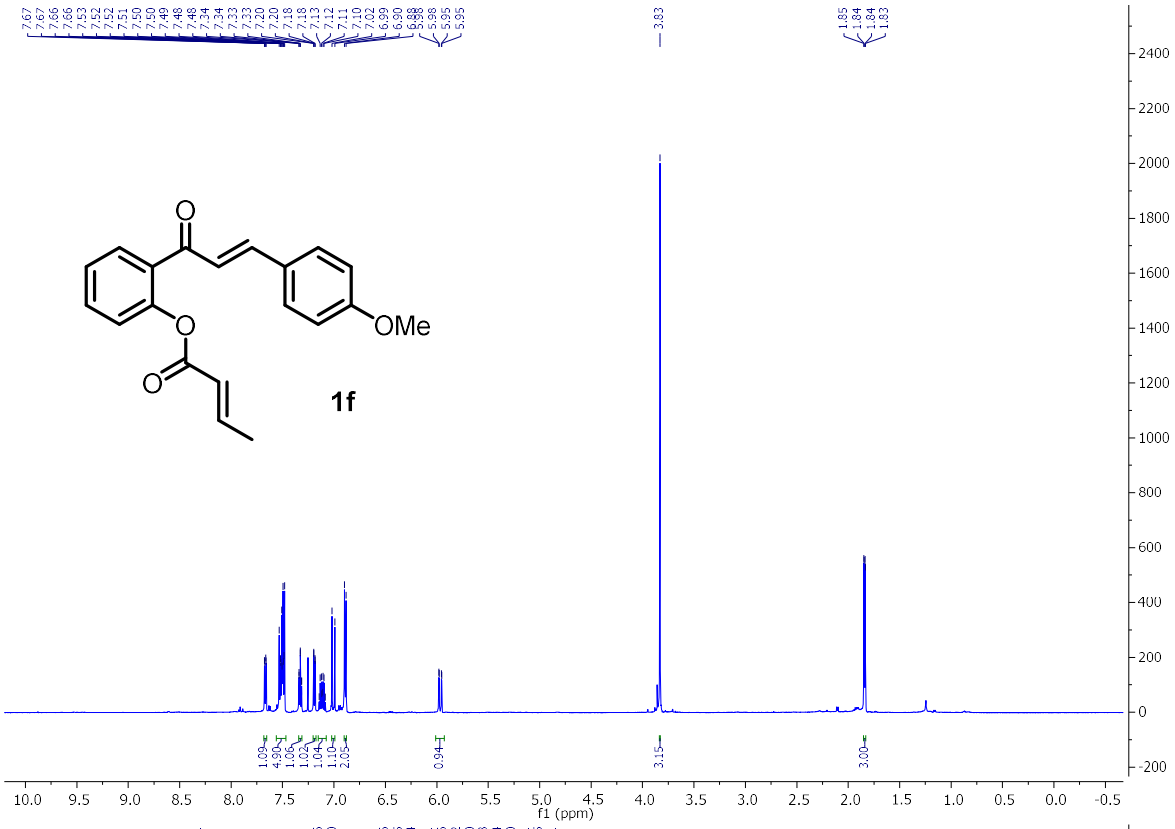
OMe
1f
f1 (ppm)

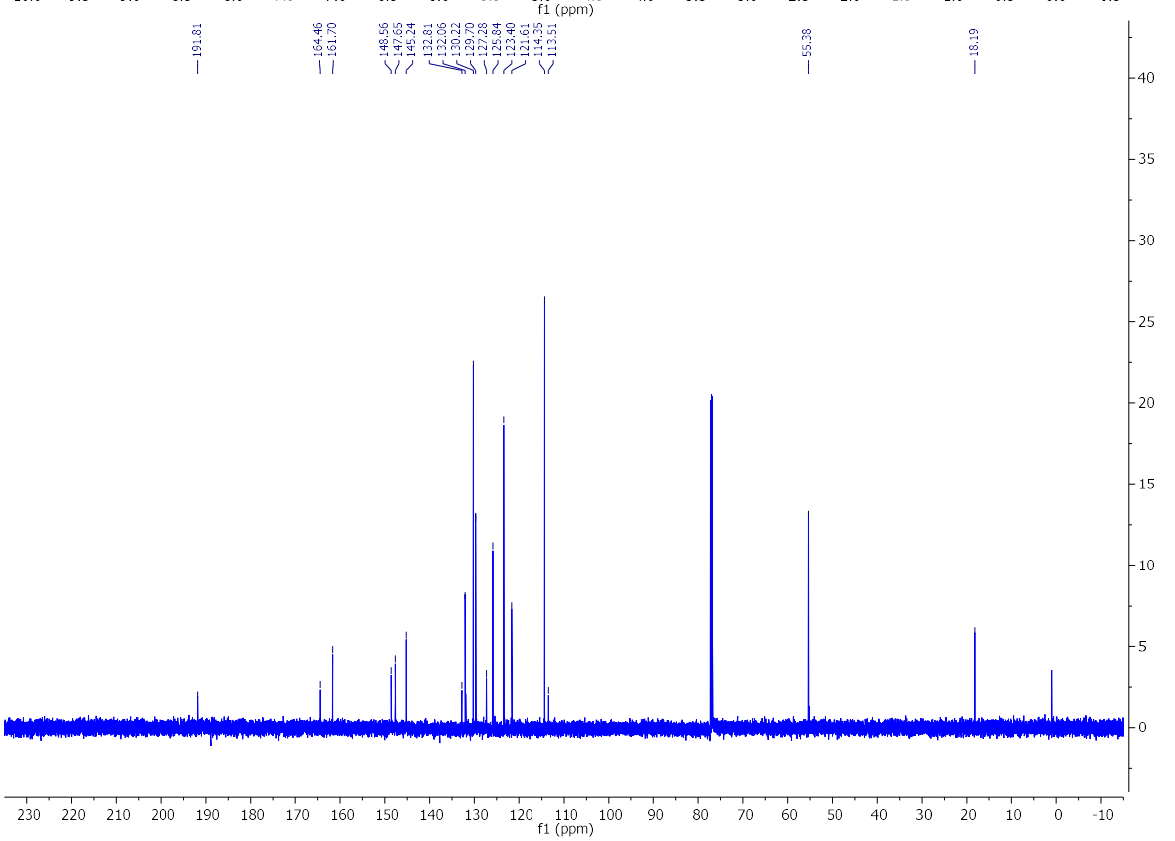
f1 (ppm)

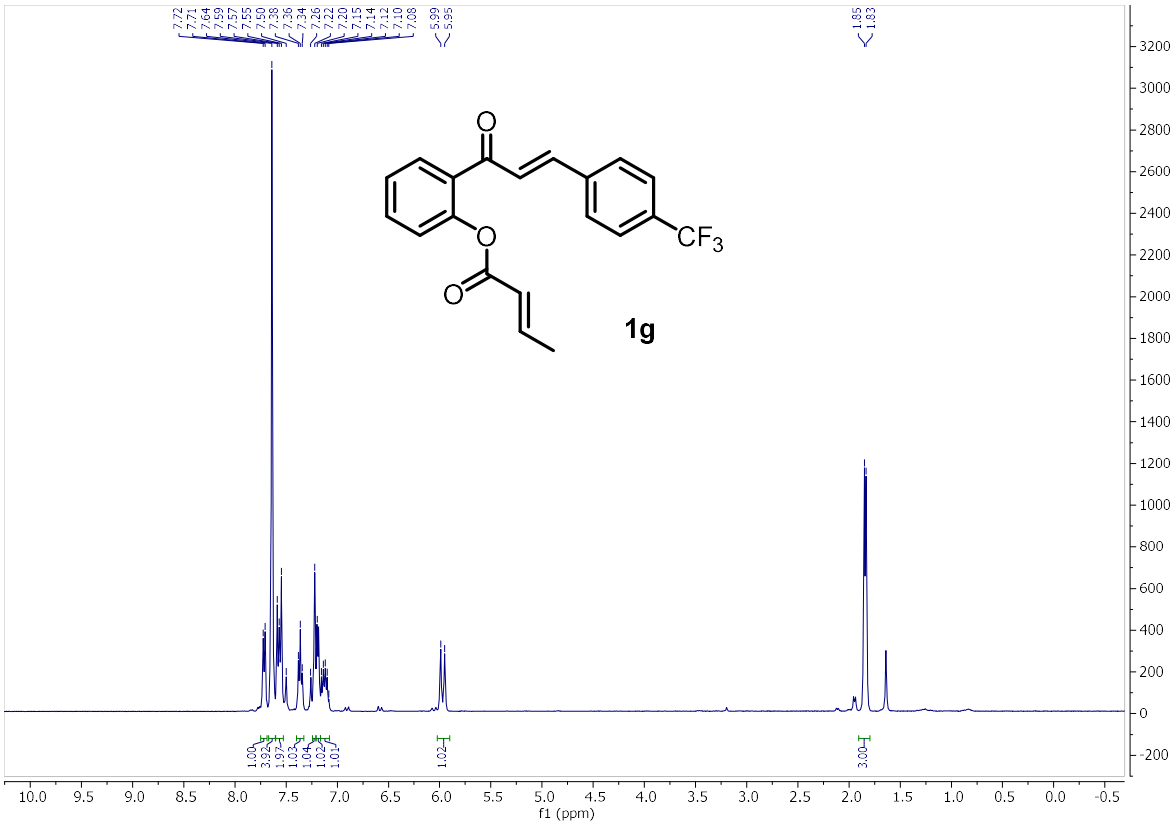
7.72
7.71
7.64
7.59
7.57
7.55
7.50
7.38
7.36
7.34
7.26
7.22
7.20
7.15
7.14
7.12
7.10
7.08
5.99
5.95
1.85
1.83
O
O
O
CF3
1g
1.00
3.92
1.91
1.03
1.04
1.02
1.01
1.02
3.00
f1 (ppm)

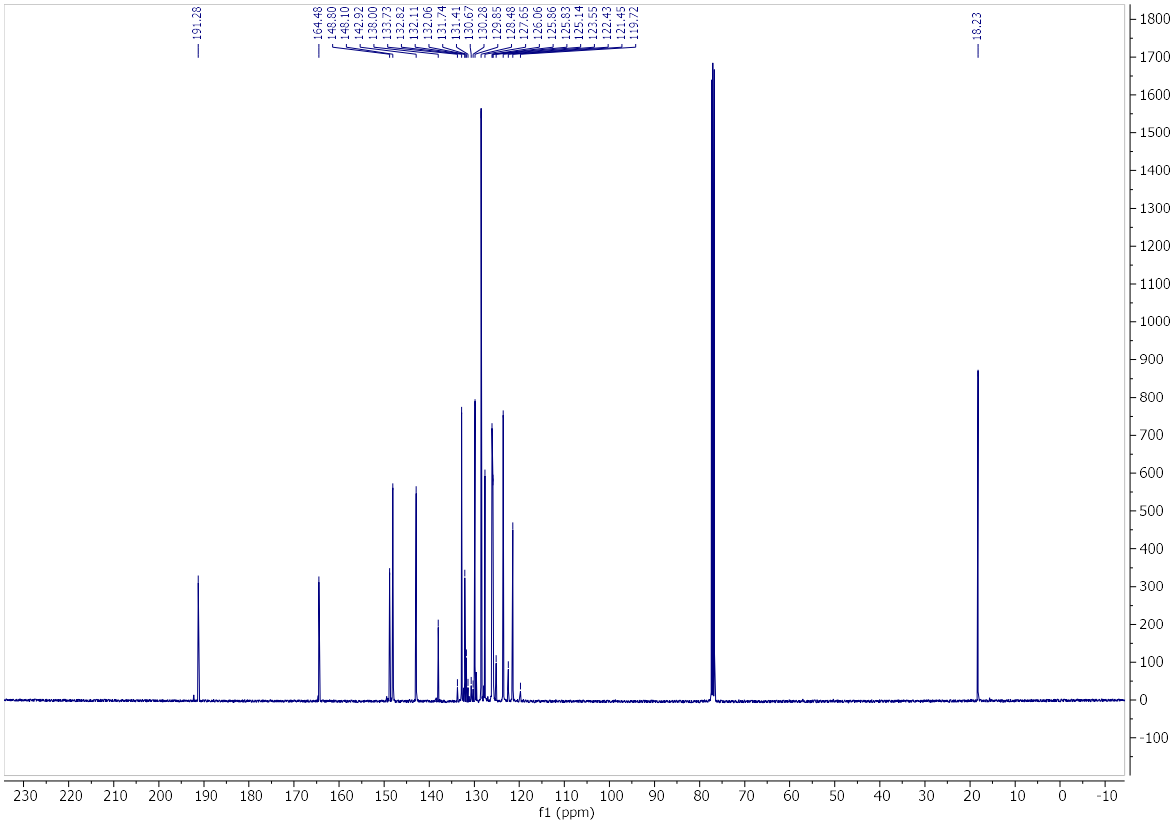
191.28
164.48
148.80
148.10
142.92
138.00
133.73
132.62
132.11
132.06
131.74
131.41
130.67
130.28
129.85
128.48
127.65
126.06
125.86
125.83
125.14
123.55
122.43
121.45
119.72
18.23
f1 (ppm)

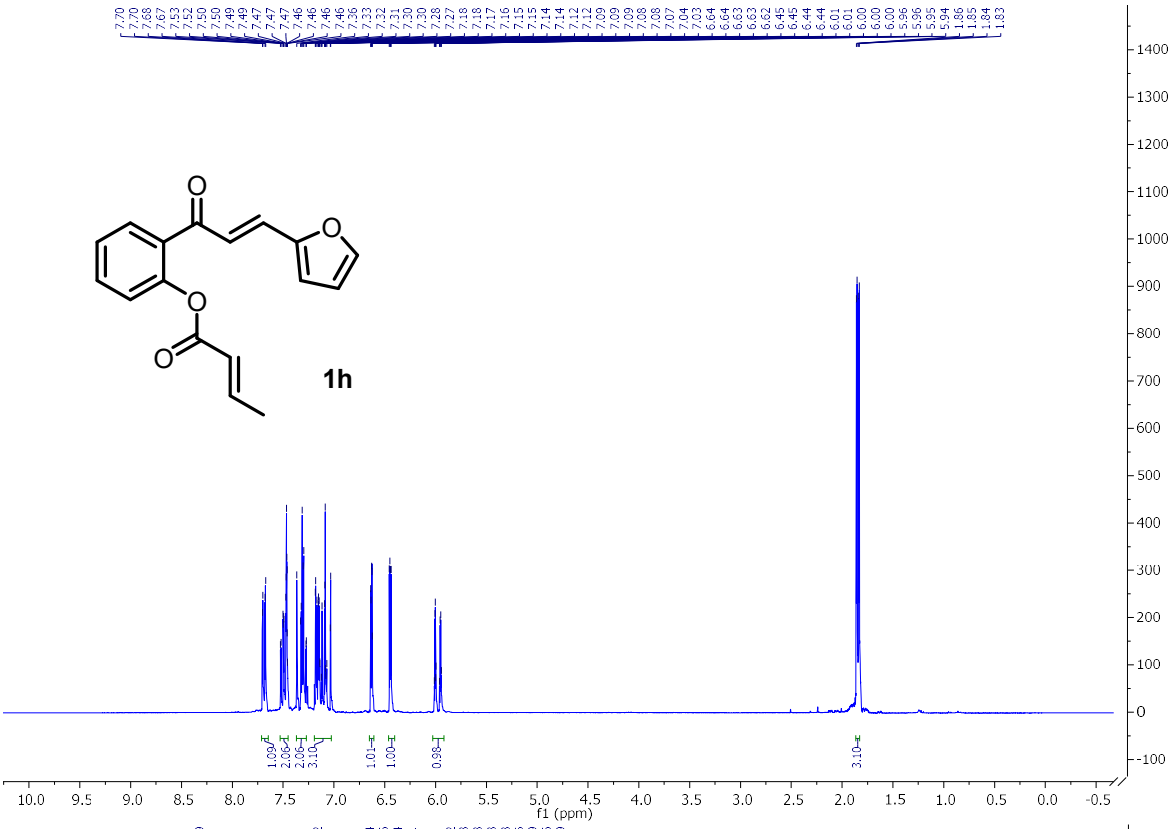
1h
f1 (ppm)

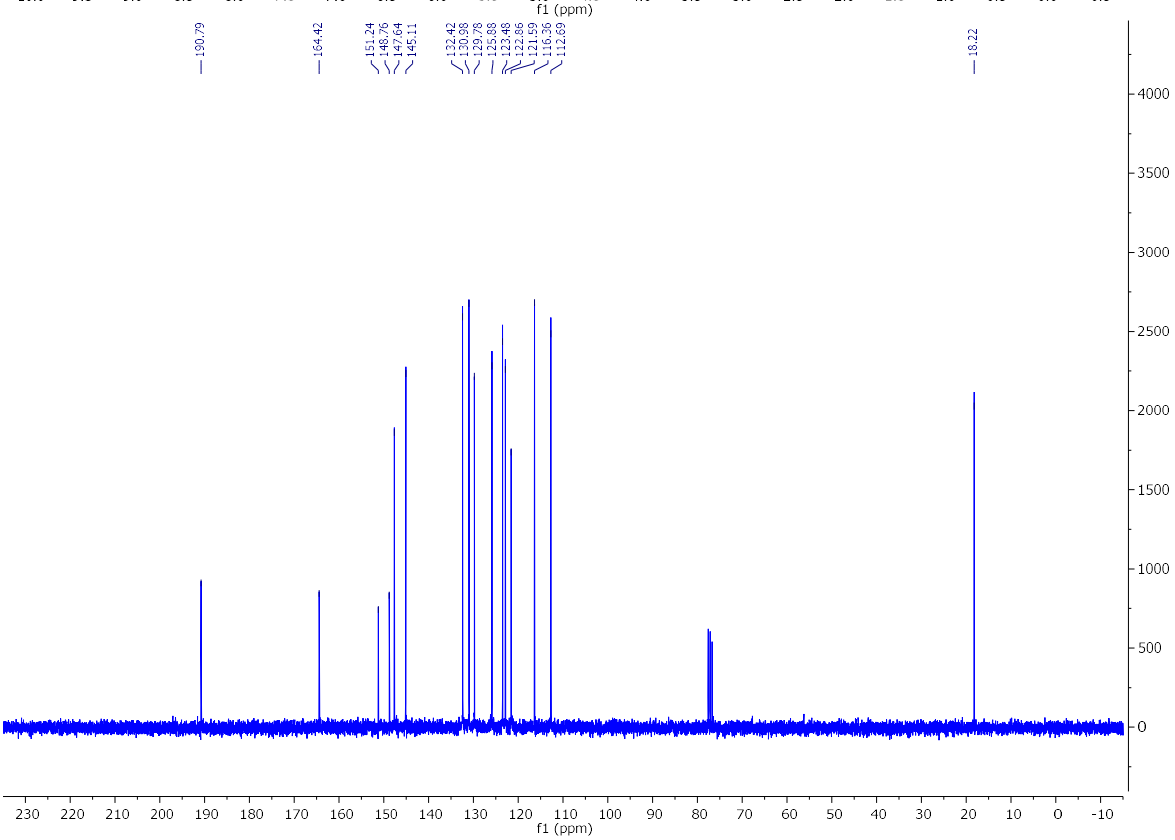
190.79
164.42
151.24
148.76
147.64
145.11
132.42
130.98
129.78
125.88
123.48
122.86
121.59
116.36
112.69
18.22
f1 (ppm)

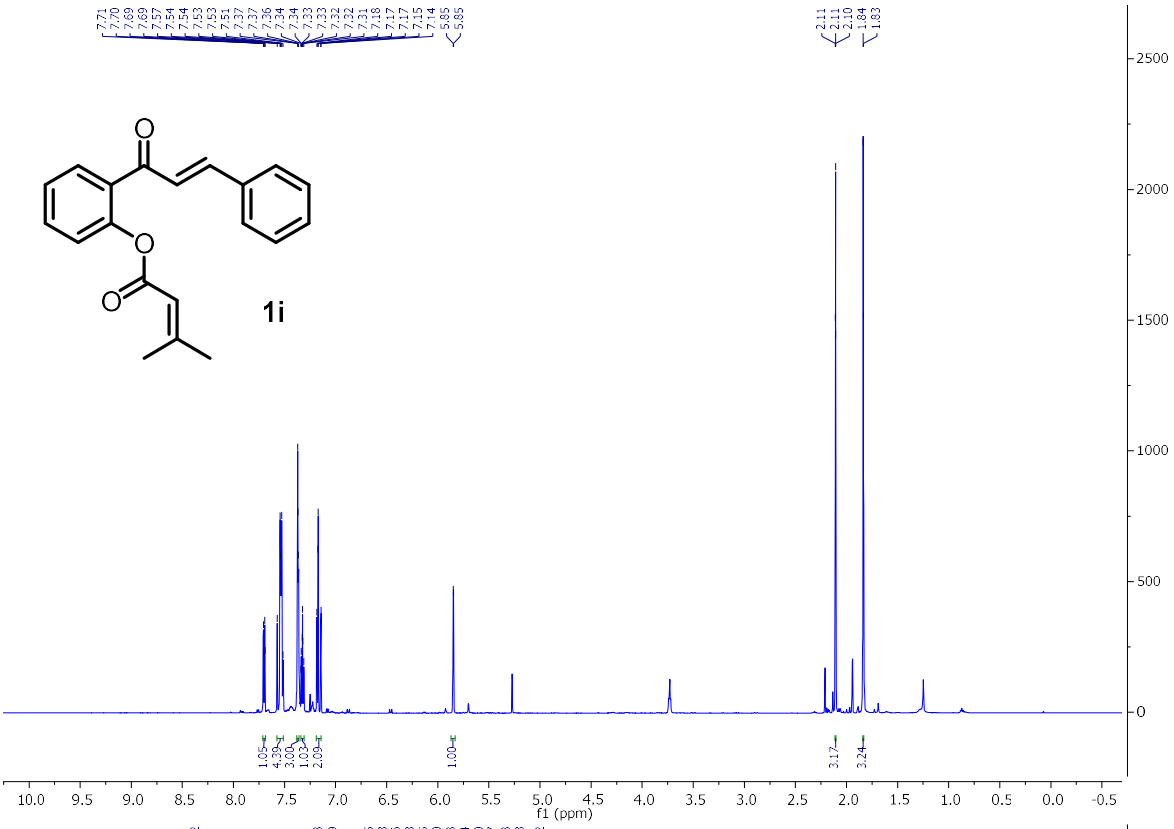
1i
f1 (ppm)

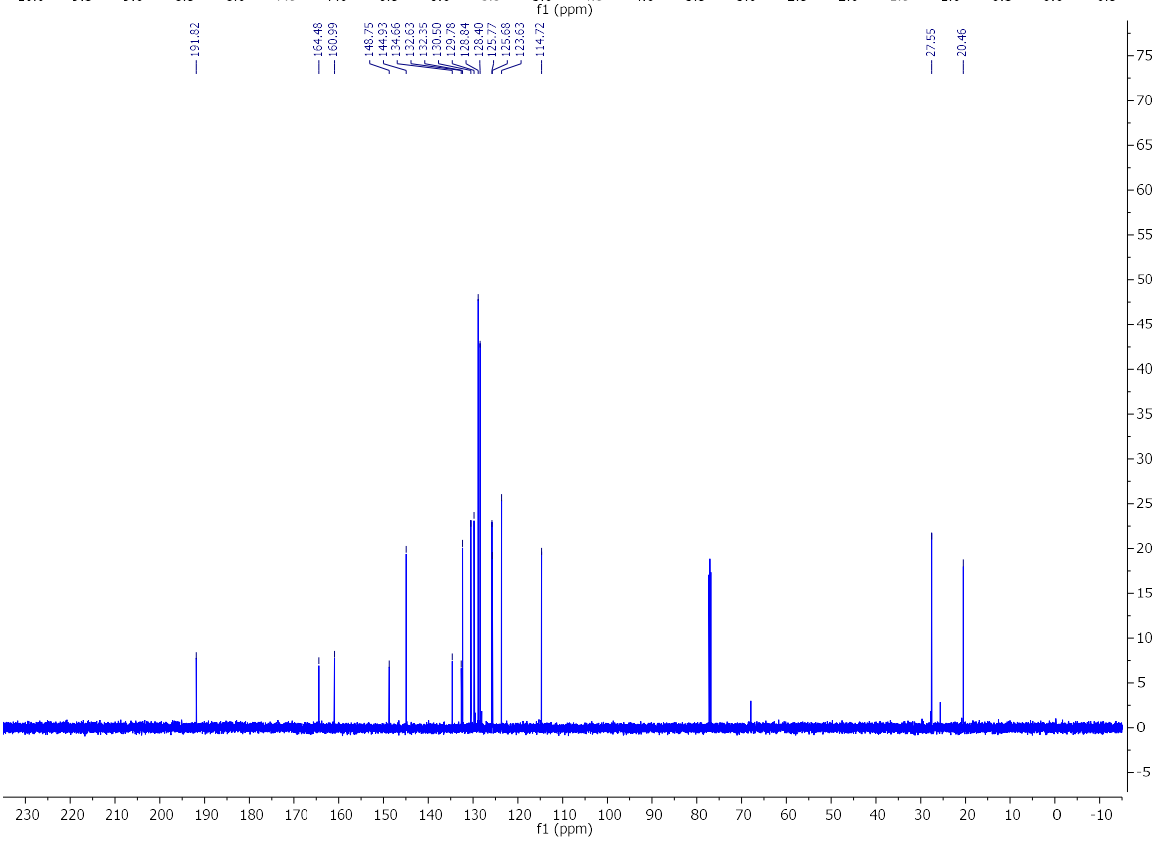
f1 (ppm)

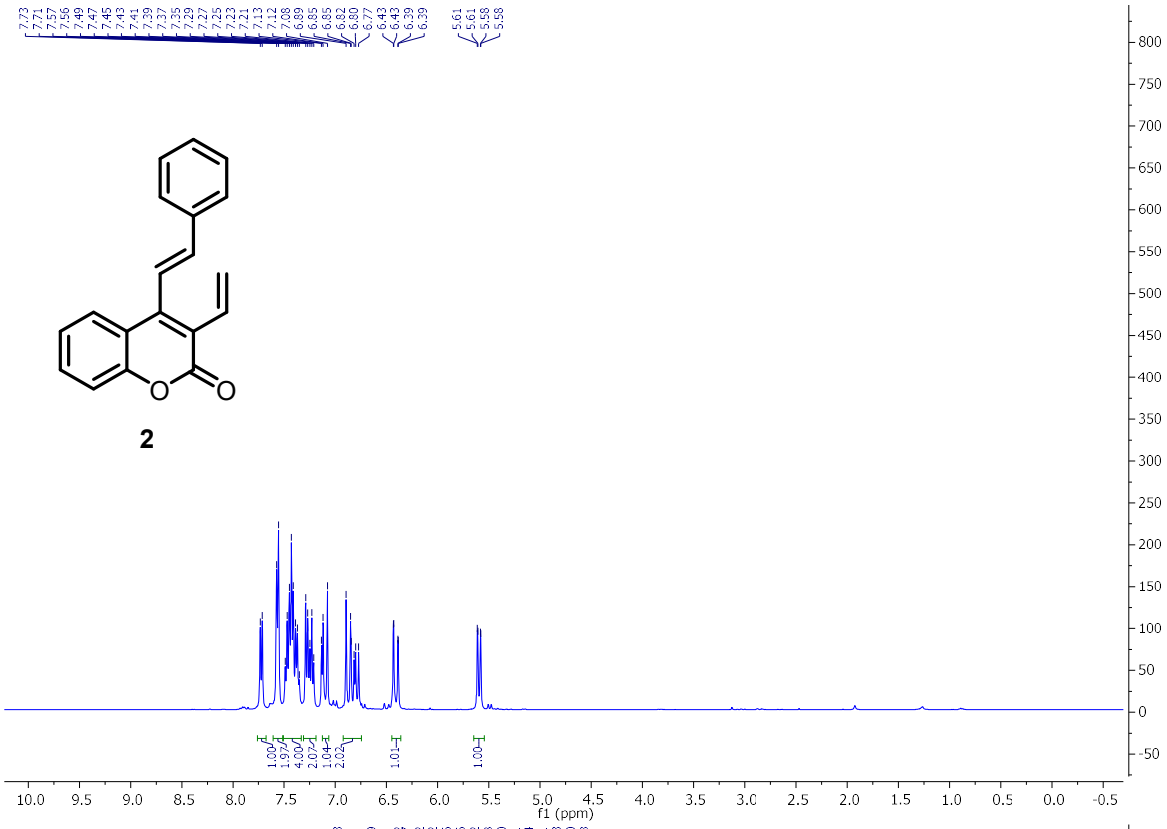
7.73
7.71
7.57
7.56
7.49
7.47
7.45
7.43
7.41
7.39
7.37
7.35
7.29
7.27
7.25
7.23
7.21
7.13
7.12
7.08
6.89
6.85
6.82
6.80
6.77
6.43
6.43
6.39
6.39
5.61
5.61
5.58
5.58
O
O
1.00
1.97
4.00
2.07
1.04
2.02
1.01
1.00
f1 (ppm)

2

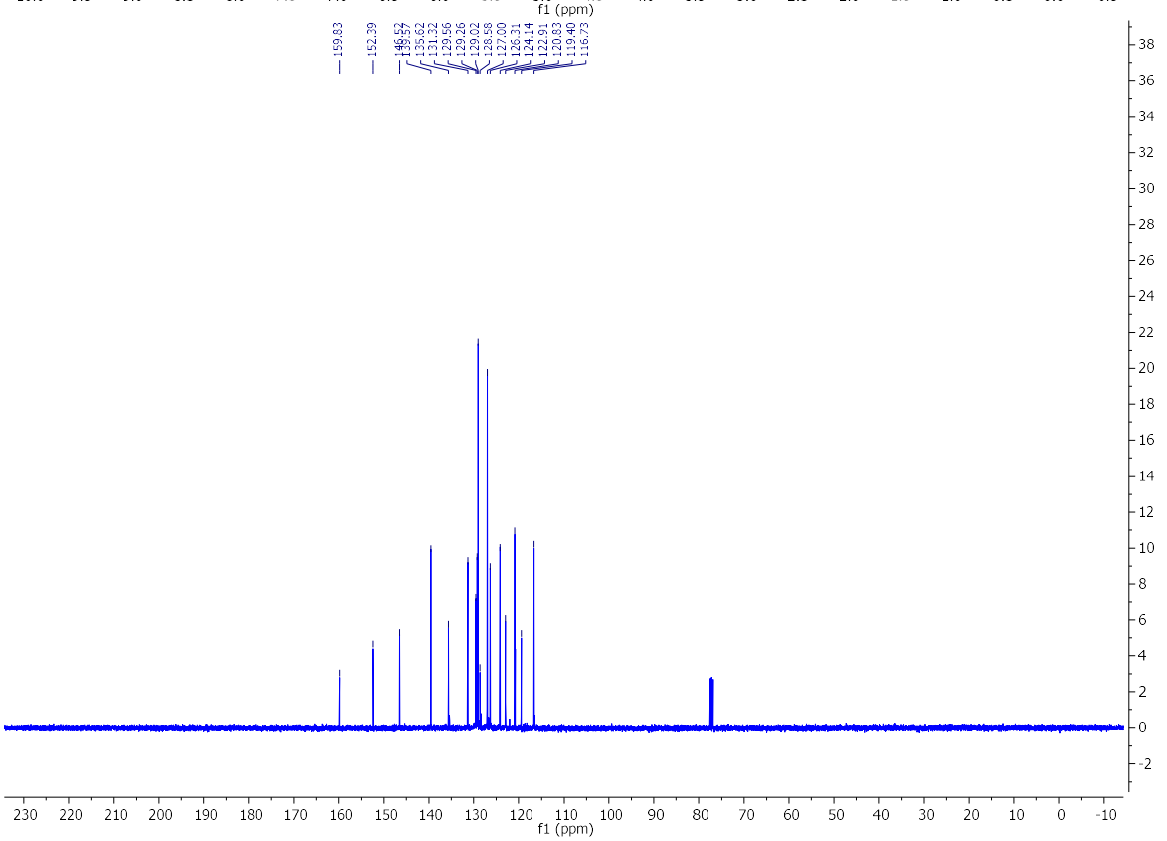
159.83
152.39
146.52
139.57
135.62
131.32
129.56
129.26
129.02
125.58
124.30
124.14
122.91
120.83
119.40
116.73
f1 (ppm)

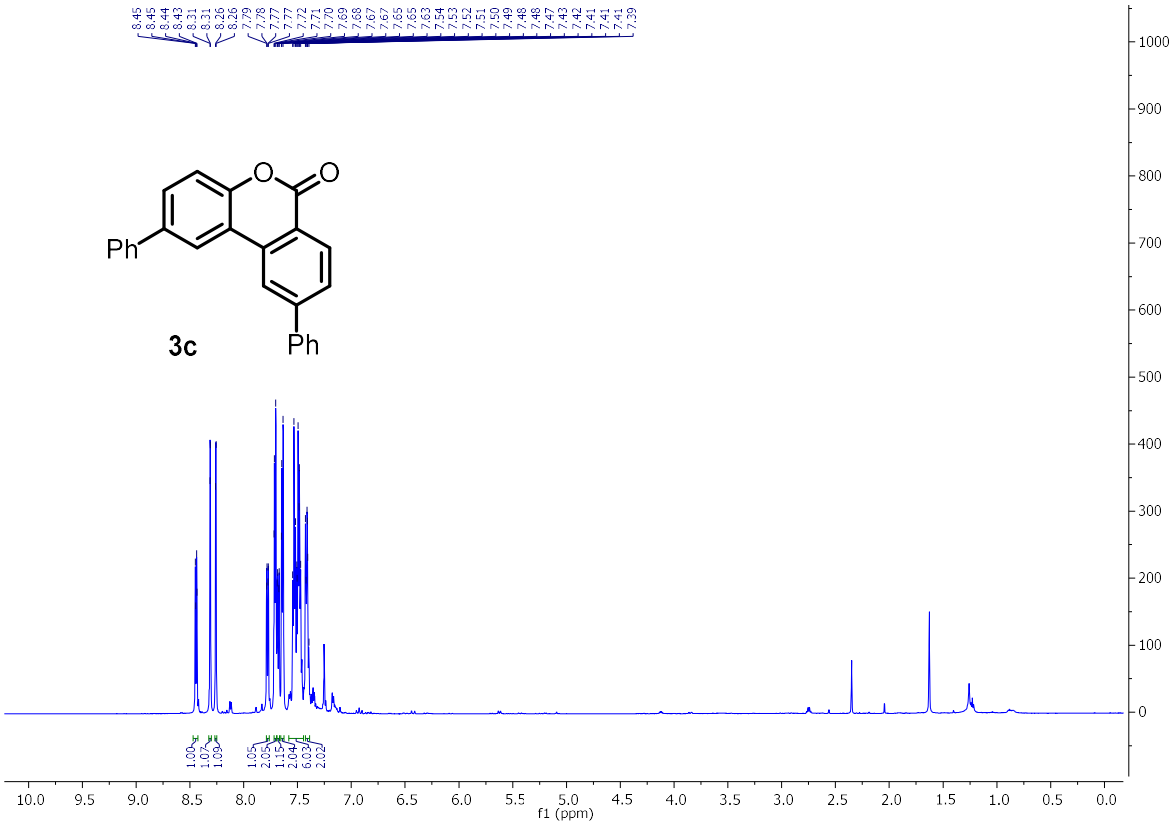
8.45
8.45
8.44
8.43
8.31
8.31
8.26
8.26
7.79
7.78
7.77
7.77
7.72
7.71
7.70
7.69
7.68
7.67
7.67
7.65
7.65
7.63
7.54
7.53
7.52
7.51
7.50
7.49
7.48
7.48
7.47
7.43
7.42
7.41
7.41
7.41
7.39
O
O
Ph
Ph
3c
1.00
1.07
1.09
1.05
2.05
1.15
2.04
6.03
2.02
f1 (ppm)

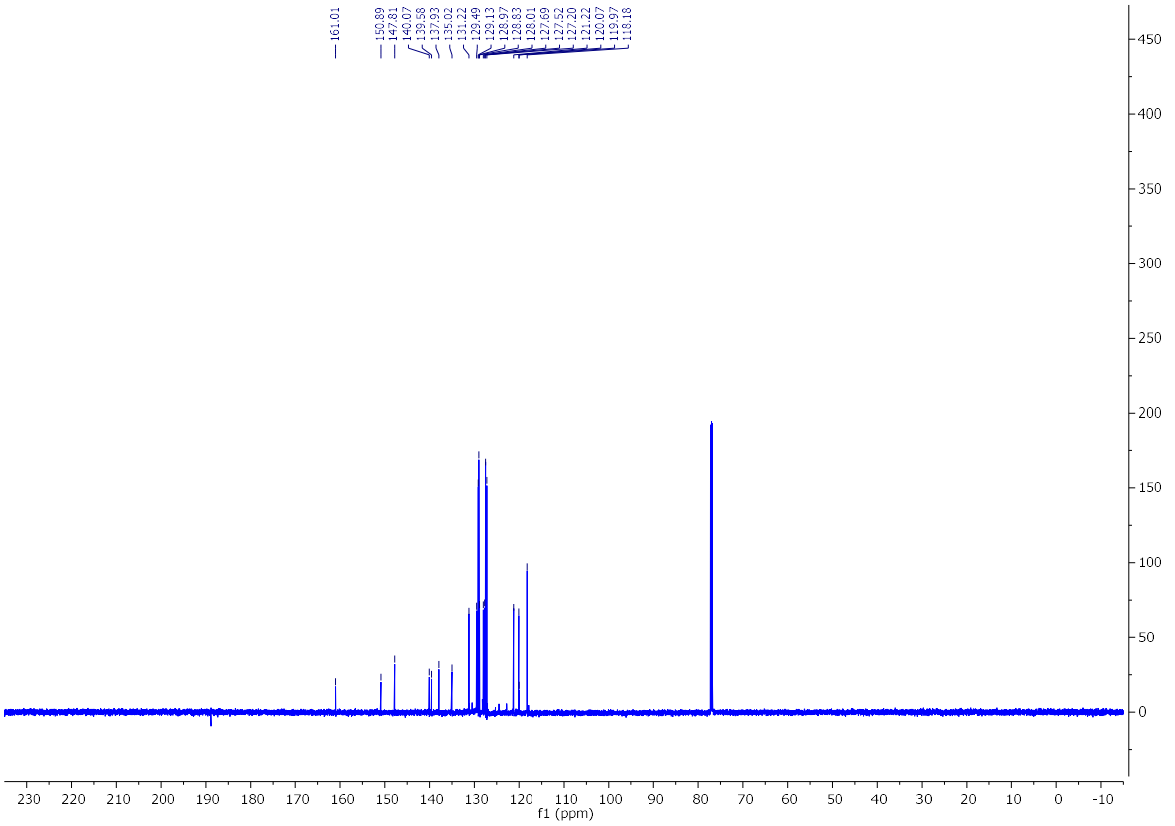
161.01
150.89
147.81
140.07
139.58
137.93
135.02
131.22
129.49
129.13
128.97
128.83
128.01
127.69
127.52
127.20
121.22
120.07
119.97
118.18
f1 (ppm)

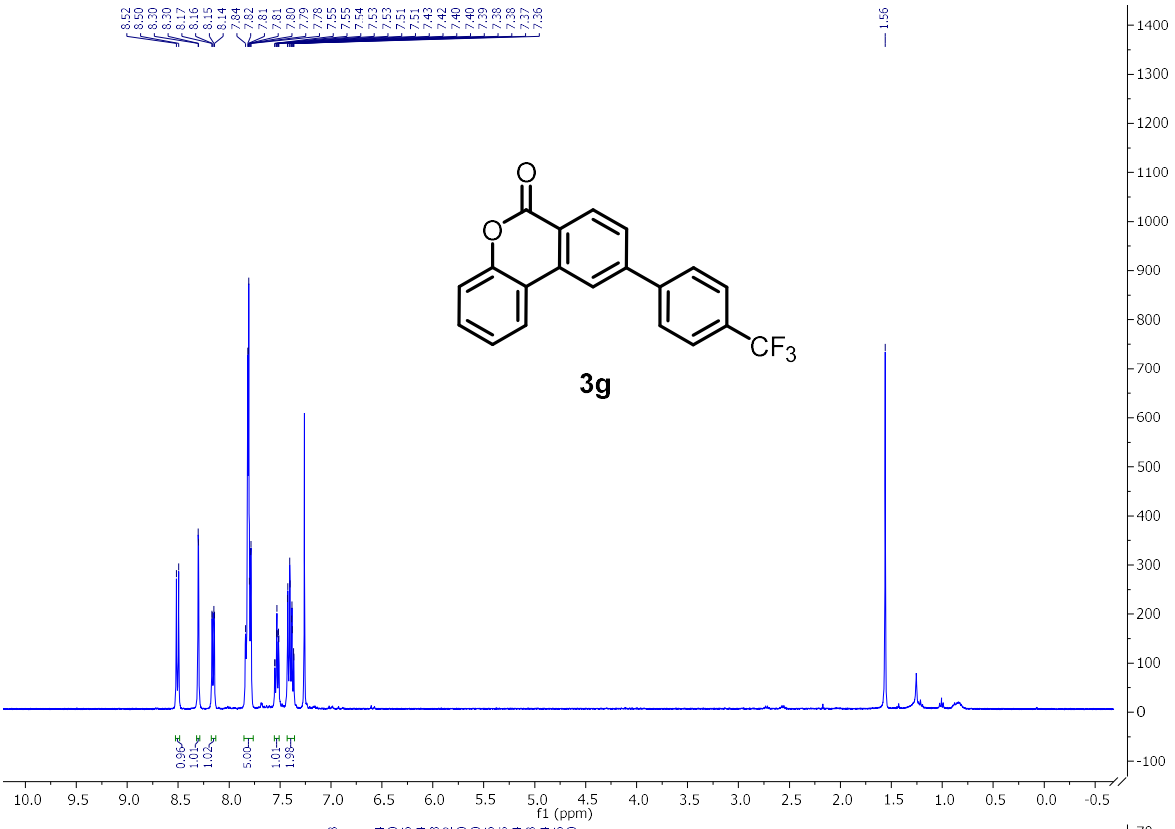
8.52
8.50
8.30
8.30
8.17
8.16
8.15
8.14
7.84
7.82
7.81
7.81
7.80
7.79
7.78
7.55
7.55
7.54
7.53
7.53
7.51
7.51
7.43
7.42
7.40
7.40
7.39
7.38
7.38
7.37
7.36
1.56
O
O
CF3
3g
0.96
1.01
1.02
5.00
1.01
1.98
f1 (ppm)

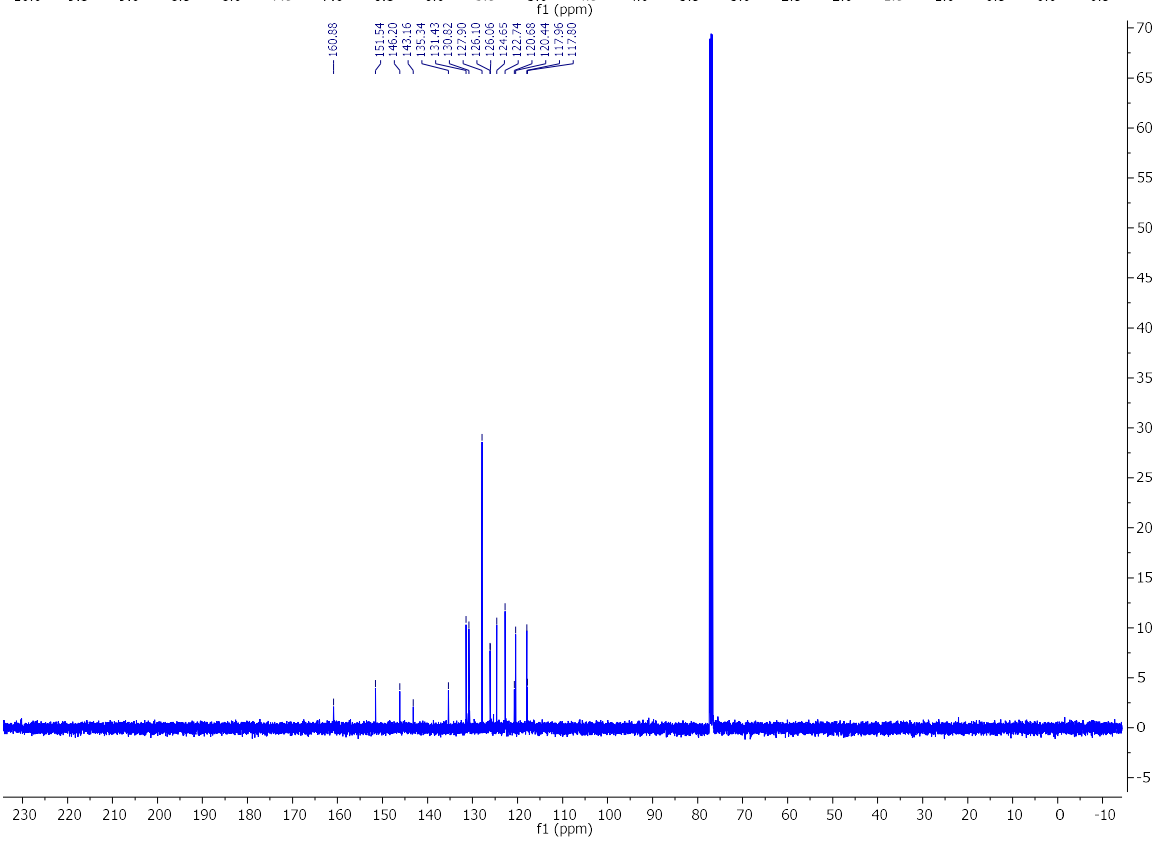
160.88
151.54
146.20
143.16
135.34
131.43
130.82
127.90
126.10
126.06
124.65
122.74
120.68
120.44
117.96
117.80
f1 (ppm)

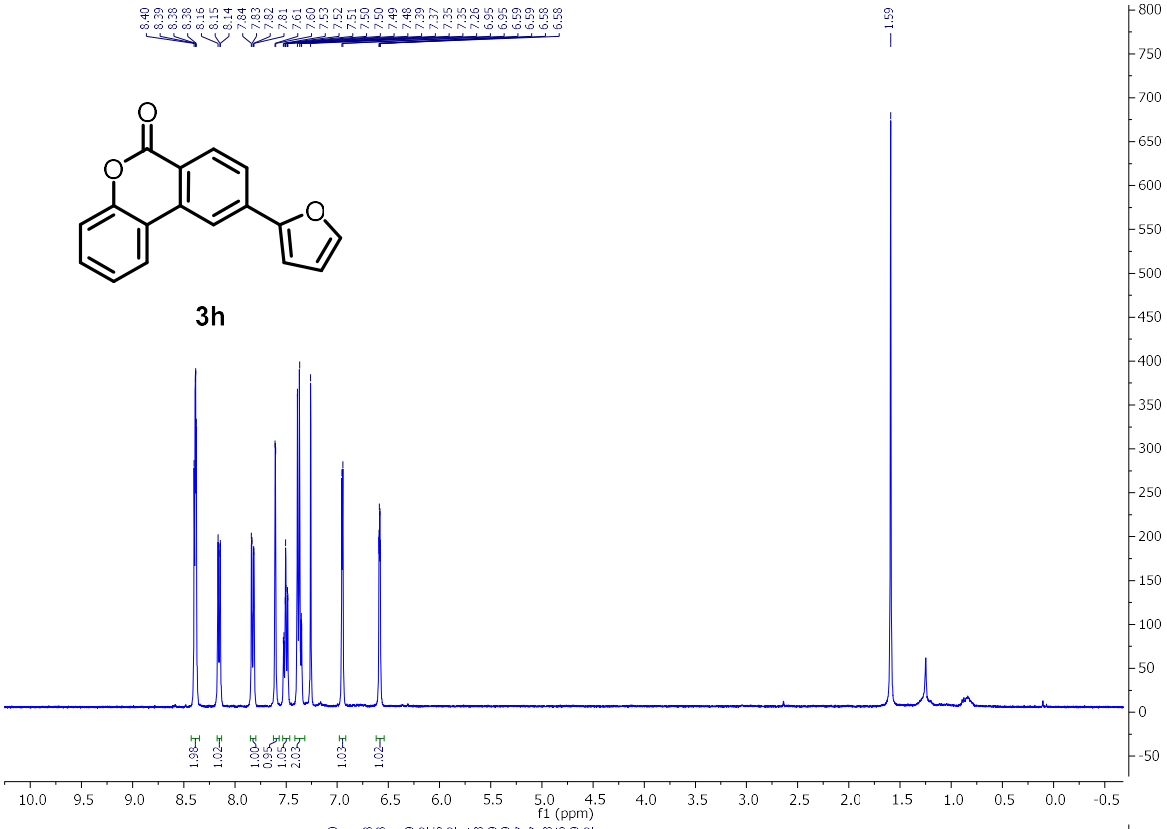
8.40
8.39
8.38
8.38
8.16
8.15
8.14
7.84
7.83
7.82
7.81
7.61
7.60
7.53
7.52
7.51
7.50
7.50
7.49
7.48
7.39
7.37
7.35
7.35
7.26
6.65
6.59
6.59
6.58
6.58
1.59
3h
1.98
1.02
1.00
0.96
1.05
2.03
1.03
1.02
f1 (ppm)

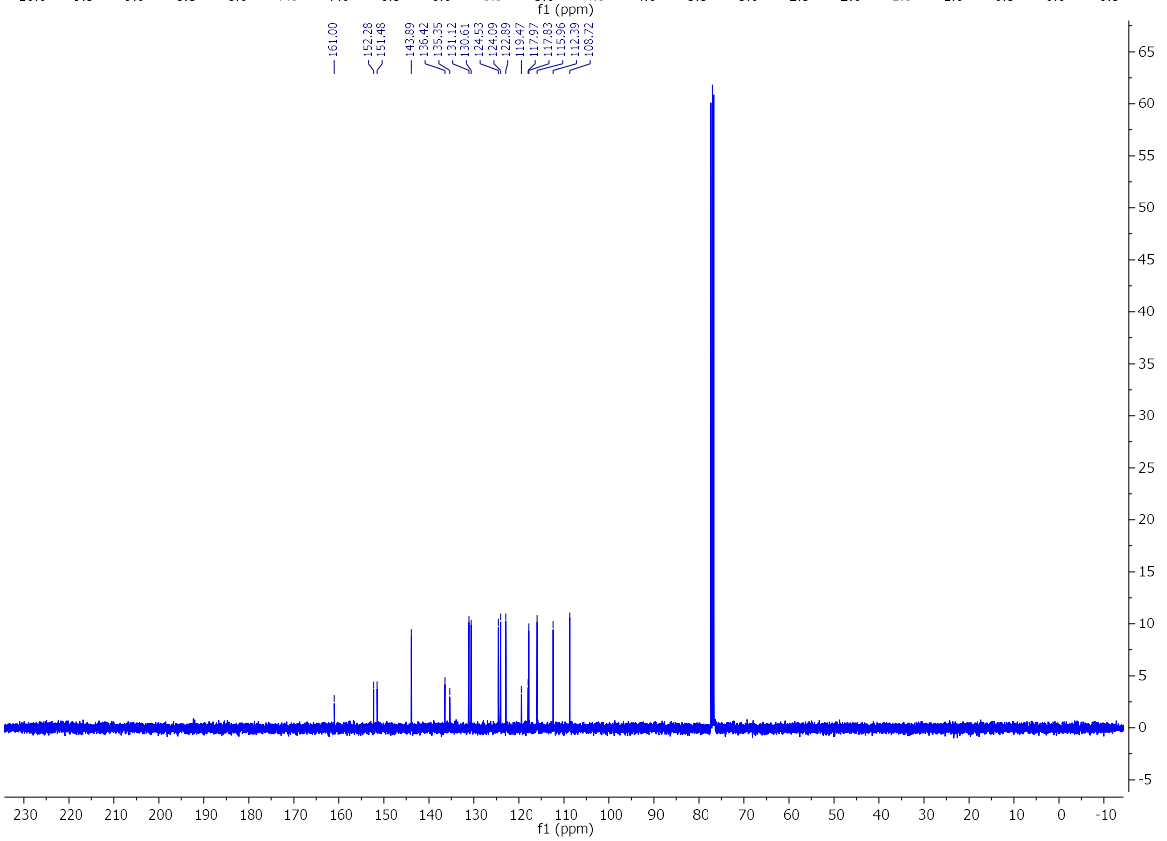
161.00
152.28
151.48
143.89
136.42
135.35
131.12
130.61
124.53
124.09
122.89
119.47
117.97
117.83
115.96
112.39
108.72
f1 (ppm)

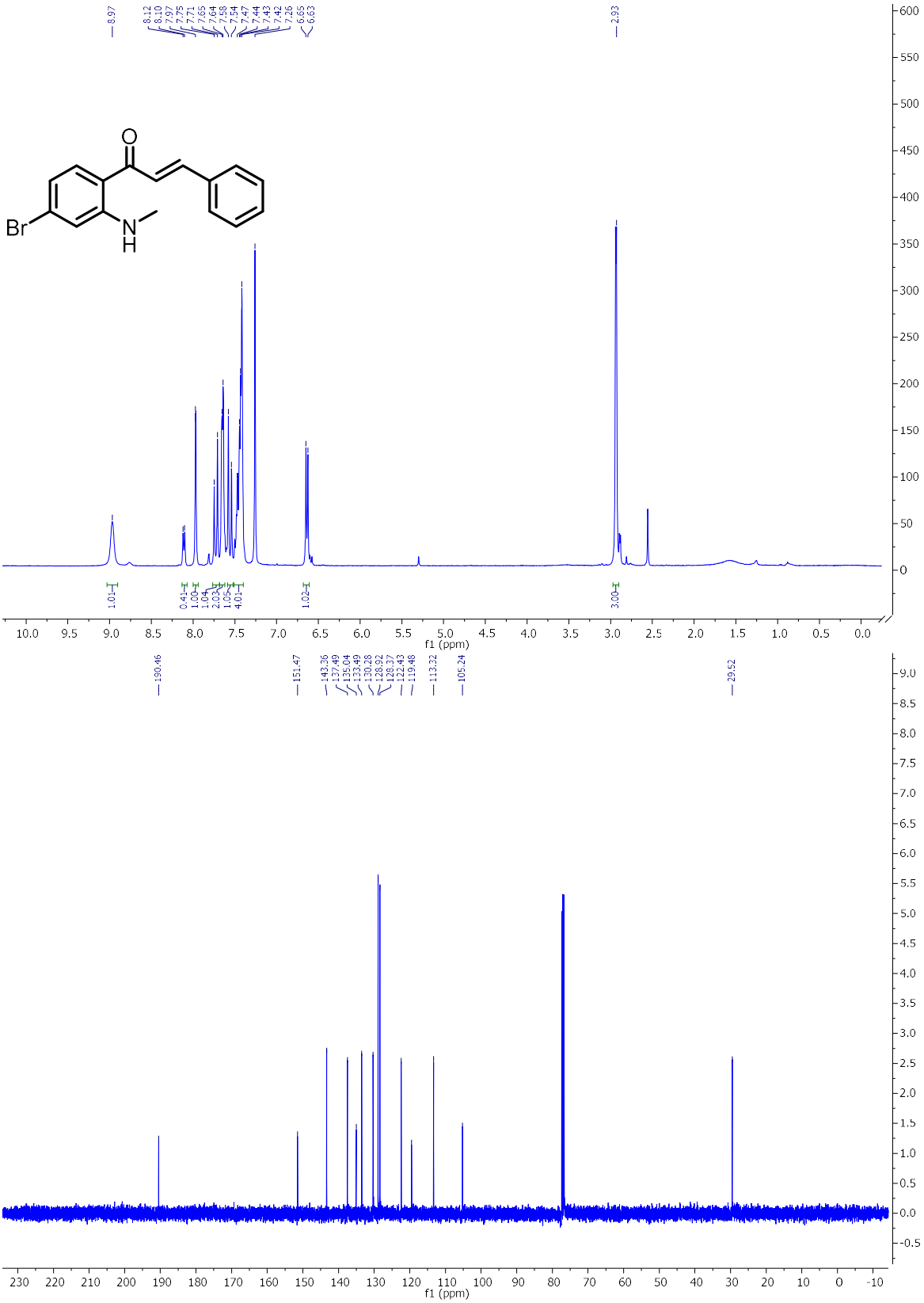
8.97
8.12
8.10
7.97
7.75
7.71
7.65
7.64
7.58
7.54
7.47
7.44
7.43
7.42
7.26
6.65
6.63
2.93
O
Br
N
H
1.01
0.41
1.00
1.04
2.05
1.85
4.01
1.02
3.00
f1 (ppm)
190.46
151.47
143.36
137.49
135.04
133.49
130.28
128.92
128.37
122.43
119.48
113.32
105.24
29.52
f1 (ppm)

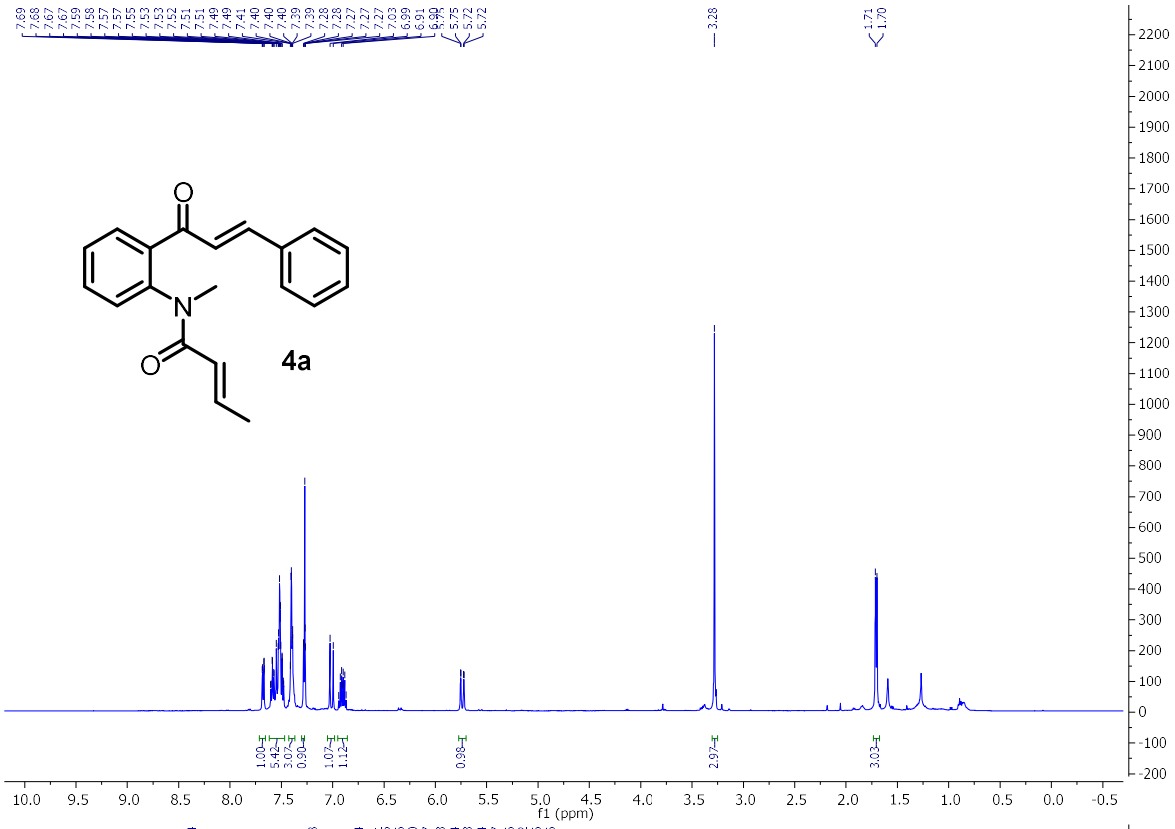
4a
f1 (ppm)

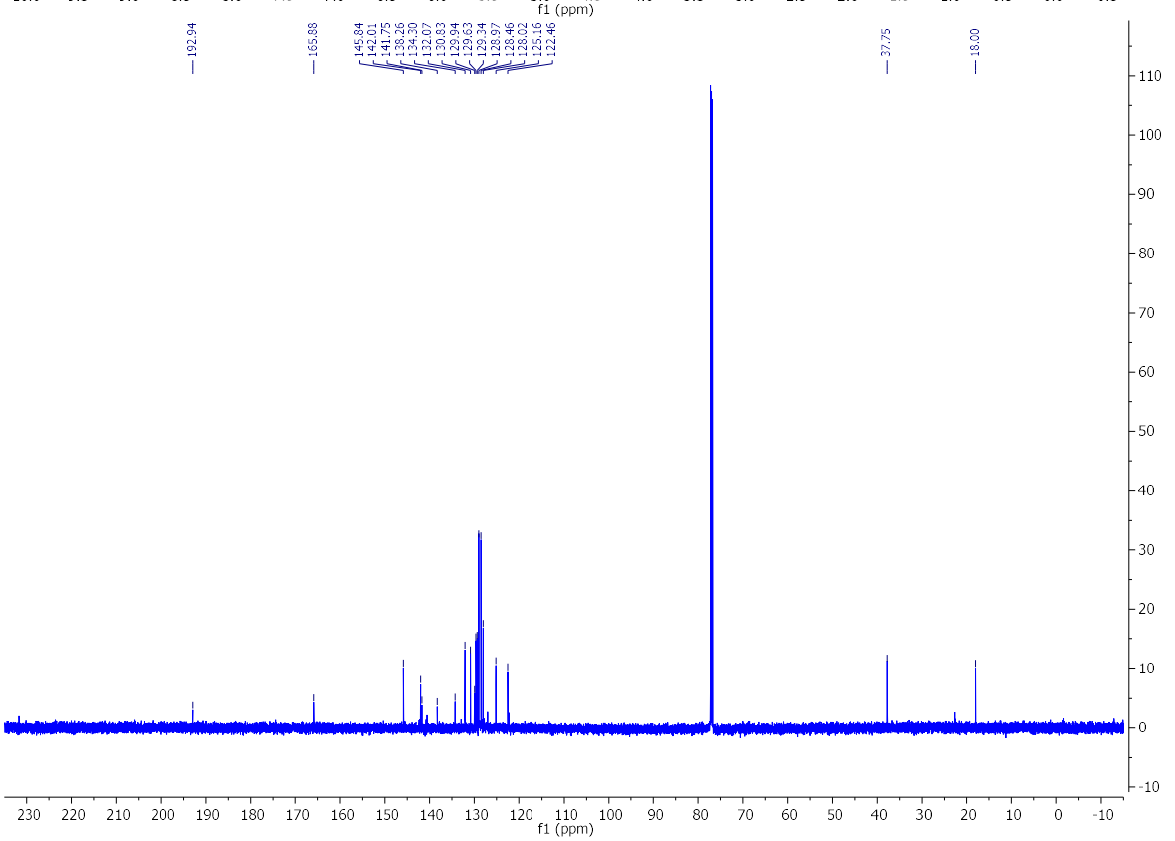
f1 (ppm)

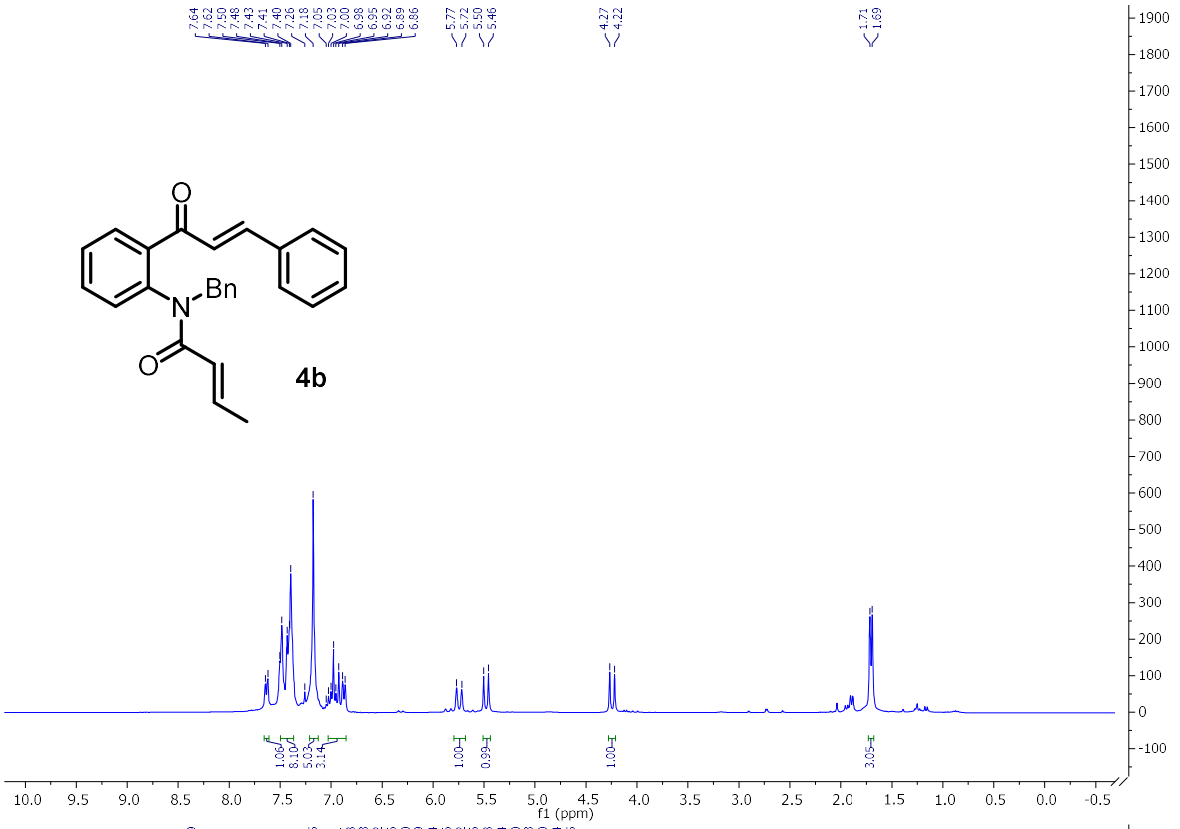
7.64
7.62
7.50
7.48
7.43
7.41
7.40
7.26
7.18
7.05
7.03
7.00
6.98
6.95
6.92
6.89
6.86
5.77
5.72
5.50
5.46
4.27
4.22
1.71
1.69
O
N
Bn
O
4b
1.08
8.10
5.03
3.14
1.00
0.99
1.00
3.05
f1 (ppm)

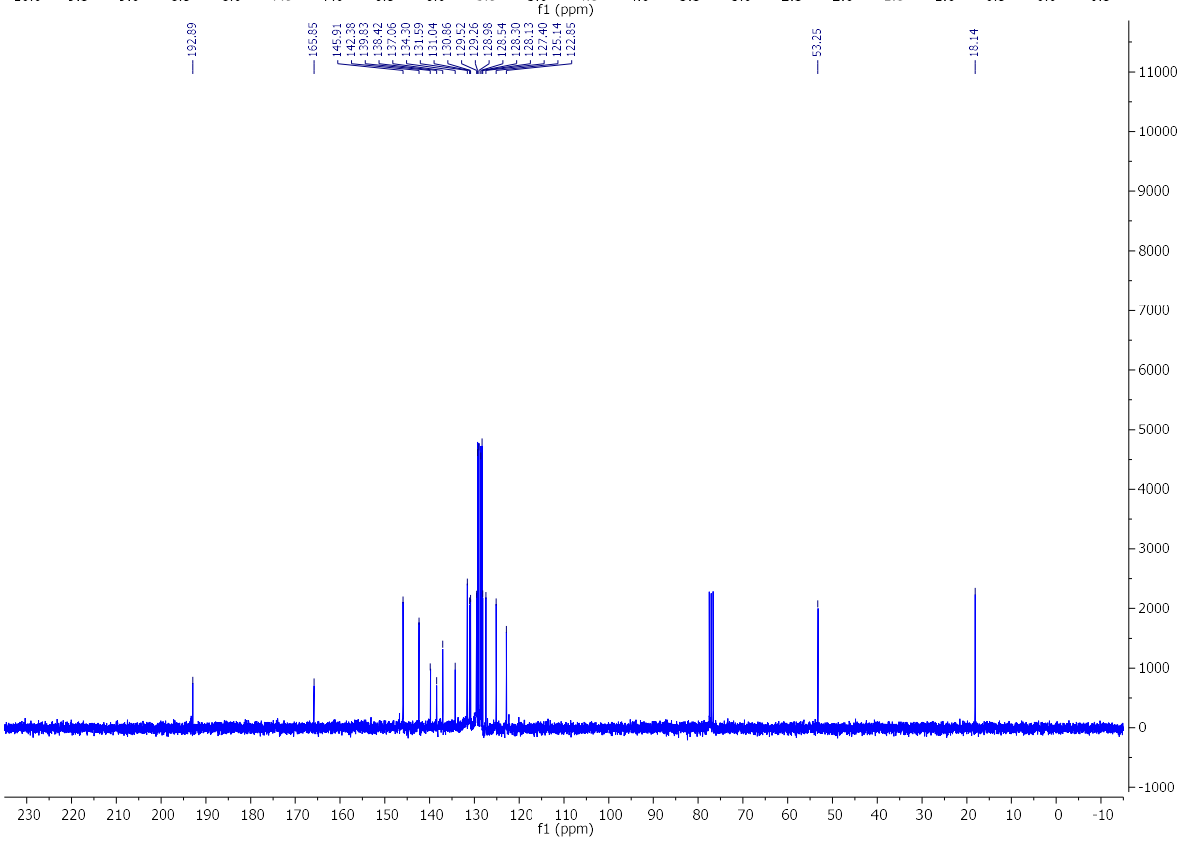
192.89
165.85
145.91
142.38
139.83
138.42
137.06
134.30
131.59
131.04
130.86
129.52
129.26
128.98
128.34
128.13
127.40
126.14
122.85
53.25
18.14
f1 (ppm)

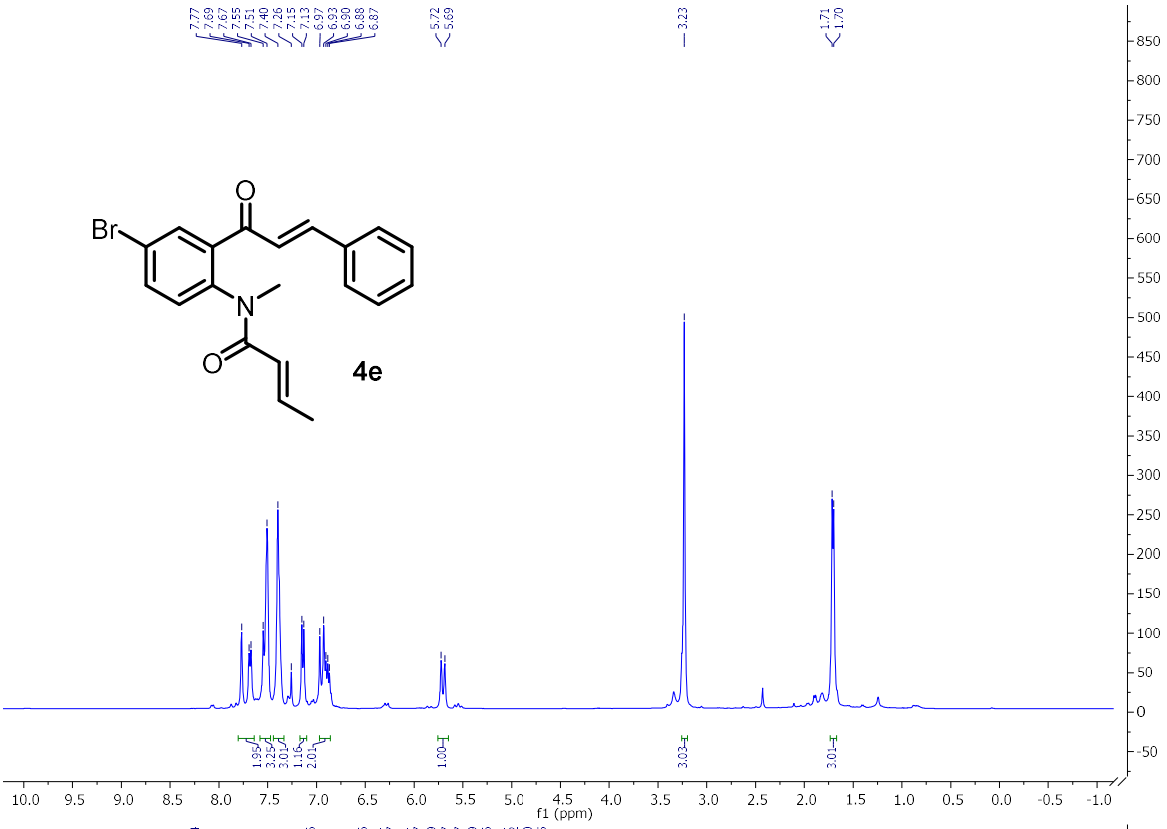
7.77
7.69
7.67
7.55
7.51
7.40
7.26
7.15
7.13
6.97
6.93
6.90
6.88
6.87
5.72
5.69
3.23
1.71
1.70
Br
O
N
O
4e
1.92
3.25
3.01
1.16
2.01
1.00
3.03
3.01
f1 (ppm)

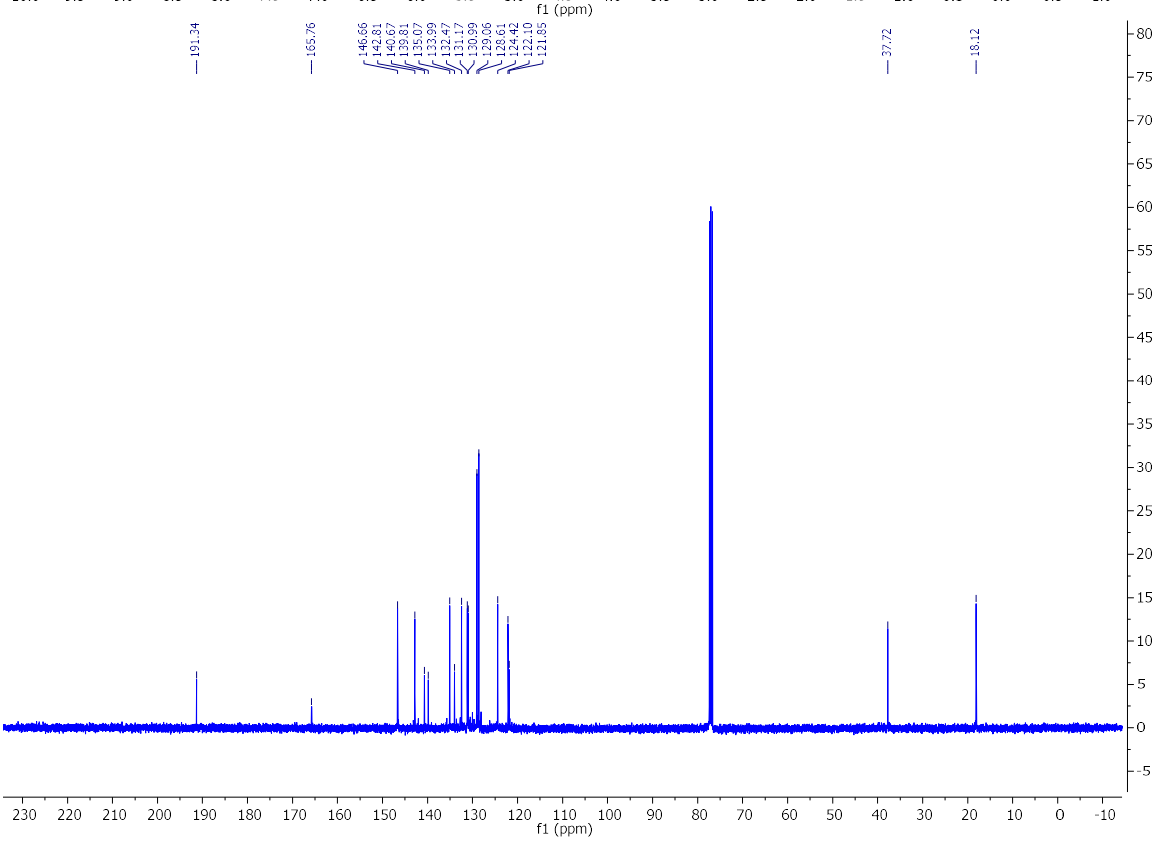
191.34
165.76
146.66
142.81
140.67
139.81
135.07
133.99
132.47
131.17
130.99
129.06
128.61
124.42
122.10
121.85
37.72
18.12
f1 (ppm)

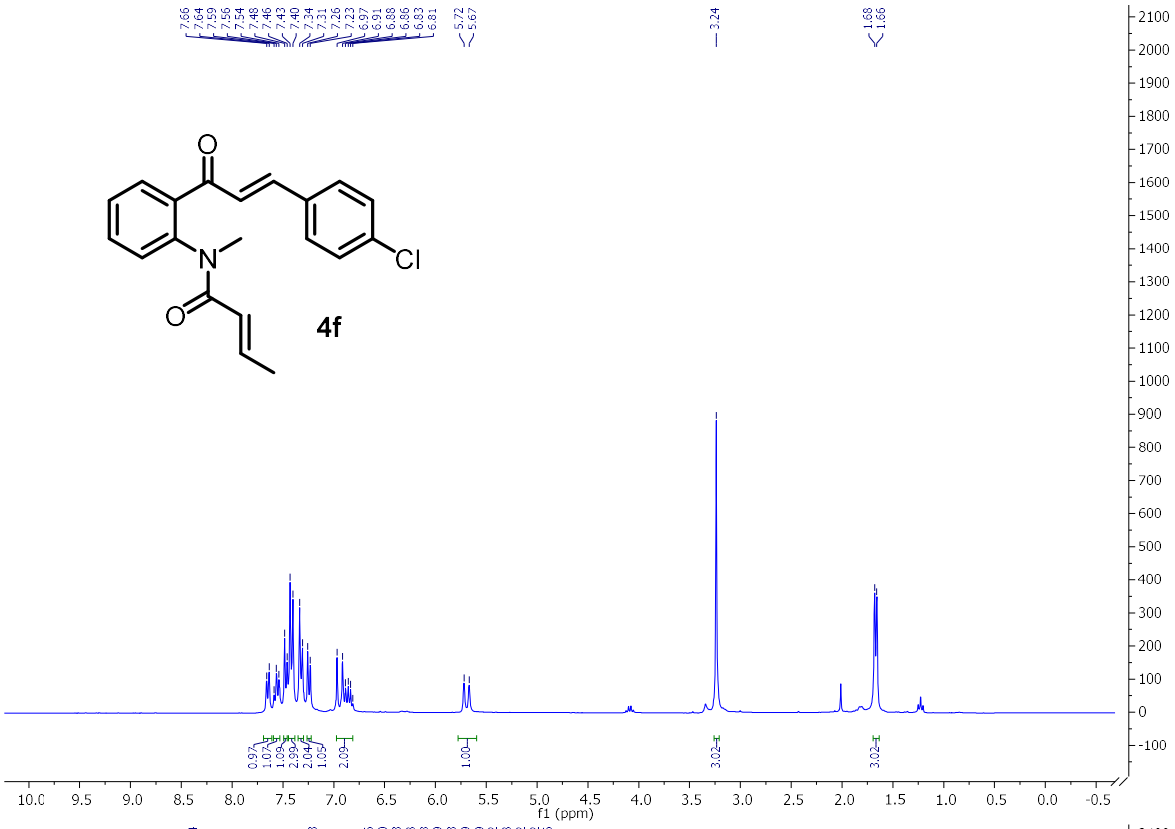
7.66
7.64
7.59
7.56
7.54
7.48
7.46
7.43
7.40
7.34
7.31
7.26
7.23
6.97
6.91
6.88
6.86
6.83
6.81
5.72
5.67
3.24
1.68
1.66
O
N
Cl
O
4f
0.97
1.07
1.05
2.99
2.04
1.09
2.09
1.00
3.02
3.02
f1 (ppm)

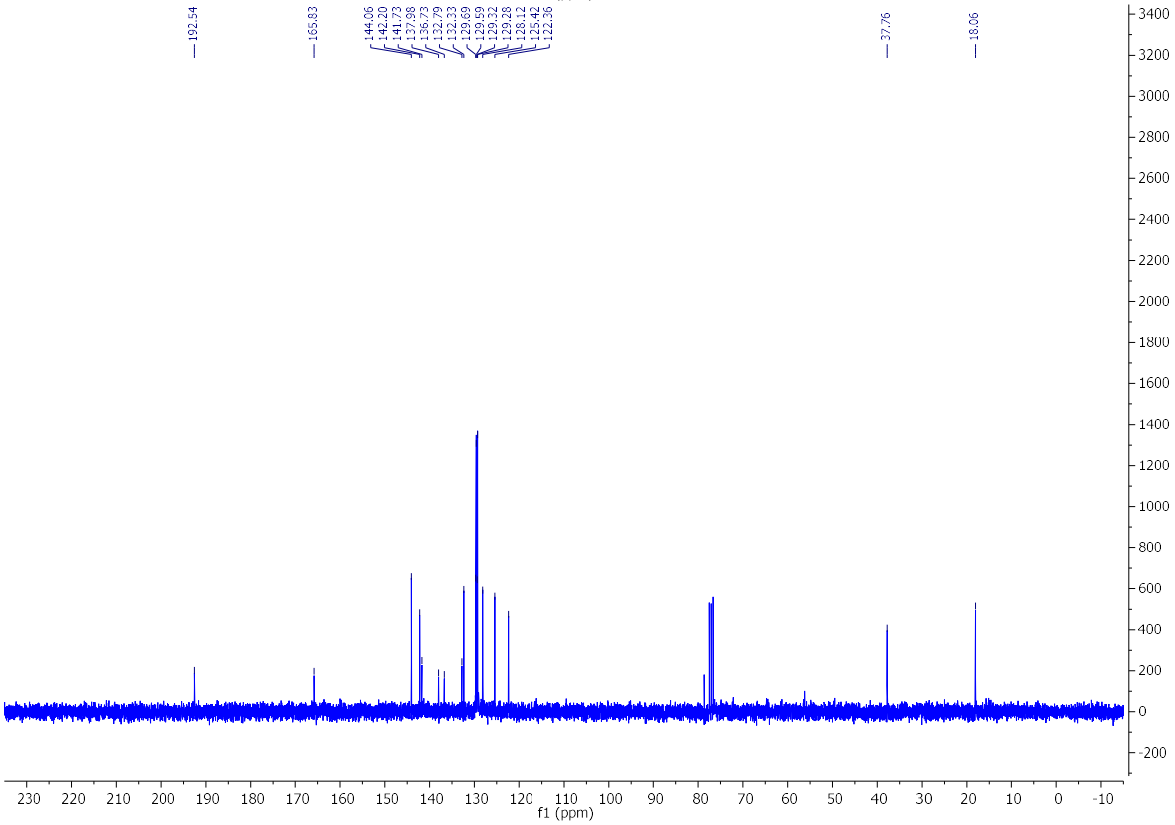
192.54
165.83
144.06
142.20
141.73
137.98
136.73
132.79
132.33
129.69
129.59
129.32
129.28
128.12
125.42
122.36
37.76
18.06
f1 (ppm)

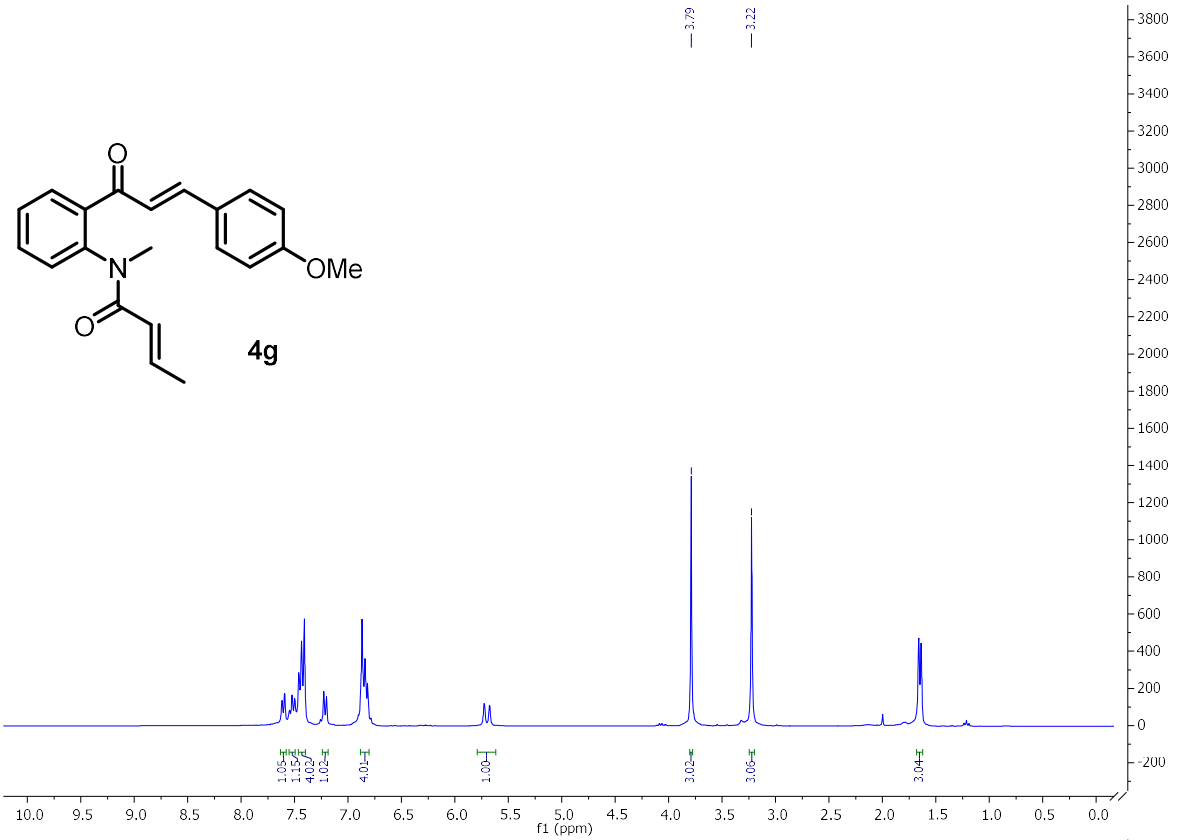
3.79
3.22
1.05
1.15
4.02
1.02
4.01
1.00
3.02
3.06
3.04
f1 (ppm)

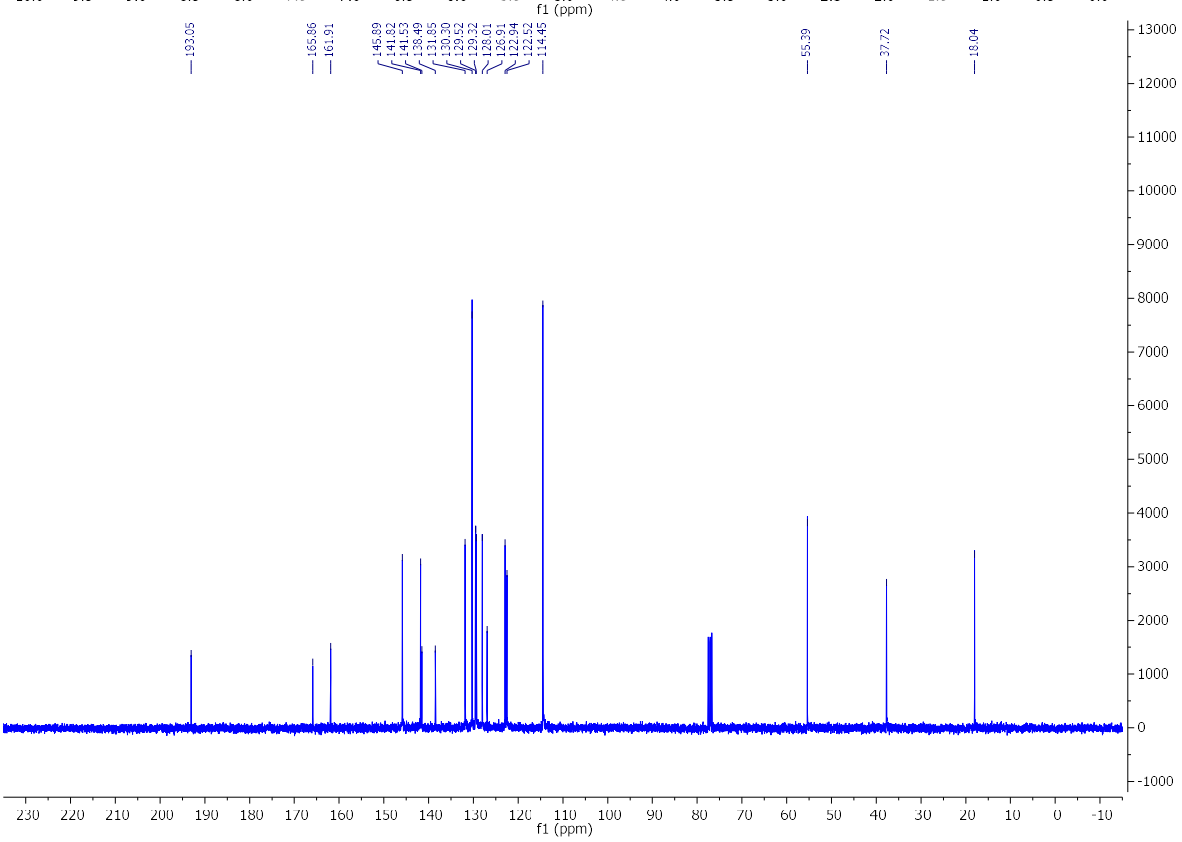
193.05
165.86
161.91
145.89
141.82
141.53
138.49
131.85
130.30
129.52
128.22
128.01
126.91
122.94
122.52
114.45
55.39
37.72
18.04
f1 (ppm)

4g

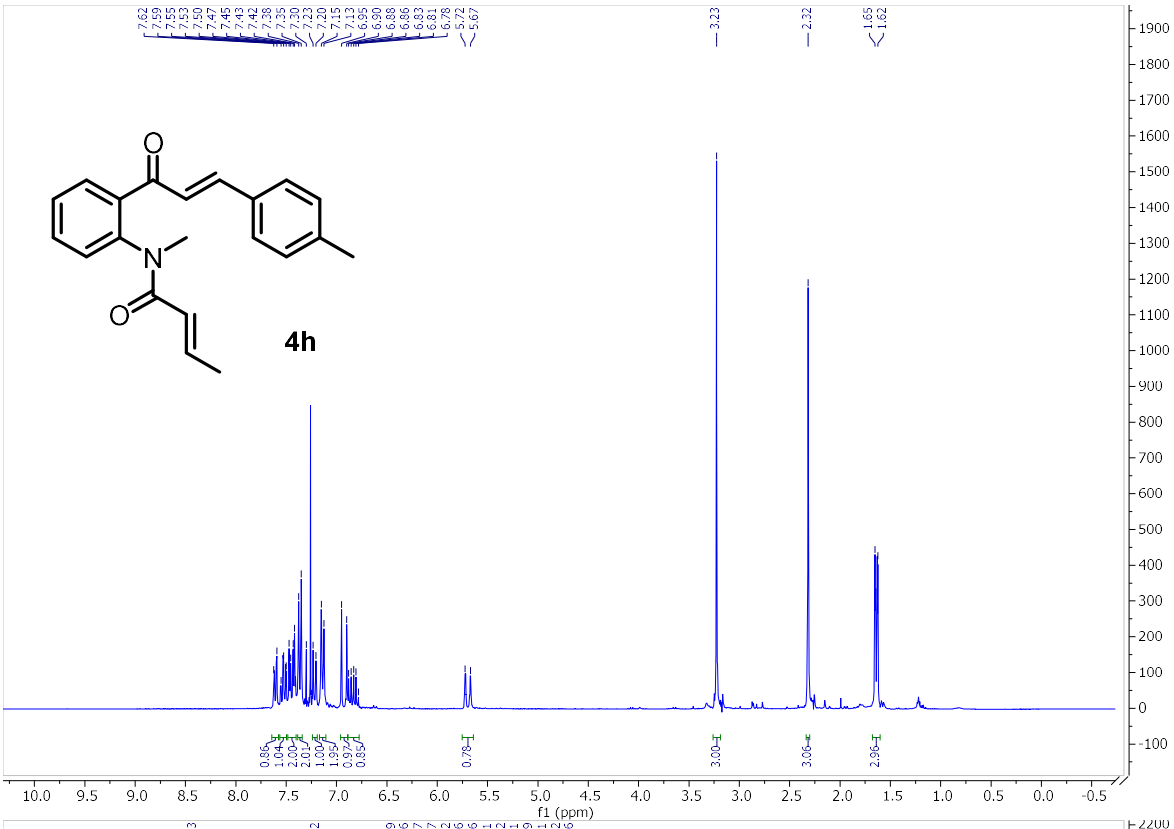
4h
f1 (ppm)

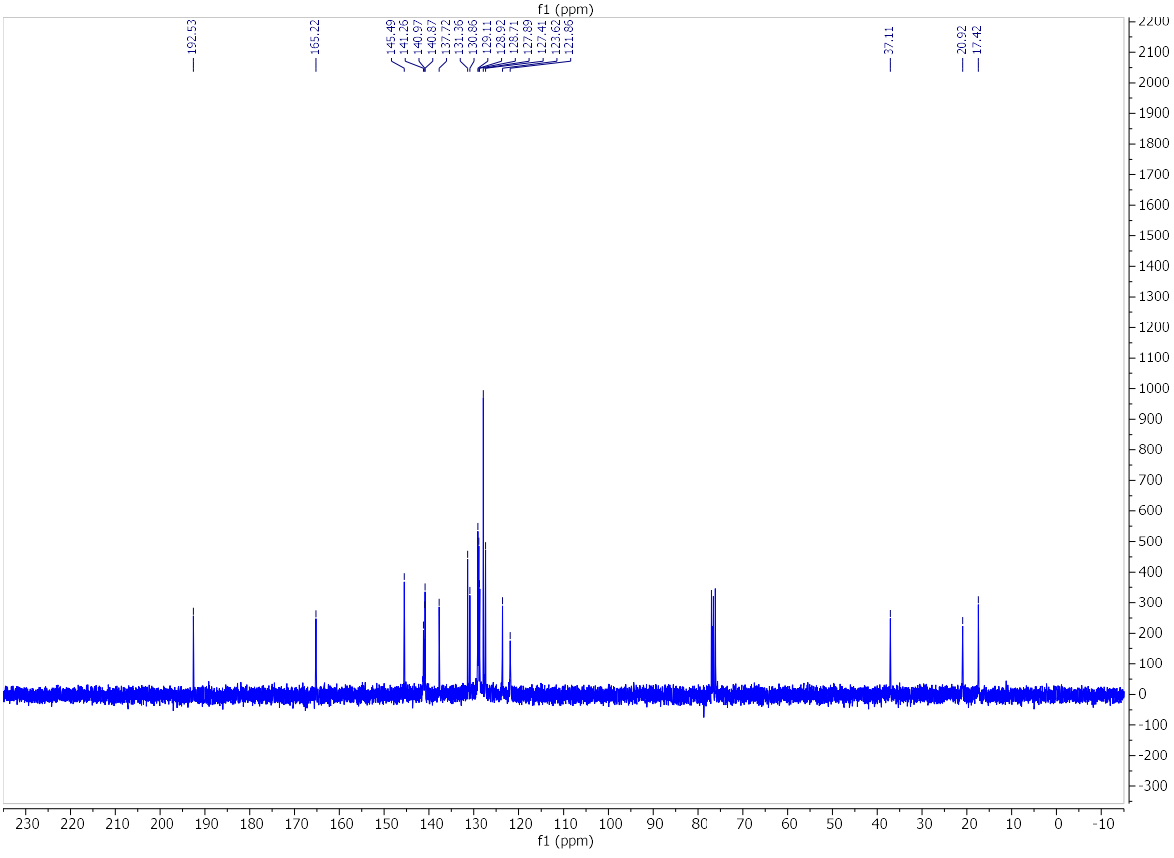
f1 (ppm)

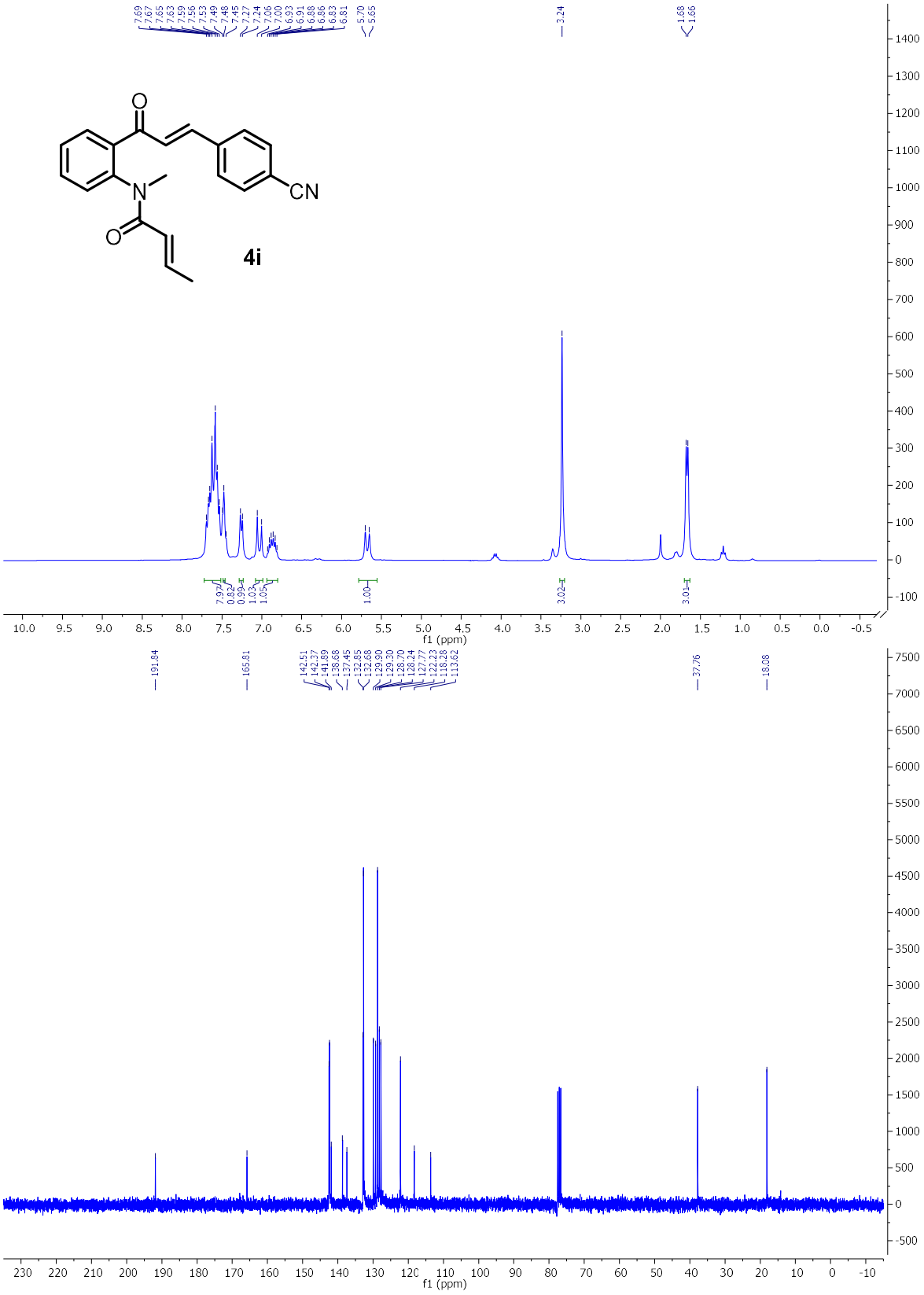
4i
CN
f1 (ppm)
f1 (ppm)

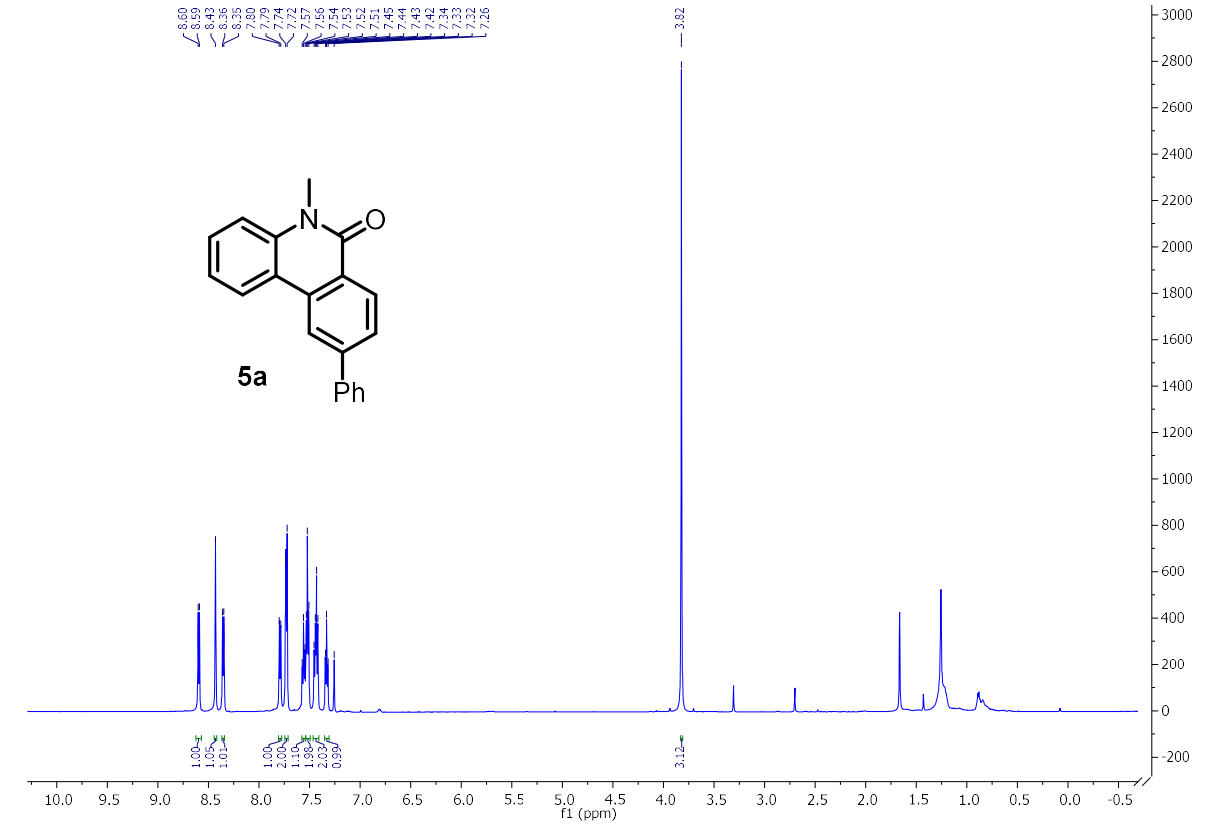
8.60
8.59
8.43
8.36
8.35
7.80
7.79
7.74
7.72
7.57
7.56
7.54
7.53
7.52
7.51
7.45
7.44
7.43
7.42
7.34
7.33
7.32
7.26
3.82
N
O
5a
Ph
1.00
1.05
1.01
1.00
2.00
1.10
1.98
2.03
0.99
3.12
f1 (ppm)

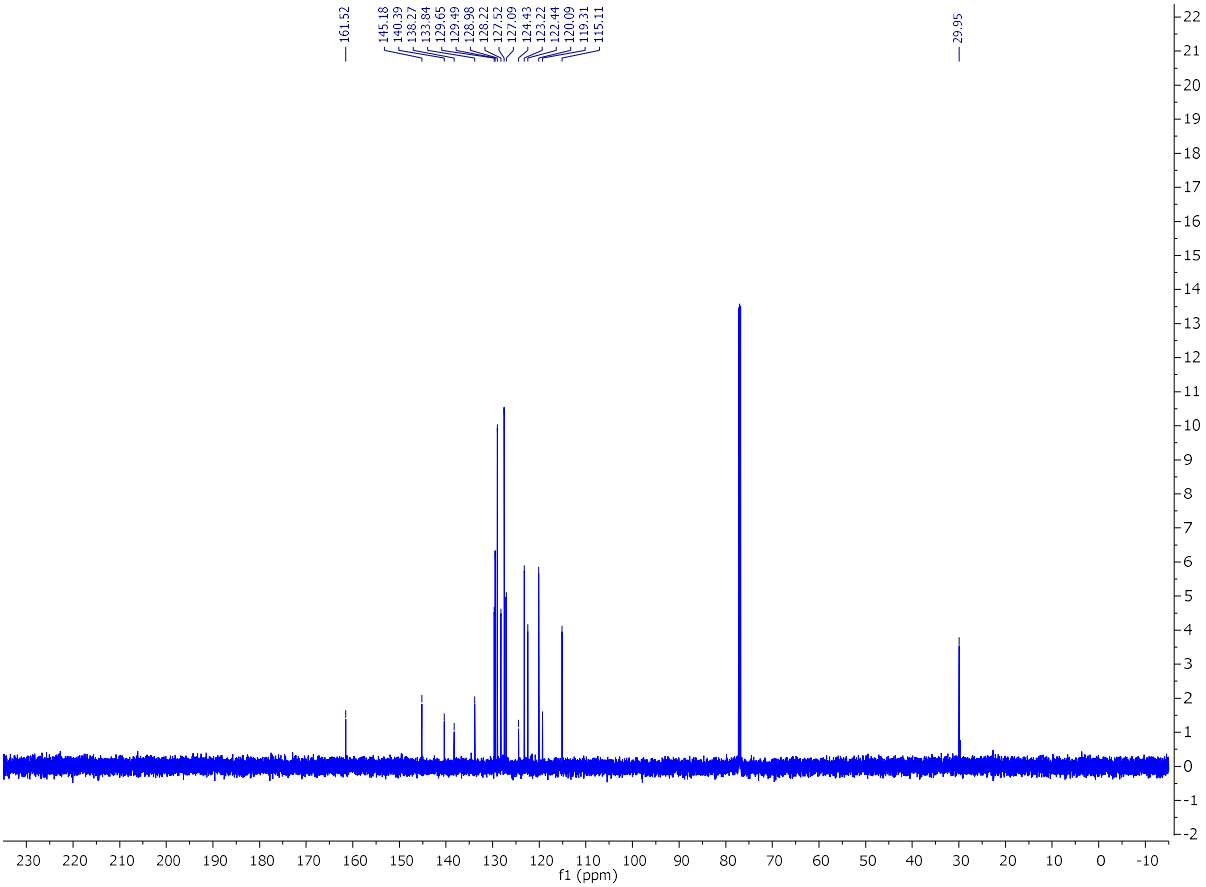
161.52
145.18
140.39
138.27
133.84
129.65
129.49
128.98
128.22
127.52
127.09
124.43
123.22
122.44
120.09
119.31
115.11
29.95
f1 (ppm)

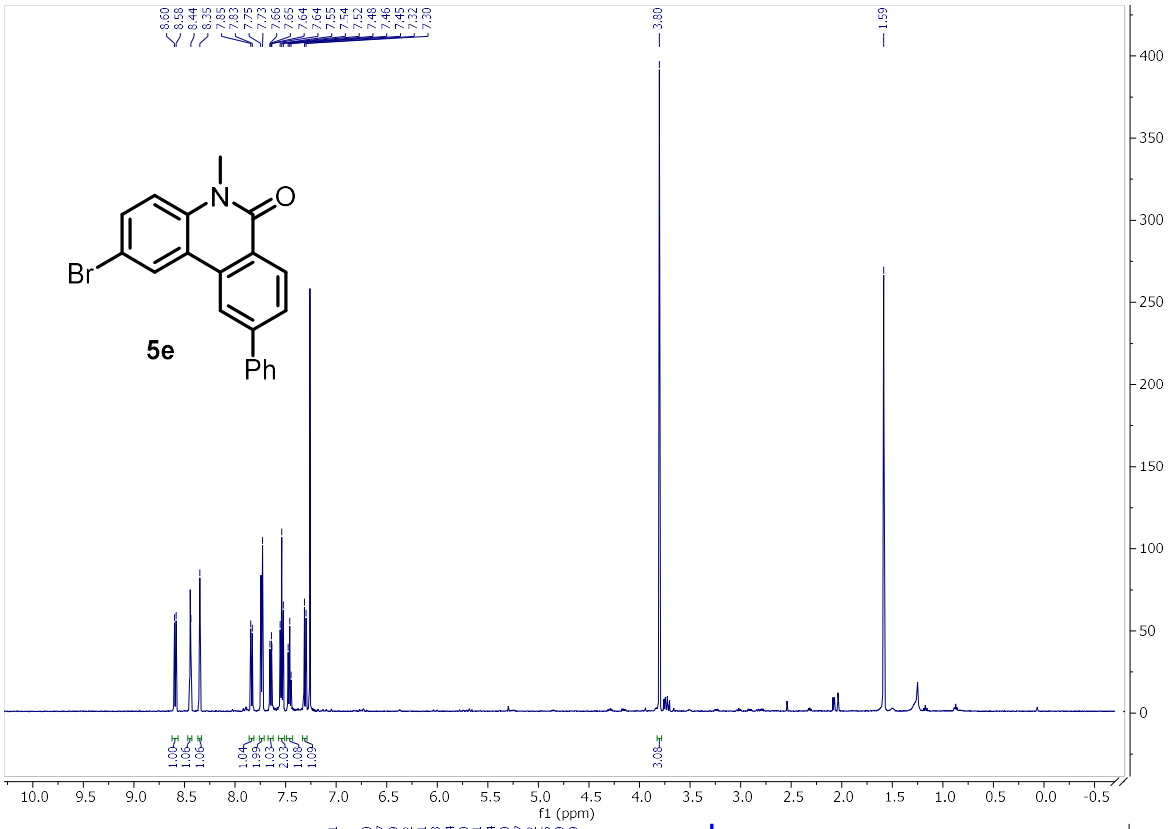
8.60
8.58
8.44
8.35
7.85
7.83
7.75
7.73
7.66
7.65
7.64
7.64
7.55
7.54
7.52
7.48
7.46
7.45
7.32
7.30
3.80
1.59
Br
N
O
Ph
5e
1.00
1.06
1.06
1.04
1.99
1.03
2.03
1.08
1.09
3.08
f1 (ppm)

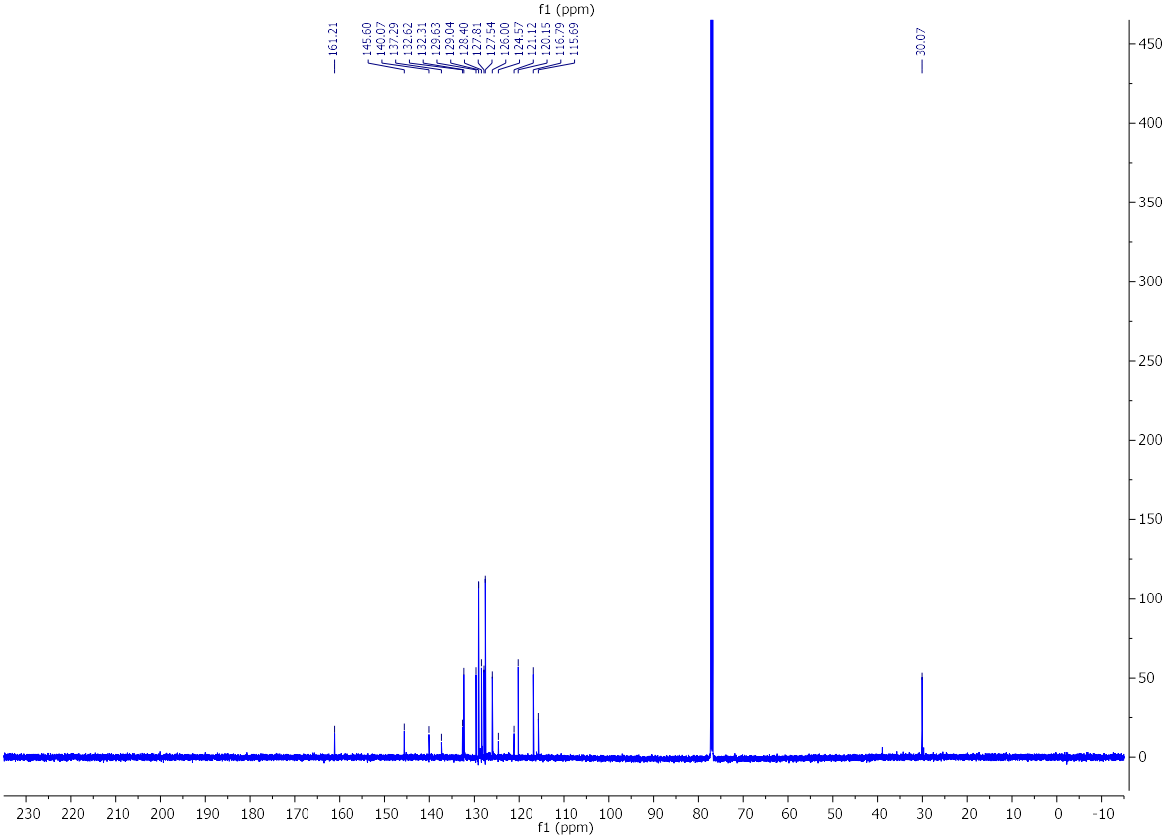
161.21
145.60
140.07
137.29
132.62
132.31
129.63
129.04
128.40
127.81
127.54
126.00
124.57
121.12
120.15
116.79
115.69
30.07
f1 (ppm)

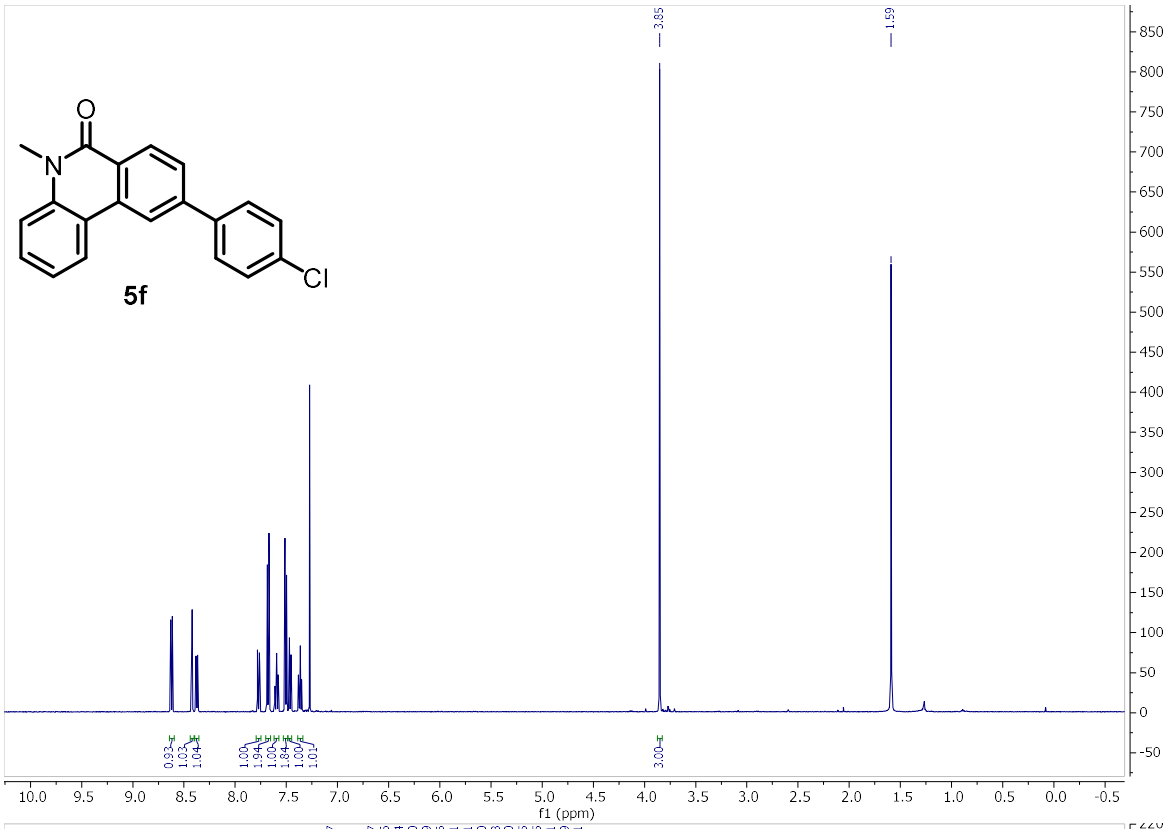
O
N
Cl
5f
3.85
1.59
0.93
1.03
1.04
1.00
1.94
1.00
1.84
1.00
1.01
3.00
f1 (ppm)

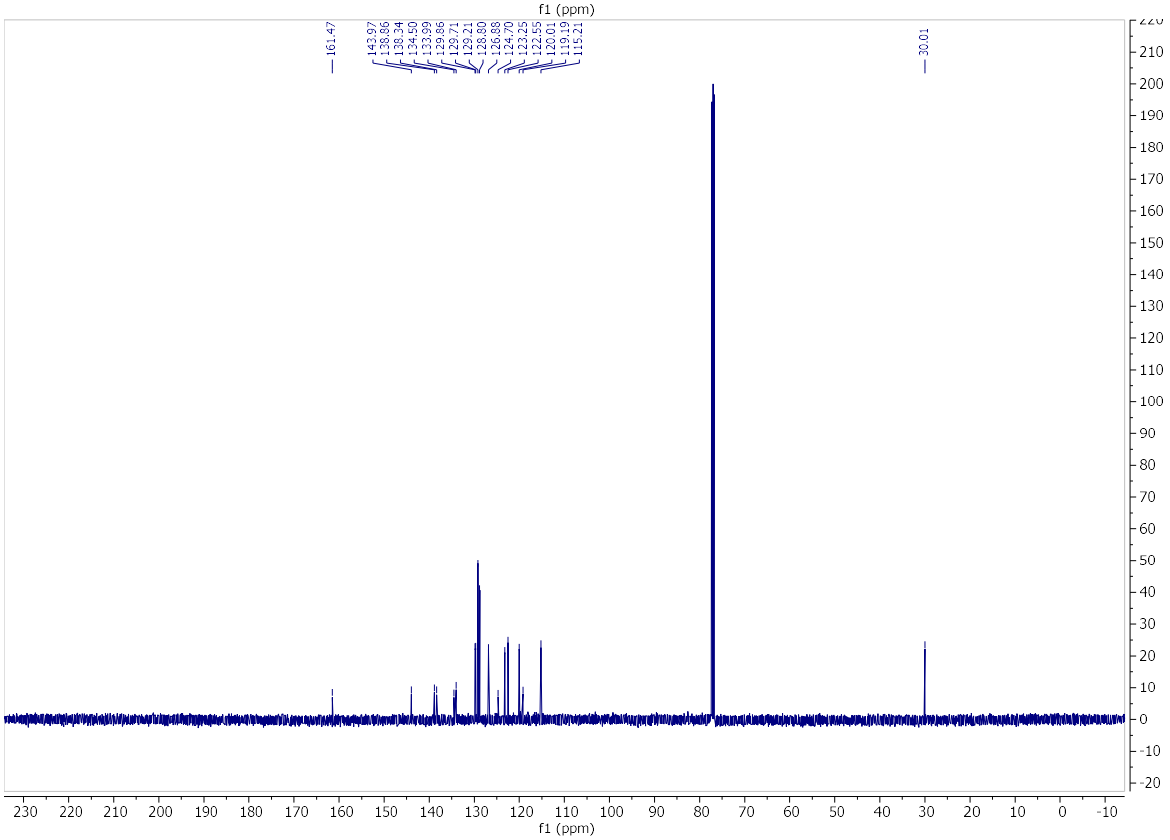
161.47
143.97
138.86
138.34
134.50
133.99
129.86
129.71
129.21
128.80
126.88
124.70
123.25
122.55
120.01
119.19
115.21
30.01
f1 (ppm)

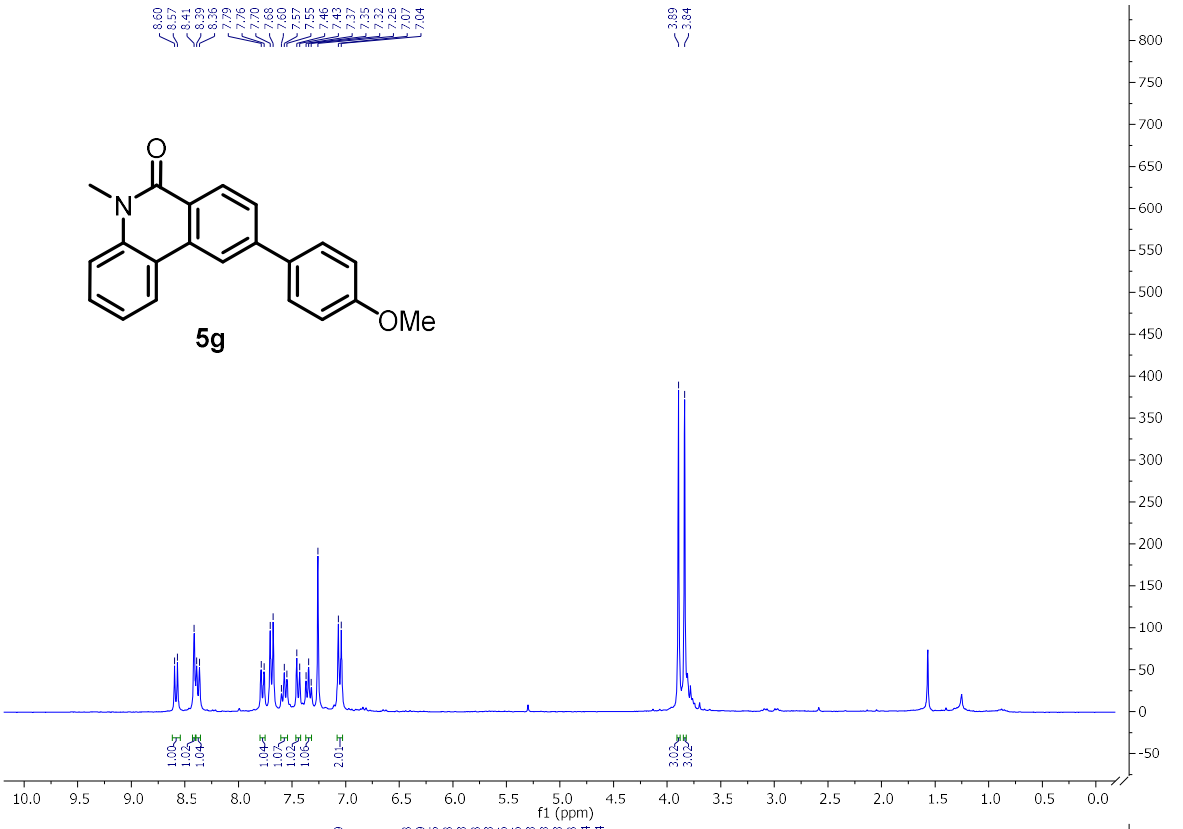
8.60
8.57
8.41
8.39
8.36
7.79
7.76
7.70
7.68
7.60
7.57
7.55
7.46
7.43
7.37
7.35
7.32
7.26
7.07
7.04
3.89
3.84
O
N
OMe
5g
1.00
1.02
1.04
1.04
1.07
1.02
1.06
2.01
3.02
3.02
f1 (ppm)

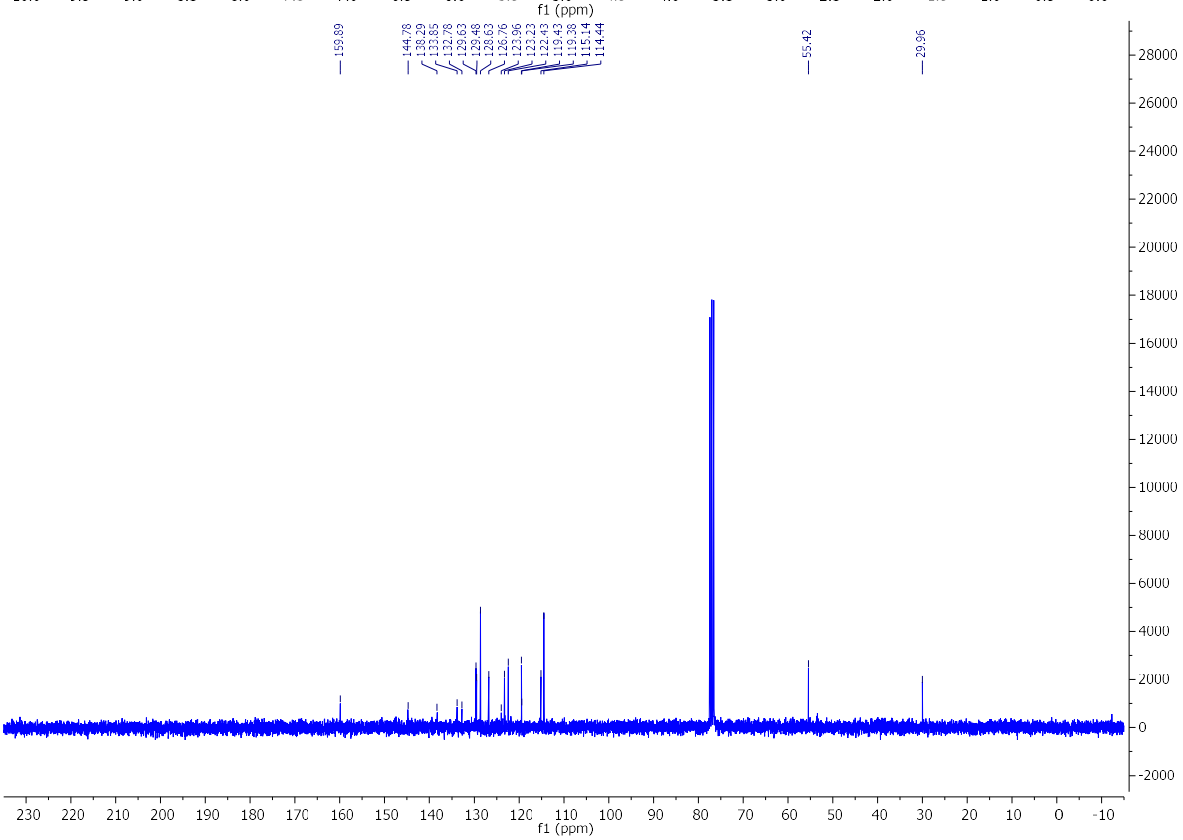
159.89
144.78
138.29
133.85
132.78
129.63
129.46
128.83
126.76
123.96
123.23
122.43
119.43
119.38
115.14
114.44
55.42
29.96
f1 (ppm)

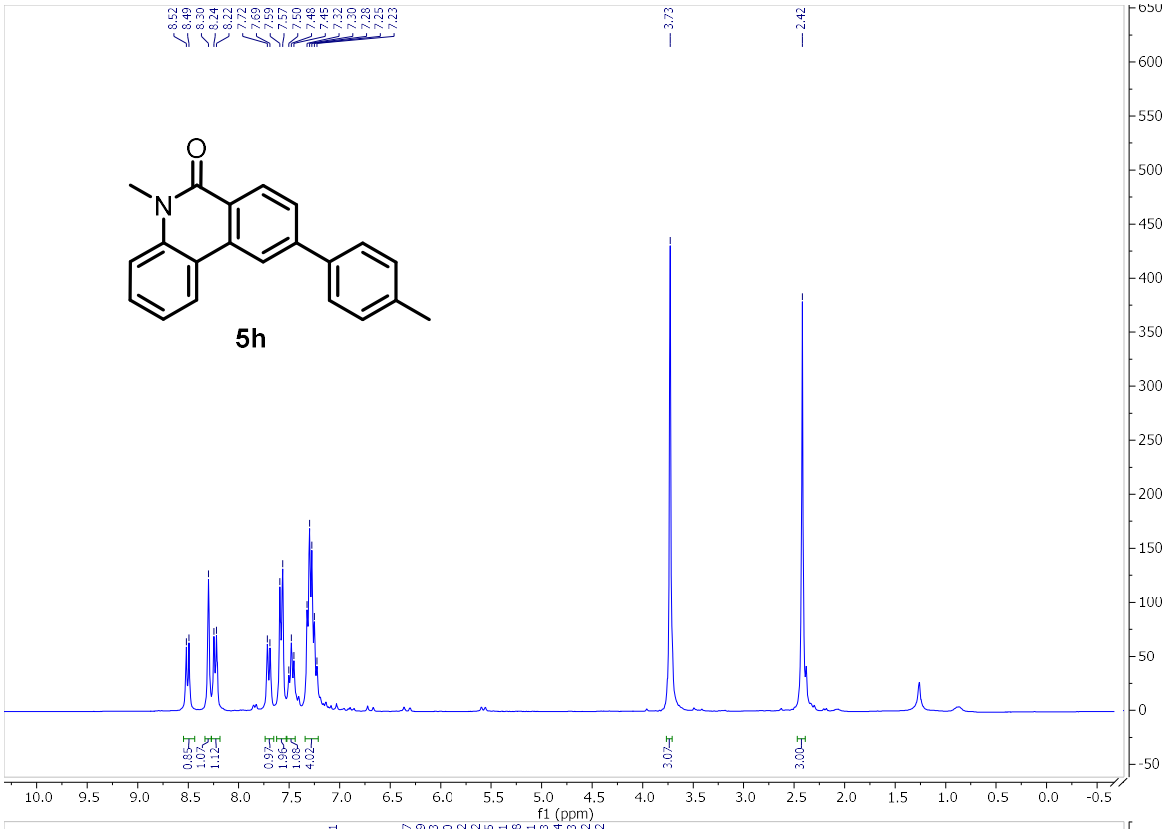
8.52
8.49
8.30
8.24
8.22
7.72
7.69
7.59
7.57
7.50
7.48
7.45
7.32
7.30
7.28
7.25
7.23
3.73
2.42
O
N
5h
0.85
1.07
1.12
0.97
1.96
1.08
4.02
3.07
3.00
f1 (ppm)

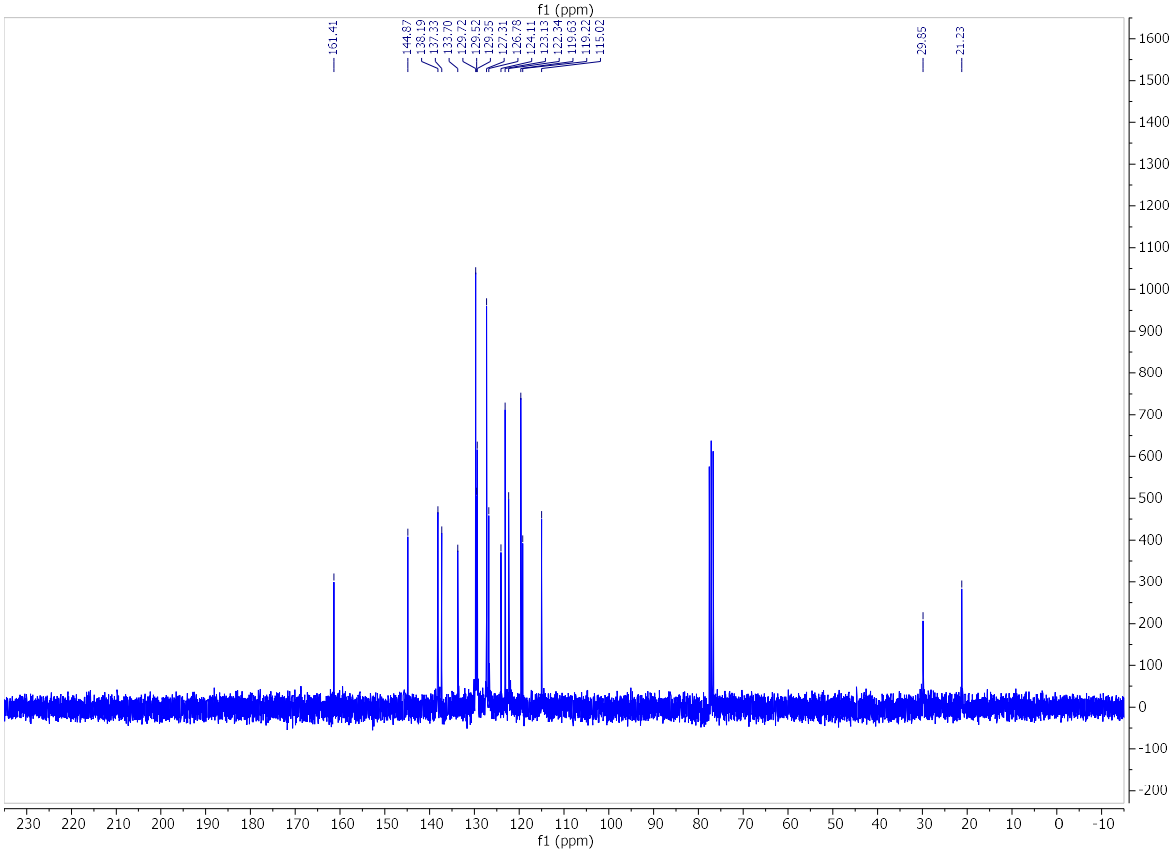
161.41
144.87
138.19
137.33
133.70
129.72
129.52
129.35
127.31
126.78
124.11
123.13
122.34
119.55
119.22
115.02
29.85
21.23
f1 (ppm)

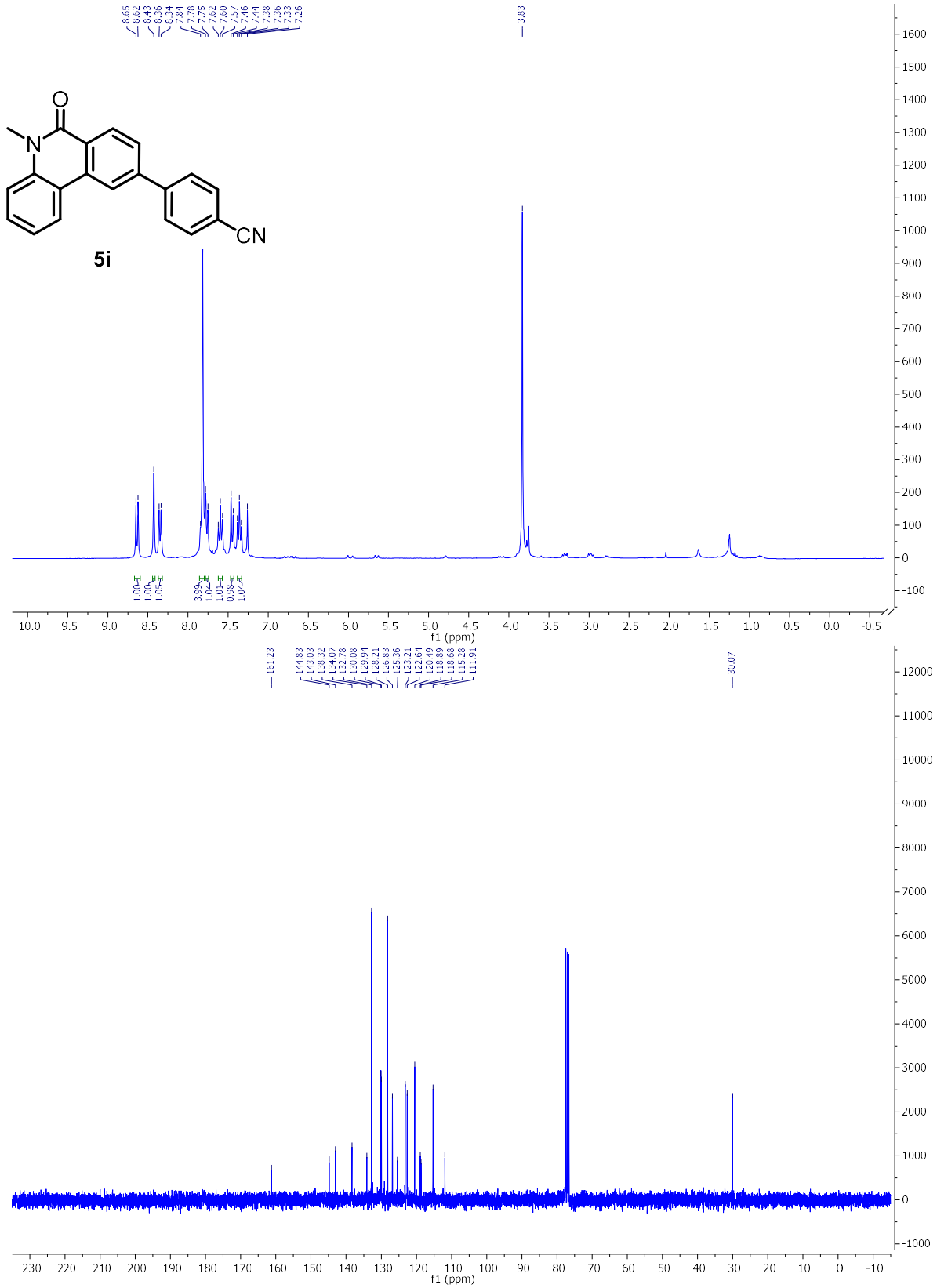
8.65
8.62
8.43
8.36
8.34
7.84
7.78
7.75
7.62
7.60
7.57
7.46
7.44
7.38
7.36
7.33
7.26
3.83
O
N
CN
5i
1.00
1.00
1.05
3.99
1.04
1.01
0.98
1.04
f1 (ppm)
161.23
144.83
143.03
138.32
134.07
132.78
130.08
129.94
128.21
126.83
125.36
123.21
122.64
120.49
118.89
118.68
115.28
111.91
30.07
f1 (ppm)

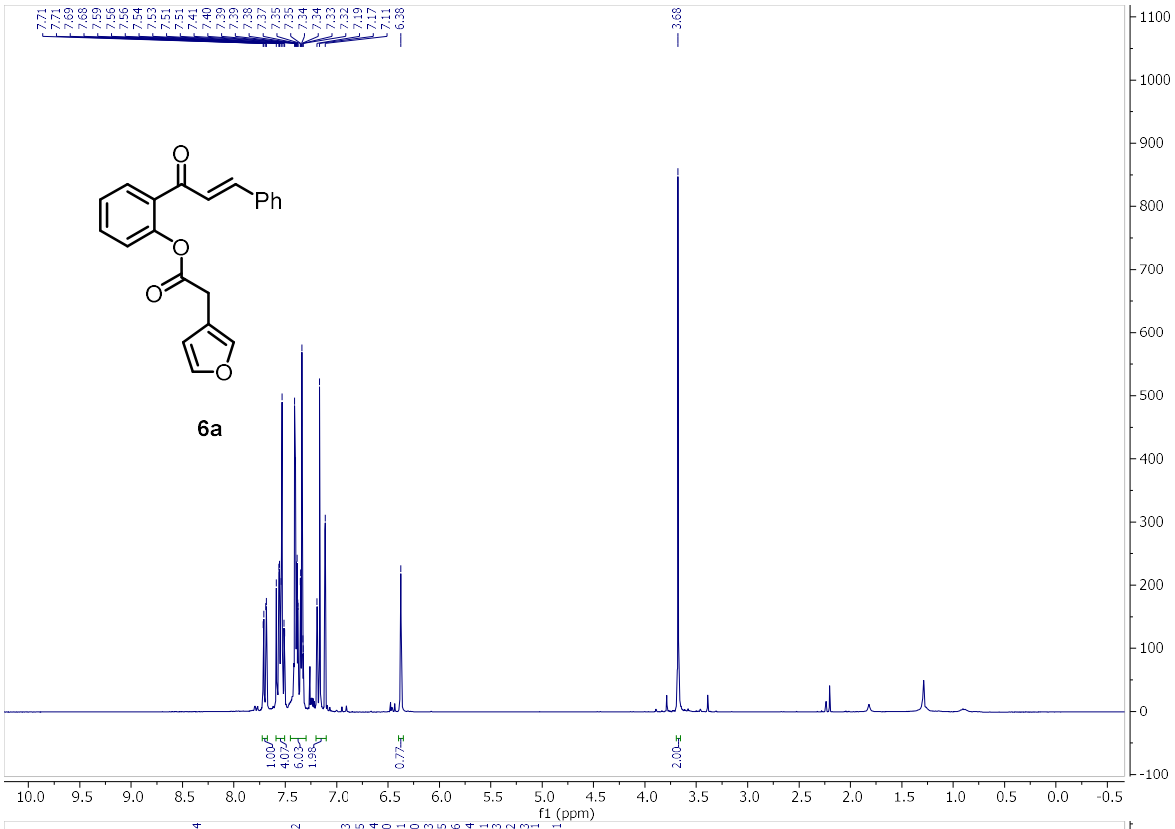
7.71
7.71
7.69
7.68
7.59
7.56
7.56
7.54
7.53
7.51
7.41
7.40
7.39
7.39
7.38
7.37
7.35
7.34
7.34
7.33
7.32
7.19
7.17
7.11
6.38
3.68
O
Ph
O
O
O
6a
1.00
4.07
6.03
1.96
0.77
2.00
f1 (ppm)

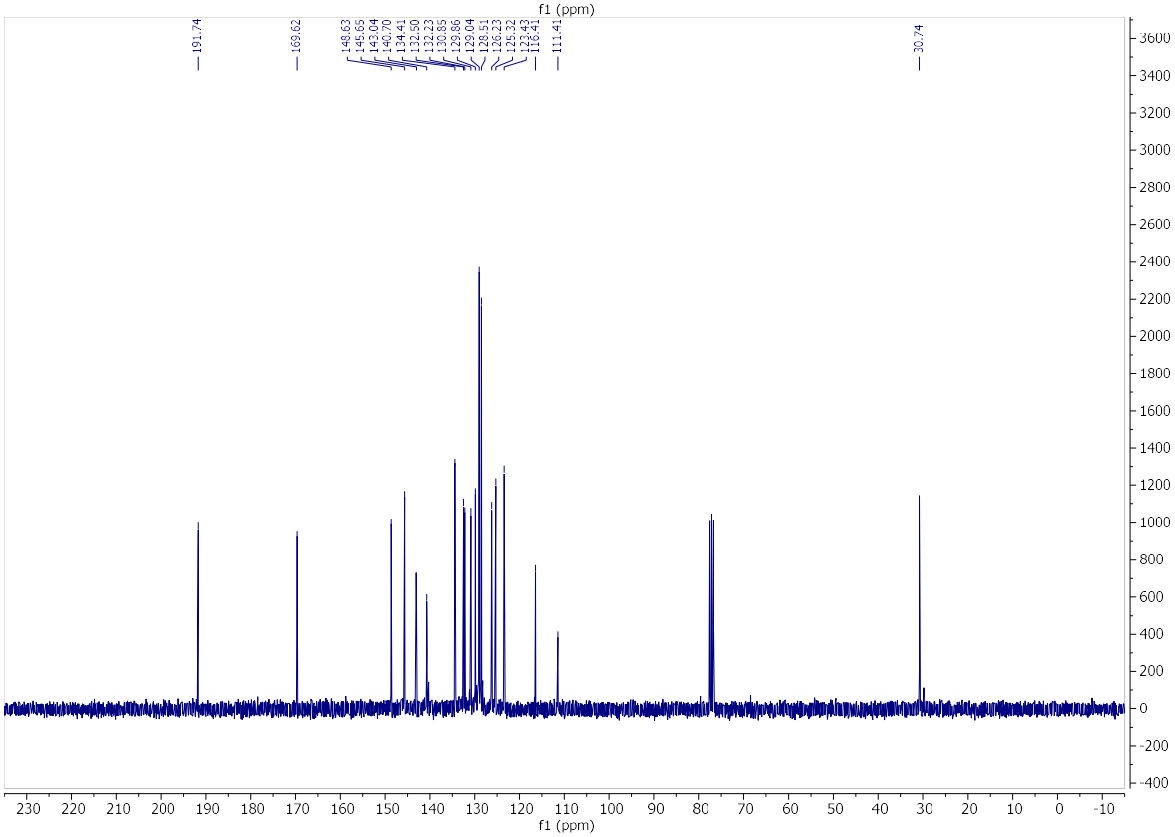
191.74
169.62
148.63
145.65
143.04
140.70
134.41
132.50
132.23
130.85
129.86
129.04
128.51
126.23
125.32
123.43
116.41
111.41
30.74
f1 (ppm)

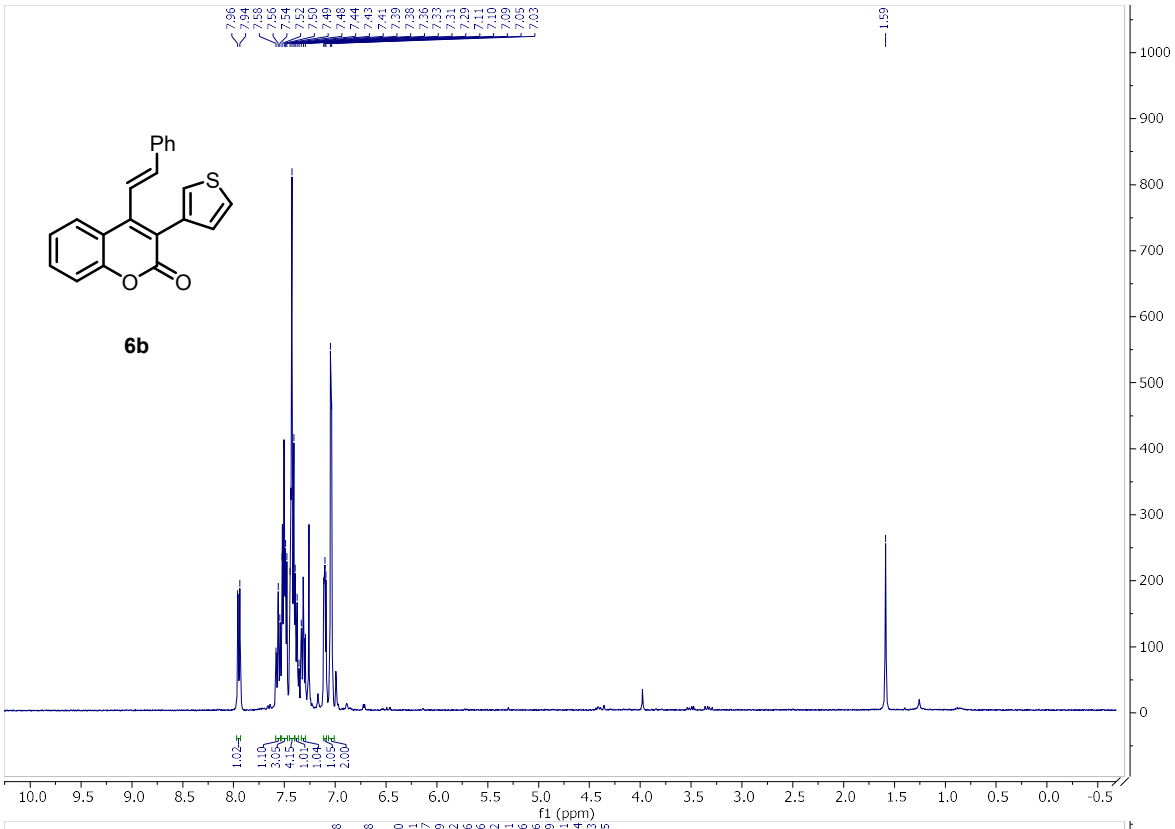
Ph
S
O
O
6b
f1 (ppm)

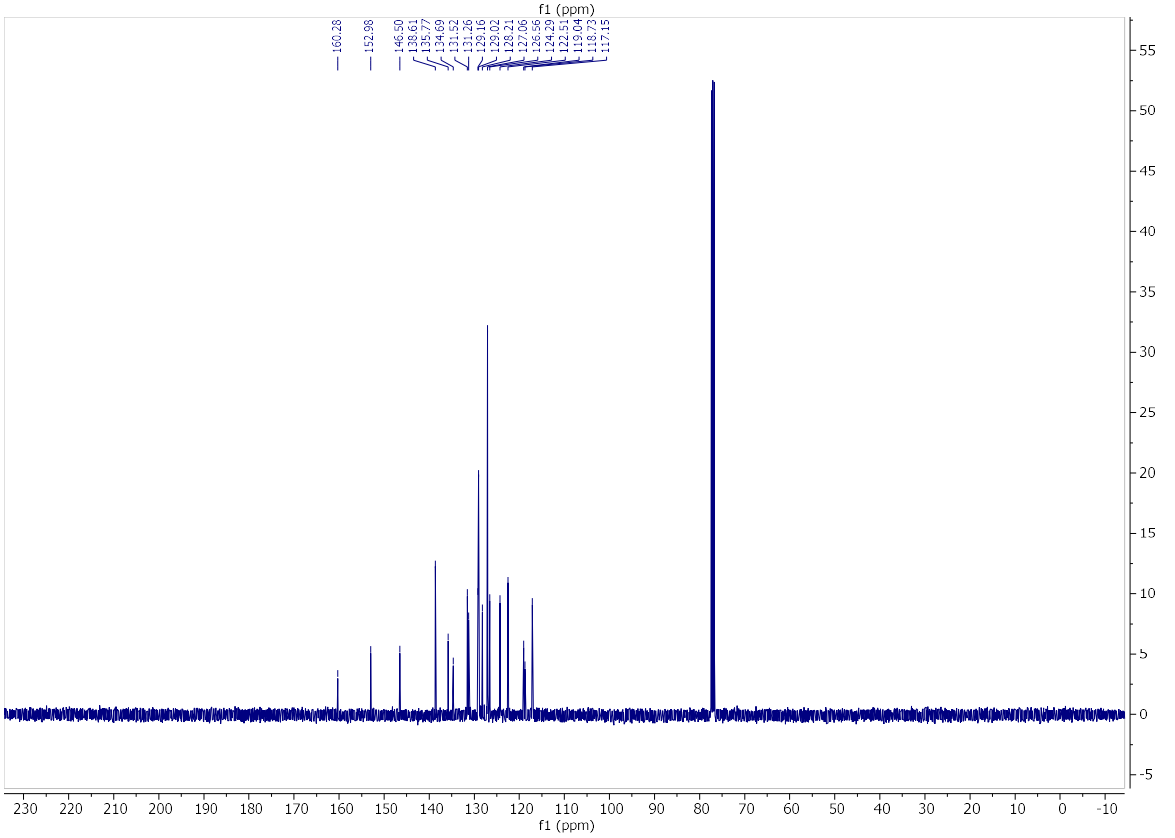
f1 (ppm)

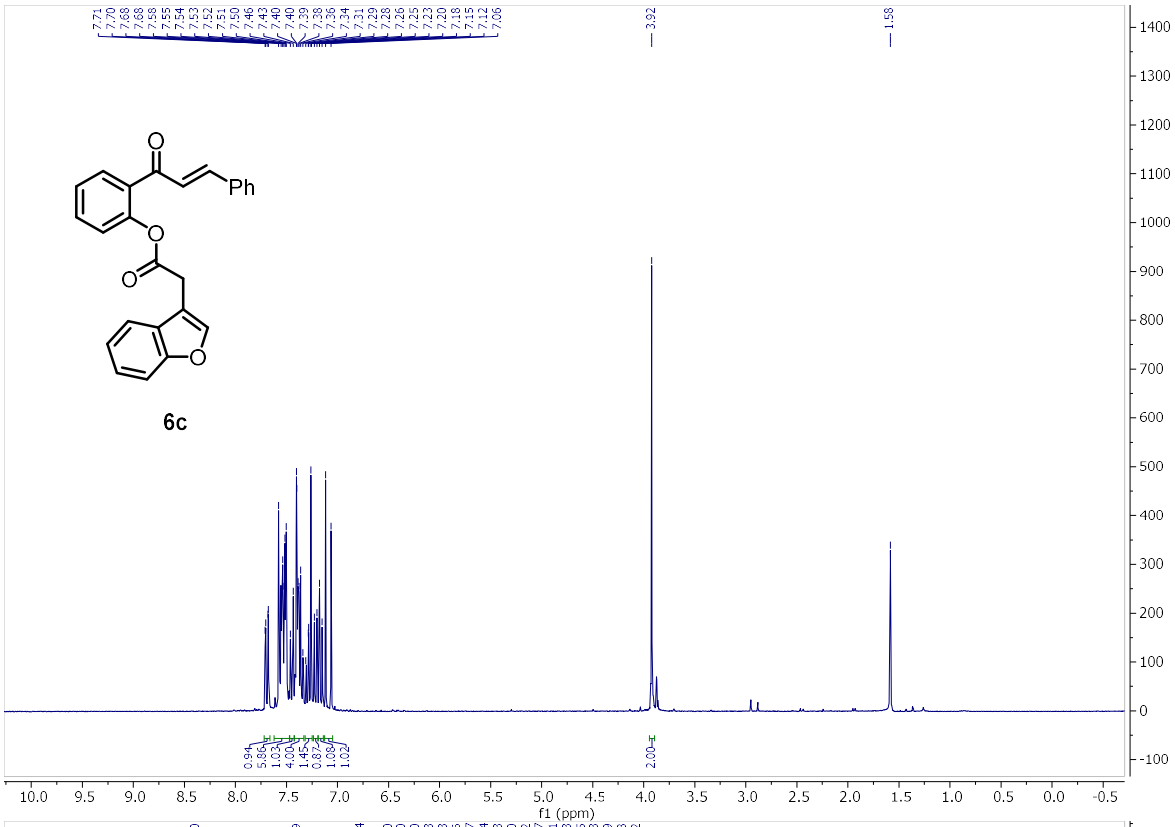
7.71
7.70
7.68
7.68
7.58
7.55
7.54
7.53
7.52
7.51
7.50
7.46
7.43
7.40
7.40
7.39
7.38
7.36
7.34
7.31
7.29
7.28
7.26
7.25
7.23
7.20
7.18
7.15
7.12
7.06
3.92
1.58
Ph
O
O
O
O
6c
0.94
5.86
1.03
4.00
1.45
0.87
1.08
1.02
2.00
f1 (ppm)

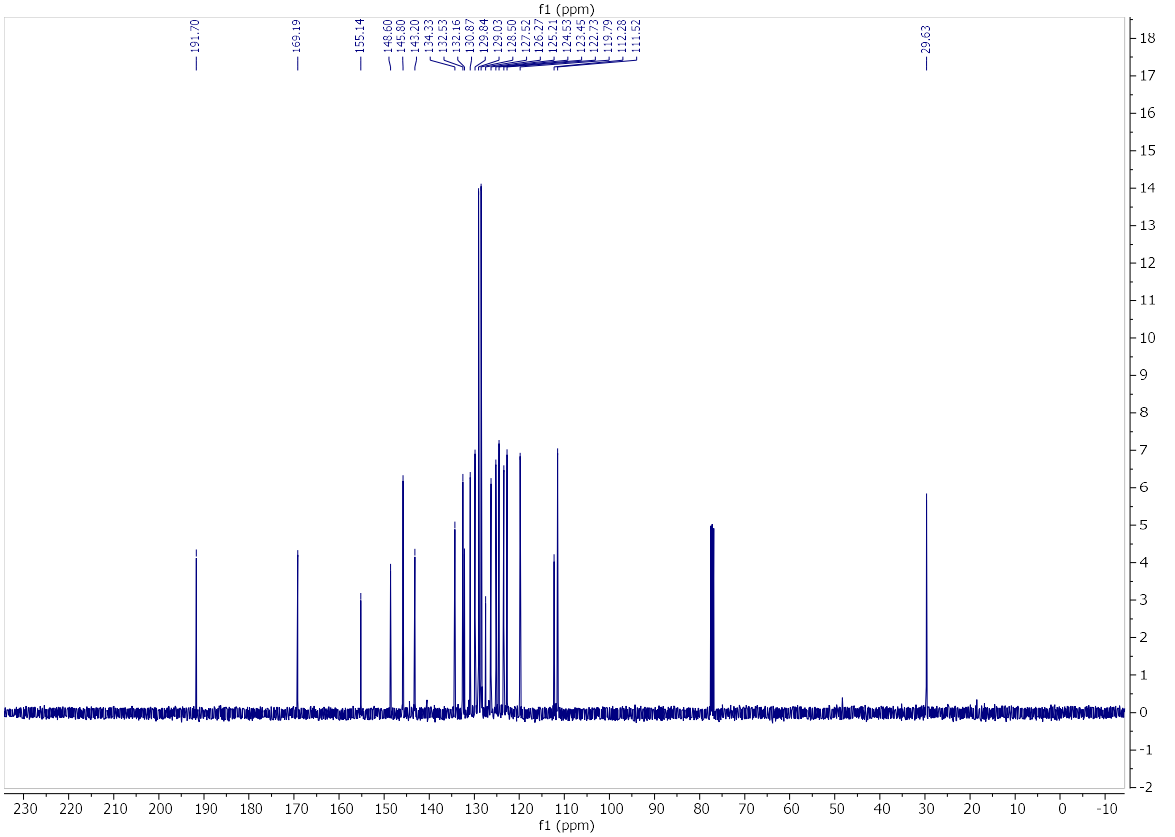
191.70
169.19
155.14
148.60
145.80
143.20
134.33
132.53
132.16
130.87
129.84
129.03
128.50
127.52
126.27
125.21
124.53
123.45
122.73
119.79
112.28
111.52
29.63
f1 (ppm)

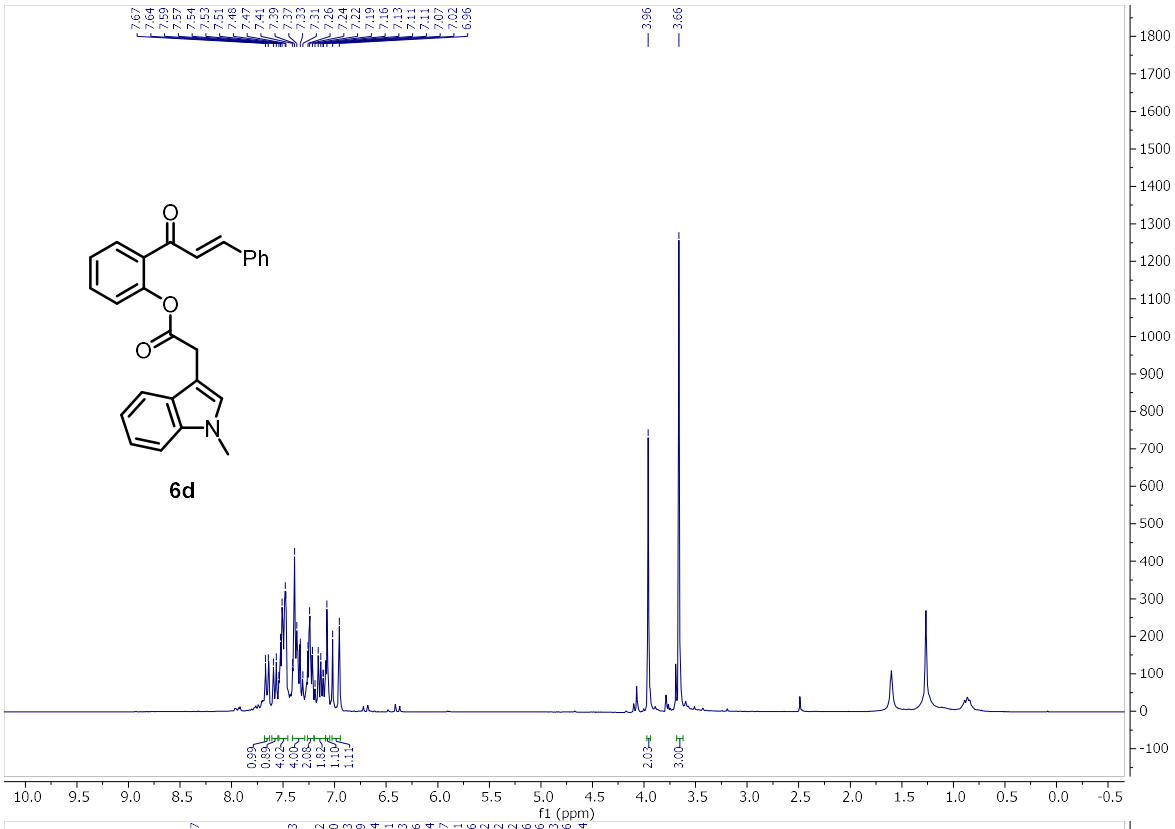
7.67
7.64
7.59
7.57
7.54
7.53
7.51
7.48
7.47
7.41
7.39
7.37
7.33
7.31
7.26
7.24
7.22
7.19
7.16
7.13
7.11
7.11
7.07
7.02
6.96
3.96
3.66
O
Ph
O
O
N
6d
0.99
0.89
4.02
4.00
2.08
1.82
1.10
1.11
2.03
3.00
f1 (ppm)

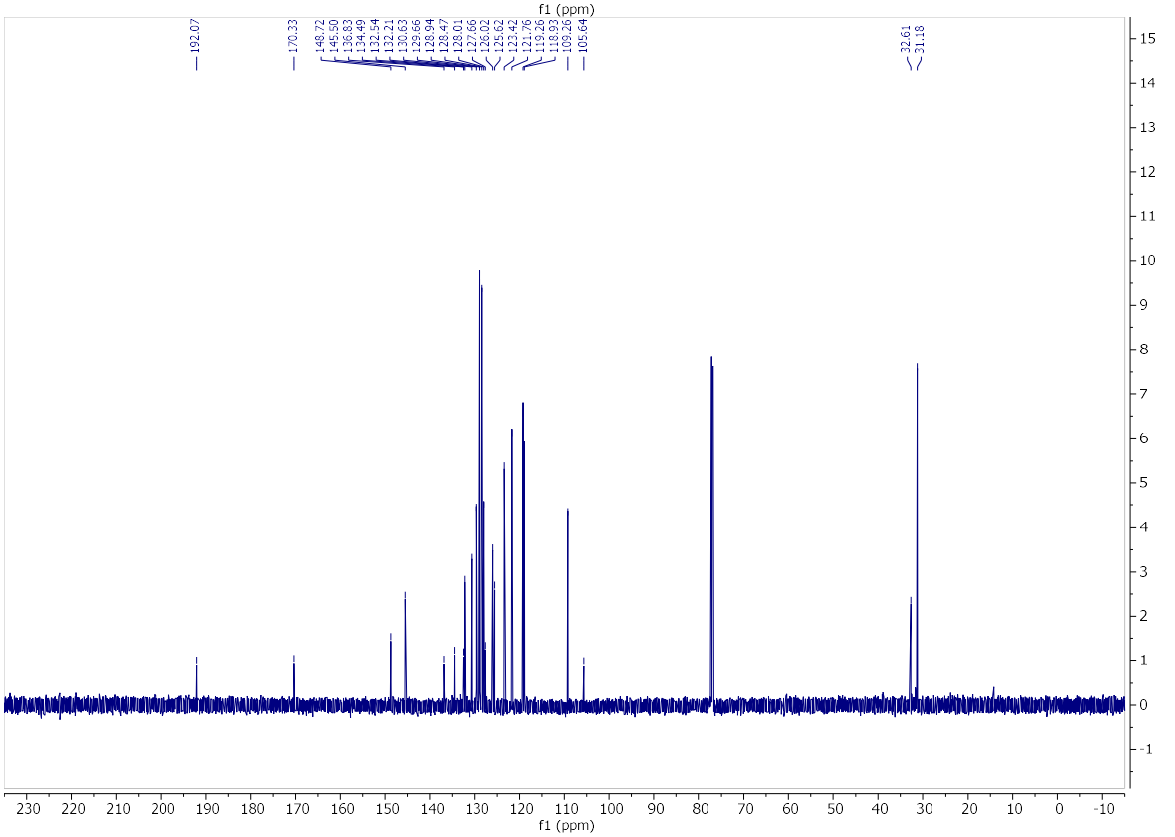
192.07
170.33
148.72
145.60
136.83
134.49
132.21
132.54
130.63
129.86
128.94
128.47
128.01
127.66
126.02
125.62
123.42
121.76
119.26
118.93
109.26
105.64
32.61
31.18
f1 (ppm)

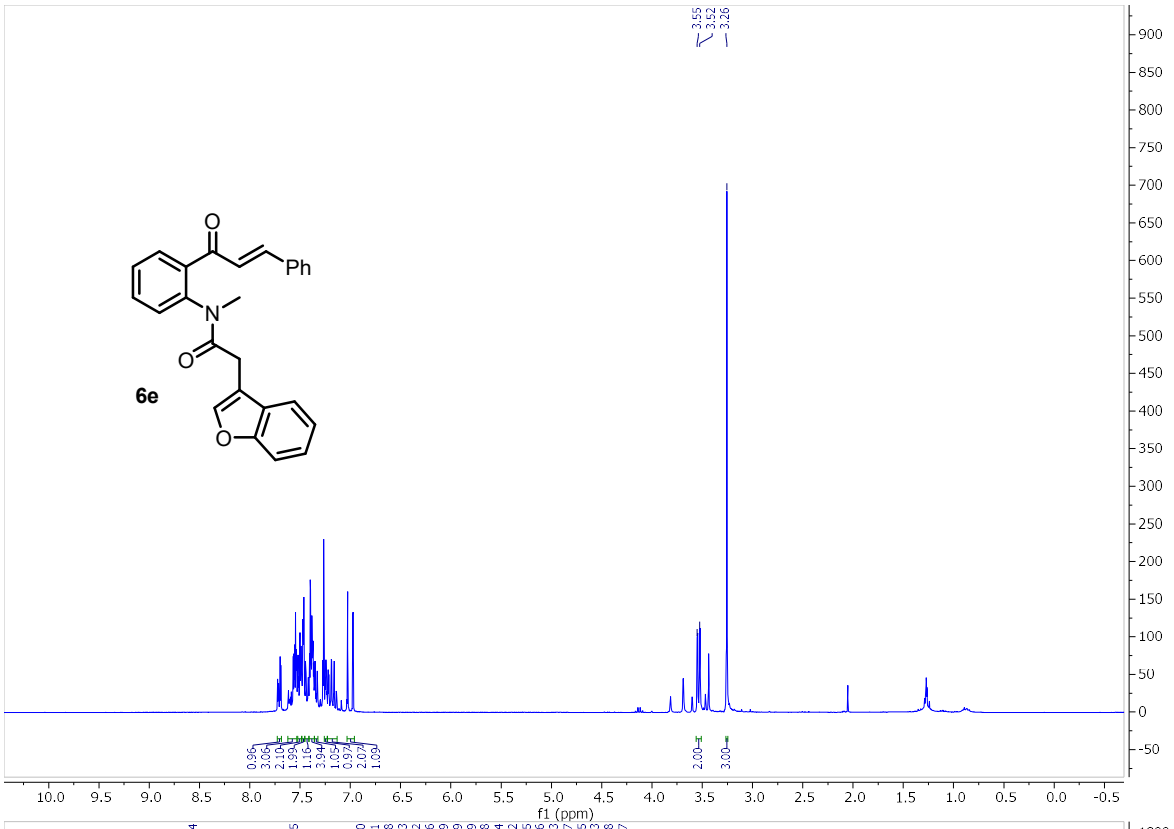
3.55
3.52
3.26
Ph
N
O
O
O
6e
0.96
3.06
2.15
1.99
1.16
3.94
1.02
0.97
2.07
1.09
2.00
3.00
f1 (ppm)

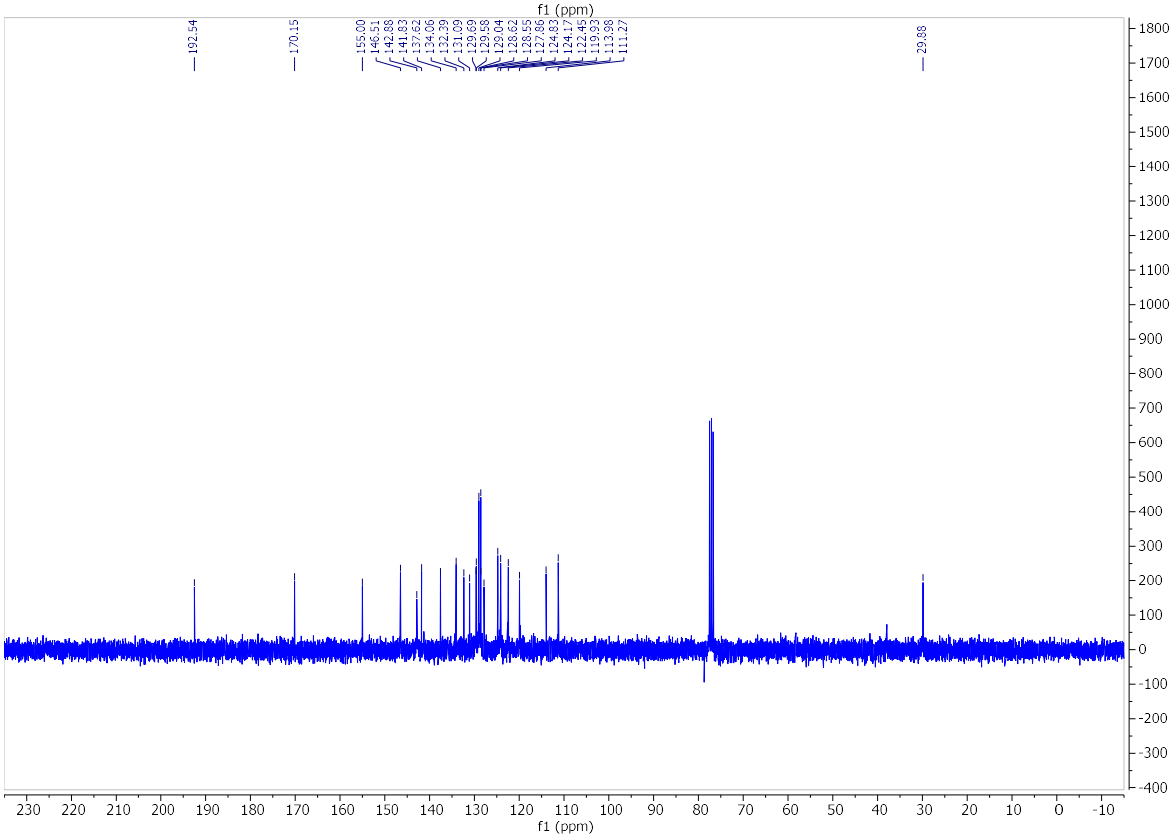
192.54
170.15
155.00
146.51
142.88
141.83
137.62
134.06
132.39
131.09
129.69
129.56
129.04
128.62
128.55
127.86
124.83
124.17
122.45
119.93
113.98
111.27
29.88
f1 (ppm)

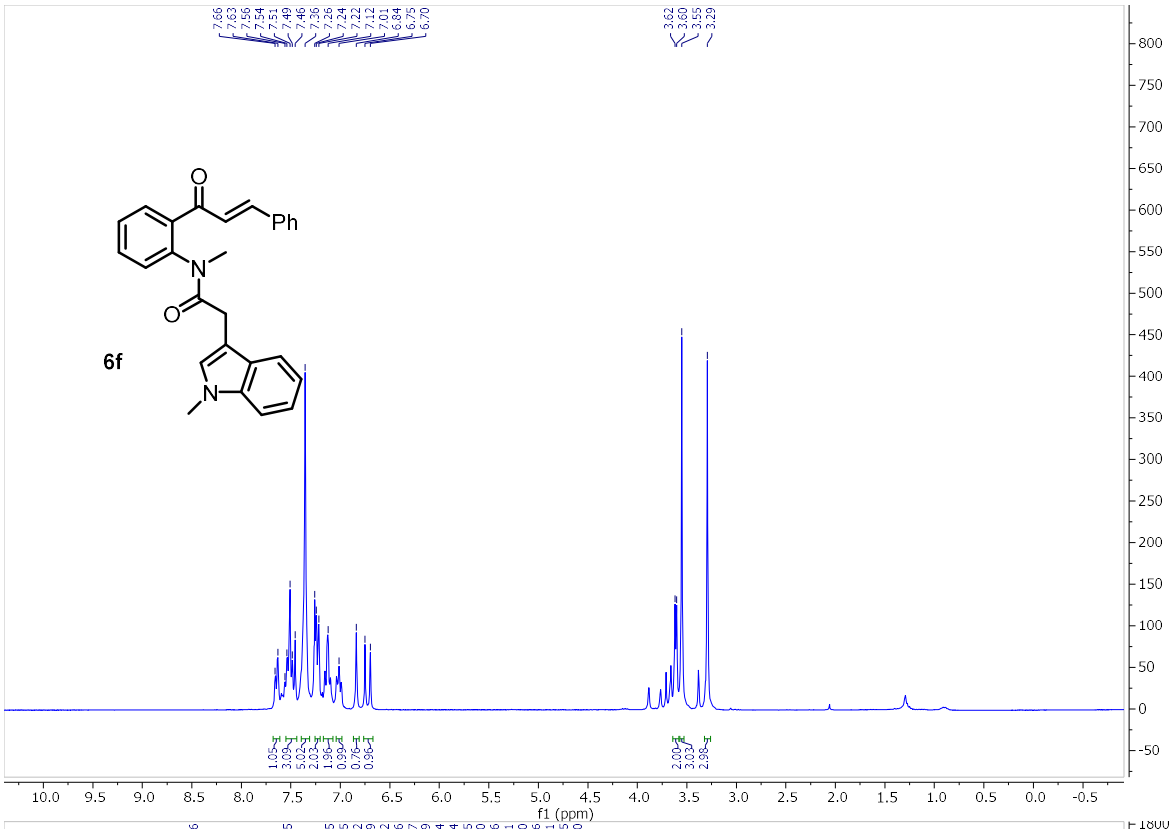
7.66
7.63
7.56
7.54
7.51
7.49
7.46
7.36
7.26
7.24
7.22
7.12
7.01
6.84
6.75
6.70
3.62
3.60
3.55
3.29
O
Ph
N
O
N
6f
1.05
3.09
5.02
2.03
1.96
0.99
0.76
0.96
2.00
3.03
2.96
f1 (ppm)

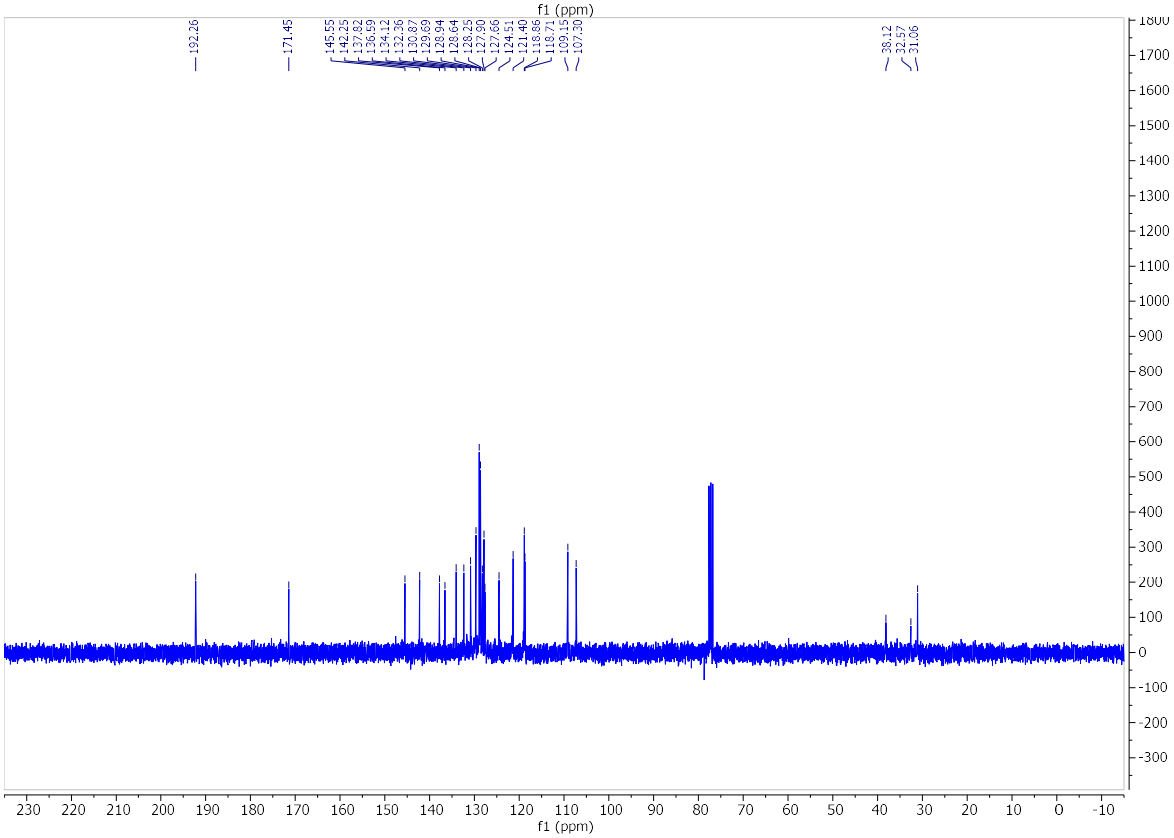
192.26
171.45
145.55
142.25
137.82
136.59
134.12
132.36
130.87
129.69
128.94
128.64
128.25
127.90
127.66
124.51
121.40
118.86
118.71
109.15
107.30
38.12
32.57
31.06
f1 (ppm)

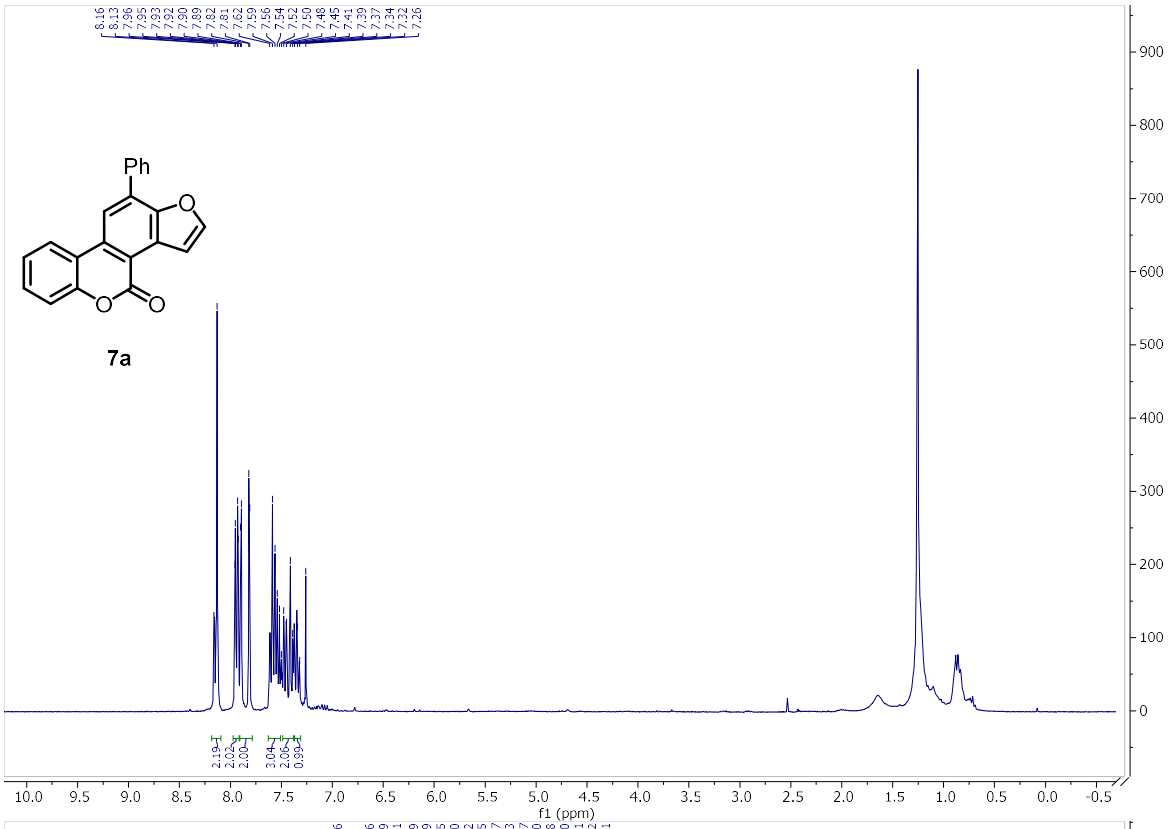
8.16
8.13
7.96
7.95
7.93
7.92
7.90
7.89
7.82
7.81
7.62
7.59
7.56
7.54
7.52
7.50
7.48
7.45
7.41
7.39
7.37
7.34
7.32
7.26
Ph
O
O
O
7a
2.19
2.02
2.00
3.04
2.06
0.99
f1 (ppm)

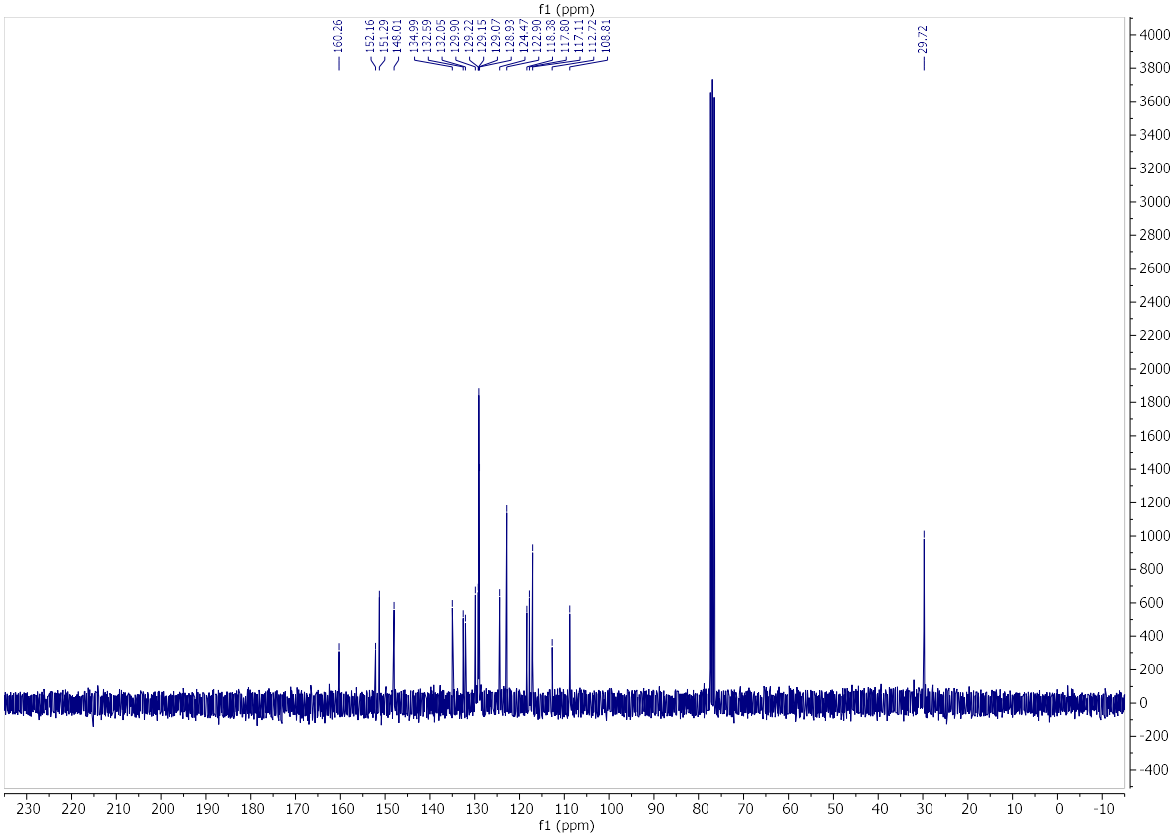
160.26
152.16
151.29
148.01
134.99
132.59
132.05
129.90
129.22
129.15
129.07
128.93
124.47
122.90
118.38
117.80
117.11
112.72
108.81
29.72
f1 (ppm)

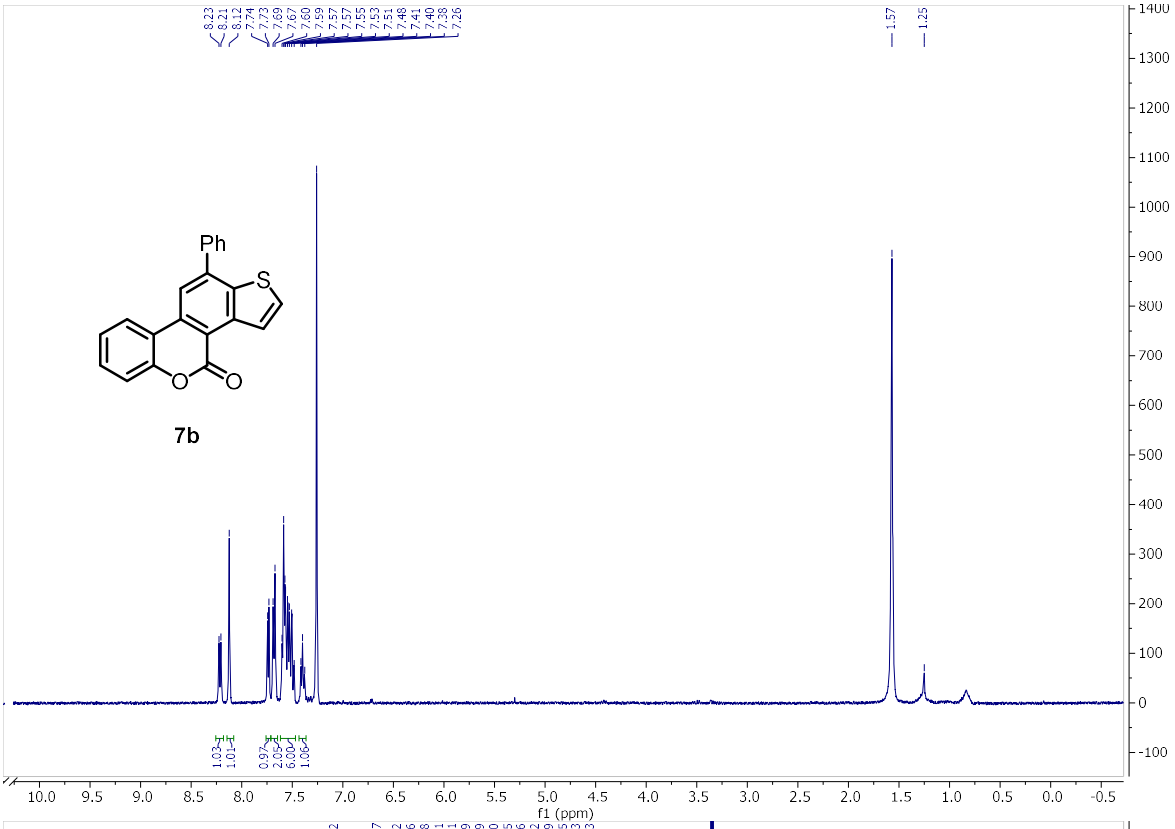
8.23
8.21
8.12
7.74
7.73
7.69
7.67
7.60
7.59
7.57
7.57
7.55
7.53
7.51
7.48
7.41
7.40
7.38
7.26
1.57
1.25
Ph
S
O
O
7b
1.03
1.01
0.97
2.05
6.00
1.06
f1 (ppm)

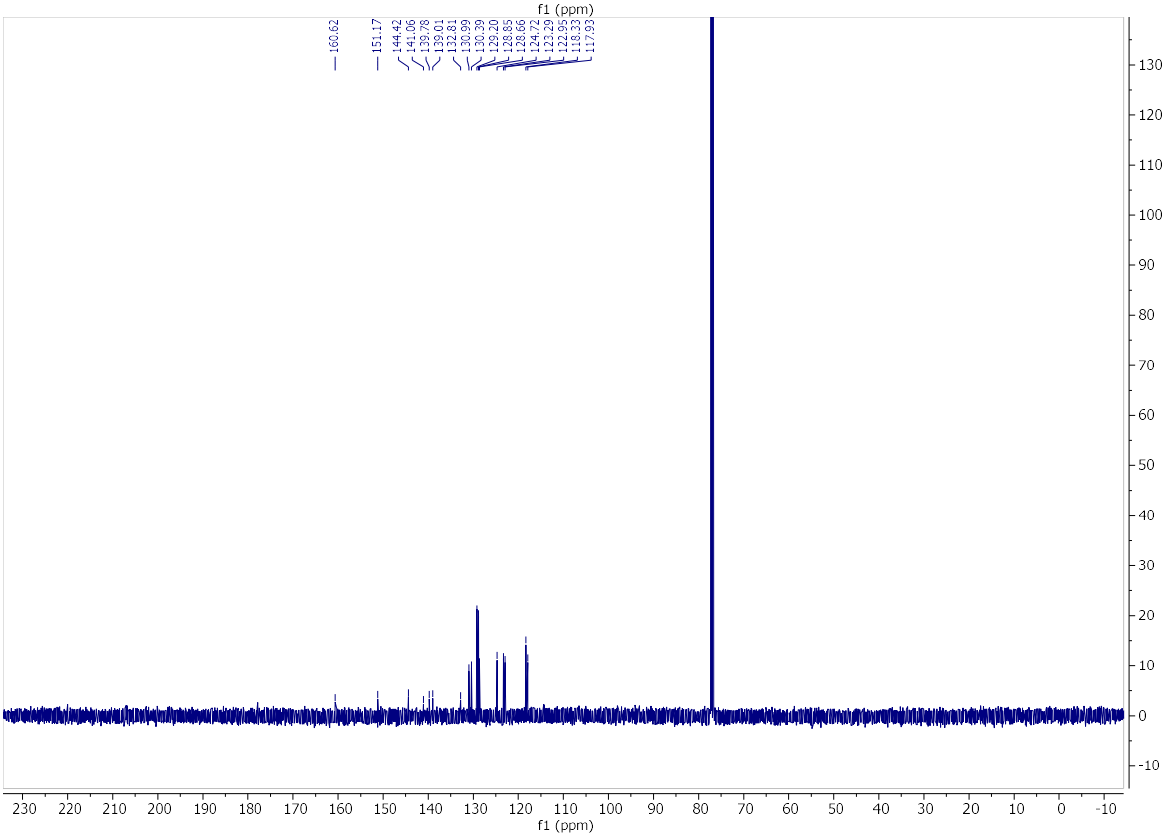
160.62
151.17
144.42
141.06
139.78
139.01
132.81
130.99
130.39
129.20
128.85
128.66
124.72
123.29
122.95
118.33
117.93
f1 (ppm)

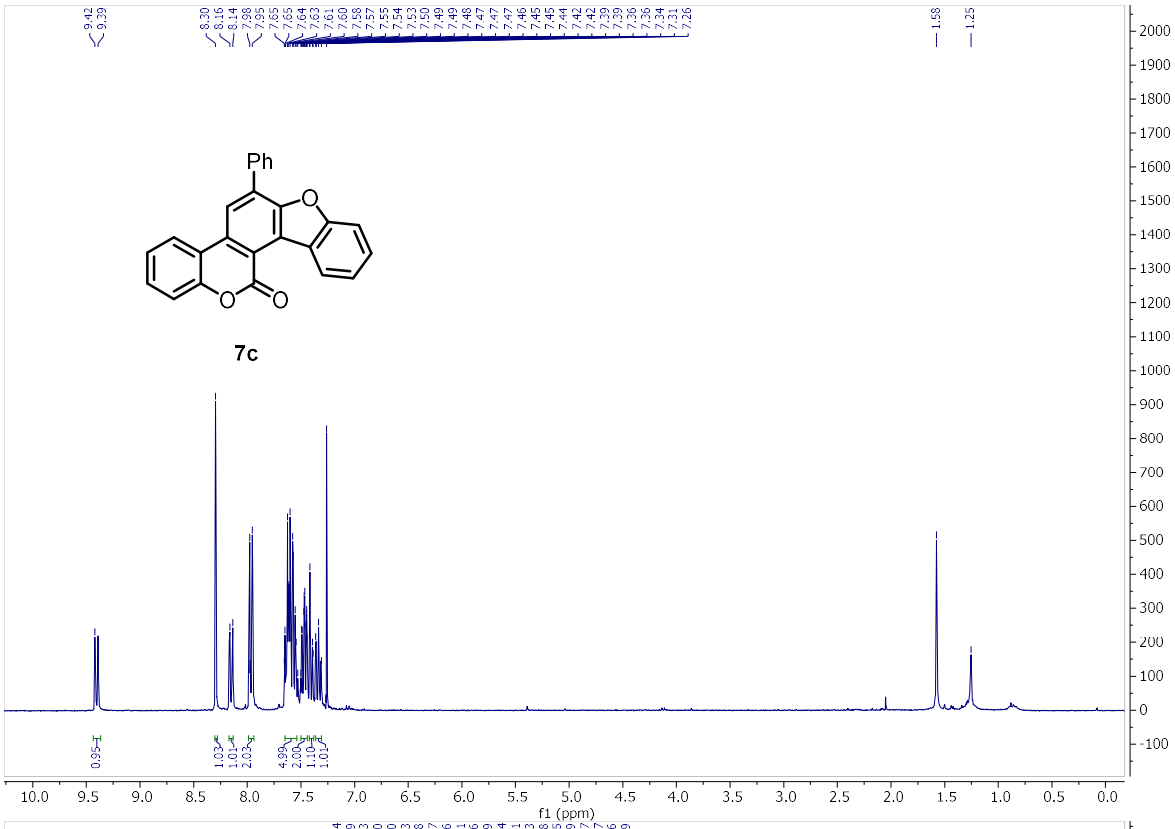
Ph
O
O
O
7c
f1 (ppm)

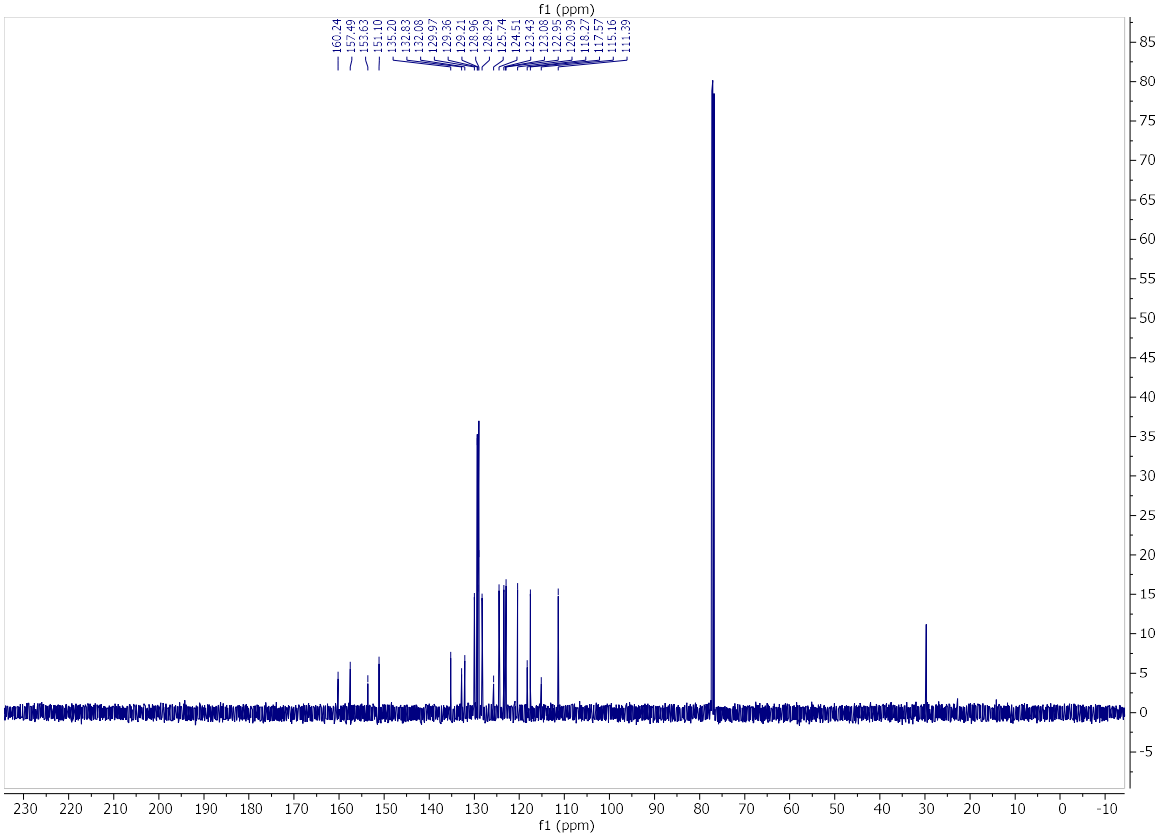
f1 (ppm)

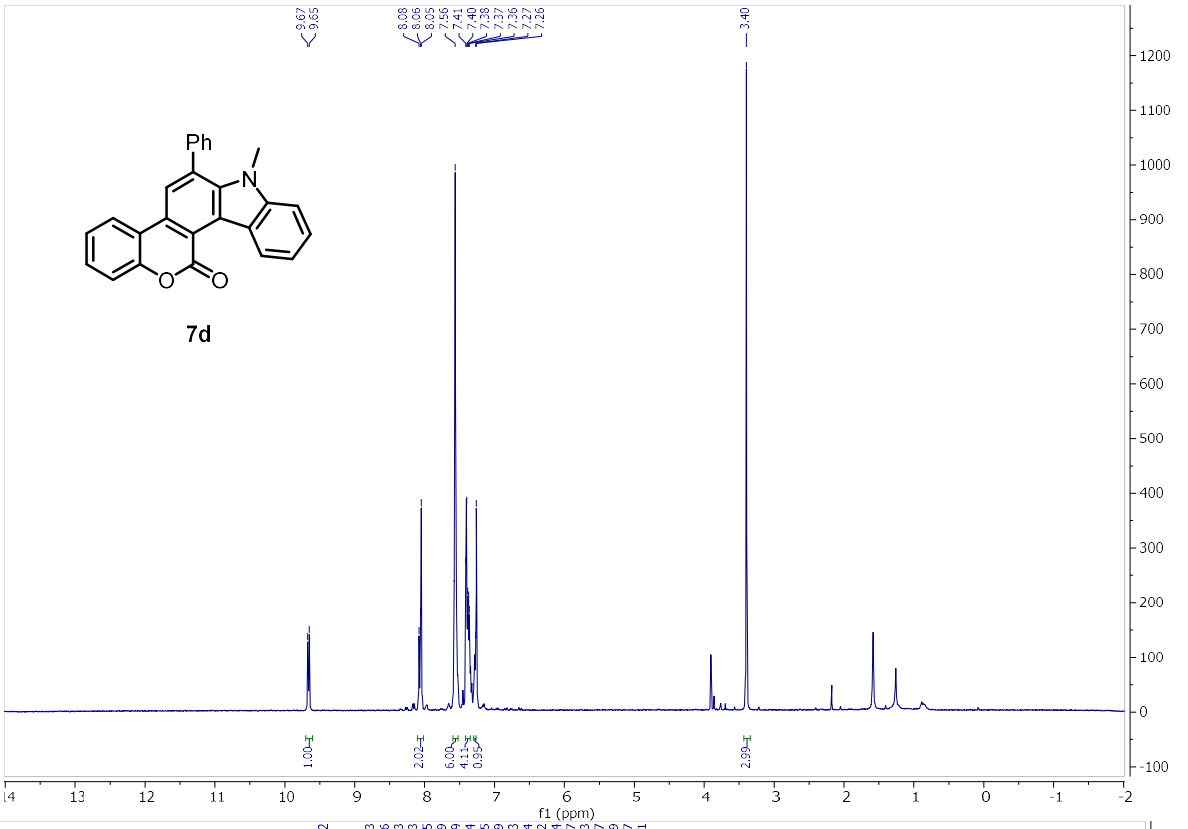
9.67
9.65
8.08
8.06
8.05
7.56
7.41
7.40
7.38
7.37
7.36
7.27
7.26
3.40
Ph
N
O
O
1.00
2.02
6.00
4.11
0.95
2.99
f1 (ppm)

7d

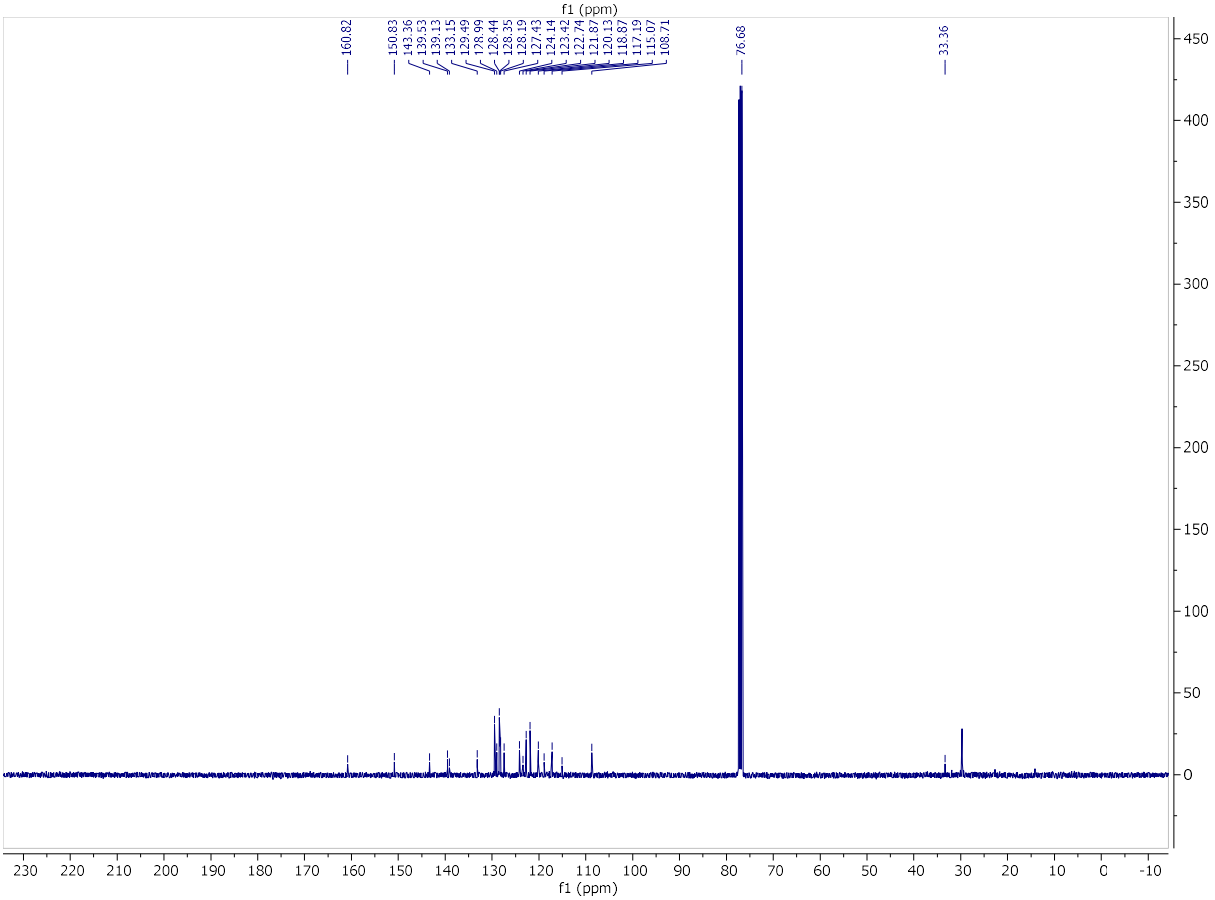
160.82
150.83
143.36
139.53
139.13
133.15
129.49
128.99
128.44
128.35
128.19
127.43
124.14
123.42
122.74
121.67
120.13
118.87
117.49
115.07
108.71
76.68
33.36
f1 (ppm)

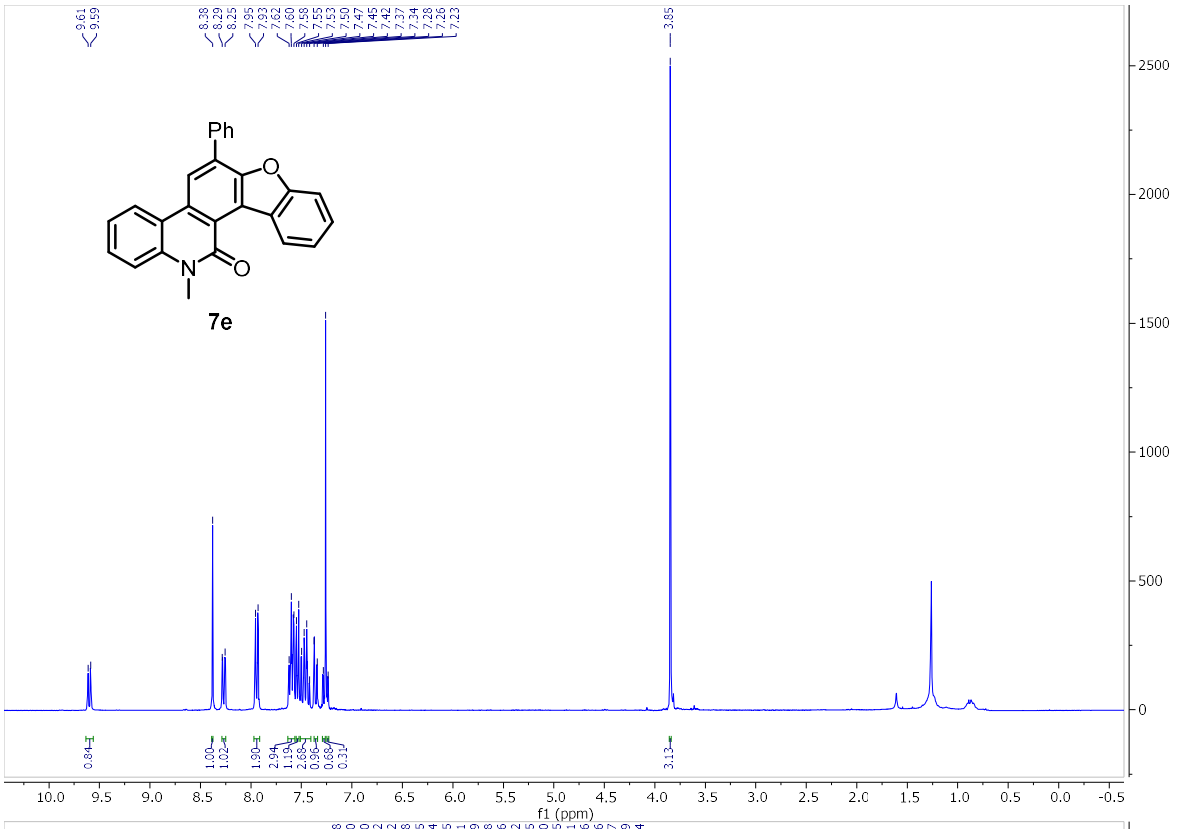
9.61
9.59
8.38
8.29
8.25
7.95
7.93
7.62
7.60
7.58
7.55
7.53
7.50
7.47
7.45
7.42
7.37
7.34
7.28
7.26
7.23
3.85
Ph
O
N
O
7e
0.84
1.00
1.02
1.90
2.94
1.19
2.68
0.96
0.68
0.31
3.13
f1 (ppm)

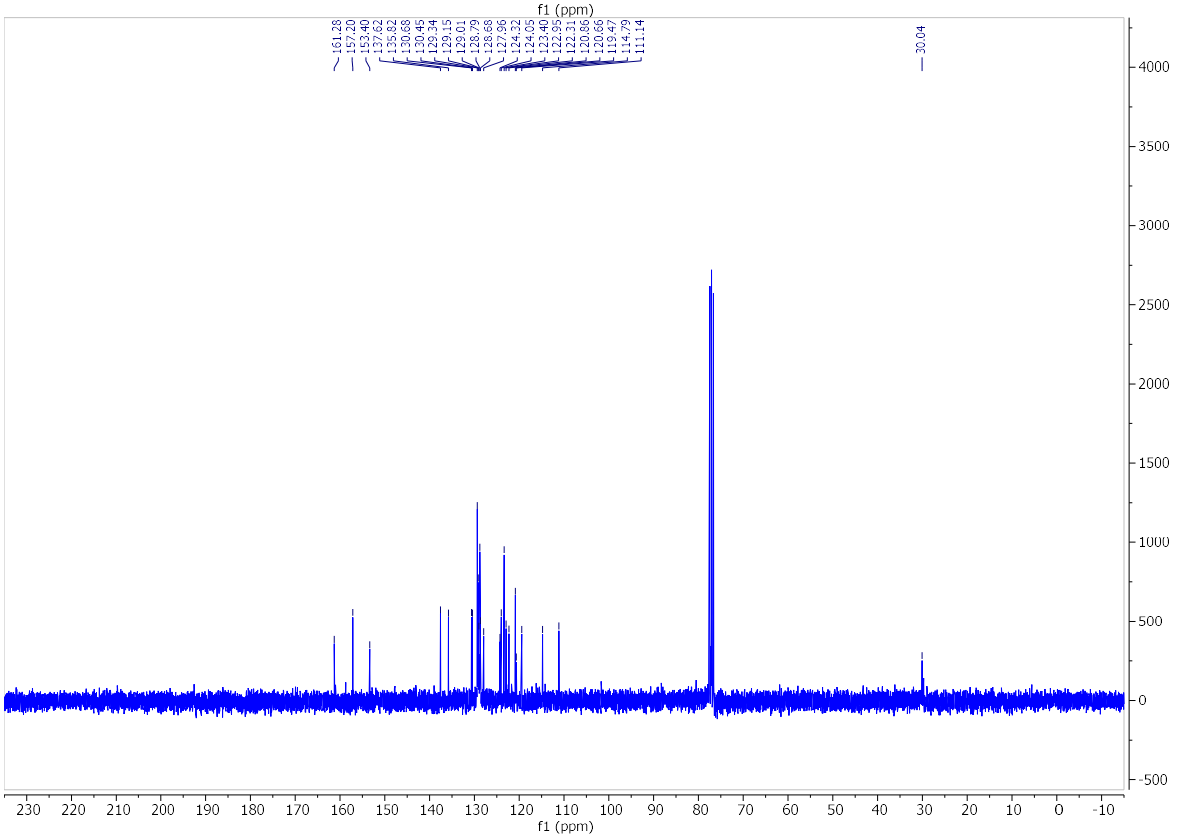
161.28
157.20
153.40
137.62
135.82
130.68
130.45
129.34
129.15
129.01
128.79
128.68
127.36
124.32
124.05
123.49
122.31
120.86
120.66
119.47
114.79
111.14
30.04
f1 (ppm)

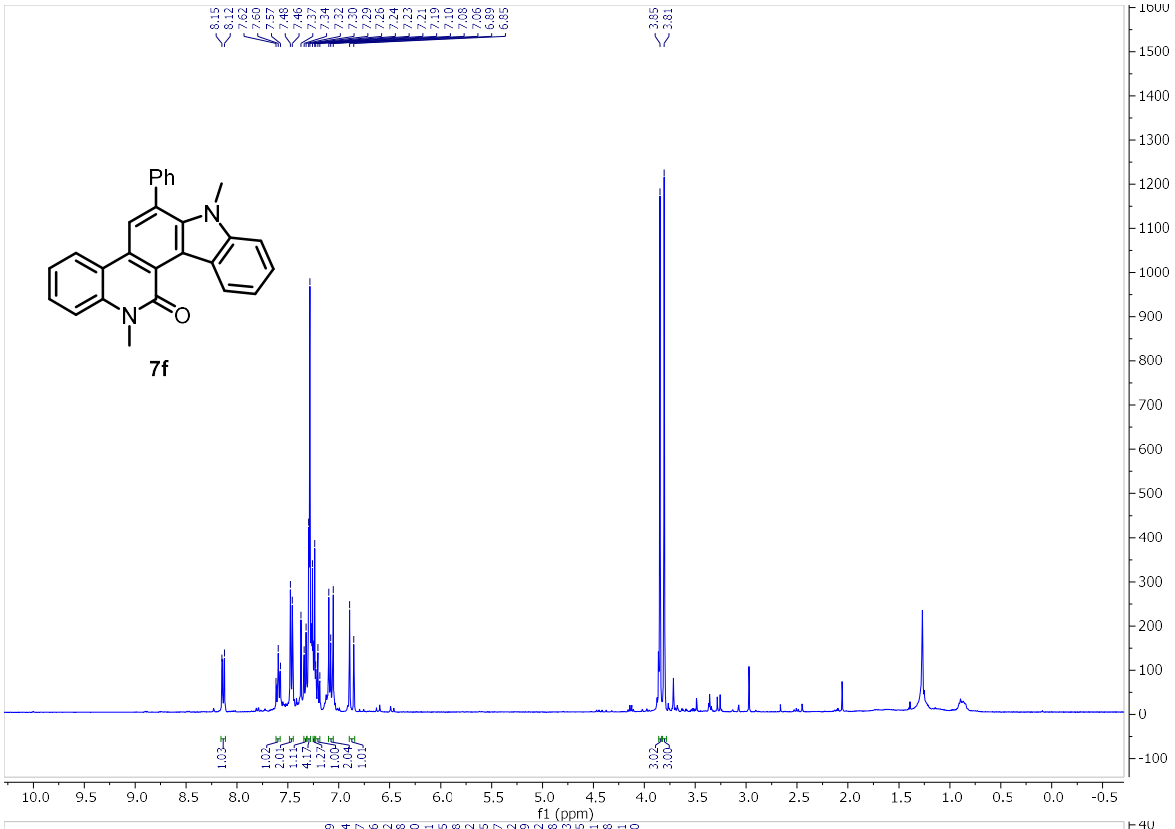
Ph
N
N
O
7f
f1 (ppm)

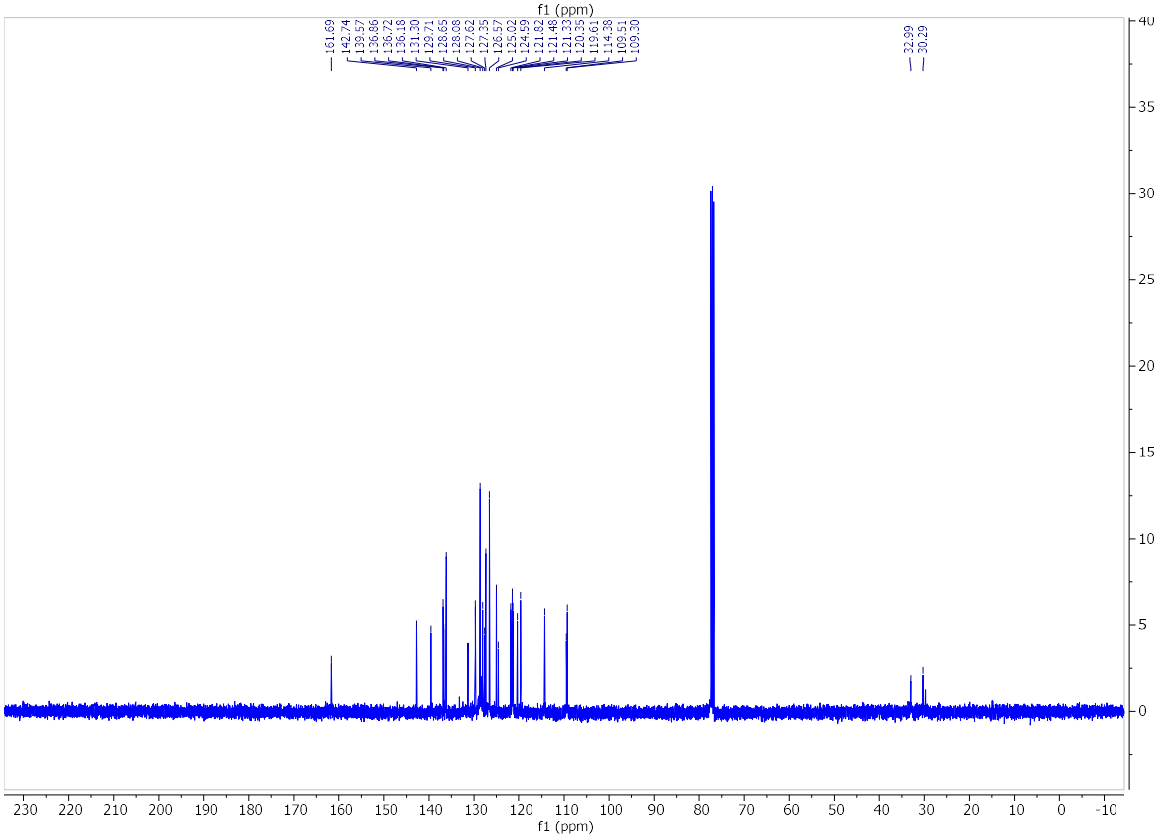
f1 (ppm)

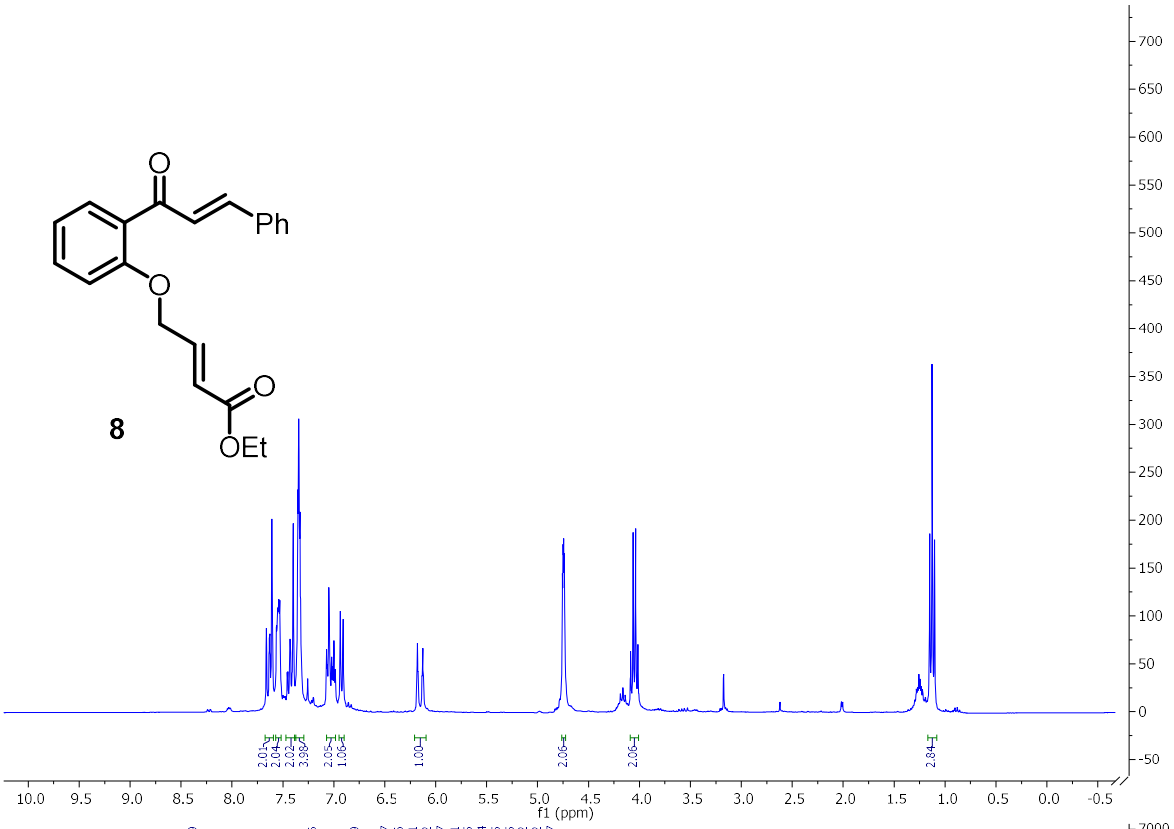
O
Ph
O
O
OEt
8
2.01
2.04
2.02
3.98
2.05
1.06
1.00
2.06
2.06
2.84
f1 (ppm)

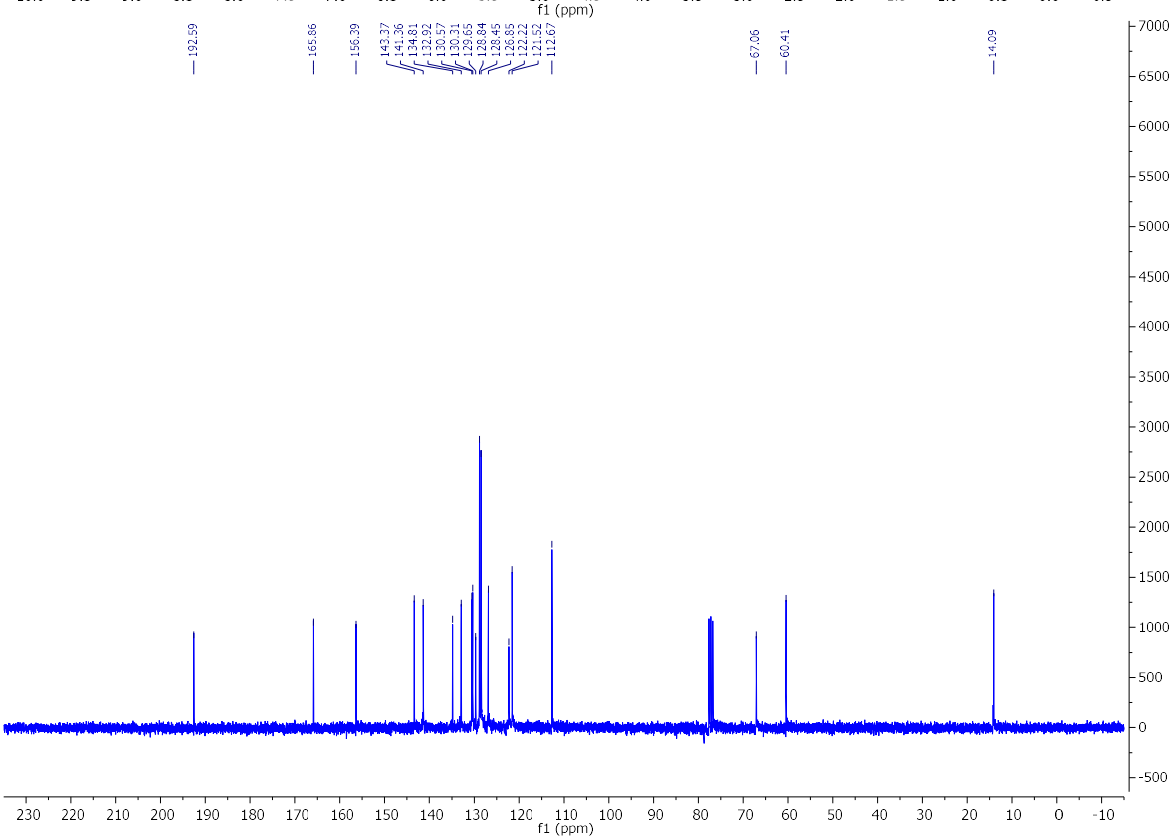
192.59
165.86
156.39
143.37
141.36
134.81
132.92
130.57
130.31
129.65
128.84
128.45
126.85
122.22
121.52
112.67
67.06
60.41
14.09
f1 (ppm)

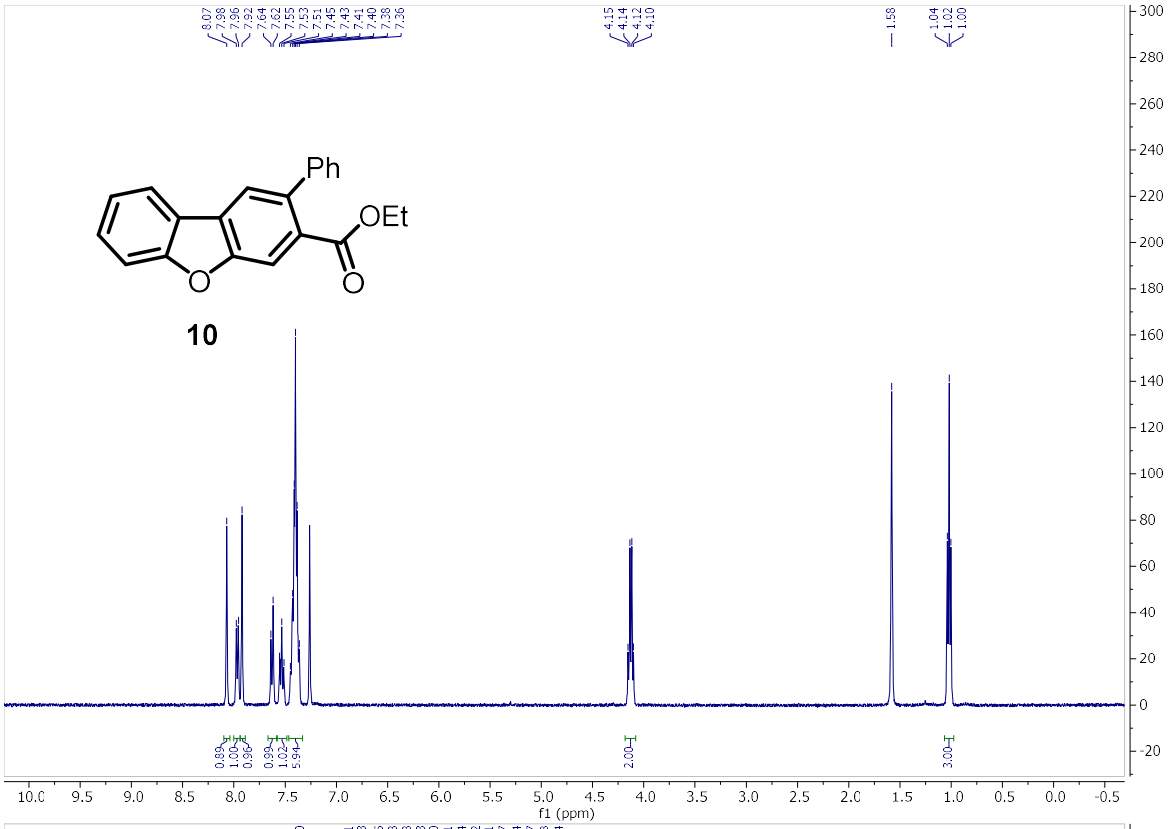
8.07
7.98
7.96
7.92
7.64
7.62
7.55
7.53
7.51
7.45
7.43
7.41
7.40
7.38
7.36
4.15
4.14
4.12
4.10
1.58
1.04
1.02
1.00
Ph
OEt
O
O
10
0.89
1.00
0.98
0.99
1.02
5.94
2.00
3.00
f1 (ppm)

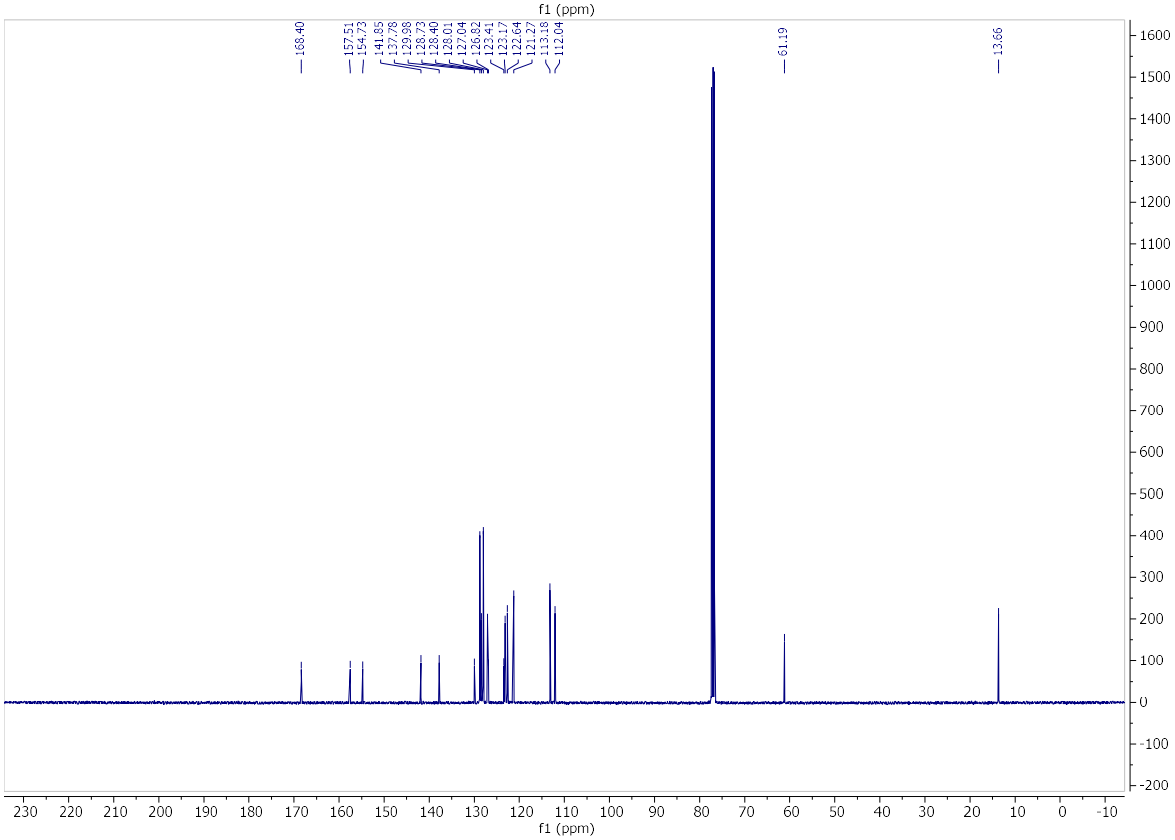
168.40
157.51
154.73
141.85
137.78
129.98
128.73
128.40
128.01
127.04
126.82
123.41
123.17
122.64
121.27
113.18
112.04
61.19
13.66
f1 (ppm)

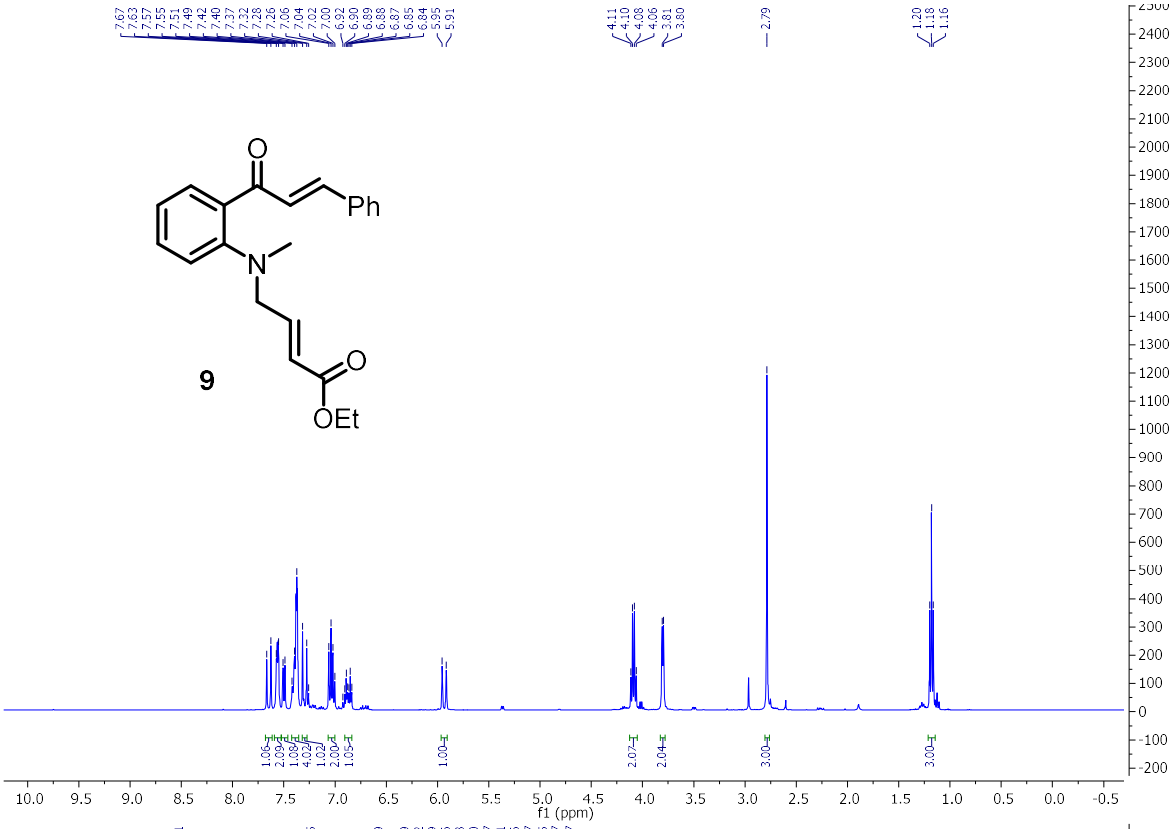
7.67
7.63
7.57
7.55
7.51
7.49
7.42
7.40
7.37
7.32
7.28
7.26
7.06
7.04
7.02
7.00
6.92
6.90
6.89
6.88
6.87
6.85
6.84
5.95
5.91
4.11
4.10
4.08
4.06
3.81
3.80
2.79
1.20
1.18
1.16
O
Ph
N
O
OEt
9
1.06
2.09
1.09
4.02
1.02
2.00
1.05
1.00
2.07
2.04
3.00
3.00
f1 (ppm)

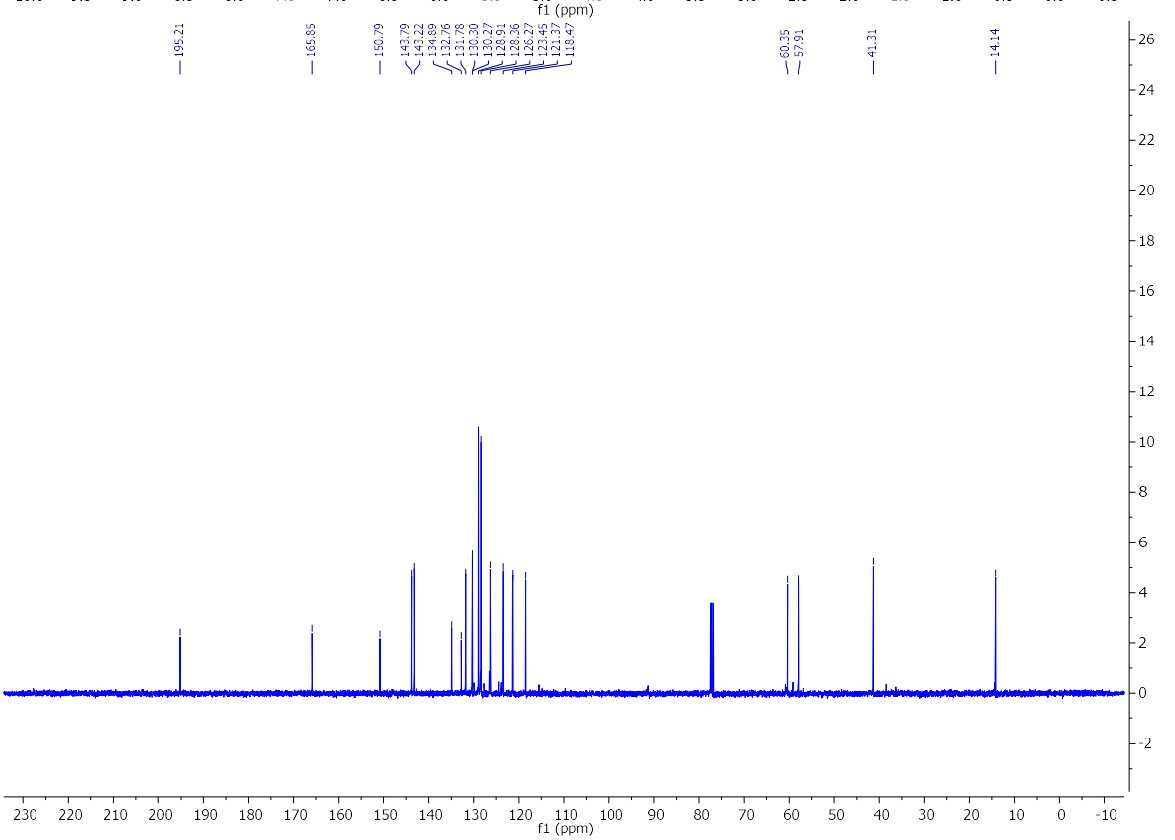
195.21
165.85
150.79
143.79
143.22
139.69
132.76
131.78
130.39
130.01
128.91
128.36
126.27
123.45
121.37
118.47
60.35
57.91
41.31
14.14
f1 (ppm)

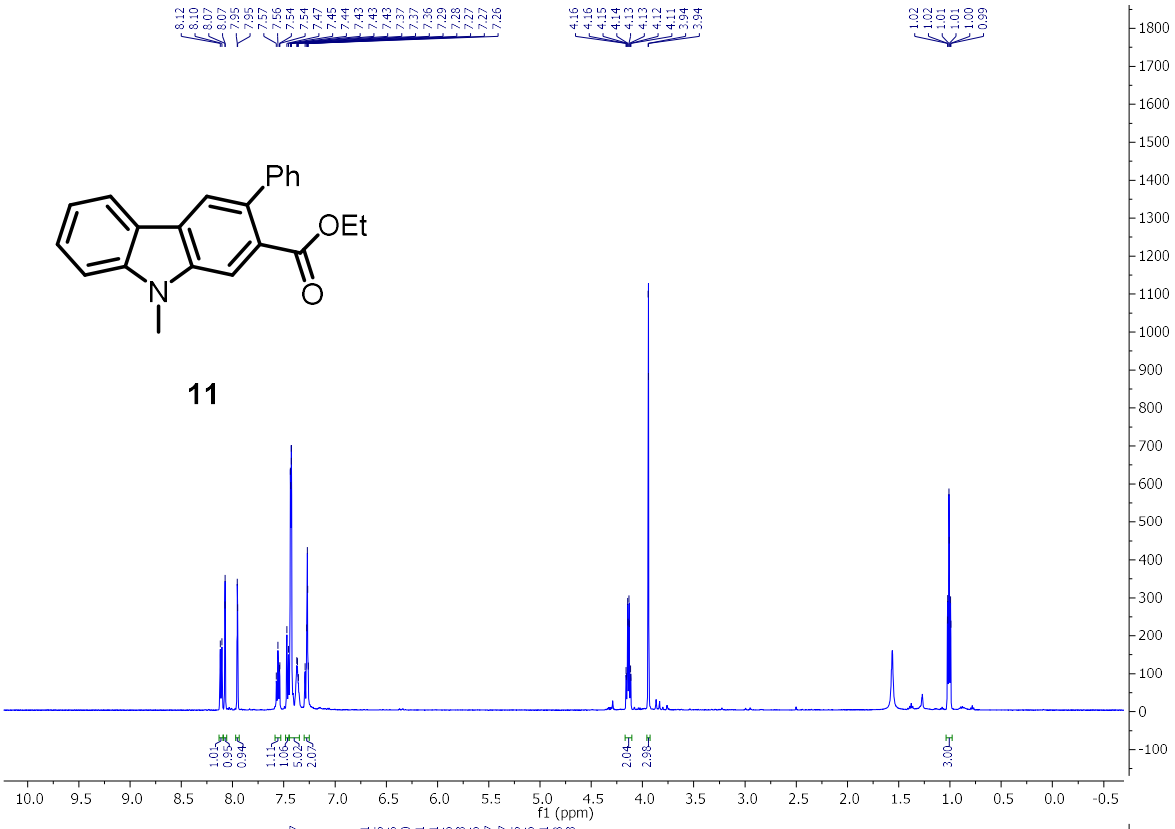
Ph
OEt
O
N
11
f1 (ppm)

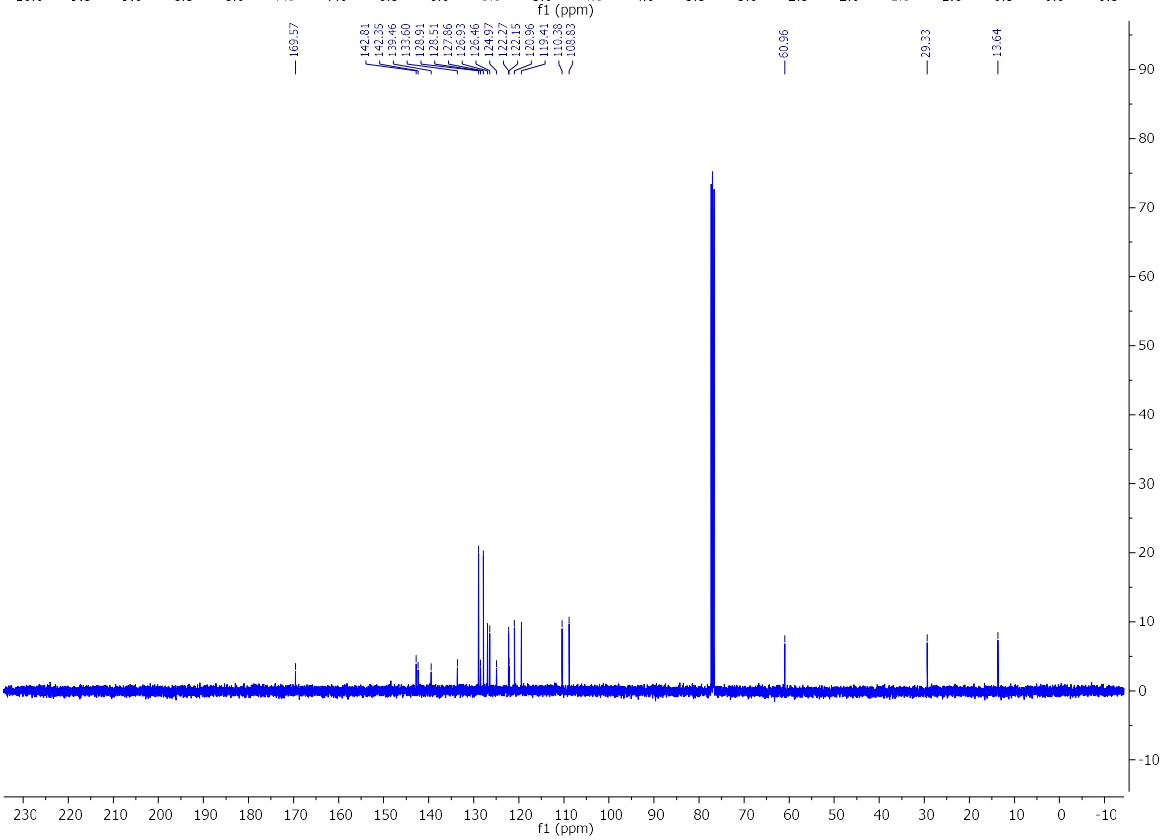
169.57
142.81
142.35
139.46
133.60
128.91
128.51
127.86
126.93
126.46
124.97
122.27
122.15
120.96
119.41
119.38
108.83
60.96
29.33
13.64
f1 (ppm)

CHAPTER 5

Conclusions

As drug development has shifted its focus towards straightforward, planar molecules in the 21st century which can be quickly and conveniently synthesized, there exists a need to expand the chemical space of the drug development process to encompass molecules with a higher degree of structural complexity. The current trend in combinatorial chemistry has shifted development of pharmaceuticals to flat, aromatic compounds; because biological targets like proteins and receptors are complex three-dimensional structures, carefully designed, structurally complex small molecules are capable of binding with a high degree of selectivity, mitigating undesired side effects of off-target binding. Since the cost of a drug is directly related to the number of synthetic steps used to prepare the compound, we have formed a central research hypothesis utilizing reactive intermediates to form such compounds in a cascade fashion, directly reducing the number of steps in their synthesis. Ultimately, culmination of this research effort

has produced new methods of generating spiroethers, carbocycles, spirothiophenes, and an array of aromatic heterocycles.

First, we have employed a catalytic cocktail comprised of $Rh_2(esp)_2$ and Au^+, which had been previously used for the formation of γ-butyrolactones from α-diazocarbonyl compounds through an acid O–H insertion/Conia-ene cascade, towards the formation of tetrahydrofurans (**Chapter 2**). This approach has proven general for a range of ketoester, diketone, and malonate diazo substrates with primary and secondary alkynols. We have also shown that this approach could be applied to cyclic diazo substrates, for the formation of spiroethers. Targeting the core of the natural product Berkeleyamide D, we were able to synthesize α-spiro-γ-lactams with a high degree of stereocontrol. These efforts were not met without challenges however, as we observed reduced yields and diastereoselectivity when chiral secondary alkynols were used with these lactam diazos.

Next, we pursued the applications of using underexplored S–H and sp^3 C–H nucleophiles in a cascade fashion (**Chapter 3**). When secondary mercaptynes were exposed to $Rh_2(esp)_2$ in the presence of a linear diazo substrate, we were able to isolate the corresponding insertion product then induce a Conia-ene cyclization in a stepwise fashion by exposing this compound to Au^+. However, when the mercaptyne and diazo were exposed to all catalysts in a one-pot fashion, we instead isolated a thiofuranofuran product, which we expect formed via undesired 5-endo-dig cyclization of the mercaptyne before S–H insertion could occur. By altering our cascade approach to an intramolecular insertion/Conia-ene strategy, we were able to develop a diazo substrate capable of producing 3-spiroinden-2-ones through benzylic sp^3 C-H insertion. These conditions

however did not prove general for the 5-membered and 7-membered Conia-ene cyclization however, as we had previously observed in a sp^2 C–H insertion/Conia-ene cascade.

Lastly, in an orthogonal research effort, we have discovered a metal-free cascade approach to four classes of heterocycles (**Chapter 4**). The reaction cascade is commenced by an intramolecular aldol condensation generating a 1,3,5-triene intermediate; the triene undergoes a 6π electrocyclization and oxidative aromatization to generate a new aromatic ring. The cascade precursors are conveniently accessed through coupling of readily accessible 2'-hydroxy/aminochalcones with vinylic carboxylic acids/acyl chlorides. The reaction conditions were suitable scale-up to gram scale without significant decrease in yields, and could also utilize aromatic components in the electrocyclization reaction to generate tetracyclic frameworks.

AUTOBIOGRAPHICAL STATEMENT

Education

08/2015-present	**Ph.D. Candidate in Organic Chemistry** University of Oklahoma (Advisor : Dr. Indrajeet Sharma) Doctoral Dissertation "*Cascade reactions to Access Bioactive Scaffolds*"
08/2011-05/2015	**B.S. in Chemistry Miami University** in Oxford, Ohio (Undergraduate Research Advisor : Dr. Benjamin W. Gung)

Publications

1. **Schlitzer, S. C**.; Dhanarajan, A.; Stevens, K. G.; Sharma, I. "A Metal-Free Cascade for the Synthesis of Diverse Heterocycles. Org. Chem. Front., 2020, 7(7), 913-918. ***Cover Page Article.*** DOI: 10.1039/c9qo01336a

2. **Schlitzer, S. C.**; Hunter, A. H.; Stevens, J. C.; Almutwalli, B.; Sharma, I. "A Convergent Approach to Diverse Spiroethers through Stereoselective Trapping of Rhodium Carbenoids with Gold-Activated Alkynols." *J. Org. Chem.,* **2018**, 83(5), 2744-2752. DOI: 10.1021/acs.joc.7b03196

3. Hunter, A. C.; **Schlitzer, S. C.**; Sharma, I. "Synergistic Diazo-OH Insertion/Conia-Ene Cascade Catalysis for the Stereoselective Synthesis of γ-Butyrolactones and Tetrahydrofurans." *Chem. Eur. J.* **2016**, 22(45), 16062-16065. DOI: 10.1002/chem.201603934

4. Gung, B. W.; **Schlitzer, S. C.** "Can Hydrogen-Bonding Donors Abstract Chloride from LAu(I)Cl Complexes: A Computational Study." *Tet. Lett.,* **2015**, 56(35), 5043-5047. DOI: 10.1016/j.tetlet.2015.07.019

Memberships

American Chemical Society (ACS)

Society for Chemistry and Biochemistry Researchers (CBR)

Honors and Awards

04/2020 **Roland E. Lehr Scholarship**
Established to provide scholarships to full-time graduate students with priority consideration given to students in physical, inorganic, or materials chemistry.

04/2016 **Outstanding Graduate Teaching Assistant Award**
Selected on the basis of exceptional performance as a TA in our undergraduate laboratories.

03/2016 **Provost's Certification for Distinction in Teaching**
Awarded to one teaching assistant per course who receives student evaluations in the top 10% of instructors.

05/2014 **Sigma Xi Grant**
Awarded to undergraduate students to pursue research during the summer semester. Designed a spectroscopy database webpage with undergraduate advisor for teaching purposes.

Teaching and Leadership Experience

CHEM 1415 General Chemistry II Laboratory — Laboratory Teaching Assistant

Led two 24-student sections through experiments that covered the fundamentals of chemistry, including basic reactions, titrations, redox chemistry, and green chemistry principles.

CHEM 3152 Organic Chemistry Laboratory — Laboratory Teaching Assistant

Led two 24-student sections through experiments that introduced students to fundamental techniques in organic chemistry including distillations, extraction techniques, basic spectroscopy, and experimental optimization culminating in a multi-step synthesis experiment.

CHEM 3053 Organic Chemistry I: Biological Emphasis — Lecture Teaching Assistant

Assisted professors in large-lecture courses (>300 students) by generating exam questions, formulating weekly problem sets, holding weekly office hours, and grading assessment materials.

CHEM 4444 Inorganic Chemistry & Spectroscopic Characterization — Laboratory Teaching Assistant, Head Teaching Assistant

Led small sections of senior students (12 – 16 students) in learning the fundamentals of inorganic synthesis, including anhydrous techniques and formation of coordination compounds. Highly focused on developing independent skills in the laboratory and in spectroscopy, including acquisition and analysis of NMR, IR, UV-Vis, and CV data.